

CLINICAL PATHS FOR SOLUBLE EPOXIDE HYDROLASE INHIBITORS

EDITED BY: John D. Imig and Christophe Morisseau
PUBLISHED IN: Frontiers in Pharmacology





frontiers

Frontiers eBook Copyright Statement

The copyright in the text of individual articles in this eBook is the property of their respective authors or their respective institutions or funders. The copyright in graphics and images within each article may be subject to copyright of other parties. In both cases this is subject to a license granted to Frontiers.

The compilation of articles constituting this eBook is the property of Frontiers.

Each article within this eBook, and the eBook itself, are published under the most recent version of the Creative Commons CC-BY licence.

The version current at the date of publication of this eBook is CC-BY 4.0. If the CC-BY licence is updated, the licence granted by Frontiers is automatically updated to the new version.

When exercising any right under the CC-BY licence, Frontiers must be attributed as the original publisher of the article or eBook, as applicable.

Authors have the responsibility of ensuring that any graphics or other materials which are the property of others may be included in the CC-BY licence, but this should be checked before relying on the CC-BY licence to reproduce those materials. Any copyright notices relating to those materials must be complied with.

Copyright and source acknowledgement notices may not be removed and must be displayed in any copy, derivative work or partial copy which includes the elements in question.

All copyright, and all rights therein, are protected by national and international copyright laws. The above represents a summary only. For further information please read Frontiers' Conditions for Website Use and Copyright Statement, and the applicable CC-BY licence.

ISSN 1664-8714

ISBN 978-2-88966-161-9

DOI 10.3389/978-2-88966-161-9

About Frontiers

Frontiers is more than just an open-access publisher of scholarly articles: it is a pioneering approach to the world of academia, radically improving the way scholarly research is managed. The grand vision of Frontiers is a world where all people have an equal opportunity to seek, share and generate knowledge. Frontiers provides immediate and permanent online open access to all its publications, but this alone is not enough to realize our grand goals.

Frontiers Journal Series

The Frontiers Journal Series is a multi-tier and interdisciplinary set of open-access, online journals, promising a paradigm shift from the current review, selection and dissemination processes in academic publishing. All Frontiers journals are driven by researchers for researchers; therefore, they constitute a service to the scholarly community. At the same time, the Frontiers Journal Series operates on a revolutionary invention, the tiered publishing system, initially addressing specific communities of scholars, and gradually climbing up to broader public understanding, thus serving the interests of the lay society, too.

Dedication to Quality

Each Frontiers article is a landmark of the highest quality, thanks to genuinely collaborative interactions between authors and review editors, who include some of the world's best academicians. Research must be certified by peers before entering a stream of knowledge that may eventually reach the public - and shape society; therefore, Frontiers only applies the most rigorous and unbiased reviews. Frontiers revolutionizes research publishing by freely delivering the most outstanding research, evaluated with no bias from both the academic and social point of view. By applying the most advanced information technologies, Frontiers is catapulting scholarly publishing into a new generation.

What are Frontiers Research Topics?

Frontiers Research Topics are very popular trademarks of the Frontiers Journals Series: they are collections of at least ten articles, all centered on a particular subject. With their unique mix of varied contributions from Original Research to Review Articles, Frontiers Research Topics unify the most influential researchers, the latest key findings and historical advances in a hot research area! Find out more on how to host your own Frontiers Research Topic or contribute to one as an author by contacting the Frontiers Editorial Office: researchtopics@frontiersin.org

CLINICAL PATHS FOR SOLUBLE EPOXIDE HYDROLASE INHIBITORS

Topic Editors:

John D. Imig, Medical College of Wisconsin, United States

Christophe Morisseau, University of California, Davis, United States

Citation: Imig, J. D., Morisseau, C., eds. (2020). Clinical Paths for Soluble Epoxide Hydrolase Inhibitors. Lausanne: Frontiers Media SA. doi: 10.3389/978-2-88966-161-9

Table of Contents

- 05 Editorial: Clinical Paths for Soluble Epoxide Hydrolase Inhibitors**
John D. Imig and Christophe Morisseau
- 08 Sexually Dimorphic Regulation of EET Synthesis and Metabolism: Roles of Estrogen**
An Huang and Dong Sun
- 16 Inhibition of Soluble Epoxide Hydrolase for Renal Health**
Jun-Yan Liu
- 27 Deficiency of Soluble Epoxide Hydrolase Protects Cardiac Function Impaired by LPS-Induced Acute Inflammation**
Victor Samokhvalov, K. Lockhart Jamieson, Ahmed M. Darwesh, Hedieh Keshavarz-Bahaghighat, Tim Y. T. Lee, Matthew Edin, Fred Lih, Darryl C. Zeldin and John M. Seubert
- 43 Pharmacological Blockade of Soluble Epoxide Hydrolase Attenuates the Progression of Congestive Heart Failure Combined With Chronic Kidney Disease: Insights From Studies With Fawn-Hooded Hypertensive Rats**
Šárka Vacková, Libor Kopkan, Soňa Kikerlová, Zuzana Husková, Janusz Sadowski, Elzbieta Kompanowska-Jezierska, Bruce D. Hammock, John D. Imig, Miloš Táborský, Vojtěch Melenovský and Luděk Červenka
- 59 Role of Soluble Epoxide Hydrolase in Metabolism of PUFAs in Psychiatric and Neurological Disorders**
Kenji Hashimoto
- 69 Soluble Epoxide Hydrolase Inhibition for Ocular Diseases: Vision for the Future**
Bomina Park and Timothy W. Corson
- 78 Epoxyeicosatrienoic Acid-Based Therapy Attenuates the Progression of Postischemic Heart Failure in Normotensive Sprague-Dawley but Not in Hypertensive Ren-2 Transgenic Rats**
Jaroslav Hrdlička, Jan Neckář, František Papoušek, Zuzana Husková, Soňa Kikerlová, Zdenka Vaňourková, Zdenka Vernerová, Firat Akat, Jana Vašinová, Bruce D. Hammock, Sung Hee Hwang, John D. Imig, John R. Falck, Luděk Červenka and František Kolář
- 90 Zafirlukast is a Dual Modulator of Human Soluble Epoxide Hydrolase and Peroxisome Proliferator-Activated Receptor γ**
Tamara Göbel, Olaf Diehl, Jan Heering, Daniel Merk, Carlo Angioni, Sandra K. Wittmann, Estel.la Buscato, Ramona Kottke, Lilia Weizel, Tim Schader, Thorsten J. Maier, Gerd Geisslinger, Manfred Schubert-Zsilavecz, Dieter Steinhilber, Ewgenij Proschak and Astrid S. Kahnt
- 105 Soluble Epoxide Hydrolase Inhibitor: A Novel Potential Therapeutic or Prophylactic Drug for Psychiatric Disorders**
Qian Ren
- 111 Docosahexaenoic Acid Increases the Potency of Soluble Epoxide Hydrolase Inhibitor in Alleviating Streptozotocin-Induced Alzheimer's Disease-Like Complications of Diabetes**
Rohit Pardeshi, Nityanand Bolshette, Kundlik Gadhave, Mohammad Arfeen, Sahabuddin Ahmed, Rohitash Jamwal, Bruce D. Hammock, Mangala Lahkar and Sumanta Kumar Goswami

- 124** *In vitro and in vivo Metabolism of a Potent Inhibitor of Soluble Epoxide Hydrolase, 1-(1-Propionylpiperidin-4-yl)-3-(4-(trifluoromethoxy)phenyl) urea*
Debin Wan, Jun Yang, Cindy B. McReynolds, Bogdan Barnych, Karen M. Wagner, Christophe Morisseau, Sung Hee Hwang, Jia Sun, René Blöcher and Bruce D. Hammock
- 142** *Epoxyeicosatrienoic Acid Analog EET-A Blunts Development of Lupus Nephritis in Mice*
Md. Abdul Hye Khan, Anna Stavniichuk, Mohammad Abdul Sattar, John R. Falck and John D. Imig
- 152** *Dimethyl Sulfoxide Decreases Levels of Oxylipin Diols in Mouse Liver*
Poonamjot Deol, Jun Yang, Christophe Morisseau, Bruce D. Hammock and Frances M. Sladek
- 159** *Pharmaceutical Effects of Inhibiting the Soluble Epoxide Hydrolase in Canine Osteoarthritis*
Cindy B. McReynolds, Sung Hee Hwang, Jun Yang, Debin Wan, Karen Wagner, Christophe Morisseau, Dongyang Li, William K. Schmidt and Bruce D. Hammock
- 171** *Epoxy-Oxylipins and Soluble Epoxide Hydrolase Metabolic Pathway as Targets for NSAID-Induced Gastroenteropathy and Inflammation-Associated Carcinogenesis*
Ryan D. Jones, Jie Liao, Xin Tong, Dandan Xu, Leyu Sun, Haonan Li and Guang-Yu Yang
- 182** *Effect Of Dual sEH/COX-2 Inhibition on Allergen-Induced Airway Inflammation*
Mythili Dileepan, Stephanie Rastle-Simpson, Yana Greenberg, Dayanjan S. Wijesinghe, Naren Gajenthra Kumar, Jun Yang, Sung Hee Hwang, Bruce D. Hammock, P. Sriramarao and Savita P. Rao



Editorial: Clinical Paths for Soluble Epoxide Hydrolase Inhibitors

John D. Imig^{1*} and Christophe Morisseau²

¹ Cardiovascular Center, Medical College of Wisconsin, Milwaukee, WI, United States, ² Department of Entomology and Nematology, University of California at Davis, Davis, CA, United States

Keywords: eicosanoids, oxylipins, heart disease, neurological diseases, kidney disease, pain, inflammation

Editorial on the Research Topic

Clinical Paths for Soluble Epoxide Hydrolase Inhibitors

INTRODUCTION

Soluble epoxide hydrolase (sEH) is an enzyme that contributes importantly to metabolism of endogenous, biologically active arachidonic acid derived epoxyeicosatrienoic acids (EETs) (Imig and Hammock, 2009). Soluble epoxide hydrolase inhibitors (sEHIs) were developed as a means to increase lipid epoxides, including EETs. sEHIs were found to reduce blood pressure, improve insulin sensitivity, and decrease inflammation (Imig and Hammock, 2009). Further sEH development led to initial clinical trials for hypertension and diabetes (Imig and Hammock, 2009). In recent years, there has been significant expansion of the potential clinical paths for sEHIs including clinical trials for COPD, with positive initial findings demonstrating improved endothelial function in smokers with COPD (Yang et al., 2017). There have also been great advances in sEH development in the areas of chronic kidney disease, neuropathic pain, and metabolic diseases with clinical trials scheduled to begin for targeting diabetic neuropathic pain (Imig, 2018).

This Research Topic captures the increasingly broad scope of potential applications for sEHIs, covering cancer, ocular diseases, pulmonary, kidney, heart, liver, and neural pathologies. Research publications span preclinical animal studies, human studies, and the development of multi-target sEH drugs. This Research Topic contains sixteen contributions that demonstrate the exciting clinical paths for sEHIs to treat human diseases.

OPEN ACCESS

Edited and reviewed by:

Alastair George Stewart,
The University of Melbourne, Australia

*Correspondence:

John D. Imig
jdlimig@mcw.edu

Specialty section:

This article was submitted to
Translational Pharmacology,
a section of the journal
Frontiers in Pharmacology

Received: 25 August 2020

Accepted: 07 September 2020

Published: 25 September 2020

Citation:

Imig JD and Morisseau C (2020)
Editorial: Clinical Paths for Soluble
Epoxide Hydrolase Inhibitors.
Front. Pharmacol. 11:598858.
doi: 10.3389/fphar.2020.598858

MINI REVIEWS AND REVIEWS

Six review contributions to the Research Topic provide insight into the impact for sEH on physiological function and broad clinical potential for sEHIs. The influence of estrogen and sex on sEH and EET regulation and vascular function was the focus of a mini-review (Huang and Sun). The increased impact for sEHIs on cardiovascular performance and ischemic diseases for woman was compared to the potential for adverse impact on the pulmonary circulation (Huang and Sun). Another mini-review focused on the potential for sEHIs to treat ocular diseases (Park and Corson). This review covered eye diseases such as macular degeneration, retinopathy of prematurity, and diabetic retinopathy. A mini-review and review provided insight on psychiatric disorders and neurological diseases. These reviews expanded to include the epoxy fatty acids beyond EETs that sEHs can regulate also. The therapeutic potential for sEHIs to regulate EETs and

epoxydocosapentaenoic acids (EDPs) for psychiatric disorders was highlighted in a mini-review (Ren). Neural inflammation and sEH metabolism of polyunsaturated fatty acids (PUFAs) were the focus of a review (Hashimoto). This review covered sEHs potential for treating depression and Parkinson's disease (Hashimoto). A multi-target sEH and cyclooxygenase (COX) inhibitor to enhance gastroenteropathy and inflammation-associated carcinogenesis was reviewed (Jones et al.). This review highlighted the ability for combined sEH and COX inhibition to impact mitochondrial function, reactive oxygen species, and inflammation (Jones et al.). Renal health in several kidney diseases and sEHs was covered in a review (Liu). The potential for sEHs to treat acute kidney injury, chronic kidney disease, hypertension induced kidney damage, and diabetic nephropathy were covered (Liu). These mini-reviews and reviews demonstrate the broad potential for sEHs to treat diseases ranging from cardiovascular diseases, neurological diseases, kidney diseases, and ocular diseases.

DRUG METABOLISM AND OXYLIPIN REGULATION

Drug and oxylipin metabolism are the topics in two scientific reports that are published in this Research Topic. The metabolism of an sEH (TPPU) was investigated in rats and liver S-9 fractions from several species (Wan et al.). Findings demonstrated the ability to translate pharmacokinetic data for TPPU from rats to humans which facilitates clinical development of sEHs (Wan et al.). Next, the effect of dimethylsulfoxide (DMSO) on oxylipin levels in mouse liver were investigated (Deol et al.). Data provided evidence that DMSO can decrease levels of oxylipin diols in mouse level and indicate caution when using DMSO as a vehicle for animal studies (Deol et al.). These studies highlight the predictability of rat studies for sEH clinical development and that there are potential for vehicles in animal studies to influence oxylipin profiles.

HEART DISEASE

The potential for sEHs and EETs as a treatment for heart disease was the focus of three scientific studies published in this Research Topic. Lipopolysaccharide (LPS) myocardial inflammation and cardiotoxicity were studied in sEH null mice and in the presence of sEH (Samokhvalov et al.). Accumulation of diols can contribute to LPS-induced cardiac cell mitochondrial dysfunction that can be combatted by sEHs (Samokhvalov et al.). More chronic heart conditions can also be alleviated by sEHs. The ability for sEH to attenuate the progression of heart failure under conditions of chronic kidney disease were demonstrated in the Fawn-Hooded hypertensive rats (Vacková et al.). Another heart study evaluated the sEH, c-AUCB, and EET analog, EET-A, to decrease postischemic heart failure in normotensive and hypertensive rats (Hrdlička et al.). Findings

from this study indicate that sEH or EET-based treatment attenuates the progression of post-myocardial infarction heart failure in normotensive but not hypertensive rats (Hrdlička et al.). Future studies are needed to translate these findings in animal studies for sEHs and EET analogs to treat acute and chronic heart diseases in humans.

OTHER DISEASES

Three scientific articles in this Research Topic demonstrate the wide-ranging diseases that sEHs and EET analogs could potentially treat. The first of these scientific articles evaluated sEH to treat osteoarthritis a degenerative joint inflammatory disease (McReynolds et al.). In this study, 5 day treatment with the sEH, EC1728, resulted in reduced inflammation and relieved pain in arthritic dogs (McReynolds et al.). The effect of sEHs combined with docosahexaenoic acid to enhance the therapeutic ability in diabetic rats and neurological complications (Pardeshi et al.). This study demonstrates the beneficial anti-inflammatory and anti-oxidative actions of EDPs and sEH on the brain to improve the memory response of diabetic rats (Pardeshi et al.). Lupus nephritis and treatment with the EET analog, EET-A, was the focus of the third scientific article (Hye Khan et al.). This study revealed decreased inflammation and fibrosis in lupus nephritis mice treated with EET-A that prevented progression of renal damage (Hye Khan et al.). These three scientific articles highlight the common threads of anti-inflammatory and anti-oxidative actions for sEHs, the various avenues to manipulate epoxy fatty acids to achieve beneficial actions, and the breadth of human diseases that sEHs and manipulating fatty acids have the potential to treat.

DUAL INHIBITORS

One area where development of sEHs has been expanding is as one component of multi-target drugs. The rational design of drugs that act on specific multiple targets has gained interest due to the recognition that the balanced modulation of two targets can provide a superior therapeutic effect and side effect profile. This balanced modulation is demonstrated in the scientific article demonstrating the effects of zafirlukast on 3T3-L1 adipocytes (Göbel et al.). Zafirlukast, which is a marketed CysLT1 receptor antagonist, provides the structural starting point for developing dual sEH and proliferator-activated receptor γ activator (PPAR γ) drugs that would have decrease inflammation, as well as, resolve inflammation to potentially treat chronic inflammatory diseases (Göbel et al.). The second multi-target sEH is combined with COX-2 inhibition (PTUPB) and compared to a sEH (*t*-TUCB) in an allergen-induced airway inflammation (Dileepan et al.). In this study the multi-target drug, PTUPB failed to provide additional advantage compared to *t*-TUCB; however, PTUPB could be useful in treating conditions where eosinophil and pain-associated inflammation co-exist

(Dileepan et al.). These findings are two examples of the ever expanding multi-drug compounds with sEHI that are being developed. There is ample evidence that a multi-target drug with sEHI activity could eventually be successful in treating human diseases.

CONCLUSIONS

The Research Topic Clinical Paths for Soluble Epoxide Hydrolase Inhibitors demonstrates the exciting potential for sEHIs to treat human diseases and improve quality of life. This collection of sixteen articles demonstrates that sEHIs can reduce inflammation, improve mitochondrial function, and decrease oxidative stress as mechanisms to combat disease. Therefore, there is great promise that an sEHI will be treating either ocular diseases, pulmonary diseases, kidney diseases, cardiovascular diseases, or neurological disorders in the near future.

REFERENCES

- Imig, J. D., and Hammock, B. D. (2009). Soluble epoxide hydrolase as a therapeutic target for cardiovascular diseases. *Nat. Rev. Drug Discovery* 8 (10), 794–805. doi: 10.1038/nrd2875
- Imig, J. D. (2018). Prospective for cytochrome P450 epoxygenase cardiovascular and renal therapeutics. *Pharmacol. Ther.* 192, 1–19. doi: 10.1016/j.pharmthera.2018.06.015
- Yang, L., Cheriyan, J., Gutterman, D. D., Mayer, J. M., Ament, Z., Griffin, J. L., et al. (2017). Mechanisms of Vascular Dysfunction in COPD and Effects of a Novel Soluble Epoxide Hydrolase Inhibitor in Smokers. *Chest* 151 (3), 555–563. doi: 10.1016/j.chest.2016.10.058

AUTHOR CONTRIBUTIONS

JJ: conceived the content and drafted the manuscript. JJ and CM: revised and approved the final manuscript.

FUNDING

This work was supported, in part, by the National Institute of Diabetes and Digestive and Kidney Diseases Grant DK103616, the National Institute of Environmental Health Sciences (NIEHS) Grant R35ES030443, NIEHS Superfund Research Program P42 ES004699, and the Dr. Ralph and Marian Falk Medical Research Trust Bank of America, N.A., Trustee.

ACKNOWLEDGMENT

We thank Wojciech K. Jankiewicz for designing the Research Topics picture.

Conflict of Interest: JJ has patents that cover the composition of matter for EET analogs and bifunctional sEH inhibitors. CM is an inventor on patents owned by UC Davis for composition of matter and usage of sEH inhibitors.

Copyright © 2020 Imig and Morisseau. This is an open-access article distributed under the terms of the Creative Commons Attribution License (CC BY). The use, distribution or reproduction in other forums is permitted, provided the original author(s) and the copyright owner(s) are credited and that the original publication in this journal is cited, in accordance with accepted academic practice. No use, distribution or reproduction is permitted which does not comply with these terms.



Sexually Dimorphic Regulation of EET Synthesis and Metabolism: Roles of Estrogen

An Huang* and Dong Sun

Department of Physiology, New York Medical College, Valhalla, NY, United States

OPEN ACCESS

Edited by:

John D. Imig,
Medical College of Wisconsin,
United States

Reviewed by:

Mohammed A. Nayeem,
West Virginia University, United States
Yi Zhu,
Tianjin Medical University, China

*Correspondence:

An Huang
an_huang@nymc.edu

Specialty section:

This article was submitted to
Translational Pharmacology,
a section of the journal
Frontiers in Pharmacology

Received: 04 September 2018

Accepted: 08 October 2018

Published: 29 October 2018

Citation:

Huang A and Sun D (2018)
Sexually Dimorphic Regulation of EET
Synthesis and Metabolism:
Roles of Estrogen.
Front. Pharmacol. 9:1222.
doi: 10.3389/fphar.2018.01222

Epoxyeicosatrienoic acids (EETs) are metabolites of arachidonic acid via cytochrome P450 (CYP)/epoxygenase and are hydrolyzed by soluble epoxide hydrolase (sEH). Circulating and tissue levels of EETs are controlled by CYP (EET synthesis) and sEH (EET degradation). Therefore, both increases in CYP activity and decreases in sEH expression potentiate EET bioavailability, responses that prevail in the female sex as a function of estrogen. This mini review, based on subtitles listed, briefly summarizes studies focusing specifically on (1) female-specific potentiation of CYP/epoxygenase activity to compensate for the endothelial dysfunction; and (2) estrogen-dependent downregulation of sEH expression, which yields divergent actions in both systemic and pulmonary circulation, respectively.

Estrogen-Potentiating EET Synthesis in Response to Endothelial Dysfunction:

This section summarizes the current understanding regarding the roles of estrogen in facilitating EET synthesis in response to endothelial dysfunction. In this regard, estrogen recruitment of EET-driven signaling serves as a back-up mechanism, which compensates for NO deficiency to preserve endothelium-dependent vasodilator responses and maintain normal blood pressure.

Estrogen-Dependent Downregulation of *Ephx2*/sEH Expression: This section focuses on molecular mechanisms responsible for the female-specific downregulation of sEH expression.

Roles of EETs in Systemic Circulation, as a Function of Estrogen-Dependent Downregulation of sEH:

This section summarizes studies conducted on animals that are either deficient in the *Ephx2* gene (sEH-KO) or have been treated with sEH inhibitors (sEHIs), and exhibit EET-mediated cardiovascular protections in the cerebral, coronary, skeletal, and splanchnic circulations. In particular, the estrogen-inherent silencing of the *Ephx2* gene duplicates the action of sEH deficiency, yielding comparable adaptations in attenuated myogenic vasoconstriction, enhanced shear stress-induced vasodilation, and improved cardiac contractility among female WT mice, male sEH-KO and sEH-treated mice.

Roles of Estrogen-Driven EET Production in Pulmonary Circulation: This section reviews epidemiological and clinical studies that provide the correlation between the

polymorphism, or mutation of gene(s) involving estrogen metabolism and female predisposition to pulmonary hypertension, and specifically addresses an intrinsic causation between the estrogen-dependent downregulation of *Ephx2* gene/sEH expression and female-susceptibility of being pulmonary hypertensive, a topic that has never been explored before. Additionally, the issue of the “estrogen paradox” in the incidence and prognosis of pulmonary hypertension is discussed.

Keywords: epoxyeicosatrienoic acids, soluble epoxide hydrolase, sex, estrogen, pulmonary hypertension

INTRODUCTION

It is established that oxidative metabolism of arachidonic acid through the cyclooxygenase (COX) and lipoxygenase pathways to biologically activate eicosanoids plays a critical role in the regulation of pathophysiological processes. To date, a dubbed “third pathway” of the cytochrome P450 (CYP)/epoxygenase system has come to the forefront of research with aims to evaluate the pathophysiological significance of its biologically active mediators, epoxyeicosatrienoic acids (EETs) (Roman, 2002). EETs possess cardiovascular protective properties in the systemic circulation via endothelium-derived hyperpolarizing factor (EDHF)-based vasodilator responses (Archer et al., 2003; Fleming, 2004; Huang et al., 2004, 2005) to lower blood pressure in both physiological (Imig, 2012; Sun et al., 2014) and pathological conditions (Lee et al., 2010; Ma et al., 2013). The contribution of EETs toward the cardiovascular protection can be controlled by soluble epoxide hydrolase (sEH), an enzyme that hydrolyzes EETs to their biologically inactive diols (dihydroxyeicosatrienoic acids, DHETs) (Newman et al., 2005). As such, either the potentiation of EET synthesis or the reduction of EET metabolism is able to increase EET bioavailability, and therefore, both CYP/epoxygenase and sEH can be therapeutic targets for cardiovascular diseases. More importantly, both enzymatic activities are regulated by female hormones/estrogens, leading to a sex disparity in the presentation of EET-mediated contributions. In general, beneficial actions of EETs in the cardiovascular system have been well reviewed (Roman, 2002; Imig, 2012), however, the sexually dimorphic phenotype, in terms of female-favorable contributions of EETs is much less addressed. Thus, this mini-review will summarize studies from the authors', as well as others' laboratories, focusing on (1) female-specific potentiation of CYP activity to compensate for the endothelial dysfunction; and (2) estrogen-dependent suppression of sEH expression that yields divergent actions in the systemic and pulmonary circulation, respectively.

ESTROGEN-FAVORABLE EET SYNTHESIS IN RESPONSE TO NITRIC OXIDE DEFICIENCY

Cytochrome P450 are encoded by a complex superfamily of genes; they are located in the endoplasmic reticulum and add an epoxide across one of the four double bonds of arachidonic acid to produce four EET regiosomers: 5,6-EET, 8,9-EET, 11,12-EET

and 14,15-EET. The CYP2C and CYP2J families are responsible for the majority of EET generation in mammals (Imig, 2012). Specifically, CYP2C29 and CYP2C7 are EET synthase in mouse and rat vascular endothelium, and express predominantly in female vessels deficient in NO synthesis (Sun et al., 2010, 2011).

One of rationales for investigating CYP/epoxygenase function is its compensatory nature, characterized by the fact that the enzymatic activity and its contribution to the regulation of cardiovascular function are dampened under physiological conditions, and become discernible in most instances, only with endothelial dysfunction, manifested as impaired NO bioavailability. Therefore, most *in vitro* studies aiming to evaluate CYP activities were performed in the presence of inhibitors of endothelial nitric oxide synthase (eNOS) and COX. More intriguingly, the CYP/EET-evoked compensatory action exerts in a female favorable manner, as indicated by the evidence that in eNOS and COX-1 double knockout (KO) mice, EET-mediated responses via an EDHF-based event contribute significantly to the preservation of endothelium-dependent relaxation, coinciding with normal blood pressure in female animals (Scotland et al., 2005), with little of this compensation in their male counterparts that display hypertension, associated with impaired endothelium-dependent vasodilations (Brandes et al., 2000). The same responsive pattern was also observed in the high fructose-induced metabolic syndrome or chronic insulin-loading animal models, where only hyperinsulinemic male rats, not females, developed hypertension, even though both sexes displayed endothelial dysfunction (Galipeau et al., 2002; Vasudevan et al., 2005); moreover, female ovariectomy (OV) prevented, and OV with estrogen replacement (OVE) restored the normotension (Galipeau et al., 2002; Song et al., 2005). These findings clarify estrogen as an essential player in the compensation against endothelial dysfunction (deficiency of NO and/or PGs), via perhaps, recruiting EET/EDHF-dependent signaling.

In the microcirculation, estrogen, in response to NO deficiency, affords protection via unveiling the EET/EDHF-mediated pathway as a back-up mechanism, to maintain normal microcirculatory resistance. For instance, in female eNOS-KO mice and female rats treated with L-NAME, estrogen via activation of estrogen receptors (ERs), evokes a solely EET-mediated response that fully preserves shear stress-induced vasodilation (SSID, one of the most important local regulators in the control of microcirculatory resistance) (Huang et al., 2001a,b; Wu et al., 2001), reminiscent of a significantly smaller magnitude of SSID mediated by COX-derived prostaglandins

(PGs) in male eNOS-KO and L-NAME treated counterparts (Sun et al., 1999, 2006). Therefore, the female phenotype of SSID is defined as augmented vasodilator responses mediated by EETs in an EDHF-based approach, as a function of either decreased NO, or increased EET bioactivities (Huang and Kaley, 2004), highlighting further, a reverse interaction between the two endothelial mediators (NO vs. EETs). The female phenotypic SSID (EET-mediation) can be changed to male phenotype of SSID (PG mediation) when gonad-intact females are ovariectomized (Huang et al., 2001b); vice versa, *in vitro* exposure of male vessels to a physiological concentration of estrogen enables to elicit a female phenotype of SSID (Huang et al., 2004). Thus, in the deficiency/impairment of NO bioactivity, vascular release of EETs to maintain a normal endothelial sensitivity to shear stress is dependent of estrogen and occurs via an ER-mediated activation of a PI3K/Akt pathway to upregulate CYP2C29 and CYP2C7 genes (Huang et al., 2004; Sun et al., 2011).

ESTROGEN-DEPENDENT DOWNREGULATION OF *Ephx2*/sEH EXPRESSION

Mammalian sEH is encoded by the *Ephx2* gene and extensively expressed in multiple organs/tissues including vasculatures; it converts epoxides to diols by adding water to open the epoxide, thus inactivating EETs (Harris and Hammock, 2013). The majority of cardiovascular protective actions elicited by pharmacological inhibition of sEH activity using sEH inhibitors (sEHIs) or genetic deletion of the *Ephx2* gene have been ascribed to be due to increases in circulating and tissue/cellular EET levels (Fang et al., 2004; Deng et al., 2011).

Noteworthy, the estrogen-potential of EET production takes place primarily in the presence of endothelial dysfunction, whereas estrogen-downregulation of sEH occurs inherently in physiological conditions. The identification of sexual dimorphism of sEH was originally reported around the 1980's, where sEH activity was found to be remarkably higher in organs/tissues of male and OV female mice in comparison to intact females (Denlinger and Vesell, 1989; Pinot et al., 1995), and further validated by a female-specific downregulation of sEH expression (Zhang et al., 2009; Kandhi et al., 2015; Froogh et al., 2016; Qin et al., 2016). This is reminiscent of the phenomenon known as the "male-specific hypotensive response to sEH deficiency," where the deletion of the *Ephx2* gene in male mice elicited a significant reduction in blood pressure, with minimal hypotensive effects on female mice (Sinal et al., 2000). We found that KO of the *Ephx2* gene (sEH-KO) or treatment with sEHIs in male mice reduced their blood pressure to the level comparable to that of wild type (WT) females; in the latter, disruption of the *Ephx2* gene further reduced blood pressure but with significantly smaller decrement than in male counterparts (Kandhi et al., 2015; Qin et al., 2015a; 2016; Froogh et al., 2016). This dose-dependent-like phenomenon implies that females may heritably possess a mechanism that imitates an action caused by the deletion of the *Ephx2* gene in males, making females less sensitive to an additional disruption of the gene. By using

in vivo and *in vitro* models, we demonstrate that estrogen, through ERs, methylates the *Ephx2* gene promoter to silence its transcriptional activity, a response that involves multiple transcription factor-driven regulatory signaling (Yang et al., 2018). This study provides mechanistically based explanations for the sexually dimorphic expression of sEH and all the consequences arising therefrom, that will be discussed in the forthcoming sections.

ROLES OF EETs IN SYSTEMIC CIRCULATION, AS A FUNCTION OF ESTROGEN-DEPENDENT DOWNREGULATION OF sEH

Female-specific downregulation of sEH expression stabilizes EETs and functionally potentiates EET bioavailability.

In the cerebral circulation, studies using animal models of ischemia demonstrated that estrogen suppression of sEH was responsible for the female-favorable protection against cerebral ischemic damages in an EET-dependent manner (Fairbanks et al., 2012; Davis et al., 2013).

In the coronary circulation, our laboratories have provided evidence indicating sex-different adaptation of cardiac performance, by conducting experiments on Langendorff-perfusion preparations. In physiological conditions, challenged with same increases in preload, female hearts displayed significantly greater cardiac contractility, associated with enhanced coronary blood flow and lower vascular resistance compared to male hearts (Qin et al., 2016). Isolated coronary arteries from female hearts exhibited significantly attenuated pressure-induced myogenic vasoconstriction compared to male arteries, responses that were prevented by 14,15-EEZE (a putative inhibitor of EETs) (Froogh et al., 2016; Qin et al., 2016). These female-specific adaptations were also observed in male sEH-KO mice, implying that estrogen downregulation of sEH duplicates actions of *Ephx2* deletion, yielding identical patterns of attenuated coronary myogenic responses, enhanced coronary perfusion and improved cardiac contractility, along with similar cardiac EET metabolic profiles (a great ratio of EETs/DHETs) among female WT, male sEH-KO mice and male WT mice treated with sEHIs (Sun et al., 2014; Qin et al., 2015b). In pathological conditions, Seubert's group using cardiac ischemia models provided strong evidence indicating an EET-driven protection against ischemia/reperfusion-induced cardiac injury in sEH deficient animals (Chaudhary et al., 2009).

In the skeletal muscle and splanchnic circulations, isolated arterioles from female WT mice exhibited significantly greater magnitude of EET-mediated SSID, accompanied with attenuated arteriolar tone than those of male WT controls, responses that were also elicited in vessels isolated from male sEH-KO mice (Sun et al., 2014; Qin et al., 2015a).

Collectively, the evidence of estrogen-dependent suppression of *Ephx2*/sEH expression provides a novel mechanistic explanation, in addition to the estrogen potentiation of NO-mediated responses (Huang and Kaley, 2004), for the

better cardiac performance and lower incidence of ischemic cardiovascular diseases in women than men.

ROLES OF ESTROGEN-DRIVEN EET PRODUCTION IN PULMONARY CIRCULATION

The systemic circulation is benefited from EETs, which then, creates a question as to whether the increase in pulmonary EETs is a “friend or foe?” In addition to the typical feature of low oxygenated blood in the pulmonary artery (PA), there are other two unique features in the pulmonary circulation that differ from the systemic circulation: (1) hypoxia pulmonary vasoconstriction (HPV) (Sylvester et al., 2012) that is reminiscent of hypoxia-induced vasodilation in systemic vasculatures (Busse et al., 1983) and (2) EET-induced pulmonary vasoconstriction via perhaps, depolarizing PA smooth muscle cells (SMC) (Zhu et al., 2000; Kandhi et al., 2016) in contrast to EET-induced vasodilation in systemic vasculatures via hyperpolarizing vascular SMC. Although currently, there is no specific explanation for the divergent responsiveness to hypoxia and EETs in the pulmonary circulation, both features seem to be relevant to estrogens, which therefore, sheds light upon the categorization of pulmonary hypertension (PH) as a disease with female-specific prevalence (Miller, 2012).

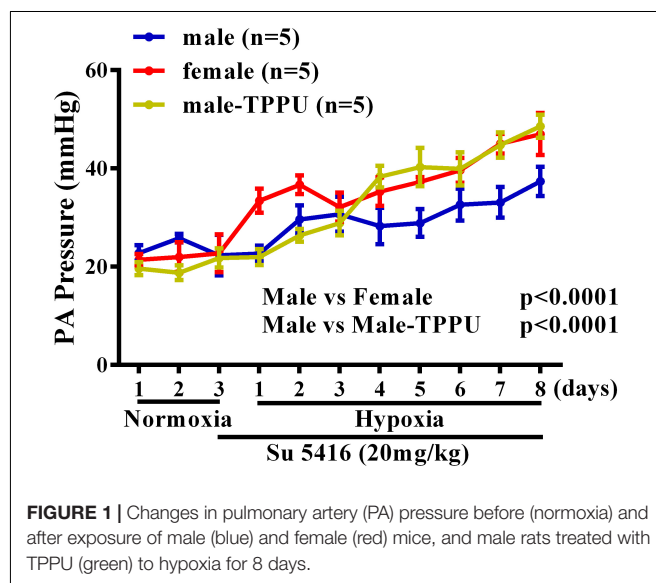
Thus, human studies show a female to male ratio of 4.3:1 among the total PH patients (Walker et al., 2006), and 4.1:1 in the idiopathic PH (IPAH) subcategory (Badesch et al., 2010). This sexual dimorphism in PH is evoked at least in part, by estrogen, as evidenced by a high PH prevalence in women who have taken oral contraceptives (Kleiger et al., 1976), received hormone replacement therapy (Sweeney and Voelkel, 2009) or had enhanced aromatase activity (Roberts et al., 2009). Also, male IPAH patients exist with significantly higher plasma estrogen levels, or a greater ratio of estrogen to testosterone than healthy males (Wu et al., 2018).

Clinical studies provide correlations between the polymorphism of gene(s) involving estrogen metabolisms and the female predisposition to PH (Austin et al., 2009). In general, the mutation in the *BMPR2* gene turns out to be one of the most important genetic-based alterations responsible for the sex-bias in IPAH (Morse et al., 2001; Austin et al., 2013; Dempsey et al., 2011; White et al., 2011), as the penetrance of PH among *BMPR2* mutation carriers shows a 42% penetrance in females vs. 14% in males (Larkin et al., 2012). Female *BMPR2* mutation carriers with PH exhibit a ten-fold reduction in *CYP1B1* gene expression (West et al., 2008; White et al., 2012), followed by altered estrogen metabolism, manifested by a significantly lower ratio of 2-OHE^{1/2} to 16 α -OHE₁ (Austin et al., 2009). This estrogen dysmetabolism shifts the balance away from 2-OHE^{1/2}-induced anti-mitogenic effects toward 16 α -OHE₁-stimulated pulmonary mitogenic and genotoxic pathways (Austin et al., 2013). Direct binding of ER α to the promoter of *BMPR2* gene silences its expression, which disrupts downstream signaling of bone morphogenetic protein-dependent ligand binding, kinase

activation and heteromeric dimer formation etc. (Lane et al., 2000; Austin et al., 2012; Johansen et al., 2016).

To date, there is little attention paid to the intrinsic causation between the estrogen-driven physiological downregulation of *Ephx2* gene/sEH and female-susceptibility to be pulmonary hypertensive, a topic that is being investigated in our laboratories. As reported, increases in pulmonary EETs caused by estrogen downregulation of sEH, knockdown of sEH and treatment with sEHIs propel HPV and promote elevation of PA pressure in response to acute hypoxia (Keseru et al., 2010; Kandhi et al., 2015, 2017). Underlying mechanisms responsible for the EET-dependent potentiation of HPV and hypoxia-induced pulmonary hypertension (HPH) remain elusive; however, roles of vasoconstrictor prostanoids and Rho kinase in this process have emerged, as shown that enhanced hypoxic responses were prevented by 14,15-EEZE, and by inhibition of COXs and Rho kinase, respectively (Keseru et al., 2008; Kandhi et al., 2017). Additionally, the membrane translocation of a TRPC6-V5 fusion protein within PASMC was sensitive to 14,15-EEZE, and hypoxia-induced EET-mediated increases in pulmonary pressure failed to be elicited in mouse lungs that were deficient in TRPC6 (Keseru et al., 2008). Thus, the interaction among estrogen/ERs, sEH/EETs and hypoxia/TRPC6/Rho kinase/PGs works reciprocally, forming a feedback loop in a pattern of cause and result for one another, to elevate PA pressure.

Furthermore, the sex disparity during the development of HPH was evaluated by using radio-telemetry to dynamically monitor changes in rat PA pressure. **Figure 1** shows that under a comparable basal/normoxic PA pressure, male and female rats displayed a time-dependent elevation of PA pressure in response to hypoxia, which, however, occurred earlier accompanied with greater magnitude in females than males, revealing female oversensitivity to hypoxia. This hypoxic responsiveness in female rats was also observed in sEH-treated male rats, indicating the role of EETs in the event. Noteworthy, during the process of

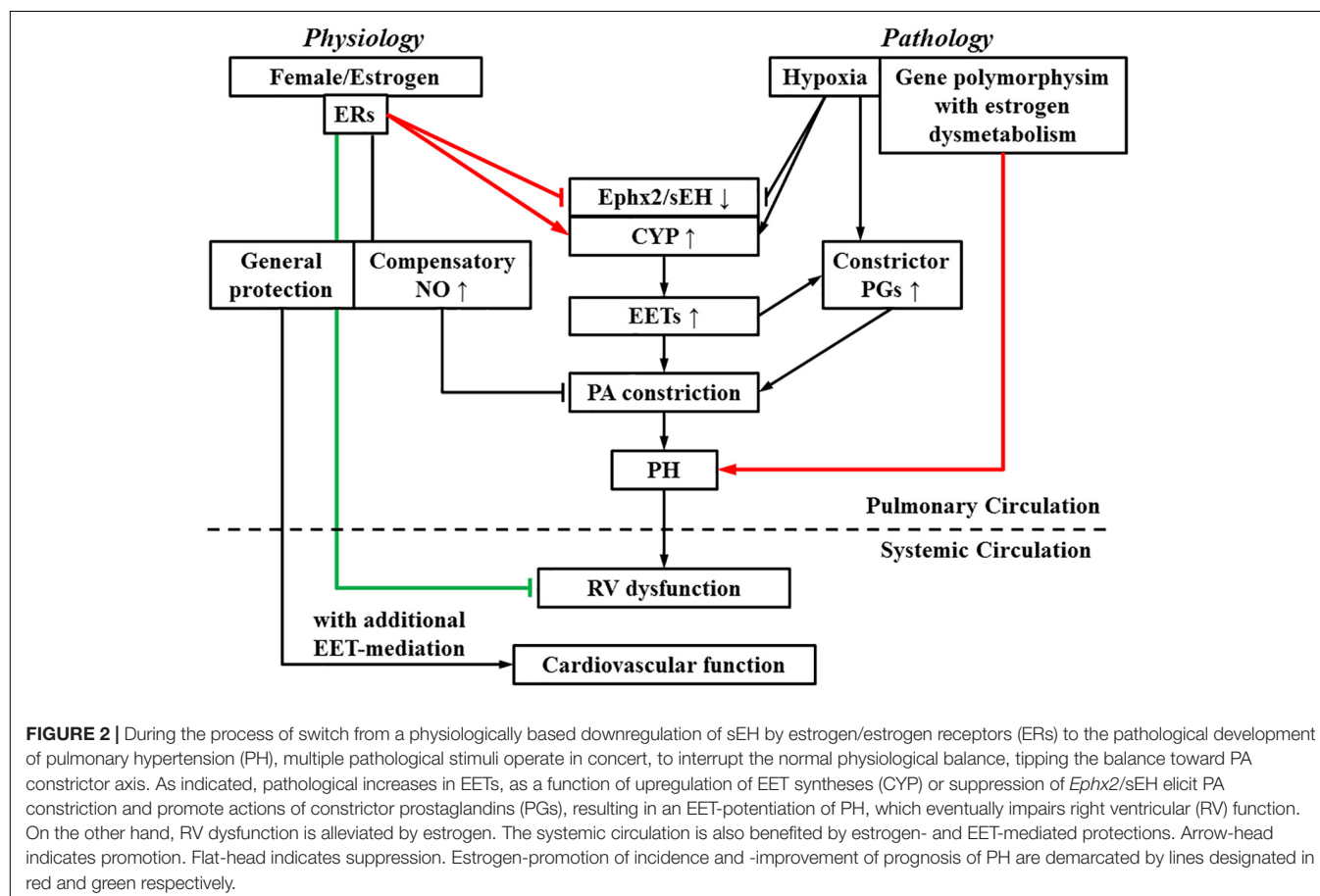


HPH development, hypoxia *per se*, enables to stimulate EET synthesis (Michaelis et al., 2005) and suppress sEH expression in a sex-independent manner (Petruzzelli et al., 1992), which exacerbate EET-mediated HPV in both genders. Alternatively, when PH is ultimately established, female patients paradoxically exhibited less impairment in right ventricle (RV) function, indicating better PH prognosis compared to males (Mair et al., 2014).

A lack of consensus regarding to roles of estrogen in PH is presumably, due to the presence of the “estrogen paradox” that is characterized by divergent actions (detrimental and beneficial) of estrogens in the incidence and prognosis of PH (Lahm et al., 2014). **Figure 2** interprets “estrogen paradox” to mean that *Ephx2*/sEH and CYP are intimately involved in the pathogenesis of HPH, via being targeted and dysregulated by estrogen and hypoxia to increase pulmonary EET bioavailability. Female PAs are capable of maintaining a normal pressure in response to physiological increases in pulmonary EETs due to the presence of compensatory balancing mechanisms such as estrogen-upregulation of eNOS/NO, but bear hyper-responsiveness to acquired pathological challenges such as hypoxia or altered estrogen metabolism, leading to the female susceptibility to PH. Alternatively, all types of PH regardless of their specific etiologies, undergo/share a common progressive process that involves multiple pathological alterations including but not

limited to, the endothelial dysfunction, enhanced oxidative stress and inflammation, vascular remodeling and formation of occlusive lesions, leading to RV hypertrophy and dysfunction, and eventually right heart failure (Rabinovitch, 2012), whereas, all of these pathological alterations can be challenged against by estrogens. For instance, in sugen-hypoxia (SuHx-HP)-induced PH, estrogen improves RV function via inotropic effects on myocardium (Liu et al., 2014) and restoration of conduit PA compliance (Liu et al., 2015). In monocrotaline (MCT)-induced PH, estrogen prevents MCT-induced impairment of antioxidant capacity to preserve myocardial function (Bal et al., 2013). This points to a non-specific pattern of estrogen-driven improvement of PH prognosis, which is neither selectively triggered by a specific model of PH, nor does it direct particular target(s), and provides explanations for the better prognosis with higher survival rate in female than male PH patients.

Currently, clinical trials designed to evaluate the protection of sEHs if any, for patients with chronic obstructive pulmonary diseases (COPD) revealed that GSK alleviated endothelial dysfunction in COPD patients (Lazaar et al., 2016; Yang et al., 2017). Since HPH, as well as COPD, is associated with downregulation of sEH and upregulation of EET production, the improvement of endothelial function elicited by GKS in COPD patents may not be purely, mediated by the inhibition of sEH *per se*, but rather by alternative pathways. Indeed, in



addition to targeting sEH, sEHs are capable of binding with other enzymes due to the presence of multi-target ligands. For instance, PTUPB is a tight COX-2 binder (Hwang et al., 2018) and TPPU selectively inhibits p38 β kinase to block downstream-located NF- κ B-dependent signaling (Liang et al., 2018). As such, pharmacological inhibition of sEH to stabilize EETs may instigate PA vasoconstriction but somehow, mitigate pathological progression in the pulmonary circulation.

SUMMARY AND PERSPECTIVES

We briefly summarized the pathophysiological significance of potentiating EET production and/or inhibiting EET hydrolysis, as a function of estrogen, in the regulation of systemic and pulmonary circulations. In the systemic circulation, increases in EETs afford better cardiovascular performance and lower incidence of ischemic diseases in women. In the pulmonary circulation, clinical development of PH appears to require “two hits” that can be triggered by either genetics (sex and

gene polymorphisms), environmental factors (hypoxia and sex hormone dysmetabolism), or both (female with hypoxia). Thus, from a pros and cons point of view, targeting CYP and sEH may prove to be a double-edged sword with beneficial and adverse effects on systemic and pulmonary circulatory systems; this brings concerns surrounding the use of sEHs as therapeutic regimens, or the consideration of sEH-related clinical trials in female populations who bear hyper-responsiveness to acquired pathological insults (as second hits) to the respiratory system.

AUTHOR CONTRIBUTIONS

AH and DS contributed equally to the literature search, figures, and writing, and gave their final approval of the manuscript.

FUNDING

This work was supported by grants HL070653 and HL129797.

REFERENCES

- Archer, S. L., Gragasin, F. S., Wu, X., Wang, S., McMurtry, S., Kim, D. H., et al. (2003). Endothelium-derived hyperpolarizing factor in human internal mammary artery is 11,12-epoxyeicosatrienoic acid and causes relaxation by activating smooth muscle BK(Ca) channels. *Circulation* 107, 769–776. doi: 10.1161/01.CIR.0000047278.28407.C2
- Austin, E. D., Cogan, J. D., West, J. D., Hedges, L. K., Hamid, R., Dawson, E. P., et al. (2009). Alterations in oestrogen metabolism: implications for higher penetrance of familial pulmonary arterial hypertension in females. *Eur. Respir. J.* 34, 1093–1099. doi: 10.1183/09031936.00010409
- Austin, E. D., Hamid, R., Hemnes, A. R., Loyd, J. E., Blackwell, T., Yu, C., et al. (2012). BMPR2 expression is suppressed by signaling through the estrogen receptor. *Biol. Sex Differ.* 3:6. doi: 10.1186/2042-6410-3-6
- Austin, E. D., Lahm, T., West, J., Tofovic, S. P., Johansen, A. K., MacLean, M. R., et al. (2013). Gender, sex hormones and pulmonary hypertension. *Pulm. Circ.* 3, 294–314. doi: 10.4103/2045-8932.114756
- Badesch, D. B., Raskob, G. E., Elliott, C. G., Krichman, A. M., Farber, H. W., Frost, A. E., et al. (2010). Pulmonary arterial hypertension: baseline characteristics from the REVEAL Registry. *Chest* 137, 376–387. doi: 10.1378/chest.09-1140
- Bal, E., Ilgin, S., Atli, O., Ergun, B., and Sirmagul, B. (2013). The effects of gender difference on monocrotaline-induced pulmonary hypertension in rats. *Hum. Exp. Toxicol.* 32, 766–774. doi: 10.1177/0960327113477874
- Brandes, R. P., Schmitz-Winnenthal, F. H., Feletou, M., Godecke, A., Huang, P. L., Vanhoutte, P. M., et al. (2000). An endothelium-derived hyperpolarizing factor distinct from NO and prostacyclin is a major endothelium-dependent vasodilator in resistance vessels of wild-type and endothelial NO synthase knockout mice. *Proc. Natl. Acad. Sci. U.S.A.* 97, 9747–9752. doi: 10.1073/pnas.97.17.9747
- Busse, R., Pohl, U., Kellner, C., and Klemm, U. (1983). Endothelial cells are involved in the vasodilatory response to hypoxia. *Pflügers Arch.* 397, 78–80. doi: 10.1007/BF00585175
- Chaudhary, K. R., Batchu, S. N., and Seubert, J. M. (2009). Cytochrome P450 enzymes and the heart. *IUBMB Life* 61, 954–960. doi: 10.1002/iub.241
- Davis, C. M., Fairbanks, S. L., and Alkayed, N. J. (2013). Mechanism of the sex difference in endothelial dysfunction after stroke. *Transl. Stroke Res.* 4:381–389. doi: 10.1007/s12975-012-0227-0
- Dempsey, Y., Nilsen, M., White, K., Mair, K. M., Loughlin, L., Ambartsumian, N., et al. (2011). Development of pulmonary arterial hypertension in mice over-expressing S100A4/Mts1 is specific to females. *Respir. Res.* 12, 159. doi: 10.1186/1465-9921-12-159
- Deng, Y., Edin, M. L., Theken, K. N., Schuck, R. N., Flake, G. P., Kannon, M. A., et al. (2011). Endothelial CYP epoxygenase overexpression and soluble epoxide hydrolase disruption attenuate acute vascular inflammatory responses in mice. *FASEB J.* 25, 703–713. doi: 10.1096/fj.10-171488
- Denlinger, C. L., and Vesell, E. S. (1989). Hormonal regulation of the developmental pattern of epoxide hydrolases. Studies in rat liver. *Biochem. Pharmacol.* 38, 603–610. doi: 10.1016/0006-2952(89)90205-0
- Fairbanks, S. L., Young, J. M., Nelson, J. W., Davis, C. M., Koerner, I. P., and Alkayed, N. J. (2012). Mechanism of the sex difference in neuronal ischemic cell death. *Neuroscience* 219, 183–191. doi: 10.1016/j.neuroscience.2012.05.048
- Fang, X., Weintraub, N. L., McCaw, R. B., Hu, S., Harmon, S. D., Rice, J. B., et al. (2004). Effect of soluble epoxide hydrolase inhibition on epoxyeicosatrienoic acid metabolism in human blood vessels. *Am. J. Physiol. Heart Circ. Physiol.* 287, H2412–H2420. doi: 10.1152/ajpheart.00527.2004
- Fleming, I. (2004). Cytochrome P450 epoxygenases as EDHF synthase(s). *Pharmacol. Res.* 49, 525–533. doi: 10.1016/j.phrs.2003.11.016
- Froogh, G., Qin, J., Kandhi, S., Le, Y., Jiang, H., Luo, M., et al. (2016). Female-favorable attenuation of coronary myogenic constriction via reciprocal activations of epoxyeicosatrienoic acids and nitric oxide. *Am. J. Physiol. Heart Circ. Physiol.* 310, H1448–H1454. doi: 10.1152/ajpheart.00906.2015
- Galipeau, D., Verma, S., and McNeill, J. H. (2002). Female rats are protected against fructose-induced changes in metabolism and blood pressure. *Am. J. Physiol. Heart Circ. Physiol.* 283, H2478–H2484. doi: 10.1152/ajpheart.00243.2002
- Harris, T. R., and Hammock, B. D. (2013). Soluble epoxide hydrolase: gene structure, expression and deletion. *Gene* 526, 61–74. doi: 10.1016/j.gene.2013.05.008
- Huang, A., and Kaley, G. (2004). Gender-specific regulation of cardiovascular function: estrogen as key player. *Microcirculation* 11, 9–38. doi: 10.1080/107396804902666162
- Huang, A., Sun, D., Carroll, M. A., Jiang, H., Smith, C. J., Connetta, J. A., et al. (2001a). EDHF mediates flow-induced dilation in skeletal muscle arterioles of female eNOS-KO mice. *Am. J. Physiol. Heart Circ. Physiol.* 280, H2462–H2469.
- Huang, A., Wu, Y., Sun, D., Koller, A., and Kaley, G. (2001b). Effect of estrogen on flow-induced dilation in NO deficiency: role of prostaglandins and EDHF. *J. Appl. Physiol.* 91, 2561–2566.
- Huang, A., Sun, D., Jacobson, A., Carroll, M. A., Falck, J. R., and Kaley, G. (2005). Epoxyeicosatrienoic acids are released to mediate shear stress-dependent hyperpolarization of arteriolar smooth muscle. *Circ. Res.* 96, 376–383. doi: 10.1161/01.RES.0000155332.17783.26
- Huang, A., Sun, D., Wu, Z., Yan, C., Carroll, M. A., Jiang, H., et al. (2004). Estrogen elicits cytochrome P450-mediated flow-induced dilation of arterioles in NO

- deficiency: role of PI3K-Akt phosphorylation in genomic regulation. *Circ. Res.* 94, 245–252. doi: 10.1161/01.RES.0000111525.96232.46
- Hwang, S. H., Gaine, S., Morisseau, C., Yang, J., Wagner, K., Gilson, M. K., et al. (2018). Dual inhibitors of cyclooxygenase-2 and soluble epoxide hydrolase: studies of binding modes and the active sites and time-dependency of inhibition and development of water-soluble prodrug. *FASEB J.* 32.
- Imig, J. D. (2012). Epoxides and soluble epoxide hydrolase in cardiovascular physiology. *Physiol. Rev.* 92, 101–130. doi: 10.1152/physrev.00021.2011
- Johansen, A. K., Dean, A., Morecroft, I., Hood, K., Nilsen, M., Loughlin, L., et al. (2016). The serotonin transporter promotes a pathological estrogen metabolic pathway in pulmonary hypertension via cytochrome P450 1B1. *Pulm. Circ.* 6:82–92. doi: 10.1086/685023
- Kandhi, S., Froogh, G., Qin, J., Luo, M., Wolin, M. S., Huang, A., et al. (2016). EETs Elicit Direct Increases in Pulmonary Arterial Pressure in Mice. *Am. J. Hypertens.* 29, 598–604. doi: 10.1093/ajh/hpv148
- Kandhi, S., Qin, J., Froogh, G., Jiang, H., Luo, M., Wolin, M. S., et al. (2015). EET-dependent potentiation of pulmonary arterial pressure: sex-different regulation of soluble epoxide hydrolase. *Am. J. Physiol. Lung Cell. Mol. Physiol.* 309, L1478–L1486. doi: 10.1152/ajplung.00208.2015
- Kandhi, S., Zhang, B., Froogh, G., Qin, J., Alruwaili, N., Le, Y., et al. (2017). EETs promote hypoxic pulmonary vasoconstriction via constrictor prostanoids. *Am. J. Physiol. Lung Cell. Mol. Physiol.* 313, L350–L359. doi: 10.1152/ajplung.00038.2017
- Keseru, B., Barbosa-Sicard, E., Popp, R., Fisslthaler, B., Dietrich, A., Gudermann, T., et al. (2008). Epoxyeicosatrienoic acids and the soluble epoxide hydrolase are determinants of pulmonary artery pressure and the acute hypoxic pulmonary vasoconstrictor response. *FASEB J.* 22, 4306–4315. doi: 10.1096/fj.08-112821
- Keseru, B., Barbosa-Sicard, E., Schermuly, R. T., Tanaka, H., Hammock, B. D., Weissmann, N., et al. (2010). Hypoxia-induced pulmonary hypertension: comparison of soluble epoxide hydrolase deletion vs. inhibition. *Cardiovasc. Res.* 85, 232–240. doi: 10.1093/cvr/cvp281
- Kleiger, R. E., Boxer, M., Ingham, R. E., and Harrison, D. C. (1976). Pulmonary hypertension in patients using oral contraceptives. A report of six cases. *Chest* 69, 143–147. doi: 10.1378/chest.69.2.143
- Lahm, T., Tuder, R. M., and Petrache, I. (2014). Progress in solving the sex hormone paradox in pulmonary hypertension. *Am. J. Physiol. Lung Cell. Mol. Physiol.* 307, L7–L26. doi: 10.1152/ajplung.00337.2013
- Lane, K. B., Machado, R. D., Pauciuolo, M. W., Thomson, J. R., Phillips, J. A., Loyd, J. E., et al. (2000). Heterozygous germline mutations in BMPR2, encoding a TGF-beta receptor, cause familial primary pulmonary hypertension. *Nat. Genet.* 26, 81–84. doi: 10.1038/79226
- Larkin, E. K., Newman, J. H., Austin, E. D., Hemnes, A. R., Wheeler, L., Robbins, I. M., et al. (2012). Longitudinal analysis casts doubt on the presence of genetic anticipation in heritable pulmonary arterial hypertension. *Am. J. Respir. Crit. Care Med.* 186, 892–896. doi: 10.1164/rccm.201205-0886OC
- Lazaar, A. L., Yang, L., Boardley, R. L., Goyal, N. S., Robertson, J., Baldwin, S. J., et al. (2016). Pharmacokinetics, pharmacodynamics and adverse event profile of GSK2256294, a novel soluble epoxide hydrolase inhibitor. *Br. J. Clin. Pharmacol.* 81, 971–979. doi: 10.1111/bcp.12855
- Lee, J., Dahl, M., Grande, P., Tybjaerg-Hansen, A., and Nordestgaard, B. G. (2010). Genetically reduced soluble epoxide hydrolase activity and risk of stroke and other cardiovascular disease. *Stroke* 41, 27–33. doi: 10.1161/STROKEAHA.109.567768
- Liang, Z., Morisseau, C., Hwang, S. H., Hammock, B. D., Li, Q. X. (2018). A dual-inhibitor of soluble epoxide hydrolase and p3 kinase alleviating Tau hyperphosphorylation and amyloid neurotoxicity for potential treatment of neuroinflammation in Alzheimer's disease. *FASEB J.* 32.
- Liu, A., Schreier, D., Tian, L., Eickhoff, J. C., Wang, Z., Hacker, T. A., et al. (2014). Direct and indirect protection of right ventricular function by estrogen in an experimental model of pulmonary arterial hypertension. *Am. J. Physiol. Heart Circ. Physiol.* 307, H273–H283. doi: 10.1152/ajpheart.00758.2013
- Liu, A., Tian, L., Golob, M., Eickhoff, J. C., Boston, M., and Chesler, N. C. (2015). 17beta-Estradiol Attenuates Conduit Pulmonary Artery Mechanical Property Changes With Pulmonary Arterial Hypertension. *Hypertension* 66, 1082–1088. doi: 10.1161/HYPERTENSIONAHA.115.05843
- Ma, B., Xiong, X., Chen, C., Li, H., Xu, X., Li, X., et al. (2013). Cardiac-specific overexpression of CYP2J2 attenuates diabetic cardiomyopathy in male streptozotocin-induced diabetic mice. *Endocrinology* 154, 2843–2856. doi: 10.1210/en.2012-2166
- Mair, K. M., Johansen, A. K., Wright, A. F., Wallace, E., and MacLean, M. R. (2014). Pulmonary arterial hypertension: basis of sex differences in incidence and treatment response. *Br. J. Pharmacol.* 171, 567–579. doi: 10.1111/bph.12281
- Michaelis, U. R., Fisslthaler, B., Barbosa-Sicard, E., Falck, J. R., Fleming, I., and Busse, R. (2005). Cytochrome P450 epoxygenases 2C8 and 2C9 are implicated in hypoxia-induced endothelial cell migration and angiogenesis. *J. Cell. Sci.* 118, 5489–5498. doi: 10.1242/jcs.02674
- Miller, V. M. (2012). In pursuit of scientific excellence: sex matters. *Am. J. Physiol. Heart Circ. Physiol.* 302, H1771–H1772. doi: 10.1152/ajpheart.00073.2012
- Morse, J. H., Deng, Z., and Knowles, J. A. (2001). Genetic aspects of pulmonary arterial hypertension. *Ann. Med.* 33, 596–603. doi: 10.3109/07853890109002105
- Newman, J. W., Morisseau, C., and Hammock, B. D. (2005). Epoxide hydrolases: their roles and interactions with lipid metabolism. *Prog. Lipid Res.* 44, 1–51. doi: 10.1016/j.plipres.2004.10.001
- Petruzzelli, S., Franchi, M., Gronchi, L., Janni, A., Oesch, F., Pacifici, G. M., et al. (1992). Cigarette smoke inhibits cytosolic but not microsomal epoxide hydrolase of human lung. *Hum. Exp. Toxicol.* 11, 99–103. doi: 10.1177/096032719201100207
- Pinot, F., Grant, D. F., Spearow, J. L., Parker, A. G., and Hammock, B. D. (1995). Differential regulation of soluble epoxide hydrolase by clofibrate and sexual hormones in the liver and kidneys of mice. *Biochem. Pharmacol.* 50, 501–508. doi: 10.1016/0006-2952(95)00167-X
- Qin, J., Kandhi, S., Froogh, G., Jiang, H., Luo, M., Sun, D., et al. (2015a). Sexually dimorphic phenotype of arteriolar responsiveness to shear stress in soluble epoxide hydrolase-knockout mice. *Am. J. Physiol. Heart Circ. Physiol.* 309, H1860–H1866. doi: 10.1152/ajpheart.00568.2015
- Qin, J., Sun, D., Jiang, H., Kandhi, S., Froogh, G., Hwang, S. H., et al. (2015b). Inhibition of soluble epoxide hydrolase increases coronary perfusion in mice. *Physiol. Rep.* 3:e12427. doi: 10.14814/phy2.12427
- Qin, J., Le, Y., Froogh, G., Kandhi, S., Jiang, H., Luo, M., et al. (2016). Sexually dimorphic adaptation of cardiac function: roles of epoxyeicosatrienoic acid and peroxisome proliferator-activated receptors. *Physiol. Rep.* 4:e12838. doi: 10.14814/phy2.12838
- Rabinovitch, M. (2012). Molecular pathogenesis of pulmonary arterial hypertension. *J. Clin. Invest.* 122, 4306–4313. doi: 10.1172/JCI60658
- Roberts, K. E., Fallon, M. B., Krowka, M. J., Brown, R. S., Trotter, J. F., Peter, I., et al. (2009). Genetic risk factors for portopulmonary hypertension in patients with advanced liver disease. *Am. J. Respir. Crit. Care Med.* 179, 835–842. doi: 10.1164/rccm.200809-1472OC
- Roman, R. J. (2002). P-450 metabolites of arachidonic acid in the control of cardiovascular function. *Physiol. Rev.* 82, 131–185. doi: 10.1152/physrev.00021.2001
- Scotland, R. S., Madhani, M., Chauhan, S., Moncada, S., Andresen, J., Nilsson, H., et al. (2005). Investigation of vascular responses in endothelial nitric oxide synthase/cyclooxygenase-1 double-knockout mice: key role for endothelium-derived hyperpolarizing factor in the regulation of blood pressure in vivo. *Circulation* 111, 796–803. doi: 10.1161/01.CIR.0000155238.70797.4E
- Sinal, C. J., Miyata, M., Tohkin, M., Nagata, K., Bend, J. R., and Gonzalez, F. J. (2000). Targeted disruption of soluble epoxide hydrolase reveals a role in blood pressure regulation. *J. Biol. Chem.* 275, 40504–40510. doi: 10.1074/jbc.M008106200
- Song, D., Arikawa, E., Galipeau, D. M., Yeh, J. N., Battell, M. L., Yuen, V. G., et al. (2005). Chronic estrogen treatment modifies insulin-induced insulin resistance and hypertension in ovariectomized rats. *Am. J. Hypertens.* 18, 1189–1194. doi: 10.1016/j.amjhyper.2005.04.003
- Sun, D., Cuevas, A. J., Gotlinger, K., Hwang, S. H., Hammock, B. D., Schwartzman, M. L., et al. (2014). Soluble epoxide hydrolase-dependent regulation of myogenic response and blood pressure. *Am. J. Physiol. Heart Circ. Physiol.* 306, H1146–H1153. doi: 10.1152/ajpheart.00920.2013
- Sun, D., Huang, A., Smith, C. J., Stackpole, C. J., Connetta, J. A., Shesely, E. G., et al. (1999). Enhanced release of prostaglandins contributes to flow-induced

- arteriolar dilation in eNOS knockout mice. *Circ. Res.* 85, 288–293. doi: 10.1161/01.RES.85.3.288
- Sun, D., Jiang, H., Wu, H., Yang, Y., Kaley, G., and Huang, A. (2011). A novel vascular EET synthase: role of CYP2C7. *Am. J. Physiol. Regul. Integr. Comp. Physiol.* 301, R1723–R1730. doi: 10.1152/ajpregu.00382.2011
- Sun, D., Liu, H., Yan, C., Jacobson, A., Ojaimi, C., Huang, A., et al. (2006). COX-2 contributes to the maintenance of flow-induced dilation in arterioles of eNOS-knockout mice. *Am. J. Physiol. Heart Circ. Physiol.* 291, H1429–H1435. doi: 10.1152/ajpheart.01130.2005
- Sun, D., Yang, Y. M., Jiang, H., Wu, H., Ojaimi, C., Kaley, G., et al. (2010). Roles of CYP2C29 and RXR gamma in vascular EET synthesis of female mice. *Am. J. Physiol. Regul. Integr. Comp. Physiol.* 298, R862–R869. doi: 10.1152/ajpregu.00575.2009
- Sweeney, L., and Voelkel, N. F. (2009). Estrogen exposure, obesity and thyroid disease in women with severe pulmonary hypertension. *Eur. J. Med. Res.* 14, 433–442. doi: 10.1186/2047-783X-14-10-433
- Sylvester, J. T., Shimoda, L. A., Aaronson, P. I., and Ward, J. P. (2012). Hypoxic pulmonary vasoconstriction. *Physiol. Rev.* 92, 367–520. doi: 10.1152/physrev.00041.2010
- Vasudevan, H., Xiang, H., and McNeill, J. H. (2005). Differential regulation of insulin resistance and hypertension by sex hormones in fructose-fed male rats. *Am. J. Physiol. Heart Circ. Physiol.* 289, H1335–H1342. doi: 10.1152/ajpheart.00399.2005
- Walker, A. M., Langleben, D., Korelitz, J. J., Rich, S., Rubin, L. J., Strom, B. L., et al. (2006). Temporal trends and drug exposures in pulmonary hypertension: an American experience. *Am. Heart J.* 152, 521–526. doi: 10.1016/j.ahj.2006.02.020
- West, J., Cogan, J., Geraci, M., Robinson, L., Newman, J., Phillips, J. A., et al. (2008). Gene expression in BMPR2 mutation carriers with and without evidence of pulmonary arterial hypertension suggests pathways relevant to disease penetrance. *BMC Med. Genomics* 1:45. doi: 10.1186/1755-8794-1-45
- White, K., Johansen, A. K., Nilsen, M., Ciuculan, L., Wallace, E., Paton, L., et al. (2012). Activity of the estrogen-metabolizing enzyme cytochrome P450 1B1 influences the development of pulmonary arterial hypertension. *Circulation* 126, 1087–1098. doi: 10.1161/CIRCULATIONAHA.111.062927
- White, K., Loughlin, L., Maqbool, Z., Nilsen, M., McClure, J., Dempsie, Y., et al. (2011). Serotonin transporter, sex, and hypoxia: microarray analysis in the pulmonary arteries of mice identifies genes with relevance to human PAH. *Physiol. Genomics* 43, 417–437. doi: 10.1152/physiolgenomics.00249.2010
- Wu, W. H., Yuan, P., Zhang, S. J., Jiang, X., Wu, C., Li, Y., et al. (2018). Impact of Pituitary-Gonadal Axis Hormones on Pulmonary Arterial Hypertension in Men. *Hypertension* 72, 151–158. doi: 10.1161/HYPERTENSIONAHA.118.10963
- Wu, Y., Huang, A., Sun, D., Falck, J. R., Koller, A., and Kaley, G. (2001). Gender-specific compensation for the lack of NO in the mediation of flow-induced arteriolar dilation. *Am. J. Physiol. Heart Circ. Physiol.* 280, H2456–H2461. doi: 10.1152/ajpheart.2001.280.6.H2456
- Yang, L., Cheriyan, J., Gutterman, D. D., Mayer, R. J., Ament, Z., Griffin, J. L., et al. (2017). Mechanisms of Vascular Dysfunction in COPD and Effects of a Novel Soluble Epoxide Hydrolase Inhibitor in Smokers. *Chest* 151, 555–563. doi: 10.1016/j.chest.2016.10.058
- Yang, Y. M., Sun, D., Kandhi, S., Froogh, G., Zhuge, J., Huang, W., et al. (2018). Estrogen-dependent epigenetic regulation of soluble epoxide hydrolase via DNA methylation. *Proc. Natl. Acad. Sci. U.S.A.* 115, 613–618. doi: 10.1073/pnas.1716016115
- Zhang, W., Iliff, J. J., Campbell, C. J., Wang, R. K., Hurn, P. D., and Alkayed, N. J. (2009). Role of soluble epoxide hydrolase in the sex-specific vascular response to cerebral ischemia. *J. Cereb. Blood Flow Metab.* 29, 1475–1481. doi: 10.1038/jcbfm.2009.65
- Zhu, D., Bousamra, M., Zeldin, D. C., Falck, J. R., Townsley, M., Harder, D. R., et al. (2000). Epoxyeicosatrienoic acids constrict isolated pressurized rabbit pulmonary arteries. *Am. J. Physiol. Lung Cell. Mol. Physiol.* 278, L335–L343. doi: 10.1152/ajplung.2000.278.2.L335

Conflict of Interest Statement: The authors declare that the research was conducted in the absence of any commercial or financial relationships that could be construed as a potential conflict of interest.

Copyright © 2018 Huang and Sun. This is an open-access article distributed under the terms of the Creative Commons Attribution License (CC BY). The use, distribution or reproduction in other forums is permitted, provided the original author(s) and the copyright owner(s) are credited and that the original publication in this journal is cited, in accordance with accepted academic practice. No use, distribution or reproduction is permitted which does not comply with these terms.



Inhibition of Soluble Epoxide Hydrolase for Renal Health

Jun-Yan Liu^{1,2*}

¹ Center for Nephrology and Metabolomics, Tongji University School of Medicine, Shanghai, China, ² Division of Nephrology, Shanghai Tenth Peoples Hospital, Tongji University School of Medicine, Shanghai, China

A soluble epoxide hydrolase (sEH) mediates the metabolism of epoxy fatty acids to form the corresponding vicinal diols, which are usually inactive or less active than the epoxide substrates. The sEH enzyme presents in many organs, including but not limited to the liver, heart, spleen, lung, and kidney. Here we summarized the changes in the expression and activity of sEH in multiple renal diseases, such as acute kidney injury (AKI), diabetic nephrology (DN), chronic kidney diseases (CKD), hypertension-mediated renal damage, and other renal dysfunctions. We also discussed the pharmacologic effects and the underlying mechanisms of sEH inhibition by using an inhibitor of sEH and/or the generic deletion of sEH on multiple renal diseases. We believe that sEH is a potential therapeutic target for renal dysfunction although the target disease needs further investigation.

Keywords: chronic kidney disease, acute kidney disease, soluble epoxide hydrolase, epoxyeicosatrienoic acid, renal dysfunction

OPEN ACCESS

Edited by:

John D. Imig,
Medical College of Wisconsin,
United States

Reviewed by:

John M. Seubert,
University of Alberta, Canada
Md Abdul Hye Khan,
Medical College of Wisconsin,
United States
Craig R. Lee,
University of North Carolina at
Chapel Hill, United States

*Correspondence:

Jun-Yan Liu
jyliu@tongji.edu.cn
orcid.org/0000-0002-3018-0335

Specialty section:

This article was submitted to
Translational Pharmacology,
a section of the journal
Frontiers in Pharmacology

Received: 20 October 2018

Accepted: 19 December 2018

Published: 10 January 2019

Citation:

Liu J-Y (2019) Inhibition of Soluble Epoxide Hydrolase for Renal Health. *Front. Pharmacol.* 9:1551. doi: 10.3389/fphar.2018.01551

INTRODUCTION

A soluble epoxide hydrolase (sEH), a member of epoxide hydrolases (EH) family, presents in almost all living organisms (Newman et al., 2005; Morisseau and Hammock, 2013). In humans, sEH is encoded by the gene *EPHX2* (Larsson et al., 1995; Sandberg and Meijer, 1996). The sEH has been well known to mediate the metabolism of epoxides to form the corresponding vicinal diols (Newman et al., 2005). The epoxides that could serve as the substrates for a sEH have been well documented previously, one member of which is epoxy fatty acids, such as the epoxy metabolites of PUFAs, including but not limited to linoleic acid [LA, 18:2 (n-6)], arachidonic acid [ARA, 20:4 (n-6)], alpha-linolenic acid [ALA, 18:3 (n-3)], eicosapentaenoic acid [EPA, 20:5 (n-3)], and docosahexaenoic acid [DHA, 22:6 (n-3)] (Figure 1; Newman et al., 2005).

Many epoxy fatty acids are multifunctional mediators *in vivo* and *in vitro*. For example, EETs, the epoxide metabolites of ARA, are anti-inflammatory (Node et al., 1999), analgesic (Inceoglu et al., 2008), and EDHF (Campbell et al., 1996). However, the sEH-mediated diol metabolites of epoxide fatty acids are usually inactive or less active than their respective epoxide precursors (Newman et al., 2005; Morisseau and Hammock, 2013). The substrate selectivity for the sEH-mediated metabolism of epoxide fatty acids was reported previously (Zeldin et al., 1995; Deng et al., 2017). Although the active epoxy fatty acids could be degraded easily, the circulation

Abbreviations: AKI, acute kidney injury; ALA, alpha-linolenic acid; AR9273, 1-adamantan-1-yl-3-(1-methylsulfonyl-piperidin-4-yl-urea); ARA, arachidonic acid; AUDA, 12-(3-adamantan-1-yl-ureido)-dodecanoic acid; BUN, blood urea nitrogen; c-AUCB, *cis*-4-[4-(3-adamantan-1-yl-ureido)cyclohexyloxy]benzoic acid; CDU, 1-cyclohexyl-3-dodecyl urea; CKD, chronic kidney disease; CYP, cytochrome P450; DHA, docosahexaenoic acid; DHOME, dihydroxyoctadecanoic acid; DN, diabetic nephrology; EDHF, endothelium-derived hyperpolarizing factor; EET, epoxyeicosatrienoic acid; EH, soluble epoxide hydrolase; EPA, eicosapentaenoic acid; EpOME, epoxyoctadecanoic acid; GBM, glomerular basement membrane; 20-HETE, 20-hydroxyeicosatetraenoic acid; IgAN, IgA nephropathy; IHC, immunohistochemical or immunohistochemistry; LA, linoleic acid; nbAUDA, n-butyl ester of 12-(3-adamantan-1-yl-ureido)-dodecanoic acid; PUFA, polyunsaturated fatty acid; SNP, single nucleotide polymorphism; STZ, streptozotocin; t-AUCB, *trans*-AUCB; TPPU, 1-trifluoromethoxyphenyl-3-(1-propionylpiperidin-4-yl)urea; UUO, unilateral ureteral obstruction.

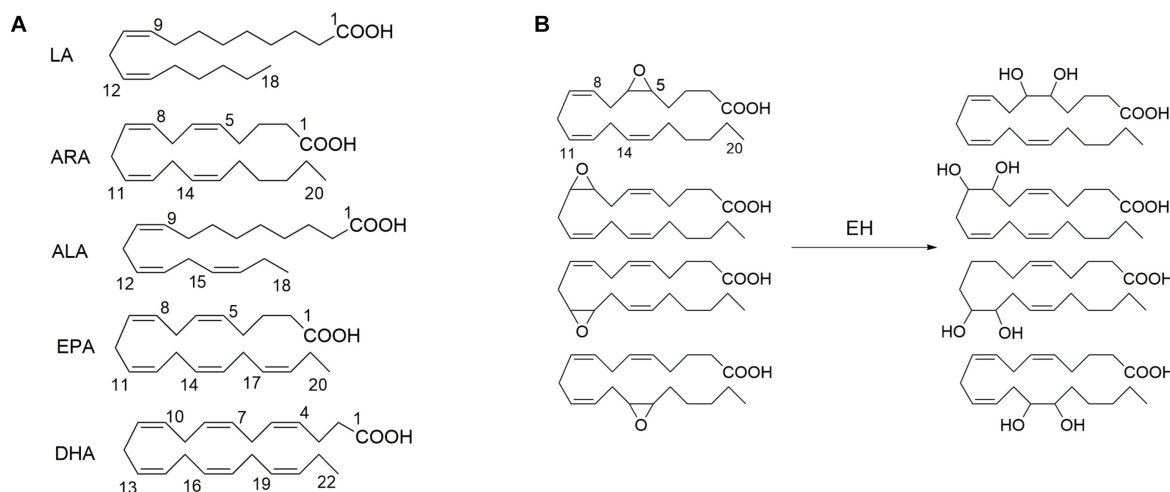


FIGURE 1 | The exemplified polyunsaturated fatty acids **(A)** that are the common substrates for epoxide hydrolase (EH) and **(B)** four epoxide regioisomers of ARA that could be metabolized to form the respective diols in the presence of EH such as soluble epoxide hydrolase (sEH) and microsomal epoxide hydrolase (mEH). LA, linoleic acid [18:2 (n-6)]; ARA, arachidonic acid [20:4 (n-6)]; ALA, alpha-linolenic acid [18:3 (n-3)]; EPA, eicosapentaenoic acid [20:5 (n-3)]; and DHA, docosahexaenoic acid [22:6 (n-3)].

and tissue levels of active epoxy fatty acids could be stabilized by both pharmacological interventions of an inhibitor of sEH and target gene disruption of *EPHX2*. Therefore, sEH inhibitors have been extensively reported to be anti-inflammatory, analgesic, anti-hypertensive, anti-fibrotic, cardioprotective and renoprotective, and other functions *in vivo* and *in vitro* (Imig and Hammock, 2009; Morisseau and Hammock, 2013; Sirish et al., 2013; Li et al., 2014; Fan et al., 2015; He et al., 2016).

The sEH presents in almost all mammal organs, such as heart, liver, lung, spleen, intestine, stomach, brain, and urinary and developmental organs¹. Kidneys, as the vital part of the urinary and excretory system, also express sEH. The expression and activity were reported upregulated in many kidney diseases for human and animals. Inhibition of sEH was therefore reported to be renoprotective in many

renal diseases. As illustrated in **Figure 2**, the attention to the sEH and kidneys has been consistently rising in the last 10 years. Here we summarized the pathophysiological and pharmacological function of sEH in the onset, prevention, and treatment in multiple kidney-associated diseases. The underlying molecular mechanisms of sEH inhibition on renal diseases were also discussed in this review paper.

THE PRESENCE AND LOCALIZATION OF sEH IN THE KIDNEYS

The enzyme sEH was expressed in all the organs investigated including but not limited to liver, kidney, brain, stomach, intestines, pancreas, prostate, heart, lung, and skin¹. The sEH has been reported to present in human and animal kidneys at both transcription and protein levels (**Table 1**). By using IHC

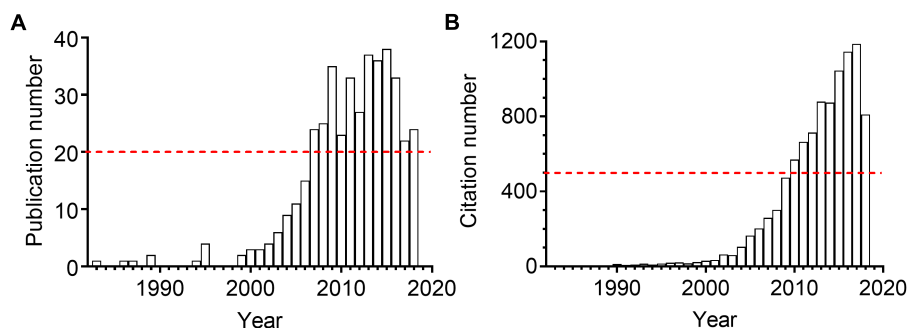


FIGURE 2 | The annual publication numbers **(A)** and the resulting citation numbers **(B)** of the scientific paper regarding sEH and kidney. The results were generated by searching the Web of Science with the topic "sEH" combined the topic "kidney or renal" on October 1, 2018.

TABLE 1 | The location and co-location of sEH in kidneys from different species.

Localization/colocalization	Species	Detection methods	Reference
Proximal tubules	Human	Immunohistochemistry	Enayetallah et al., 2004
Peroxisomal and cytosolic compartments of renal proximal tubules	Human	Immunofluorescence	Enayetallah et al., 2006
Tubular epithelial cells	Human	Immunohistochemistry	Wang et al., 2018
Proximal tubular cells	Human	Immunohistochemistry	Wang et al., 2013
Vasculature	Human	Immunohistochemistry	Yu et al., 2004
Proximal tubular epithelial cells	Rat	Immunoblotting	Wang et al., 2013
Renal proximal tubular epithelial cells	Rat	Immunoblotting	Liang et al., 2015
Kidney	Rat	q-PCR, ELISA	Abramova et al., 2013 Chábová et al., 2018 Cervenka et al., 2015 Seubert et al., 2005 Imig et al., 2002; Walkowska et al., 2010
Kidney	Rat	q-PCR	
Kidney	Rat	q-PCR, immunoblotting	
Kidney	Rat	Immunoblotting	
Kidney	Rat	cDNA microarray, immunoblotting	
Cortex	Rat	Immunoblotting	Zhao et al., 2004 Patel et al., 1986 Bettaieb et al., 2017b,a Chiang et al., 2015 Chen G. et al., 2012; Kim et al., 2014, 2015
Microvessels and cortex	Rat	Immunoblotting	
Soluble fraction	Mice	Product diol	
Kidney, podocytes	Mice	Immunoblotting, q-PCR, immunofluorescence	
Kidney	Mice	Immunohistochemistry, immunoblotting	
Kidney	Mice	immunoblotting	Oguro et al., 2009; Jung et al., 2010; Luo et al., unpublished Roche et al., 2015
Cortex	Mice	q-PCR, immunoblotting	
Cortex	Mice	q-PCR	

staining, Enayetallah et al. (2004) reported the distribution and expression of sEH in an array of normal human tissues. They found that sEH was frequently expressed in the human kidneys ($n = 15$) with a high level in the renal proximal tubules but a low level in the renal distal tubules and meager presence in the glomeruli (Enayetallah et al., 2004). In a follow-up study, Enayetallah et al. (2006) found that the sEH is presented in the proximal and cytosolic compartments in hepatocytes and renal proximal tubules. Wang et al. (2013, 2018) also reported that sEH expressed in the renal tubules in the patients with IgAN and other glomerulonephritis. In contrast, Yu et al. (2004) reported the cellular localization of sEH in the human kidneys by examining the biopsies taken from the patients with multiple non-end-stage renal diseases ($n = 8$) and those without known renal disorders ($n = 7$). Yu et al. (2004) found that sEH was preferentially expressed in the renal vasculature, mostly in the smooth muscle layers of the arterial wall, while relatively low levels in the surrounding tubules. Also, Yu et al. (2004) reported that sEH expressed in the normal kidneys in a similar pattern to those in the diseased kidneys in the samples investigated. The inconsistent observations among these studies may be due to the different sampling locations of renal biopsies. In addition, the sEH was also reported to be present in the murine and rodent kidneys (Patel et al., 1986; Johansson et al., 1995). The presence of sEH in human and animal kidneys opens a possibility that sEH could be associated by multiple renal diseases.

PRECLINICAL STUDIES OF THE TREATMENT OF RENAL DYSFUNCTION BY REGULATION OF sEH

Although there has been no drug clinically used as a sEH inhibitor yet, a large amount of pre-clinically experimental evidence supports that sEH may be a potential therapeutic target for several kidney-associated diseases, such as acute kidney injury (AKI), chronic kidney disease (CKD), diabetic nephrology (DN), and hypertension-associated kidney damage.

Regulation of sEH for the Treatment of AKI

AKI is a common fatal disease in hospitals characterized by a sudden and sustained reduction in renal function with the phenotypes of an abrupt decrease in urine output and a dramatic increase in serum creatinine level. The mechanisms underlying the pathogenesis of AKI vary, including but not limited to ischemia/reperfusion, septic shock, toxicant exposure, and inflammation-caused decrease in kidney blood flow, resulting in the damage to renal tissues, and eventually renal dysfunction (Kusch et al., 2013; Persson, 2013; Glodowski and Wagener, 2015; Takaori and Yanagita, 2016), which involve the impairment in glomerulus and renal tubular epithelial cells (Kusch et al., 2013; Prieto-Garcia et al., 2016), and activation of NFκB and GSK-3β (Liu et al., 2012; Kusch et al., 2013; Deng et al., 2017).

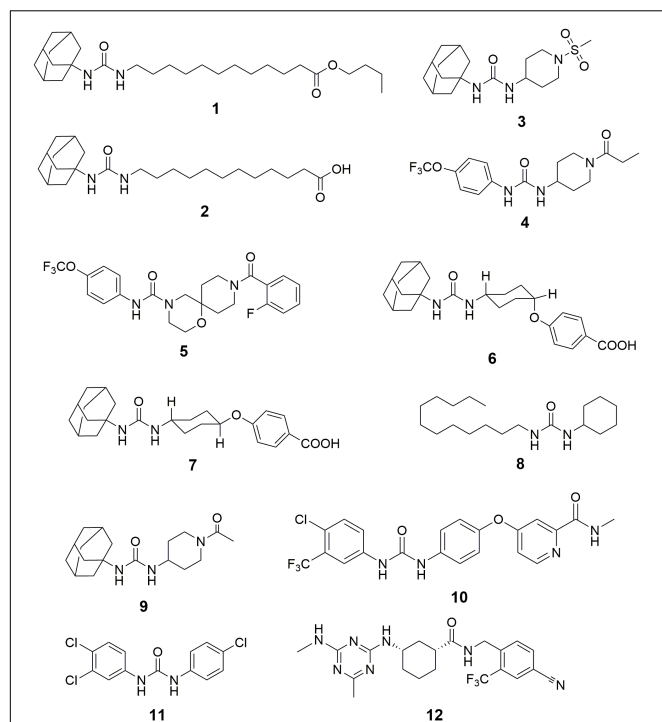


FIGURE 3 | The chemical structures of the inhibitors of sEH summarized in this paper. 1, n-butyl ester of 12-(3-adamantan-1-yl-ureido)-dodecanoic acid (nbAUDA); 2, 12-(3-adamantan-1-yl-ureido)-dodecanoic acid (AUDA); 3, 1-adamantan-1-yl-3-(1-methylsulfonyl-piperidin-4-yl)-urea (AR9273); 4, 1-(4-(2-fluorobenzoyl)-N-[4-(trifluoromethoxy)phenyl]-1-oxa-4,9-diazaspiro[5.5]undecane-4-carboxamide; 5, *cis*-4-[4-(3-adamantan-1-yl-ureido)cyclohexyloxy]benzoic acid (*c*-AUCB); 6, *trans*-4-[4-(3-adamantan-1-yl-ureido)cyclohexyloxy]benzoic acid (*t*-AUCB); 7, 1-cyclohexyl-3-dodecylurea (CDU); 8, 1-(1-acetypiperidin-4-yl)-3-adamantan-1-yl-urea (AR9281); 9, 4-[4-(4-chloro-3-(trifluoromethyl)phenyl)carbamoylamino]phenoxy-N-methylpyridine-2-carboxamide (Sorafenib); 10, 3-(4-chlorophenyl)-1-(3,4-dichlorophenyl)-urea (Triclocarban); 11, 1-(1R,3S)-N-[4-cyano-2-(trifluoromethyl)benzyl]-3-[(4-methyl-6-(methylamino)-1,3,5-triazin-2-yl)amino]cyclohexane-1-carboxamide (GSK2256294).

Inhibition of sEH has been reported to attenuate the renal injury in multiple murine models of AKI. Although Hashimoto et al. (2015) reported that cisplatin administration decrease the activity and expression of sEH in the kidneys of male ddY mice, Parrish et al. (2009) found that subcutaneous (*s.c.*) injection of a sEH inhibitor n-butyl ester of 12-(3-adamantan-1-yl-ureido)-dodecanoic acid (nbAUDA, 1, **Figure 3**), a pro-drug of AUDA (Newman et al., 2005) significantly attenuated the renal injury in a C3H mice model of AKI caused by intraperitoneal (*i.p.*) injection of cisplatin, which was supported by the blood levels of urea nitrogen (BUN) and histological analysis of kidneys. Also, in a murine model of AKI caused by *i.p.* injection of cisplatin, Liu et al. reported that oral administration of another sEH inhibitor, 1-adamantan-1-yl-3-(1-methylsulfonyl-piperidin-4-yl)-urea (AR9273, 3) that is structurally different from AUDA, markedly attenuated renal injury, which was supported by the

serum levels of urea nitrogen and creatinine, and histological evidence of renal tubular damage and neutrophil infiltration (Liu et al., 2012, 2013). Also, the renoprotective effects of AR9273 were consistent with those in the sEH knockout mice (Liu et al., 2012). It should be noted that the sEH inhibitors were administered 1 day before cisplatin treatment in both studies. Therefore, the renoprotective effects of sEH inhibitors are prophylactic rather than therapeutic effects.

In a murine model of AKI caused by ischemia/reperfusion, Deng et al. (2017) reported that administration of a sEH inhibitor, TPPU, 4 attenuated renal injury, which was supported by plasma creatinine, survival time, and histological analysis. In contrast, Zhu et al. (2016) also reported that sEH knockout exacerbated renal injury caused by ischemia/reperfusion in a murine model. Interestingly, Zhu et al. (2016) found that the renal level of 20-HETE and one of its synthetic enzymes, Cyp4a12a, were increased significantly in sEH knockout mice when compared with those of wildtype mice. 20-HETE is a potent nephrotoxic compound, which may abate the renoprotective effects of increased EETs caused by sEH deficiency.

In a murine model of AKI caused by lipopolysaccharide (LPS), Bettaieb et al. (2017a) reported that podocyte-specific sEH deficiency ameliorated the LPS-caused mice renal injury, which was supported by the favorable changes in proteinuria, BUN, and renal mRNA levels and serum levels of inflammatory cytokines. In addition, the *in vivo* renal protective effect of podocyte-specific sEH knockout was further supported by the *in vitro* data from the treatment of a sEH inhibitor TPPU to the E11 murine podocytes (Bettaieb et al., 2017a).

Inhibition of sEH for the Treatment of CKD

CKD is one of the top public health problems and leading diseases for all-cause mortality globally (Xie et al., 2018). The putative mechanisms regarding the pathogenesis and progression of CKD have been well documented previously (Fogo, 2007; Malyszko, 2010; Eddy et al., 2012; Yang et al., 2017; Cheung et al., 2018; Mihai et al., 2018; Moradi and Vaziri, 2018; Rossi et al., 2018). Briefly, both generic factor-caused genital abnormality of renal development, and other factors (e.g., inflammation, hypertension, diabetes, dyslipidemia, disorder of cytokines and growth factors, proteinuria, podocyte loss, etc.) can cause irreversible scarring in kidney, resulting in progressive renal fibrosis, and eventually end-stage renal disease, which needs renal replacement therapy, such as hemodialysis and renal transplantation. The progression of CKD has been reported to be associated with the damage to renal glomerulus and renal epithelial cells, accelerating the cell migration and epithelial-mesenchymal transition, and repressing the proliferation of podocytes, which may be mediated by angiotensin-II, PPAR- γ , AMPK, CYPs, and sEH (Fogo, 2007; Malyszko, 2010; Decleves et al., 2011; Kim et al., 2014; Fan et al., 2015).

Inhibition of sEH by both pharmacological interventions with a sEH inhibitor and target gene disruption of sEH has been reported to attenuate the renal injury in several murine and rodent models. Kato et al. (2014) reported that a potent sEH

inhibitor, 9-(2-fluorobenzoyl)-N-[4-(trifluoromethoxy)phenyl]-1-oxa-4,9-diazaspiro[5.5]undecane-4-carboxamide (Node et al., 1999), ameliorated renal injury in a rat model of anti-glomerular basement membrane glomerulonephritis evidenced by time-dependently reducing the rat serum creatinine. Liang et al. (2015) reported that the treatment of AUDA abated the proteinuria-induced epithelial-mesenchymal transition *in vivo* and *in vitro*.

By using a rodent model of CKD caused by 5/6 nephrectomy (5/6 NX) in Ren-2 transgenic rats, Kujal et al. (2014) reported that the treatment of a sEH inhibitor, *cis*-4-[4-(3-adamantan-1-yl-ureido)cyclohexyloxy]benzoic acid (*c*-AUCB, 6) attenuated the renal and cardiac injuries of the diseased rats by modification of the survival rate, blood pressure, cardiac hypertrophy, proteinuria, degree of glomerular and tubulointerstitial injury, and glomerular volume toward the normative status. In addition, Chábová et al. (2018) reported that co-administration of *c*-AUCB with a standard renin-angiotensin system (RAS) blockade resulted in additional therapeutic effects in the improvement of rat survival rate, reduce in albuminuria, glomerular and tubulointerstitial injury when compared with the standard RAS blockade alone.

In a murine model of obstructive nephropathy caused by UUO surgery, Kim et al. (2014) reported that the deficiency of sEH abolished the renal interstitial fibrosis and inflammation. Consistently, Chiang et al. (2015) found that renal expression of sEH protein was increased in the UUO-treated mice when compared with the sham mice. In addition, the target gene disruption of sEH abated the UUO-caused renal injury, such as hydronephrosis, renal tubular injury, inflammation, and fibrosis. Also, oral administration of a sEH inhibitor, *trans*-4-[4-(3-adamantan-1-yl-ureido)cyclohexyloxy]benzoic acid (*t*-AUCB, 7) resulted in the similar fibro-protective and anti-inflammatory effects to sEH gene knockout (Kim et al., 2014, 2015). Interestingly, Yang et al. (2017) reported that treatment of AUDA resulted in similar results to *t*-AUCB in a UUO-induced mice model of renal fibrosis.

In addition, Huang et al. (2007) reported that inhibition of sEH by administration of a sEH inhibitor AUDA attenuated the renal injury by regulating the mean arterial pressure, renal vascular resistance, and glomerular filtration rate, and renal blood flow for the obese rats toward normative status. By using a target metabolomic analysis, Luo et al. (unpublished) found that renal sEH was upregulated at both transcription and protein levels time-dependently upon the challenge of high-fat diet (HFD) feeding, which was associated with the progression of renal injury. In addition, inhibition of sEH by TPPU attenuated the HFD-induced renal injury by, at least in part, activation of the Ampk-mediated macro-autophagy and Pax2-mediated chaperone-mediated autophagy.

It is worth noting that not all the study showed the favorite effect of sEH inhibition on kidney diseases. Jung et al. reported in a mice model of chronic renal failure caused by 5/6-nephrectomy that *c*-TUCB (Inceoglu et al., 2008) failed in lowering blood pressure and even aggravated albuminuria when compared with the placebo controls (El-Sherbeni et al., 2013). The authors thought that this unfavorable effect may be due to the shifts

of arachidonic metabolism into lipoxygenase pathway by sEH inhibition.

Inhibition of sEH for the Treatment of Diabetic Nephrology

We separated DN from CKD in the “Inhibition of sEH for the treatment of CKD” since DN is a leading cause of CKD and end-stage renal disease (Lin and Sheu, 2014). DN causes primary renal damage to its microvascular system including glomerular capillaries, influent and affluent arteries at the beginning, and most leading to end-stage renal disease over time (Remuzzi et al., 2006; Afsar and Elsurur, 2017), which may involve the activation of some transcription factors (e.g., activator protein 1, cAMP-response element-binding protein, nuclear factor of activated T cells, NF- κ B, stimulating protein 1, and upstream stimulatory factor 1) and may be regulated by some signal pathways such as mTOR, AMPK, GSK-3 β , and Deptor 2 (Mariappan, 2012).

Chen G. et al. (2012) reported that sEH deficiency maintained the renal function in a murine model of STZ-induced DN. Compared with the wildtype diabetic mice, sEH-deficient mice resulted in significantly decreased levels of plasma Hb A_{1c} and creatinine, BUN and urinary microalbumin excretion. Bettaieb et al. (2017b) reported that renal sEH protein was upregulated in the mice under HFD and STZ-induced hyperglycemia. In addition, podocyte-specific sEH deficiency preserved renal function *in vivo* and *in vitro* via modulation of the renal endoplasmic reticulum (ER) stress, inflammation, fibrosis, and autophagy toward normative conditions, which was further supported by the *in vitro* data from the pharmacological intervention of sEH with the sEH inhibitor TPPU (Bettaieb et al., 2017b). Katary et al. (2017) reported that in a rodent model of STZ-induced DN, the treatment with *t*-AUCB attenuated the renal injury by reducing glomerular albumin permeability, albumin, and nephrin excretion levels and restoring the decrease in glomerular α 3 integrin and nephrin expression in diabetic rats. However, this beneficial effect of sEH inhibition was unable to be enhanced by co-administration with meloxicam, a cyclooxygenase inhibitor (Katary et al., 2017).

Inhibition of sEH for the Attenuation of Hypertension-Associated Kidney Disorders

Hypertension is the second leading cause of end-stage renal disease after diabetes in the United States (U.S. Renal Data System, 2009). Although the susceptibility to hypertension-associated renal injury differs significantly in various populations, a consensus is that hypertension causes damage to glomerular arteries and capillary, and endothelial cells, leading to the injuries to glomerular filtration barrier and podocytes, eventually renal dysfunction, which may be manipulated by renin-angiotensin-aldosterone system, reactive oxidative species, endothelial dysfunction, and genetic and epigenetic factors (Mennuni et al., 2014).

Hypertension is a risk factor for the development of renal dysfunction. The renal sEH was upregulated in hypertensive status. By using a gene microarray analysis, Seubert et al. (2005)

reported that sEH was significantly upregulated in the kidneys of spontaneously hypertensive rats (SHR) when compared with the non-hypertensive Wistar-Kyoto (WKY) rats. Also, Abramova et al. (2013, 2017) found that the renal mRNA level and protein concentration of sEH were increased at in the inherited stress-induced arterial hypertension (ISIAH) rats when compared with the normative Wistar Albino Glaxo (WAG) rats. Tain et al. (2015) reported that renal sEH was upregulated in dexamethasone- and a high fructose-induced rodent model of programmed hypertension. These data suggest the possibility that inhibition of sEH could protect the kidney from injury associated with hypertension.

Zhao et al. (2004) reported that chronic administration of a sEH inhibitor 1-cyclohexyl-3-dodecyl urea (CDU, 8) significantly attenuated renal injury in an angiotensin-induced rodent model of hypertension, which was supported by the observation that CDU treatment maintained the renal vasculatures and glomerulus toward normative status. Imig et al. (2005) reported that administration of AUDA significantly lowered blood pressure and protected renal damage by decreasing the urinary microalbumin excretion in the rodent models of hypertension induced by both normal-salt angiotensin and high-salt angiotensin. Imig et al. also reported that another sEH inhibitor AR9281 attenuated glomeruli injury and reduced renal inflammation in the angiotensin-induced hypertensive rats (Imig et al., 2009). Olearczyk et al. (2009) reported that treatment with AUDA protected kidneys from glomerular and tubular damage in spontaneously diabetic Goto-Kakizaki rats induced by angiotensin II with high salt diet. Sporkova et al. (2011) reported that treatment of *c*-AUCB improved renal function by maintaining the renal blood flow toward normative status while exhibiting an anti-hypertensive effect in the 2-kidney 1 clip hypertensive rats. Imig et al. (2012) reported that *t*-AUCB treatment reversed the increase in urinary levels of albumin and kidney injury marker-1 (KIM-1) in the spontaneously hypertensive obese rats. In addition, co-administration of *t*-AUCB with rosiglitazone, an agonist of PPAR γ , resulted in additive reno-protection (Imig et al., 2012). Cervenka et al. (2015) reported that in an aorto-caval fistula-induced Ren-2 transgenic hypertensive rats model of congestive heart failure (CHF), *c*-AUCB treatment improved rats survival rate and increased renal blood flow, glomerular filtration rate and fractional sodium excretion.

ASSOCIATION OF sEH POLYMORPHISMS WITH KIDNEY-ASSOCIATED DISEASES

Several sEH polymorphisms, such as Lys55Arg, rs41507953 (K55R), rs751141 (R287Q), and rs1042032, were reported to correlate with several renal-associated diseases. Based on current data, lower sEH activity is associated with the improved renal function. Shuey et al. (2017) reported that sEH Lys55Arg polymorphism was associated with an increased incidence of AKI following cardiac surgery in patients without preexisting CKD. Also, the sEH activity that was characterized by the

ratio of DHOMEs to EpOMEs was increased in sEH 55Arg variant carriers when compared with the investigated wildtype carriers.

Lee et al. (2011) investigated the association of three single nucleotide polymorphisms [SNPs, rs41507953 (K55R), rs751141 (R287Q), and rs1042032] of sEH with IgAN progression in a retrospective cohort including 401 IgAN patients and 402 normal healthy controls. They reported that the patients carrying the variant allele (A) of rs751141 (R287Q) were associated with a better kidney survival ($P < 0.001$) and a lower sEH activity ($P < 0.05$) than those with the wildtype allele (G) (Lee et al., 2011). Also, Wang et al. (2013, 2018) reported that the level of sEH expression correlated with proteinuria and infiltration of macrophages positively in the IgAN patients and other glomerulonephritis.

Dreisbach et al. (2005) conducted a case-control study to investigate the possible correlation of multiple SNPs in sEH (sEH-Q and sEH-RR) and CYP 2C8, 2C9, and 2J2 with an increased risk of hypertension in African American individuals. They found that these SNPs are not associated with the increased risk of hypertension in the African American population (Dreisbach et al., 2005). Ma et al. (2018) reported that the A allele of an exonic polymorphism in sEH rs751141 correlated with the incidence of DN in the Chinese T2D population negatively, which could be modulated by homocysteine level status.

Gervasini et al. (2015) reported that the renal transplant recipients who carried the rs1042032GG genotype in sEH were associated with the significantly lower estimated glomerular filtration rate and higher serum creatinine levels on year after grafting compared with those with wildtype A-allele. This was consistent with the study by Lee et al. (2008), in which the presence of the rs1042032 AA genotype in sEH was reported to correlate with a protective role for allograft function for the kidney transplant recipients.

MOLECULAR MECHANISMS UNDERLYING THE REGULATION OF sEH FOR RENO-PROTECTION

The sEH has been reported to be upregulated by both endogenous and exogenous factors at both mRNA and protein levels. Wang et al. (2013, 2018) reported that the expression of sEH was increased in renal tissues in the patients with glomerulonephritis when compared with the control renal tissues by IHC analysis. Both mRNA and protein levels of sEH were found higher in the kidneys of SHR than those of the control WKY rats (Yu et al., 2000; Koeners et al., 2011). The sEH was also upregulated in the renal cortex by angiotensin-II, two-kidney-one-clip, and a HFD (Imig et al., 2002; Zhao et al., 2004; Kopkan et al., 2012; Luo et al., unpublished).

An sEH can be down-regulated by generic target gene disruption of *Ephx2* and chemical knockdown by various sEH inhibitors. In most cases, sEH is believed to be inhibited at protein level primarily due to the formation of the hydrogen bonds between the inhibitors and the active sites Tyr461 and Tyr385 in both human and mammal sEH enzymes (Argiriadi et al., 1999,

2000; Gomez et al., 2004). Recently, Luo et al. (unpublished) found that an sEH inhibitor TPPU could inhibit murine sEH transcriptionally.

The mechanisms underlying the reno-protection of sEH inhibition are summarized in **Figure 4**. The renoprotective effects of sEH inhibition are mostly believed to be ascribed to the increased renal levels of EETs resulted from pharmacological interventions with a sEH inhibitor or genetic disruption of sEH based on two main facts. The one is that the renal and/or circulation levels EETs or the intrarenal ratio of EETs to DHETs were hypothesized and observed to be increased following sEH inhibition (Zhao et al., 2004; Huang et al., 2007; Kim et al., 2014, 2015; Kujal et al., 2014; Deng et al., 2017; Luo et al., unpublished). The other is that EETs have been investigated to be the active mediators, which could result in the protection of kidneys from multiple injuries. In addition to inhibition of sEH, the metabolic pathway of EETs, upregulation of CYP2C and/or 2J, the biosynthetic pathways of EETs, is an alternative approach to stabilize the EETs level *in vivo*. Upregulation of Cyp2J was previously reported to protect the kidneys function in the 5/6-nephrectomized rat (Zhao et al., 2012), which supports that the reno-protection of EETs.

The biochemical functions of EETs have been well documented in several review papers (Spector et al., 2004; Spector and Norris, 2007; Wang and DuBois, 2012; Imig, 2015). EETs were reported to be anti-inflammatory via modulation of the NFκB/IκBK signaling pathway (Node et al., 1999). Reno-protective effects of sEH inhibition, such as anti-inflammatory and fibro-protective, were reported to be involved in the modulation of NFκB signaling pathway and cytokine orchestra toward inflammation resolution in several animal studies (Liu et al., 2012; Kim et al., 2014, 2015; Bettaieb et al., 2017a). Also, EETs are potent EDHF (Campbell et al., 1996; Archer et al., 2003). Inhibition of sEH was reported to protect the kidney from the multiple injuries associated with the improvement of the

renal microvessel dilation and renal blood flowing (Sporkova et al., 2011; Cervenka et al., 2015).

Epoxyeicosatrienoic acids have been reported to induce cell growth and inhibit the cell apoptosis (Dhanasekaran et al., 2006; Nieves and Moreno, 2007). EETs were found to protect pig kidney proximal tubule LLC-PK1 cells from cisplatin-induced p38 MAPK activation, and Bax mitochondrial trafficking (Liu et al., 2013), which was further supported by that inhibition of sEH by AR9273 treatment and sEH-deficiency significantly attenuated cisplatin-induced murine renal injury via inhibition of the p38 MAPK phosphorylation (Liu et al., 2013). The renal podocyte-specific sEH deficiency ameliorated murine kidney injury associated with decreased LPS-induced NF-κB and MAPK activation and attenuated endoplasmic reticulum stress (Bettaieb et al., 2017a). EETs were also reported to inhibit the apoptosis of renal tubular epithelial cells via, at least in part, the modulation of the phosphorylation of GSK-3β, which was also supported by the *in vivo* data from TPPU treatment in a murine model of AKI (Deng et al., 2017). Also, AUDA treatment was reported to attenuate renal injury by modulation of the PI3K-Akt-GSK-3β signaling pathway (Liang et al., 2015). Also, sEH gene inhibition and exogenous EETs significantly protected HK-2 cells from TNF-induced apoptosis *in vitro* associated with activation of the PI3K-Akt-NOS3 and AMPK signaling cascades (Chen G. et al., 2012).

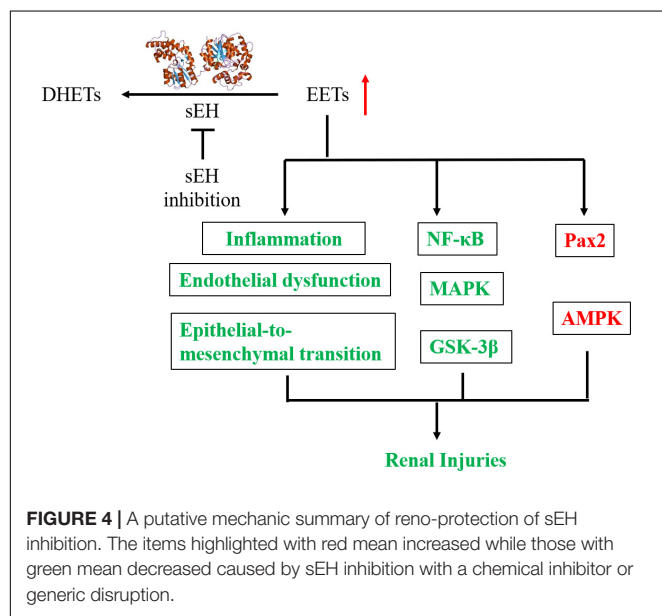
Recently, Luo et al. (unpublished) found that EETs protected the murine renal mesangial cells and tubular epithelial cells from palmitic acid-induced injury by activation of Ampk and Pax2, which was supported by the *in vivo* data from the TPPU treatment to the mice feeding on a HFD.

In addition to EETs, other epoxy fatty acids were also reported to contribute to the renoprotective role of sEH inhibition. 19(20)-epoxydocosapentaenoic acid, the principal epoxy metabolite of DHA that could also be stabilized by sEH inhibition, was found to mitigate the renal fibrosis in a mouse model of experimental UUO-induced renal fibrosis by decreasing renal epithelial-to-mesenchymal transition (Sharma et al., 2016).

Besides sEH, microsomal EH (mEH), encoded by *EPHX1*, has the similar function to sEH in mediating the hydrolysis of epoxy fatty acids (Newman et al., 2005; Rawal et al., 2009). However, mEH was found to modified slightly while sEH was up-regulated significantly in renal microvessels by the treatment of angiotensin-II infusion (Zhao et al., 2004). Recently, mEH was found to be decreased significantly while sEH altered non-significantly at mRNA level in the blood cells of the uremic patients when compared with healthy controls (Hu et al., 2018). The pathophysiological and pharmacological role of mEH in kidney diseases and other disorders needs further investigation.

CLINICAL STUDIES OF sEH INHIBITORS

As far as we know, there is no clinical drug used as a sEH inhibitor. However, some sEH chemical inhibitors failed in, or are under, or will be tested in clinical trials. In addition, some clinically used drugs or human used agents were found to be the potent sEH inhibitors although they have their specific mode



of action other than sEH inhibition. For example, sorafenib (Imig and Hammock, 2009) is a clinical drug for the treatment of advanced renal cell carcinoma, advanced hepatocellular carcinoma, and radioactive iodine resistant advanced thyroid carcinoma as an inhibitor of multi-kinase, such as VEGFR, PDGFR, and Raf family kinases (Ng and Chen, 2006; Wilhelm et al., 2008; Smalley et al., 2009; Iyer et al., 2010). However, since sorafenib has the N,N' -disubstituted substructure that is similar to many potent sEH inhibitors (Figure 3), it was found to be a potent sEH inhibitor (Liu et al., 2009). Also, triclocarban (He et al., 2016) has been widely used as an anti-microbial agent in various personal care products (Brausch and Rand, 2011; Bu et al., 2013), is also a potent inhibitor of sEH (Liu et al., 2011).

In addition, two sEH inhibitors, AR9281 and GSK2256294, finished the phase I clinical trials. AR9281 showed well-tolerated at a single oral dose (10–1000 mg) and multiple doses (100–400 mg every 8 h) during the test period (1 week) and dose-dependent blood drug concentration and activity to inhibit the blood sEH with 90% or greater inhibition. This study suggested a twice-daily or thrice-daily dosing regimen for the patients (Chen D. et al., 2012). GSK2256294 was also well-tolerated at the tested doses. Plasma drug concentration increased at a dose-related manner with a half-life of 25–43 h. The activity of GSK2256294 to inhibit sEH was dose-dependent, from an average of 41.9% (2 mg) to 99.8% (20 mg) (Lazaar et al., 2016).

Wang et al. (2018) reported that renal sEH expression was increased in patients with IgA nephropathy. Before that, Wang et al. (2013) reported that renal sEH expression was upregulated in the patients with glomerulonephritis including IgA nephropathy. These human data suggest that sEH may be a therapeutic target for some renal diseases like IgA nephropathy.

However, Hu et al. (2018) reported that the mEH (EPHX1) was downregulated while sEH was changed slightly in the whole blood cells of the uremic patients when compared with healthy controls. Therefore, further studies are needed to optimize a target renal disease for the follow-up clinical study of a sEH inhibitor.

CONCLUSION

In summary, sEH may be a promising therapeutic target for the prevention and treatment of renal disorders. Also, various small molecular sEH inhibitors were synthesized in several laboratories with favorable pharmacokinetics and pharmacodynamics in multiple animals and humans. To move sEH inhibitors toward clinical use, the next step should focus more on the functional investigation of sEH in the pathology and pathophysiology of the renal dysfunction by using human samples to target a renal disease for systemic evaluation of the pharmacological and toxicological effects of sEH inhibitors.

AUTHOR CONTRIBUTIONS

J-YL designed and wrote the paper.

FUNDING

This study was supported by the National Natural Science Foundation of China (NSFC) grant 81470588.

REFERENCES

- Abramova, T. O., Redina, O. E., Smolenskaya, S. E., and Markel, A. L. (2013). Elevated expression of the Ephx2 mRNA in the kidney of hypertensive ISIAH rats. *Mol. Biol.* 47, 821–826. doi: 10.1134/S0026893313060022
- Abramova, T. O., Ryazanova, M. A., Antonov, E. V., Redina, O. E., and Markel, A. L. (2017). Increase in the concentration of sEH protein in renal medulla of ISIAH rats with inherited stress-induced arterial hypertension. *Mol. Biol.* 51, 389–392. doi: 10.7868/S0026893417020021
- Afsar, B., and Elsurur, R. (2017). Increased renal resistive index in type 2 diabetes: clinical relevance, mechanisms and future directions. *Diabetes Metab. Syndr.* 11, 291–296. doi: 10.1016/j.dsx.2016.08.019
- Archer, S. L., Gragasin, F. S., Wu, X. C., Wang, S. H., McMurtry, S., Kim, D. H., et al. (2003). Endothelium-derived hyperpolarizing factor in human internal mammary artery is 11,12-epoxyeicosatrienoic acid and causes relaxation by activating smooth muscle BKCa channels. *Circulation* 107, 769–776. doi: 10.1161/01.CIR.0000047278.28407.C2
- Argiriadi, M. A., Morisseau, C., Goodrow, M. H., Dowdy, D. L., Hammock, B. D., and Christianson, D. W. (2000). Binding of alkylurea inhibitors to epoxide hydrolase implicates active site tyrosines in substrate activation. *J. Biol. Chem.* 275, 15265–15270. doi: 10.1074/jbc.M000278200
- Argiriadi, M. A., Morisseau, C., Hammock, B. D., and Christianson, D. W. (1999). Detoxification of environmental mutagens and carcinogens: structure, mechanism, and evolution of liver epoxide hydrolase. *Proc. Natl. Acad. Sci. U.S.A.* 96, 10637–10642. doi: 10.1073/pnas.96.19.10637
- Bettaieb, A., Koike, S., Chahed, S., Zhao, Y., Bachaalany, S., Hashoush, N., et al. (2017a). Podocyte-specific soluble epoxide hydrolase deficiency in mice attenuates acute kidney injury. *FEBS J.* 284, 1970–1986. doi: 10.1111/febs.14100
- Bettaieb, A., Koike, S., Hsu, M. F., Ito, Y., Chahed, S., Bachaalany, S., et al. (2017b). Soluble epoxide hydrolase in podocytes is a significant contributor to renal function under hyperglycemia. *Biochim. Biophys. Acta Gen. Subj.* 1861, 2758–2765. doi: 10.1016/j.bbagen.2017.07.021
- Brausch, J. M., and Rand, G. M. (2011). A review of personal care products in the aquatic environment: environmental concentrations and toxicity. *Chemosphere* 82, 1518–1532. doi: 10.1016/j.chemosphere.2010.11.018
- Bu, Q., Wang, B., Huang, J., Deng, S., and Yu, G. (2013). Pharmaceuticals and personal care products in the aquatic environment in China: a review. *J. Hazard. Mater.* 262, 189–211. doi: 10.1016/j.jhazmat.2013.08.040
- Campbell, W. B., Gebremedhin, D., Pratt, P. F., and Harder, D. R. (1996). Identification of epoxyeicosatrienoic acids as endothelium-derived hyperpolarizing factors. *Circ. Res.* 78, 415–423. doi: 10.1161/01.RES.78.3.415
- Cervenka, L., Melenovsky, V., Huskova, Z., Skaroupkova, P., Nishiyama, A., and Sadowski, J. (2015). Inhibition of soluble epoxide hydrolase counteracts the development of renal dysfunction and progression of congestive heart failure in Ren-2 transgenic hypertensive rats with aorto-caval fistula. *Clin. Exp. Pharmacol. Physiol.* 42, 795–807. doi: 10.1111/1440-1681.12419
- Chábová, V. C., Kujal, P., Skaroupkova, P., Varnourkova, Z., Vackova, S., Huskova, Z., et al. (2018). Combined inhibition of soluble epoxide hydrolase and renin-angiotensin system exhibits superior renoprotection to renin-angiotensin system blockade in 5/6 nephrectomized Ren-2 transgenic hypertensive rats with established chronic kidney disease. *Kidney Blood Press. Res.* 43, 329–349. doi: 10.1159/000487902
- Chen, D., Whitcomb, R., MacIntyre, E., Tran, V., Do, Z. N., Sabry, J., et al. (2012). Pharmacokinetics and pharmacodynamics of AR9281, an inhibitor of soluble epoxide hydrolase, in single- and multiple-dose studies in healthy human subjects. *J. Clin. Pharmacol.* 52, 319–328. doi: 10.1177/0091270010397049

Chen, G., Xu, R., Wang, Y., Wang, P., Zhao, G., Xu, X., et al. (2012). Genetic disruption of soluble epoxide hydrolase is protective against streptozotocin-induced diabetic nephropathy. *Am. J. Physiol. Endocrinol. Metab.* 303, E563–E575. doi: 10.1152/ajpendo.00591.2011

Cheung, K. L., Zakai, N. A., Callas, P. W., Howard, G., Mahmoodi, B. K., Peralta, C. A., et al. (2018). Mechanisms and mitigating factors for venous thromboembolism in chronic kidney disease: the REGARDS study. *J. Thromb. Haemost.* 16, 1743–1752. doi: 10.1111/jth.14235

Chiang, C. W., Lee, H. T., Tarng, D. C., Kuo, K. L., Cheng, L. C., and Lee, T. S. (2015). Genetic deletion of soluble epoxide hydrolase attenuates inflammation and fibrosis in experimental obstructive nephropathy. *Mediat. Inflamm.* 2015:693260. doi: 10.1155/2015/693260

Decleves, A. E., Mathew, A. V., Cunard, R., and Sharma, K. (2011). AMPK mediates the initiation of kidney disease induced by a high-fat diet. *J. Am. Soc. Nephrol.* 22, 1846–1855. doi: 10.1681/ASN.2011010026

Deng, B. Q., Luo, Y., Kang, X., Li, C. B., Morisseau, C., Yang, J., et al. (2017). Epoxide metabolites of arachidonate and docosahexaenoate function conversely in acute kidney injury involved in GSK3 beta signaling. *Proc. Natl. Acad. Sci. U.S.A.* 114, 12608–12613. doi: 10.1073/pnas.1705615114

Dhanasekaran, A., Gruenloh, S., Jacobs, E., and Medhora, M. (2006). Epoxyeicosatrienoic acids (EETs) protect cardiovascular cells from apoptosis mediated by caspase 3-dependent pathways. *FASEB J.* 20, A123–A123.

Dreisbach, A. W., Japa, S., Sigel, A., Parenti, M. B., Hess, A. E., Srinouanprachanh, S. L., et al. (2005). The prevalence of CYP2C8, 2C9, 2J2, and soluble epoxide hydrolase polymorphisms in African Americans with hypertension. *Am. J. Hypertens.* 18, 1276–1281. doi: 10.1016/j.amjhyper.2005.04.019

Eddy, A. A., Lopez-Guisa, J. M., Okamura, D. M., and Yamaguchi, I. (2012). Investigating mechanisms of chronic kidney disease in mouse models. *Pediatr. Nephrol.* 27, 1233–1247. doi: 10.1007/s00467-011-1938-2

El-Sherbeni, A. A., Aboutabl, M. E., Zordoky, B. N. M., Anwar-Mohamed, A., and El-Kadi, A. O. S. (2013). Determination of the dominant arachidonic acid cytochrome P450 monooxygenases in rat heart, lung, kidney, and liver: protein expression and metabolite kinetics. *AAPS J.* 15, 112–122. doi: 10.1208/s12248-012-9425-7

Enayetallah, A. E., French, R. A., Barber, M., and Grant, D. F. (2006). Cell-specific subcellular localization of soluble epoxide hydrolase in human tissues. *J. Histochem. Cytochem.* 54, 329–335. doi: 10.1369/jhc.5A6808.2005

Enayetallah, A. E., French, R. A., Thibodeau, M. S., and Grant, D. F. (2004). Distribution of soluble epoxide hydrolase and of cytochrome P450C8, 2C9, and 2J2 in human tissues. *J. Histochem. Cytochem.* 52, 447–454. doi: 10.1177/002215540405200403

Fan, F., Muroya, Y., and Roman, R. J. (2015). Cytochrome P450 eicosanoids in hypertension and renal disease. *Curr. Opin. Nephrol. Hypertens.* 24, 37–46. doi: 10.1097/MNH.0000000000000088

Fogo, A. B. (2007). Mechanisms of progression of chronic kidney disease. *Pediatr. Nephrol.* 22, 2011–2022. doi: 10.1007/s00467-007-0524-0

Gervasini, G., Garcia-Cerrada, M., Coto, E., Vergara, E., Garcia-Pino, G., Alvarado, R., et al. (2015). A 3'-UTR polymorphism in soluble epoxide hydrolase gene is associated with acute rejection in renal transplant recipients. *PLoS One* 10:e0133563. doi: 10.1371/journal.pone.0133563

Glodowski, S. D., and Wagener, G. (2015). New insights into the mechanisms of acute kidney injury in the intensive care unit. *J. Clin. Anesth.* 27, 175–180. doi: 10.1016/j.jclinane.2014.09.011

Gomez, G. A., Morisseau, C., Hammock, B. D., and Christianson, D. W. (2004). Structure of human epoxide hydrolase reveals mechanistic inferences on bifunctional catalysis in epoxide and phosphate ester hydrolysis. *Biochemistry* 43, 4716–4723. doi: 10.1021/bi036189j

Hashimoto, T., Fang, Y. I., Ohata, H., and Honda, K. (2015). Change in soluble epoxide hydrolase (sEH) during cisplatin-induced acute renal failure in mice. *J. Toxicol. Sci.* 40, 451–457. doi: 10.2131/jts.40.451

He, J. L., Wang, C. J., Zhu, Y., and Ai, D. (2016). Soluble epoxide hydrolase: a potential target for metabolic diseases. *J. Diabetes* 8, 305–313. doi: 10.1111/1753-0407.12358

Hu, D. Y., Luo, Y., Li, C. B., Zhou, C. Y., Li, X. H., Peng, A., et al. (2018). Oxylinin profiling of human plasma reflects the renal dysfunction in uremic patients. *Metabolomics* 14:104. doi: 10.1007/s11306-018-1402-4

Huang, H., Morisseau, C., Wang, J. F., Yang, T. X., Falck, J. R., Hammock, B. D., et al. (2007). Increasing or stabilizing renal epoxyeicosatrienoic acid production attenuates abnormal renal function and hypertension in obese rats. *Am. J. Physiol. Renal Physiol.* 293, F342–F349. doi: 10.1152/ajprenal.00004.2007

Imig, J. D. (2015). Epoxyeicosatrienoic acids, hypertension, and kidney injury. *Hypertension* 65, 476–482. doi: 10.1161/HYPERTENSIONAHA.114.03585

Imig, J. D., Carpenter, M. A., and Shaw, S. (2009). The soluble epoxide hydrolase inhibitor AR9281 decreases blood pressure, ameliorates renal injury and improves vascular function in hypertension. *Pharmaceuticals* 2, 217–227. doi: 10.3390/ph2030217

Imig, J. D., and Hammock, B. D. (2009). Soluble epoxide hydrolase as a therapeutic target for cardiovascular diseases. *Nat. Rev. Drug Discov.* 8, 794–805. doi: 10.1038/nrd2875

Imig, J. D., Walsh, K. A., Khan, M. A. H., Nagasawa, T., Cherian-Shaw, M., Shaw, S. M., et al. (2012). Soluble epoxide hydrolase inhibition and peroxisome proliferator activated receptor gamma agonist improve vascular function and decrease renal injury in hypertensive obese rats. *Exp. Biol. Med.* 237, 1402–1412. doi: 10.1258/ebm.2012.012225

Imig, J. D., Zhao, X. Y., Capdevila, J. H., Morisseau, C., and Hammock, B. D. (2002). Soluble epoxide hydrolase inhibition lowers arterial blood pressure in angiotensin II hypertension. *Hypertension* 39, 690–694. doi: 10.1161/hy0202.103788

Imig, J. D., Zhao, X. Y., Zaharis, C. Z., Olearczyk, J. J., Pollock, D. M., Newman, J. W., et al. (2005). An orally active epoxide hydrolase inhibitor lowers blood pressure and provides renal protection in salt-sensitive hypertension. *Hypertension* 46, 975–981. doi: 10.1161/01.HYP.0000176237.74820.75

Inceoglu, B., Jinks, S. L., Ulu, A., Hegedus, C. M., Georgi, K., Schmelzer, K. R., et al. (2008). Soluble epoxide hydrolase and epoxyeicosatrienoic acids modulate two distinct analgesic pathways. *Proc. Natl. Acad. Sci. U.S.A.* 105, 18901–18906. doi: 10.1073/pnas.0809765105

Iyer, R., Fetterly, G., Lugade, A., and Thanavala, Y. (2010). Sorafenib: a clinical and pharmacologic review. *Expert Opin. Pharmacother.* 11, 1943–1955. doi: 10.1517/14656566.2010.496453

Johansson, C., Stark, A., Sandberg, M., Ek, B., Rask, L., and Meijer, J. (1995). Tissue-specific basal expression of soluble murine epoxide hydrolase and effects of clofibrate on the messenger-rna levels in extrahepatic tissues and liver. *Arch. Toxicol.* 70, 61–63. doi: 10.1007/s002040050250

Jung, O., Jansen, F., Mieth, A., Barbosa-Sicard, E., Pliquet, R. U., Babelova, A., et al. (2010). Inhibition of the soluble epoxide hydrolase promotes albuminuria in mice with progressive renal disease. *PLoS One* 5:e11979. doi: 10.1371/journal.pone.0011979

Katary, M. M., Pye, C., and Elmarakby, A. A. (2017). Meloxicam fails to augment the reno-protective effects of soluble epoxide hydrolase inhibition in streptozotocin-induced diabetic rats via increased 20-HETE levels. *Prostaglandins Other Lipid Mediat.* 132, 3–11. doi: 10.1016/j.prostaglandins.2016.08.004

Kato, Y., Fuchi, N., Nishimura, Y., Watanabe, A., Yagi, M., Nakadera, Y., et al. (2014). Discovery of 1-oxa-4,9-diazaspiro[5.5]undecane-based trisubstituted urea derivatives as highly potent soluble epoxide hydrolase inhibitors and orally active drug candidates for treating of chronic kidney diseases. *Bioorg. Med. Chem. Lett.* 24, 565–570. doi: 10.1016/j.bmcl.2013.12.020

Kim, J., Imig, J. D., Yang, J., Hammock, B. D., and Padanilam, B. J. (2014). Inhibition of soluble epoxide hydrolase prevents renal interstitial fibrosis and inflammation. *Am. J. Physiol. Renal Physiol.* 307, F971–F980. doi: 10.1152/ajprenal.00256.2014

Kim, J., Yoon, S. P., Toews, M. L., Imig, J. D., Hwang, S. H., Hammock, B. D., et al. (2015). Pharmacological inhibition of soluble epoxide hydrolase prevents renal interstitial fibrogenesis in obstructive nephropathy. *Am. J. Physiol. Renal Physiol.* 308, F131–F139. doi: 10.1152/ajprenal.00531.2014

Koeners, M. P., Wesseling, S., Ulu, A., Sepulveda, R. L., Morisseau, C., Braam, B., et al. (2011). Soluble epoxide hydrolase in the generation and maintenance of high blood pressure in spontaneously hypertensive rats. *Am. J. Physiol. Endocrinol. Metab.* 300, E691–E698. doi: 10.1152/ajpendo.00710.2010

Kopkan, L., Huskova, Z., Sporkova, A., Varcabova, S., Honetschlagerova, Z., Hwang, S. H., et al. (2012). Soluble epoxide hydrolase inhibition exhibits antihypertensive actions independently of nitric oxide in mice with renovascular hypertension. *Kidney Blood Press. Res.* 35, 595–607. doi: 10.1159/000339883

Kujal, P., Chabova, V. C., Skaroupkova, P., Huskova, Z., Vernerova, Z., Kramer, H. J., et al. (2014). Inhibition of soluble epoxide hydrolase is renoprotective in

5/6 nephrectomized Ren-2 transgenic hypertensive rats. *Clin. Exp. Pharmacol. Physiol.* 41, 227–237. doi: 10.1111/1440-1681.12204

Kusch, A., Hoff, U., Bubalo, G., Zhu, Y., Fechner, M., Schmidt-Ullrich, R., et al. (2013). Novel signalling mechanisms and targets in renal ischaemia and reperfusion injury. *Acta Physiol.* 208, 25–40. doi: 10.1111/apha.12089

Larsson, C., White, I., Johansson, C., Stark, A., and Meijer, J. (1995). Localization of the human soluble epoxide hydrolase gene (Ephx2) to chromosomal region 8p21-P12. *Hum. Genet.* 95, 356–358. doi: 10.1007/BF00225209

Lazaar, A. L., Yang, L., Boardley, R. L., Goyal, N. S., Robertson, J., Baldwin, S. J., et al. (2016). Pharmacokinetics, pharmacodynamics and adverse event profile of GSK2256294, a novel soluble epoxide hydrolase inhibitor. *Br. J. Clin. Pharmacol.* 81, 971–979. doi: 10.1111/bcp.12855

Lee, J. P., Yang, S. H., Kim, D. K., Lee, H., Kim, B., Cho, J. Y., et al. (2011). In vivo activity of epoxide hydrolase according to sequence variation affects the progression of human IgA nephropathy. *Am. J. Physiol. Renal Physiol.* 300, F1283–F1290. doi: 10.1152/ajprenal.00733.2010

Lee, S. H., Lee, J., Cha, R., Park, M. H., Ha, J. W., Kim, S., et al. (2008). Genetic variations in soluble epoxide hydrolase and graft function in kidney transplantation. *Transplant. Proc.* 40, 1353–1356. doi: 10.1016/j.transproceed.2008.03.137

Li, L. J., Li, N., Pang, W., Zhang, X., Hammock, B. D., Ai, D., et al. (2014). Opposite effects of gene deficiency and pharmacological inhibition of soluble epoxide hydrolase on cardiac fibrosis. *PLoS One* 9:e94092. doi: 10.1371/journal.pone.0094092

Liang, Y. X., Jing, Z. Y., Deng, H., Li, Z. Q., Zhuang, Z., Wang, S., et al. (2015). Soluble epoxide hydrolase inhibition ameliorates proteinuria-induced epithelial-mesenchymal transition by regulating the PI3K-Akt-GSK-3 beta signaling pathway. *Biochem. Biophys. Res. Commun.* 463, 70–75. doi: 10.1016/j.bbrc.2015.05.020

Lin, Y. F., and Sheu, W. H. H. (2014). From sugar to kidney: a never-ending battle. *J. Diabetes Investig.* 5, 482–483. doi: 10.1111/jdi.12230

Liu, J. Y., Park, S. H., Morisseau, C., Hwang, S. H., Hammock, B. D., and Weiss, R. H. (2009). Sorafenib has soluble epoxide hydrolase inhibitory activity, which contributes to its effect profile in vivo. *Mol. Cancer Ther.* 8, 2193–2203. doi: 10.1158/1535-7163.MCT-09-0119

Liu, J. Y., Qiu, H., Morisseau, C., Hwang, S. H., Tsai, H. J., Ulu, A., et al. (2011). Inhibition of soluble epoxide hydrolase contributes to the anti-inflammatory effect of antimicrobial triclocarban in a murine model. *Toxicol. Appl. Pharmacol.* 255, 200–206. doi: 10.1016/j.taap.2011.06.017

Liu, Y. M., Lu, X. D., Nguyen, S., Olson, J. L., Webb, H. K., and Kroetz, D. L. (2013). Epoxyeicosatrienoic acids prevent cisplatin-induced renal apoptosis through a p38 mitogen-activated protein kinase-regulated mitochondrial pathway. *Mol. Pharmacol.* 84, 925–934. doi: 10.1124/mol.113.088302

Liu, Y. M., Webb, H. K., Fukushima, H., Micheli, J., Markova, S., Olson, J. L., et al. (2012). Attenuation of cisplatin-induced renal injury by inhibition of soluble epoxide hydrolase involves nuclear factor kappa B signaling. *J. Pharmacol. Exp. Ther.* 341, 725–734. doi: 10.1124/jpet.111.191247

Ma, L., Yan, M., Kong, X., Jiang, Y., Zhao, T., Zhao, H., et al. (2018). Association of EPHX2 R287Q polymorphism with diabetic nephropathy in Chinese type 2 diabetic patients. *J. Diabetes Res.* 2018:6. doi: 10.1155/2018/2786470

Malyszko, J. (2010). Mechanism of endothelial dysfunction in chronic kidney disease. *Clin. Chim. Acta* 411, 1412–1420. doi: 10.1016/j.cca.2010.06.019

Mariappan, M. M. (2012). Signaling mechanisms in the regulation of renal matrix metabolism in diabetes. *Exp. Diabetes Res.* 2012:749812. doi: 10.1155/2012/749812

Mennuni, S., Rubattu, S., Pierelli, G., Tocci, G., Fofi, C., and Volpe, M. (2014). Hypertension and kidneys: unraveling complex molecular mechanisms underlying hypertensive renal damage. *J. Hum. Hypertens.* 28, 74–79. doi: 10.1038/jhh.2013.55

Mihai, S., Codrici, E., Popescu, I. D., Enciu, A. M., Albulescu, L., Necula, L. G., et al. (2018). Inflammation-related mechanisms in chronic kidney disease prediction, progression, and outcome. *J. Immunol. Res.* 2018:2180373. doi: 10.1155/2018/2180373

Moradi, H., and Vaziri, N. D. (2018). Molecular mechanisms of disorders of lipid metabolism in chronic kidney disease. *Front. Biosci.* 23, 146–161. doi: 10.2741/4585

Morisseau, C., and Hammock, B. D. (2013). Impact of soluble epoxide hydrolase and epoxyeicosanoids on human health. *Annu. Rev. Pharmacol. Toxicol.* 53, 37–58. doi: 10.1146/annurev-pharmtox-011112-140244

Newman, J. W., Morisseau, C., and Hammock, B. D. (2005). Epoxide hydrolases: their roles and interactions with lipid metabolism. *Prog. Lipid Res.* 44, 1–51. doi: 10.1016/j.plipres.2004.10.001

Ng, R., and Chen, E. X. (2006). Sorafenib (BAY 43-9006): review of clinical development. *Curr. Clin. Pharmacol.* 1, 223–228. doi: 10.2174/157488406778249325

Nieves, D., and Moreno, J. J. (2007). Epoxyeicosatrienoic acids induce growth inhibition and calpain/caspase-12 dependent apoptosis in PDGF cultured 3T6 fibroblast. *Apoptosis* 12, 1979–1988. doi: 10.1007/s10495-007-0123-3

Node, K., Huo, Y. Q., Ruan, X. L., Yang, B. C., Spiecker, M., Ley, K., et al. (1999). Anti-inflammatory properties of cytochrome P450 epoxygenase-derived eicosanoids. *Science* 285, 1276–1279. doi: 10.1126/science.285.5431.1276

Oguro, A., Fujita, N., and Imaoka, S. (2009). Regulation of soluble epoxide hydrolase (sEH) in mice with diabetes: high glucose suppresses sEH expression. *Drug Metab. Pharmacokinet.* 24, 438–445. doi: 10.2133/dmpk.24.438

Olearczyk, J. J., Quigley, J. E., Mitchell, B. C., Yamamoto, T., Kim, I. H., Newman, J. W., et al. (2009). Administration of a substituted adamantyl urea inhibitor of soluble epoxide hydrolase protects the kidney from damage in hypertensive Goto-Kakizaki rats. *Clin. Sci.* 116, 61–70. doi: 10.1042/CS20080039

Parrish, A. R., Chen, G., Burghardt, R. C., Watanabe, T., Morisseau, C., and Hammock, B. D. (2009). Attenuation of cisplatin nephrotoxicity by inhibition of soluble epoxide hydrolase. *Cell Biol. Toxicol.* 25, 217–225. doi: 10.1007/s10565-008-9071-0

Patel, B. N., Mackness, M. I., Nwosu, V., and Connock, M. J. (1986). Subcellular-localization of epoxide hydrolase in mouse-liver and kidney. *Biochem. Pharmacol.* 35, 231–235. doi: 10.1016/0006-2952(86)90519-8

Persson, P. B. (2013). Mechanisms of acute kidney injury. *Acta Physiol.* 207, 430–431. doi: 10.1111/apha.12063

Prieto-Garcia, L., Pericacho, M., Sancho-Martinez, S. M., Sanchez, A., Martinez-Salgado, C., Lopez-Novoa, J. M., et al. (2016). Mechanisms of triple whammy acute kidney injury. *Pharmacol. Ther.* 167, 132–145. doi: 10.1016/j.pharmthera.2016.07.011

Rawal, S., Morisseau, C., Hammock, B. D., and Shivachar, A. C. (2009). Differential subcellular distribution and colocalization of the microsomal and soluble epoxide hydrolases in cultured neonatal rat brain cortical astrocytes. *J. Neurosci. Res.* 87, 218–227. doi: 10.1002/jnr.21827

Remuzzi, G., Benigni, A., and Remuzzi, A. (2006). Mechanisms of progression and regression of renal lesions of chronic nephropathies and diabetes. *J. Clin. Invest.* 116, 288–296. doi: 10.1172/JCI27699

Roche, C., Guerrot, D., Harouki, N., Duflot, T., Besnier, M., Remy-Jouet, I., et al. (2015). Impact of soluble epoxide hydrolase inhibition on early kidney damage in hyperglycemic overweight mice. *Prostaglandins Other Lipid Mediat.* 120, 148–154. doi: 10.1016/j.prostaglandins.2015.04.011

Rossi, G. P., Seccia, T. M., Barton, M., Danser, A. H. J., de Leeuw, P. W., Dhaun, N., et al. (2018). Endothelial factors in the pathogenesis and treatment of chronic kidney disease Part I: general mechanisms: a joint consensus statement from the European society of hypertension working group on endothelin and endothelial factors and the Japanese society of hypertension. *J. Hypertens.* 36, 451–461. doi: 10.1097/HJH.0000000000001599

Sandberg, M., and Meijer, J. (1996). Structural characterization of the human soluble epoxide hydrolase gene (EPHX2). *Biochem. Biophys. Res. Commun.* 221, 333–339. doi: 10.1006/bbrc.1996.0596

Seubert, J. M., Xu, F., Graves, J. P., Collins, J. B., Sieber, S. O., Paules, R. S., et al. (2005). Differential renal gene expression in prehypertensive and hypertensive spontaneously hypertensive rats. *Am. J. Physiol. Renal Physiol.* 289, F552–F561. doi: 10.1152/ajprenal.00354.2004

Sharma, A., Hye Khan, M. A., Levick, S. P., Lee, K. S., Hammock, B. D., and Imig, J. D. (2016). Novel Omega-3 fatty acid epoxygenase metabolite reduces kidney fibrosis. *Int. J. Mol. Sci.* 17:E751. doi: 10.3390/ijms17050751

Shuey, M. M., Billings, F. T., Wei, S. Z., Milne, G. L., Nian, H., Yu, C., et al. (2017). Association of gain-of-function EPHX2 polymorphism Lys55Arg with acute kidney injury following cardiac surgery. *PLoS One* 12:e0175292. doi: 10.1371/journal.pone.0175292

- Sirish, P., Li, N., Liu, J. Y., Lee, K. S. S., Hwang, S. H., Qiu, H., et al. (2013). Unique mechanistic insights into the beneficial effects of soluble epoxide hydrolase inhibitors in the prevention of cardiac fibrosis. *Proc. Natl. Acad. Sci. U.S.A.* 110, 5618–5623. doi: 10.1073/pnas.1221972110
- Smalley, K. S., Xiao, M., Villanueva, J., Nguyen, T. K., Flaherty, K. T., Letrero, R., et al. (2009). CRAF inhibition induces apoptosis in melanoma cells with non-V600E BRAF mutations. *Oncogene* 28, 85–94. doi: 10.1038/onc.2008.362
- Spector, A. A., Fang, X., Snyder, G. D., and Weintraub, N. L. (2004). Epoxyeicosatrienoic acids (EETs): metabolism and biochemical function. *Prog. Lipid Res.* 43, 55–90. doi: 10.1016/S0163-7827(03)00049-3
- Spector, A. A., and Norris, A. W. (2007). Action of epoxyeicosatrienoic acids on cellular function. *Am. J. Physiol. Cell Physiol.* 292, C996–C1012. doi: 10.1152/ajpcell.00402.2006
- Sporkova, A., Kopkan, L., Varcabova, S., Huskova, Z., Hwang, S. H., Hammock, B. D., et al. (2011). Role of cytochrome P-450 metabolites in the regulation of renal function and blood pressure in 2-kidney 1-clip hypertensive rats. *Am. J. Physiol. Regul. Integr. Comp. Physiol.* 300, R1468–R1475. doi: 10.1152/ajpregu.00215.2010
- Tain, Y. L., Huang, L. T., Chan, J. Y. H., and Lee, C. T. (2015). Transcriptome analysis in rat kidneys: importance of genes involved in programmed hypertension. *Int. J. Mol. Sci.* 16, 4744–4758. doi: 10.3390/ijms16034744
- Takaori, K., and Yanagita, M. (2016). Insights into the mechanisms of the acute kidney injury-to-chronic kidney disease continuum. *Nephron* 134, 172–176. doi: 10.1159/000448081
- U.S. Renal Data System (2009). *USRDS 2009 Annual Data Report: Atlas of Chronic Kidney Disease and End-Stage Renal Disease in the United States*. Bethesda, MD: National Institute of Diabetes and Digestive and Kidney Diseases.
- Walkowska, A., Skaroupkova, P., Huskova, Z., Vanourkova, Z., Chabova, V. C., Tesar, V., et al. (2010). Intrarenal cytochrome P-450 metabolites of arachidonic acid in the regulation of the nonclipped kidney function in two-kidney, one-clip Goldblatt hypertensive rats. *J. Hypertens.* 28, 582–593. doi: 10.1097/HJH.0b013e328334dfdd
- Wang, D. Z., and DuBois, R. N. (2012). Epoxyeicosatrienoic acids: a double-edged sword in cardiovascular diseases and cancer. *J. Clin. Invest.* 122, 19–22. doi: 10.1172/JCI61453
- Wang, Q., Liang, Y., Qiao, Y., Zhao, X., Yang, Y., Yang, S., et al. (2018). Expression of soluble epoxide hydrolase in renal tubular epithelial cells regulates macrophage infiltration and polarization in IgA nephropathy. *Am. J. Physiol. Renal Physiol.* 315, F915–F926. doi: 10.1152/ajprenal.00534.2017
- Wang, Q., Pang, W., Cui, Z., Shi, J. B., Liu, Y., Liu, B., et al. (2013). Upregulation of soluble epoxide hydrolase in proximal tubular cells mediated proteinuria-induced renal damage. *Am. J. Physiol. Renal Physiol.* 304, F168–F176. doi: 10.1152/ajprenal.00129.2012
- Wilhelm, S. M., Adnane, L., Newell, P., Villanueva, A., Llovet, J. M., and Lynch, M. (2008). Preclinical overview of sorafenib, a multikinase inhibitor that targets both Raf and VEGF and PDGF receptor tyrosine kinase signaling. *Mol. Cancer Ther.* 7, 3129–3140. doi: 10.1158/1535-7163.MCT-08-0013
- Xie, Y., Bowe, B., Mokdad, A. H., Xian, H., Yan, Y., Li, T. T., et al. (2018). Analysis of the Global Burden of Disease study highlights the global, regional, and national trends of chronic kidney disease epidemiology from 1990 to 2016. *Kidney Int.* 94, 567–581. doi: 10.1016/j.kint.2018.04.011
- Yang, S. H., Kim, Y. C., An, J. N., Kim, J. H., Lee, J., Lee, H. Y., et al. (2017). Active maintenance of endothelial cells prevents kidney fibrosis. *Kidney Res. Clin. Pract.* 36, 329–341. doi: 10.23876/j.krcp.2017.36.4.329
- Yu, Z. G., Davis, B. B., Morisseau, C., Hammock, B. D., Olson, J. L., Kroetz, D. L., et al. (2004). Vascular localization of soluble epoxide hydrolase in the human kidney. *Am. J. Physiol. Renal Physiol.* 286, F720–F726. doi: 10.1152/ajprenal.00165.2003
- Yu, Z. G., Xu, F. Y., Huse, L. M., Morisseau, C., Draper, A. J., Newman, J. W., et al. (2000). Soluble epoxide hydrolase regulates hydrolysis of vasoactive epoxyeicosatrienoic acids. *Circ. Res.* 87, 992–998. doi: 10.1161/01.RES.87.11.992
- Zeldin, D. C., Wei, S. Z., Falck, J. R., Hammock, B. D., Snapper, J. R., and Capdevila, J. H. (1995). Metabolism of epoxyeicosatrienoic acids by cytosolic epoxide hydrolase - substrate structural determinants of asymmetric catalysis. *Arch. Biochem. Biophys.* 316, 443–451. doi: 10.1006/abbi.1995.1059
- Zhao, G., Tu, L., Li, X. G., Yang, S. L., Chen, C., Xu, X. Z., et al. (2012). Delivery of AAV2-CYP2J2 protects remnant kidney in the 5/6-nephrectomized rat via inhibition of apoptosis and fibrosis. *Hum. Gene Ther.* 23, 688–699. doi: 10.1089/hum.2011.135
- Zhao, X. Y., Yamamoto, T., Newman, J. W., Kim, I. H., Watanabe, T., Hammock, B. D., et al. (2004). Soluble epoxide hydrolase inhibition protects the kidney from hypertension-induced damage. *J. Am. Soc. Nephrol.* 15, 1244–1253.
- Zhu, Y., Blum, M., Hoff, U., Wesser, T., Fechner, M., Westphal, C., et al. (2016). Renal ischemia/reperfusion injury in soluble epoxide hydrolase-deficient mice. *PLoS One* 11:e0145645. doi: 10.1371/journal.pone.0145645

Conflict of Interest Statement: The author declares that the research was conducted in the absence of any commercial or financial relationships that could be construed as a potential conflict of interest.

Copyright © 2019 Liu. This is an open-access article distributed under the terms of the Creative Commons Attribution License (CC BY). The use, distribution or reproduction in other forums is permitted, provided the original author(s) and the copyright owner(s) are credited and that the original publication in this journal is cited, in accordance with accepted academic practice. No use, distribution or reproduction is permitted which does not comply with these terms.



Deficiency of Soluble Epoxide Hydrolase Protects Cardiac Function Impaired by LPS-Induced Acute Inflammation

Victor Samokhvalov¹, K. Lockhart Jamieson¹, Ahmed M. Darwesh¹, Hedieh Keshavarz-Bahaghighat¹, Tim Y. T. Lee², Matthew Edin³, Fred Lih³, Darryl C. Zeldin³ and John M. Seubert^{1,2*}

¹ Faculty of Pharmacy and Pharmaceutical Sciences, University of Alberta, Edmonton, AB, Canada, ² Department of Pharmacology, Faculty of Medicine, University of Alberta, Edmonton, AB, Canada, ³ Division of Intramural Research, National Institute of Environmental Health Sciences, National Institutes of Health, Research Triangle Park, NC, United States

OPEN ACCESS

Edited by:

John D. Imig,
Medical College of Wisconsin,
United States

Reviewed by:

Beshay Zordoky,
University of Minnesota, United States
An Huang,
New York Medical College,
United States

*Correspondence:

John M. Seubert
jseubert@ualberta.ca

Specialty section:

This article was submitted to
Translational Pharmacology,
a section of the journal
Frontiers in Pharmacology

Received: 08 November 2018

Accepted: 24 December 2018

Published: 14 January 2019

Citation:

Samokhvalov V, Jamieson KL,
Darwesh AM, Keshavarz-
Bahaghighat H, Lee TYT, Edin M,
Lih F, Zeldin DC and Seubert JM
(2019) Deficiency of Soluble Epoxide
Hydrolase Protects Cardiac Function
Impaired by LPS-Induced Acute
Inflammation.
Front. Pharmacol. 9:1572.
doi: 10.3389/fphar.2018.01572

Lipopolysaccharide (LPS) is a bacterial wall endotoxin producing many pathophysiological conditions including myocardial inflammation leading to cardiotoxicity. Linoleic acid (18:2n6, LA) is an essential n-6 PUFA which is converted to arachidonic acid (20:4n6, AA) by desaturation and elongation via enzyme systems within the body. Biological transformation of PUFA through CYP-mediated hydroxylation, epoxidation, and allylic oxidation produces lipid mediators, which may be subsequently hydrolyzed to corresponding diol metabolites by soluble epoxide hydrolase (sEH). In the current study, we investigate whether inhibition of sEH, which alters the PUFA metabolite profile, can influence LPS induced cardiotoxicity and mitochondrial function. Our data demonstrate that deletion of soluble epoxide hydrolase provides protective effects against LPS-induced cardiotoxicity by maintaining mitochondrial function. There was a marked alteration in the cardiac metabolite profile with notable increases in sEH-derived vicinal diols, 9,10- and 12,13-dihydroxyoctadecenoic acid (DiHOME) in WT hearts following LPS administration, which was absent in sEH null mice. We found that DiHOMEs triggered pronounced mitochondrial structural abnormalities, which also contributed to the development of extensive mitochondrial dysfunction in cardiac cells. Accumulation of DiHOMEs may represent an intermediate mechanism through which LPS-induced acute inflammation triggers deleterious alterations in the myocardium *in vivo* and cardiac cells *in vitro*. This study reveals novel research exploring the contribution of DiHOMEs in the progression of adverse inflammatory responses toward cardiac function *in vitro* and *in vivo*.

Keywords: soluble epoxide hydrolase, cardiac function, mitochondrial function, LPS, inflammation

INTRODUCTION

Exposure to the bacterial endotoxin lipopolysaccharide (LPS), a major component of the cell wall from Gram-negative bacteria, can trigger acute systemic reactions potentially leading to multiple organ failure (Lew et al., 2013). Prevailing theories attribute these failures to uncontrolled inflammatory responses that produce numerous deleterious effects such as extensive organelle dysfunction and ultimately cell death (Lew, 2003; Kozlov et al., 2011; Lew et al., 2013). Cardiac dysfunction is a common outcome following such acute inflammatory responses, which can

ultimately lead to heart failure and subsequent death (Chagnon et al., 2005). Binding of LPS to TLR-4 receptors initiates the IKK-NF- κ B inflammatory program releasing pro-inflammatory cytokines such as TNF α , IL-1, IL-6, and MCP-1 (Frantz et al., 1999; Chagnon et al., 2005; Charalambous et al., 2007). The heart represents a particularly vulnerable target for LPS as terminally differentiated cardiomyocytes abundantly express TLR4 receptors (Kozlov et al., 2011). Furthermore, significant amounts of energy are required to sustain proper cardiac contractile function, making the heart the major consumer of energy in the body on a weight basis. During heart failure, the myocardium has low ATP content due to a decreased ability to generate ATP by oxidative metabolism thus reducing contractile work (Brealey et al., 2002). Although the precise mechanisms by which adverse acute inflammatory reactions lead to organ failure are not clear, evidence suggests mitochondrial dysfunction is an important cause in the progression of cardiac failure (Frantz et al., 1999; Callahan and Supinski, 2005; Anderson et al., 2007).

Dietary sources of n-6 polyunsaturated fatty acids (n-6 PUFA) may be obtained from liquid vegetable oils, including soybean, corn, sunflower, safflower, and cottonseed oils. Linoleic acid (18:2n6, LA) is the primary source of the essential n-6 PUFA, which is converted to arachidonic acid (20:4n6, AA) by desaturation and elongation via enzyme systems within the body (Jamieson et al., 2017a). N-6 PUFA are metabolized into a plethora of bioactive eicosanoids through three primary enzymatic systems: cyclooxygenases (COX), lipoxygenases (LOX), and cytochrome P450 (CYP) enzymes (Mabalirajan et al., 2013). CYP epoxygenases generate linoleic epoxides including 9,10-epoxyoctadecenoic acid (9,10-EpOME) and 12,13-epoxyoctadecenoic acid (12,13-EpOME), which are further metabolized by soluble epoxide hydrolase (sEH) to form the corresponding linoleic diols 9,10-dihydroxyoctadecenoic acid (9,10-DiHOME) and 12,13-dihydroxyoctadecenoic acid (12,13-DiHOME) (Mabalirajan et al., 2013; Lynes et al., 2017). The eicosanoids produced act as potent lipid mediators that regulate cellular homeostasis, including inflammatory responses and cytotoxicity (Dennis and Norris, 2015; Wagner et al., 2017). Evidence has indicated many of the cytotoxic effects attributed to EpOMes are in fact caused by their secondary metabolites DiHOMes, which are formed in the reaction catalyzed by sEH (Moghaddam et al., 1997; Fleming, 2014). For example, loss of cardioprotection observed in transgenic mice overexpressing CYP2J2 in cardiomyocytes was related to an age-related increase accumulation of cardiotoxic derivatives such as DiHOMes, which were reversed following inhibition of sEH (Chaudhary S. et al., 2013). Similarly, well documented evidence demonstrates that evoking anti-inflammatory responses can be achieved by inhibiting or deleting sEH (Schmelzer et al., 2005; Wagner et al., 2017). However, the biological effects and potency of many of the eicosanoid molecules remains largely unknown and yet to be identified in the context of orchestrating inflammatory responses in cardiovascular system.

In this study, we investigated the influence of sEH over LPS-induced acute inflammation responses and the involvement of CYP-derived metabolites of LA regarding cardiac and mitochondrial dysfunction and cellular injury. Our major

findings suggest increased levels of DiHOMes correlate with LPS-induced cardiac toxicity and markedly reduces mitochondrial function. In addition, exposure of cardiac cells to DiHOMes *in vitro* resulted in development of cellular injury leading to cell death.

MATERIALS AND METHODS

Animals

A colony of mice with targeted disruption of the *Ephx2* gene (sEH null) and wild-type littermates are maintained at the University of Alberta. All studies were carried out using male mice that were 2–3 months old and weighed 20–30 g. Mice received a single injection of LPS administered intraperitoneally (10 mg/kg) and were sacrificed 24 h later and samples collected. The dose of LPS injection was determined from previous myocardial studies and is considered a moderate dose (Lew et al., 2013; Strand et al., 2015). Body temperature was determined by measuring rectal temperature in animals using a digital thermometer (MT-Esatherm Ltd., 8172, Czechia) with a 2 mm sensor diameter. All animal experimental protocols were approved by the University of Alberta Health Sciences Welfare Committee and were performed in strict adherence to the guidelines set by the Canadian Council of Animal Care.

Blood Glucose Monitoring

The level of blood glucose was determined using a calibrated glucometer OneTouch Ultra2 from (LifeScan Inc., Switzerland). The assay was performed in accordance to guidance manufacturer instruction.

Mitochondrial Function

Hearts were ground with a mortar and pestle on dry ice and then homogenized in ice-cold buffer (20 mM Tris-HCl, 50 mM NaCl, 50 mM NaF, 5 mM sodium pyrophosphate, with 0.25 M sucrose added on the day of the experiment). Samples were centrifuged at $600 \times g$ for 10 min at 4°C to remove debris. Supernatant was collected and the protein content was measured by standard Bradford assay. The activities of citrate synthase (CS), NADH:ubiquinone oxidoreductase (complex I) and succinate dehydrogenase (SDH, complex II) were assessed spectrophotometrically as previously described (Akhnoh et al., 2016). Mitochondrial respiration was analyzed in freshly isolated cardiac mitochondria as described (Gedik et al., 2013). Briefly, heart homogenate was first centrifuged at $700 \times g$ for 10 min followed by centrifuging the supernatant at $10,000 \times g$ for 10 min, then the pellet was resuspended and washed using isolation buffer at $10,000 \times g$ for 10 min. Mitochondrial oxygen consumption was measured in isolated mitochondria (50 μ g of mitochondrial protein) added to a chamber connected to OXYGRAPH PLUS system (Hansatech Instruments Ltd., Norfolk, England). Respiration rates were measured at 30°C in 2 ml of respiration buffer. Basal respiration was recorded after the addition of 5 mM malate and 10 mM glutamate as respiratory substrates for basal oxidative respiration. ADP-stimulated respiration was initiated by addition of 1 mM ADP then recorded. The efficiency of

coupled oxidative phosphorylation was calculated and expressed as the ratio between basal and ADP-stimulated respiration rates.

ATP content was assessed using a colorimetric assay kit (ab83355, Abcam Inc., Toronto, ON, Canada). Heart powders were homogenized and centrifuged at $15000 \times g$ for 2 min and the resultant supernatant was assessed for ATP content. Standard curve for ATP and reaction mixture were prepared according to the kit manual in a 96-well plate and optical density (OD) was measured at 570 nm.

Immunoblotting

Subcellular fractions isolated from hearts were subjected to western blot analysis as previously described (Darwesh et al., 2018; Endo et al., 2018). Briefly, 25 μ g of protein from heart tissues was resolved on a 12% SDS-polyacrylamide gel and transferred to polyvinylidene difluoride membranes. Membranes were incubated with primary antibodies to sEH (1:1000, Santa Cruz Biotech, Inc., Cat No. sc22344), eNOS (1:500, Abcam, Toronto, ON, Cat No: ab76198), TLR4 (1:500, Abcam, Toronto, ON, Cat No: ab13556), succinate dehydrogenase A (SDH-A) (1:500, Cell Signaling Tech., Inc., Whitby, ON, Cat No. cs5839), CS (1:000, Abcam, Toronto, ON, Cat No: ab129095), cytochrome c oxidase subunit 1 (COX IV) (1:1,000, Cell Signaling Tech., Inc., Whitby, ON, Cat No: 4850), prohibitin (1:1000, Cell Signaling Technology, Inc., MA, Cat. NO: 2426), or GAPDH (1:5000, Cell Signaling Tech., Inc., Whitby, ON, Cat No: 5174S), secondary antibodies were used as 1:5000 dilution and expression was visualized with ECL reagent. Band intensities were expressed as fold change relative to control using Image J software (NIH, United States).

Aconitase, 20S Proteasome and Malondialdehyde Assays

Aconitase activity was used as a marker of oxidative mitochondrial damage and evaluated using an ELISA kit (Abcam, Toronto, ON, Canada). 20S proteasome activity was used as a marker of unspecific degenerative processes and determined in tissue lysates based on monitoring the release of AMC by proteolytic cleavage of the peptide Suc-LLVY-AMC (CHEMICON Inc., Billerica, MA, United States) by 20S proteasomes. Fluorescence was monitored at wavelengths of 380 nm (excitation) and 460 nm (emission). Specific activity was determined from a standard curve established with AMC. The level of MDA was used as an overall marker of lipid peroxidation and assessed in reaction with thiobarbituric acid using a kit from (Abcam, Toronto, ON, Canada). The MDA-TBA adduct was quantified colorimetrically at 540 nm wavelength.

LC – MS/MS Oxylipid Analysis

Tissue samples were stored at -80°C until processing. LC-MS/MS methods and multiple reaction monitoring have been adapted from previously established protocols (Newman et al., 2002; Edin et al., 2011). Samples were homogenized in $5 \times$ volume of 0.1% acetic acid in 5% methanol containing 1 μM *trans*-4-[4-(3-adamantan-1-yl-ureido)-cyclohexyloxy]-benzoic

acid (tAUCB), spiked with 3 ng PGE 2 -d9, d11-11,12-DHET, d11-11,12-EET (Cayman) as internal standards, extracted by liquid:liquid extraction with 3 ml ethyl acetate and dried in vacuum centrifuge. Samples were analyzed in duplicate 10 μL injections. Online liquid chromatography of extracted samples was performed with an Agilent 1200 Series capillary HPLC (Agilent Technologies, Santa Clara, CA, United States). Separations were achieved using a Halo C18 column (2.7 mm, 10062.1 mm; MAC-MOD Analytical, Chadds Ford, PA, United States), which was held at 50°C . Mobile phase A was 85:15:0.1 water:acetonitrile:acetic acid. Mobile phase B was 70:30:0.1 acetonitrile:methanol:acetic acid. Flow rate was 400 ml/min. Gradient elution was used; mobile phase percentage B and flow rate were varied as follows: 20% B at 0 min, ramp from 0 to 5 min to 40% B, ramp from 5 to 7 min to 55% B, ramp from 7 to 13 min to 64% B. From 13 to 19 min the column was flushed with 100% B at a flow rate of 550 Turbo desolation gas was heated to 425°C at a flow rate of 6 L/min. Negative ion electrospray ionization tandem mass spectrometry with multiple reaction monitoring was used for detection. Quantification was done using Analyst 1.5.1 software comparing relative response ratios for each analyte/internal standard to standard curves for each analyte.

Echocardiography Measurements

Non-invasive functional assessment was performed by transthoracic echocardiography using a Vevo 770 high-resolution imaging system with a 30 MHz transducer (RMV-707B; VisualSonics). Isoflurane (0.8% by anesthetic machine) was used to anesthetize the mice during the recordings. To assess the change in cardiac function, echocardiography was carried 24 h after LPS administration. Left ventricular end-systolic diameter (LVESD) and end-diastolic diameter (LVEDD) were obtained from M-mode images as well left atrial size was obtained by M-mode imaging in the parasternal long axis view. Systolic function was assessed by calculating ejection fraction (%EF) and fractional shortening (%FS) using the following equations $\%EF = (LVEDV - LVESV / LVEDV) \times 100$ and $\%FS = (LVEDD - LVESD / LVEDD) \times 100$. Tei index was calculated as $[\text{isovolumic contraction time (IVCT)} + \text{isovolumic relaxation time (IVRT)}] / \text{ejection time (ET)}$. Diastolic function was assessed using pulsed-wave Doppler imaging as previously described (Akhnoh et al., 2016; Jamieson et al., 2017b). VisualSonics software was used for the qualitative and quantitative measurements.

Inflammatory Response

Blood samples were collected and probed for TNF α and MCP-1 using ELISA kits (Abcam, Toronto, ON, Canada). Briefly, the sample was added into individual wells of a 96-well plate coated with a TNF α or MCP-1 mouse-specific antibody. After washing, wells were incubated with HRP-conjugated streptavidin, washed and incubated with substrate solution and measured spectrophotometrically at 450 nm. Increased color intensity occurred in a linear proportion to the amount of TNF α or MCP-1

in the samples. NF- κ B DNA binding activity was measured using an ELISA kit from Active Motif (Carlsbad, CA, United States), which is based on the specific recognition of NF- κ B response elements.

Cell Culture

HL-1 cardiac cells were a kind gift from Dr. Claycomb (New Orleans, United States). Cells were cultivated in Claycomb media supplemented with glutamine and norepinephrine as described (Samokhvalov et al., 2012). HL-1 cells were maintained at 37°C in a humidified atmosphere of 5% CO₂ and 95% air. Neonatal rat cardiomyocytes (NRCMs) were isolated from 2 to 3 day-old pups as previously described before (Samokhvalov et al., 2012) and were cultivated in DMEM medium supplemented with 10% FBS at 37°C in a humidified incubator maintaining 5% CO₂ and 95% air. Cell viability was assessed using the CCK-8 viability kit (Sigma-Aldrich, Oakville, ON, Canada) based on the production of water-soluble formazan by dehydrogenases of viable cells. HL-1 cells were treated or co-treated with either 9,10-DiHOME, 12,13-DiHOME, 9,10-EpOME, 12,13-EpOME (0.01, 0.1, or 1 μ M), and/or *t*AUCB (10 μ M) to specifically inhibit sEH activity. 9,10-DiHOME, 12,13-DiHOME, 9,10-EpOME, and 12,13-EpOME were obtained from Cayman Chemical (Ann Arbor, MI, United States) and *t*AUCB was kindly provided by Dr. Bruce Hammock, UC, Davis, United States. Caspase-3/7 activity in cardiomyocytes was detected by using the Apo-ONE assay kit (Promega, Madison, WI, United States) according to manufacturer's instructions. Aconitase 2 enzymatic activity as a marker of mitochondrial injury was assessed using a kit from (Abcam Toronto, ON, Canada).

Assessments of Mitochondrial Function and Biogenesis

In order to test mitochondrial function we measured ATP levels using a luciferase-based method (Sigma-Aldrich, Oakville, ON, Canada). Mitochondrial respiration was measured in saponin (100 μ g/ml) permeabilized HL-1 cells using Clark oxygen electrode connected to Oxygraph Plus recorder (Hansatech Instruments Ltd., Norfolk, England) (Akhnoh et al., 2016). Respiration rates were measured at 30°C before and after addition of 2 mM ADP where 5 mM malate and 10 mM glutamate were used as respiratory substrates. Respiratory control ratio (RCR) was calculated as the ratio between basal and ADP-stimulated respiration rates. Mitochondrial biogenesis was evaluated using an ELISA kit (Abcam, Toronto, ON, Canada) based on simultaneous detection of SDH-A, a subunit of complex II (nDNA-encoded protein) and COX-1, a subunit of complex IV (mtDNA-encoded).

Microscopic Analysis

HL-1 cells were plated in 6-well glass bottom plate and left until 80–90% confluency. Cells were loaded with 1 nM tetramethylrhodamine ethyl ester (TMRE) and 1 μ M Hoechst 33342 trihydrochloride, 30 min prior to treatment. TMRE was used to reflect mitochondria and Hoechst 33342 to identify cell

nuclei. Cells were treated with EpOMEs (0,10 nM or 100 nM) and DiHOMEs (0,10 nM or 100 nM) for 6 h. Images were taken by Zeiss Axio Observer Z1 inverted epifluorescence microscope, using 63X oil lens and maintained at 37°C and 5% CO₂ throughout the experiment.

Statistical Analysis

Data are presented as mean \pm SEM. Statistical analysis was based on two-way ANOVA with Tukey's *post hoc* test; *P* < 0.05 was considered statistically significant. All statistical analysis was performed using GraphPad Prism 7 software.

RESULTS

sEH Null Mice Had Attenuated Inflammatory Responses Evoked by LPS

In order to assess whether sEH deficiency provides resistance, we induced acute inflammation in WT and sEH null mice using a clinically relevant model where LPS was administered i.p. (10 mg/kg). Administration of LPS resulted in weight loss, increased body temperature and significantly reduced levels of blood glucose in WT mice (Figures 1A–C). The physiological changes we observed in WT mice following exposure to LPS reflect common responses that occur in acute murine sepsis such as fever, anorexia and subsequent hypoglycemia (Wisse et al., 2007; Yue et al., 2015). In contrast, sEH null mice had reduced physiological responses to LPS exposure compared to the WT mice (Figures 1A–C). These observations demonstrate that deficiency of sEH confers a high degree of physiological tolerance to LPS-induced acute inflammation. To determine whether sEH expression was altered following LPS injection, sEH protein expression was then assessed in WT and sEH null hearts. There were no significant changes in WT hearts exposed to LPS (Figure 1G) with no expression in either control or LPS groups in sEH null hearts as expected. In order to obtain insight into key proteins involved in immune responses we assessed hearts for expression of eNOS and TLR4 (Figures 1H, I). There were no significant differences between WT and sEH null mice in either control or LPS groups for eNOS and TLR4 proteins.

LPS-induced injury is largely mediated through robust activation of the pro-inflammatory response. Particularly, LPS-associated inflammation appears to be a driving force causing inflammatory-associated damage and dysfunction of the myocardium. First, we investigated if WT differed from sEH null mice in terms of overall inflammatory reactions developed in response to LPS administration. We found significantly lower levels of both TNF α and MCP-1 cytokines in blood of sEH null versus WT mice (Figures 1D,E), suggesting the inflammatory response was attenuated in sEH null mice. We next investigated the effect of sEH deficiency toward activation of a specific inflammatory response, NF- κ B DNA binding activity. Consistent with the reduced inflammatory response, we found NF- κ B DNA binding activity was significantly lower in myocardium of sEH null mice compared to WT (Figure 1F). Together, these data indicate that deficiency of sEH confers

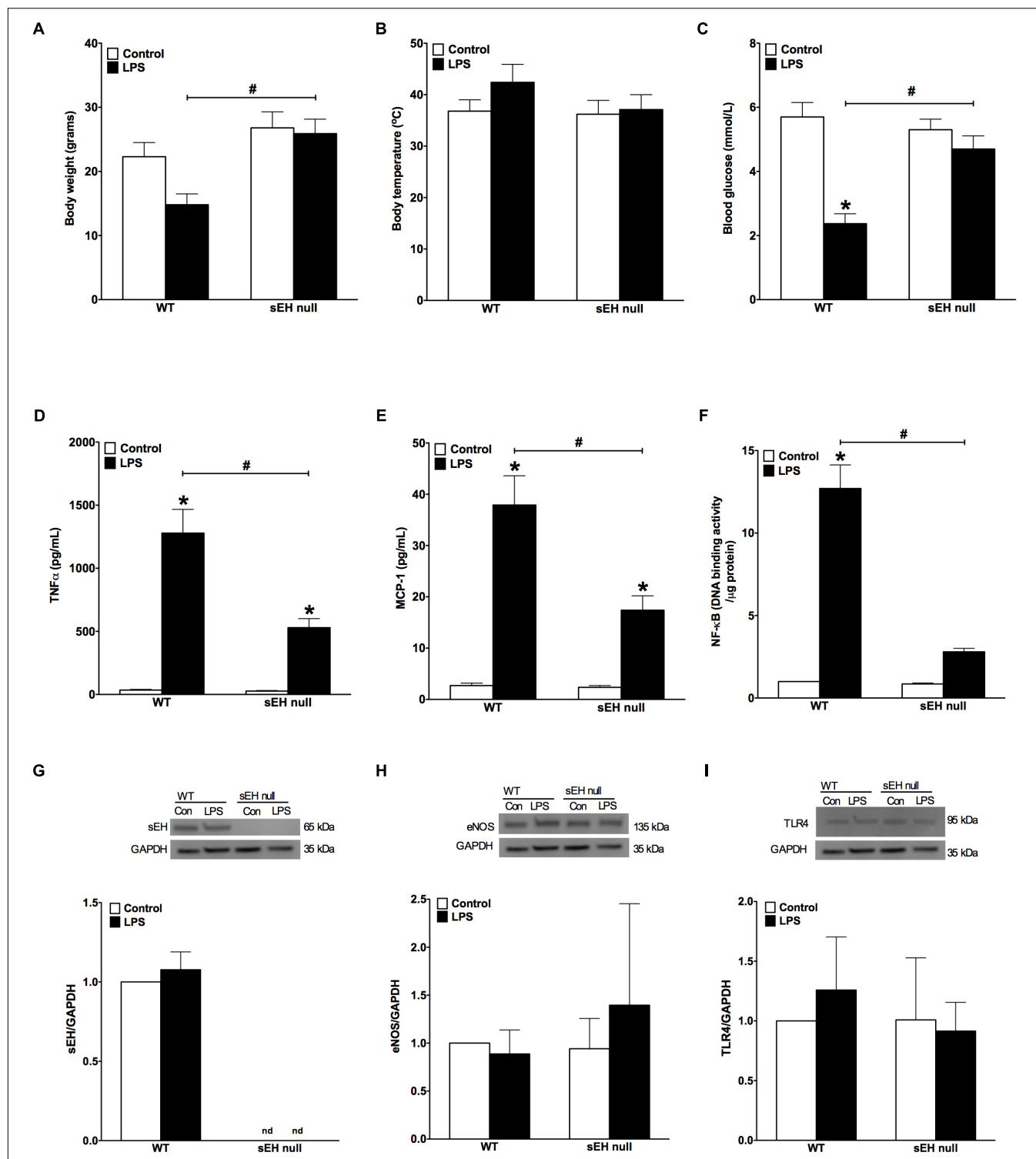


FIGURE 1 | Changes to body weight, temperature, blood glucose levels and inflammatory responses following LPS administration in WT and sEH null mice.

(A) Differences in body weight of WT and sEH null mice with or without injection of LPS, (B) differences in body temperature in WT and sEH null mice with or without injection of LPS, (C) comparing blood glucose levels for WT and sEH mice with or without injection of LPS, (D) serum levels of TNFα in WT and sEH null mice, (E) serum levels of MCP-1 in WT and sEH null mice, (F) DNA binding activity of NF-κB in hearts from WT and sEH null mice. Representative immunoblots and densitometric quantification of (G) sEH (60 kDa), (H) eNOS (135 kDa), and (I) TLR4 (95 kDa) protein expression in hearts from WT and sEH null mice. All expression was normalized to GAPDH loading control. Data presented as mean ± SEM, $N = 4-6$. Statistics: Two-way ANOVA with Tukey's *post hoc* test. * $p < 0.05$ vs. control, # $p < 0.05$ vs. LPS treatment groups.

protection against inflammation occurring in response to LPS challenge.

sEH Deficiency Attenuated Against LPS-Induced Cardiac Dysfunction

Development of LPS-induced inflammation is associated with multiple organ failure as a result of an uncontrollable innate immune response, which impacts cardiac function. We determined if sEH deficiency protects against cardiac dysfunction resulting from LPS-induced acute inflammation. Baseline heart function was similar between WT and sEH null mice; however, there was a decline in heart function in WT mice following 24 h LPS exposure (**Table 1**). No significant differences in heart rate were observed between WT and sEH null mice, suggesting any changes to LV function were not attributed to fluctuations in HR. Assessment of LV internal diameter during diastole and systole revealed LPS-mediated increases for WT hearts. The decreased ejection fraction and fractional shortening observed following LPS administration demonstrated a significant reduction of systolic function in WT mice (**Table 1**). Our previous observations demonstrated genetic deletion of sEH significantly attenuated the cardiac dysfunction following myocardial infarction (Akhnokh et al., 2016). Similarly, LPS-mediated cardiac dysfunction characterized by significantly decreased %EF, %FS, and increased LV volumes was primarily observed in WT mice with sEH mice exhibiting preserved systolic function 24 h post-LPS injection (**Table 1**).

sEH Null Mice Are Resistant to Myocardial Oxidative Injury in Response to LPS

Accumulation of oxidative injury in myocardium has been recognized as one of the key factors mediating cardiotoxicity of LPS (Suliman et al., 2004; Vanasco et al., 2008). Aconitase is an enzyme that catalyzes the reversible interconversion of citrate and isocitrate in the TCA cycle. Importantly, aconitase also stabilizes mtDNA thereby influencing mitochondrial gene expression. A decrease in aconitase activity is considered a marker of damaged mitochondrial structures. Our observations demonstrate that inflammation induced significantly stronger decrease in aconitase activity of WT mice than in those of sEH null mice (**Figure 2A**). In order to examine if sEH null mice are resistant to oxidative injury in the setting of LPS-induced inflammation, we employed a test measuring a total level of malondialdehyde (MDA). We found that LPS caused a dramatic increase in the levels of MDA in myocardium of WT mice indicative of extensive damages of cardiac structures. However, administration of LPS to sEH null mice did not result in much accumulation of myocardial MDA suggesting there was an adaptive event associated with sEH deficiency (**Figure 2B**). The accumulation of ubiquitinated proteins triggers 20S proteasome activity to remove the targeted damaged proteins. As such, in accordance to our previously published studies, 20S proteasome activity can be utilized as a marker of unspecific cellular degenerative processes occurring in myocardium. **Figure 2C**

TABLE 1 | Echocardiography data demonstrated various changes between WT and sEH null mice when treated with LPS.

	WT		sEH null	
	Control	LPS	Control	LPS
HR, beats/min	484 ± 22	466 ± 7	517 ± 24	495 ± 40
Wall measurements				
Corrected LV mass, mg	71.68 ± 5.97	80.34 ± 7.98	70.47 ± 2.65	84.95 ± 7.64
IVS-diastole, mm	0.70 ± 0.04	0.71 ± 0.03	0.74 ± 0.04	0.77 ± 0.06
IVS-systole, mm	1.18 ± 0.13	0.99 ± 0.08	1.07 ± 0.07	1.18 ± 0.12
LVPW-diastole, mm	0.72 ± 0.05	0.67 ± 0.03	0.69 ± 0.03	0.77 ± 0.08
LVPW-systole, mm	1.09 ± 0.09	0.92 ± 0.08	1.18 ± 0.03	1.18 ± 0.17
LVID-diastole, mm	3.7 ± 0.2	4.1 ± 0.2	3.7 ± 0.1	3.9 ± 0.1
LVID-systole, mm	2.3 ± 0.2	3.2 ± 0.3	2.3 ± 0.1	2.6 ± 0.3
Cardiac function				
EF, %	72.46 ± 2.08	45.78 ± 6.25*	68.06 ± 1.96	61.83 ± 6.70
FS, %	41.04 ± 1.67	22.85 ± 3.62*	37.35 ± 1.61	33.57 ± 5.19
LVEDV, μ l	55.44 ± 3.98	74.80 ± 7.78	57.84 ± 4.33	67.93 ± 4.97
LVESV, μ l	15.76 ± 2.28	41.10 ± 7.34*	18.49 ± 1.91	26.78 ± 6.17
CO, ml/min	19.03 ± 0.47	15.66 ± 2.22	20.61 ± 2.31	20.21 ± 1.26
SV, μ l	39.68 ± 1.96	33.73 ± 4.88	39.35 ± 3.06	41.18 ± 2.21
Doppler imaging				
IVRT, ms	13.1 ± 2.3	24.2 ± 1.1*	13.5 ± 0.7	19.0 ± 0.7
IVCT, ms	10.6 ± 1.5	17.6 ± 2.1*	7.6 ± 0.8	16.0 ± 1.6*
ET, ms	53.5 ± 3.1	43.1 ± 3.4	42.4 ± 2.6	45.6 ± 2.1
Tei index	0.45 ± 0.06	1.01 ± 0.16*	0.50 ± 0.04	0.77 ± 0.03

Data presented as mean ± SEM, N = 4–6, *p < 0.05 vs. control.

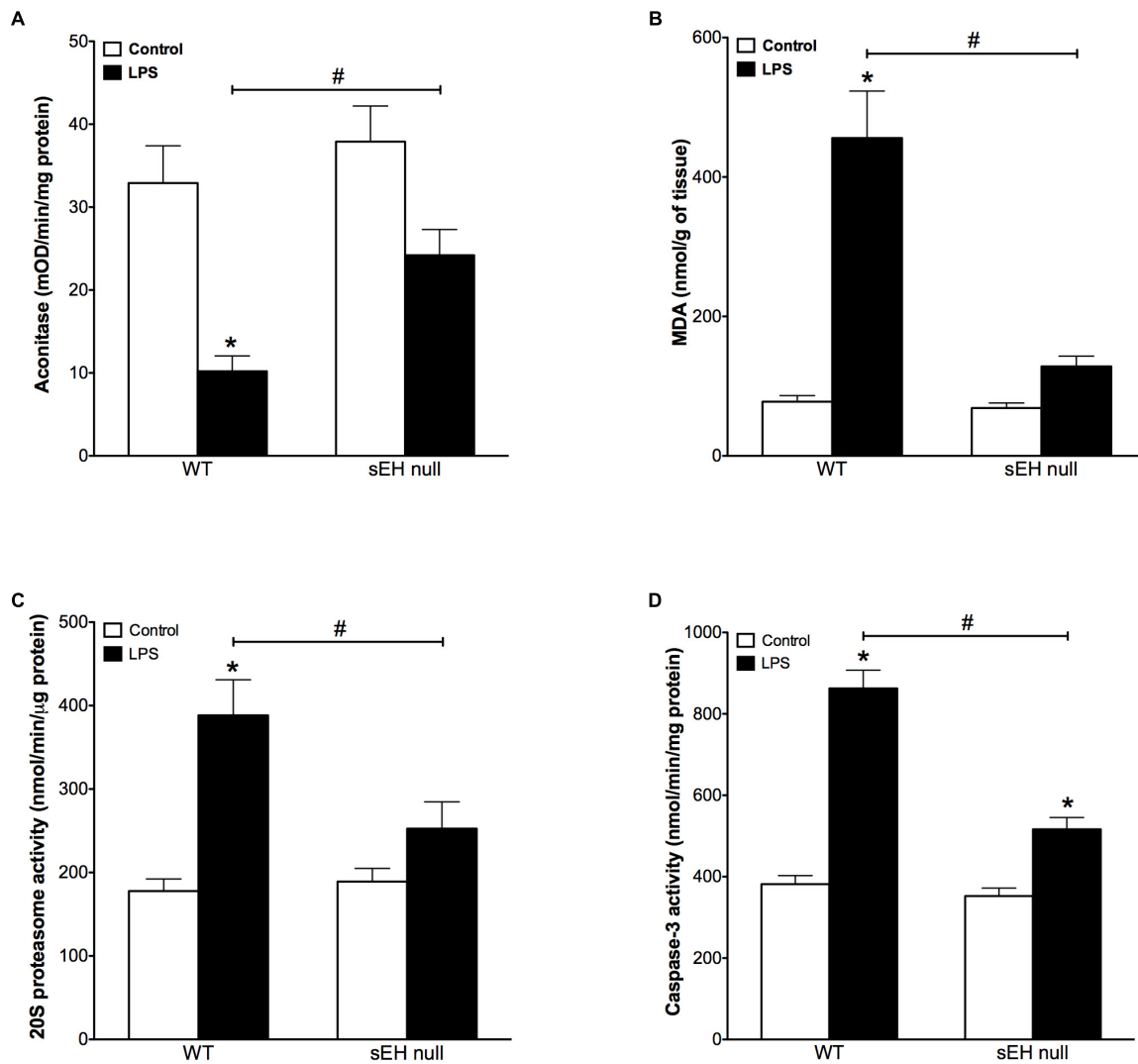


FIGURE 2 | Aconitase levels are recovered in sEH null mice after injection of LPS whereas MDA, 20S proteasome and caspase-3 activity are reduced in sEH null mice post LPS treatment. **(A)** Aconitase activity, **(B)** heart malondialdehyde (MDA) levels, **(C)** 20S proteasome activity, and **(D)** cardiac caspase-3 activity in hearts from WT and sEH null mice. Data presented as mean \pm SEM, $N = 4-6$. Statistics: Two-way ANOVA with Tukey's *post hoc* test. * $p < 0.05$ vs. control, # $p < 0.05$ vs. LPS treatment groups.

clearly demonstrates that WT mice developed a sharp elevation in 20S proteasomal activity in myocardium after being challenged with LPS. Conversely, sEH null mice displayed significantly less activation providing further evidence of cardioprotection associated with deficiency of sEH (**Figure 2C**). Finally, we measured activity of caspase 3/7 (a marker of apoptosis) in myocardium of WT and sEH null mice. These data provide indirect evidence of increased activation of apoptotic responses in the myocardium of WT mice compared to sEH null animals (**Figure 2D**).

Deletion of sEH Preserved Mitochondrial Function Following LPS Treatment

Based on our previous data demonstrating adverse effects of LPS toward cardiac mitochondria, it was important to

further evaluate alterations in mitochondrial function and whether sEH deficiency confers mitochondrial protection against LPS insult (Samokhvalov et al., 2015). Accordingly, we first measured protein content and then activity of key enzymes of mitochondrial oxidative metabolism such as citrate synthase, complex I and complex II. No significant alterations in the expression of cardiac mitochondrial proteins was observed in hearts from WT or sEH null mice, suggesting overall mitochondrial content was preserved (**Figures 3A–D**). However, LPS WT animals had significantly lower catalytic activity in the tested enzymes indicative of an overall decrease in mitochondrial function (**Figures 3E–G**). Remarkably, administration of LPS did not produce severe inhibition of enzymatic activities in the hearts of sEH null mice providing further evidence of cardioprotection was associated with preservation of mitochondrial function.

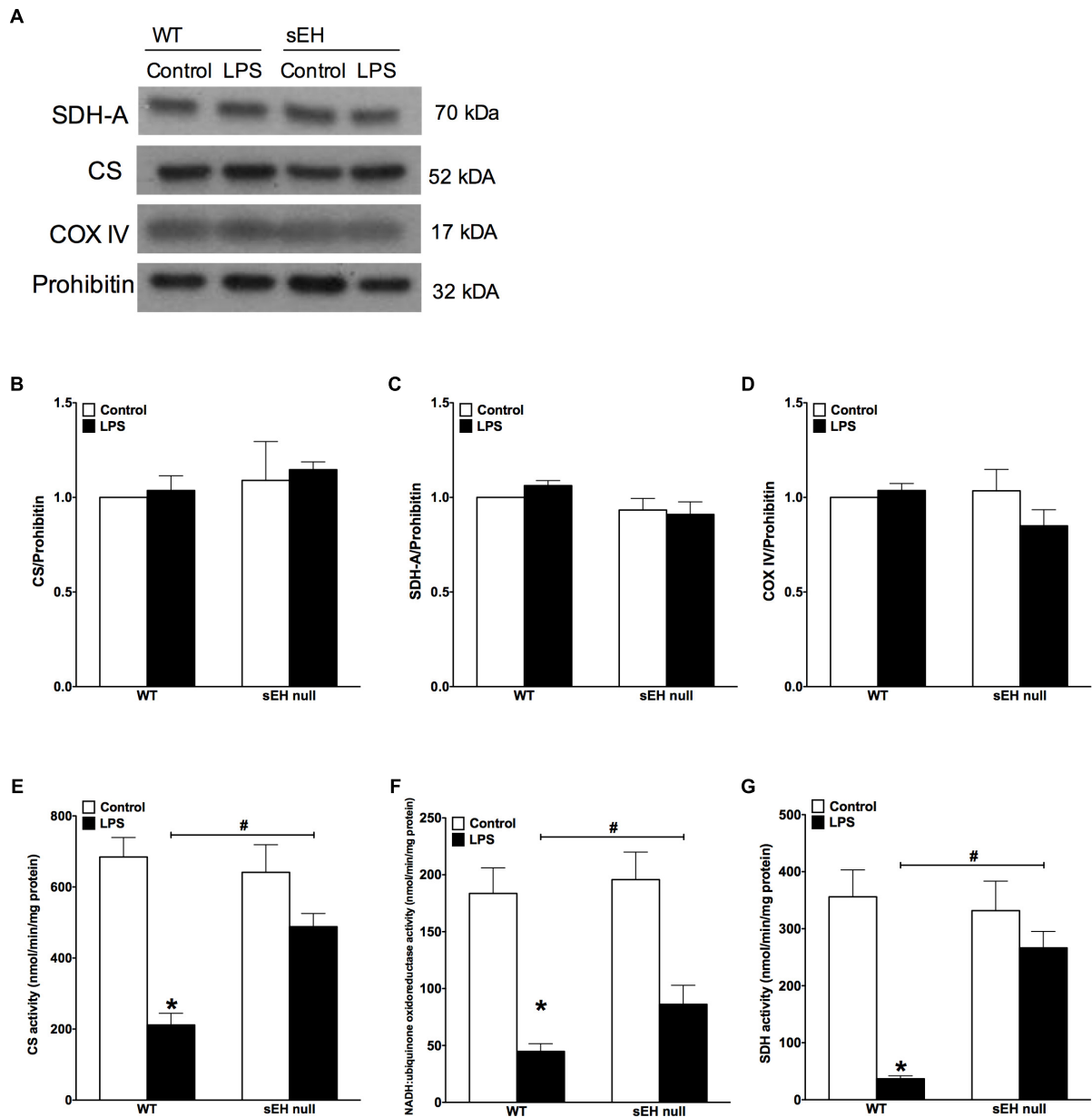
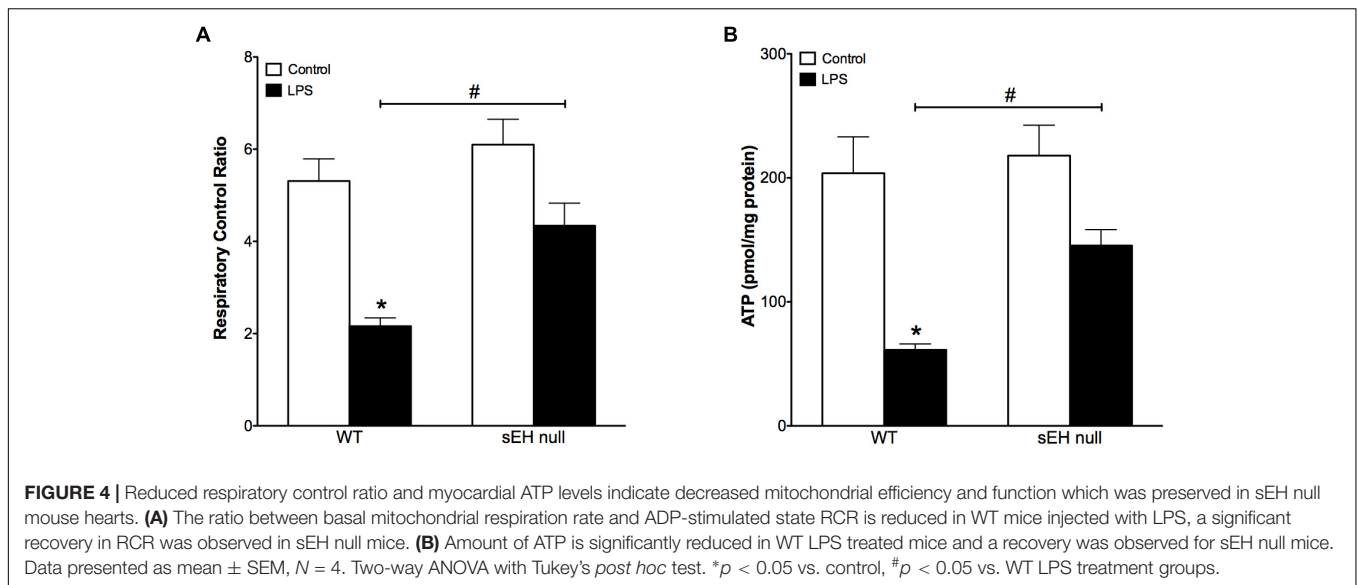


FIGURE 3 | Key mitochondrial oxidative metabolism enzyme levels had no significant change but activities in LPS treated WT mice is significantly reduced.

(A) Representative immunoblots of succinate dehydrogenase (SDH-A 70 kDa), citrate synthetase (CS 52 kDa), cytochrome c oxidase IV (COX IV 17 kDa), and loading control prohibitin (32 kDa). Densitometric quantification of (B) CS, (C) SDH-A, (D) COX IV, and (E) CS activity, (F) NADH:ubiquinone oxidoreductase activity, and (G) succinate dehydrogenase activity in hearts from WT and sEH null mice. Data presented as mean \pm SEM, $N = 5$. Statistics: Two-way ANOVA with Tukey's *post hoc* test. * $p < 0.05$ vs. control, # $p < 0.05$ vs. WT LPS treatment groups.

Analysis of mitochondrial O_2 consumption is the classical approach to characterize mitochondrial function by determining the respiratory rates during mitochondrial respiratory states such as basal state (resting or controlled respiration) and in ADP-stimulated state (active respiration, the maximal physiological rate of O_2 uptake, and ATP synthesis). The ratio between the states represents a level of physiological efficiency of mitochondria and expressed as RCR. As shown in Figure 4A, we observed a significant decline in RCR of cardiac mitochondria

isolated from LPS-exposed WT mice that was significantly attenuated in sEH null mice. Noteworthy, malate and glutamate were used as respiratory substrates. Considering the fact that oxidation of malate-glutamate is controlled exclusively by complex I, our observations tentatively suggest there was an impairment in complex I causing further limitation of the entire respiratory rates. This finding is indirectly supported by a previous report suggesting inactivation of respiratory activity following acute LPS exposure compromises optimal



mitochondrial function (Frisard et al., 2015). Myocardial ATP content is a classical marker of mitochondrial function. LPS exposure significantly decreased ATP content in the hearts of WT animals (**Figure 4B**). While a moderate drop in ATP levels was observed in sEH null mice following LPS exposure, ATP levels were significantly better in sEH null hearts compared to WT mice (**Figure 4B**). All together, these data directly suggests a metabolic collapse of the heart developed in WT mice exposed to LPS, which can be considered as a beginning of heart failure. In striking contrast, mitochondria isolated from the hearts of sEH null animals exhibited preserved hallmarks of oxidative metabolism indicative of adaptive cardioprotection originating most likely within mitochondria.

Cardiac Oxylipin Levels Following Acute Inflammation in WT and sEH Null Mice

We quantified metabolites of arachidonic acid, linoleic acid, EPA, and DHA derived epoxides and diols in myocardium from WT and sEH null mice challenged with or without LPS utilizing LC-MS/MS (**Table 2**). Genetic deletion of sEH resulted in moderate changes in epoxides derived from linoleic acid (12,13-EpOME and 9,10-EpOME), arachidonic acid, EPA, and DHA metabolites, generated via catalytic pathways mediated by COX, LOX, and CYP450. Following 24 h exposure to LPS there was an expected increase in pro-inflammatory metabolites in WT mice. This was marked by increased production of COX metabolites of AA (prostanoids), 6-keto-PGF 1α , PGF 2α , PGE 2 , and PGD 2 , reflecting a pro-inflammatory response. PGE 2 is a predominant pro-inflammatory prostanoid that enhances edema formation and leukocyte infiltration by promoting blood flow, while PGD 2 is a major product of mast cells, contributing to inflammation. The changes were attenuated in sEH null mice following LPS treatment supporting the anti-inflammatory effect. There were no statistically significant alterations in LOX-dependent metabolites of AA (5-, 8-, 12-, and 15-HETE). However, there were trends suggesting increases in LA [9- and 13-hydroxyoctadecadienoic

acid (HODE)] metabolites in WT mice following LPS exposure, which were absent in sEH null mice.

CYP epoxygenase metabolites of LA (EpOMEs), AA (EETs), EPA (17,18-EpETE), and DHA (19,20-EpDPEs) were found in significant amounts in control hearts (**Table 2**), which were higher in sEH null mice compared to WT. While LPS exposure did not significantly increase levels of 9,10-, 12,13-EpOME, and 8,9-, 11,12-, 14,15-EET, 17,18-EpETE, or 19,20-EpDPE, they were elevated in WT mice following LPS exposure. There were no changes in EpOME, EET, EpETE, or EpDPE levels observed in sEH null mice following LPS exposure. There was a significant increase in corresponding sEH-dependent diol products in WT hearts, which were significantly lower in sEH null hearts.

DiHOMEs Cause an Inflammatory Response and Cytotoxicity in Cardiac Cells

Evidence from literature indicates both beneficial and detrimental effects of EpOMEs and DiHOMEs within the cardiovascular system. As we observed large alterations in the DiHOME metabolites following LPS exposure in WT hearts, we further explored their effects in HL-1 cardiac cells and NRCMs. Treatment with 9,10- or 12,13-DiHOME resulted in a concentration-dependent decline in cell viability, beginning as low as 10 nM (**Figures 5A–C**). Conversely, HL-1 cells treated with different concentrations of 9,10-, or 12,13-EpOME in the presence of a sEH inhibitor (tAUCB) to prevent the conversion to DiHOMEs failed to cause any alteration in cell viability. In order to determine if DiHOMEs triggered a release of major pro-inflammatory cytokines such as TNF α and MCP-1 we assessed the response in HL-1 cells. Consistent, both 9,10- and 12,13-DiHOME caused massive release of TNF α and MCP-1 from HL-1 cells (**Figures 5D,E**). Together, these observations support a concept where accumulation of DiHOMEs may orchestrate an inflammatory cascade.

TABLE 2 | Cardiac oxylipin levels in WT or sEH deficient mice following LPS treatment.

	WT		sEH null	
	Control	LPS	Control	LPS
CYP epoxygenase dependent metabolism				
12,13-EpOME	29.25 ± 3.34	50.35 ± 7.99	56.95 ± 8.89	47.2 ± 7.03
9,10-EpOME	32.55 ± 3.63	59.07 ± 8.94	52.72 ± 8.52	45.2 ± 3.64
14,15-EET	2.97 ± 0.24	3.25 ± 0.5	3.2 ± 0.64	3.31 ± 0.48
11,12-EET	2.44 ± 0.24	2.74 ± 0.18	2.99 ± 0.39	2.96 ± 0.37
8,9-EET	3.25 ± 0.44	4.09 ± 0.5	3.69 ± 0.75	3.6 ± 0.52
5,6-EET	ND	ND	ND	ND
17,18-EpETE	1.19 ± 0.17	0.83 ± 0.067	2.6 ± 0.29	1.98 ± 0.95
19,20-EpDPE	72.67 ± 15.95	81.2 ± 20.89	65.42 ± 23.01	60.75 ± 11.18
sEH dependent metabolism				
12,13-DiHOME	11.58 ± 1.88	43.27 ± 2.9*	4.1 ± 0.77	3.58 ± 0.79#
9,10-DiHOME	6.28 ± 1.15	19.6 ± 0.68*	6.84 ± 1.07	7.33 ± 1.24#
14,15-DHET	0.79 ± 0.15	1.15 ± 0.23	0.24 ± 0.05	0.22 ± 0.038#
11,12-DHET	0.4 ± 0.039	0.76 ± 0.14*	0.26 ± 0.043	0.25 ± 0.026#
8,9-DHET	0.37 ± 0.039	0.96 ± 0.11*	0.28 ± 0.059	0.23 ± 0.04#
5,6-DHET	0.47 ± 0.049	0.62 ± 0.047	0.29 ± 0.087	0.35 ± 0.035#
19,20-DiHDP	3.84 ± 0.95	1.70 ± 0.23	9.15 ± 1.37	1.78 ± 0.28
CYP hydrolase dependent metabolism				
20-HETE	ND	ND	ND	ND
LOX-dependent metabolism				
15-HETE	6.24 ± 1.19	6.97 ± 0.75	5.52 ± 1.15	6.67 ± 0.82
12-HETE	13.89 ± 2.53	172.35 ± 145.55	13.76 ± 2.83	11.01 ± 1.82
11-HETE	2.71 ± 0.47	4.05 ± 0.45	2.45 ± 0.36	2.62 ± 0.2
8-HETE	50.57 ± 6.38	78.67 ± 23.16	47.35 ± 8.47	50.35 ± 7.95
5-HETE	3.39 ± 0.51	3.6 ± 0.5	3.35 ± 1.07	3.69 ± 0.49
9-HODE	38.45 ± 8.85	65.025 ± 7.89	42.8 ± 9.89	41.8 ± 5.2
13-HODE	163.35 ± 39.12	283 ± 30.7	165.17 ± 35.03	171.2 ± 21.9
COX-dependent metabolism				
6-keto-PGF1 α	4.39 ± 1.046	9.89 ± 1.86*	3.86 ± 0.59	4.39 ± 0.3#
PGF2 α	0.96 ± 0.25	1.65 ± 0.35	0.81 ± 0.16	0.63 ± 0.024
PGE2	0.61 ± 0.07	1.21 ± 0.24	0.8 ± 0.34	0.99 ± 0.25
PGD2	0.33 ± 0.05	1.23 ± 0.28*	0.39 ± 0.09	0.47 ± 0.1#

Values (pg/ml) are represented as mean ± SEM, N = 4 independent experiments, *p < 0.05 vs. WT control, #p < 0.05 vs. treatment group vs. WT-LPS.

Epifluorescence microscopy images were used to assess alterations to mitochondrial morphology in HL-1 cells treated with 10 nM 9,10-DiHOME, 9,10-EpOME, or 9,10-EpOME with *t*AUCB for 6 h (Figure 5F). Our data suggest that treatment with 10 nM 9,10-DiHOME and 9,10-EpOME alone resulted in a pronounced degradation of mitochondria, as reflected by the markedly punctuated appearance and reduced size compared to the threadlike appearance in controls (Figure 5F). However, inhibition of sEH with *t*AUCB prevented the effect of 9,10-EpOME suggesting the toxic effect mitochondrial morphology was attributable to the DiHOME metabolite. Similar to HL-1 cells, NRCM treated with 9,10- or 12,13-DiHOME (100 nM) for 24 h resulted in a decline in cell viability, release of TNF α and MCP-1 (Figures 5G–I). Interestingly, when NRCM were 9,10- or 12,13-EpOME (100 nM) alone for 24 h there was less but still a significant loss in cell viability and release of TNF α and MCP-1. Importantly, the co-treatment of 9,10- or 12,13-EpOME (100 nM) with the sEHi (*t*AUCB) attenuated the adverse effects,

again suggesting the DiHOMEs are responsible for the observed responses.

HL-1 Cardiac Cells Exposed to DiHOMEs Revealed Profound Mitochondrial Dysfunction

The most essential component of mitochondrial function is respiration coupled with generation of ATP also referred as oxidative phosphorylation. The ratio between oxygen consumption by mitochondria in basal and ADP-stimulated states indicates respiratory control ratio, which reflects bioenergetic efficiency of mitochondria. We measured mitochondrial respiration in permeabilized HL-1 cells to characterize the effects of DiHOMEs on mitochondrial function. Treatment with 9,10- or 12,13-DiHOME resulted in a strong decrease in mitochondrial RCR, suggesting there was an overall collapse in mitochondrial function, while treatment

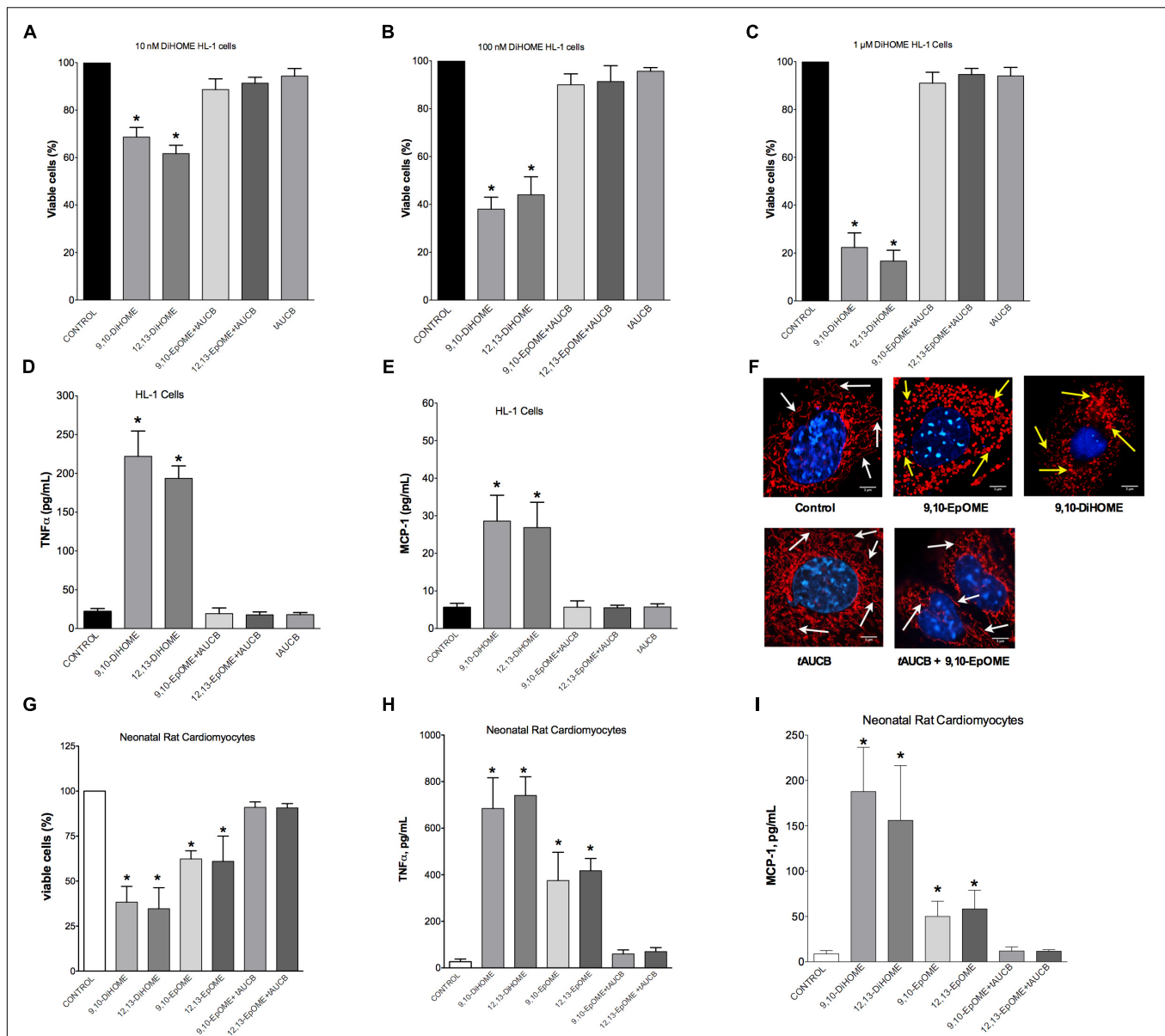
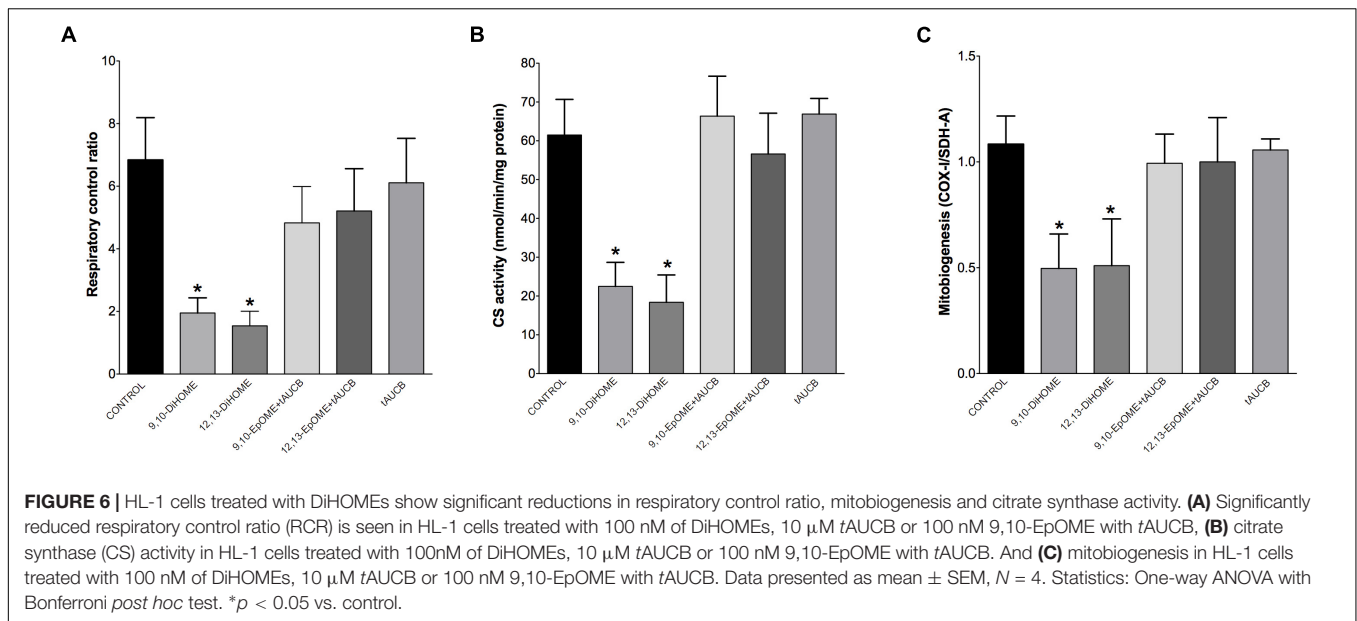


FIGURE 5 | Concentration-response in HL-1 cells and neonatal cardiomyocytes following treatment with DiHOMEs. HL-1 cell viability following 24 h treatment with (A) 10 nM of DiHOMEs, 10 μM tAUCB or 10 nM 9,10-EpOME with tAUCB, (B) 100 nM of DiHOMEs, 10 μM tAUCB or 10 nM 9,10-EpOME with tAUCB, (C) 1 μM of DiHOMEs, 10 μM tAUCB or 10 nM 9,10-EpOME with tAUCB, (D) TNFα levels secreted by HL-1 cells treated with 100 nM of DiHOMEs, 10 μM tAUCB or 10 nM 9,10-EpOME with tAUCB, (E) MCP-1 levels secreted by HL-1 cells treated 100nM of DiHOMEs, 10 μM tAUCB or 10 nM 9,10-EpOME with tAUCB. (F) Representative images of mitochondrial morphology in HL-1 cells following treatment for 6 h with 10 nM 9,10-EpOME, 10 nM 9,10-DiHOME, 10 μM tAUCB or 9,10-EpOME with tAUCB. Mitochondrial morphology, filamentous and tubular shape, of control cells are highlighted by white arrows. In contrast, treated cells exhibit significant punctate and fragmented mitochondrial morphology that are highlighted by yellow arrows. (G) Cell viability, (H) TNFα levels and (I) MCP-1 levels secreted from neonatal rat cardiomyocytes following 24 h treatment with either 100 nM 9,10-DiHOME, 100 nM 12,13-DiHOME, 100 nM 9,10-EpOME, 10 nM 12,13-EpOME, 100 nM 9,10-EpOME with 10 μM tAUCB or 100 nM 12,13-EpOME with 10 μM tAUCB. Data presented as mean ± SEM, $N = 4$. Statistics: One-way ANOVA with Bonferroni *post hoc* test. * $p < 0.05$ vs. control.

with 9,10- or 12,13-EpOME with tAUCB did not impact RCR (Figure 6A). This finding is supported by another observation where exposure to only 9,10- or 12,13-DiHOME resulted in a strong decrease in CS activity in HL-1 cardiac cells (Figure 6B). Generation of new pool of mitochondria appears to be an important physiological strategy developed to withstand stress

conditions. Numerous studies have demonstrated that disruption of mitobiogenesis causes extensive cardiac dysfunction. HL-1 cardiac cells exposed to DiHOMEs displayed a rapid decline in overall rate of mitobiogenesis, which was detected based on the ratio between expression of the mitochondrial proteins COX-1 (mtDNA-encoded) and SDH-A (nDNA-encoded)



measured simultaneously. This observation suggests that DiHOMEs trigger a negative impact toward mitobiogenesis (Figure 6C).

DISCUSSION

Excessive inflammatory responses can cause a number of injurious events at both the systemic and cellular levels, such as inhibiting mitochondrial function, activating the immune system and nonspecific degenerative processes. Cardiovascular systems are highly susceptible to deleterious effects of LPS; however, the specific mechanisms are complex and poorly understood. Although several trials have been attempted to protect the heart against LPS-induced injury, there remain no definitive effective therapies to prevent and/or limit injury (Landesberg et al., 2012; Wang et al., 2016; Zhang et al., 2017; Chen et al., 2018; Wei et al., 2018). Our understanding about the role of inflammatory mediators have in regulating injury is important for developing novel diagnostic and therapeutic approaches in sepsis and endotoxemia. In the present study we investigated the protective effect of sEH deficiency toward mitochondrial and cardiac function following LPS exposure. We have previously demonstrated that sEH deficiency is effective in protecting cardiac cells against LPS-induced injury (Samokhvalov et al., 2015). Furthermore, a recent study showed that sEH ablation attenuates the pulmonary inflammatory response in mice challenged with LPS (Wepler et al., 2016). Here, we used a mouse model of sEH deletion to demonstrate cardiac function is maintained *in vivo* following LPS-induced acute inflammation.

In our model, the acute exposure to LPS caused pronounced cardiac injury highlighted by a robust pro-inflammatory response indicated by elevated serum TNF α and MCP-1 cytokine levels as well as increased NF- κ B DNA binding

activity without any change in cardiac TLR4 or sEH protein expression. In left ventricular tissue, LPS exposure induced oxidative stress and amplified protein degradation as illustrated by elevated 20S proteasome activity, eventually leading to increased activity of the apoptotic enzyme caspase-3 and cell injury. Enhanced release of pro-inflammatory cytokines from the heart causes recruitment of mononuclear cells, which has been shown to assist in the development of cardiovascular disease (Anker and von Haehling, 2004; Zerneck et al., 2008). The therapeutic potential for limiting inflammatory-induced migration of immune cells in myocardium appears to be tremendous. Our findings illustrate that sEH deficiency reduced the serum level of pro-inflammatory response and limited cell injury in response to LPS administration. Together, the data suggest that deletion or inhibition of sEH correlates with lower rates in migration of mononuclear cells thereby limiting inflammatory associated cardiac dysfunction.

Numerous studies demonstrate that LPS is capable of damaging mitochondria by mechanisms such as oxidizing mitochondrial DNA, decreasing ATP production and increasing ROS generation, all of which contribute to cardiac dysfunction (Suliman et al., 2004; Vanasco et al., 2012). Further reports demonstrate these alterations may occur in a tissue specific manner, for example, mitochondrial oxygen consumption during state 3 respiration was reduced in cardiac and skeletal muscle in a rat model of acute inflammation (Rozenberg et al., 2006; Vanasco et al., 2008, 2012). The acute effect of LPS exposure reflect cellular responses to physiological cues that lead to mitochondrial uncoupling, altered respiration and a switch to a more rapidly metabolized substrate for ATP production (e.g., glucose) (Zhang et al., 2014; Frisard et al., 2015). Furthermore, the subsequent increased ROS production may stem from increased mitochondrial proton leak and uncoupling through either UCP3 dependent or

independent mechanisms resulting in decreased mitochondrial efficiency directly leading to cardiovascular collapse (Frisard et al., 2015). The present study demonstrates LPS triggered mitochondrial damage and impaired the catalytic activity of key markers of oxidative phosphorylation resulting in a decline in mitochondrial respiration and ATP content, indicative of impaired mitochondrial function. Considering we did not observe changes in mitochondrial protein levels but decreased function in WT mice compared to sEH null, our data suggest the pool of mitochondria found in sEH null hearts was healthier. As such, the adverse effects in WT mice may be attributed to either direct impact on function and/or impeded mitochondrial quality control mechanisms.

In response to inflammation and cell injury succinate can accumulate in the mitochondria, inhibiting complex I activity and inducing generation of ROS. This results in the lower rates of electron transfer through complex I observed in acute inflammation, which critically restricts ATP synthesis and results in a situation further exacerbating organ damage through a self-sustaining process. Thus, acute inflammation provokes a suppression of cardiac mitochondrial function accompanied by increased accumulation of injury (Galkin et al., 2009; Navarro et al., 2009, 2010). Compounding all factors presented, the synergetic magnitude of these events instigated cardiac collapse. Ultimately, these changes contributed to the pronounced dilation of the myocardium accompanied by drastic decrease in ejection fraction we observed in the WT mice, indicative of a progression to early heart failure. In striking contrast, sEH null animals presented conserved oxidative metabolism suggesting adaptive cardioprotection originating most likely in the mitochondria. These data indicate that deficiency of sEH confers protection against cardiac inflammation and mitochondrial damage upon LPS challenge. Intriguingly, these data are associated with fundamental changes in the LA-derived epoxides.

The anti-inflammatory effects of epoxides have been extensively studied since it was discovered inflammation plays a critical role in cardiovascular diseases. A tight functional connection between inflammation and epoxigenase enzymes has been established (Dennis and Norris, 2015). The anti-inflammatory actions of epoxides appear to be mediated through suppression of NF- κ B activation. Activated NF- κ B is a critical signaling molecule for the induction of numerous inflammatory mediators in all cells types including cardiomyocytes. Previously, we demonstrated that EETs effectively inhibit the activation of inflammatory reactions in cardiac cells in response to LPS (Samokhvalov et al., 2014). An important outcome of this study proposes that protective effects of sEH deficiency can be explained by an increased level of endogenously produced EETs as their metabolic degradation would be strongly suppressed. These findings have provided the framework for the notion sEH is a promising therapeutic target for the treatment of cardiac dysfunction associated with upregulated inflammatory response in the setting of LPS-induced acute inflammation. We and others have shown sEH deficiency and EETs, particularly 11,12-EET, are cardioprotective in models of cardiovascular injury and aging (Batchu et al., 2011; Akhnokh et al., 2016; Jamieson et al., 2017a). Moreover, sEH deficiency in pulmonary LPS-induced toxicity

was associated with improved recovery and increased levels of EETs (Wepler et al., 2016). There is convincing evidence in the literature that EETs suppress NF- κ B-mediated induction and the subsequent pro-inflammatory response through inhibition of IKK complex activity (Node et al., 1999; Deng et al., 2010; Zhao et al., 2012). Interestingly, in this model we saw no change in overall EET levels 24 h following LPS administration in either WT or sEH null mice. However, DHET levels were significantly reduced, suggesting that sEH deficiency lengthens the half-life of the EETs rather than increasing basal levels. The body may also compensate to the genetic ablation by reducing the production of EETs to preserve homeostasis, resulting in overall preserved EET levels.

Importantly, the acute LPS challenge markedly altered the cardiac oxylipin profile in the hearts, which included changes to various different metabolites. While this suggests multiple lipid mediators may be involved in effects we observed following LPS administration, the current study focused on the effect of DiHOMEs. Lipid mediators generated from eicosanoid metabolism have been demonstrated to modulate functional activity of mitochondria. Several models show pathological concentrations of LA uncouple oxidative phosphorylation, induce mitochondrial permeability transition, and activate processes leading to cell death (Schonfeld and Bohnensack, 1997; Moran et al., 2000, 2001; Schonfeld et al., 2000; Konkel and Schunck, 2011). This is supported by studies demonstrating pathological concentrations of 12,13-EpOMes and 12,13-DiHOMes are toxic to cardiac cells (Moran et al., 2000, 2001; Konkel and Schunck, 2011). Conversely, several studies suggest EpOMes may be cardioprotective via maintenance of mitochondrial function (Moghaddam et al., 1997; Nowak et al., 2004; Hou et al., 2012). Although the specific roles of EpOMes in inflammation and cellular homeostasis remain poorly understood, evidence indicates many of the cytotoxic effects attributed to EpOMes are in fact caused by their secondary metabolites DiHOMes. The accumulation of DiHOMes in the heart is associated with impaired cardiac function, including that resulting from LPS-induced endotoxemic shock (Edin et al., 2011; Chaudhary K.R. et al., 2013). Therefore, DiHOMes may be considered the crucial metabolites mediating the toxicity of LA epoxides (Moghaddam et al., 1997; Zeldin, 2001; Zheng et al., 2001; Fleming, 2014). Consistent with previous reports, 24 h after LPS administration the levels of DiHOMes were elevated in left ventricular tissue revealing activation of the CYP P450 epoxigenase-sEH metabolic pathway during LPS-induced toxicity (Schmelzer et al., 2005; Tao et al., 2016). In contrast, deletion of sEH significantly attenuated DiHOME accumulation in left ventricular tissue following LPS administration, increasing the levels of EpOME relative to DiHOME production. Data from our cell studies indicated inhibition of EpOME metabolism with an sEH inhibitor prevented cytotoxic effects suggesting the DiHOME metabolite was causing the adverse response. Taken together, these data indicate sEH deletion serves as a twofold cardioprotective strategy to decrease DiHOME production while simultaneously preserve EET levels, ultimately acting to protect cardiac mitochondria and thus maintain overall cardiac function.

In summary, our results demonstrate that accumulation of DiHOMEs correlates with LPS-induced cardiac toxicity and markedly reduces mitochondrial function and cell survival. However, preventing the metabolism of the EpOMEs in cardiac tissue through sEH deficiency preserves a pool of healthy mitochondria thereby limiting LPS-induced cytotoxicity and ultimately preserving cardiac function.

AUTHOR CONTRIBUTIONS

VS performed and planned the experiments, data analyses and writing of the manuscript. KLJ was involved with echocardiography, data analysis and writing the manuscript. AD and TL were involved in the experiments, data analysis and writing of the manuscript. HK-B performed immunoblot experiments and data analyses. ME, FL, and DZ performed the LC/MS metabolite profile and scientific evaluation. JMS is the

primary investigator. JMS was involved in the planning and experimental design, data analyses and writing of the manuscript.

FUNDING

This work was supported by a grant from the National Sciences and Engineering Research Council of Canada (NSERC RGPIN-2018-05696) (JMS).

ACKNOWLEDGMENTS

The authors would like to thank Donna Beker for her expertise in the echocardiography portion of this study as well as Paul Jurasz and Ayman El-Kadi for their generous gift of antibodies.

REFERENCES

- Akhnoh, M. K., Yang, F. H., Samokhvalov, V., Jamieson, K. L., Cho, W. J., Wagg, C., et al. (2016). Inhibition of soluble epoxide hydrolase limits mitochondrial damage and preserves function following ischemic injury. *Front. Pharmacol.* 7:133. doi: 10.3389/fphar.2016.00133
- Anderson, P. D., Mehta, N. N., Wolfe, M. L., Hinkle, C. C., Pruscino, L., Comiskey, L. L., et al. (2007). Innate immunity modulates adipokines in humans. *J. Clin. Endocrinol. Metab.* 92, 2272–2279. doi: 10.1210/jc.2006-2545
- Anker, S. D., and von Haehling, S. (2004). Inflammatory mediators in chronic heart failure: an overview. *Heart* 90, 464–470. doi: 10.1136/hrt.2002.007005
- Batchu, S. N., Lee, S. B., Qadhi, R. S., Chaudhary, K. R., El-Sikhry, H., Kodala, R., et al. (2011). Cardioprotective effect of a dual acting epoxyeicosatrienoic acid analogue towards ischaemia reperfusion injury. *Br. J. Pharmacol.* 162, 897–907. doi: 10.1111/j.1476-5381.2010.01093.x
- Brealey, D., Brand, M., Hargreaves, I., Heales, S., Land, J., Smolenski, R., et al. (2002). Association between mitochondrial dysfunction and severity and outcome of septic shock. *Lancet* 360, 219–223. doi: 10.1016/S0140-6736(02)09459-X
- Callahan, L. A., and Supinski, G. S. (2005). Downregulation of diaphragm electron transport chain and glycolytic enzyme gene expression in sepsis. *J. Appl. Physiol.* 99, 1120–1126. doi: 10.1152/jappphysiol.01157.2004
- Chagnon, F., Metz, C. N., Bucala, R., and Lesur, O. (2005). Endotoxin-induced myocardial dysfunction: effects of macrophage migration inhibitory factor neutralization. *Circ. Res.* 96, 1095–1102. doi: 10.1161/01.RES.0000168327.22888.4d
- Charalambous, B. M., Stephens, R. C., Feavers, I. M., and Montgomery, H. E. (2007). Role of bacterial endotoxin in chronic heart failure: the gut of the matter. *Shock* 28, 15–23. doi: 10.1097/shk.0b013e318033ebc5
- Chaudhary, K. R., Zordoky, B. N., Edin, M. L., Alsaleh, N., El-Kadi, A. O., Zeldin, D. C., et al. (2013). Differential effects of soluble epoxide hydrolase inhibition and CYP2J2 overexpression on postischemic cardiac function in aged mice. *Prostaglandins Other Lipid Mediat.* 10, 8–17. doi: 10.1016/j.prostaglandins.2012.08.001
- Chaudhary, S., Thukral, A., Kataria, M., Ghosh, S., Mukherjee, S., and Chowdhury, S. (2013). Comment on: besser et al. lessons from the mixed-meal tolerance test: use of 90-minute and fasting C-peptide in pediatric diabetes. *Diabetes care* 2013;36:195–201. *Diabetes Care* 36:e221. doi: 10.2337/dc13-0369
- Chen, J., Wang, B., Lai, J., Braunstein, Z., He, M., Ruan, G., et al. (2018). Trimetazidine attenuates cardiac dysfunction in endotoxemia and sepsis by promoting neutrophil migration. *Front. Immunol.* 9:2015. doi: 10.3389/fimmu.2018.02015
- Darwesh, A. M., Jamieson, K. L., Wang, C., Samokhvalov, V., and Seubert, J. M. (2018). Cardioprotective effects of CYP-derived epoxy metabolites of docosahexaenoic acid involve limiting NLRP3 inflammasome activation. *Can. J. Physiol. Pharmacol.* doi: 10.1139/cjpp-2018-0480 [Epub ahead of print].
- Deng, Y., Theken, K. N., and Lee, C. R. (2010). Cytochrome P450 epoxygenases, soluble epoxide hydrolase, and the regulation of cardiovascular inflammation. *J. Mol. Cell. Cardiol.* 48, 331–341. doi: 10.1016/j.yjmcc.2009.10.022
- Dennis, E. A., and Norris, P. C. (2015). Eicosanoid storm in infection and inflammation. *Nat. Rev. Immunol.* 15, 511–523. doi: 10.1038/nri3859
- Edin, M. L., Wang, Z., Bradbury, J. A., Graves, J. P., Lih, F. B., DeGraff, L. M., et al. (2011). Endothelial expression of human cytochrome P450 epoxygenase CYP2C8 increases susceptibility to ischemia-reperfusion injury in isolated mouse heart. *FASEB J.* 25, 3436–3447. doi: 10.1096/fj.11-188300
- Endo, T., Samokhvalov, V., Darwesh, A. M., Khey, K. M. W., El-Sherbeni, A. A., El-Kadi, A. O. S., et al. (2018). DHA and 19,20-EDP induce lysosomal-proteolytic-dependent cytotoxicity through de novo ceramide production in H9c2 cells with a glycolytic profile. *Cell Death Discov.* 4:88. doi: 10.1038/s41420-018-0090-1
- Fleming, I. (2014). The pharmacology of the cytochrome P450 epoxygenase/soluble epoxide hydrolase axis in the vasculature and cardiovascular disease. *Pharmacol. Rev.* 66, 1106–1140. doi: 10.1124/pr.113.007781
- Frantz, S., Kobzik, L., Kim, Y. D., Fukazawa, R., Medzhitov, R., Lee, R. T., et al. (1999). Toll4 (TLR4) expression in cardiac myocytes in normal and failing myocardium. *J. Clin. Invest.* 104, 271–280. doi: 10.1172/JCI6709
- Frisard, M. I., Wu, Y., McMillan, R. P., Voelker, K. A., Wahlberg, K. A., Anderson, A. S., et al. (2015). Low levels of lipopolysaccharide modulate mitochondrial oxygen consumption in skeletal muscle. *Metabolism* 64, 416–427. doi: 10.1016/j.metabol.2014.11.007
- Galkin, A., Abramov, A. Y., Frakich, N., Duchon, M. R., and Moncada, S. (2009). Lack of oxygen deactivates mitochondrial complex I: implications for ischemic injury? *J. Biol. Chem.* 284, 36055–36061. doi: 10.1074/jbc.M109.054346
- Gedik, N., Heusch, G., and Skyschally, A. (2013). Infarct size reduction by cyclosporine A at reperfusion involves inhibition of the mitochondrial permeability transition pore but does not improve mitochondrial respiration. *Arch. Med. Sci.* 9, 968–975. doi: 10.5114/aoms.2013.38175
- Hou, H. H., Hammock, B. D., Su, K. H., Morisseau, C., Kou, Y. R., Imaoka, S., et al. (2012). N-terminal domain of soluble epoxide hydrolase negatively regulates the VEGF-mediated activation of endothelial nitric oxide synthase. *Cardiovasc. Res.* 93, 120–129. doi: 10.1093/cvr/cvr267
- Jamieson, K. L., Endo, T., Darwesh, A. M., Samokhvalov, V., and Seubert, J. M. (2017a). Cytochrome P450-derived eicosanoids and heart function. *Pharmacol. Ther.* 179, 47–83. doi: 10.1016/j.pharmthera.2017.05.005
- Jamieson, K. L., Samokhvalov, V., Akhnoh, M. K., Lee, K., Cho, W. J., Takawale, A., et al. (2017b). Genetic deletion of soluble epoxide hydrolase provides cardioprotective responses following myocardial infarction in

- aged mice. *Prostaglandins Other Lipid Mediat.* 132, 47–58. doi: 10.1016/j.prostaglandins.2017.01.001
- Konkel, A., and Schunck, W. H. (2011). Role of cytochrome P450 enzymes in the bioactivation of polyunsaturated fatty acids. *Biochim. Biophys. Acta* 1814, 210–222. doi: 10.1016/j.bbapap.2010.09.009
- Kozlov, A. V., Bahrami, S., Calzia, E., Dungal, P., Gille, L., Kuznetsov, A. V., et al. (2011). Mitochondrial dysfunction and biogenesis: do ICU patients die from mitochondrial failure? *Ann. Intensive Care* 1:41. doi: 10.1186/2110-5820-1-41
- Landesberg, G., Gilon, D., Meroz, Y., Georgieva, M., Levin, P. D., Goodman, S., et al. (2012). Diastolic dysfunction and mortality in severe sepsis and septic shock. *Eur. Heart J.* 33, 895–903. doi: 10.1093/eurheartj/ehs351
- Lew, W. Y. (2003). Endotoxin attacks the cardiovascular system: black death at the tollgate. *J. Am. Coll. Cardiol.* 42, 1663–1665. doi: 10.1016/j.jacc.2003.08.006
- Lew, W. Y., Bayna, E., Molle, E. D., Dalton, N. D., Lai, N. C., Bhargava, V., et al. (2013). Recurrent exposure to subclinical lipopolysaccharide increases mortality and induces cardiac fibrosis in mice. *PLoS One* 8:e61057. doi: 10.1371/journal.pone.0061057
- Lynes, M. D., Leiria, L. O., Lundh, M., Bartelt, A., Shamsi, F., Huang, T. L., et al. (2017). The cold-induced lipokine 12,13-diHOME promotes fatty acid transport into brown adipose tissue. *Nat. Med.* 23, 631–637. doi: 10.1038/nm.4297
- Mabalirajan, U., Rehman, R., Ahmad, T., Kumar, S., Singh, S., Leishangthem, G. D., et al. (2013). Linoleic acid metabolite drives severe asthma by causing airway epithelial injury. *Sci. Rep.* 3:1349. doi: 10.1038/srep01349
- Moghaddam, M. F., Grant, D. F., Cheek, J. M., Greene, J. F., Williamson, K. C., and Hammock, B. D. (1997). Bioactivation of leukotoxins to their toxic diols by epoxide hydrolase. *Nat. Med.* 3, 562–566. doi: 10.1038/nm0597562
- Moran, J. H., Mitchell, L. A., Bradbury, J. A., Qu, W., Zeldin, D. C., Schnellmann, R. G., et al. (2000). Analysis of the cytotoxic properties of linoleic acid metabolites produced by renal and hepatic P450s. *Toxicol. Appl. Pharmacol.* 168, 268–279. doi: 10.1006/taap.2000.9053
- Moran, J. H., Nowak, G., and Grant, D. F. (2001). Analysis of the toxic effects of linoleic acid, 12,13-cis-epoxyoctadecenoic acid, and 12,13-dihydroxyoctadecenoic acid in rabbit renal cortical mitochondria. *Toxicol. Appl. Pharmacol.* 172, 150–161. doi: 10.1006/taap.2001.9149
- Navarro, A., Bandez, M. J., Gomez, C., Repetto, M. G., and Boveris, A. (2010). Effects of rotenone and pyridaben on complex I electron transfer and on mitochondrial nitric oxide synthase functional activity. *J. Bioenerg. Biomembr.* 42, 405–412. doi: 10.1007/s10863-010-9309-4
- Navarro, A., Boveris, A., Bandez, M. J., Sanchez-Pino, M. J., Gomez, C., Muntane, G., et al. (2009). Human brain cortex: mitochondrial oxidative damage and adaptive response in Parkinson disease and in dementia with Lewy bodies. *Free Radic. Biol. Med.* 46, 1574–1580. doi: 10.1016/j.freeradbiomed.2009.03.007
- Newman, J. W., Watanabe, T., and Hammock, B. D. (2002). The simultaneous quantification of cytochrome P450 dependent linoleate and arachidonate metabolites in urine by HPLC-MS/MS. *J. Lipid Res.* 43, 1563–1578. doi: 10.1194/jlr.D200018-JLR200
- Node, K., Huo, Y., Ruan, X., Yang, B., Spiecker, M., Ley, K., et al. (1999). Anti-inflammatory properties of cytochrome P450 epoxygenase-derived eicosanoids. *Science* 285, 1276–1279. doi: 10.1126/science.285.5431.1276
- Nowak, G., Grant, D. F., and Moran, J. H. (2004). Linoleic acid epoxide promotes the maintenance of mitochondrial function and active Na⁺ transport following hypoxia. *Toxicol. Lett.* 147, 161–175. doi: 10.1016/j.toxlet.2003.11.002
- Rozenberg, S., Besse, S., Brisson, H., Jozefowicz, E., Kandoussi, A., Mebazaa, A., et al. (2006). Endotoxin-induced myocardial dysfunction in senescent rats. *Crit. Care* 10:R124.
- Samokhvalov, V., Jamieson, K. L., Vriend, J., Quan, S., and Seubert, J. M. (2015). CYP-epoxygenase metabolites of docosahexaenoic acid protect HL-1 cardiac cells against LPS-induced cytotoxicity Through SIRT1. *Cell Death Discov.* 1:15054. doi: 10.1038/cddiscovery.2015.54
- Samokhvalov, V., Ussher, J. R., Fillmore, N., Armstrong, I. K., Keung, W., Moroz, D., et al. (2012). Inhibition of malonyl-CoA decarboxylase reduces the inflammatory response associated with insulin resistance. *Am. J. Physiol. Endocrinol. Metab.* 303, E1459–E1468. doi: 10.1152/ajpendo.00018.2012
- Samokhvalov, V., Vriend, J., Jamieson, K. L., Akhnokh, M. K., Manne, R., Falck, J. R., et al. (2014). PPARgamma signaling is required for mediating EETs protective effects in neonatal cardiomyocytes exposed to LPS. *Front. Pharmacol.* 5:242. doi: 10.3389/fphar.2014.00242
- Schmelzer, K. R., Kubala, L., Newman, J. W., Kim, I. H., Eiserich, J. P., and Hammock, B. D. (2005). Soluble epoxide hydrolase is a therapeutic target for acute inflammation. *Proc. Natl. Acad. Sci. U.S.A.* 102, 9772–9777. doi: 10.1073/pnas.0503279102
- Schonfeld, P., and Bohnensack, R. (1997). Fatty acid-promoted mitochondrial permeability transition by membrane depolarization and binding to the ADP/ATP carrier. *FEBS Lett.* 420, 167–170. doi: 10.1016/S0014-5793(97)01511-1
- Schonfeld, P., Wieckowski, M. R., and Wojtczak, L. (2000). Long-chain fatty acid-promoted swelling of mitochondria: further evidence for the protonophoric effect of fatty acids in the inner mitochondrial membrane. *FEBS Lett.* 471, 108–112. doi: 10.1016/S0014-5793(00)01376-4
- Strand, M. E., Aronsen, J. M., Braathen, B., Sjaastad, I., Kvaloy, H., Tonnessen, T., et al. (2015). Shedding of syndecan-4 promotes immune cell recruitment and mitigates cardiac dysfunction after lipopolysaccharide challenge in mice. *J. Mol. Cell. Cardiol.* 88, 133–144. doi: 10.1016/j.yjmcc.2015.10.003
- Suliman, H. B., Welty-Wolf, K. E., Carraway, M., Tatro, L., and Piantadosi, C. A. (2004). Lipopolysaccharide induces oxidative cardiac mitochondrial damage and biogenesis. *Cardiovasc. Res.* 64, 279–288. doi: 10.1016/j.cardiores.2004.07.005
- Tao, W., Li, P. S., Yang, L. Q., and Ma, Y. B. (2016). Effects of a soluble epoxide hydrolase inhibitor on lipopolysaccharide-induced acute lung injury in mice. *PLoS One* 11:e0160359. doi: 10.1371/journal.pone.0160359
- Vanasco, V., Cimolai, M. C., Evelson, P., and Alvarez, S. (2008). The oxidative stress and the mitochondrial dysfunction caused by endotoxemia are prevented by alpha-lipoic acid. *Free Radic. Res.* 42, 815–823. doi: 10.1080/10715760802438709
- Vanasco, V., Magnani, N. D., Cimolai, M. C., Valdez, L. B., Evelson, P., Boveris, A., et al. (2012). Endotoxemia impairs heart mitochondrial function by decreasing electron transfer, ATP synthesis and ATP content without affecting membrane potential. *J. Bioenerg. Biomembr.* 44, 243–252. doi: 10.1007/s10863-012-9426-3
- Wagner, K. M., McReynolds, C. B., Schmidt, W. K., and Hammock, B. D. (2017). Soluble epoxide hydrolase as a therapeutic target for pain, inflammatory and neurodegenerative diseases. *Pharmacol. Ther.* 180, 62–76. doi: 10.1016/j.pharmthera.2017.06.006
- Wang, H., Bei, Y., Huang, P., Zhou, Q., Shi, J., Sun, Q., et al. (2016). Inhibition of miR-155 protects against LPS-induced cardiac dysfunction and apoptosis in mice. *Mol. Ther. Nucleic Acids* 5:e374. doi: 10.1038/mtna.2016.80
- Wei, W. Y., Ma, Z. G., Zhang, N., Xu, S. C., Yuan, Y. P., Zeng, X. F., et al. (2018). Overexpression of CTRP3 protects against sepsis-induced myocardial dysfunction in mice. *Mol. Cell. Endocrinol.* 476, 27–36. doi: 10.1016/j.mce.2018.04.006
- Wepler, M., Beloiartsev, A., Buswell, M. D., Panigrahy, D., Malhotra, R., Buys, E. S., et al. (2016). Soluble epoxide hydrolase deficiency or inhibition enhances murine hypoxic pulmonary vasoconstriction after lipopolysaccharide challenge. *Am. J. Physiol. Lung Cell. Mol. Physiol.* 311, L1213–L1221. doi: 10.1152/ajplung.00394.2016
- Wisse, B. E., Ogimoto, K., Tang, J., Harris, M. K. Jr., Raines, E. W., and Schwartz, M. W. (2007). Evidence that lipopolysaccharide-induced anorexia depends upon central, rather than peripheral, inflammatory signals. *Endocrinology* 148, 5230–5237. doi: 10.1210/en.2007-0394
- Yue, Y., Wang, Y., Li, D., Song, Z., Jiao, H., and Lin, H. (2015). A central role for the mammalian target of rapamycin in LPS-induced anorexia in mice. *J. Endocrinol.* 224, 37–47. doi: 10.1530/JOE-14-0523
- Zeldin, D. C. (2001). Epoxygenase pathways of arachidonic acid metabolism. *J. Biol. Chem.* 276, 36059–36062. doi: 10.1074/jbc.R100030200
- Zernecke, A., Bernhagen, J., and Weber, C. (2008). Macrophage migration inhibitory factor in cardiovascular disease. *Circulation* 117, 1594–1602. doi: 10.1161/CIRCULATIONAHA.107.729125
- Zhang, S., Hulver, M. W., McMillan, R. P., Cline, M. A., and Gilbert, E. R. (2014). The pivotal role of pyruvate dehydrogenase kinases in metabolic flexibility. *Nutr. Metab.* 11:10. doi: 10.1186/1743-7075-11-10
- Zhang, W. B., Zhang, H. Y., Zhang, Q., Jiao, F. Z., Zhang, H., Wang, L. W., et al. (2017). Glutamine ameliorates lipopolysaccharide-induced cardiac dysfunction

- by regulating the toll-like receptor 4/mitogen-activated protein kinase/nuclear factor- κ B signaling pathway. *Exp. Ther. Med.* 14, 5825–5832. doi: 10.3892/etm.2017.5324
- Zhao, G., Wang, J., Xu, X., Jing, Y., Tu, L., Li, X., et al. (2012). Epoxyeicosatrienoic acids protect rat hearts against tumor necrosis factor- α -induced injury. *J. Lipid Res.* 53, 456–466. doi: 10.1194/jlr.M017319
- Zheng, J., Plopper, C. G., Lakritz, J., Storms, D. H., and Hammock, B. D. (2001). Leukotoxin-diol: a putative toxic mediator involved in acute respiratory distress syndrome. *Am. J. Respir. Cell Mol. Biol.* 25, 434–438. doi: 10.1165/ajrcmb.25.4.4104
- Conflict of Interest Statement:** The authors declare that the research was conducted in the absence of any commercial or financial relationships that could be construed as a potential conflict of interest.

Copyright © 2019 Samokhvalov, Jamieson, Darwesh, Keshavarz-Bahaghighat, Lee, Edin, Lih, Zeldin and Seubert. This is an open-access article distributed under the terms of the Creative Commons Attribution License (CC BY). The use, distribution or reproduction in other forums is permitted, provided the original author(s) and the copyright owner(s) are credited and that the original publication in this journal is cited, in accordance with accepted academic practice. No use, distribution or reproduction is permitted which does not comply with these terms.



Pharmacological Blockade of Soluble Epoxide Hydrolase Attenuates the Progression of Congestive Heart Failure Combined With Chronic Kidney Disease: Insights From Studies With Fawn-Hooded Hypertensive Rats

Šárka Vacková^{1,2}, Libor Kopkan¹, Soňa Kikerlová¹, Zuzana Husková¹, Janusz Sadowski³, Elzbieta Kompanowska-Jezierska³, Bruce D. Hammock⁴, John D. Imig⁵, Miloš Táborský⁶, Vojtěch Melenovský⁷ and Luděk Červenka^{1,8*}

OPEN ACCESS

Edited by:

Lei Xi,
Virginia Commonwealth University,
United States

Reviewed by:

Mohammed A. Nayeem,
West Virginia University, United States
Ningjun Li,
Virginia Commonwealth University,
United States

*Correspondence:

Luděk Červenka
luce@ikem.cz;
luce@medicon.cz

Specialty section:

This article was submitted to
Translational Pharmacology,
a section of the journal
Frontiers in Pharmacology

Received: 02 October 2018

Accepted: 08 January 2019

Published: 23 January 2019

Citation:

Vacková Š, Kopkan L, Kikerlová S,
Husková Z, Sadowski J,
Kompanowska-Jezierska E,
Hammock BD, Imig JD, Táborský M,
Melenovský V and Červenka L (2019)
Pharmacological Blockade of Soluble
Epoxide Hydrolase Attenuates
the Progression of Congestive Heart
Failure Combined With Chronic
Kidney Disease: Insights From
Studies With Fawn-Hooded
Hypertensive Rats.
Front. Pharmacol. 10:18.
doi: 10.3389/fphar.2019.00018

¹ Center for Experimental Medicine, Institute for Clinical and Experimental Medicine, Prague, Czechia, ² Department of Physiology, Faculty of Science, Charles University, Prague, Czechia, ³ Department of Renal and Body Fluid Physiology, Mossakowski Medical Research Centre, Polish Academy of Sciences, Warsaw, Poland, ⁴ Department of Entomology, UCD Cancer Center, University of California, Davis, Davis, CA, United States, ⁵ Department of Pharmacology and Toxicology, Medical College of Wisconsin, Milwaukee, WI, United States, ⁶ Department of Internal Medicine I, Cardiology, University Hospital Olomouc, Palacký University, Olomouc, Czechia, ⁷ Department of Cardiology, Institute for Clinical and Experimental Medicine, Prague, Czechia, ⁸ Department of Pathophysiology, Second Faculty of Medicine, Charles University, Prague, Czechia

An association between congestive heart failure (CHF) and chronic kidney disease (CKD) results in extremely poor patient survival rates. Previous studies have shown that increasing kidney epoxyeicosatrienoic acids (EETs) by blocking soluble epoxide hydrolase (sEH), an enzyme responsible for EETs degradation, improves the survival rate in CHF induced by aorto-caval fistula (ACF) and attenuates CKD progression. This prompted us to examine if sEH inhibitor treatment would improve the outcome if both experimental conditions are combined. Fawn-hooded hypertensive (FHH) rats, a genetic model showing early CKD development was employed, and CHF was induced by ACF. Treatment with an sEH inhibitor was initiated 4 weeks after ACF creation, in FHH and in fawn-hooded low-pressure (FHL) rats, a control strain without renal damage. The follow-up period was 20 weeks. We found that ACF FHH rats exhibited substantially lower survival rates (all the animals died by week 14) as compared with the 64% survival rate observed in ACF FHL rats. The former group showed pronounced albuminuria (almost 30-fold higher than in FHL) and reduced intrarenal EET concentrations. The sEH inhibitor treatment improved survival rate and distinctly reduced increases in albuminuria in ACF FHH and in ACF FHL rats, however, all the beneficial actions were more pronounced in the hypertensive strain. These data indicate that pharmacological blockade of sEH could be a novel therapeutic approach for the treatment of CHF, particularly under conditions when it is associated with CKD.

Keywords: congestive heart failure, chronic kidney disease, soluble epoxide hydrolase inhibitor, hypertension, renin-angiotensin-aldosterone system

INTRODUCTION

Congestive heart failure (CHF) presents a serious medical problem affecting about 4% of the adult population (Ziaieian and Fonarow, 2016; Benjamin et al., 2017). The incidence of chronic kidney disease (CKD) is also increasing, reaching a level of 8–16% worldwide (Jha et al., 2013; U.S. Renal Data System, 2015) which makes it a growing public health problem. It will be noticed that CHF and CKD can have deleterious effects on each other, through the activation of vicious cycles resulting ultimately in extremely poor outcomes in patients with CHF and CKD associated (Braam et al., 2014; Schefold et al., 2016; Mullens et al., 2017; Arrigo et al., 2018; House, 2018). In spite of an array of therapeutic approaches applied, the survival prognosis of patients with CHF who exhibit kidney disease remains bleak. Therefore, there is an obvious need for focused experimental studies that would examine the value of novel therapeutic approaches.

Within the research of the pathophysiological background of hypertension, CHF, and CKD, considerable attention has been focused on the role of epoxyeicosatrienoic acids (EETs), cytochrome P-450 (CYP)-dependent metabolites of arachidonic acid (AA). Indeed, increased EETs levels was reported to have important antihypertensive and organ-protective actions (Elmarakby, 2012; Kujal et al., 2014; Fan and Roman, 2017; Imig, 2018). However, direct therapeutic potential of EETs is limited because they are rapidly metabolized to biologically inactive dihydroxyeicosatrienoic acids (DHETEs) by soluble epoxide hydrolase (sEH). On the other hand, blocking sEH and increasing tissue EETs bioavailability produced antihypertensive and cardio- and renoprotective effects (Imig, 2018). Moreover, in the spontaneously hypertensive heart failure rat, an inbred, genetically homogenous model that mirrors human hypertension-associated heart failure (McCune et al., 1990), an alteration of the gene encoding sEH (*Ephx2*) facilitated CHF progression and was identified as a heart failure susceptibility gene (Monti et al., 2008).

Collectively, these findings suggest that pharmacological blockade of sEH could present a new approach for CHF treatment, particularly when CHF is combined with CKD. However, no evidence is so far available to indicate that chronic sEH inhibition results in a prolongation of life in individuals with advanced CHF associated with evident kidney disease.

In order to study the pathophysiological mechanism(s) of CHF and possible novel therapeutic measures, rats with aorto-caval fistula (ACF) in which CHF is induced by volume overload was introduced 40 years ago (Hatt et al., 1980). This model has many features similar to untreated human CHF (Brower et al., 1996; Abassi et al., 2011; Melenovsky et al., 2012, 2018; Cohen-Segev et al., 2014; Červenka et al., 2015) and is now recommended by American Heart Association for testing therapeutic strategies for CHF (Houser et al., 2012). In addition, fawn-hooded hypertensive rats (FHH) represent a unique genetic model of spontaneous hypertension characterized by early development of kidney disease (Prooovost, 1994; Doleželová et al., 2016). Thus, FHH seems to be an optimal experimental model to study the course of combined CHF and CKD.

Making use of suitable experimental models, we have undertaken to evaluate the effects of sEH inhibitor treatment on morbidity and mortality in male FHH with ACF-induced CHF. To gain a more detailed insight in the possible mechanism(s) underlying the expected beneficial action of chronic sEH inhibition, we determined concentrations of CYP-derived AA metabolites. Given the established role of the renin-angiotensin system (RAS) promoting the progression of CHF (Braunwald, 2015; Ziaieian and Fonarow, 2016; Packer and McMurray, 2017 CEPP), urinary angiotensinogen excretion and concentrations of angiotensin II (ANG II) were also determined. All these indices were compared between sham-operated FHH and either untreated or treated ACF FHH on one side and their sham-operated and either untreated or treated ACF normotensive counterparts [fawn-hooded low-pressure (FHL) rats] on the other side, the latter strain reportedly resistant to renal damage (Prooovost, 1994; Doleželová et al., 2016). Finally, to further elucidate possible mechanism(s) underlying the beneficial effects of the treatment with sEH inhibitor on the course of ACF-induced CHF, we assessed the cardiac structure and function, using echocardiography and invasive pressure-volume analyses of the left ventricle (LV). This was done after 2-weeks of treatment, because at this stage (i.e., 6 weeks after induction of ACF) untreated ACF FHH still exhibited 100% survival rate. On the other hand, this was just 1 week before the rats began to die and it was particularly interesting to find out if the treatment regime applied at this stage would beneficially influence cardiac function.

MATERIALS AND METHODS

General Methodological Procedures

Ethical Approval and Animals

The studies followed the guidelines and practices established by the Animal Care and Use Committee of the Institute for Clinical and Experimental Medicine, which accord with the national law and with American Physiological Society guiding principles for the care and use of vertebrate animals in research and training, and were approved by the Animal Care and Use Committee of the Institute for Clinical and Experimental Medicine and, consequently, by the Ministry of Health of the Czechia (project decision 17124/2016-OZV-30.0.8.3.16/2).

Male FHH and FHL rats, at the initial age of 12 weeks, derived from several litters, were randomly assigned to experimental groups. In order to obtain reliable data regarding the effects of the treatment regimen on the survival rate, high initial *n*-values were employed (not so for sham-operated animals) to enable valid comparison of the long-term survival rate.

CHF Model, Pharmacological Therapeutic Regimen and General Methodological Procedures

Rats were anesthetized (tiletamine + zolazepam, Virbac SA, Carros Cedex, France, 8 mg/kg; and xylazine, Spofa, Czechia, 4 mg/kg intramuscularly) and CHF was induced by volume overload caused by ACF created using needle technique as employed and validated by many investigators including our

own group (Oliver-Dussault et al., 2010; Abassi et al., 2011; Melenovsky et al., 2012, 2018; Cohen-Segev et al., 2014; Brower et al., 2015; Červenka et al., 2015, 2016; Kala et al., 2018). Briefly, after exposure of the abdominal aorta and inferior vena cava between the renal arteries and iliac bifurcation, the aorta was temporarily occluded at this segment for about 40 s. An 18-gauge needle (diameter 1.2 mm) was inserted into the abdominal aorta and advanced across its wall into the inferior vena cava to create ACF. Thereafter the needle was withdrawn and the puncture site was sealed with cyanoacrylate tissue glue. Successful creation of ACF was confirmed by inspection of pulsatile flow of oxygenated blood from the abdominal aorta into the vena cava. Sham-operated rats underwent an identical procedure but without creating ACF. To inhibit sEH, *cis*-4-[4-(3-adamantan-1-yl-ureido) cyclohexyloxy]benzoic acid (*c*-AUCB) was used, which was prepared freshly and given in drinking water at 3 mg/L. The appropriate amount of *c*-AUCB was dissolved under gentle warming in polyethylene glycol and added with rapid stirring to warm drinking water to obtain 0.1% aqueous solution of polyethylene glycol. The dose of *c*-AUCB was selected based on our recent studies where it elicited substantial increases in tissue concentration of EETs without altering RAS activity (Sporková et al., 2014; Červenka et al., 2015; Kala et al., 2018).

Rat total angiotensinogen concentrations were measured in urine samples by a solid phase sandwich Enzyme-linked Immunosorbent Assay, using the commercially available ELISA kit (JP27414, IBL Int., Hamburg, Germany) as described in our recent study (Čertíková Chábová et al., 2018).

The samples for measurement of plasma and kidney ANG II concentrations were obtained from conscious decapitated rats because it is established that they are higher than those measured under anesthesia (Husková et al., 2006a,b). ANG II concentrations were assessed by radioimmunoassay based on the original procedure developed by Fox et al. (1992) and further modified and validated in our laboratory (Husková et al., 2016). This method is described in detail in our recent publication (Čertíková Chábová et al., 2018).

The levels of arachidonic acid metabolites: EETs (specifically: 5,6-EET, 8,9-EET, 11,12-EET, and 14,15-EET) and DHETEs (the biologically active and inactive, respectively, products of CYP epoxygenase pathway) were measured in the kidney cortex and the LV myocardium. The EETs/DHETEs ratio was calculated from total concentrations of EETs and of DHETEs. In the same cortex samples the levels of hydroxyeicosatetraenoic acids (HETEs), the products of CYP ω -hydroxylase pathway were determined, specifically 5-HETE, 8-HETE, 11-HETE, 12-HETE, 15-HETE, 19-HETE, and 20-HETE, which were separately determined and pooled for presentation: these metabolites are biologically the most active products of the CYP epoxygenase and hydroxylase pathways (Jamieson et al., 2017; Imig, 2018). For these analyses, 20–40 mg of tissue was used. Homogenized tissue samples were subjected to alkaline hydrolysis and solid-phase extraction was performed as described by Rivera et al. (2004). Thereafter the samples were analyzed using high performance liquid chromatography (using Agilent 1200SL with tandem mass spectroscopy (MS) and Agilent 6460 for quantification) as described in detail previously

(Alánová et al., 2015; Jíchová et al., 2016; Čertíková Chábová et al., 2018).

Detailed Experimental Design

Series 1: Comparison of the Survival Rate, Albuminuria and Urinary Angiotensinogen Excretion Between ACF FHH and ACF FHL Rats and Effects of the Treatment With sEH Inhibitor

Animals underwent either sham-operation or ACF creation as described above (at the week labeled -4) and were left without treatment for 4 weeks. Previous studies have shown that after this time CHF features are fully developed but the animals are still in the compensation phase (Oliver-Dussault et al., 2010; Melenovsky et al., 2012, 2018; Červenka et al., 2015, 2016; Kala et al., 2018). At this time point (week 0) the rats were divided into the following experimental groups:

1. Sham-operated FHL + placebo (initial $n = 10$).
2. ACF FHL + placebo (initial $n = 26$).
3. ACF FHL + sEH inhibitor (initial $n = 26$).
4. Sham-operated FHH + placebo (initial $n = 10$).
5. ACF FHH + placebo (initial $n = 29$).
6. ACF FHH + sEH inhibitor (initial $n = 27$).

The follow-up period was 20 weeks (until week +20). In the weeks labeled -5 (i.e., 1 week before ACF creation), +4, +6, +8, +10, +20 after appropriate habituation training the animals were placed in individual metabolic cages and their 24-h urine was collected for determination of albuminuria and urinary angiotensinogen excretion.

Series 2: Effects of 10-Week Treatment With sEH Inhibitor on ANG II, EETs, DHETEs, and HETEs Concentrations and on Organ Weights

Animals were prepared as described in series 1 and in the week 0 the pharmacological treatment was initiated for a period of 10 weeks in the same experimental groups as described in series 1. At the end of experiment (in the week +10) the rats were killed by decapitation and plasma ANG II, kidney, and heart LV concentrations of ANG II, EETs, DHETEs, and HETEs were measured as described above ($n = 10$ in each experimental group). The aim of this series was to evaluate the degree of RAS activation and the activity of CYP-dependent epoxygenase and hydroxylase pathways and the effects of sEH inhibitor treatment.

Series 3: Effects of 2-Week Treatment With sEH Inhibitor on Basal Cardiac Function Parameters Assessed by Echocardiography and by Pressure-Volume Analysis

Animals were prepared as described in series 1 and in the week 0 the pharmacological treatment was applied for 2 weeks. At this time point (week +2) experiments were performed in the following groups:

1. Sham-operated FHL + placebo (water).
2. Sham-operated FHL + sEH inhibitor.
3. ACF FHL + placebo.

4. ACF FHL + sEH inhibitor.
5. Sham-operated FHH + placebo.
6. Sham-operated FHH + sEH inhibitor.
7. ACF FHH + placebo.
8. ACF FHH + sEH inhibitor.

($n = 6$ in each group). At the end of the experimental protocol, animals were anesthetized by intraperitoneal (i.p.) ketamine/midazolam combination (50 mg and 5 mg/kg of body weight, respectively) and echocardiography was performed as described in our earlier studies (Benes et al., 2011; Červenka et al., 2015). Subsequently, the rats were intubated with an appropriate cannula, relaxed with pancuronium (Pavulon, 0.16 mg/kg) and artificially ventilated (rodent ventilator Ugo Basile, Italy, $\text{FiO}_2 = 21\%$). LV function was invasively assessed using a 2F Pressure-Volume (P-V) micromanometry catheter (Millar Instruments) introduced into the LV cavity via the right carotid artery after previous vagal blockade (atropine 0.10 mg/kg), as described previously (Benes et al., 2011; Červenka et al., 2015). The volume signal was calibrated by determining end-diastolic and end-systolic volume by echocardiography, shortly before invasive recordings. The data were acquired using an 8-channel Power Lab recorder and were analyzed by Labchart Pro software (ADInstruments, Australia). The aim of this series was to evaluate the degree of the impairment of cardiac function at the stage when untreated ACF FHH began to die, and to examine the effects of treatment on cardiac function.

Statistical Analysis

Statistical analysis of the data was performed using Graph-Pad Prism software (Graph Pad Software, San Diego, CA, United States). Comparison of survival curves was performed by log-rank (Mantel-Cox) test followed by Gehan-Breslow-Wilcoxon test. Statistical comparison of other results was made by Student's t -test, Wilcoxon's signed-rank test for unpaired data or one-way ANOVA when appropriate. The values are expressed as mean \pm SEM. P -values below 0.05 were considered statistically significant.

RESULTS

Series 1: Comparison of the Survival Rate, Albuminuria and Urinary Angiotensinogen Excretion in ACF FHH and ACF FHL Rats and Effects of the Treatment With sEH Inhibitor

Figures 1, 2 present the data on survival rate, albuminuria and urinary angiotensinogen excretion in untreated experimental animals.

All sham-operated FHH and FHL rats survived until the end of the experiment (Figure 1). ACF FHH rats began to die at week 2 (i.e., 6 weeks after ACF creation) and all the animals died by week 14. In contrast, untreated ACF FHL rats showed higher survival rate throughout the study and the final rate at week 20 (i.e., 24 weeks after creation of ACF) was 64%.

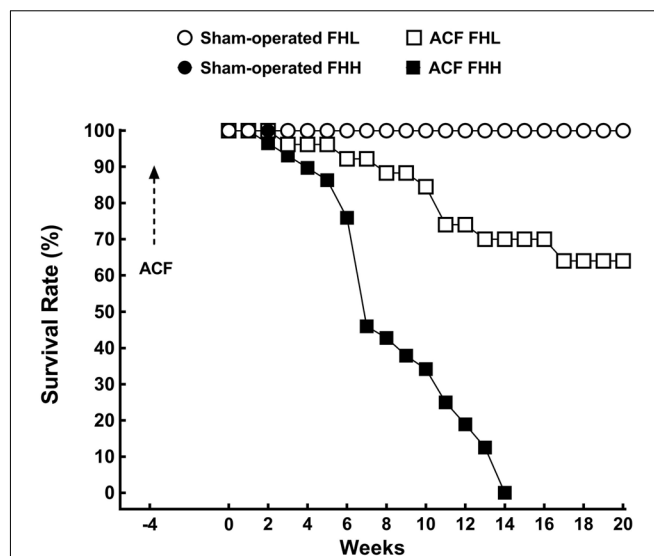
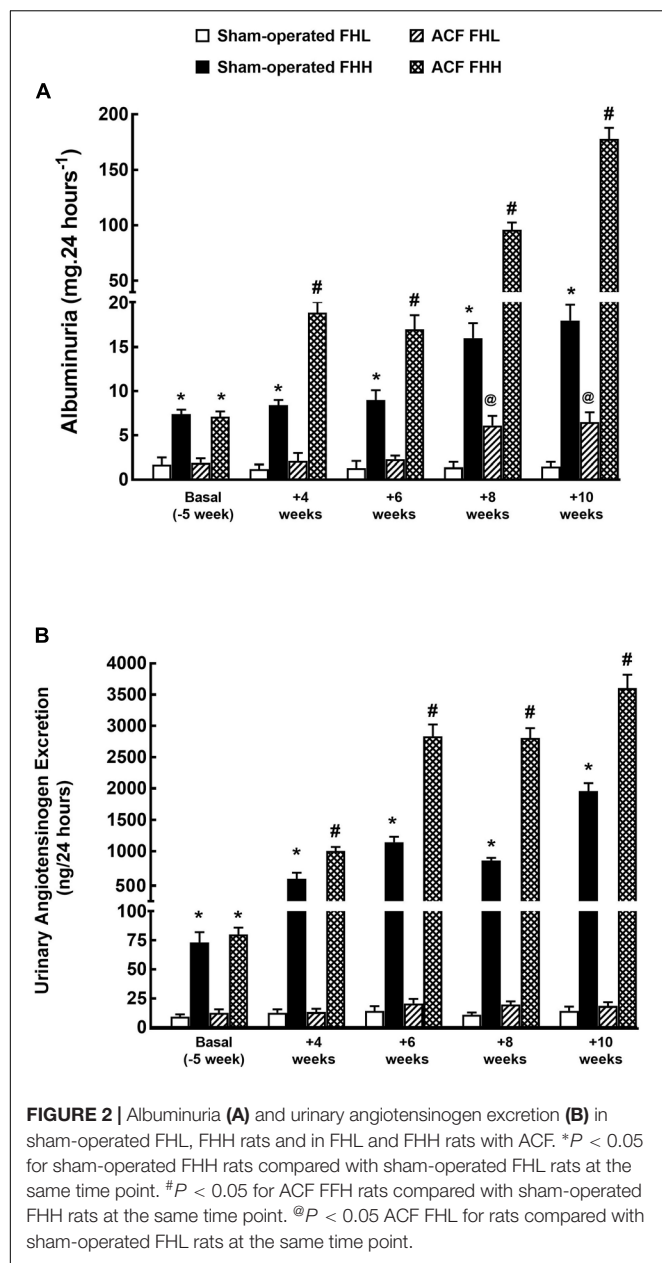


FIGURE 1 | Survival rates in sham-operated fawn-hooded low-pressure (FHL), sham-operated hypertensive (FHH) rats and in untreated FHL, and FHH rats with aorto-caval fistula (ACF). The survival profiles (straight line) for sham-operated FHL and FHH were superimposable and are depicted by one symbol only (blank circles). The survival rate of ACF FHL was significantly lower than in sham-operated FHL rats and in ACF FHH it was the lowest of all experimental groups (analyzed by log-rank Mantel-Cox test followed by Gehan-Breslow-Wilcoxon test).

Figure 2A shows that at the start the sham-operated FHH rats showed albuminuria that was about three-fold higher than in sham-operated FHL rats. In FHL rats it remained stable throughout the study whereas it progressively increased in sham-operated FHH: in the end it was 12-fold higher than in sham-operated FHL. Albuminuria was gradually but only slightly increasing during the study in ACF FHL rats but was still significantly lower than in sham-operated FHH rats. By contrast, in ACF FHH rats the albuminuria exhibited a progressive increase which was much steeper than in sham-operated FHH rats: at week 10 (i.e., 14 weeks after creation of ACF) it was 10-fold higher, despite the fact that the animals with the most pronounced albuminuria died early and have not been included in the final calculation.

As shown in Figure 2B, at the start (i.e., before either sham-operation or creation of ACF) the urinary angiotensinogen excretion was about seven-fold higher in sham-operated FHH rats than in the corresponding FHL group. Thereafter angiotensinogen showed a marked progressive increase throughout the experiment and at the end it was already 140-fold higher. Untreated ACF FHL rats displayed significant increases in the urinary angiotensinogen excretion, unlike the stable levels observed in the sham-operated FHL group. In untreated ACF FHH rats urinary angiotensinogen excretion dramatically increased, significantly more than in the corresponding sham-operated group: at the end it was about 90-fold higher than in untreated ACF FHL rats.

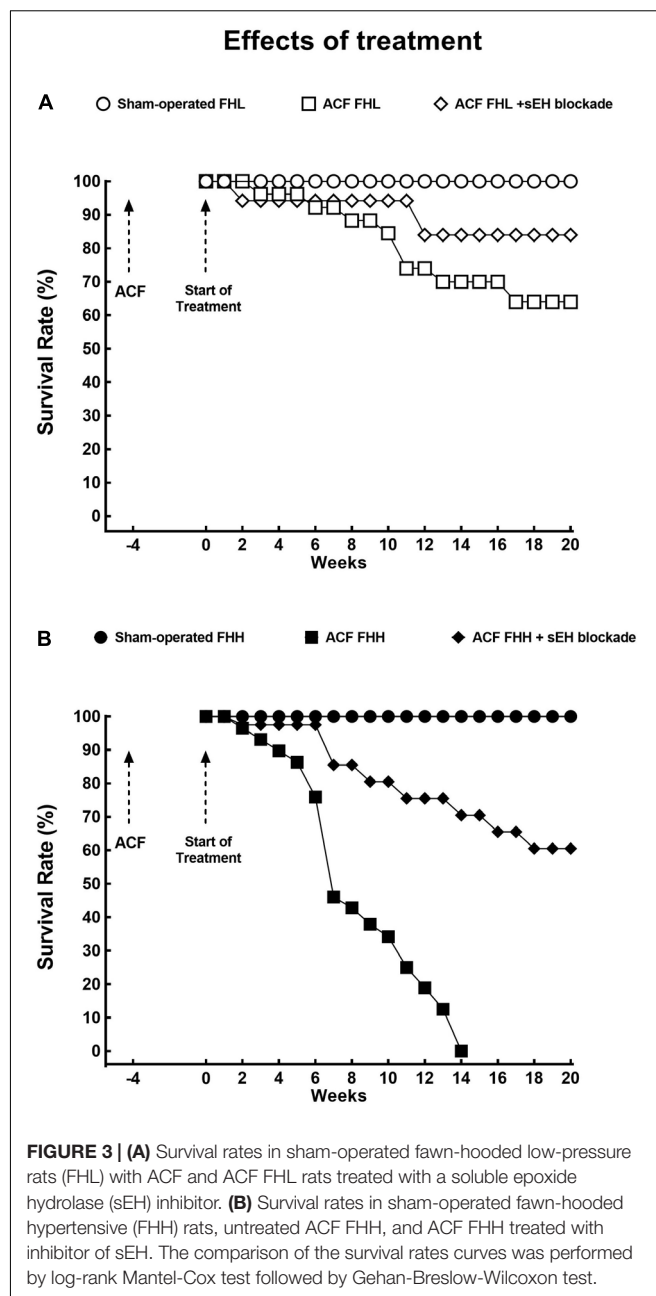
As shown in Figure 3, sEH inhibitor treatment improved the survival rate in ACF FHL rats as well as in ACF FHH rats,



but the improvement was much more pronounced in the latter group: in ACF FHL the final (week 20) survival rate was 61% whereas untreated ACF FHH rats did not survive beyond week 14 (Figure 3B).

Figure 4 presents the data on the effects of sEH inhibition on the development of albuminuria in ACF animals: evidently, the long-term treatment eliminated increases in albuminuria after ACF creation in FHL rats. In the FHH group the therapeutic effect was somewhat less pronounced but at the end of the study albuminuria was not different from that observed in sham-operated animals.

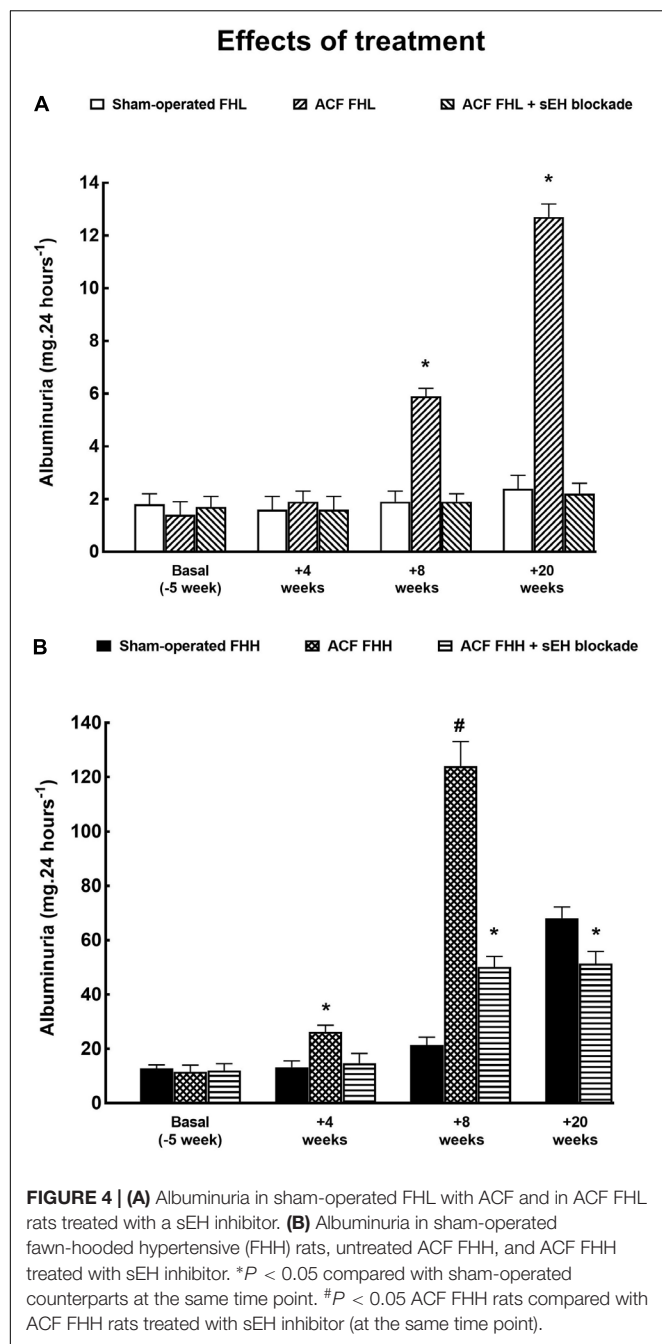
As shown in Figure 5, urinary angiotensinogen excretion increased progressively and significantly during the study in ACF FHH but not in ACF FHL rats. The treatment with sEH inhibitor



did not alter the course of urinary angiotensinogen excretion, similarly in ACF FHL and in ACF FHH rats.

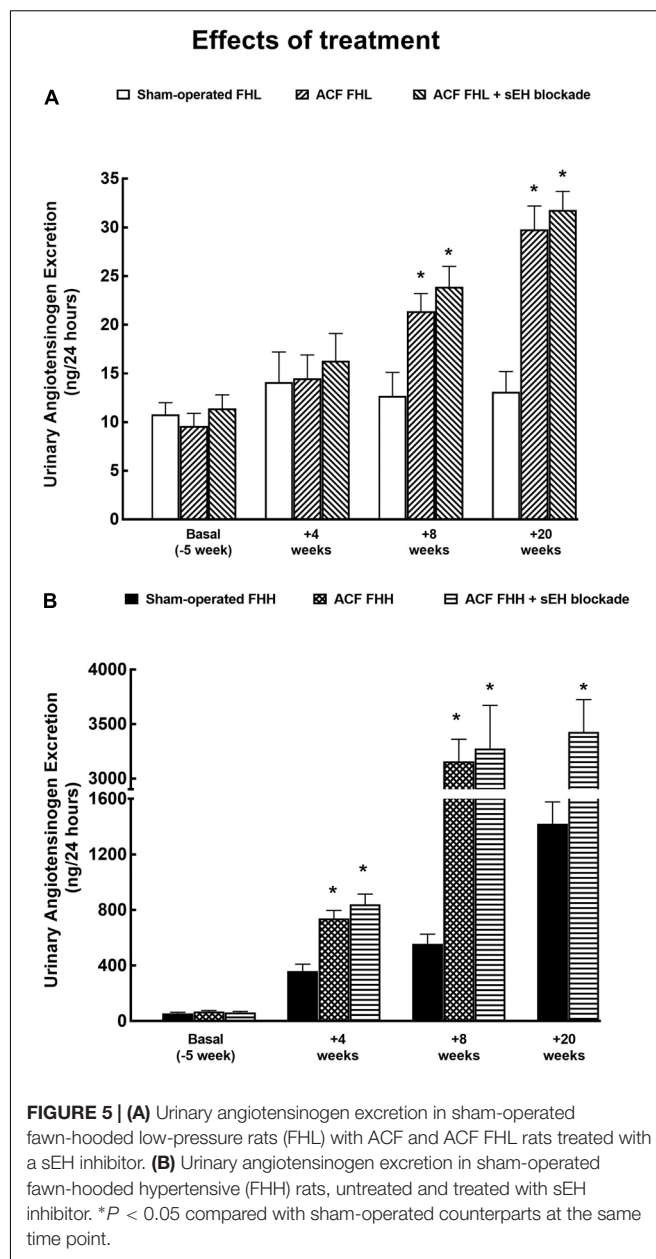
Series 2: Effects of 10-Week Treatment With sEH Inhibitor on ANG II, EETs, DHETEs and HETEs Concentrations and on Organ Weights

As shown in Figure 6, there were no significant differences in plasma, kidney, and LV concentrations of ANG II between sham-operated FHL and sham-operated FHH rats. The levels of plasma and kidney ANG II levels were significantly higher in untreated ACF FHL and ACF FHH rats than in their



sham-operated counterparts. In contrast, LV concentrations of ANG II were not significantly higher in untreated ACF FHL and ACF FHH rats than in their sham-operated counterparts (**Figure 6C**). The treatment with sEH inhibitor did not modify plasma, kidney, and LV concentrations of ANG II, similarly in ACF FHL and ACF FHH rats.

Figure 7A shows that there were no significant differences in renal tissue concentrations of HETEs (ω -hydroxylase AA metabolites) between the experimental FHL and FHH groups. Similarly, there were no significant differences in the renal tissue availability of biologically active epoxygenase metabolites



of AA (expressed as the ratio of EETs to DHETEs) (**Figure 7B**). Untreated ACF FHL as well as ACF FHH rats displayed significantly lower ratios as compared with the sham-operated animals. The sEH inhibitor treatment markedly increased EETs/DHETEs ratios in ACF FHL rats and in ACF FHH rats to values that were even significantly higher than observed in sham-operated FHL and FHH rats.

Figure 7C demonstrates that LV tissue concentrations of HETEs did not significantly differ between the experimental groups of FHL and FHH rats. In addition, it shows that LV concentrations of HETEs were about 40% lower than observed in the kidney.

Figure 7D shows that untreated ACF FHL and ACF FHH did not exhibit lower EETs/DHETEs ratios in the LV as compared

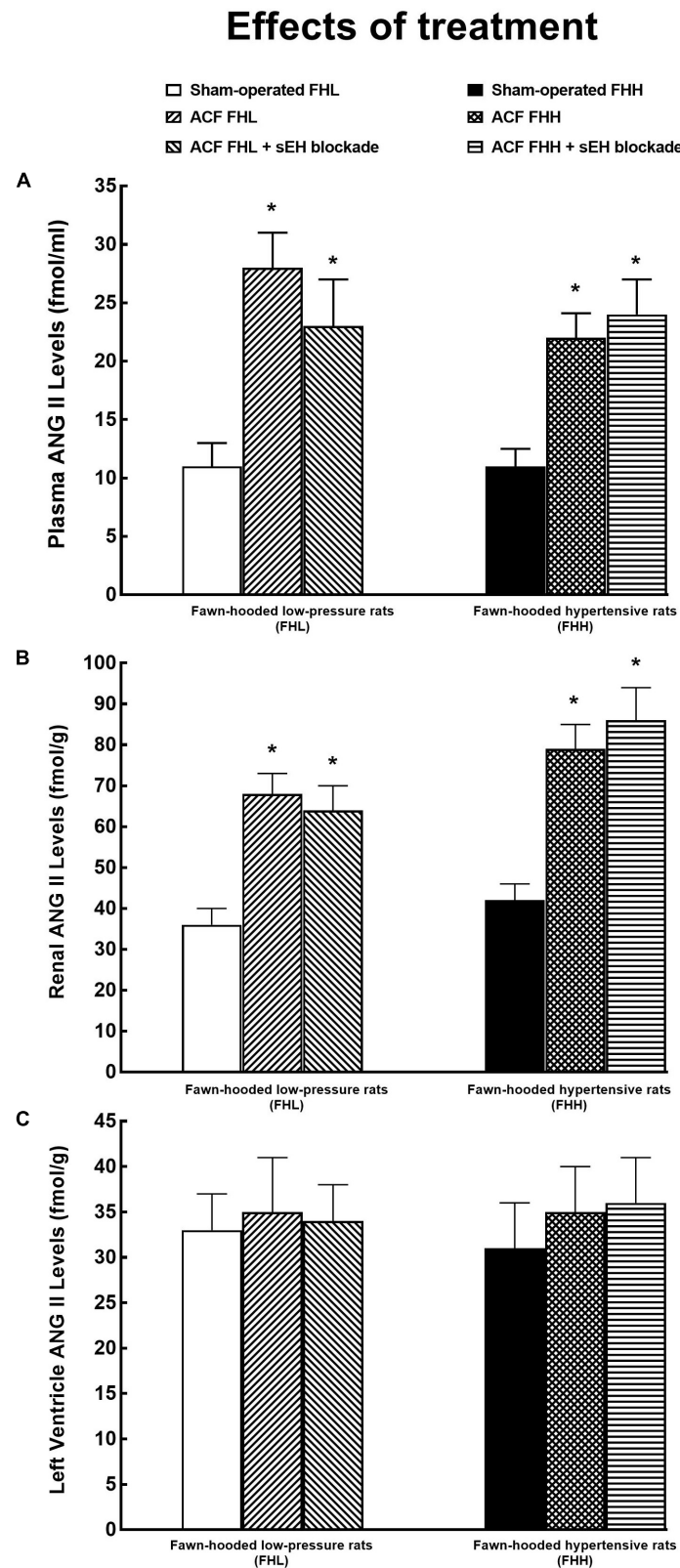
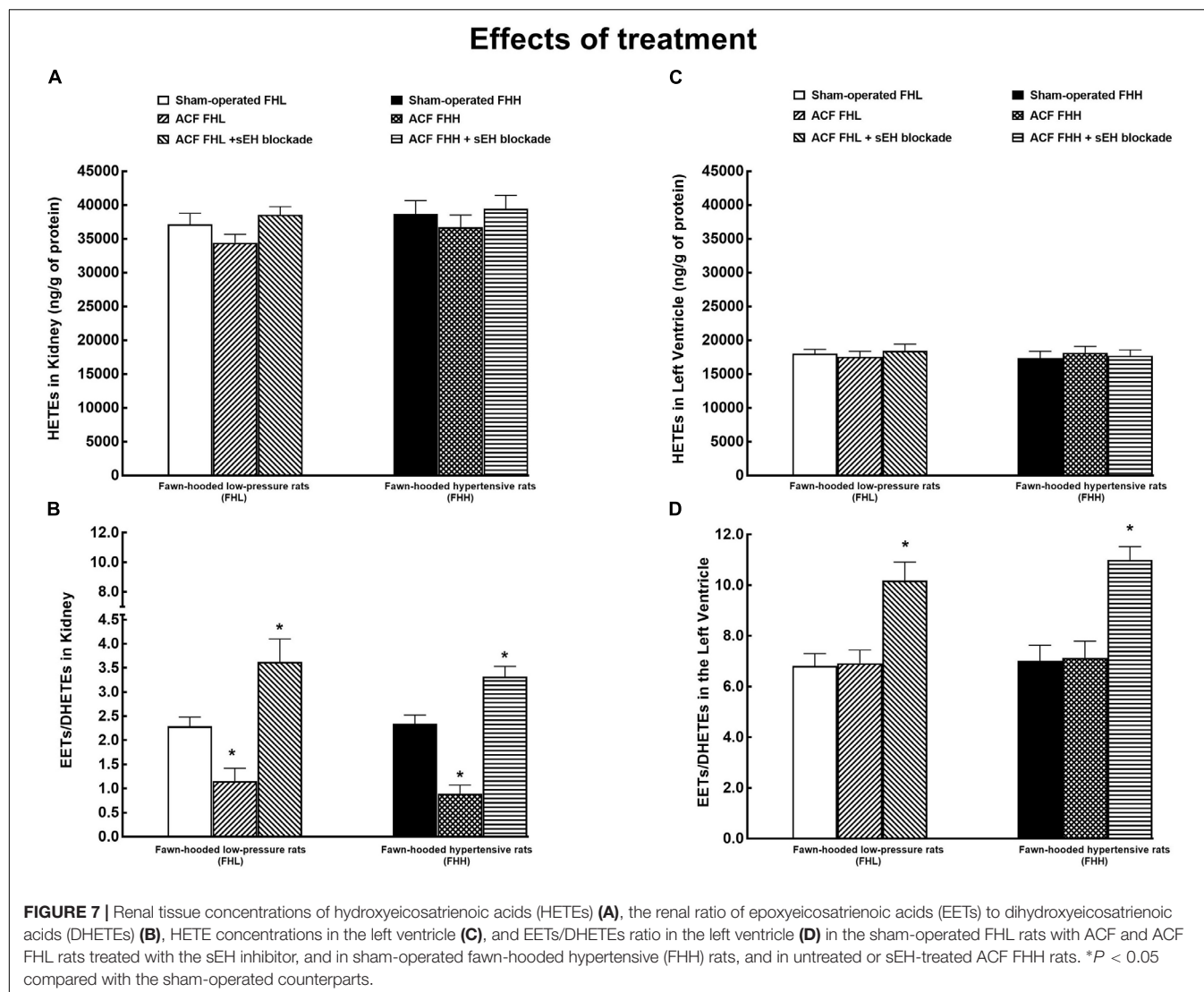


FIGURE 6 | Plasma (A), kidney (B), and left ventricle (C) angiotensin II (ANG II) levels in sham-operated fawn-hooded low-pressure rats (FHL) with ACF and ACF FHL rats treated with a sEH inhibitor, and in sham-operated fawn-hooded hypertensive (FHH) rats, untreated and treated with sEH inhibitor. * $P < 0.05$ compared with the sham-operated counterparts at the same time point.



with their sham-operated counterparts. However, the treatment with sEH inhibitor markedly increased EETs/DHETEs ratio in ACF FHL rats and in ACF FHH rats as compared with the sham-operated FHL and FHH rats. (more important I would be to say as compared with the untreated ACF FHL and ACF FHH rats) In addition, EETs/DHETEs ratio in the LV are was about three-fold higher than in the kidney.

Figure 8 shows the data on renal tissue availability of four biologically active epoxygenase products of AA. It is seen that ACF creation significantly decreased the levels of all EET regioisomers, to the same extent in FHL and FHH rats. The treatment with the sEH inhibitor restored these bioavailability values to levels observed in sham-operated animals of both strains. In addition, the data show that in FHL and in FHH rats 14,15-EET and 5,6-EET prevail among CYP-dependent epoxygenase metabolites of AA, which agrees with the results of previous studies indicating the critical importance of 14,15-EET in kidney tissue (Roman, 2002; Fleming, 2014; Capdevila et al., 2015; Jíchová et al., 2016; Imig, 2018).

Figure 9 shows the data on LV tissue availability of four biologically active epoxygenase products of AA. It demonstrates that there were no significant differences in any of EET regioisomer concentrations between FHL and FHH rats in the LV. ACF creation did not alter LV concentrations of the EET regioisomers, similarly in FHL and FHH rats. The treatment with the sEH inhibitor increased LV levels of all EET regioisomers in FHL as well as in FHH rats to the same extent. In addition, the data show that in FHL and FHH rats 11,12-EET, and 14,15-EET prevail, which agrees with previous reports (Fleming, 2014; Jamieson et al., 2017). Moreover our data indicate that, quantitatively, increased concentrations of 11,12-EET and 14,15-EET are mostly responsible for the overall increment in LV tissue concentrations of biologically active epoxygenase products of AA.

As shown in **Figure 10A**, untreated ACF FHH rats exhibited significantly lower body weight as compared with all the other experimental groups.

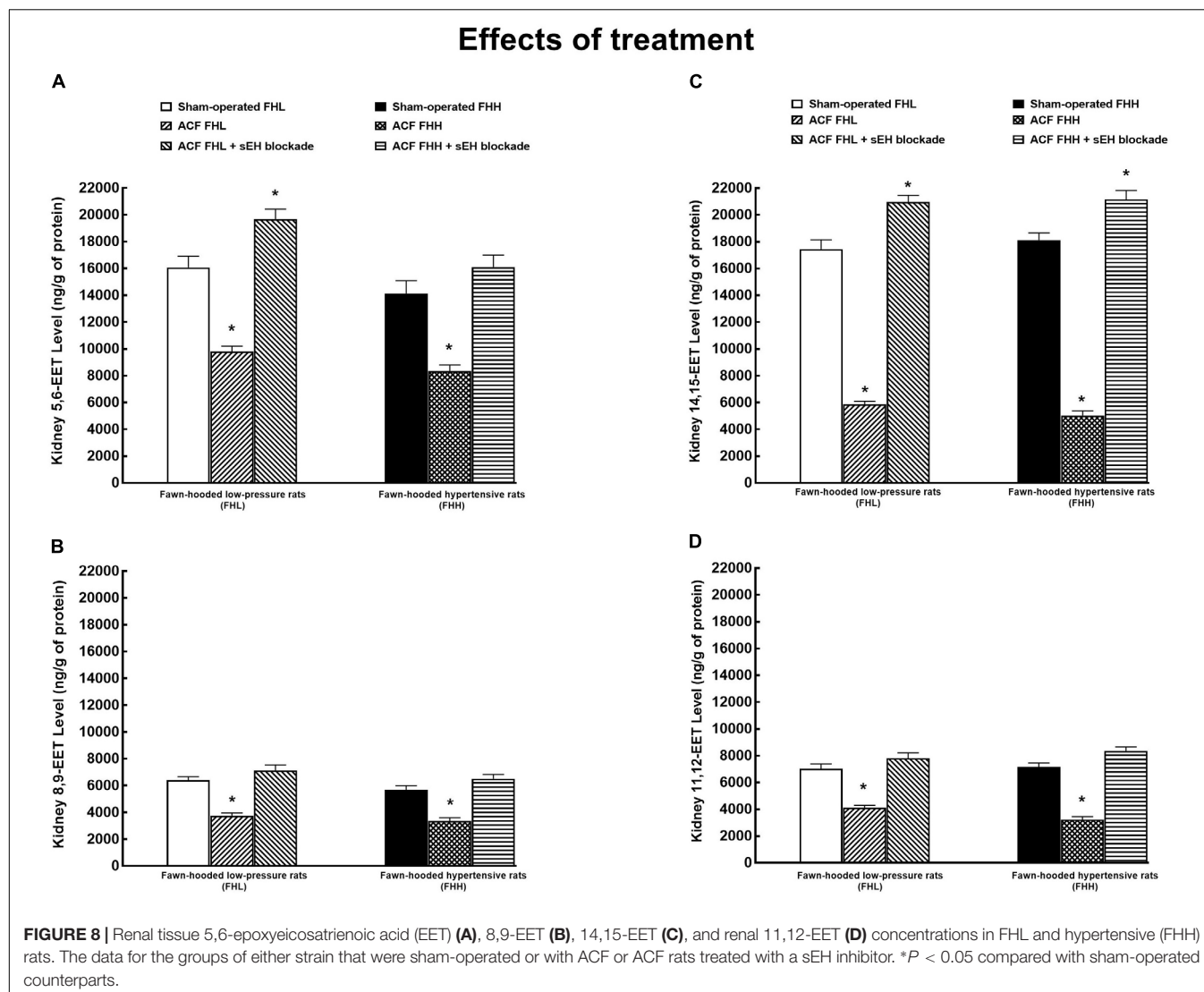


Figure 10B shows that untreated ACF FHL as well as ACF FHH rats displayed significantly higher ratio of lung-to-body weight than their sham-operated counterparts, the increase was more pronounced in the ACF FHH group. These findings indicate the development of important lung congestion in ACF animals, particularly in untreated ACF FHH rats. The treatment with sEH inhibitor did not alter the ratio in ACF FHL but lowered it in ACF FHH rats. However, the ratio remained significantly higher than in sham-operated FHH rats.

There were no significant differences between experimental groups in the kidney weight when normalized to body weight (**Figure 10C**) and the liver weight (data not shown).

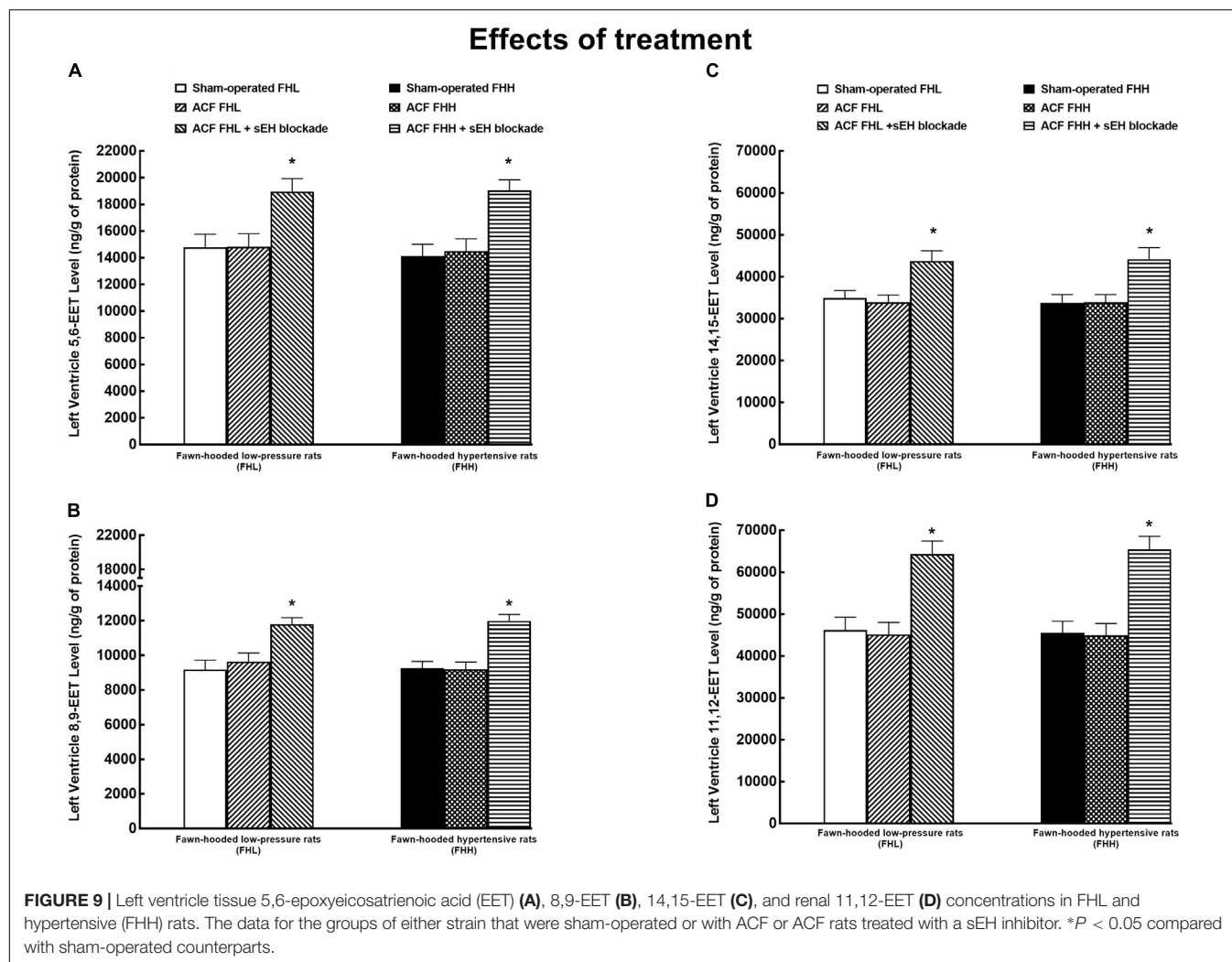
As shown in **Figures 11A,B**, sham-operated FHH rats exhibited significant cardiac hypertrophy [expressed as whole heart weight (HW) to body weight ratio], with marked left ventricle (LV) hypertrophy [expressed as LV weight (LVW) to body weight ratio] as compared with sham-operated FHL rats. **Figure 11C** shows that there were no significant differences

in right ventricle (RV) weight (RVW) (expressed as RVW to body weight ratio) between sham-operated FHH and FHL rats.

Untreated ACF FHL and ACF FHH rats exhibited marked cardiac hypertrophy as compared with their sham-operated counterparts. The treatment with sEH inhibitor did not modify the development of cardiac hypertrophy in ACF FHL but, in contrast, attenuated it in ACF FHH rats (**Figures 11A–C**).

Series 3: Effects of 2-Week Treatment With sEH Inhibitor on Basal Cardiac Function Parameters Assessed by Echocardiography and by Pressure-Volume Analysis

Table 1 summarizes the evaluation of cardiac function by echocardiography. The data confirms that sham-operated FHH displayed cardiac hypertrophy as compared with FHL rats and the induction of ACF caused marked cardiac hypertrophy, to



the same extent in FHL and FHH, as soon as 6 weeks after ACF creation. The treatment with sEH inhibitor did not alter the degree of cardiac hypertrophy, similarly in sham-operated FHH or ACF FHL rats and ACF FHH rats. Untreated ACF FHL as well as ACF FHH rats showed increased stroke volume and cardiac output (dependent on the presence of the shunt), significant increases in LV and RV diameter, a decrease in the relative LV wall thickness (indicating the development of eccentric hypertrophy) and a significant decrease in LV fractional shortening (indication of LV systolic dysfunction) as compared with sham-operated FHL and FHH rats. The treatment with sEH inhibitor did not change any of these parameters, similarly in sham-operated FHL and FHH rats, and in ACF FHL and ACF FHH rats.

Table 2 summarizes the assessment of cardiac function by LV pressure-volume analysis. Sham-operated FHH displayed only higher LV peak pressure as compared with sham-operated FHL rats (confirming a slight hypertension in FHH rats). With regard to all the other parameters there were no significant differences between sham-operated FHL and sham-operated FHH rats (indicating that sham-operated FHH rats do not exhibit

any substantial impairment of basal cardiac function) and the treatment with sEH inhibitor did not change any parameter in sham-operated FHL and FHH rats.

Untreated ACF FHL as well as ACF FHH rats showed markedly higher LV end-diastolic pressure and LV end-diastolic volume as compared with their sham-operated counterparts which indicated a significant degree of CHF in the two former groups. There were no significant differences in the maximum rate of pressure rise $[(+dP/dt)_{max}]$ and maximum rate of pressure fall $[-(dP/dt)_{max}]$ between the experimental groups. Untreated ACF FHL as well as ACF FHH rats showed markedly lower end-systolic pressure-volume relationship as compared with sham-operated FHL and sham-operated FHH rats, which indicated impairment of myocardial contractility in ACF animals. Untreated ACF FHL and ACF FHH rats also showed lower end-diastolic pressure volume relationship compared with their sham-operated counterparts, which indicated enhanced LV compliance resulting from the chamber eccentric remodeling. There were no significant differences in any measured parameter between ACF FHL and ACF FHH rats, and the treatment with sEH inhibitor did not significantly

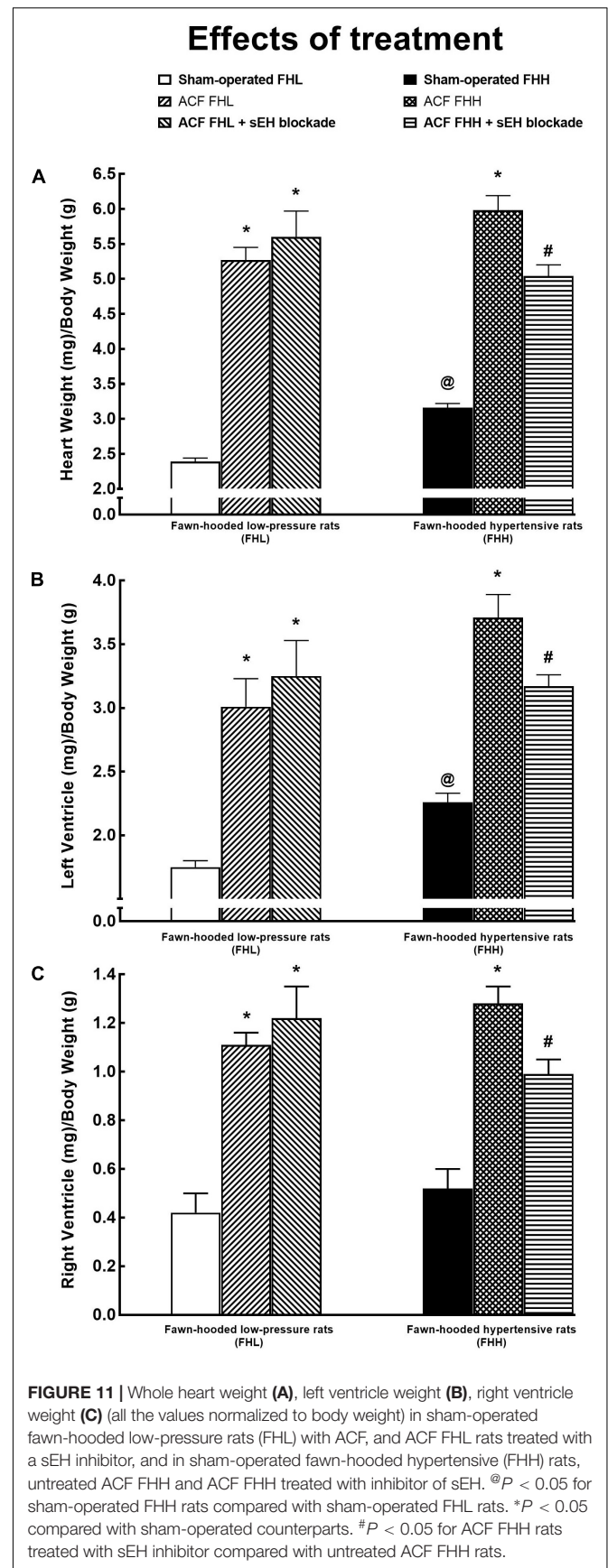
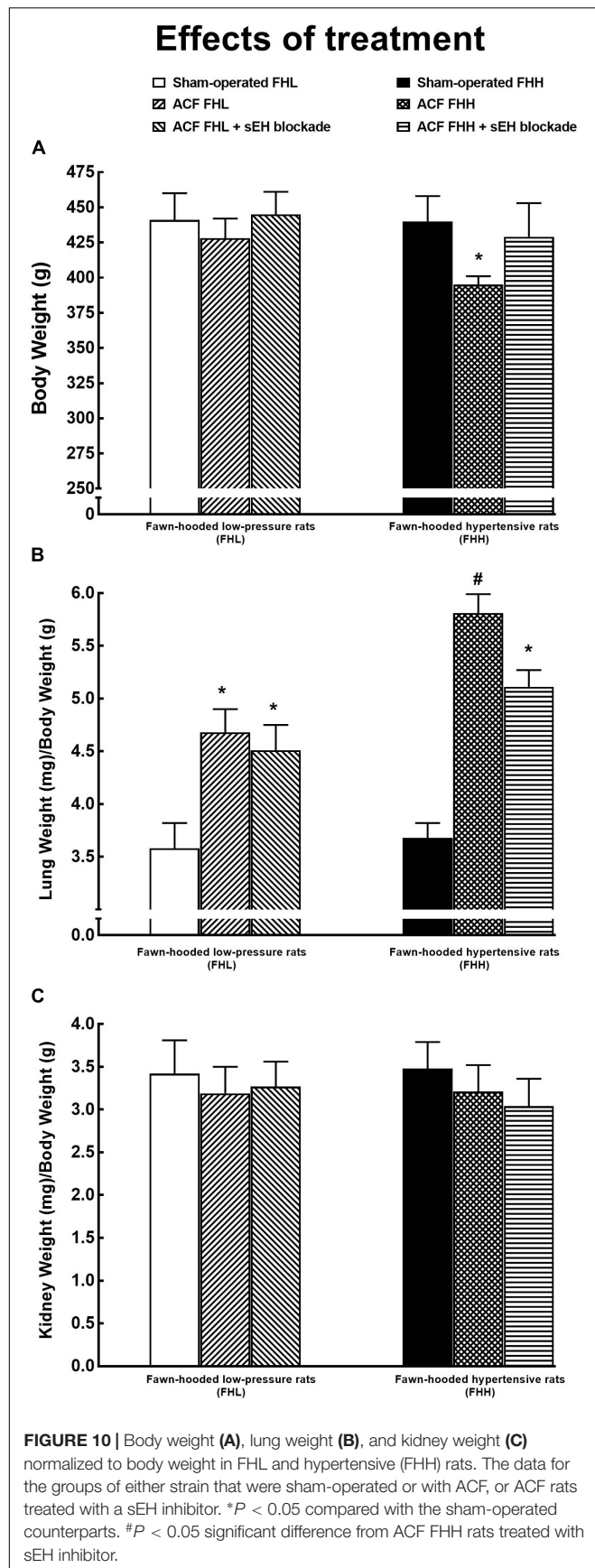


TABLE 1 | Echocardiography at week 6 after induction of the aorto-caval fistula and after 2 weeks of treatment with the soluble epoxide hydrolase inhibitor.

Parameter	Group					
	FHL + water	FHL + sEHi	ACF FHL + water	ACF FHL + sEHi	FHH + water	FHH + sEHi
Heart weight (mg)/Body weight (g)	2.78 ± 0.09	2.84 ± 0.08	4.99 ± 0.21*	5.12 ± 0.26*	3.21 ± 0.08 [#]	3.22 ± 0.09 [#]
RV diastolic diameter (mm)	3.25 ± 0.24	3.41 ± 0.29	6.19 ± 0.27*	6.24 ± 0.26*	3.31 ± 0.22	3.36 ± 0.27
LV diastolic diameter (mm)	6.19 ± 0.43	6.16 ± 0.47	11.02 ± 0.39*	10.99 ± 0.41*	6.17 ± 0.31	6.22 ± 0.33
LV systolic diameter (mm)	3.14 ± 0.38	3.17 ± 0.34	7.14 ± 0.38*	7.08 ± 0.34*	3.26 ± 0.21	3.27 ± 0.23
LV posterior wall thickness in diastole (mm)	2.36 ± 0.31	2.31 ± 0.29	2.27 ± 0.31	2.26 ± 0.29	2.96 ± 0.11	2.98 ± 0.10
Interventricular septum thickness (mm)	2.25 ± 0.18	2.23 ± 0.17	2.17 ± 0.17	2.18 ± 0.09	2.61 ± 0.17	2.63 ± 0.18
LV relative wall thickness (mm)	0.71 ± 0.05	0.69 ± 0.04	0.41 ± 0.03*	0.39 ± 0.04*	0.78 ± 0.04	0.79 ± 0.04
LV fractional shortening (%)	63 ± 3	61 ± 3	47 ± 2*	46 ± 2*	61 ± 3	62 ± 3
Stroke volume (μl)	206 ± 9	211 ± 8	556 ± 2*	562 ± 31*	209 ± 11	207 ± 9
Cardiac output (ml.min ⁻¹)	108 ± 9	111 ± 12	308 ± 14*	318 ± 13*	112 ± 10	111 ± 9

Values are means ± SEM. RV, right ventricle; FHL, fawn-hooded low-pressure rats; FHH, fawn-hooded hypertensive rats; ACF, aorto-caval fistula; sEHi, soluble epoxide hydrolase inhibitor. * $P < 0.05$ compared with sham-operated counterparts. [#] $P < 0.05$ FHH vs. FHL.

TABLE 2 | Invasive hemodynamics at week 6 after induction of aorto-caval fistula and after 2 weeks of treatment with soluble epoxide hydrolase inhibitor.

Parameter	Group					
	FHL + water	FHL + sEHi	ACF FHL + water	ACF FHL + sEHi	FHH + water	FHH + sEHi
Heart rate (s ⁻¹)	435 ± 19	432 ± 21	419 ± 27	4271 ± 22	416 ± 29	418 ± 31
LV peak pressure (mmHg)	137 ± 4	139 ± 4	112 ± 4*	114 ± 4*	149 ± 4 [#]	150 ± 3 [#]
LV end-diastolic pressure (mmHg)	1.9 ± 0.5	1.9 ± 0.4	8.6 ± 0.8*	8.9 ± 0.7*	1.7 ± 0.6	1.8 ± 0.4
LV end-diastolic volume (ml)	0.29 ± 0.09	0.30 ± 0.08	0.99 ± 0.06*	1.04 ± 0.10*	0.31 ± 0.06	0.32 ± 0.09
+(dP/dt) _{max} (mmHg.s ⁻¹)	10972 ± 986	10732 ± 896	10742 ± 886	10963 ± 971	11563 ± 1001	11042 ± 952
-(dP/dt) _{max} (mmHg.s ⁻¹)	-9156 ± 832	-9063 ± 776	-9192 ± 874	-9098 ± 836	-9272 ± 914	-9154 ± 857
ESPVR _{max} (mmHg.ml ⁻¹)	286 ± 39	256 ± 33	57 ± 17*	61 ± 13*	261 ± 37	256 ± 36
EDPVR _{max} (mmHg.ml ⁻¹)	43 ± 9	39 ± 7	14 ± 4*	15 ± 4*	42 ± 6	40 ± 6
LV relaxation constant, tau (ms)	13 ± 2	14 ± 3	27 ± 4*	28 ± 3*	11 ± 3	12 ± 3

Values are means ± SEM. LV, left ventricle; +(dP/dt)_{max}, maximum rates of pressure rise; -(dP/dt)_{min}, maximum rates of pressure fall; ESPVR_{max}, maximum end-systolic pressure-volume relationship; EDPVR_{max}, maximum end-diastolic pressure-volume relationship; FHL, fawn-hooded low-pressure rats; FHH, fawn-hooded hypertensive rats; ACF, aorto-caval fistula; sEHi, soluble epoxide hydrolase inhibitor. * $P < 0.05$ compared with sham-operated counterparts. [#] $P < 0.05$ FHH vs. FHL.

alter this situation, similarly in ACF FHL and ACF FHH rats.

DISCUSSION

Our interest in this study focused on the differences in the course of ACF-induced CHF in FHL versus FHH rats: first, we found that the latter animals exhibited substantially lower survival rate. It is emphasized that at the stage when ACF was induced, FHH rats showed only minimally increased albuminuria as compared with FHL rats. It will be noticed that while in adult FHH rats blood pressure (BP) is significantly higher than in FHL rats, at the age of 3–6 months FHHs are only slightly hypertensive. This was shown by our earlier radiotelemetry BP measurements: at the respective ages they reached mean BP levels of 138 and 148 mmHg, (Doleželová et al., 2016).

During the present follow-up study albuminuria increased to a greater extent in ACF FHH than in ACF FHL rats; at the week 10 (i.e., 14 weeks after creation of ACF) it was almost 30-fold higher and this was so despite the fact that ACF FHH rats with the most prominent albuminuria died earlier. In addition, our results show that urinary angiotensinogen excretion, a recognized index of the dynamics of intrarenal RAS activity (Kobori et al., 2003; Kobori and Urushihara, 2013) increased considerably more (almost 90-fold) in ACF FHH than in ACF FHL rats, indicating its much greater activation in the former. Furthermore, it was seen that ACF FHL rats as well as ACF FHH rats displayed reduced renal tissue availability of biologically active epoxygenase metabolites of AA, assessed as the ratio of EETs to DHETES (approximately 60% reduction as compared with sham-operated animals). In contrast, we found that myocardial tissue availability of biologically active epoxygenase metabolites of AA in ACF FHL rats or ACF FHH rats was not reduced as compared with their sham-operated counterparts. Broadly speaking, sham-operated FHH rats showed only slight BP increase (estimated from LV peak pressure) and only moderate cardiac hypertrophy as compared with sham-operated FHL rats whereas all the other indices of cardiac function as well as the response to sEH inhibitor were not altered. Creation of ACF resulted in similar responses in cardiac structure and function in FHL and FHH rats. Six weeks before ACF FHH rats began definitely to die, untreated ACF FHL as well as untreated ACF FHH rats developed marked eccentric LV remodeling and cardiac hypertrophy linked to increased cardiac output, the result of blood recirculation via the fistula. Even though the load-dependent measures of LV contractility $[+(dp/dt)_{\max}]$ were at this stage not impaired, the suppression of the end-systolic pressure-volume slope and decreased LV fractional shortening imply significant impairment of systolic function. In addition, ACF FHL rats as well as ACF FHH rats also showed a suppression of the end-diastolic pressure-volume slope and prolongation of the LV relaxation, indicating impairment of early diastolic function. These findings are in accordance with the results of previous studies in this volume overload model of CHF (Brower et al., 1996; Oliver-Dussault et al., 2010; Červenka et al., 2015).

However, the most important are our findings that there were no significant differences between ACF FHL rats and ACF FHH rats and that the treatment with sEH inhibitor, which significantly increased LV tissue availability of EETs, did not improve cardiac morphology and cardiac performance in ACF FHH rats, despite the fact that it dramatically improved the survival rate. These findings suggest that beneficial effects on BP or on the LV dysfunction are probably not the mechanism(s) responsible for the improvement of survival rate in ACF FHH rats treated with sEH inhibitor. In this context it is important to recognize that one important limitation of our present study is that the results provide only one time-point information on BP and cardiac function. It is still possible that in the advanced phase of CHF, alterations in cardiac function and/or BP might influence the outcome in ACF FHH rats. To achieve more meaningful comparative data, comprehensive long term telemetric studies are required that would evaluate BP and LV function. Unfortunately, technical difficulties, and relatively short durability of implantable telemetric probes limit at present the feasibility of such prolonged experiments.

Nevertheless, despite this limitation and after considering all our present data, we can conclude that even moderate kidney damage dramatically worsens the course of ACF-induced CHF in FHH rats. This further strengthens the notion on the critical importance of the heart and kidney interaction in the pathophysiology of progression of CHF. The two organs interact in a complex bidirectional mode, which can critical influence the outcome in patients with CHF (Braam et al., 2014; Schefold et al., 2016; Mullens et al., 2017; Arrigo et al., 2018; House, 2018).

The most important set of findings is that chronic pharmacological inhibition of sEH substantially improved survival rate and prevented increases in albuminuria in ACF FHL as well as ACF FHH rats. The beneficial effects of the treatment, particularly on the survival rate, were more pronounced in ACF FHH rats. In addition, our results show that, in accordance with previous findings (Oliver-Dussault et al., 2010; Melenovsky et al., 2012, 2018; Červenka et al., 2015, 2016; Kala et al., 2018), after creation of ACF the animals displayed signs of pronounced cardiac hypertrophy, involving both ventricles. Remarkably, this was associated with distinct lung congestion, indicating LV failure without signs of RV failure (no liver congestion). However, the signs of LV failure were more pronounced in ACF FHH rats and the treatment with sEH inhibitor attenuated cardiac hypertrophy and lung congestion in the hypertensive strain only, which further indicates that beneficial actions of the treatment are here more prominent. They were also associated with increases in intrarenal EETs availability; notably, *c*-AUCB-treated rats, both ACF FHL and ACF FHH strains, showed higher EETs/DHETEs ratio than found in their sham-operated counterparts. These findings accord with our recent report that in rats after 5/6 renal mass reduction (5/6 NX), a commonly used model of CKD, specific renoprotective effects (unrelated to the RAS blockade) are indeed associated with normalization of the intrarenal EETs availability (Čertíková Chábová et al., 2018).

In this context we have to acknowledge another important limitation of our present study: it did not evaluate the effects

of chronic sEH inhibition on the development of hypertension and CKD in sham-operated FHH rats. In our previous study, we found (Doleželová et al., 2016) that renal concentrations of EETs were similar in young FHL and FHH rats, but in the latter renal EETs concentrations progressively decreased with age. This is important because of the known organ-protective actions of EETs (Elmarakby, 2012; Fan and Roman, 2017; Imig, 2018). Moreover, renal EETs deficiency was shown to significantly contribute to the pathophysiology of hypertension and renal damage in several models (Honetschlagerova et al., 2011; Elmarakby, 2012; Kopkan et al., 2012; Fan and Roman, 2017; Imig, 2018). Therefore, one can assume that progressively decreasing renal tissue EETs could contribute to the development of CKD in FHH rats and chronic pharmacologic sEH inhibition should attenuate it. Future long term, appropriately focused studies should address this issue, however, the present study (with a different focus) provides a necessary background for such studies.

On the other hand, our results show that intrarenal and myocardial activity of CYP-dependent ω -hydroxylase products (HETEs) was not significantly altered in ACF FHL or ACF FHH rats, and was not modified by chronic pharmacological sEH inhibition. These findings are important because increased activity of CYP-dependent ω -hydroxylase pathway of AA metabolism and increased production/action of HETEs (mainly 20-HETE) is proposed to substantially contribute to the pathophysiology of cardio-renal diseases (Jamieson et al., 2017; Rocic and Schwartzman, 2018). Our findings do not support this view, at least with the rat strain and experimental model used here. On the contrary, the results speak against the role of renal and myocardial alterations of the CYP-dependent ω -hydroxylase pathway of AA in the progression of CHF in ACF FHH rats.

In addition, our results show that, when assessed 14 weeks after ACF creation, ACF FHL and ACF FHH rats exhibited similar striking activation of both systemic and intrarenal vasoconstrictor/sodium retaining axis of the RAS, as indicated by elevation of plasma and kidney ANG II levels. However, it is striking that in ACF FHH rats urinary angiotensinogen excretion was dramatically higher (about 1000-fold) than observed in the ACF FHL strain. This suggests that the course of ACF-induced CHF in FHH rats is characterized by activation of intrarenal RAS that is more pronounced than observed in animals that are resistant to renal damage and development of CKD. We cannot provide satisfactory explanation why urinary angiotensinogen excretion and not renal tissue ANG II was the distinguishing feature between ACF FHH and ACF FHL rats. However, one should consider that ANG II levels were measured at the one time-point only and despite all precautions the very procedure of tissue sampling can alter the results (Husková et al., 2006a,b). On the other hand, urinary angiotensinogen excretion was performed repeatedly throughout the study and despite some technical limitations it allegedly presents a reliable marker for non-invasive evaluation of intrarenal RAS activity (Kobori et al., 2003; Kobori and Urushihara, 2013). At variance with the present observations, in a recent study of 5/6 NX rats we showed a high correlation between renal ANG II concentrations and urinary angiotensinogen excretion (Sedláková et al., 2017; Čertíková

Chábová et al., 2018). Nevertheless, regardless of the reason(s) for the discrepancy between urinary angiotensinogen excretion and renal ANG II concentrations, an assessment of both parameters clearly shows that the intrarenal RAS system was activated, and that sEH inhibition did not alter this activation, quite, similarly so in ACF FHL and ACF FHH rats. This indicates that the beneficial effects of chronic sEH inhibition are not related to alterations of the vasoconstrictor/sodium retaining axis of the RAS, which further supports the notion that CHF is not simply a hemodynamic disorder. Apparently, compensatory activation of systemic and tissue neurohormonal systems, perhaps also outside the heart and the kidney, plays an important role in the progression of CHF and can in the long-term can adversely affect the outcome of CHF, probably due to inappropriate activation of the RAS and/or insufficient activation of the CYP epoxigenase enzymatic pathway (Dube and Weber, 2011; Hartupée and Mann, 2017; Packer and McMurray, 2017).

CONCLUSION

We believe that the results of our present study provide further evidence that an association of even mild form of CKD has a strikingly negative impact on the course of ACF-induced CHF and that the reduced renal availability of EETs plays an important role. We found that sEH inhibitor treatment normalized renal availability of EETs and improved the long-term survival rate, without altering RAS activity. The results provide the rationale for attempts to increase the generation of EETs, possibly by reducing their degradation by sEH, as a new therapeutic approach for the treatment of CHF, particularly of its forms associated with CKD.

AUTHOR CONTRIBUTIONS

ŠV, LK, JS, EK-J, JI, MT, VM, and LČ primarily conceived and designed the study, analyzed, and interpreted the data, and wrote the manuscript. ŠV, LK, and LČ performed all surgical procedures in this study. SK and ZH performed the biochemical analyses. BH designed and synthesized the sEH inhibitor. MT and VM performed studies evaluating cardiac function. All authors were involved in the final analysis and interpretation of the data and contributed to the intellectual content and editing of the manuscript, and approved its final version.

FUNDING

This study was primarily supported by the Ministry of Health of the Czechia grant no. 17-28220A awarded to MT. All rights reserved. BH was supported by the National Institute of Health R01ES002710, P42ES004699, and R01DK103616 grants. A National Institute of Health (NIH) grant (DK103616) and Dr. Ralph and Marian Falk Medical Research Trust Bank of America, N.A., Trustee grant to JI supported this study.

REFERENCES

- Abassi, Z., Goltsmna, I., Karram, T., Winaver, J., and Horrman, A. (2011). Aortocaval fistula in rat: a unique model of volume-overload congestive heart failure and cardiac hypertrophy. *J. Biomed. Biotechnol.* 2011:729497. doi: 10.1155/2011/729497
- Alánová, P., Husková, Z., Kopkan, L., Sporková, A., Jíchová, Š., Neckář, J., et al. (2015). Orally active epoxyeicosatrienoic acid analog does not exhibit antihypertensive and reno- or cardioprotective actions in two-kidney, one-clip Goldblatt hypertensive rats. *Vasc. Pharmacol.* 73, 45–56. doi: 10.1016/j.vph.2015.08.013
- Arrigo, M., Cippa, P. E., and Mebazaa, A. (2018). Cardiorenal interactions revisited: how to improve heart failure outcomes in patients with chronic kidney disease. *Curr. Heart Fail.* doi: 10.1007/s11897-018-0406-8 [Epub ahead of print].
- Benes, J., Kazdova, L., Drahota, Z., Houstek, J., Medrikova, D., Kopecky, J., et al. (2011). Effect of metformin therapy on cardiac function and survival in a volume-overload model of heart failure in rats. *Clin. Sci.* 121, 29–41. doi: 10.1042/CS20100527
- Benjamin, E. J., Blaha, M. J., Chiuve, S. E., Cushman, M., Das, S. R., de Ferranti, S. D., et al. (2017). Heart disease and stroke statistics-2017 update: a report from the American Heart Association. *Circulation* 135, e146–e603. doi: 10.1161/CIR.0000000000000485
- Braam, B., Joles, J. A., Daniswar, A. H., and Gaillard, C. A. (2014). Cardiorenal syndrome – current understanding and future perspectives. *Nat. Rev. Nephrol.* 10, 48–55. doi: 10.1038/nrneph.2013.250
- Braunwald, E. (2015). The war against heart failure. *Lancet* 385, 812–824. doi: 10.1016/S0140-6736(14)61889-4
- Brower, G. L., Henegar, J. R., and Janicki, J. S. (1996). Temporal evaluation of left ventricular remodeling and function in rats with chronic volume overload. *Am. J. Physiol.* 40, H2071–H2078. doi: 10.1152/ajpheart.1996.271.5.H2071
- Brower, G. L., Levick, S. P., and Janicki, J. S. (2015). Differential effects of prevention and reversal treatment with lisinopril on left ventricular remodeling in a rat model of heart failure. *Heart Lung Circ.* 24, 919–924. doi: 10.1016/j.hlc.2015.02.023
- Capdevila, J. H., Wang, W., and Falck, J. R. (2015). Arachidonic acid monooxygenase: genetic and biochemical approaches to physiological/pathophysiological relevance. *Prostaglandins Other Lipid Mediat.* 120, 40–49. doi: 10.1016/j.prostaglandins.2015.05.004
- Čertíková Chábová, V., Kujal, P., Škaroupková, P., Vaňourková, Z., Vacková, Š., Husková, Z., et al. (2018). Combined inhibition of soluble epoxide hydrolase and renin-angiotensin system exhibits superior renoprotection to renin-angiotensin system blockade in 5/6 nephrectomized Ren-2 transgenic hypertensive rats with established chronic kidney disease. *Kidney Blood Press Res.* 43, 329–349. doi: 10.1159/000487902
- Červenka, L., Melenovský, V., Husková, Z., Škaroupková, P., Nishiyama, A., and Sadowski, J. (2015). Inhibition of soluble epoxide hydrolase counteracts the development of renal dysfunction and progression of congestive heart failure in Ren-2 transgenic hypertensive rats with aorto-caval fistula. *Clin. Exp. Pharmacol. Physiol.* 42, 795–807. doi: 10.1111/1440-1681.12419
- Červenka, L., Škaroupková, P., Kompanowska-Jeziarska, E., and Sadowski, J. (2016). Sex-linked differences in the course of chronic kidney disease and congestive heart failure: a study in 5/6 nephrectomized Ren-2 transgenic hypertensive rats with volume overload induced using aorto-caval fistula. *Clin. Exp. Pharmacol. Physiol.* 43, 883–895. doi: 10.1111/1440-1681.12619
- Cohen-Segev, R., Francis, B., Abu-Saleh, N., Awad, H., Lazarovich, A., Kabala, A., et al. (2014). Cardiac and renal distribution of ACE and ACE-2 in rats with heart failure. *Acta Histochem.* 116, 1342–1349. doi: 10.1016/j.acthis.2014.08.006
- Doleželová, Š., Jíchová, Š., Husková, Z., Vojtíšková, A., Kujal, P., Hošková, L., et al. (2016). Progression of hypertension and kidney disease in aging fawn-hooded rats is mediated by enhanced influence of renin-angiotensin system and suppression of nitric oxide system and epoxyeicosanoids. *Clin. Exp. Hypertens.* 38, 644–651. doi: 10.1080/10641963.2016.1182182
- Dube, P., and Weber, K. T. (2011). Congestive heart failure: pathophysiologic consequences of neurohormonal activation and the potential for recovery: part I. *Am. J. Med. Sci.* 342, 348–351. doi: 10.1097/MAJ.0b013e318232750d
- Elmarakby, A. A. (2012). Reno-protective mechanisms of epoxyeicosatrienoic acids in cardiovascular disease. *Am. J. Physiol.* 302, R321–R330. doi: 10.1152/ajpregu.00606.2011
- Fan, F., and Roman, R. J. (2017). Effect of cytochrome P450 metabolites of arachidonic acid in nephrology. *J. Am. Soc. Nephrol.* 28, 2845–2855. doi: 10.1681/ASN.2017030252
- Fleming, I. (2014). The pharmacology of the cytochrome P450 epoxigenase/soluble epoxide hydrolase axis in the vasculature and cardiovascular disease. *Pharmacol. Rev.* 66, 1106–1140. doi: 10.1124/pr.113.007781
- Fox, J., Guan, S., Hymel, A. A., and Navar, L. G. (1992). Dietary Na and ACE inhibition effects on renal tissue angiotensin I and II and ACE activity in rats. *Am J Physiol.* 262, F902–F909. doi: 10.1152/ajprenal.1992.262.5.F902
- Hartupée, J., and Mann, D. L. (2017). Neurohormonal activation in heart failure with reduced ejection fraction. *Nat. Rev. Cardiol.* 14, 30–38. doi: 10.1038/nrcardio.2016.163
- Hatt, P. Y., Rakusan, K., Gastineau, P., Laplace, M., and Cluzeaud, F. (1980). Aorto-caval fistula in the rat. An experimental model of heart volume overloading. *Basic Res. Cardiol.* 75, 105–108. doi: 10.1007/BF02001401
- Honetschlagerova, Z., Husková, Z., Vaňourková, Z., Sporková, A., Kramer, H. J., Hwang, S. H., et al. (2011). Renal mechanisms contributing to the antihypertensive action of soluble epoxide hydrolase inhibition in Ren-2 transgenic rats with inducible hypertension. *J. Physiol.* 589, 207–219. doi: 10.1113/jphysiol.2010.199505
- House, A. A. (2018). Management of heart failure in advancing CKD: core curriculum 2018. *Am. J. Kidney Dis.* 72, 284–295. doi: 10.1053/j.ajkd.2017.12.006
- Houser, S. R., Margulies, K. B., Murphy, A. M., Spinale, F. G., Francis, G. S., Prabhu, S. D., et al. (2012). Animal models of heart failure: a scientific statement from the American Heart Association. *Circ. Res.* 111:e54. doi: 10.1161/RES.0b013e3182582523
- Husková, Z., Kopkan, L., Červenková, L., Doleželová, Š., Vaňourková, Z., Škaroupková, P., et al. (2016). Intrarenal alterations of the angiotensin-converting type 2/angiotensin 1-7 complex of the renin-angiotensin system do not alter the course of malignant hypertension in Cyp1a1-Ren-2 transgenic rats. *Clin. Exp. Pharmacol. Physiol.* 43, 438–449. doi: 10.1111/1440-1681.12553
- Husková, Z., Kramer, H. J., Thumová, M., Vaňourková, Z., Burgerová, M., Teplan, V., et al. (2006a). Effects of anesthesia on plasma and kidney ANG II levels in normotensive and ANG II-dependent hypertensive rats. *Kidney Blood Press Res.* 29, 74–83.
- Husková, Z., Kramer, H. J., Vaňourková, Z., and Červenka, L. (2006b). Effects of changes in sodium balance on plasma and kidney angiotensin II levels in anesthetized and conscious Ren-2 transgenic rats. *J Hypertens.* 24, 517–522.
- Imig, J. D. (2018). Prospective for cytochrome P450 epoxigenase cardiovascular and renal therapies. *Pharmacol. Ther.* doi: 10.1016/j.pharmthera.2018.06.015 [Epub ahead of print].
- Jamieson, K. L., Endo, T., Darwesh, A. M., Samokhvalov, V., and Seubert, J. M. (2017). Cytochrome P450-derived eicosanoids and heart function. *Pharmacol. Ther.* 179, 47–83. doi: 10.1016/j.pharmthera.2017.05.005
- Jha, V., Garcia-Garcia, G., Iseki, K., Li, Z., Naicker, S., Plattner, B., et al. (2013). Chronic kidney disease: global dimension and perspectives. *Lancet* 382, 260–272. doi: 10.1016/S0140-6736(13)60687-X
- Jíchová, Š., Doleželová, Š., Kopkan, L., Kompanowska-Jeziarska, E., Sadowski, J., and Červenka, L. (2016). Fenebricate attenuates malignant hypertension by suppression of the renin-angiotensin system: a study in Cyp1a1-Ren-2 transgenic rats. *Am. J. Med. Sci.* 352, 618–630. doi: 10.1016/j.amjms.2016.09.008
- Kala, P., Sedláková, L., Škaroupková, P., Kopkan, L., Vaňourková, Z., Táborský, M., et al. (2018). Effect of angiotensin-converting enzyme blockade, alone or combined with blockade of soluble epoxide hydrolase, on the course of congestive heart failure and occurrence of renal dysfunction in Ren-2 transgenic hypertensive rats with aorto-caval fistula. *Physiol. Res.* 67, 401–415.
- Kobori, H., Nishiyama, A., Harrison-Bernard, L. M., and Navar, L. G. (2003). Urinary angiotensinogen as an indicator of intrarenal angiotensin status in hypertension. *Hypertension* 41, 42–49. doi: 10.1161/01.HYP.0000050102.90932.CF
- Kobori, H., and Urushihara, M. (2013). Augmented intrarenal and urinary angiotensinogen in hypertension and chronic kidney disease. *Pflugers Arch.* 465, 3–12. doi: 10.1007/s00424-012-1143-6

- Kopkan, L., Husková, Z., Sporková, A., Varcabová, Š., Honetschlagerová, Z., Hwan, S. H., et al. (2012). Soluble epoxide hydrolase inhibition exhibits antihypertensive actions independently of nitric oxide in mice with renovascular hypertension. *Kidney Blood Press Res.* 35, 595–607. doi: 10.1159/000339883
- Kujal, P., Čertíková Chábová, V., Škaroupková, P., Husková, Z., Vernerová, Z., Kramer, H. J., et al. (2014). Inhibition of soluble epoxide hydrolase is renoprotective in 5/6 nephrectomized Ren-2 transgenic hypertensive rats. *Clin. Exp. Pharmacol. Physiol.* 41, 227–237. doi: 10.1111/1440-1681.12204
- McCune, S., Baker, P. B., and Stills, F. H. (1990). SHF/Mcc-cp rat: model of obesity, non-insulin-dependent diabetes, and congestive heart failure. *Ilar News* 32, 23–27. doi: 10.1093/ilar.32.3.23
- Melenovsky, V., Cervenka, L., Viklicky, O., Franekova, J., Havlenova, T., Behounek, M., et al. (2018). Kidney response to heart failure: proteomic analysis of cardiorenal syndrome. *Kidney Blood Press Res.* 43, 1437–1450. doi: 10.1159/000493657
- Melenovsky, V., Skaroupkova, P., Benes, J., Torresova, V., Kopkan, L., and Cervenka, L. (2012). The course of heart failure development and mortality in rats with volume overload due to aorto-caval fistula. *Kidney Blood Press Res.* 35, 167–173. doi: 10.1159/000331562
- Monti, J., Fischer, J., Paskas, S., Heining, M., Schulz, H., and Gosele, C. (2008). Soluble epoxide hydrolase is a susceptibility factor for heart failure in a rat model of human disease. *Nat. Genet.* 40, 529–537. doi: 10.1038/ng.129
- Mullens, W., Verbrugge, F. H., Nijst, P., and Tang, W. H. W. (2017). Renal sodium avidity in heart failure: from pathophysiology to treatment strategies. *Eur. Heart J.* 38, 1872–1882. doi: 10.1093/eurheartj/ehx035
- Oliver-Dussault, C., Ascah, A., Marcil, M., Matas, J., Picard, S., Pibarot, P., et al. (2010). Early predictors of cardiac decompensation in experimental volume overload. *Mol. Cell Biochem.* 2010, 271–281. doi: 10.1007/s11010-009-0361-5
- Packer, M., and McMurray, J. J. V. (2017). Importance of endogenous compensatory vasoactive peptides in broadening the effects of inhibitors of the renin-angiotensin system for the treatment of heart failure. *Lancet* 389, 1831–1840. doi: 10.1016/S0140-6736(16)30969-2
- Provoost, A. P. (1994). Spontaneous glomerulosclerosis: insights from the fawn-hooded rat. *Kidney Int. Suppl.* 45, S2–S5.
- Rivera, J., Ward, N., Hodgson, J., Hodgson, J., Puddey, I. B., Falck, J. R., et al. (2004). Measurement of 20-hydroxyeicosatetraenoic acid in human urine by gas chromatography-mass spectrometry. *Clin. Chem.* 50, 224–226. doi: 10.1373/clinchem.2003.025775
- Rocic, P., and Schwartzman, M. L. (2018). 20-HETE in the regulation of vascular and cardiac function. *Pharmacol. Ther.* 192, 74–87. doi: 10.1016/j.pharmthera.2018.07.004
- Roman, R. J. (2002). P-450 metabolites of arachidonic acid in the control of cardiovascular function. *Physiol. Rev.* 82, 131–185. doi: 10.1152/physrev.00021.2001
- Scheffold, J. C., Filippatos, G., Hasenfuss, G., Anker, S. D., and von Haehling, S. (2016). Heart failure and kidney dysfunction: epidemiology, mechanisms and management. *Nat. Rev. Cardiol.* 12, 610–623. doi: 10.1038/nrneph.2016.113
- Sedláková, L., Čertíková Chábová, V., Doleželová, Š., Škaroupková, P., Kopkan, L., Husková, Z., et al. (2017). Renin-angiotensin system blockade alone or combined with ETA receptor blockade: effects on the course of chronic kidney disease in 5/6 nephrectomized Ren-2 transgenic rats. *Clin. Exp. Hypertens.* 39, 183–195. doi: 10.1080/10641963.2016.1235184
- Sporková, A., Jichová, Š., Husková, Z., Kopkan, L., Nishiyama, A., Hwang, S. H., et al. (2014). Different mechanisms of acute versus long-term antihypertensive effects of soluble epoxide hydrolase inhibition: studies in Cyp1a1-Ren-2 transgenic rats. *Clin. Exp. Pharmacol. Physiol.* 41, 1003–1013. doi: 10.1111/1440-1681.12310
- U.S. Renal Data System (2015). *USRDS. Annual Data Report 2015*. Seattle, WA: Epidemiology of kidney disease in the United States.
- Ziaeeian, B., and Fonarow, G. C. (2016). Epidemiology and aetiology of heart failure. *Nat. Rev. Cardiol.* 13, 368–378. doi: 10.1038/nrcardio.2016.25

Conflict of Interest Statement: The authors declare that the research was conducted in the absence of any commercial or financial relationships that could be construed as a potential conflict of interest.

Copyright © 2019 Vacková, Kopkan, Kikerlová, Husková, Sadowski, Kompanowska-Jezierska, Hammock, Imig, Táborský, Melenovský and Červenka. This is an open-access article distributed under the terms of the Creative Commons Attribution License (CC BY). The use, distribution or reproduction in other forums is permitted, provided the original author(s) and the copyright owner(s) are credited and that the original publication in this journal is cited, in accordance with accepted academic practice. No use, distribution or reproduction is permitted which does not comply with these terms.



Role of Soluble Epoxide Hydrolase in Metabolism of PUFAs in Psychiatric and Neurological Disorders

Kenji Hashimoto*

Division of Clinical Neuroscience, Center for Forensic Mental Health, Chiba University, Chiba, Japan

OPEN ACCESS

Edited by:

John D. Imig,
Medical College of Wisconsin,
United States

Reviewed by:

Hui-Ching Lin,
National Yang-Ming University, Taiwan
Artiom Gruzdev,
National Institute of Environmental
Health Sciences (NIEHS),
United States
Aldrin V. Gomes,
University of California, Davis,
United States

*Correspondence:

Kenji Hashimoto
hashimoto@faculty.chiba-u.jp

Specialty section:

This article was submitted to
Translational Pharmacology,
a section of the journal
Frontiers in Pharmacology

Received: 08 November 2018

Accepted: 14 January 2019

Published: 30 January 2019

Citation:

Hashimoto K (2019) Role
of Soluble Epoxide Hydrolase
in Metabolism of PUFAs in Psychiatric
and Neurological Disorders.
Front. Pharmacol. 10:36.
doi: 10.3389/fphar.2019.00036

Inflammation plays a key role in the pathogenesis of a number of psychiatric and neurological disorders. Soluble epoxide hydrolases (sEH), enzymes present in all living organisms, metabolize epoxy fatty acids (EpFAs) to corresponding 1,2-diols by the addition of a molecule of water. Accumulating evidence suggests that sEH in the metabolism of polyunsaturated fatty acids (PUFAs) plays a key role in inflammation. Preclinical studies demonstrated that protein expression of sEH in the prefrontal cortex, striatum, and hippocampus from mice with depression-like phenotype was higher than control mice. Furthermore, protein expression of sEH in the parietal cortex from patients with major depressive disorder was higher than controls. Interestingly, *Ephx2* knock-out (KO) mice exhibit stress resilience after chronic social defeat stress. Furthermore, the sEH inhibitors have antidepressant effects in animal models of depression. In addition, pharmacological inhibition or gene KO of sEH protected against dopaminergic neurotoxicity in the striatum after repeated administration of MPTP (1-methyl-4-phenyl-1,2,3,6-tetrahydropyridine) in an animal model of Parkinson's disease (PD). Protein expression of sEH in the striatum from MPTP-treated mice was higher than control mice. A number of studies using postmortem brain samples showed that the deposition of protein aggregates of α -synuclein, termed Lewy bodies, is evident in multiple brain regions of patients from PD and dementia with Lewy bodies (DLB). Moreover, the expression of the sEH protein in the striatum from patients with DLB was significantly higher compared with controls. Interestingly, there was a positive correlation between sEH expression and the ratio of phosphorylated α -synuclein to α -synuclein in the striatum. In the review, the author discusses the role of sEH in the metabolism of PUFAs in inflammation-related psychiatric and neurological disorders.

Keywords: α -synuclein, cytochrome P450, dementia of Lewy bodies, depression, epoxy fatty acids, inflammation, Parkinson's disease, stress resilience

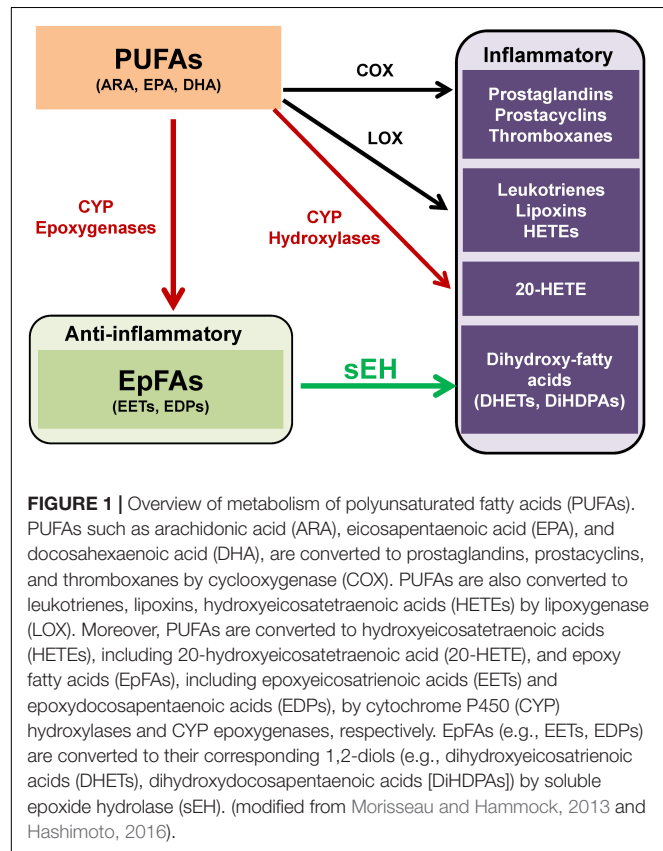
INTRODUCTION

Polyunsaturated fatty acids (PUFAs) are generally considered to be necessary for maintaining normal physiology (Jump, 2002; Bazinet and Layé, 2014; Layé et al., 2018). PUFAs are known to regulate both the structure and the function of neurons, glial cells, and endothelial cells in the brain (Bazinet and Layé, 2014; Layé et al., 2018). Importantly, PUFAs

need to be provided by the diet since they cannot be produced in mammals. There are two main families (ω -3 and ω -6) of PUFAs. Linoleic acid, the predominant plant-derived dietary ω -6 PUFA, is a precursor of arachidonic acid (ARA). α -linolenic acid, the predominant plant-derived dietary ω -3 PUFA, is a precursor of eicosapentaenoic acid (EPA) and docosahexaenoic acid (DHA).

Polyunsaturated fatty acids (PUFAs) are metabolized into bioactive derivatives by the main enzymes such as cyclooxygenases (COXs), lipoxygenases (LOXs), and cytochrome P450s (CYPs) (Imig and Hammock, 2009; Arnold et al., 2010; Imig, 2012, 2018; Morisseau and Hammock, 2013; Bazinet and Layé, 2014; Urquhart et al., 2015; Westphal et al., 2015; **Figure 1**). The COX pathway leads to the formation of prostaglandins, prostacyclins and thromboxanes, the LOX pathway leads to leukotrienes, lipoxins, and hydroxyl-eicosatetraenoic acids (HETEs). The CYP pathway leads to 20-HETE by CYP hydroxylases, and epoxy fatty acids (EpFAs) such as epoxy-eicosatrienoic acids (EETs) and epoxydocosapentaenoic acids (EDPs) by CYP epoxigenases (**Figure 1**).

In the review, the author would like to discuss the role of soluble epoxide hydrolase (sEH) in the CYP-mediated metabolism of PUFAs which might be involved in the pathogenesis of psychiatric and neurological disorders. Furthermore, we also refer to the clinical significance of sEH inhibitors for these disorders.



SOLUBLE EPOXIDE HYDROLASE IN CYP SYSTEM

The CYP system is a superfamily of enzymes, which are involved in the metabolism of exogenous and endogenous compounds. The CYP in the eicosanoid pathway was first described in 1980 and is comprised of two enzymatic pathways such as hydroxylases and epoxigenases. The CYP isoforms metabolize a number of ω -3 and ω -6 PUFAs, including ARA, EPA and DHA into bioactive lipid mediators, termed eicosanoids (Imig and Hammock, 2009; Imig, 2012, 2018; Morisseau and Hammock, 2013; Urquhart et al., 2015; Westphal et al., 2015; Jamieson et al., 2017). The CYP system produces both the pro-inflammatory, terminally hydroxylated metabolite 20-HETE and the anti-inflammatory EpFAs, including EETs from ARA and EDPs from DHA (**Figure 1**).

In contrast, EpFAs such as EETs, and EDPs are rapidly metabolized by a number of pathways including the soluble epoxide hydrolase (sEH) (Imig and Hammock, 2009; Morisseau and Hammock, 2013). The sEH was first identified in the cytosolic fraction of mouse liver through its activity on epoxide containing substances such as juvenile hormone and lipid epoxides (Hammock et al., 1976; Gill and Hammock, 1980; Ota and Hammock, 1980). Human sEH is a 62 kDa enzyme composed of two domains separately by a short proline-rich linker (Harris and Hammock, 2013). The N-terminal domain has a phosphatase activity that hydrolyzes lipid phosphates, while the C-terminal domain has an epoxide hydrolase activity that converts epoxides to their corresponding diols (Newman et al., 2003). The human *EPHX2* gene codes for the sEH protein is widely expressed in a number of tissues, including the liver, lungs, kidney, heart, brain, adrenals, spleen, intestines, urinary bladder, placenta, skin, mammary gland, testis, leukocytes, vascular endothelium, and smooth muscle. Interestingly, the sEH protein is most highly expressed in the liver and kidney (Gill and Hammock, 1980; Newman et al., 2005; Imig, 2012).

Accumulating evidence suggests that EETs, EDPs and some other EpFAs have potent anti-inflammatory properties (Wagner et al., 2014, 2017; López-Vicario et al., 2015) which are implicated in the pathogenesis of a number of psychiatric and neurological disorders (Denis et al., 2015; Hashimoto, 2015, 2016, 2018; Gumusoglu and Stevens, 2018; Polokowski et al., 2018).

INFLAMMATION IN DEPRESSION AND SEH

Depression, one of the most common disorders in the world, is a major psychiatric disorder with a high rate of relapse. The World Health Organization (WHO) estimates that more than 320 million individuals of all ages suffer from depression (World Health Organization [WHO], 2017). Multiple lines of evidence demonstrate inflammatory processes in the pathophysiology of depression and in the antidepressant actions of the certain compounds (Dantzer et al., 2008; Miller et al., 2009, 2017; Raison et al., 2010; Hashimoto, 2015, 2016, 2018; Mechawar and Savitz, 2016; Miller and Raison, 2016; Zhang et al.,

2016a,b, 2017b,a). Meta-analysis showed higher levels of pro-inflammatory cytokines in the blood of drug-free or medicated depressed patients compared to healthy controls (Dowlati et al., 2010; Young et al., 2014; Haapakoski et al., 2015; Eyre et al., 2016; Köhler et al., 2018). Collectively, it is likely that inflammation plays a key role in the pathophysiology of depression.

Several reports using meta-analysis demonstrated that ω -3 PUFAs could reduce depressive symptoms beyond placebo (Lin et al., 2010, 2017; Sublette et al., 2011; Mello et al., 2014; Grosso et al., 2016; Hallahan et al., 2016; Mocking et al., 2016; Sarris et al., 2016; Bai et al., 2018; Hsu et al., 2018). Dietary intake of ω -3 PUFAs is known to be associated with lower risk of depression. Importantly, EPA-rich ω -3 PUFAs could be recommended for the treatment of depression (Sublette et al., 2011; Mocking et al., 2016; Sarris et al., 2016). Importantly, brain EPA levels are 250–300-fold lower than DHA compared to about 4- (plasma), 5- (erythrocyte), 14- (liver), and 86-fold (heart) lower levels of EPA versus DHA (Chen and Bazinet, 2015; Dylla, 2015).

Given the role of inflammation in depression, it is likely that sEH might contribute to the pathophysiology of depression. A single injection of lipopolysaccharide (LPS) is known to produce depression-like phenotypes in rodents after sickness behaviors (Dantzer et al., 2008; Zhang et al., 2014, 2016a, 2017b; Ma et al., 2017; Yang et al., 2017). Ren et al. (2016) reported that the sEH inhibitor TPPU [1-(1-propionylpiperidin-4-yl)-3-(4-(trifluoromethoxy)phenyl)urea] (Figure 2) conferred prophylactic and antidepressant effects in the LPS-induced inflammation model of depression while the current antidepressants showed no therapeutic effects in this model (Zhang et al., 2014). Chronic social defeat stress (CSDS) model of depression is widely used as an animal model of depression (Nestler and Hyman, 2010; Golden et al., 2011; Yang et al., 2015, 2017, 2018). Pretreatment with TPPU before

social defeat stress showed resilience to CSDS. In addition, TPPU showed rapid antidepressant effects in susceptible mice after CSDS (Ren et al., 2016). Interestingly, the sEH KO mice showed stress resilience to repeated social defeat stress. Increased brain-derived neurotrophic factor (BDNF) and its receptor TrkB signaling in the prefrontal cortex and hippocampus of the KO mice might be responsible for stress resilience (Ren et al., 2016). Furthermore, repeated treatment with TPPU for 7 days increased interaction time of socially defeated mice in a CSDS model, and improvement by TPPU was blocked by TrkB antagonist K252a (Wu et al., 2017), suggesting a role of BDNF-TrkB signaling in TPPU's beneficial effects. Interestingly, higher protein levels of sEH were shown in the brain regions of mice with a depression-like phenotype in the inflammation and CSDS models, suggesting that increased levels of sEH may play a role in depression-like phenotypes in rodents (Ren et al., 2016). We found higher sEH protein levels in the parietal cortex (Brodmann area 7) from patients with major depressive disorder, pointing to a possible role for increased sEH levels in depression (Ren et al., 2016). Taken together, this study highlights a key function for sEH in the pathophysiology of depression, and for its inhibitors as potential therapeutic or prophylactic drugs for depression (Hashimoto, 2016; Ren et al., 2016; Swardfager et al., 2018; Figure 3).

A study using euthymic patients with a history of major depressive disorder with seasonal depression showed changes in CYP- and sEH-derived eicosanoids in patients with winter depression (Hennebelle et al., 2017). The ω -6 derived sEH product 12,13-DiHOME [12,13-dihydroxy-9-octadecenoic acid] increased in winter depression. Total 14,15-EpETE [14,15-epoxy-5Z,8Z,11Z,17Z-eicosatetraenoic acid], a sEH substrate, as well as sEH-derived free 14,15-DiHETrE [14,15-dihydroxy-5Z,8Z,11Z-eicosatrienoic acid], decreased during winter

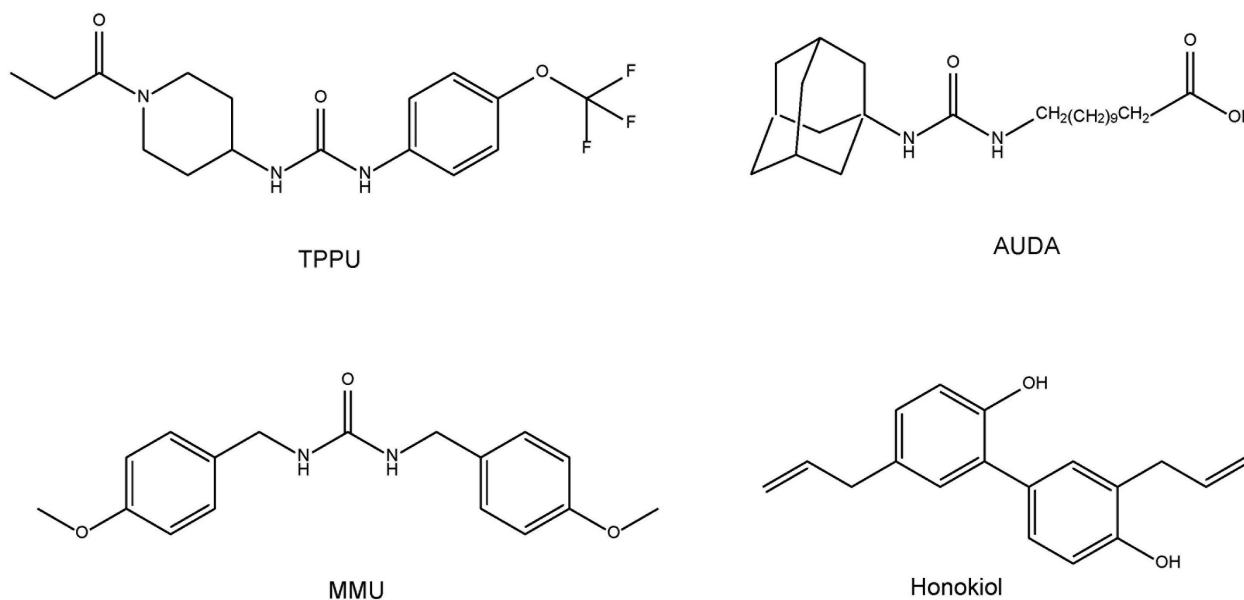


FIGURE 2 | Chemical structure of sEH inhibitors TPPU, AUDA, MMU, and honokiol.

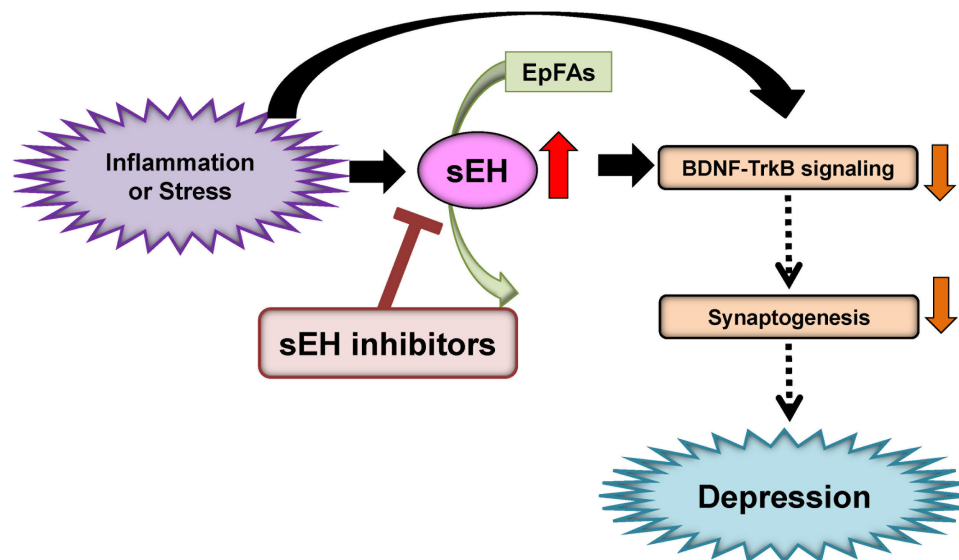


FIGURE 3 | Proposed mechanism of the role of sEH in depression. Inflammation or stress can increase the expression of sEH in the brain, resulting in enhanced metabolism of anti-inflammatory PUFA epoxides (EpFAs). Subsequently, increased expression of sEH can decrease BDNF-TrkB signaling and synaptogenesis, leading to depressive symptoms. The sEH inhibitors may have antidepressant actions in depressed patients. (modified from Hashimoto, 2016).

compared to summer-fall, while sEH-derived total 7,8-DiHDPE [7,8-dihydroxy-4Z,10Z,13Z,16Z,19Z-docosapentaenoic acid], total 19,20-DiHDPE [19,20-dihydroxy-4Z,7Z,10Z,13Z,16Z-docosapentaenoic acid], and total 12,13-DiHOME [12,13-dihydroxy-9Z-octadecenoic acid] were increased during winter. These findings suggest that seasonal shifts in ω -6 and ω -3 PUFAs metabolism mediated by sEH may underlie inflammatory states in symptomatic depression with seasonal pattern (Hennebelle et al., 2017). Given the crucial role of sEH in the metabolism of ω -3 PUFAs, ω -3 PUFAs such as EPA in combination with a sEH inhibitor would be a novel therapeutic approach for depression (Figure 3).

EATING DISORDERS AND ADHD

Anorexia nervosa (AN) is a serious eating disorder characterized by the persistent restriction of energy intake, intense fear of gaining weight, and distribution in self-perceived weight or shape. The Epoxide Hydrolase 2 (*EPHX2*) gene was found to harbor several common and rare risk variants for AN (Scott-Van Zeeland et al., 2014). Subsequently, the patients with AN show elevated plasma levels of ω -3 PUFAs (ARA, EPA, DHA) compared to controls (Shih et al., 2016). Interestingly, 15,16-DiHODE [15,16-dihydroxy-9Z,12Z-octadecadienoic acid]/15,16-EpODE [15,16-epoxy-9Z,12Z-octadecadienoic acid] ratio derived from ARA and 19,20-DiHDPE [19,20-dihydroxy-4Z,7Z,10Z,13Z,16Z-docosapentaenoic acid]/19,20-EpDPE [19,20-epoxy-4Z,7Z,10Z,13Z,16Z-docosapentaenoic acid] ratio derived from DHA in AN patients were higher than controls, suggesting a higher *in vivo* sEH activity, concentration, or efficiency in AN (Shih et al., 2016; Shih, 2017). These data suggest the role of *EPHX2*-associated eicosanoid dysregulations in AN.

Collectively, sEH inhibitors might be potential therapeutic drugs for AN (Shih et al., 2016; Shih, 2017).

Attention deficit hyperactivity disorder (ADHD) is one of the most common psychiatric disorders affecting children. Symptoms of ADHD include inattention, hyperactivity and impulsivity. However, biological mechanisms underlying ADHD remain unknown. A meta-analysis shows that children and youth with ADHD have elevated ratios of both blood ω -6/ ω -3 PUFAs compared to controls (LaChance et al., 2016), suggesting an elevated ω -6/ ω -3, and more specifically ARA/EPA ratio may represent the underlying disturbance in essential PUFAs levels in patients with ADHD. A recent meta-analysis shows that children and adolescents with ADHD have lower levels of DHA, EPA, and total ω -3 PUFAs (Chang et al., 2018). Furthermore, supplementation of ω -3 PUFAs, particularly with high doses of EPA, was modestly effective in the treatment of ADHD (Bloch and Qawasmi, 2011; Chang et al., 2018). Collectively, it is of great interest to study whether blood levels of EpFAs and their corresponding diols are altered in the patients with ADHD. Furthermore, it is also interesting to investigate the role of sEH in the pathogenesis of ADHD since there are no reports showing the role of sEH in ADHD.

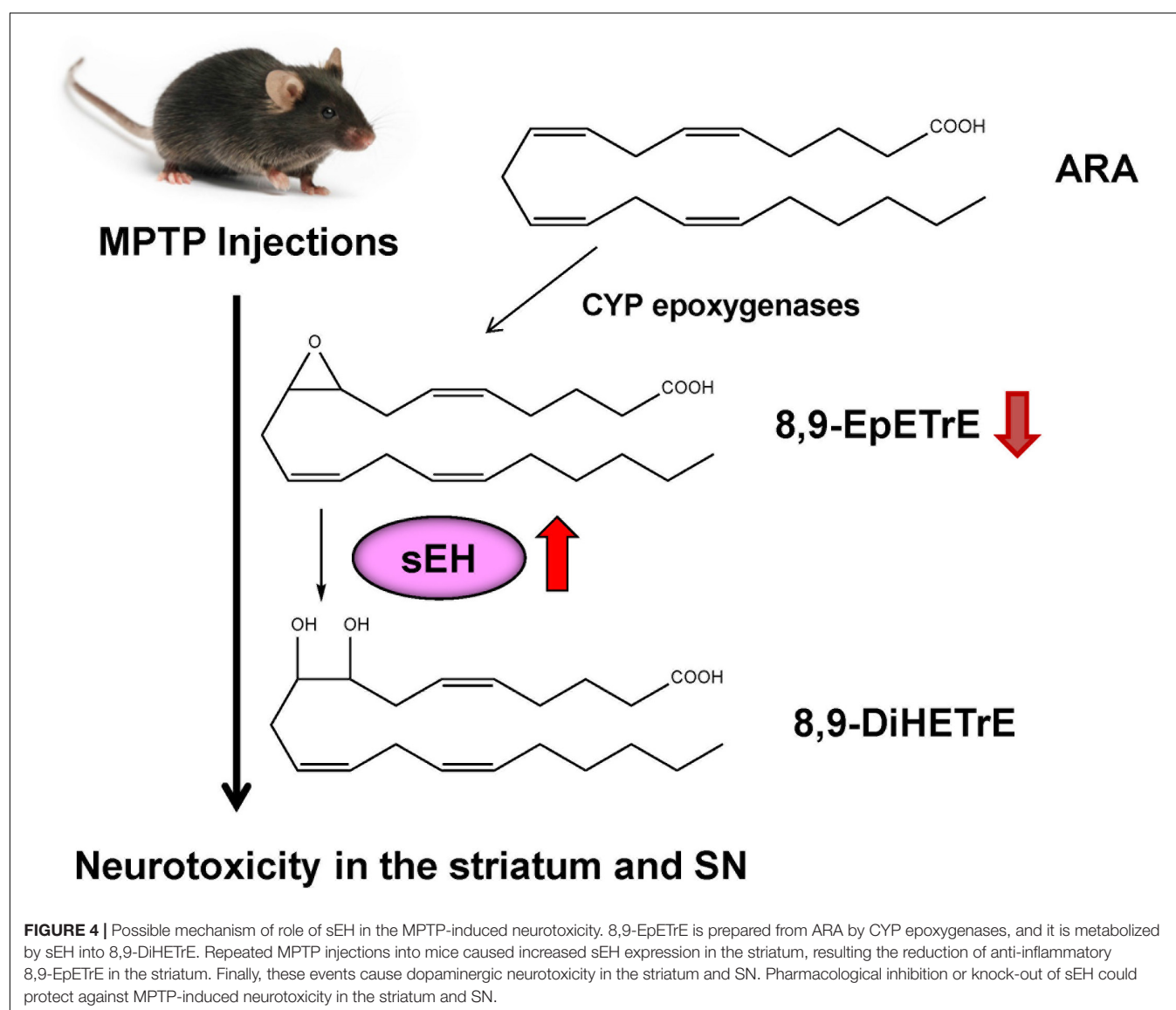
INFLAMMATION IN PARKINSON'S DISEASE AND SEH

Parkinson's disease (PD) is the second most common neurodegenerative disease after Alzheimer's disease. Although the precise pathogenesis of PD is unknown, the pathological hallmark of PD involves the progressive loss of dopaminergic neurons in the substantia nigra (SN) (Kalia and Lang, 2015;

Ascherio and Schwarzschild, 2016). In addition, the deposition of aggregates of α -synuclein, termed Lewy bodies, is evident in multiple brain regions of patients from PD and dementia with Lewy bodies (DLB) (Spillantini et al., 1997). There are, to date, no agents with a disease-modifying or neuroprotective indication for PD has been approved (Dehay et al., 2015). Interestingly, it is noteworthy that PD or DLB patients have depressive symptoms (Cummings, 1992; Takahashi et al., 2009; Goodarzi et al., 2016; Schapira et al., 2017), indicating that management of depression in these patients is also important. Therefore, the development of new drugs possessing disease-modifying and/or neuroprotective properties is unmet medical need.

ω -3 PUFAs appear to be neuroprotective for several neurological disorders. It is reported that dietary intake of PUFAs is associated with lower risk of PD (Kamel et al., 2014; Seidl et al., 2014). MPTP (1-methyl-4-phenyl-1,2,3,6-tetrahydropyridine)-induced neurotoxicity in the striatum and SN has been widely

used as an animal model of PD (Sedelis et al., 2001; Jackson-Lewis and Przedborski, 2007). A diet rich in EPA diminished MPTP-induced hypokinesia in mice and ameliorated procedural memory deficit (Luchtman et al., 2012). Recently, we reported that MPTP-induced neurotoxicity [e.g., loss of dopamine transporter (DAT), loss of tyrosine hydrolase (TH)-positive cells, increased endoplasmic reticulum (ER) stress] in the striatum and SN was attenuated after subsequent repeated oral administration of TPPU (Ren et al., 2018). MPTP-induced loss of TH-positive cells in the SN is also attenuated by pretreatment with another sEH inhibitor, AUDA [12-(((tricyclo(3.3.1.1^{3,7})dec-1-ylamino)carbonyl)amino)-dodecanoic acid] (Figure 2), although posttreatment with AUDA did not attenuate MPTP-induced neurotoxicity (Qin et al., 2015). Furthermore, deletion of the sEH gene protected against MPTP-induced neurotoxicity in the mouse striatum (Huang et al., 2018; Ren et al., 2018), while overexpression of sEH in the striatum significantly enhanced



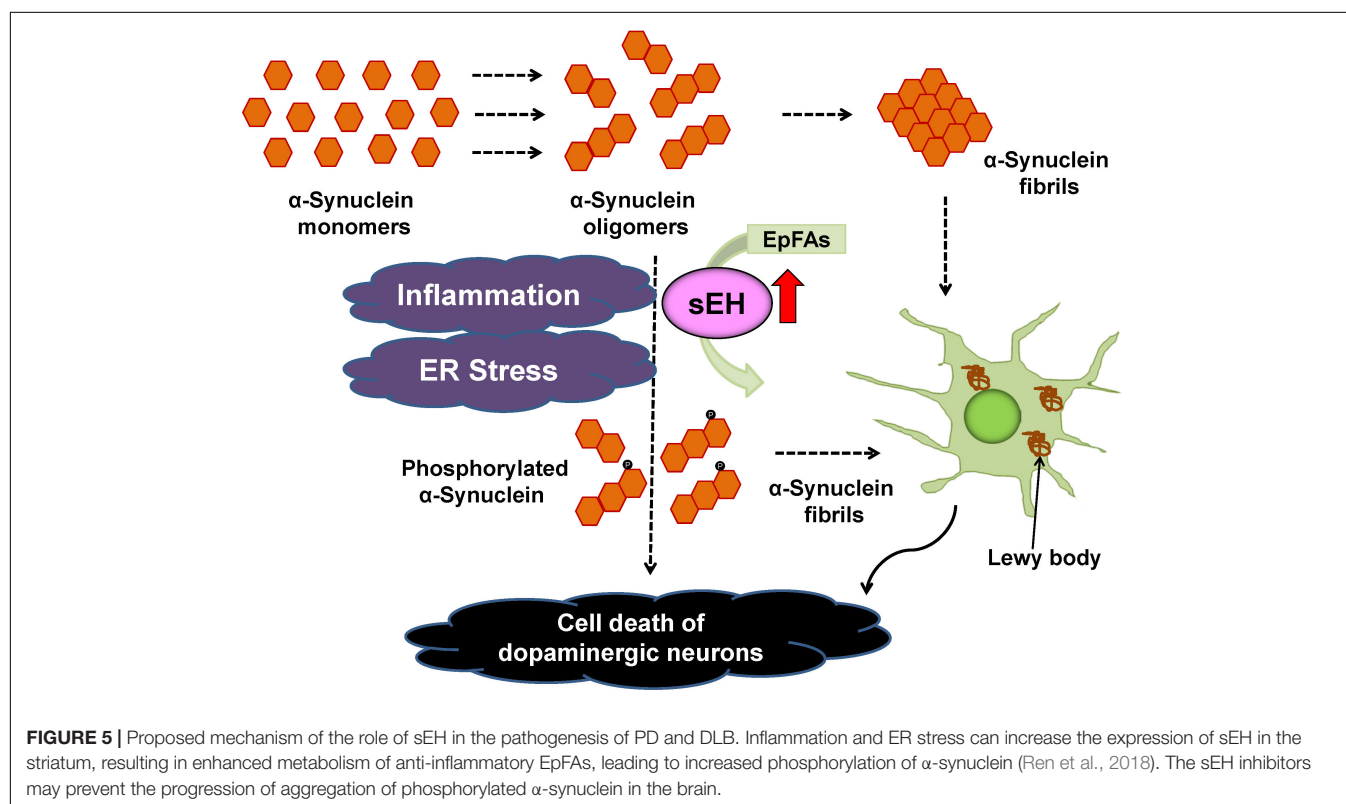
MPTP-induced neurotoxicity (Ren et al., 2018). Moreover, the expression of the sEH protein in the striatum from MPTP-treated mice was significantly higher than control group. Interestingly, there was a positive correlation between sEH expression and phosphorylation of α -synuclein in the striatum, suggesting that sEH may play a role in the phosphorylation of α -synuclein in the mouse striatum (Ren et al., 2018). Oxylipin analysis showed reduced levels of 8,9-epoxy-5Z,11Z,14Z-eicosatrienoic acid (8,9-EpETrE) prepared from ARA in the striatum of MPTP-treated mice, suggesting increased activity of sEH in this region (Figure 4).

Deposition of α -synuclein has been shown in multiple brain regions of PD and DLB patients (Spillantini et al., 1997). Interestingly, the high levels of DHA in brain areas containing α -synuclein in PD patients may support the possible interaction between α -synuclein and DHA (Fecchio et al., 2018). Protein levels of sEH in the striatum from DLB patients were significantly higher than those of the controls, whereas protein levels of DAT and TH in the striatum from DLB patients were significantly lower than those of controls (Ren et al., 2018). Furthermore, the ratio of phosphorylated α -synuclein to α -synuclein in the striatum from DLB patients was significantly higher than that of controls (Ren et al., 2018). Interestingly, there was a positive correlation between sEH levels and the ratio of phosphorylated α -synuclein to α -synuclein in all subjects (Ren et al., 2018). Collectively, it is likely that increased sEH and resulting increase in phosphorylation of α -synuclein may play a role in the pathogenesis of PD.

The PARK2 is one of the familial forms of PDs caused by a mutation in the *PARKIN* gene (Imaizumi et al., 2012). In addition, the expression of *EPHX2* mRNA in human PARK2 iPSC-derived neurons was higher than that of healthy control group. Treatment with TPPU protected against apoptosis in human PARK2 iPSC-derived neurons (Ren et al., 2018). These findings suggest that increased activity of sEH in the striatum plays a key role in the pathogenesis of neurological disorders such as PD and DLB although common polymorphisms within *EPHX2* do not appear to be important risk factors for PD (Farin et al., 2001). Accumulation of aggregated α -synuclein is the pathological hallmark of PD and DLB although its precise role is not understood. Our data suggest a possible interaction between phosphorylation of α -synuclein and sEH expression in the striatum from DLB patients. Taken all together, it is likely that sEH could represent a promising therapeutic target for α -synuclein-related neurological disorders such as PD and DLB (Borlongan, 2018; Ren et al., 2018; Figure 5). In addition, there are also several approaches (e.g., a small-interfering RNA, immunotherapies, enhancement of autophagy) to reduce α -synuclein production (Stoker et al., 2018).

CONCLUSION REMARKS AND FUTURE PERSPECTIVE

Many patients with depression become chronically ill, with several relapses or later recurrences, following initial short-term improvement or remission. Relapses occur at a rate of over 85



percent within a decade of an index depressive episode (Forte et al., 2015; Sim et al., 2015). Therefore, the prevention of relapse and recurrence is important in the management of depression. Taken together, it seems that sEH inhibitors could be prophylactic drugs to prevent or minimize relapses triggered by inflammation and/or stress in remitted patients with depression (Hashimoto, 2016; Ren et al., 2016). In addition, given the comorbidity of depressive symptoms in PD or DLB patients (Cummings, 1992; Takahashi et al., 2009; Goodarzi et al., 2016; Schapira et al., 2017), it is also likely that sEH inhibitors may serve as prophylactic drugs to prevent the progression of PD or DLB in patients.

Some natural compounds with sEH inhibitory action were reported. MMU [1,3-bis (4-methoxybenzyl)urea] (Figure 2), the most abundant (45.3 µg/g dry root weight from the plant *Pentadiplandra brazzeana*), showed an IC₅₀ of 92 nM via fluorescent assay and a Ki of 54 nM via radioactivity-based assay on human sEH (Kitamura et al., 2015). MMU is about 8-fold more potent than previously reported natural product sEH inhibitor honokiol (Lee et al., 2014; Kitamura et al., 2015; Figure 2). These findings may explain partly the pharmacological mechanisms of the traditional medicinal use of the root of *P. brazzeana*. Therefore, it is of interest to study whether the use of the root of *P. brazzeana* has beneficial effects in patients with psychiatric and neurological disorders.

Another topic is the systemic anti-inflammatory effects of sEH inhibition or genetic disruption (Liu et al., 2012; Shahabi et al., 2014). Therefore, it is possible that systemic sEH inhibition may play a role in the beneficial effects in CNS disorders through systemic anti-inflammatory actions of sEH inhibition although

further study on the role of systemic anti-inflammation effects of sEH inhibition is needed. It is also suggested that a paracrine role of EET signaling is responsible for a lot of the beneficial effects of EETs (Spector, 2009; Imig, 2016). Therefore, it is possible that up-regulation of sEH, which results in decreased paracrine EET signaling that exacerbates the disease state although further study on the role of paracrine role of EETs and sEH is needed.

In conclusion, considering the role of sEH in the metabolism of EpFAs (e.g., EETs, EDPs), treatment of ω-3 PUFAs in combination with a sEH inhibitor could represent a novel therapeutic approach for psychiatric and neurological disorders. This approach may well bridge the currently unmet medical needs for these CNS disorders.

AUTHOR CONTRIBUTIONS

The author confirms being the sole contributor of this work and has approved it for publication.

FUNDING

This study was partly supported by grants from AMED, Japan (to KH, JP18dm0107119).

ACKNOWLEDGMENTS

I would like to thank my collaborators who are listed as the co-authors of our papers in the reference list.

REFERENCES

- Arnold, C., Konkel, A., Fischer, R., and Schunck, W. H. (2010). Cytochrome P450-dependent metabolism of omega-6 and omega-3 long-chain polyunsaturated fatty acids. *Pharmacol. Rep.* 62, 536–547. doi: 10.1016/S1734-1140(10)70311-X
- Ascherio, P. A., and Schwarzschild, M. A. (2016). The epidemiology of Parkinson's disease: risk factors and prevention. *Lancet Neurol.* 15, 1257–1272. doi: 10.1016/S1474-4422(16)30230-7
- Bai, Z. G., Bo, A., Wu, S. J., Gai, Q. Y., and Chi, I. (2018). Omega-3 polyunsaturated fatty acids and reduction of depressive symptoms in older adults: a systematic review and meta-analysis. *J. Affect. Disord.* 241, 241–248. doi: 10.1016/j.jad.2018.07.057
- Bazinet, R. P., and Layé, S. (2014). Polyunsaturated fatty acids and their metabolites in brain function and disease. *Nat. Rev. Neurosci.* 15, 771–785. doi: 10.1038/nrn3820
- Bloch, M. H., and Qawasmi, A. (2011). Omega-3 fatty acid supplementation for the treatment of children with attention-deficit/hyperactivity disorder symptomatology: systematic review and meta-analysis. *J. Am. Acad. Child Adolesc. Psychiatry* 50, 991–1000. doi: 10.1016/j.jaac.2011.06.008
- Borlongan, C. V. (2018). Fatty acid chemical mediator provides insights into the pathology and treatment of Parkinson's disease. *Proc. Natl. Acad. Sci. U.S.A.* 115, 6322–6324. doi: 10.1073/pnas.1807276115
- Chang, J. P., Su, K. P., Mondelli, V., and Pariante, C. M. (2018). Omega-3 polyunsaturated fatty acids in youths with attention deficit hyperactivity disorder: a systematic review and meta-analysis of clinical trials and biological studies. *Neuropsychopharmacology* 43, 534–545. doi: 10.1038/npp.2017.160
- Chen, C. T., and Bazinet, R. P. (2015). β-oxidation and rapid metabolism, but not uptake regulate brain eicosapentaenoic acid levels. *Prostaglandins Leukot. Essent. Fatty Acids* 92, 33–40. doi: 10.1016/j.plefa.2014.05.007
- Cummings, J. L. (1992). Depression and Parkinson's disease: a review. *Am. J. Psychiatry* 149, 443–454. doi: 10.1176/ajp.149.4.443
- Dantzer, R., O'Connor, J. C., Freund, G. G., Johnson, R. W., and Kelley, K. W. (2008). From inflammation to sickness and depression: when the immune system subjugates the brain. *Nat. Rev. Neurosci.* 9, 46–57. doi: 10.1038/nrn2297
- Dehay, B., Bourdenx, M., Gorry, P., Przedborski, S., Vila, M., Hunot, S., et al. (2015). Targeting α-synuclein for treatment of Parkinson's disease: mechanistic and therapeutic considerations. *Lancet Neurol.* 14, 855–866. doi: 10.1016/S1474-4422(15)00006-X
- Denis, I., Potier, B., Heberden, C., and Vancassel, S. (2015). Omega-3 polyunsaturated fatty acids and brain aging. *Curr. Opin. Clin. Nutr. Metab. Care* 18, 139–146. doi: 10.1097/MCO.0000000000000141
- Dowlati, Y., Herrmann, N., Swardfager, W., Liu, H., Sham, L., Reim, E. K., et al. (2010). A meta-analysis of cytokines in major depression. *Biol. Psychiatry* 67, 446–457. doi: 10.1016/j.biopsych.2009.09.033
- Dyall, S. C. (2015). Long-chain omega-3 fatty acids and the brain: a review of the independent and shared effects of EPA, DPA and DHA. *Front. Aging Neurosci.* 7:52. doi: 10.3389/fnagi.2015.00052
- Eyre, H. A., Air, T., Pradhan, A., Johnston, J., Lavretsky, H., Stuart, M. J., et al. (2016). A meta-analysis of chemokines in major depression. *Prog. Neuropsychopharmacol. Biol. Psychiatry* 68, 1–8. doi: 10.1016/j.pnpbp.2016.02.006
- Farin, F. M., Janssen, P., Quigley, S., Abbott, D., Hassett, C., Smith-Weller, T., et al. (2001). Genetic polymorphisms of microsomal and soluble epoxide hydrolase

- and the risk of Parkinson's disease. *Pharmacogenetics* 11, 703–708. doi: 10.1097/00008571-200111000-00009
- Fecchio, C., Palazzi, L., and de Laureto, P. P. (2018). α -Synuclein and polyunsaturated fatty acids: molecular basis of the interaction and implication in neurodegeneration. *Molecules* 23:E1531. doi: 10.3390/molecules23071531
- Forste, A., Baldessarini, R. J., Tondo, L., Vázquez, G. H., Pompili, M., and Girardi, P. (2015). Long-term morbidity in bipolar-I, bipolar-II, and unipolar major depressive disorders. *J. Affect. Disord.* 178, 71–78. doi: 10.1016/j.jad.2015.02.011
- Gill, S. S., and Hammock, B. D. (1980). Distribution and properties of a mammalian soluble epoxide hydrolase. *Biochem. Pharmacol.* 29, 389–395. doi: 10.1016/0006-2952(80)90518-3
- Golden, S. A., Covington, H. E., Berton, O., and Russo, S. J. (2011). A standardized protocol for repeated social defeat stress in mice. *Nat. Protoc.* 6, 1183–1191. doi: 10.1038/nprot.2011.361
- Goodarzi, Z., Mirkas, K. J., Roberts, D. J., Jette, N., Pringsheim, T., and Holroyd-Leduc, J. (2016). Detecting depression in Parkinson disease: a systematic review and meta-analysis. *Neurology* 87, 426–437. doi: 10.1212/WNL.0000000000002898
- Grosso, G., Micek, A., Marventano, S., Castellano, S., Mistretta, A., Pajak, A., et al. (2016). Dietary n-3 PUFA, fish consumption and depression: a systematic review and meta-analysis of observational studies. *J. Affect. Disord.* 205, 269–281. doi: 10.1016/j.jad.2016.08.011
- Gumusoglu, S. B., and Stevens, H. E. (2018). Maternal inflammation and neurodevelopmental programming: a review of preclinical outcomes and implications for translational psychiatry. *Biol. Psychiatry* 85, 107–121. doi: 10.1016/j.biopsych.2018.08.008
- Haapakoski, R., Mathieu, J., Ebmeier, K. P., Alenius, H., and Kivimäki, M. (2015). Cumulative meta-analysis of interleukins 6 and 1 β , tumour necrosis factor α and C-reactive protein in patients with major depressive disorder. *Brain Behav. Immun.* 49, 206–215. doi: 10.1016/j.bbi.2015.06.001
- Hallahan, B., Ryan, T., Hibbeln, J. R., Murray, I. T., Glynn, S., Ramsden, C. E., et al. (2016). Efficacy of omega-3 highly unsaturated fatty acids in the treatment of depression. *Br. J. Psychiatry* 209, 192–201. doi: 10.1192/bjp.bp.114.160242
- Hammock, B. D., Gill, S. S., Stamoudis, V., and Gilbert, L. I. (1976). Soluble mammalian epoxide hydratase: action on juvenile hormone and other terpenoid epoxides. *Comp. Biochem. Physiol. B* 53, 263–265. doi: 10.1016/0305-0491(76)90045-6
- Harris, T. R., and Hammock, B. D. (2013). Soluble epoxide hydrolase: gene structure, expression and deletion. *Gene* 526, 61–74. doi: 10.1016/j.gene.2013.05.008
- Hashimoto, K. (2015). Inflammatory biomarkers as differential predictors of antidepressant response. *Int. J. Mol. Sci.* 16, 7796–7801. doi: 10.3390/ijms16047796
- Hashimoto, K. (2016). Soluble epoxide hydrolase: a new therapeutic target for depression. *Expert Opin. Ther. Targets* 20, 1149–1151. doi: 10.1080/14728222.2016.1226284
- Hashimoto, K. (2018). Essential role of Keap1-Nrf2 signaling in mood disorders: overview and future perspective. *Front. Pharmacol.* 9:1182. doi: 10.3389/fphar.2018.01182
- Hennebelle, M., Otaki, Y., Yang, J., Hammock, B. D., Levitt, A. J., Taha, A. Y., et al. (2017). Altered soluble epoxide hydrolase-derived oxylipins in patients with seasonal major depression: an exploratory study. *Psychiatry Res.* 252, 94–101. doi: 10.1016/j.psychres.2017.02.056
- Hsu, M. C., Tung, C. Y., and Chen, H. E. (2018). Omega-3 polyunsaturated fatty acid supplementation in prevention and treatment of maternal depression: putative mechanism and recommendation. *J. Affect. Disord.* 238, 47–61. doi: 10.1016/j.jad.2018.05.018
- Huang, H. J., Wang, Y. T., Lin, H. C., Lee, Y. H., and Lin, A. M. Y. (2018). Soluble epoxide hydrolase inhibition attenuates MPTP-induced in the nigrostriatal dopaminergic system: involvement of α -synuclein aggregation and ER stress. *Mol. Neurobiol.* 55, 138–144. doi: 10.1007/s12035-017-0726-9
- Imaizumi, Y., Okada, Y., Akamatsu, W., Koike, M., Kuzumaki, N., Hayakawa, H., et al. (2012). Mitochondrial dysfunction associated with increased oxidative stress and α -synuclein accumulation in PARK2 iPSC-derived neurons and postmortem brain tissue. *Mol. Brain* 5:35. doi: 10.1186/1756-6606-5-35
- Imig, J. D. (2012). Epoxides and soluble epoxide hydrolase in cardiovascular physiology. *Physiol. Rev.* 92, 101–130. doi: 10.1152/physrev.00021.2011
- Imig, J. D. (2016). Epoxyeicosatrienoic acids and 20-hydroxyeicosatetraenoic acid on endothelial and vascular function. *Adv. Pharmacol.* 77, 105–141. doi: 10.1016/bs.apha.2016.04.003
- Imig, J. D. (2018). Prospective for cytochrome P450 epoxigenase cardiovascular and renal therapeutics. *Pharmacol. Ther.* 192, 1–19. doi: 10.1016/j.pharmthera.2018.06.015
- Imig, J. D., and Hammock, B. D. (2009). Soluble epoxide hydrolase as a therapeutic target for cardiovascular diseases. *Nat. Rev. Drug Discov.* 8, 794–805. doi: 10.1038/nrd2875
- Jackson-Lewis, V., and Przedborski, S. (2007). Protocol for the MPTP mouse model of Parkinson's disease. *Nat. Protoc.* 2, 141–151. doi: 10.1038/nprot.2006.342
- Jamieson, K. L., Endo, T., Darwesh, A. M., Samokhvalov, V., and Seubert, J. M. (2017). Cytochrome P450-derived eicosanoids and heart function. *Pharmacol. Ther.* 179, 47–83. doi: 10.1016/j.pharmthera.2017.05.005
- Jump, D. B. (2002). The biochemistry of n-3 polyunsaturated fatty acids. *J. Biol. Chem.* 277, 8755–8758. doi: 10.1074/jbc.R100062200
- Kalia, L. V., and Lang, A. E. (2015). Parkinson's disease. *Lancet* 386, 896–912. doi: 10.1016/S0140-6736(14)61393-3
- Kamel, F., Goldman, S. M., Umbach, D. M., Chen, H., Richardson, G., Barber, M. R., et al. (2014). Dietary fat intake, pesticide use, and Parkinson's disease. *Parkinsonism Relat. Disord.* 20, 82–87. doi: 10.1016/j.parkreldis.2013.09.023
- Kitamura, S., Morisseau, C., Inceoglu, B., Kamita, S. G., De Nicola, G. R., Nyegue, M., et al. (2015). Potent natural soluble epoxide hydrolase inhibitors from *Pentadiplandra brazzeana* baillon: synthesis, quantification, and measurement of biological activities *in vitro* and *in vivo*. *PLoS One* 10:e0117438. doi: 10.1371/journal.pone.0117438
- Köhler, C. A., Freitas, T. H., Stubbs, B., Maes, M., Solmi, M., Veronese, N., et al. (2018). Peripheral alterations in cytokine and chemokine levels after antidepressant drug treatment for major depressive disorder: systematic review and meta-analysis. *Mol. Neurobiol.* 55, 4195–4206. doi: 10.1007/s12035-017-0632-1
- LaChance, L., McKenzie, K., Taylor, V. H., and Vigod, S. N. (2016). Omega-6 to omega-3 fatty acid ratio in patients with ADHD: a meta-analysis. *J. Can. Acad. Child Adolesc. Psychiatry* 25, 87–96.
- Layé, S., Nadjjar, A., Joffe, C., and Bazinet, R. P. (2018). Anti-inflammatory effects of omega-3 fatty acids in the brain: physiological mechanisms and relevance to pharmacology. *Pharmacol. Rev.* 70, 12–38. doi: 10.1124/pr.117.014092
- Lee, G. H., Ch, S. J., Lee, S. Y., Lee, J. Y., Ma, J. Y., Kim, Y. H., et al. (2014). Discovery of soluble epoxide hydrolase inhibitors from natural products. *Food Chem. Toxicol.* 64, 225–230. doi: 10.1016/j.fct.2013.11.042
- Lin, P. Y., Chang, C. H., Chong, M. F., Chen, H., and Su, K. P. (2017). Polyunsaturated fatty acids in perinatal depression: a systematic review and meta-analysis. *Biol. Psychiatry* 82, 560–569. doi: 10.1016/j.biopsych.2017.02.1182
- Lin, P. Y., Huang, S. Y., and Su, K. P. (2010). A meta-analytic review of polyunsaturated fatty acid compositions in patients with depression. *Biol. Psychiatry* 68, 140–147. doi: 10.1016/j.biopsych.2010.03.018
- Liu, Y., Dang, H., Li, D., Pang, W., Hammock, B. D., and Zhu, Y. (2012). Inhibition of soluble epoxide hydrolase attenuates high-fat-diet-induced hepatic steatosis by reduced systemic inflammatory status in mice. *PLoS One* 7:e39165. doi: 10.1371/journal.pone.0039165
- López-Vicario, C., Alcaraz-Quiles, J., García-Alonso, V., Rius, B., Hwang, S. H., Titos, E., et al. (2015). Inhibition of soluble epoxide hydrolase modulates inflammation and autophagy in obese adipose tissue and liver: role for omega-3 epoxides. *Proc. Natl. Acad. Sci. U.S.A.* 112, 536–541. doi: 10.1073/pnas.1422590112
- Luchtman, D. W., Meng, Q., and Song, C. (2012). Ethyl-eicosapentaenoate (E-EPA) attenuates motor impairments and inflammation in the MPTP-probenecid mouse model of Parkinson's disease. *Behav. Brain Res.* 226, 386–396. doi: 10.1016/j.bbr.2011.09.033
- Ma, M., Ren, Q., Yang, C., Zhang, J. C., Yao, W., Dong, C., et al. (2017). Antidepressant effects of combination of brexpiprazole and fluoxetine on depression-like behavior and dendritic changes in mice after inflammation. *Psychopharmacology* 234, 525–533. doi: 10.1007/s00213-016-4483-7
- Mechawar, N., and Savitz, J. (2016). Neuropathology of mood disorders: do we see the stigmata of inflammation? *Transl. Psychiatry* 6:e946. doi: 10.1038/tp.2016.212

- Mello, A. H., Gassenferth, A., Souza, L. R., Fortunato, J. J., and Rezin, G. T. (2014). ω -3 and major depression: a review. *Acta Neuropsychiatr.* 26, 178–185. doi: 10.1017/neu.2013.52
- Miller, A. H., Haroon, E., and Felger, J. C. (2017). Therapeutic implications of brain-immune interactions: treatment in translation. *Neuropsychopharmacology* 42, 334–359. doi: 10.1038/npp.2016.167
- Miller, A. H., Maletic, V., and Raison, C. L. (2009). Inflammation and its discontents: the role of cytokines in the pathophysiology of major depression. *Biol. Psychiatry* 65, 732–741. doi: 10.1016/j.biopsych.2008.11.029
- Miller, A. H., and Raison, C. L. (2016). The role of inflammation in depression: from evolutionary imperative to modern treatment target. *Nat. Rev. Immunol.* 16, 22–34. doi: 10.1038/nri.2015.5
- Mocking, R. J., Harmsen, I., Assies, J., Koeter, M. W., Ruhé, H. G., and Schene, A. H. (2016). Meta-analysis and meta-regression of omega-3 polyunsaturated fatty acid supplementation for major depressive disorder. *Transl. Psychiatry* 6:e756. doi: 10.1038/tp.2016.29
- Morisseau, C., and Hammock, B. D. (2013). Impact of soluble epoxide hydrolase and epoxyeicosanoids on human health. *Annu. Rev. Pharmacol. Toxicol.* 53, 37–58. doi: 10.1146/annurev-pharmtox-011112-140244
- Nestler, E. J., and Hyman, S. E. (2010). Animal models of neuropsychiatric disorders. *Nat. Rev. Neurosci.* 13, 1161–1169. doi: 10.1038/nn.2647
- Newman, J. W., Morisseau, C., and Hammock, B. D. (2005). Epoxide hydrolases: their roles and interactions with lipid metabolism. *Prog. Lipid Res.* 44, 1–51. doi: 10.1016/j.plipres.2004.10.001
- Newman, J. W., Morisseau, C., Harris, T. R., and Hammock, B. D. (2003). The soluble epoxide hydrolase encoded by EPXH2 is a bifunctional enzyme with novel lipid phosphate phosphatase activity. *Proc. Natl. Acad. Sci. U.S.A.* 100, 1558–1563. doi: 10.1073/pnas.0437724100
- Ota, K., and Hammock, B. D. (1980). Cytosolic and microsomal epoxide hydrolases: differential properties in mammalian liver. *Science* 207, 1479–1481. doi: 10.1126/science.7361100
- Polokowski, A. R., Shakil, H., Carmichael, C. L., and Reigada, L. C. (2018). Omega-3 fatty acids and anxiety: a systematic review of the possible mechanisms at play. *Nutr. Neurosci.* 28, 1–11. doi: 10.1080/1028415X.2018.1525092
- Qin, X., Wu, Q., Lin, L., Sun, A., Liu, S., Li, X., et al. (2015). Soluble epoxide hydrolase deficiency or inhibition attenuates MPTP-induced Parkinsonism. *Mol. Neurobiol.* 52, 187–195. doi: 10.1007/s12035-014-8833-3
- Raison, C. L., Lowry, C. A., and Rook, G. A. (2010). Inflammation, sanitation, and consternation: loss of contact with coevolved, tolerogenic microorganisms and the pathophysiology and treatment of major depression. *Arch. Gen. Psychiatry* 67, 1211–1224. doi: 10.1001/archgenpsychiatry.2010.161
- Ren, Q., Ma, M., Ishima, T., Morisseau, C., Yang, J., Wagner, K. M., et al. (2016). Gene deficiency and pharmacological inhibition of soluble epoxide hydrolase confers resilience to repeated social defeat stress. *Proc. Natl. Acad. Sci. U.S.A.* 113, E1944–E1952. doi: 10.1073/pnas.1601532113
- Ren, Q., Ma, M., Yang, J., Nonaka, R., Yamaguchi, A., Ishikawa, K. I., et al. (2018). Soluble epoxide hydrolase plays a key role in the pathogenesis of Parkinson's disease. *Proc. Natl. Acad. Sci. U.S.A.* 115, E5815–E5823. doi: 10.1073/pnas.1802179115
- Sarris, J., Murphy, J., Mischoulon, D., Papakostas, G. I., Fava, M., Berk, M., et al. (2016). Adjunctive nutraceuticals for depression: a systematic review and meta-analyses. *Am. J. Psychiatry* 173, 575–587. doi: 10.1176/appi.ajp.2016.15091228
- Schapira, A. H. V., Chaudhuri, K. R., and Jenner, P. (2017). Non-motor features of Parkinson disease. *Nat. Rev. Neurosci.* 18, 435–450. doi: 10.1038/nnrn.2017.62
- Scott-Van Zeeland, A. A., Bloss, C. S., Tewhey, R., Bansal, V., Torkamani, A., Libiger, O., et al. (2014). Evidence for the role of EPHX2 gene variants in anorexia nervosa. *Mol. Psychiatry* 19, 724–732. doi: 10.1038/mp.2013.91
- Sedelis, M., Schwarting, R. K. W., and Huston, J. P. (2001). Behavioral phenotyping of the MPTP mouse model of Parkinson's disease. *Behav. Brain Res.* 125, 109–125. doi: 10.1016/S0166-4328(01)00309-6
- Seidl, S. E., Santiago, J. A., Bilyk, H., and Potashkin, J. A. (2014). The emerging role of nutrition in Parkinson's disease. *Front. Aging Neurosci.* 6:36. doi: 10.3389/fnagi.2014.00036
- Shahabi, P., Siest, G., and Visvikis-siest, S. (2014). Influence of inflammation on cardiovascular protective effects of cytochrome P450 epoxygenase-derived epoxyeicosatrienoic acids. *Drug Metab. Rev.* 46, 33–56. doi: 10.3109/03602532.2013.837916
- Shih, P. B. (2017). Integrating multi-omics biomarkers and postprandial metabolism to develop personalized treatment for anorexia nervosa. *Prostaglandins Other Lipid Mediat.* 132, 69–76. doi: 10.1016/j.prostaglandins.2017.02.002
- Shih, P. B., Yang, J., Morisseau, C., German, J. B., Zeeland, A. A., Armando, A. M., et al. (2016). Dysregulation of soluble epoxide hydrolase and lipidomic profiles in anorexia nervosa. *Mol. Psychiatry* 21, 537–546. doi: 10.1038/mp.2015.26
- Sim, K., Lau, W. K., Sim, J., Sum, M. Y., and Baldessarini, R. J. (2015). Prevention of relapse and recurrence in adults with major depressive disorder: systematic review and meta-analyses of controlled trials. *Int. J. Neuropsychopharmacol.* 18:pyv076.
- Spector, A. A. (2009). Arachidonic acid cytochrome P450 epoxygenase pathway. *J. Lipid Res.* 50(Suppl.), S52–S56. doi: 10.1194/jlr.R800038-JLR200
- Spillantini, M. G., Schmidt, M. L., Lee, V. M. Y., Trojanowsky, J. Q., Jakes, R., and Goedert, M. (1997). α -synuclein in Lewy bodies. *Nature* 388, 839–840. doi: 10.1038/42166
- Stoker, T. B., Torsney, K. M., and Barker, R. A. (2018). Emerging treatment approaches for Parkinson's disease. *Front. Neurosci.* 12:693. doi: 10.3389/fnins.2018.00693
- Sublette, M. E., Ellis, S. P., Geant, A. L., and Mann, J. J. (2011). Meta-analysis of the effects of eicosapentaenoic acid (EPA) in clinical trials in depression. *J. Clin. Psychiatry* 72, 1577–1584. doi: 10.4088/JCP.10m06634
- Swardfager, W., Hennebelle, M., Yu, D., Hammock, B. D., Levitt, A. J., Hashimoto, K., et al. (2018). Metabolic/inflammatory/vascular comorbidity in psychiatric disorders; soluble epoxide hydrolase (sEH) as a possible new target. *Neurosci. Biobehav. Rev.* 87, 56–66. doi: 10.1016/j.neubiorev.2018.01.010
- Takahashi, S., Mizukami, K., Yasuno, F., and Asada, T. (2009). Depression associated with dementia with Lewy bodies (DLB) and the effect of somatotherapy. *Psychogeriatrics* 9, 56–61. doi: 10.1111/j.1479-8301.2009.00292.x
- Urquhart, P., Nicolaou, A., and Woodward, D. F. (2015). Endocannabinoids and their oxygenation by cyclo-oxygenases, lipoxygenases and other oxygenases. *Biochim. Biophys. Acta* 1851, 366–376. doi: 10.1016/j.bbali.2014.12.015
- Wagner, K., Vito, S., Inceoglu, B., and Hammock, B. D. (2014). The role of long chain fatty acids and their epoxide metabolites in nociceptive signaling. *Prostaglandins Other Lipid Mediat.* 11, 2–12. doi: 10.1016/j.prostaglandins.2014.09.001
- Wagner, K. M., McReynolds, C. B., Schmidt, W. K., and Hammock, B. D. (2017). Soluble epoxide hydrolase as a therapeutic target for pain, inflammatory and neurodegenerative diseases. *Pharmacol. Ther.* 180, 62–76. doi: 10.1016/j.pharmthera.2017.06.006
- Westphal, C., Konkel, A., and Schunck, W. H. (2015). Cytochrome p450 enzymes in the bioactivation of polyunsaturated Fatty acids and their role in cardiovascular disease. *Adv. Exp. Med. Biol.* 851, 151–187. doi: 10.1007/978-3-319-16009-2_6
- World Health Organization [WHO] (2017). *Depression*. Available at: <http://www.who.int/en/news-room/fact-sheets/detail/depression>
- Wu, Q., Cai, H., Song, J., and Chang, Q. (2017). The effects of sEH inhibitor on depression-like behavior and neurogenesis in male mice. *J. Neurosci. Res.* 95, 2483–2492. doi: 10.1002/jnr.24080
- Yang, C., Qu, Y., Abe, M., Nozawa, D., Chaki, S., and Hashimoto, K. (2017). (R)-Ketamine shows greater potency and longer lasting antidepressant effects than its metabolite (2R,6R)-hydroxynorketamine. *Biol. Psychiatry* 82, e43–e44. doi: 10.1016/j.biopsych.2016.12.020
- Yang, C., Ren, Q., Qu, Y., Zhang, J. C., Ma, M., Dong, C., et al. (2018). Mechanistic target of rapamycin-independent antidepressant effects of (R)-ketamine in a social defeat stress model. *Biol. Psychiatry* 83, 18–28. doi: 10.1016/j.biopsych.2017.05.016
- Yang, C., Shirayama, Y., Zhang, J. C., Ren, Q., Yao, W., Ma, M., et al. (2015). R-ketamine: a rapid-onset and sustained antidepressant without psychotomimetic side effects. *Transl. Psychiatry* 5:e632. doi: 10.1038/tp.2015.136
- Young, J. J., Bruno, D., and Pomara, N. (2014). A review of the relationship between pro-inflammatory cytokines and major depressive disorder. *J. Affect. Disord.* 169, 15–20. doi: 10.1016/j.jad.2014.07.032

- Zhang, J. C., Wu, J., Fujita, Y., Yao, W., Ren, Q., Yang, C., et al. (2014). Antidepressant effects of TrkB ligands on depression-like behavior and dendritic changes in mice after inflammation. *Int. J. Neuropsychopharmacol.* 18:pyu077. doi: 10.1093/ijnp/pyu077
- Zhang, J. C., Yao, W., Dong, C., Yang, C., Ren, Q., Ma, M., et al. (2017a). Blockade of interleukin-6 receptor in the periphery promotes rapid and sustained antidepressant actions: a possible role of gut-microbiota-brain axis. *Transl. Psychiatry* 7:e1138. doi: 10.1038/tp.2017.112
- Zhang, J. C., Yao, W., Dong, C., Yang, C., Ren, Q., Ma, M., et al. (2017b). Prophylactic effects of sulforaphane on depression-like behavior and dendritic changes in mice after inflammation. *J. Nutr. Biochem.* 39, 134–144. doi: 10.1016/j.jnutbio.2016.10.004
- Zhang, J. C., Yao, W., and Hashimoto, K. (2016a). Brain-derived neurotrophic factor (BDNF)-TrkB signaling in inflammation-related depression and potential therapeutic targets. *Curr. Neuropharmacol.* 14, 721–731.
- Zhang, J. C., Yao, W., Ren, Q., Yang, C., Dong, C., Ma, M., et al. (2016b). Depression-like phenotype by deletion of $\alpha 7$ nicotinic acetylcholine receptor: role of BDNF-TrkB in nucleus accumbens. *Sci. Rep.* 6:36705. doi: 10.1038/srep36705

Conflict of Interest Statement: The author declares that the research was conducted in the absence of any commercial or financial relationships that could be construed as a potential conflict of interest.

Copyright © 2019 Hashimoto. This is an open-access article distributed under the terms of the Creative Commons Attribution License (CC BY). The use, distribution or reproduction in other forums is permitted, provided the original author(s) and the copyright owner(s) are credited and that the original publication in this journal is cited, in accordance with accepted academic practice. No use, distribution or reproduction is permitted which does not comply with these terms.



Soluble Epoxide Hydrolase Inhibition for Ocular Diseases: Vision for the Future

Bomina Park^{1,2} and Timothy W. Corson^{1,2,3*}

¹ Department of Ophthalmology, Eugene and Marilyn Glick Eye Institute, Indiana University School of Medicine, Indianapolis, IN, United States, ² Department of Pharmacology and Toxicology, Indiana University School of Medicine, Indianapolis, IN, United States, ³ Department of Biochemistry and Molecular Biology, Indiana University School of Medicine, Indianapolis, IN, United States

OPEN ACCESS

Edited by:

John D. Imig,
Medical College of Wisconsin,
United States

Reviewed by:

Zhongjie Fu,
Boston Children's Hospital and
Harvard Medical School,
United States
Artiom Gruzdev,
National Institute of Environmental
Health Sciences (NIEHS),
United States
Sumanta Kumar Goswami,
University of California, Davis,
United States

*Correspondence:

Timothy W. Corson
tcorson@iu.edu

Specialty section:

This article was submitted to
Translational Pharmacology,
a section of the journal
Frontiers in Pharmacology

Received: 07 November 2018

Accepted: 24 January 2019

Published: 07 February 2019

Citation:

Park B and Corson TW (2019)
Soluble Epoxide Hydrolase Inhibition
for Ocular Diseases: Vision
for the Future.
Front. Pharmacol. 10:95.
doi: 10.3389/fphar.2019.00095

Ocular diseases cause visual impairment and blindness, imposing a devastating impact on quality of life and a substantial societal economic burden. Many such diseases lack universally effective pharmacotherapies. Therefore, understanding the mediators involved in their pathophysiology is necessary for the development of therapeutic strategies. To this end, the hydrolase activity of soluble epoxide hydrolase (sEH) has been explored in the context of several eye diseases, due to its implications in vascular diseases through metabolism of bioactive epoxygenated fatty acids. In this mini-review, we discuss the mounting evidence associating sEH with ocular diseases and its therapeutic value as a target. Substantial data link sEH with the retinal and choroidal neovascularization underlying diseases such as wet age-related macular degeneration, retinopathy of prematurity, and proliferative diabetic retinopathy, although some conflicting results pose challenges for the synthesis of a common mechanism. sEH also shows therapeutic relevance in non-proliferative diabetic retinopathy and diabetic keratopathy, and sEH inhibition has been tested in a uveitis model. Various approaches have been implemented to assess sEH function in the eye, including expression analyses, genetic manipulation, pharmacological targeting of sEH, and modulation of certain lipid metabolites that are upstream and downstream of sEH. On balance, sEH inhibition shows considerable promise for treating multiple eye diseases. The possibility of local delivery of inhibitors makes the eye an appealing target for future sEH drug development initiatives.

Keywords: soluble epoxide hydrolase, small molecule inhibitor, age-related macular degeneration, diabetic retinopathy, diabetic keratopathy, uveitis, angiogenesis

INTRODUCTION

Visual impairment and blindness from ocular diseases can profoundly compromise patients' quality of life, and imposes a substantial economic burden of \$35.4 billion per year in the United States (Rein et al., 2006). The development of anti-vascular endothelial growth factor (anti-VEGF) therapies has advanced treatment for neovascular eye diseases, but these drugs have drawbacks and there is a lack of pharmacotherapies for other ocular diseases (**Figure 1A**) despite consistent and intense expansion in market potential for ocular therapeutics (Kompella et al., 2010).

Understanding the mediators involved in pathophysiology and identification of therapeutic targets and inhibitors are necessary in order to address these unmet therapeutic needs.

There is a growing awareness of the importance of bioactive lipid metabolism to ocular structure, function, and pathology. Especially, the unique lipid profile of the retina gives an outsized role for docosahexaenoic acid (DHA, 22:6 ω -3) and DHA-derived polyunsaturated fatty acid (PUFA) metabolites in the eye (**Figure 1B**). DHA is a major structural component of the membrane phospholipids in the retina (Querques et al., 2011), constituting 50–60% of the total fatty acids in the outer segments of photoreceptors (Stinson et al., 1991; Bush et al., 1994; Stillwell and Wassall, 2003), in contrast to most tissues that contain only a small portion (~5%) of their fatty acids as DHA. In parallel with the arachidonic acid (ARA, 20:4 ω -6) cascade, the metabolism of DHA involves three branches of oxylipin synthesis enzymes: cyclooxygenase (COX), lipoxygenase (LOX), and cytochrome P450 (CYP) epoxygenases, of which the CYPs are responsible for generating bioactive epoxygenated fatty acids (EpFAs) (Morisseau et al., 2010; Zhang et al., 2013; Malamas et al., 2017). EpFAs like epoxyeicosatrienoic acids (EETs) from ω -6 ARA and epoxydocosapentaenoic acids (EDPs) from ω -3 DHA have garnered much attention in vascular disorders due to their vasodilatory and anti-inflammatory properties (Ye et al., 2002; Zhang et al., 2014; Capozzi et al., 2016).

Epoxygenated fatty acids are physiologically unstable because they are rapidly metabolized, mainly by soluble epoxide hydrolase (sEH) (Chacos et al., 1983; **Figure 1B**). sEH, encoded by the *EPHX2* gene, has a C-terminal hydrolase function that acts on lipid epoxides, plus a poorly studied N-terminal phosphatase activity (Harris and Hammock, 2013). Inhibition of sEH stabilizes EpFAs, enhancing their biological activities, which vary among EpFAs derived from ω -6 and ω -3 PUFAs. EETs and EDPs have vasodilatory (Oltman et al., 1998; Zhang et al., 2001; Ye et al., 2002) and analgesic effects, reducing inflammatory pain (Inceoglu et al., 2008; Morisseau et al., 2010; Wagner et al., 2014). But they have contradictory effects on angiogenesis: EETs usually have proangiogenic effects depending on the experimental context (Pozzi et al., 2005; Michaelis et al., 2008; Xu et al., 2013), whereas EDPs have antiangiogenic effects (Zhang et al., 2013; Capozzi et al., 2014; Hasegawa et al., 2017; Hu et al., 2017). Moreover, sEH mediated metabolism of EpFAs produces lipid diols like dihydroxydocosapentaenoic acids (DHDP) (**Figure 1B**). Thus, sEH inhibition can result in tissue specific effects by modulating different classes of EpFAs depending on the abundance of individual PUFAs in the given tissue.

Genetic manipulation of CYP/sEH expression and small molecule mediated targeting of sEH have allowed investigation of the role of EpFAs in eye diseases, in particular diseases mediated by inflammation and angiogenesis. Through the metabolism of bioactive EpFAs and production of corresponding diols, sEH plays a role in the regulation of angiogenesis and inflammation relevant to the pathogenesis of numerous eye diseases. This mini-review discusses sEH as a therapeutic target for eye diseases and the role of PUFA metabolites of CYP and sEH in ocular neovascularization and other ocular disorders.

SEH AND NEOVASCULAR EYE DISEASES

Ocular neovascularization (abnormal angiogenesis) is a prominent feature of blinding eye diseases including proliferative diabetic retinopathy (PDR), retinopathy of prematurity (ROP), and neovascular “wet” age-related macular degeneration (wet AMD) (Das and McGuire, 2003; **Figure 1A**). The new blood vessels that form in these diseases are leaky and prone to rupture, thereby causing vascular leakage, scarring, and even retinal detachment that can lead to permanent vision loss (Hageman et al., 2008). Efforts to treat neovascular eye diseases are hampered by resistance or refractory response to the current standard of care, anti-VEGF therapies (Lux et al., 2007). Therefore, identification of novel therapeutic targets and inhibitors is needed to address the unmet needs in antiangiogenic treatment. Metabolites of ω -3 PUFAs from the CYP-sEH pathway are emerging as important mediators of angiogenesis (Shao et al., 2014; Yanai et al., 2014; Gong et al., 2016a,b).

EpFAs and Angiogenesis

Epoxydocosapentaenoic acids are anti-angiogenic *in vitro*: all the chemically stable EDP regioisomers inhibited VEGF-induced angiogenesis in a Matrigel plug assay (Zhang et al., 2013). Of note, 19,20-EDP, which is the least efficient substrate for sEH, therefore most abundant isomer (Zhang et al., 2014), had no effect on endothelial cell proliferation but strongly inhibited human umbilical vein endothelial cell tubular network formation and migration and weakly inhibited matrix metalloproteinase 2 (MMP-2) activity via a VEGF receptor 2 dependent manner (Zhang et al., 2013), although the exact mechanism through which EDPs crosstalk with VEGF signaling remains to be clarified.

ω -3 EpFAs also have anti-inflammatory and anti-angiogenic effects in animal models of ocular angiogenesis. Dietary intake of ω -3 PUFAs but not ω -6 PUFAs reduces murine laser-induced choroidal neovascularization (L-CNV) (Yanai et al., 2014), a widely used model in which laser ruptures Bruch's membrane, resulting in angiogenesis from the choroid into the subretinal space. This recapitulates key features of wet AMD and serves as a model in which to test anti-angiogenic therapies (Lambert et al., 2013).

Dietary intake of ω -3 PUFAs in mice substantially enhanced levels of 17,18-epoxyeicosatetraenoic acid (EEQ) and 19,20-EDP in the serum lipid profile. However, it did not increase levels of EDPs in the retinal lipid profile. Interestingly, dietary intake of 17,18-EEQ or 19,20-EDP also suppressed CNV, suggesting that the protective effect of ω -3 PUFAs against CNV could be mediated by its downstream epoxy metabolites that are generated by CYP. In addition, dietary ω -3 PUFAs interfered with leukocyte invasion into the CNV lesions, while ω -6 PUFA did not (Yanai et al., 2014). These effects were associated with anti-inflammatory properties of EpFAs. Specifically, they modulated leukocyte rolling velocity by changing the expression of adhesion molecules on the surfaces of leukocytes and in

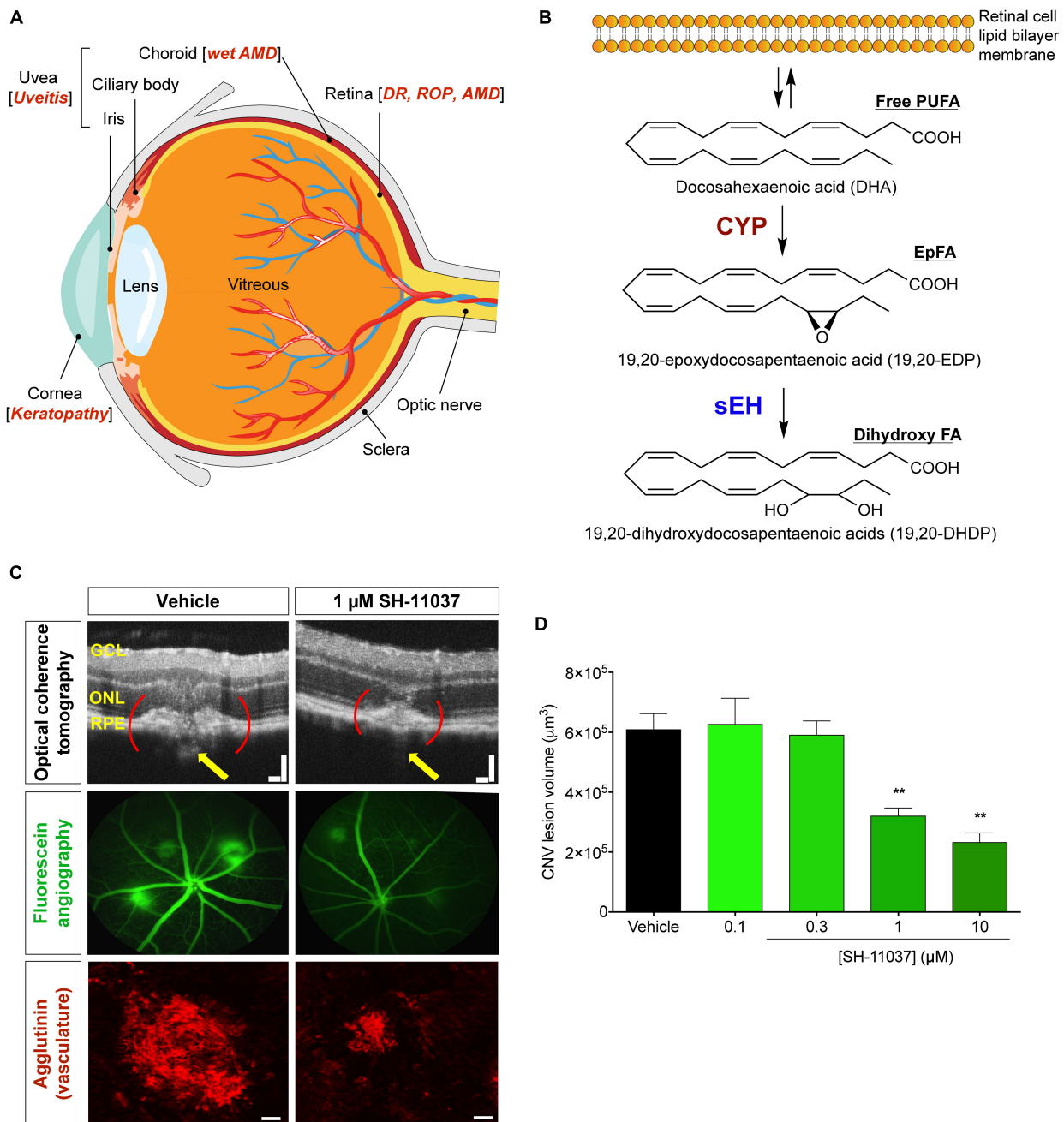


FIGURE 1 | Schematic representation of the eye and PUFA metabolism by the CYP-sEH pathway, and effects of sEH inhibition *in vivo*. **(A)** Common eye diseases and associated structures in the human eye. **(B)** Retina has the highest concentration of ω -3 docosahexaenoic acid of all fatty acids. The regulation of bioactive epoxygenated fatty acids takes place through production by cytochrome P450 epoxygenase and degradation by soluble epoxide hydrolase (sEH). ω -3 fatty acids shown; the same pathway acts on ω -6 fatty acids. **(C,D)** sEH inhibitor SH-11037 dose-dependently suppresses L-CNV lesion volumes. Figure modified from Sulaiman et al. (2016). **(C)** Representative imaging data. Optical coherence tomography obtained 7 days post-laser. Yellow arrows highlight regions containing CNV. Scale bars = 100 μ m. Fluorescein angiography images 14 days post-laser and confocal microscopy images for agglutinin-stained CNV lesions 14 days post-laser. Scale bars = 50 μ m. **(D)** Quantification of CNV lesion volumes from Z-stack images at day 14 using ImageJ software. ** P < 0.01, one-way ANOVA, Tukey's *post hoc* tests, Mean \pm SEM, n = 12 eyes/treatment. AMD, age-related macular degeneration; CYP, cytochrome P450 epoxygenase; DR, diabetic retinopathy; EpFA, epoxygenated fatty acid; FA, fatty acid; PUFA, polyunsaturated fatty acid; ROP, retinopathy of prematurity; sEH, soluble epoxide hydrolase.

the CNV lesions (Hasegawa et al., 2017). In transgenic mice overexpressing CYP2C8 in endothelial cells, the dietary intake of ω -3 PUFAs, which increased production of 17,18-EEQ and

19,20-EDP in serum, reduced CNV lesions (Hasegawa et al., 2017). Likewise, dietary ω -3 PUFAs reduced CNV lesions in *Ephx2*^{-/-} mice. These mice also had increased plasma levels of

17,18-EEQ and 19,20-EDP, since sEH-dependent degradation of these epoxides into corresponding diols was blocked. In contrast, dietary ω -3 PUFAs did not confer inhibitory effects on CNV in mice overexpressing sEH.

The relevance of sEH to CNV was further supported by our recent study that showed an increase in the expression of sEH in the eyes of L-CNV mice and human wet AMD patients (Sulaiman et al., 2018). Interestingly, sEH was upregulated in the photoreceptors, and ocular enzymatic activity of sEH was increased upon L-CNV induction in adult mice. The lipid profile of retina/choroidal tissue of the mice revealed that the ratio of 19,20-EDP to 19,20-DHDP was significantly reduced in L-CNV, suggesting enhanced sEH activity (Sulaiman et al., 2018). In the developing mouse retina, sEH is highly expressed in Müller glia, and DHDP produced by sEH contributes to retinal angiogenesis (Hu et al., 2014). Müller glia span the entire retina radially, providing structural and metabolic support for retinal neurons (Reichenbach and Bringmann, 2013). The Müller cell specific knockout of sEH or systemic deletion of sEH significantly impaired developmental retinal angiogenesis and altered the retinal lipid profile. The level of 19,20-DHDP was significantly reduced in the retina of *Ephx2*^{-/-} mice. Intravitreal injection of 19,20-DHDP rescued impaired retinal angiogenesis in *Ephx2*^{-/-} mice. 19,20-DHDP was also found to be a signaling molecule, downregulating the endothelial Notch signaling pathway by inhibiting presenilin-1 dependent γ -secretase activity, which is required for release of the Notch intracellular domain (Hu et al., 2014). Interestingly, the crosstalk between Notch and VEGF pathways in angiogenesis has been reported in numerous studies, where activation of Notch signaling modulates VEGF signaling (Hellström et al., 2007; Li and Harris, 2009). Given this, inhibition of sEH not only stabilizes the anti-angiogenic and anti-inflammatory ω -3 EpFAs, but also inhibits production of pro-angiogenic DHDP.

Small Molecule sEH Inhibition and Ocular Angiogenesis

Targeting sEH with small molecule inhibitors effectively reduces ocular angiogenesis (Table 1). SH-11037, a synthetic homoisoflavonoid that we developed in cell-based assays and subsequently identified as an sEH inhibitor (Sulaiman et al., 2018), effectively blocked key angiogenic properties of human retinal endothelial cells (HRECs) – proliferation, migration and tube formation – without inducing cell death (Basavarajappa et al., 2015). As well, SH-11037 reduced angiogenesis in an *ex vivo* choroidal sprouting assay and inhibited developmental ocular angiogenesis in zebrafish larvae (Sulaiman et al., 2016). Local application of SH-11037 (1 μ M) into the eye via intravitreal injection significantly suppressed CNV lesions (Sulaiman et al., 2016; Figures 1C,D) and was also effective in reducing retinal neovascularization in the oxygen-induced retinopathy (OIR) model (Basavarajappa et al., 2015), in which neonatal mouse pups are subjected to hyperoxia during their developmental retinal vascularization, causing ischemia-induced angiogenesis on return to normoxia (Scott and Fruttiger, 2009; Kim et al., 2016). Structural, morphological and vascular examination of retina

and electroretinography showed that up to 100 μ M intravitreal SH-11037 does not exert ocular toxicity (Sulaiman et al., 2016). Excitingly, SH-11037 also synergized with anti-VEGF therapy to reduce L-CNV (Sulaiman et al., 2016).

Intravitreal injection of other known sEH inhibitors *t*-AUCB (1–10 μ M) and “compound 7” (10–30 μ M) also suppressed L-CNV lesions (Sulaiman et al., 2018; Table 1). Moreover, intravitreal 10 μ M SH-11037 or *t*-AUCB treatment effectively normalized CNV-induced sEH enzymatic activity and increased the ratio of 19,20-EDP to 19,20-DHDP, indicating that local pharmacological inhibition of sEH can alter the lipid metabolism in the eye (Sulaiman et al., 2018). These studies used 6–15 mice per treatment, plus vehicle injected controls (Basavarajappa et al., 2015; Sulaiman et al., 2016, 2018), which should be sufficient to avoid any confounding effects of inflammation, which is a concern with this delivery route (Chiu et al., 2007). An inhibitory effect on ocular angiogenesis was also reported for other routes of administration of sEH inhibitors. Oral administration of TPPU (1 mg/kg/day) not only reduced CNV lesions and vascular leakage, but also its coadministration with i.p. injection of 17,18-EEQ or 19,20-EDP (50 μ g/kg/day) potentiated anti-angiogenic effects on CNV (Hasegawa et al., 2017). In addition, normal neonatal mice that received i.p. injection of *t*-AUCB (2 mg/kg, twice/day) from 1 to 4 days had significantly reduced retinal vascularization (Hu et al., 2014). Together, these studies support the therapeutic potential of sEH inhibitors for ocular neovascularization.

Conflicts and Controversies

However, some studies do not support the finding that sEH inhibition reduces ocular angiogenesis (Gong et al., 2017). Shao et al. (2014) found that EDP is pro-angiogenic and inhibition of CYP epoxygenase rather than sEH reduced retinal neovascularization in OIR. Systemic overexpression of the CYP epoxygenase CYP2C8 and downregulation of sEH expression in the retina of OIR mice were reflected in the increased and decreased retinal EDP to DHDP ratio, respectively. Dietary ω -3 PUFAs enhanced OIR-induced retinal neovascularization in CYP2C8 overexpressing mice and reduced retinal neovascularization in sEH overexpressing mice. In the aortic ring assay, DHA had an anti-angiogenic effect which was abolished by CYP2C8 overexpression, whereas 19,20-EDP alone had no effect but 19,20-EDP + sEH overexpression reduced aortic sprouting (Shao et al., 2014). However, the macrovessels of the aortic ring do not fully recapitulate microvascular features of the choroid capillaries (Shao et al., 2013).

Panigrahy and colleagues showed that CYP2CJ and CYP2C8 overexpressing mice and *Ephx2*^{-/-} mice had enhanced corneal and neonatal retinal vascularization (Panigrahy et al., 2013) and enhanced tumor dependent corneal angiogenesis (Panigrahy et al., 2012). CYP2C8 inhibition with montelukast further inhibited OIR and L-CNV in mice fed with ω -3 and ω -6 PUFAs, as opposed to sEH inhibition with i.p. injection of UC1770 (0.3 mg/kg) which enhanced OIR and L-CNV (Gong et al., 2016a). Also, UC1770 promoted aortic ring and choroidal sprouting, while montelukast enhanced the anti-angiogenic effects of DHA on aortic and choroidal sprouting,

and HREC proliferation, which were all rescued by 19,20-EDP (Gong et al., 2016a). CYP2C8 inhibition with fenofibrate also further reduced OIR and L-CNV in animals fed with dietary ω -3 PUFAs (Gong et al., 2016b). Again, 19,20-EDP reversed the anti-angiogenic effects of fenofibrate in aortic and choroidal sprouting, HREC migration, and tube formation, in contrast to DHA which enhanced fenofibrate's anti-angiogenic effects (Gong et al., 2016b). Thus, these studies present conflicting results regarding sEH as a therapeutic target for ocular angiogenesis.

Reconciling Disparate Findings

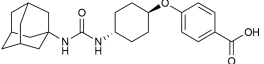
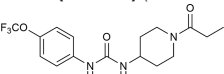
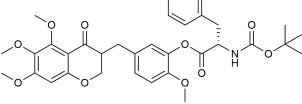
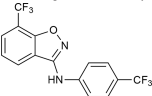
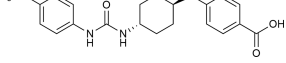
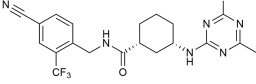
There are important factors to consider in attempting to integrate the conflicting experimental data: stability of EpFAs, routes of administration of CYP or sEH inhibitors and systemic or local modulation of sEH/CYP expression, modulation of other lipid mediator pathways, and experimental design considerations.

First, we cannot conclude that 19,20-EDP promotes ocular angiogenesis when studies added 19,20-EDP into growth media without modulating sEH activity in the aortic ring and choroidal sprouting assay (Gong et al., 2016a,b). Although 19,20-EDP is a fairly stable isomer, it can be converted into its corresponding diol 19,20-DHDP by sEH. Co-treatment with an sEH inhibitor

is required to stabilize 19,20-EDP to ascertain that a change in phenotype is due to 19,20-EDP and to minimize effects from 19,20-DHDP that is generated by sEH activity. Indeed, Hasegawa et al. (2017) demonstrated greater inhibitory effects on L-CNV upon oral administration of sEH inhibitor TPPU + 17,18-EEQ or 19,20-EDP compared to 17,18-EEQ or 19,20-EDP alone. Additionally, aortic rings from *Ephx2*^{-/-} mice treated with 19,20-EDP or 17,18-EEQ did not show any effect on angiogenic sprouting. One explanation for this lack of effect is that the lipid concentration used (1 μ M) (Shao et al., 2014) may be below the inhibitory threshold; further characterization of dose dependent effects of these compounds on angiogenesis may be necessary.

Second, the studies suggesting that inhibition of sEH promotes ocular angiogenesis employed sEH blockade via constitutive *Ephx2*^{-/-} mice (Panigrahy et al., 2013) or oral administration (Gong et al., 2016b) or systemic i.p. injection of sEH inhibitors (Gong et al., 2016a). It is difficult to compare such results to those from tissue specific local targeting of sEH, considering the potential confounding effect of the blood-retina barrier (BRB) and the unique retinal lipid profile. To validate sEH as a key player in ocular angiogenesis, local targeting of

TABLE 1 | Soluble epoxide hydrolase inhibitors tested in ocular disease animal models.

sEH inhibitor (Reference)	Routes	Dose	Model	Reference
t-AUCB (UC1471) (Hwang et al., 2007) 	Oral	2 mg/L	Mouse diabetic retinopathy, sEHI in drinking water for 10 months	Hu et al., 2017
	Intravitreal	1–10 μ M	Mouse L-CNV, single sEHI injection	
	Intraperitoneal	2 mg/kg	Mouse neonatal retinal angiogenesis, twice a day sEHI injections for postnatal (P) days 1–4	Hu et al., 2014
	Subconjunctival	10 nM	Mouse diabetic keratopathy, single sEHI delivery	Sun et al., 2018
TPPU (UC1770) (Rose et al., 2010) 	Intraperitoneal	0.3 mg/kg	Mouse OIR, daily sEHI injections from P12–P16	Gong et al., 2016a
	Oral	1 mg/kg	Mouse L-CNV, daily sEHI injections from day 0–6	
SH-11037 (Basavarajappa et al., 2015) 	Intravitreal	0.1–100 μ M	Mouse ocular toxicity	Sulaiman et al., 2016
		1–10 μ M	Mouse L-CNV, single sEHI injection	
	Systemic (in larvae water)	1–10 μ M	Ocular angiogenesis in zebrafish larvae, sEHI treatment 2–5 days post fertilization (dpf)	Basavarajappa et al., 2015
	Intravitreal	1 μ M	Mouse OIR, single sEHI injection	
“Compound 7” (Shen et al., 2009) 	Intravitreal	10–30 μ M	Mouse L-CNV, single sEHI injection	Sulaiman et al., 2018
t-TUCB (UC1728) (Hwang et al., 2007) 	Subcutaneous	3 mg/kg	Rabbit LPS-induced uveitis, daily sEHI injections	McLellan et al., 2016
GSK2256294A (Podolin et al., 2013) 	Subconjunctival	10 nM	Mouse diabetic keratopathy, single sEHI delivery	Sun et al., 2018

L-CNV, laser-induced choroidal neovascularization; LPS, lipopolysaccharide; OIR, oxygen-induced retinopathy; P, postnatal; sEHI, soluble epoxide hydrolase inhibitor.

sEH (e.g., tissue-specific knockout, intraocular injection, or topical therapy) is necessary. Moreover, sEH inhibition can have opposite effects on angiogenesis depending on tissue levels of fatty acids that are parent to EpFAs. EETs and EDPs are the most abundant epoxy substrates of sEH in ω -6 ARA and ω -3 DHA rich tissues, respectively. EETs usually have proangiogenic effects (Pozzi et al., 2005; Michaelis et al., 2008; Xu et al., 2013) while EDPs have antiangiogenic effects (Zhang et al., 2013; Capozzi et al., 2014; Hasegawa et al., 2017; Hu et al., 2017). Systemic targeting of sEH could accumulate EETs and their effects on angiogenesis could outweigh those of EDPs. Conversely, local targeting of sEH in the eye would predominantly accumulate EDPs since ω -3 DHA is most enriched in retina (Querques et al., 2011). Likewise, levels of EDPs are substantially greater than EETs in retina (Hu et al., 2014).

Third, the studies that showed that DHA delivery and CYP inhibition are antiangiogenic do not necessarily lead to the conclusion that downstream EpFA metabolites are proangiogenic, since CYP inhibition and the resulting accumulation of DHA could lead to accumulation of metabolites from the COX and LOX pathway. The dietary intake of DHA reduced retinal (Connor et al., 2007; Stahl et al., 2010b; Shao et al., 2014; Gong et al., 2016b) and choroidal neovascularization (Moghaddam-Taaheri et al., 2011; Gong et al., 2016a,b), but the inhibition of CYP epoxygenase potentiated the beneficial effect of DHA against ocular angiogenesis, suggesting that the resulting accumulation of DHA or reduced generation of EDP or both are playing a role in ocular angiogenesis. In addition, the results can also be partially explained by studies that show DHA derived metabolites of LOX and COX such as resolvins and neuroprotectin are anti-inflammatory and inhibit retinal angiogenesis (Connor et al., 2007). It is likely that the beneficial effects of exogenous DHA plus CYP blockade are mediated by increasing free DHA that can efficiently compete with ARA for the two other major metabolic pathways, LOX and COX, which produce ARA-derived pro-inflammatory metabolites such as prostaglandins and leukotrienes (Calder, 2010). In addition, certain COX metabolites from EETs were shown to be pro-angiogenic (Rand et al., 2017). Even though inhibition of CYP would reduce the formation of EDP, the effect of increased DHA leading to reduction in COX/LOX-dependent ARA derived pro-inflammatory and pro-angiogenic metabolites, and increase in COX/LOX dependent DHA derived anti-inflammatory metabolites could outweigh the loss of EDP.

Finally, experimental design factors should be considered. The ω -3/ ω -6 lipid composition of mouse chow can vary between facilities, potentially influencing findings. Sex differences in animal models matter, too, given the estrogen dependent suppression of sEH expression (Yang et al., 2018). This could possibly reduce the response to sEH loss/inhibition in female mice whereas response to sEH loss/inhibition could be more apparent in male mice. Among the studies discussed above, many did not specify the sex (Connor et al., 2007; Stahl et al., 2010b; Hu et al., 2014; Shao et al., 2014; Basavarajappa et al., 2015; Gong et al., 2016a,b) while some studies reported using male mice (Panigrahy et al., 2012, 2013; Yanai et al., 2014;

Hasegawa et al., 2017) or female mice (Sulaiman et al., 2016, 2018), thus posing a challenge in assessing potential variability in results due to sex differences. In addition, sex differences and age are critical factors in the L-CNV model, as aged female mice (>9 months) develop more severe CNV lesions than age-matched male mice whereas sex differences are not significant in younger mice (Gong et al., 2015). Reassuringly, mice at 6–8 weeks of age were used in all relevant studies (Yanai et al., 2014; Gong et al., 2016a; Sulaiman et al., 2016, 2018), which is an ideal age range for the L-CNV model (Gong et al., 2015). Likewise, all studies showed rigor in use of littermate controls for the OIR model (Panigrahy et al., 2012; Shao et al., 2014; Basavarajappa et al., 2015; Gong et al., 2016a,b), which is important as mice from larger litters with poor postnatal weight gain develop more severe OIR (Stahl et al., 2010a; Kim et al., 2016).

NON-PROLIFERATIVE DIABETIC RETINOPATHY

Soluble epoxide hydrolase has also been implicated in non-proliferative diabetic retinopathy. This early phase of the disease is characterized by pericyte loss and increased vascular permeability, distinct from the late, proliferative phase characterized by neovascularization (Hammes et al., 2002; **Figure 1A**). A recent study (Hu et al., 2017) reveals that increased retinal expression of sEH and corresponding production of 19,20-DHDP contribute to the progression of non-proliferative diabetic retinopathy in hyperglycemic *Ins2^{Akita}* mouse retinas and in the retinas and vitreous of human diabetic patients. Under normal conditions, retinal endothelial cells are connected by tight junction proteins and supported by pericytes. During the early phase of diabetic retinopathy, 19,20-DHDP alters the distribution of presenilin 1 in lipid rafts of the cell membrane, thereby preventing interaction between presenilin 1 and cadherins and disrupting endothelial cell to pericyte and endothelial cell-to-cell contacts. Treatment with sEH inhibitor *t*-AUCB (**Table 1**) in drinking water (2 mg/L) significantly reduced the retinal level of 19,20-DHDP and normalized vascular defects (reduced pericyte number, enhanced migration of vascular pericytes to the extravascular space, increased acellular capillaries and increased vascular permeability) that were present in the eyes of diabetic mice. Overexpression of sEH (delivered by intravitreal adenovirus) in retinal Müller glia increased retinal 19,20-DHDP and induced retinopathy in non-diabetic mice, highlighting that sEH may play a causative role in progression of the disease (Hu et al., 2017). This mechanism – disrupting endothelial cell junctions of the BRB by sEH-dependent production of 19,20-DHDP – is worth investigating further since defects in the BRB contribute to other eye diseases (Campochiaro et al., 1999; Green, 1999). Furthermore, a recent study reported that sEH inhibitor TPPU reduces fasting glucose level in rats (Minaz et al., 2018). Given this, the antihyperglycemic effect of sEH inhibitors in relation to diabetic retinopathy is also worth exploring.

DIABETIC KERATOPATHY

Diabetic keratopathy is characterized by delayed corneal epithelial wound healing and epithelial erosion, resulting in a compromised defense system against corneal injury and infective agents (Kaji, 2005). sEH is a potential therapeutic target for diabetic keratopathy, as tested in a mouse model where corneal erosions develop upon a single corneal debridement wound (Sun et al., 2018). The expression and enzymatic activity of sEH were increased in the corneal epithelial cells of streptozotocin-induced diabetic epithelial unwounded and wounded mice compared to control mice. *Ephx2*^{-/-} mice with streptozotocin-induced diabetes showed an increase in the rate of epithelial wound healing, decreased sensory nerve degeneration of corneas, and did not develop diabetes-associated dry eye symptoms. The loss of sEH also restored wound-induced STAT3 signaling and heme oxygenase-1 (HO-1) expression that were downregulated by hyperglycemic conditions. Similarly, sEH inhibition with subconjunctival 10 nM *t*-AUCB or clinical candidate inhibitor GSK2256294A (**Table 1**) promoted epithelial wound healing and restored HO-1 expression in diabetic mouse corneas (Sun et al., 2018).

UVEITIS

Uveitis refers to numerous intraocular inflammatory conditions often involving the uvea but not limited to this pigmented tissue layer (Brady et al., 2016; **Figure 1A**). Inhibition of sEH has anti-inflammatory effects in different models of inflammation (Askari et al., 2014; Hasegawa et al., 2017; Zhou et al., 2017). Given that a specific sEH inhibitor UC1728 (*t*-TUCB) (**Table 1**) had anti-inflammatory and analgesic effects in laminitis horses (Guedes et al., 2013), with a favorable pharmacokinetic profile in mice, it was proposed that subcutaneous injection of UC1728 might attenuate lipopolysaccharide (LPS)-induced inflammatory uveitis in rabbits (McLellan et al., 2016). In this model, *Escherichia coli*-derived LPS is injected into the anterior chamber (intracameral injection), inducing acute inflammation. Contrary to the hypothesis, treatment with UC1728 (3 mg/kg) was not efficacious in attenuating this uveitis. However, it is perhaps premature to conclude that sEH does not play a role in uveitis. Analysis of sEH expression and lipid profiles in the affected site may yet reveal sEH involvement that might respond to local treatment.

CONCLUSION AND FUTURE DIRECTIONS

Overall, there is strong evidence that stabilization of anti-inflammatory and anti-angiogenic EpFAs through sEH inhibition could be promising therapies for eye diseases. The unique anatomical and physiological features of the eye as a self-contained unit pose both advantages and disadvantages in drug discovery and delivery. Unlike other parts of the central nervous system, the eye is clinically accessible, allowing targeted drug

delivery via routes of topical eye drops or intraocular injections, thus systemic side effects can be minimized. Conversely, barriers such as the cornea, blood aqueous-barrier and BRB hinder drug transport and absorption (Lee and Pelis, 2016). Therefore, implementing local routes of administration for lipid metabolites or sEH inhibitors in the eye is crucial, as is exploring the rich variety of sEH inhibitors that have been developed both preclinically and clinically (Shen and Hammock, 2012; **Table 1**).

Over the past decade, intravitreal anti-VEGF therapy has significantly advanced the treatment of neovascular eye diseases. But the only current delivery route for anti-VEGF agents, due to their large molecular weight, is intravitreal injection. This can be associated with intraocular inflammation, infection, hemorrhage, elevation of intraocular pressure, and cataract (Geroski and Edelhauser, 2000; Falavarjani and Nguyen, 2013), as well as patient inconvenience. Small molecule sEH inhibitors could provide advantages over anti-VEGF agents as they might be administered through non-invasive routes such as eye drops. Future studies may also reveal certain sEH inhibitors to be BRB permeable when delivered systemically, considering that a blood-brain barrier permeable sEH inhibitor, TPPU, has been characterized (Inceoglu et al., 2013).

Of course, adverse effects are still possible with sEH inhibitors if administered systemically, or if local delivery results in systemic exposure. Some of the compounds discussed here (such as TPPU and *t*-TUCB) have been tested for target specificity, with minimal non-specific binding to pharmacologically important proteins, rendering unexpected adverse effects unlikely (Lee et al., 2014). Nonetheless, it will also be important to assess the overall risk and benefit ratio of sEH inhibitors in the eye regardless of specificity. But polypharmacology can also offer therapeutic benefit: A COX-2/sEH dual inhibitor has been characterized as a potent agent against tumor angiogenesis and tumor growth (Wang et al., 2018). Utilization of such dual inhibitors or combined treatment of sEH inhibitors with other anti-inflammatory agents could also provide therapeutic potential against neovascular and inflammatory eye diseases. Understanding not only the biological activities of EpFAs and diols, but also the mechanisms by which they exert their biological effects in the eye is critical to develop sEH-mediated therapeutic approaches.

AUTHOR CONTRIBUTIONS

BP and TC wrote the manuscript, edited the manuscript, and approved the final version of the manuscript.

FUNDING

Related work in the laboratory of TC was supported by NIH/NEI R01EY025641 and NIH/NCATS UL1TR001108, the Retina Research Foundation, the International Retinal Research Foundation, the BrightFocus Foundation, the Carl Marshall and Mildred Almen Reeves Foundation, and the Indiana Center for Biomedical Innovation.

REFERENCES

- Askari, A. A., Thomson, S., Edin, M. L., Lih, F. B., Zeldin, D. C., and Bishop-Bailey, D. (2014). Basal and inducible anti-inflammatory epoxigenase activity in endothelial cells. *Biochem. Biophys. Res. Commun.* 446, 633–637. doi: 10.1016/j.bbrc.2014.03.020
- Basavarajappa, H. D., Lee, B., Lee, H., Sulaiman, R. S., An, H., Magana, C., et al. (2015). Synthesis and biological evaluation of novel homoisoflavonoids for retinal neovascularization. *J. Med. Chem.* 58, 5015–5027. doi: 10.1021/acs.jmedchem.5b00449
- Brady, C. J., Villanti, A. C., Law, H. A., Rahimy, E., Reddy, R., Sieving, P. C., et al. (2016). Corticosteroid implants for chronic non-infectious uveitis. *Cochrane Database Syst. Rev.* 2:CD010469. doi: 10.1002/14651858.CD010469.pub2
- Bush, R. A., Malnoe, A., Reme, C. E., and Williams, T. P. (1994). Dietary deficiency of N-3 fatty acids alters rhodopsin content and function in the rat retina. *Invest. Ophthalmol. Vis. Sci.* 35, 91–100.
- Calder, P. C. (2010). Omega-3 fatty acids and inflammatory processes. *Nutrients* 2, 355–374. doi: 10.3390/nu2030355
- Campochiaro, P. A., Soloway, P., Ryan, S. J., and Miller, J. W. (1999). The pathogenesis of choroidal neovascularization in patients with age-related macular degeneration. *Mol. Vis.* 5:34.
- Capozzi, M. E., Hammer, S. S., McCollum, G. W., and Penn, J. S. (2016). Epoxygenated fatty acids inhibit retinal vascular inflammation. *Sci. Rep.* 6:39211. doi: 10.1038/srep39211
- Capozzi, M. E., McCollum, G. W., and Penn, J. S. (2014). The role of cytochrome P450 epoxigenases in retinal angiogenesis. *Invest. Ophthalmol. Vis. Sci.* 55, 4253–4260. doi: 10.1167/iops.14-14216
- Chacos, N., Capdevila, J., Falck, J. R., Manna, S., Martin-Wixtrom, C., Gill, S. S., et al. (1983). The reaction of arachidonic acid epoxides (epoxyeicosatrienoic acids) with a cytosolic epoxide hydrolase. *Arch. Biochem. Biophys.* 223, 639–648. doi: 10.1016/0003-9861(83)90628-8
- Chiu, K., Chang, R. C.-C., and So, K.-F. (2007). Intravitreal injection for establishing ocular diseases model. *J. Vis. Exp.* 2007:313. doi: 10.3791/313
- Connor, K. M., SanGiovanni, J. P., Lofqvist, C., Aderman, C. M., Chen, J., Higuchi, A., et al. (2007). Increased dietary intake of omega-3-polyunsaturated fatty acids reduces pathological retinal angiogenesis. *Nat. Med.* 13, 868–873. doi: 10.1038/nm1591
- Das, A., and McGuire, P. G. (2003). Retinal and choroidal angiogenesis: pathophysiology and strategies for inhibition. *Prog. Retin. Eye Res.* 22, 721–748. doi: 10.1016/j.preteyeres.2003.08.001
- Falavarjani, K. G., and Nguyen, Q. D. (2013). Adverse events and complications associated with intravitreal injection of anti-VEGF agents: a review of literature. *Eye* 27, 787–794. doi: 10.1038/eye.2013.107
- Geroski, D. H., and Edelhauser, H. F. (2000). Drug delivery for posterior segment eye disease. *Invest. Ophthalmol. Vis. Sci.* 41, 961–964.
- Gong, Y., Fu, Z., Edin, M. L., Liu, C.-H., Wang, Z., Shao, Z., et al. (2016a). Cytochrome P450 oxidase 2C inhibition adds to ω -3 long-chain polyunsaturated fatty acids protection against retinal and choroidal neovascularization. *Arterioscler. Thromb. Vasc. Biol.* 36, 1919–1927. doi: 10.1161/ATVBAHA.116.307558
- Gong, Y., Shao, Z., Fu, Z., Edin, M. L., Sun, Y., Liegl, R. G., et al. (2016b). Fenofibrate inhibits cytochrome P450 epoxigenase 2C activity to suppress pathological ocular angiogenesis. *eBioMedicine* 13, 201–211. doi: 10.1016/j.ebiom.2016.09.025
- Gong, Y., Fu, Z., Liegl, R., Chen, J., Hellström, A., and Smith, L. E. (2017). ω -3 and ω -6 long-chain PUFAs and their enzymatic metabolites in neovascular eye diseases. *Am. J. Clin. Nutr.* 106, 16–26. doi: 10.3945/ajcn.117.153825
- Gong, Y., Li, J., Sun, Y., Fu, Z., Liu, C.-H., Evans, L., et al. (2015). Optimization of an image-guided laser-induced choroidal neovascularization model in mice. *PLoS One* 10:e0132643. doi: 10.1371/journal.pone.0132643
- Green, W. R. (1999). Histopathology of age-related macular degeneration. *Mol. Vis.* 5:27.
- Guedes, A. G. P., Morisseau, C., Sole, A., Soares, J. H. N., Ulu, A., Dong, H., et al. (2013). Use of a soluble epoxide hydrolase inhibitor as an adjunctive analgesic in a horse with laminitis. *Vet. Anaesth. Analg.* 40, 440–448. doi: 10.1111/vaa.12030
- Hageman, G. S., Gaehrs, K., Johnson, L. V., and Anderson, D. (2008). “Age-related macular degeneration (AMD),” in *The Organization of the Retina and Visual System*, eds H. Kolb, R. Nelson, E. Fernandez, and B. Jones (Salt Lake, UT: University of Utah Health Sciences Center).
- Hammes, H.-P., Lin, J., Renner, O., Shani, M., Lundqvist, A., Betsholtz, C., et al. (2002). Pericytes and the pathogenesis of diabetic retinopathy. *Diabetes* 51, 3107–3112. doi: 10.2337/diabetes.51.10.3107
- Harris, T. R., and Hammock, B. D. (2013). Soluble epoxide hydrolase: gene structure, expression and deletion. *Gene* 526, 61–74. doi: 10.1016/j.gene.2013.05.008
- Hasegawa, E., Inafuku, S., Mulki, L., Okunuki, Y., Yanai, R., Smith, K. E., et al. (2017). Cytochrome P450 monooxygenase lipid metabolites are significant second messengers in the resolution of choroidal neovascularization. *Proc. Natl. Acad. Sci. U.S.A.* 114, E7545–E7553. doi: 10.1073/pnas.1620898114
- Hellström, M., Phng, L.-K., and Gerhardt, H. (2007). VEGF and notch signaling: the yin and yang of angiogenic sprouting. *Cell Adh. Migr.* 1, 133–136. doi: 10.4161/cam.1.3.4978
- Hu, J., Dziubla, S., Lin, J., Bibli, S. I., Zukunft, S., de Mos, J., et al. (2017). Inhibition of soluble epoxide hydrolase prevents diabetic retinopathy. *Nature* 552, 248–252. doi: 10.1038/nature25013
- Hu, J., Popp, R., Fromel, T., Ehling, M., Awwad, K., Adams, R. H., et al. (2014). Muller glia cells regulate notch signaling and retinal angiogenesis via the generation of 19,20-dihydroxydocosapentaenoic acid. *J. Exp. Med.* 211, 281–295. doi: 10.1084/jem.20131494
- Hwang, S. H., Tsai, H.-J., Liu, J.-Y., Morisseau, C., and Hammock, B. D. (2007). Orally bioavailable potent soluble epoxide hydrolase inhibitors. *J. Med. Chem.* 50, 3825–3840. doi: 10.1021/jm070270t
- Inceoglu, B., Jinks, S. L., Ulu, A., Hegedus, C. M., Georgi, K., Schmelzer, K. R., et al. (2008). Soluble epoxide hydrolase and epoxyeicosatrienoic acids modulate two distinct analgesic pathways. *Proc. Natl. Acad. Sci. U.S.A.* 105, 18901–18906. doi: 10.1073/pnas.0809765105
- Inceoglu, B., Zolkowska, D., Yoo, H. J., Wagner, K. M., Yang, J., Hackett, E., et al. (2013). Epoxy fatty acids and inhibition of the soluble epoxide hydrolase selectively modulate GABA mediated neurotransmission to delay onset of seizures. *PLoS One* 8:e80922. doi: 10.1371/journal.pone.0080922
- Kaji, Y. (2005). Prevention of diabetic keratopathy. *Br. J. Ophthalmol.* 89, 254–255. doi: 10.1136/bjo.2004.055541
- Kim, C. B., D’Amore, P. A., and Connor, K. M. (2016). Revisiting the mouse model of oxygen-induced retinopathy. *Eye Brain* 8, 67–79. doi: 10.2147/EB.S94447
- Kompella, U. B., Kadam, R. S., and Lee, V. H. L. (2010). Recent advances in ophthalmic drug delivery. *Ther. Deliv.* 1, 435–456. doi: 10.4155/TDE.10.40
- Lambert, V., Lecomte, J., Hansen, S., Blacher, S., Gonzalez, M. L., Struman, I., et al. (2013). Laser-induced choroidal neovascularization model to study age-related macular degeneration in mice. *Nat. Protoc.* 8, 2197–2211. doi: 10.1038/nprot.2013.135
- Lee, J., and Pelis, R. M. (2016). Drug transport by the blood–aqueous humor barrier of the eye. *Drug Metab. Dispos.* 44, 1675–1681. doi: 10.1124/dmd.116.069369
- Lee, K. S. S., Liu, J.-Y., Wagner, K. M., Pakhomova, S., Dong, H., Morisseau, C., et al. (2014). Optimized inhibitors of soluble epoxide hydrolase improve *in vitro* target residence time and *in vivo* efficacy. *J. Med. Chem.* 57, 7016–7030. doi: 10.1021/jm500694p
- Li, J. L., and Harris, A. L. (2009). Crosstalk of VEGF and Notch pathways in tumour angiogenesis: therapeutic implications. *Front. Biosci.* 14, 3094–3110. doi: 10.2741/3438
- Lux, A., Llacer, H., Heussen, F. M., and Joussen, A. M. (2007). Non-responders to bevacizumab (Avastin) therapy of choroidal neovascular lesions. *Br. J. Ophthalmol.* 91, 1318–1322. doi: 10.1136/bjo.2006.113902
- Malamas, A., Chranioti, A., Tsakalidis, C., Dimitrakos, S. A., and Mataftsi, A. (2017). The omega-3 and retinopathy of prematurity relationship. *Int J Ophthalmol* 10, 300–305. doi: 10.18240/ijo.2017.02.19
- McLellan, G. J., Aktas, Z., Hennes-Beane, E., Kolb, A. W., Larsen, I. V., Schmitz, E. J., et al. (2016). Effect of a soluble epoxide hydrolase inhibitor, UC1728, on LPS-induced uveitis in the rabbit. *J. Ocul. Biol.* 4:24. doi: 10.13188/2334-2838.1000024
- Michaelis, U. R., Xia, N., Barbosa-Sicard, E., Falck, J. R., and Fleming, I. (2008). Role of cytochrome P450 2C epoxigenases in hypoxia-induced cell migration and angiogenesis in retinal endothelial cells. *Invest. Ophthalmol. Vis. Sci.* 49, 1242–1247. doi: 10.1167/iops.07-1087
- Minaz, N., Razdan, R., Hammock, B. D., and Goswami, S. K. (2018). An inhibitor of soluble epoxide hydrolase ameliorates diabetes-induced learning and memory impairment in rats. *Prostaglandins Other Lipid Mediat.* 136, 84–89. doi: 10.1016/j.prostaglandins.2018.05.004
- Moghaddam-Taaheri, S., Agarwal, M., Amaral, J., Fedorova, I., Agron, E., Salem, N. Jr., et al. (2011). Effects of docosahexaenoic acid in preventing experimental

- choroidal neovascularization in rodents. *J. Clin. Exp. Ophthalmol.* 2:187. doi: 10.4172/2155-9570.1000187
- Morisseau, C., Inceoglu, B., Schmelzer, K., Tsai, H. J., Jinks, S. L., Hegedus, C. M., et al. (2010). Naturally occurring monoepoxides of eicosapentaenoic acid and docosahexaenoic acid are bioactive antihyperalgesic lipids. *J. Lipid Res.* 51, 3481–3490. doi: 10.1194/jlr.M006007
- Oltman, C. L., Weintraub, N. L., VanRollins, M., and Dellsperger, K. C. (1998). Epoxyeicosatrienoic acids and dihydroxyeicosatrienoic acids are potent vasodilators in the canine coronary microcirculation. *Circ. Res.* 83, 932–939. doi: 10.1161/01.RES.83.9.932
- Panigrahy, D., Edin, M. L., Lee, C. R., Huang, S., Bielenberg, D. R., Butterfield, C. E., et al. (2012). Epoxyeicosanoids stimulate multiorgan metastasis and tumor dormancy escape in mice. *J. Clin. Invest.* 122, 178–191. doi: 10.1172/JCI58128
- Panigrahy, D., Kalish, B. T., Huang, S., Bielenberg, D. R., Le, H. D., Yang, J., et al. (2013). Epoxyeicosanoids promote organ and tissue regeneration. *Proc. Natl. Acad. Sci. U.S.A.* 110, 13528–13533. doi: 10.1073/pnas.1311565110
- Podolin, P. L., Bolognese, B. J., Foley, J. F., Long, E. III, Peck, B., Umbrecht, S., et al. (2013). *In vitro* and *in vivo* characterization of a novel soluble epoxide hydrolase inhibitor. *Prostaglandins Other Lipid Mediat.* 104–105, 25–31. doi: 10.1016/j.prostaglandins.2013.02.001
- Pozzi, A., Macias-Perez, I., Abair, T., Wei, S., Su, Y., Zent, R., et al. (2005). Characterization of 5,6- and 8,9-epoxyeicosatrienoic acids (5,6- and 8,9-EET) as potent *in vivo* angiogenic lipids. *J. Biol. Chem.* 280, 27138–27146. doi: 10.1074/jbc.M501730200
- Querques, G., Forte, R., and Souied, E. H. (2011). Retina and omega-3. *J. Clin. Nutr. Metab.* 2011:748361. doi: 10.1155/2011/748361
- Rand, A. A., Barnych, B., Morisseau, C., Cajka, T., Lee, K. S. S., Panigrahy, D., et al. (2017). Cyclooxygenase-derived proangiogenic metabolites of epoxyeicosatrienoic acids. *Proc. Natl. Acad. Sci. U.S.A.* 114, 4370–4375. doi: 10.1073/pnas.1616893114
- Reichenbach, A., and Bringmann, A. (2013). New functions of muller cells. *Glia* 61, 651–678. doi: 10.1002/glia.22477
- Rein, D. B., Zhang, P., Wirth, K. E., Lee, P. P., Hoerger, T. J., McCall, N., et al. (2006). The economic burden of major adult visual disorders in the United States. *Arch. Ophthalmol.* 124, 1754–1760. doi: 10.1001/archoph.124.12.1754
- Rose, T. E., Morisseau, C., Liu, J. Y., Inceoglu, B., Jones, P. D., Sanborn, J. R., et al. (2010). 1-Aryl-3-(1-acylpiperidin-4-yl)urea inhibitors of human and murine soluble epoxide hydrolase: structure-activity relationships, pharmacokinetics, and reduction of inflammatory pain. *J. Med. Chem.* 53, 7067–7075. doi: 10.1021/jm100691c
- Scott, A., and Fruttiger, M. (2009). Oxygen-induced retinopathy: a model for vascular pathology in the retina. *Eye* 24, 416–421. doi: 10.1038/eye.2009.306
- Shao, Z., Friedlander, M., Hurst, C. G., Cui, Z., Pei, D. T., Evans, L. P., et al. (2013). Choroid sprouting assay: an *ex vivo* model of microvascular angiogenesis. *PLoS One* 8:e69552. doi: 10.1371/journal.pone.0069552
- Shao, Z., Fu, Z., Stahl, A., Joyal, J.-S., Hatton, C., Juan, A., et al. (2014). Cytochrome P450 2C8 ω 3-long-chain polyunsaturated fatty acid metabolites increase mouse retinal pathologic neovascularization—brief report. *Arterioscler. Thromb. Vasc. Biol.* 34, 581–586. doi: 10.1161/ATVBAHA.113.302927
- Shen, H. C., Ding, F.-X., Deng, Q., Xu, S., Tong, X., Zhang, X., et al. (2009). A strategy of employing aminoheterocycles as amide mimics to identify novel, potent and bioavailable soluble epoxide hydrolase inhibitors. *Bioorg. Med. Chem. Lett.* 19, 5716–5721. doi: 10.1016/j.bmcl.2009.08.006
- Shen, H. C., and Hammock, B. D. (2012). Discovery of inhibitors of soluble epoxide hydrolase: a target with multiple potential therapeutic indications. *J. Med. Chem.* 55, 1789–1808. doi: 10.1021/jm201468j
- Stahl, A., Chen, J., Sapienza, P., Seaward, M. R., Krah, N. M., Dennison, R. J., et al. (2010a). Postnatal weight gain modifies severity and functional outcome of oxygen-induced proliferative retinopathy. *Am. J. Pathol.* 177, 2715–2723. doi: 10.2353/ajpath.2010.100526
- Stahl, A., Sapienza, P., Connor, K. M., Sangiovanni, J. P., Chen, J., Aderman, C. M., et al. (2010b). Short communication: PPAR gamma mediates a direct antiangiogenic effect of omega 3-PUFAs in proliferative retinopathy. *Circ. Res.* 107, 495–500. doi: 10.1161/circresaha.110.221317
- Stillwell, W., and Wassall, S. R. (2003). Docosahexaenoic acid: membrane properties of a unique fatty acid. *Chem. Phys. Lipids* 126, 1–27. doi: 10.1016/S0009-3084(03)00101-4
- Stinson, A. M., Wiegand, R. D., and Anderson, R. E. (1991). Recycling of docosahexaenoic acid in rat retinas during n-3 fatty acid deficiency. *J. Lipid Res.* 32, 2009–2017.
- Sulaiman, R. S., Merrigan, S., Quigley, J., Qi, X., Lee, B., Boulton, M. E., et al. (2016). A novel small molecule ameliorates ocular neovascularisation and synergises with anti-VEGF therapy. *Sci. Rep.* 6:25509. doi: 10.1038/srep25509
- Sulaiman, R. S., Park, B., Sheik Pran Babu, S. P., Si, Y., Kharwadkar, R., Mitter, S. K., et al. (2018). Chemical proteomics reveals soluble epoxide hydrolase as a therapeutic target for ocular neovascularization. *ACS Chem. Biol.* 13, 45–52. doi: 10.1021/acschembio.7b00854
- Sun, H., Lee, P., Yan, C., Gao, N., Wang, J., Fan, X., et al. (2018). Inhibition of soluble epoxide hydrolase 2 ameliorates diabetic keratopathy and impaired wound healing in mouse corneas. *Diabetes* 67, 1162–1172. doi: 10.2337/db17-1336
- Wagner, K., Vito, S., Inceoglu, B., and Hammock, B. D. (2014). The role of long chain fatty acids and their epoxide metabolites in nociceptive signaling. *Prostaglandins Other Lipid Mediat.* 11, 2–12. doi: 10.1016/j.prostaglandins.2014.09.001
- Wang, F., Zhang, H., Ma, A. H., Yu, W., Zimmermann, M., Yang, J., et al. (2018). COX-2/SEH dual inhibitor PTUPB potentiates the antitumor efficacy of cisplatin. *Mol. Cancer Ther.* 17, 474–483. doi: 10.1158/1535-7163.Mct-16-0818
- Xu, D. Y., Davis, B. B., Wang, Z. H., Zhao, S. P., Wasti, B., Liu, Z. L., et al. (2013). A potent soluble epoxide hydrolase inhibitor, t-AUCB, acts through PPARgamma to modulate the function of endothelial progenitor cells from patients with acute myocardial infarction. *Int. J. Cardiol.* 167, 1298–1304. doi: 10.1016/j.ijcard.2012.03.167
- Yanai, R., Mulki, L., Hasegawa, E., Takeuchi, K., Sweigard, H., Suzuki, J., et al. (2014). Cytochrome P450-generated metabolites derived from ω -3 fatty acids attenuate neovascularization. *Proc. Natl. Acad. Sci. U.S.A.* 111, 9603–9608. doi: 10.1073/pnas.1401191111
- Yang, Y. M., Sun, D., Kandhi, S., Froogh, G., Zhuge, J., Huang, W., et al. (2018). Estrogen-dependent epigenetic regulation of soluble epoxide hydrolase via DNA methylation. *Proc. Natl. Acad. Sci. U.S.A.* 115, 613–618. doi: 10.1073/pnas.1716016115
- Ye, D., Zhang, D., Oltman, C., Dellsperger, K., Lee, H. C., and VanRollins, M. (2002). Cytochrome p-450 epoxygenase metabolites of docosahexaenoate potentially dilate coronary arterioles by activating large-conductance calcium-activated potassium channels. *J. Pharmacol. Exp. Ther.* 303, 768–776. doi: 10.1124/jpet.303.2.768
- Zhang, G., Kodani, S., and Hammock, B. D. (2014). Stabilized epoxygenated fatty acids regulate inflammation, pain, angiogenesis and cancer. *Prog. Lipid Res.* 53, 108–123. doi: 10.1016/j.plipres.2013.11.003
- Zhang, G., Panigrahy, D., Mahakian, L. M., Yang, J., Liu, J.-Y., Stephen Lee, K. S., et al. (2013). Epoxy metabolites of docosahexaenoic acid (DHA) inhibit angiogenesis, tumor growth, and metastasis. *Proc. Natl. Acad. Sci. U.S.A.* 110, 6530–6535. doi: 10.1073/pnas.1304321110
- Zhang, Y., Oltman, C. L., Lu, T., Lee, H. C., Dellsperger, K. C., and VanRollins, M. (2001). EET homologs potentially dilate coronary microvessels and activate BK(Ca) channels. *Am. J. Physiol. Heart Circ. Physiol.* 280, H2430–H2440. doi: 10.1152/ajpheart.2001.280.6.H2430
- Zhou, Y., Liu, T., Duan, J. X., Li, P., Sun, G. Y., Liu, Y. P., et al. (2017). Soluble epoxide hydrolase inhibitor attenuates lipopolysaccharide-induced acute lung injury and improves survival in mice. *Shock* 47, 638–645. doi: 10.1097/shk.0000000000000767

Conflict of Interest Statement: TC is a named inventor on patent applications related to this topic and has received related research support from Inclera Therapeutics.

The remaining author declares that the research was conducted in the absence of any commercial or financial relationships that could be construed as a potential conflict of interest.

Copyright © 2019 Park and Corson. This is an open-access article distributed under the terms of the Creative Commons Attribution License (CC BY). The use, distribution or reproduction in other forums is permitted, provided the original author(s) and the copyright owner(s) are credited and that the original publication in this journal is cited, in accordance with accepted academic practice. No use, distribution or reproduction is permitted which does not comply with these terms.



Epoxyeicosatrienoic Acid-Based Therapy Attenuates the Progression of Postischemic Heart Failure in Normotensive Sprague-Dawley but Not in Hypertensive *Ren-2* Transgenic Rats

Jaroslav Hrdlička^{1,2}, Jan Neckář^{1,3*}, František Papoušek¹, Zuzana Husková³, Soňa Kikerlová³, Zdenka Vaňourková³, Zdenka Vernerová³, Firat Akat^{1,4}, Jana Vašinová¹, Bruce D. Hammock⁵, Sung Hee Hwang⁵, John D. Imig⁶, John R. Falck⁷, Luděk Červenka³ and František Kolář¹

OPEN ACCESS

Edited by:

Ali H. Eid,
American University of Beirut,
Lebanon

Reviewed by:

Raffaële Altara,
Oslo University Hospital, Norway
Ning Li,
The Ohio State University,
United States

*Correspondence:

Jan Neckář
jan.neckar@fgu.cas.cz

Specialty section:

This article was submitted to
Translational Pharmacology,
a section of the journal
Frontiers in Pharmacology

Received: 08 November 2018

Accepted: 11 February 2019

Published: 01 March 2019

Citation:

Hrdlička J, Neckář J, Papoušek F, Husková Z, Kikerlová S, Vaňourková Z, Vernerová Z, Akat F, Vašinová J, Hammock BD, Hwang SH, Imig JD, Falck JR, Červenka L and Kolář F (2019) Epoxyeicosatrienoic Acid-Based Therapy Attenuates the Progression of Postischemic Heart Failure in Normotensive Sprague-Dawley but Not in Hypertensive *Ren-2* Transgenic Rats. *Front. Pharmacol.* 10:159. doi: 10.3389/fphar.2019.00159

¹ Institute of Physiology of the Czech Academy of Sciences, Prague, Czechia, ² Department of Physiology, Faculty of Science, Charles University, Prague, Czechia, ³ Center for Experimental Medicine, Institute for Clinical and Experimental Medicine, Prague, Czechia, ⁴ Department of Physiology, Faculty of Medicine, Ankara University, Ankara, Turkey, ⁵ Department of Entomology and Nematology, UC Davis Comprehensive Cancer Center, University of California, Davis, Davis, CA, United States, ⁶ Department of Pharmacology and Toxicology, Medical College of Wisconsin, Milwaukee, WI, United States, ⁷ Department of Biochemistry, University of Texas Southwestern, Dallas, TX, United States

Epoxyeicosatrienoic acids (EETs) and their analogs have been identified as potent antihypertensive compounds with cardio- and renoprotective actions. Here, we examined the effect of EET-A, an orally active EET analog, and c-AUCB, an inhibitor of the EETs degrading enzyme soluble epoxide hydrolase, on the progression of post-myocardial infarction (MI) heart failure (HF) in normotensive Hannover Sprague-Dawley (HanSD) and in heterozygous *Ren-2* transgenic rats (TGR) with angiotensin II-dependent hypertension. Adult male rats (12 weeks old) were subjected to 60-min left anterior descending (LAD) coronary artery occlusion or sham (non-MI) operation. Animals were treated with EET-A and c-AUCB (10 and 1 mg/kg/day, respectively) in drinking water, given alone or combined for 5 weeks starting 24 h after MI induction. Left ventricle (LV) function and geometry were assessed by echocardiography before MI and during the progression of HF. At the end of the study, LV function was determined by catheterization and tissue samples were collected. Ischemic mortality due to the incidence of sustained ventricular fibrillation was significantly higher in TGR than in HanSD rats (35.4 and 17.7%, respectively). MI-induced HF markedly increased LV end-diastolic pressure (P_{ed}) and reduced fractional shortening (FS) and the peak rate of pressure development $[(+dP/dt)_{max}]$ in untreated HanSD compared to sham (non-MI) group [P_{ed} : 30.5 ± 3.3 vs. 9.7 ± 1.3 mmHg; FS: 11.1 ± 1.0 vs. $40.8 \pm 0.5\%$; $(+dP/dt)_{max}$: 3890 ± 291 vs. 5947 ± 309 mmHg/s]. EET-A and c-AUCB, given alone, tended to improve LV function parameters in HanSD rats. Their combination amplified the cardioprotective effect of single therapy and reached significant differences compared to untreated HanSD controls [P_{ed} : 19.4 ± 2.2 mmHg; FS: $14.9 \pm 1.0\%$; $(+dP/dt)_{max}$: 5278 ± 255 mmHg/s].

In TGR, MI resulted in the impairment of LV function like HanSD rats. All treatments reduced the increased level of albuminuria in TGR compared to untreated MI group, but neither single nor combined EET-based therapy improved LV function. Our results indicate that EET-based therapy attenuates the progression of post-MI HF in HanSD, but not in TGR, even though they exhibited renoprotective action in TGR hypertensive rats.

Keywords: epoxyeicosatrienoic acid, soluble epoxide hydrolase, chronic heart failure, hypertension, myocardial infarction, echocardiography

INTRODUCTION

Current experimental and clinical research into pathophysiological mechanisms of cardiovascular diseases provided series of evidences suggesting an increased activity of soluble epoxide hydrolase (sEH) in several heart and kidney disorders (Imig, 2012; Oni-Orisan et al., 2014; Campbell et al., 2017). sEH is an enzyme responsible for rapid conversion of cytochrome P450 arachidonic acid epoxigenase metabolites, the epoxyeicosatrienoic acids (EETs), to inactive or less active dihydroxyeicosatrienoic acids (DHETs). It has been shown that EETs have beneficial action to combat many cardiovascular diseases and their progression including hypertension, ischemic heart diseases, chronic heart failure (CHF), diabetes mellitus, chronic kidney diseases etc. (reviewed in Qiu et al., 2011; Jamieson et al., 2017; Imig, 2018). Therefore, sEH inhibitors represent a potential class of drugs for treating various cardiovascular diseases.

Despite major improvements in the therapy of cardiac disorders, the prevalence of CHF is rising (Braunwald, 2013). In most instances, CHF is the irreversible and final consequence of heart injury associated with high morbidity and mortality. The progression of left ventricle (LV) dysfunction following acute myocardial infarction (MI) is a predominant cause of CHF (Roger, 2013). Regarding the therapeutic effects of EETs on post-MI remodeling, it has been shown that chronic treatment of normotensive rats or mice with sEH inhibitors reduce the progression of LV systolic dysfunction (Li et al., 2009; Merabet et al., 2012; Kompa et al., 2013; Sirish et al., 2013).

It is well known that specific metabolic pathways, including sEH, quickly terminate the biological activity of EETs (Spector and Norris, 2007). To circumvent this limitation of endogenous EETs, several synthetic and more stable EET analogs with markedly longer half-life and promising cardioprotective actions have been developed (Campbell et al., 2017). Previously, it has been shown that NUDSA, the first generation EET analog, increased LV function and decreased cardiac fibrosis in mice after MI (Cao et al., 2015).

Altogether, the EET therapy based on EET analogs or sEH inhibitors can limit a harmful myocardial remodeling associated with the progression of post-MI CHF, however, their combined action was never analyzed. Therefore, here we examined the effect of EET-A (a third generation of EET analog with better water solubility and improved oral bioavailability) and *c*-AUCB (sEH inhibitor), given alone or combined, on the progression of post-MI CHF in normotensive Hannover Sprague-Dawley (HanSD) and in heterozygous *Ren-2* transgenic rats (TGR)

with angiotensin II (Ang II)-dependent form of hypertension. Previously, it has been shown that *c*-AUCB reduced mortality in TGR subjected to aorto-caval fistula, a well-defined model of CHF due to volume overload (Červenka et al., 2015a). Moreover, the same EET-based therapy (EET-A and *c*-AUCB) administered before MI effectively reduced high blood pressure and decreased the incidence of life-threatening ventricular fibrillation in hypertensive TGR (Červenka et al., 2018).

MATERIALS AND METHODS

Animals and Experimental Protocol

HanSD rats and TGR were bred at the Center of Experimental Medicine of the Institute for Clinical and Experimental Medicine in Prague and housed in a controlled environment (23°C, 12 h light-dark cycle; light from 6:00 AM) with free access to water and standard chow diet. The study was conducted in accordance with the Guide for the Care and Use of Laboratory Animals published by the National Academy of Science, National Academy Press, Washington, DC. The experimental protocols were approved by the Animal Care and Use Committee of the Institute of Physiology of the Czech Academy of Sciences.

Adult male HanSD rats and TGR (12 weeks old; *n* = 76 and 90, respectively) were subjected to 60-min regional ischemia or sham operation as described earlier (Hrdlička et al., 2016). Briefly, animals were anesthetized with sodium pentobarbital (60 mg/kg, i.p., Sigma-Aldrich, United States). Intubated rats were ventilated (Ugo Basile, Italy) with room air at 68 strokes/min (tidal volume of 1.2 ml/100 g body weight) and their rectal temperature was maintained between 36.5 and 37.5°C with a heating pad. A left thoracotomy was performed and the pericardium was removed to reveal the location of the left anterior descending (LAD) coronary artery. Then a silk ligature 6/0 (Chirmax, Czech Republic) was placed around the LAD coronary artery about 1–2 mm distal to the origin and an occlusive snare was placed around it. The ends of the suture were threaded through a polyethylene tube. After the surgical preparation, the rats were allowed to stabilize for 10 min before the ischemic intervention. Myocardial ischemia was induced by tightening the ligature around the coronary artery. Sham (non-MI) surgery was performed identically without occlusion. Characteristic changes in myocardial color and the incidence of ischemic arrhythmias verified the complete coronary artery occlusion. At the start of reperfusion, the snare was released, the chest was closed, air was removed from the thorax and spontaneously breathing

animals recovering from anesthesia were housed in separate cages and received analgesia (Ibuprofen, 6 mg/day p.o.) for 3 consecutive days.

Twenty-four hours after surgery, rats of both strains were randomly assigned based on their treatment to the following groups: (i) untreated Sham-operated (non-MI), (ii) post-MI untreated controls, and rats treated by (iii) EET-A (10 mg/kg/day, p.o.), (iv) *c*-AUCB (1 mg/kg/day, p.o.), and (v) a combination of EET-A and *c*-AUCB (10 mg/kg/day and 1 mg/kg/day, respectively, p.o.).

Echocardiography

LV geometry and function were assessed by echocardiography 3 days prior to MI and 5 weeks post-MI using GE Vivid 7 Dimension (GE Vingmed Ultrasound, Horten, Norway) with a 12 MHz linear matrix probe M12L (Hrdlička et al., 2016). Animals were anesthetized with 2% isoflurane (Forane, Abbott Laboratories, Queenborough, United Kingdom) mixed with room air, placed on a heating pad and their rectal temperature was maintained between 36.5 and 37.5°C. Basic 2-D and M-mode in both long and short axis and 4-D mitral flow and pulmonary artery (PA) pulse Doppler measurements were recorded. Heart rate (HR) and following parameters of LV geometry were assessed: end-diastolic and systolic LV cavity diameter (LVDd, LVDs), LV cavity length (LVLd, LVLs), LV cavity area in short axis (LVAd, LVAs), anterior wall thickness (AWTd, AWTs), and posterior wall thickness (PWTd, PWTs). Fractional shortening (FS) and relative wall thickness (RWT) were derived as follows: $FS = 100 * [(LVDd - LVDs) / LVDd]$; $RWT = 100 * [(AWTd + PWTd) / LVDd]$.

Heart Catheterization

At the end of the study, rats anesthetized with 2% isoflurane were subjected to LV catheterization through the right carotid artery using the SPR-407 microtip pressure catheter as described previously (Lee et al., 2008) and data were acquired using MPVS 300 (Millar, Houston, TX, United States), PowerLab 8/30 (ADInstruments, Oxford, United Kingdom). End-diastolic, systolic, and developed pressure and peak rate of pressure development and decline ($+dP/dt$)_{max}, ($-dP/dt$)_{max}, respectively) were assessed from 5 consecutive pressure cycles using LabChart Pro (ADInstruments, Oxford, United Kingdom).

Plasma Monocyte Chemoattractant Protein-1 (MCP-1)

After catheterization, blood was collected from the right ventricle, centrifuged and plasma samples were frozen in liquid nitrogen and stored in -80°C. Plasma concentration of MCP-1 was measured by a quantitative sandwich enzyme immunoassay technique, using a commercially available ELISA kit (BMS631INST, Invitrogen by Thermo Fischer Scientific, Austria).

Kidney Injury Markers

Twenty-four hour urine samples were collected at the end of the five-week post-MI follow-up period. Albumin and cystatin C

were measured by a quantitative sandwich enzyme immunoassay technique, using a commercially available ELISA kits (ERA3201-1, AssayPro, MO, United States; EK1109, BOSTER Biological Technology Co., Ltd., CA, United States). Urine creatinine was determined using Liquick Cor-Creatinine kit without deproteinization (PZ Cormay S.A., Poland). In alkaline solution, picrate reacts with creatinine to form a yellow-red 2,4,6-trinitrocyclohexadienate. The color intensity measured by a photometer at 500 nm is proportional to the creatinine concentration. Albumin data were normalized to the creatinine data. Sodium and potassium levels in urine samples were measured using flame photometer BWB-XP (BWB Technologies, Great Britain).

Kidneys were immersion-fixed in 10% neutral buffered formalin and paraffin embedded. Tissue sections were cut into 4 µm slices for use in histology protocols. Tissue slices were de-paraffinized, re-hydrated and stained with hematoxylin/eosin and periodic acid-Schiff reaction and examined using Nikon Eclipse Ni-E. Slides were evaluated in a blind fashion. Renal damage was expressed as a total index, the sum of glomerulosclerosis and cortical tubulointerstitial injury (CTI).

Glomerulosclerosis/hyalinosis (GSI) was defined as segmental solidification of glomerular capillary tuft, segmental collapse, obliteration of capillary lumen and accumulation of hyaline. One hundred glomeruli per section were randomly selected and evaluated using semiquantitative scoring method. Degree of sclerosis in each glomerulus was graded subjectively: grade 0, normal; grade 1, sclerotic area up to 25% (minimal); grade 2, sclerotic area 25–50% (moderate); grade 3, sclerotic area 50–75% (moderate-severe); and grade 4, sclerotic area 75–100% (severe). GSI index was calculated using the following formula: $GSI = [(1 * n_1) + (2 * n_2) + (3 * n_3) + (4 * n_4)] / (n_0 + n_1 + n_2 + n_3 + n_4)$, where *n* is the number of glomeruli in each grade of glomerulosclerosis.

Cortical tubulointerstitial injury (CTI) was defined as inflammatory cell infiltration, tubular dilatation and/or atrophy, or interstitial fibrosis. Lesions were assessed for at least 30 random and non-overlapping fields in a cortex and were graded semiquantitatively using the following scale: 0, no abnormal findings; 1, mild (up to 25% of the cortex); 2, moderate (25–50% of the cortex); 3, severe (more than 50% of cortex). CTI index was calculated using the following formula: $CTI = [(1 * n_1) + (2 * n_2) + (3 * n_3)] / 30$ (fields), where *n_x* is the number of fields in each grade.

Statistical Analysis

Data are expressed as mean ± SEM. Statistical evaluation were done using GraphPad Prism 6 (GraphPad Software, San Diego, CA, United States). The incidence of mortality was evaluated by Fisher's exact test. For multiple comparison of between group differences one-way analysis of variance (ANOVA) and Holm-Sidak's multiple comparison *post hoc* test were used. The values exceeding 95% probability limits (*P* < 0.05) were considered statistically significant.

RESULTS

Weight Parameters, Mortality, and Plasma MCP-1 Level

At the beginning of the study, the experimental groups did not differ in body weight (BW). A slight reduction in BW was observed one week after MI. From week two post-MI, BW gain occurred and by the end of the study BW did not differ among the groups (Figures 1A,B).

In HanSD rats, the acute ischemic mortality was 17.7% due to the incidence of sustained ventricular fibrillation (sVF); mortality increased to 25.0% by 24 h after MI (Figures 1C,D). Only two additional untreated HanSD rats died during 5 weeks of post-MI period. In TGR, the acute and 24 h mortality were significantly higher (35.4 and 42.7%, respectively) compared to HanSD rats (Figures 1C,D). Moreover, three untreated rats and four rats from each therapy group of TGR died during post-MI period; the post-MI mortality did not differ among TGR groups. Overall, 72.1% (49 out of 68) of HanSD rats and 39.0% (32 out of 82) of TGR subjected to MI survived till the end of the study.

As summarized in Table 1, in untreated HanSD rats MI led to the significant increase in the relative heart weight (HW/BW) compared to Sham (non-MI) group (3.23 ± 0.14 mg/g vs. 2.71 ± 0.14 mg/g). Sham (non-MI) TGR exhibited higher

HW/BW (3.22 ± 0.11 mg/g) than HanSD rats. As compared to HanSD rats, MI had no significant effect on the relative heart weight in TGR (Table 1). Neither single nor combined EET-based therapy significantly affected HW/BW in both strains compared to corresponding untreated MI groups.

The progression of post-MI CHF was associated with significant increase in lungs weight by 139 and 123%, respectively, in untreated HanSD rats and TGR compared to corresponding non-MI controls. In HanSD rats (but not in TGR) treated with EET-A alone or combined with *c*-AUCB, relative lung weight increased only by 65 and 63%, respectively (Table 1). Nevertheless, the observed decreases did not reach statistical significance compared to untreated HanSD rats.

The concentration of MCP-1, a chemotactic cytokine, was analyzed as a marker of systemic inflammation in plasma. As shown in Supplementary Figure S1, neither MI nor EET-based therapy significantly affected MCP-1 levels in both strains at the end of study.

Kidney Injury Markers

Neither MI nor EET-based therapy affected kidney weight, albuminuria, and kidney total injury score in HanSD rats (Table 1 and Figure 2). In untreated TGR, increased levels of kidney injury markers were observed. MI slightly decreased the relative

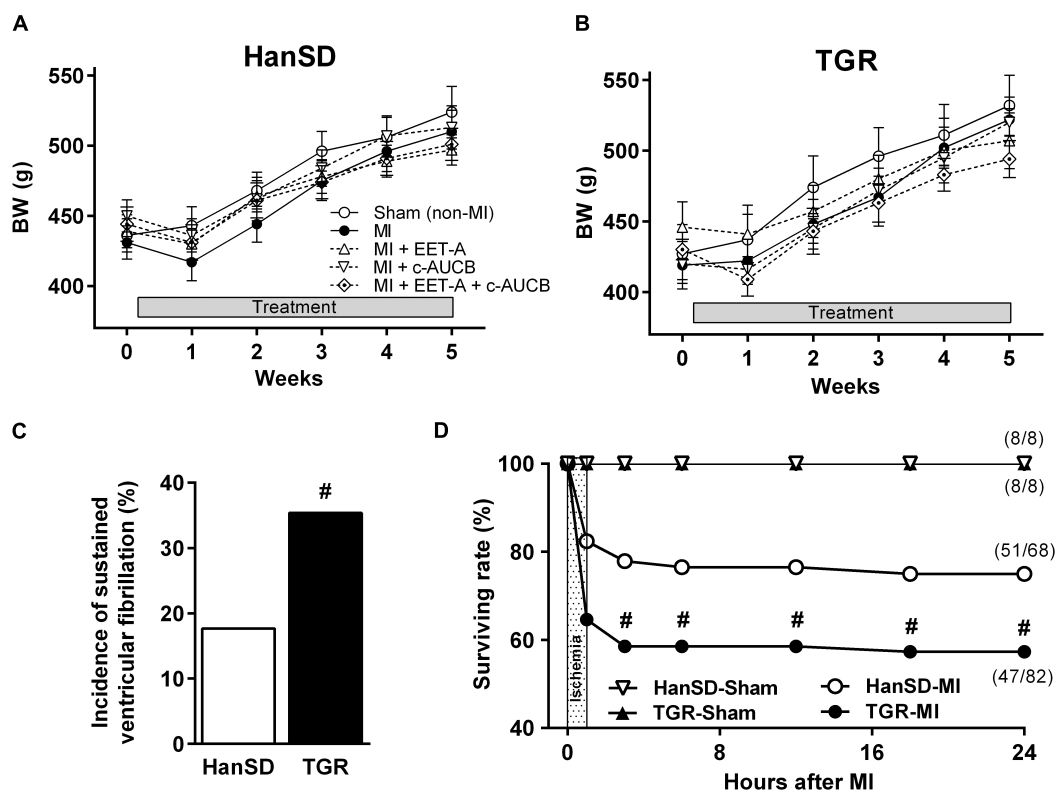


FIGURE 1 | Body weight of Hannover Sprague-Dawley (HanSD; **A**) and *Ren-2* transgenic rats (TGR; **B**) before myocardial infarction (MI) and during 5 weeks of post-MI period and in Sham (non-MI) operated animals. Rats were treated with epoxyeicosatrienoic acid analog (EET-A) or soluble epoxide hydrolase inhibitor (*c*-AUCB), given alone or combined. The incidence of sustained ventricular fibrillation during ischemia (**C**) and 24 h survival rate (**D**) in HanSD and TGR subjected to MI. Values are means \pm SEM. #*P* < 0.05 vs. HanSD.

kidney weight, albuminuria and kidney total injury score (by 13, 45, and 27%). EET-based therapy had no additional effects on kidney weight. EET-A decreased albuminuria in TGR by 56%, though the effect was not significant. However, *c*-AUCB and the combined treatment reduced albuminuria significantly (by 72 and 87%, respectively). EET-based therapy decreased the total index of kidney injury by 43–57% in TGR (**Figure 2B**) but the differences did not reach statistical significances. Finally, neither MI nor EET-based therapy significantly affected urinary excretion of sodium and potassium as well as cystatin C, a marker of renal tubular dysfunction, at the end of study (**Supplementary Figure S2**).

Heart Geometry and Function Assessed by Echocardiography

At the beginning of the study (before MI), AWTd and PWTd reached 2.10 ± 0.07 mm and 2.09 ± 0.04 mm, respectively, in Sham (non-MI) HanSD rats; LV systolic function, determined as FS, was $42.1 \pm 0.9\%$. In Sham (non-MI) TGR, concentric LV hypertrophy and systolic dysfunction was observed (AWTd: 2.60 ± 0.09 mm; PWTd: 2.61 ± 0.07 mm; FS: $36.9 \pm 1.6\%$). Similar differences in diastolic wall thickness and systolic function between Sham (non-MI) HanSD rats and TGR were also observed at the end of study (**Table 2** and **Figure 3**).

As summarized in **Table 2**, MI without treatment resulted in significant decreases in diastolic and systolic AWT and increased LVD in both strains compared to corresponding Sham (non-MI) groups. In the untreated MI group of HanSD rats, systolic PWT was also significantly decreased. These changes in LV geometry were reflected in significantly decreased RWT in both strains (by 31% in HanSD rats and 48% in TGR; **Table 2**). In HanSD rats (but not in TGR), EET-A or *c*-AUCB, given alone, decreased both diastolic (11.24 ± 0.17 and 11.13 ± 0.16 mm,

respectively) and systolic (9.65 ± 0.17 and 9.62 ± 0.20 mm, respectively) LVD compared with untreated MI controls (LVDd: 11.70 ± 0.17 ; LVDs: 10.37 ± 0.21) but the differences did not reach statistical significances. The combined treatment decreased LVDs significantly (9.50 ± 0.29 mm) compared to untreated MI group. Other parameters of LV geometry were not significantly affected by the treatments in any strain (**Table 2**).

MI markedly decreased LV systolic function expressed as FS in untreated animals of both strains (to $11.1 \pm 1.0\%$ and $11.0 \pm 0.9\%$, respectively; **Figure 3**). In HanSD rats, EET-A and *c*-AUCB, given alone, improved FS to $14.1 \pm 0.8\%$ and $13.5 \pm 0.9\%$, respectively, but the increase was not statistically significant. The combined administration of EET-A and *c*-AUCB amplified the cardioprotective effect of single therapy and significantly improved FS to $14.9 \pm 1.0\%$ compared with untreated HanSD controls. In TGR, neither single nor combined EET-based therapy affected LV systolic function (**Figure 3**).

Progression of post-MI heart failure was associated with changes of mitral flow time parameters. In both untreated HanSD rats and TGR, MI significantly increased the LV filling peak velocity, prolonged the isovolumic contraction time, and shortened the filling time, but had no effect on the ejection time and isovolumic relaxation time (**Table 3**). In HanSD rats, *c*-AUCB alone significantly reduced the prolongation of isovolumic contraction time. Combined EET-based therapy shortened the isovolumic contraction time and also prolonged the filling time compared to MI untreated controls. Neither single nor combined EET-based therapy affected CHF-associated changes in time parameters of mitral flow in TGR.

MI reduced the PA peak and mean velocities, but did not change the PA ejection time and acceleration time in both untreated post-MI groups (**Table 3**). In HanSD rats, the PA mean velocity significantly increased after *c*-AUCB as well as combined treatments. Neither single nor combined EET-based therapy affected CHF-associated changes in PA flow in TGR.

TABLE 1 | Relative weights of lung, heart and right kidney of Hannover Sprague-Dawley (HanSD) and *Ren-2* transgenic rats (TGR) subjected to sham operation (non-MI) or myocardial infarction (MI) and treated with epoxyeicosatrienoic acid analog (EET-A) or soluble epoxide hydrolase inhibitor (*c*-AUCB), given alone or combined, for 5 weeks since 24 h after MI.

	n	Heart/BW (mg/g)	Lungs/BW (mg/g)	Kidney/BW (mg/g)
HanSD				
Sham (non-MI)	8	2.71 ± 0.14	2.94 ± 0.07	3.20 ± 0.07
MI	11	$3.23 \pm 0.14^\dagger$	$7.04 \pm 0.82^\dagger$	3.17 ± 0.15
MI + EET-A	14	3.03 ± 0.09	4.84 ± 0.64	3.43 ± 0.06
MI + <i>c</i> -AUCB	10	3.10 ± 0.10	6.63 ± 1.28	3.44 ± 0.09
MI + EET-A + <i>c</i> -AUCB	14	3.00 ± 0.05	4.78 ± 0.75	3.46 ± 0.04
TGR				
Sham (non-MI)	8	3.22 ± 0.11	3.05 ± 0.13	3.57 ± 0.10
MI	8	3.44 ± 0.11	$6.82 \pm 0.59^\dagger$	$3.11 \pm 0.09^\dagger$
MI + EET-A	8	3.19 ± 0.08	6.46 ± 0.97	3.19 ± 0.04
MI + <i>c</i> -AUCB	10	3.19 ± 0.14	6.93 ± 0.74	3.14 ± 0.09
MI + EET-A + <i>c</i> -AUCB	6	3.11 ± 0.11	7.55 ± 1.29	3.07 ± 0.04

BW, body weight; n, number of animals. Values are means \pm SEM. $^\dagger P < 0.05$ MI vs. corresponding Sham (non-MI) group.

Heart Function and Blood Pressure Assessed by Catheterization

As demonstrated in **Figure 4**, the progression of post-MI CHF resulted in impaired LV contractile function. In MI untreated HanSD and TGR groups, the peak rate of pressure development $[(+dp/dt)_{\max}]$ markedly decreased to 3890 ± 291 and 3485 ± 417 mmHg/s, respectively, compared to corresponding Sham (non-MI) groups (5947 ± 301 and 6910 ± 462 mmHg/s, respectively, **Figure 4A**). In HanSD rats, EET-A or *c*-AUCB, given alone, improved $[(+dp/dt)_{\max}]$ to 4596 ± 297 and 4442 ± 287 mmHg/s, respectively, though the effect was not significant. The combined treatment provided the stronger cardioprotective effect (5278 ± 255 mmHg/s) than single therapies reaching significant difference compared to untreated HanSD controls; the peak value of pressure decline $[-(dp/dt)_{\max}]$ exhibited similar changes (**Figure 4A**).

In untreated HanSD and TGR, MI induced significant systolic blood pressure reduction to 104.7 ± 2.6 and 97.0 ± 6.4 mmHg, respectively, compared to corresponding Sham (non-MI) animals (117.7 ± 3.7 and 139.6 ± 4.4 mmHg, respectively). Neither single

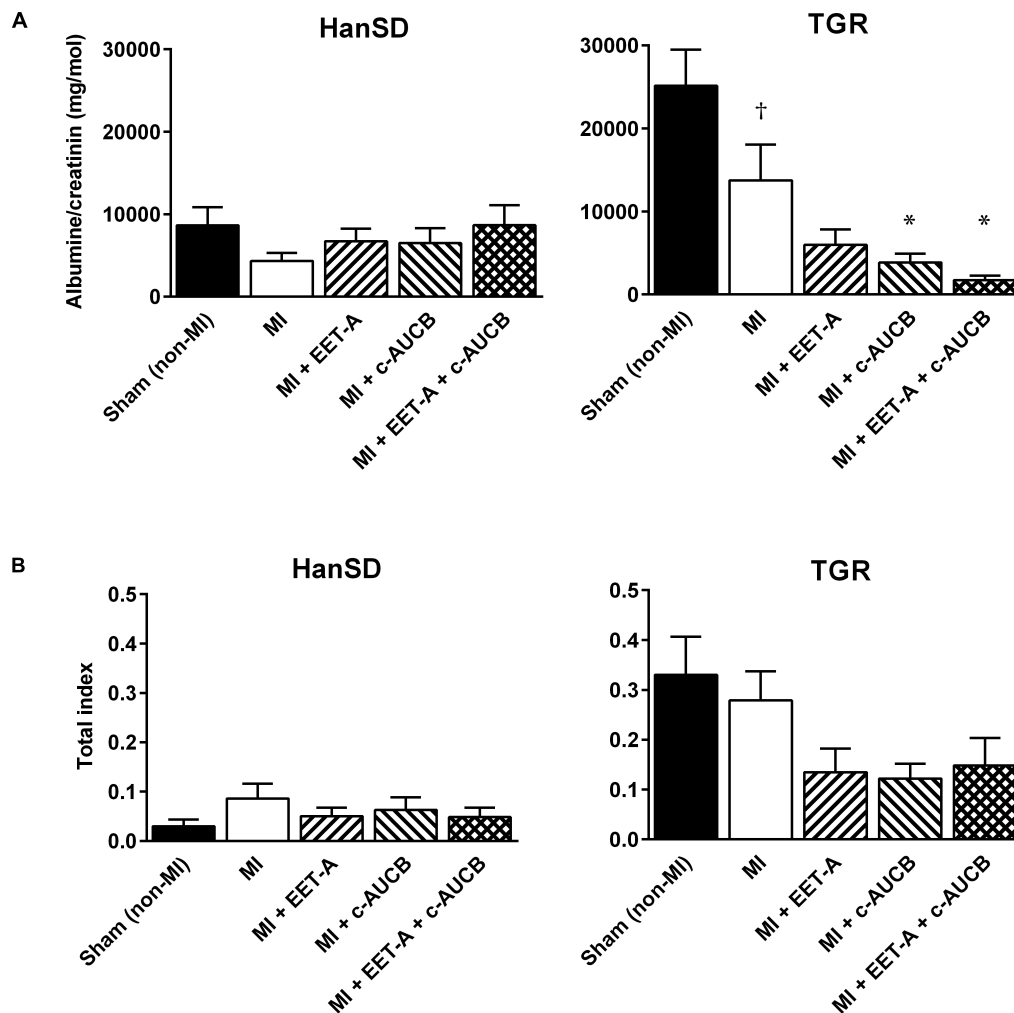


FIGURE 2 | Albumine/Creatinine clearance (**A**) and the total index of kidney injury (the sum of glomerulosclerosis and cortical tubulointerstitial injury; **B**) in Hannover Sprague-Dawley (HanSD) and *Ren-2* transgenic rats (TGR) subjected to sham operation (non-MI) or myocardial infarction (MI) and treated with epoxyeicosatrienoic acid analog (EET-A) or soluble epoxide hydrolase inhibitor (c-AUCB), given alone or combined for 5 weeks since 24 h after MI. Values are means \pm SEM; [†] $P < 0.05$ MI vs. corresponding Sham (non-MI) group; ^{*} $P < 0.05$ vs. corresponding MI group.

nor combined treatment affected systolic blood pressure which varied between 102 and 108 mmHg in HanSD rats and 93–99 mmHg in TGR. In both strains, EET-based therapy did not significantly affect LV developed pressure in animals subjected to MI (**Figure 4B**). However, EET-A treatment, given alone or in combination, significantly reduced high LV end-diastolic pressure to 20.6 ± 2.5 and 19.4 ± 2.2 mmHg, respectively, compared with 30.5 ± 3.3 mmHg in untreated HanSD rats (**Figure 4C**). In TGR, neither single nor combined EET-based therapy affected post-MI LV dysfunction (**Figure 4**).

DISCUSSION

The main finding of the study is that the therapeutic administration of combined EET-based therapy after MI slowed down the progression of post-MI CHF in HanSD rats. As

compared to normotensive strain, neither single nor combined treatment by EET analog and sEH inhibitor affected the progression of post-MI CHF in transgenic rats with Ang II-dependent hypertension. These effects were demonstrated by echocardiography as well as the direct LV catheterization.

In the present study, TGR were used as a well characterized experimental model of monogenetic hypertension of renal origin. The TGR strain [TGR(mRen2)27] was created by Mullins et al. (1990) as a rat model with an additional expression of the murine renin. Heterozygous TGR males reach maximum blood pressure at the age of 8–9 weeks (Lee et al., 1996). It has been demonstrated that TGR develop pathophysiological changes of the heart such as LV hypertrophy and myocardial fibrosis (Bachmann et al., 1992). With respect to the heart function, TGR exhibited unchanged (Habibi et al., 2011; Ma et al., 2012; Neckář et al., 2012; Červenka et al., 2015a; Kovács et al., 2016) or slightly lower LV systolic function (Whaley-Connell et al., 2007;

TABLE 2 | Echocardiographic parameters of left ventricle (LV) and heart rate (HR) in Hannover Sprague-Dawley (HanSD) and *Ren-2* transgenic rats (TGR) subjected to sham operation (non-MI) and myocardial infarction (MI) and treated with epoxyeicosatrienoic acid analog (EET-A) or soluble epoxide hydrolase inhibitor (*c*-AUCB), given alone or combined for 5 weeks since 24 h after MI.

	AWTd (mm)	LVDd (mm)	PWTd (mm)	AWTs (mm)	LVDs (mm)	PWTs (mm)	RWT (%)	HR (bpm)
HanSD								
Sham (non-MI)	2.21 ± 0.09	8.82 ± 0.20	2.28 ± 0.09	3.44 ± 0.11	5.27 ± 0.16	3.39 ± 0.10	51.1 ± 2.1	360 ± 14
MI	1.69 ± 0.08 [†]	11.70 ± 0.17 [†]	2.41 ± 0.10	1.66 ± 0.07 [†]	10.37 ± 0.21 [†]	2.88 ± 0.13 [†]	35.1 ± 0.9 [†]	327 ± 11
MI + EET-A	1.61 ± 0.05	11.24 ± 0.17	2.26 ± 0.07	1.62 ± 0.06	9.65 ± 0.17	2.92 ± 0.09	34.6 ± 0.7	347 ± 8
MI + <i>c</i> -AUCB	1.61 ± 0.05	11.13 ± 0.16	2.34 ± 0.10	1.62 ± 0.05	9.62 ± 0.20	2.95 ± 0.11	35.6 ± 1.2	355 ± 7
MI + EET-A + <i>c</i> -AUCB	1.60 ± 0.07	11.13 ± 0.24	2.16 ± 0.05	1.70 ± 0.12	9.50 ± 0.29*	2.83 ± 0.07	34.0 ± 1.1	356 ± 7
TGR								
Sham (non-MI)	2.64 ± 0.10	8.52 ± 0.17	2.57 ± 0.10	3.66 ± 0.14	5.44 ± 0.13	3.42 ± 0.10	65.1 ± 2.8	373 ± 13
MI	1.95 ± 0.08 [†]	11.65 ± 0.29 [†]	2.41 ± 0.09	2.03 ± 0.15 [†]	10.35 ± 0.33 [†]	3.16 ± 0.11	35.0 ± 1.6 [†]	353 ± 11
MI + EET-A	1.88 ± 0.08	11.19 ± 0.30	2.41 ± 0.05	1.93 ± 0.13	9.90 ± 0.35	3.17 ± 0.06	38.1 ± 2.2	351 ± 15
MI + <i>c</i> -AUCB	1.84 ± 0.06	11.54 ± 0.17	2.40 ± 0.09	1.96 ± 0.14	10.28 ± 0.24	3.00 ± 0.09	35.3 ± 1.0	343 ± 10
MI + EET-A + <i>c</i> -AUCB	1.85 ± 0.08	11.47 ± 0.16	2.43 ± 0.11	1.94 ± 0.18	10.30 ± 0.16	3.10 ± 0.14	35.4 ± 1.7	321 ± 16

AWTd, diastolic anterior wall thickness; LVDd, diastolic LV diameter; PWTd, diastolic posterior wall thickness; AWTs, systolic anterior wall thickness; LVDs, systolic LV diameter; PWTs, systolic posterior wall thickness; RWT, relative wall thickness; bpm, beats per minute. Values are means ± SEM; [†]*P* < 0.05 MI vs. corresponding Sham (non-MI) group; **P* < 0.05 vs. corresponding MI group.

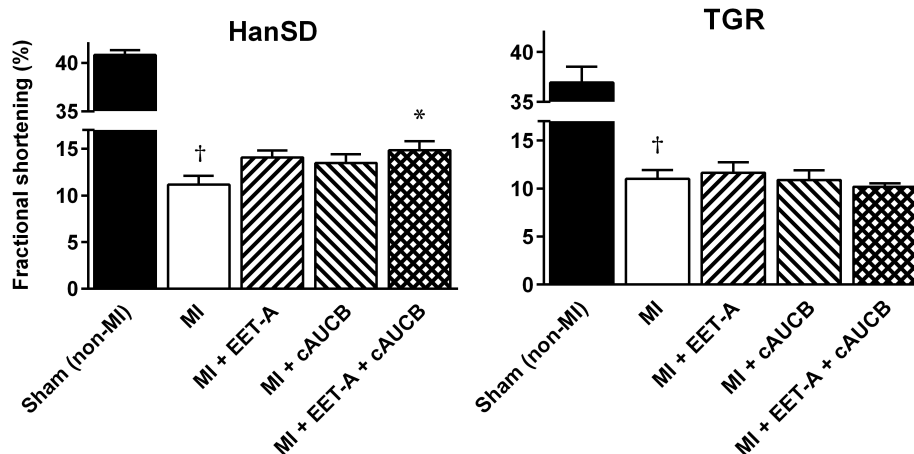


FIGURE 3 | Fractional shortening in Hannover Sprague-Dawley (HanSD) and *Ren-2* transgenic rats (TGR) subjected to Sham (non-MI) operation or myocardial infarction (MI) and treated with epoxyeicosatrienoic acid analog (EET-A) or soluble epoxide hydrolase inhibitor (*c*-AUCB), given alone or combined for 5 weeks since 24 h after MI. Values are means ± SEM; [†]*P* < 0.05 MI vs. corresponding Sham (non-MI) group; **P* < 0.05 vs. corresponding MI group.

De Mello et al., 2013), depending on measured heart parameters and used methods. Further, it has been shown that TGR have increased mortality compared to normotensive HanSD rats when subjected to volume overload (Červenka et al., 2015a,b; Kala et al., 2018). Finally, there is a single paper dealing with the progression of post-MI CHF in TGR (Connelly et al., 2013). Using TGR females, it demonstrated the LV function impairment after MI comparable to our present study. It also showed that combined pharmacological treatment with angiotensin converting enzyme and direct renin inhibition blunted the progression of post-MI CHF.

The present study follows on from our recent report (Červenka et al., 2018) which analyzed the preventive effect of the same EET-based therapy on the acute cardiac ischemic tolerance in HanSD rats and TGR. We demonstrated that EET-A and *c*-AUCB, given alone or combined before MI (two-week

treatment), did not affect the infarct size in both strains and had no additional effects on hearts of HanSD rats. However, both single and combined EET-based therapy lowered high blood pressure, decreased LV hypertrophy and reduced the increased incidence of ischemia-induced ventricular fibrillation in hypertensive TGR (Červenka et al., 2018). These findings provided the impetus to conduct the current experimental study to determine effects of EET-A and *c*-AUCB, given alone or combined after MI.

Here we examined effects of single and combined EET-A treatment on the progression of post-MI CHF. The third generation of orally active EET agonist analogs, including EET-A, demonstrated great potential for therapy of cardiovascular and kidney diseases in rat and mouse models. Indeed, the most promising compounds (EET-A and EET-B) were validated as powerful 14,15-EET analogs (Falck et al., 2014; Khan

TABLE 3 | Doppler echocardiography of mitral and pulmonary artery flow in Hannover Sprague-Dawley (HanSD) and *Ren-2* transgenic rats (TGR) subjected to sham operation (non-MI) and myocardial infarction (MI) and treated with epoxyeicosatrienoic acid analog (EET-A) or soluble epoxide hydrolase inhibitor (*c*-AUCB), given alone or combined for 5 weeks since 24 h after MI.

	Mitral flow					Pulmonary artery flow			
	Vm _{max} (m.s ⁻¹)	FT (ms)	IVCT (ms)	ET (ms)	IVRT (ms)	Vpa _{max} (m.s ⁻¹)	Vpa _{mean} (m.s ⁻¹)	AT (ms)	ETpa (ms)
HanSD									
Sham (non-MI)	1.11 ± 0.04	64.1 ± 3.6	13.9 ± 1.2	67.9 ± 4.4	23.7 ± 1.8	1.06 ± 0.05	0.46 ± 0.02	27.5 ± 1.5	95.1 ± 3.0
MI	1.32 ± 0.04 [†]	45.2 ± 1.7 [†]	49.2 ± 5.3 [†]	61.5 ± 2.0	29.5 ± 1.8	0.77 ± 0.05 [†]	0.31 ± 0.02 [†]	25.4 ± 1.6	92.1 ± 2.2
MI + EET-A	1.29 ± 0.04	49.6 ± 1.6	40.0 ± 5.5	63.7 ± 1.8	25.5 ± 2.2	0.92 ± 0.04	0.39 ± 0.02*	28.0 ± 1.4	91.1 ± 1.2
MI + <i>c</i> -AUCB	1.31 ± 0.06	46.6 ± 1.8	30.5 ± 3.2*	59.9 ± 3.5	30.6 ± 2.7	0.89 ± 0.04	0.37 ± 0.02	27.5 ± 1.9	89.5 ± 2.4
MI + EET-A + <i>c</i> -AUCB	1.17 ± 0.05	54.0 ± 2.0*	31.4 ± 3.7*	57.9 ± 1.9	26.3 ± 1.4	0.92 ± 0.04	0.39 ± 0.02*	27.1 ± 1.4	90.7 ± 1.3
TGR									
Sham (non-MI)	1.20 ± 0.04	59.5 ± 3.0	14.6 ± 1.6	63.8 ± 2.0	21.4 ± 2.6	1.08 ± 0.03	0.47 ± 0.02	28.2 ± 1.3	89.8 ± 1.7
MI	1.51 ± 0.06 [†]	44.8 ± 1.9 [†]	35.9 ± 4.7 [†]	59.1 ± 3.8	32.0 ± 4.3	0.80 ± 0.06 [†]	0.32 ± 0.03 [†]	25.2 ± 1.4	88.1 ± 1.5
MI + EET-A	1.36 ± 0.06	47.0 ± 1.3	41.3 ± 7.3	61.2 ± 4.8	31.3 ± 7.2	0.89 ± 0.05	0.37 ± 0.03	25.4 ± 0.7	87.7 ± 1.5
MI + <i>c</i> -AUCB	1.38 ± 0.06	47.0 ± 2.5	46.1 ± 5.8	64.8 ± 2.9	20.7 ± 1.7	0.83 ± 0.04	0.34 ± 0.03	26.3 ± 1.3	90.4 ± 2.0
MI + EET-A + <i>c</i> -AUCB	1.27 ± 0.09	43.1 ± 3.5	56.2 ± 9.4	61.0 ± 4.7	29.0 ± 3.8	0.75 ± 0.04	0.30 ± 0.03	26.7 ± 1.7	91.2 ± 1.3

Vm_{max}, left ventricle filling peak velocity; FT, filling time; IVCT, isovolumic contraction time; ET, left ventricle ejection time; IVRT, isovolumic relaxation time; Vpa_{max}, peak velocity; Vpa_{mean}, mean velocity; AT, acceleration time; ETpa, pulmonary artery ejection time. Values are means ± SEM; [†]P < 0.05 MI vs. corresponding Sham (non-MI) group; *P < 0.05 vs. corresponding MI group.

et al., 2014; Campbell et al., 2017). It has been shown that these novel and orally active EET analogs provided heart and kidney protection comparable with that of native EETs (Skibba et al., 2017; Neckář et al., 2018). Previously, Imig's group demonstrated that EET-A markedly reduced cisplatin-induced nephrotoxicity and mitigated radiation nephropathy in rats (Khan et al., 2013; Hye Khan et al., 2016). EET-A also ameliorated the deleterious effects of high fat diet-induced metabolic abnormalities in obese mice (Singh et al., 2016). In the same mouse model (db/db mice), EET-A treatment improved LV systolic function (Cao et al., 2017). Recently, we have shown that the continuous treatment by another 14,15-EET analog EET-B before and after MI reduced post-MI mortality and the progression of LV systolic dysfunction in spontaneously hypertensive rats (Neckář et al., unpublished). Compared to predominant EET analogs-mediated protection against end-organ injury, their antihypertensive action is rather inconsistent; rodent models with various genetic background of hypertension differ in their sensitivity to EET-based therapy. Hence, EET-A reduced blood pressure in various forms of Ang II-dependent models of hypertension in rats (Neckář et al., 2012; Hye Khan et al., 2014; Červenka et al., 2018) and in mice with high fat diet-induced obesity (Singh et al., 2016). On the other hand, EET-A or EET-B did not exhibit any antihypertensive action in Dahl salt-sensitive rats, Goldblatt hypertensive rats, Cyp11a1-Ren-2 transgenic rats, and in spontaneously hypertensive rats (Hye Khan et al., 2013; Alánová et al., 2015; Jířková et al., 2016; Neckář et al., unpublished). Therefore, it seems that the protective action of EET analogs against end-organ injury is independent of blood pressure reduction in hypertensive animal models.

The progression of post-MI CHF in the present study was associated with decreased albuminuria and the total index of

kidney injury in untreated TGR compared to Sham (non-MI) controls. We speculate that these findings can reflect blood pressure reduction after MI. Indeed, it is well known that post-MI CHF decreases blood pressure in hypertensive rats due to insufficient myocardial function (Nishikimi et al., 1995; Mori et al., 1998; Wiemer et al., 2001) which can result in reduced kidney injury. Further, EET-based therapy almost eliminated albuminuria and decreased kidney injury score in TGR. This finding is not surprising because sEH inhibitors and EET analogs, respectively, represent promising and powerful therapies to prevent the progression of various chronic kidney diseases to renal failure (Imig, 2015; Fan and Roman, 2017). Similarly, preventive treatment of TGR by the same EET-based therapy before MI resulted in kidney protection (Červenka et al., 2018). The absence of any differences in other urinary markers of renal injury suggests that post-MI progression of CHF did not substantially damage kidney in both strains.

Previously, it has been demonstrated that acute exogenous administration of EETs or inhibition of sEH attenuated the increase of endothelial cell permeability and lung injury after acute ischemia/reperfusion or lipopolysaccharides administration (Townsend et al., 2010; Chen et al., 2015; Tao et al., 2016). Further, long-lasting sEH inhibitor treatment reduced bleomycin-induced pulmonary injury (Dong et al., 2017). It seems that EETs can protect against various lung diseases associated with inflammation and oxidative stress like asthma and chronic obstructive pulmonary disease (Yang et al., 2015, 2017). In line with these observations, EET-based therapy moderately limited CHF-induced lungs edema and improved PA flow in HanSD rats in the present study.

It has been shown that chronic treatment with sEH inhibitors reduced the progression of post-MI LV systolic dysfunction in normotensive animals (Li et al., 2009; Merabet et al., 2012;

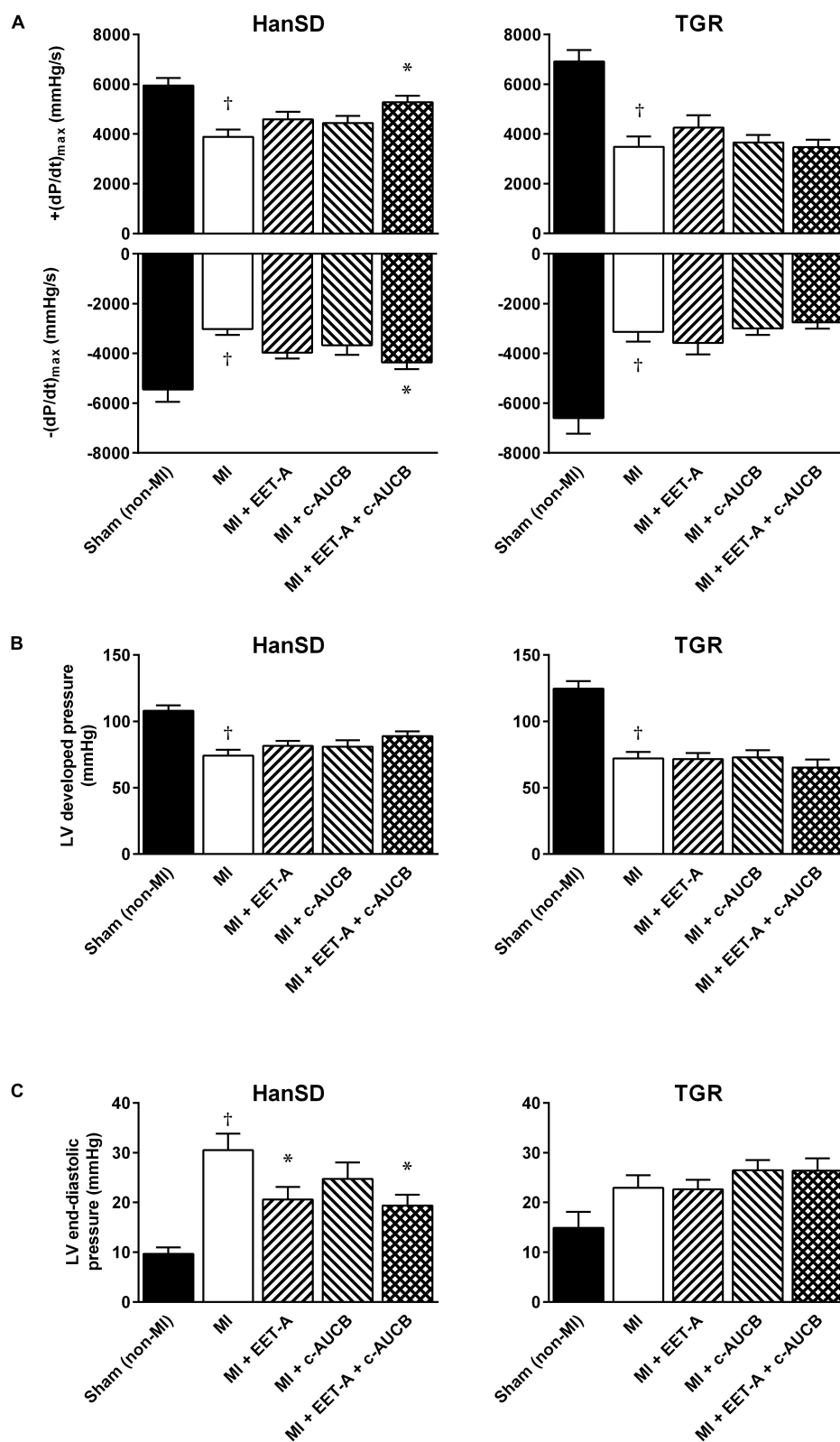


FIGURE 4 | Left ventricle peak rates of pressure development and fall **(A)**, developed pressure **(B)**, and end-diastolic pressure **(C)** in Hannover Sprague-Dawley (HanSD) and *Ren-2* transgenic rats (TGR) subjected to Sham (non-MI) operation or myocardial infarction (MI) and treated with epoxyeicosatrienoic acid analog (EET-A) or soluble epoxide hydrolase inhibitor (c-AUCB), given alone or combined for 5 weeks since 24 h after MI. Values are means \pm SEM; $^{\dagger}P < 0.05$ MI vs. corresponding Sham (non-MI) group; $*P < 0.05$ vs. corresponding MI group.

Kompa et al., 2013; Sirish et al., 2013). The beneficial effect of different sEH inhibitors was associated with increased EETs levels (Li et al., 2009; Sirish et al., 2013). Similarly, *c*-AUCB (given alone or in combination with EET-A) increased the myocardial concentration of endogenous EETs in both HanSD rats and TGR (Červenka et al., 2018). Moreover, Merabet et al. (2012) demonstrated that the cardioprotective action of sEH treatment was abolished by co-administration with an inhibitor of cytochrome P450 epoxygenase, the enzyme producing EETs from arachidonic acid. Therefore, EETs can play a role in the progression of post-MI CHF in normotensive rats, which is in line with our present study.

The effect of sEH inhibitors on the progression of CHF associated etiologies other than ischemic heart disease is inconsistent. Indeed, it has been reported that other sEH inhibitors such as AEPu, AUDA and TPPU reduced the development of cardiac hypertrophy and diminished adverse cardiac remodeling in normotensive mice subjected to pressure overload due to thoracic aortic constriction (Xu et al., 2006; Sirish et al., 2013). On the other hand, another sEH inhibitor GSK2256294 did not reverse LV dysfunction induced by pressure overload in both mice and rats, in spite of the fact that the increased an EETs-to-DHETs ratio was observed (Morgan et al., 2013). Similarly, *c*-AUCB did not alter LV contractility in hypertensive TGR and Fawn-hooded rats as well as normotensive HanSD and Fawn-hooded low-pressure rats subjected to volume overload (Červenka et al., 2015a,b; Vacková et al., 2019).

The overall biology of both mimics of epoxy fatty acids (EpFA) and sEH inhibitors are anticipated to be similar and in some cases additive. An intrinsic problem with sEH inhibitors is that they can only preserve the EpFA that are present. This has the advantage of making it difficult to over dose, but a disadvantage is that the sEH inhibitors cannot correct for abnormally low levels of EpFA. The mimics on the other hand do not require endogenous production of EpFA for their biological activity. However, the mimics only mimic a single isomer of the complex array of EpFAs present in an organism while sEH inhibitors to some degree preserve all EpFA. The preservation is likely to be related to the endogenous ratios of endogenous EpFA. Thus each pharmaceutical approach offers endogenous advantages and limitations. One can anticipate situations where the effect of the two drug classes would likely be additive. As individual EpFA mimics and sEH inhibitors are selected for development each will present unique pharmacokinetic parameters which will offer specific limitations and assets (Shen and Hammock, 2012).

CONCLUSION

In conclusion, our results showed that combined EET-based therapy reduced the progression of post-MI CHF in normotensive HanSD rats. Even though they exhibited renoprotective action, neither single nor combined treatment by EET-A and *c*-AUCB affected the extent of post-MI CHF in *Ren*-2 transgenic rats with Ang II-dependent form of hypertension. Cardioprotective efficacy of EET-based therapy against the

progression of CHF varies depending on experiment model and protocol, and associated comorbidities.

DATA AVAILABILITY

All datasets generated for this study are included in the manuscript and/or the **Supplementary Files**.

AUTHOR CONTRIBUTIONS

JN primarily conceived and designed the study, performed experiments, and wrote the manuscript. JH performed experiments, analyzed and interpreted the data, and wrote the manuscript. BH, SH, JI, and JF designed and synthesized *c*-AUCB and EET-A. FP, ZH, SK, ZVa, ZVe, FA, JV, LČ, and FK were involved in performing the experiments, data collection, analysis and interpretation, contributed to the intellectual content and editing of the manuscript, and approved its final version.

FUNDING

JH was supported by the Charles University, Project GAUK No. 1064317. JN was supported by grant of Ministry of Health of the Czech Republic (Grant No. 15-27735A), and the Institutional Research Projects 67985823 (Institute of Physiology, CAS) and 00023001 (IKEM). BH was supported by NIEHS R01 ES002710 and Superfund Research Program P42 ES004699. JI was supported by the Dr. Ralph and Marian Falk Medical Research Trust Bank of America, N.A., Trustee. JF was supported by Robert Welch Foundation (I-0011).

ACKNOWLEDGMENTS

We wish to thank Mrs. M. Pešková for excellent technical assistance.

SUPPLEMENTARY MATERIAL

The Supplementary Material for this article can be found online at: <https://www.frontiersin.org/articles/10.3389/fphar.2019.00159/full#supplementary-material>

FIGURE S1 | Plasma concentration of monocyte chemoattractant protein-1 (MCP-1) at the end of study in Hannover Sprague-Dawley (HanSD) and *Ren*-2 transgenic rats (TGR) subjected to Sham (non-MI) operation or myocardial infarction (MI) and treated with epoxyeicosatrienoic acid analog (EET-A) or soluble epoxide hydrolase inhibitor (*c*-AUCB), given alone or combined for 5 weeks since 24 h after MI. Values are means \pm SEM.

FIGURE S2 | Urinary sodium (A), potassium (B) and cystatin c (C) excretion at the end of study in Hannover Sprague-Dawley (HanSD) and *Ren*-2 transgenic rats (TGR) subjected to Sham (non-MI) operation or myocardial infarction (MI) and treated with epoxyeicosatrienoic acid analog (EET-A) or soluble epoxide hydrolase inhibitor (*c*-AUCB), given alone or combined for 5 weeks since 24 h after MI. Values are means \pm SEM.

REFERENCES

- Alánová, P., Husková, Z., Kopkan, L., Sporková, A., Jíchová, Š., Neckář, J., et al. (2015). Orally active epoxyeicosatrienoic acid analog does not exhibit antihypertensive and reno- or cardioprotective actions in two-kidney, one-clip Goldblatt hypertensive rats. *Vasc. Pharmacol.* 73, 45–56. doi: 10.1016/j.vph.2015.08.013
- Bachmann, S., Peters, J., Engler, E., Ganten, D., and Mullins, J. (1992). Transgenic rats carrying the mouse renin gene-morphological characterization of a low-renin hypertension model. *Kidney Int.* 41, 24–36. doi: 10.1038/ki.1992.4
- Braunwald, E. (2013). Heart failure. *JACC Heart Fail.* 1, 1–20. doi: 10.1016/j.jchf.2012.10.002
- Campbell, W. B., Imig, J. D., Schmitz, J. M., and Falck, J. R. (2017). Orally active epoxyeicosatrienoic acid analogs. *J. Cardiovasc. Pharmacol.* 70, 211–224. doi: 10.1097/fjc.0000000000000523
- Cao, J., Singh, S. P., McClung, J. A., Joseph, G., Vanella, L., Barbagallo, I., et al. (2017). EET intervention on Wnt1, NOV, and HO-1 signaling prevents obesity-induced cardiomyopathy in obese mice. *Am. J. Physiol. Heart Circ. Physiol.* 313, H368–H380. doi: 10.1152/ajpheart.00093.2017
- Cao, J., Tsenovoy, P. L., Thompson, E. A., Falck, J. R., Touchon, R., Sodhi, K., et al. (2015). Agonists of epoxyeicosatrienoic acids reduce infarct size and ameliorate cardiac dysfunction via activation of HO-1 and Wnt1 canonical pathway. *Prostaglandins Other Lipid Mediat.* 11, 76–86. doi: 10.1016/j.prostaglandins.2015.01.002
- Červenka, L., Husková, Z., Kopkan, L., Kikerlová, S., Sedláková, L., Vaňourková, Z., et al. (2018). Two pharmacological epoxyeicosatrienoic acid-enhancing therapies are effectively antihypertensive and reduce the severity of ischemic arrhythmias in rats with angiotensin II-dependent hypertension. *J. Hypertens.* 36, 1326–1341. doi: 10.1097/hjh.0000000000001708
- Červenka, L., Melenovský, V., Husková, Z., Škaroupková, P., Nishiyama, A., and Sadowski, J. (2015a). Inhibition of soluble epoxide hydrolase counteracts the development of renal dysfunction and progression of congestive heart failure in Ren-2 transgenic hypertensive rats with aorto-caval fistula. *Clin. Exp. Pharmacol. Physiol.* 42, 795–807. doi: 10.1111/1440-1681.12419
- Červenka, L., Melenovský, V., Husková, Z., Sporková, A., Bürgelová, M., Škaroupková, P., et al. (2015b). Inhibition of soluble epoxide hydrolase does not improve the course of congestive heart failure and the development of renal dysfunction in rats with volume overload induced by aorto-caval fistula. *Physiol. Res.* 64, 857–873.
- Chen, W., Yang, S., Ping, W., Fu, X., Xu, Q., and Wang, J. (2015). CYP2J2 and EETs protect against lung ischemia/reperfusion injury via anti-inflammatory effects in vivo and in vitro. *Cell. Physiol. Biochem.* 35, 2043–2054. doi: 10.1159/000374011
- Connelly, K. A., Advani, A., Advani, S., Zhang, Y., Thai, K., Thomas, S., et al. (2013). Combination angiotensin converting enzyme and direct renin inhibition in heart failure following experimental myocardial infarction. *Cardiovasc. Ther.* 31, 84–91. doi: 10.1111/j.1755-5922.2011.00292.x
- De Mello, W., Rivera, M., Rabell, A., and Gerena, Y. (2013). Aliskiren, at low doses, reduces the electrical remodeling in the heart of the TGR(mRen2)27 rat independently of blood pressure. *J. Renin Angiotensin Aldosterone Syst.* 14, 23–33. doi: 10.1177/1470320312463832
- Dong, X. W., Jia, Y. L., Ge, L. T., Jiang, B., Jiang, J. X., Shen, J., et al. (2017). Soluble epoxide hydrolase inhibitor AUDA decreases bleomycin-induced pulmonary toxicity in mice by inhibiting the p38/Smad3 pathways. *Toxicology* 389, 31–41. doi: 10.1016/j.tox.2017.07.002
- Falck, J. R., Koduru, S. R., Mohapatra, S., Manne, R., Atcha, K. R., Atcha, R., et al. (2014). 14,15-Epoxyeicosa-5,8,11-trienoic Acid (14,15-EET) surrogates: carboxylate modifications. *J. Med. Chem.* 57, 6965–6972. doi: 10.1021/jm500262m
- Fan, F., and Roman, R. J. (2017). Effect of cytochrome P450 metabolites of arachidonic acid in nephrology. *J. Am. Soc. Nephrol.* 28, 2845–2855. doi: 10.1681/ASN.2017030252
- Habibi, J., DeMarco, V. G., Ma, L., Pulakat, L., Rainey, W. E., Whaley-Connell, A. T., et al. (2011). Mineralocorticoid receptor blockade improves diastolic function independent of blood pressure reduction in a transgenic model of RAAS overexpression. *Am. J. Physiol. Heart. Circ. Physiol.* 300, H1484–H1491. doi: 10.1152/ajpheart.01000.2010
- Hrdlička, J., Neckář, J., Papoušek, F., Vašinová, J., Alánová, P., Kolář, F., et al. (2016). Beneficial effect of continuous normobaric hypoxia on ventricular dilatation in rats with post-infarction heart failure. *Physiol. Res.* 65, 867–870.
- Hye Khan, M. A., Fish, B., Wahl, G., Sharma, A., Falck, J. R., Paudyal, M. P., et al. (2016). Epoxyeicosatrienoic acid analogue mitigates kidney injury in a rat model of radiation nephropathy. *Clin. Sci.* 130, 587–599. doi: 10.1042/cs20150778
- Hye Khan, M. A., Neckář, J., Manthathi, V., Errabelli, R., Pavlov, T. S., Staruschenko, A., et al. (2013). Orally active epoxyeicosatrienoic acid analog attenuates kidney injury in hypertensive Dahl salt-sensitive rat. *Hypertension* 62, 905–913. doi: 10.1161/hypertensionaha.113.01949
- Hye Khan, M. A., Pavlov, T. S., Christain, S. V., Neckář, J., Staruschenko, A., Gauthier, K. M., et al. (2014). Epoxyeicosatrienoic acid analogue lowers blood pressure through vasodilation and sodium channel inhibition. *Clin. Sci.* 127, 463–474. doi: 10.1042/CS20130479
- Imig, J. D. (2012). Epoxides and soluble epoxide hydrolase in cardiovascular physiology. *Physiol. Rev.* 92, 101–130. doi: 10.1152/physrev.00021.2011
- Imig, J. D. (2015). Epoxyeicosatrienoic acids, hypertension, and kidney injury. *Hypertension* 65, 476–482. doi: 10.1161/HYPERTENSIONAHA
- Imig, J. D. (2018). Prospective for cytochrome P450 epoxygenase cardiovascular and renal therapeutics. *Pharmacol. Ther.* 192, 1–19. doi: 10.1016/j.pharmthera.2018.06.015
- Jamieson, K. L., Endo, T., Darwesh, A. M., Samokhvalov, V., and Seubert, J. M. (2017). Cytochrome P450-derived eicosanoids and heart function. *Pharmacol. Ther.* 179, 47–83. doi: 10.1016/j.pharmthera.2017.05.005
- Jíchová, Š., Kopkan, L., Husková, Z., Doleželová, Š., Neckář, J., Kujal, P., et al. (2016). Epoxyeicosatrienoic acid analog attenuates the development of malignant hypertension, but does not reverse it once established: a study in Cyp11a1-Ren-2 transgenic rats. *J. Hypertens.* 34, 2008–2025. doi: 10.1097/hjh.0000000000001029
- Kala, P., Sedláková, L., Škaroupková, P., Kopkan, L., Vaňourková, Z., Táborský, M., et al. (2018). Effect of angiotensin-converting enzyme blockade, alone or combined with blockade of soluble epoxide hydrolase, on the course of congestive heart failure and occurrence of renal dysfunction in Ren-2 transgenic hypertensive rats with aorto-caval fistula. *Physiol. Res.* 67, 401–415.
- Khan, A. H., Falck, J. R., Manthathi, V. L., Campbell, W. B., and Imig, J. D. (2014). Epoxyeicosatrienoic acid analog attenuates angiotensin II hypertension and kidney injury. *Front. Pharmacol.* 23:216. doi: 10.3389/fphar.2014.00216
- Khan, M. A., Liu, J., Kumar, G., Skapek, S. X., Falck, J. R., and Imig, J. D. (2013). Novel orally active epoxyeicosatrienoic acid (EET) analogs attenuate cisplatin nephrotoxicity. *FASEB J.* 27, 2946–2956. doi: 10.1096/fj.12-218040
- Kompa, A. R., Wang, B. H., Xu, G., Zhang, Y., Ho, P. Y., Eisennagel, S., et al. (2013). Soluble epoxide hydrolase inhibition exerts beneficial anti-remodeling actions post-myocardial infarction. *Int. J. Cardiol.* 167, 210–219. doi: 10.1016/j.ijcard.2011.12.062
- Kovács, Á., Fülöp, G. Á., Kovács, A., Csipő, T., Bódi, B., Priks, D., et al. (2016). Renin overexpression leads to increased titin-based stiffness contributing to diastolic dysfunction in hypertensive mRen2 rats. *Am. J. Physiol. Heart Circ. Physiol.* 310, H1671–H1682. doi: 10.1152/ajpheart.00842.2015
- Lee, M. A., Böhm, M., Paul, M., Bader, M., Ganten, U., and Ganten, D. (1996). Physiological characterization of the hypertensive transgenic rat TGR(mRen2)27. *Am. J. Physiol.* 270, E919–E929. doi: 10.1152/ajpendo.1996.270.6.e919
- Lee, T. M., Lin, M. S., and Chang, N. C. (2008). Effect of ATP-sensitive potassium channel agonists on ventricular remodeling in healed rat infarcts. *J. Am. Coll. Cardiol.* 51, 1309–1318. doi: 10.1016/j.jacc.2007.11.067
- Li, N., Liu, J. Y., Timofeyev, V., Qiu, H., Hwang, S. H., Tuteja, D., et al. (2009). Beneficial effects of soluble epoxide hydrolase inhibitors in myocardial infarction model: insight gained using metabolomic approaches. *J. Mol. Cell Cardiol.* 47, 835–845. doi: 10.1016/j.yjmcc.2009.08.017
- Ma, L., Gul, R., Habibi, J., Yang, M., Pulakat, L., Whaley-Connell, A., et al. (2012). Nebivolol improves diastolic dysfunction and myocardial remodeling through reductions in oxidative stress in the transgenic (mRen2) rat. *Am. J. Physiol. Heart. Circ. Physiol.* 302, H2341–H2351. doi: 10.1152/ajpheart.01126.2011
- Merabet, N., Bellien, J., Glevarec, E., Nicol, L., Lucas, D., Remy-Jouet, I., et al. (2012). Soluble epoxide hydrolase inhibition improves myocardial perfusion and function in experimental heart failure. *J. Mol. Cell Cardiol.* 52, 660–666. doi: 10.1016/j.yjmcc.2011.11.015

- Morgan, L. A., Olzinski, A. R., Upson, J. J., Zhao, S., Wang, T., Eisennagel, S. H., et al. (2013). Soluble epoxide hydrolase inhibition does not prevent cardiac remodeling and dysfunction after aortic constriction in rats and mice. *J. Cardiovasc. Pharmacol.* 61, 291–301. doi: 10.1097/FJC.0b013e31827fe59c
- Mori, T., Nishimura, H., Okabe, M., Ueyama, M., Kubota, J., and Kawamura, K. (1998). Cardioprotective effects of quinapril after myocardial infarction in hypertensive rats. *Eur. J. Pharmacol.* 348, 229–234. doi: 10.1016/S0014-2999(98)00155-1
- Mullins, J. J., Peters, J., and Ganten, D. (1990). Fulminant hypertension in transgenic rats harbouring the mouse Ren-2 gene. *Nature* 344, 541–544. doi: 10.1038/344541a0
- Neckář, J., Hsu, A., Hye Khan, M. A., Gross, G. J., Nithipatikom, K., Cyprová, M., et al. (2018). Infarct size-limiting effect of epoxyeicosatrienoic acid analog EET-B is mediated by hypoxia-inducible factor-1 α via downregulation of prolyl hydroxylase 3. *Am. J. Physiol. Heart Circ. Physiol.* 315, H1148–H1158. doi: 10.1152/ajpheart.00726.2017
- Neckář, J., Kopkan, L., Husková, Z., Kolář, F., Papoušek, F., Kramer, H. J., et al. (2012). Inhibition of soluble epoxide hydrolase by cis-4-[4-(3-adamantan-1-ylureido)cyclohexyl-oxy]benzoic acid exhibits antihypertensive and cardioprotective actions in transgenic rats with angiotensin II-dependent hypertension. *Clin. Sci.* 122, 513–525. doi: 10.1042/CS20110622
- Nishikimi, T., Yamagishi, H., Takeuchi, K., and Takeda, T. (1995). An angiotensin II receptor antagonist attenuates left ventricular dilatation after myocardial infarction in the hypertensive rat. *Cardiovasc. Res.* 29, 856–861. doi: 10.1016/S0008-6363(96)88623-8
- Oni-Orisan, A., Alsaleh, N., Lee, C. R., and Seubert, J. M. (2014). Epoxyeicosatrienoic acids and cardioprotection: the road to translation. *J. Mol. Cell Cardiol.* 74, 199–208. doi: 10.1016/j.yjmcc.2014.05.016
- Qiu, H., Li, N., Liu, J. Y., Harris, T. R., Hammock, B. D., and Chiamvimonvat, N. (2011). Soluble epoxide hydrolase inhibitors and heart failure. *Cardiovasc. Ther.* 29, 99–111. doi: 10.1111/j.1755-5922.2010.00150.x
- Roger, V. L. (2013). Epidemiology of heart failure. *Circ. Res.* 113, 646–659. doi: 10.1161/circresaha.113.300268
- Shen, H., and Hammock, B. D. (2012). Discovery of inhibitors of soluble epoxide hydrolase: a target with multiple potential therapeutic indications. *J. Med. Chem.* 55, 1789–1808. doi: 10.1021/jm201468j
- Singh, S. P., Schragenheim, J., Cao, J., Falck, J. R., Abraham, N. G., and Bellner, L. (2016). PGC-1 α regulates HO-1 expression, mitochondrial dynamics and biogenesis: role of epoxyeicosatrienoic acid. *Prostaglandins Other Lipid Mediat.* 125, 8–18. doi: 10.1016/j.prostaglandins.2016.07.004
- Sirish, P., Li, N., Liu, J. Y., Lee, K. S., Hwang, S. H., Qiu, H., et al. (2013). Unique mechanistic insights into the beneficial effects of soluble epoxide hydrolase inhibitors in the prevention of cardiac fibrosis. *Proc. Natl. Acad. Sci. U.S.A.* 110, 5618–5623. doi: 10.1073/pnas.1221972110
- Skibba, M., Hye Khan, M. A., Kolb, L. L., Yeboah, M. M., Falck, J. R., Amaradhi, R., et al. (2017). Epoxyeicosatrienoic acid analog decreases renal fibrosis by reducing epithelial-to-mesenchymal transition. *Front. Pharmacol.* 8:406. doi: 10.3389/fphar.2017.00406
- Spector, A. A., and Norris, A. W. (2007). Action of epoxyeicosatrienoic acids on cellular function. *Am. J. Physiol. Cell Physiol.* 292, C996–C1012. doi: 10.1152/ajpcell.00402.2006
- Tao, W., Li, P. S., Yang, L. Q., and Ma, Y. B. (2016). Effects of a soluble epoxide hydrolase inhibitor on lipopolysaccharide-induced acute lung injury in mice. *PLoS One* 11:e0160359. doi: 10.1371/journal.pone.0160359
- Townsley, M. I., Morisseau, C., Hammock, B., and King, J. A. (2010). Impact of epoxyeicosatrienoic acids in lung ischemia-reperfusion injury. *Microcirculation* 17, 137–146. doi: 10.1111/j.1549-8719.2009.00013.x
- Vacková, Š., Kopkan, L., Kikerlová, S., Husková, Z., Sadowski, J., Kompanowska-Jezierska, E., et al. (2019). Pharmacological blockade of soluble epoxide hydrolase attenuates the progression of congestive heart failure combined with chronic kidney disease: insights from studies with Fawn-hooded hypertensive rats. *Front. Pharmacol.* 10:18. doi: 10.3389/fphar.2019.00018
- Whaley-Connell, A., Govindarajan, G., Habibi, J., Hayden, M. R., Cooper, S. A., Wei, Y., et al. (2007). Angiotensin II-mediated oxidative stress promotes myocardial tissue remodeling in the transgenic (mRen2) 27 Ren2 rat. *Am. J. Physiol. Endocrinol. Metab.* 293, E355–E363. doi: 10.1152/ajpendo.00632.2006
- Wiemer, G., Itter, G., Malinski, T., and Linz, W. (2001). Decreased nitric oxide availability in normotensive and hypertensive rats with failing hearts after myocardial infarction. *Hypertension* 38, 1367–1371. doi: 10.1161/hy1101.096115
- Xu, D., Li, N., He, Y., Timofeyev, V., Lu, L., Tsai, H. J., et al. (2006). Prevention and reversal of cardiac hypertrophy by soluble epoxide hydrolase inhibitors. *Proc. Natl. Acad. Sci. U.S.A.* 103, 18733–18738. doi: 10.1073/pnas.0609158103
- Yang, J., Bratt, J., Franz, L., Liu, J. Y., Zhang, G., Zeki, A. A., et al. (2015). Soluble epoxide hydrolase inhibitor attenuates inflammation and airway hyperresponsiveness in mice. *Am. J. Respir. Cell Mol. Biol.* 52, 46–55. doi: 10.1165/rcmb.2013-0440OC
- Yang, L., Cheriyan, J., Gutterman, D. D., Mayer, R. J., Ament, Z., Griffin, J. L., et al. (2017). Mechanisms of vascular dysfunction in COPD and effects of a novel soluble epoxide hydrolase inhibitor in smokers. *Chest* 151, 555–563. doi: 10.1016/j.chest.2016.10.058

Conflict of Interest Statement: The authors declare that the research was conducted in the absence of any commercial or financial relationships that could be construed as a potential conflict of interest.

Copyright © 2019 Hrdlička, Neckář, Papoušek, Husková, Kikerlová, Vaňourková, Vernerová, Akat, Vašinová, Hammock, Hwang, Imig, Falck, Červenka and Kolář. This is an open-access article distributed under the terms of the Creative Commons Attribution License (CC BY). The use, distribution or reproduction in other forums is permitted, provided the original author(s) and the copyright owner(s) are credited and that the original publication in this journal is cited, in accordance with accepted academic practice. No use, distribution or reproduction is permitted which does not comply with these terms.



Zafirlukast Is a Dual Modulator of Human Soluble Epoxide Hydrolase and Peroxisome Proliferator-Activated Receptor γ

OPEN ACCESS

Edited by:

John D. Imig,
Medical College of Wisconsin,
United States

Reviewed by:

Luca Vanella,
Università degli Studi di Catania, Italy
Komal Sodhi,
Marshall University, United States

*Correspondence:

Ewgenij Proschak
proschak@pharmchem.uni-
frankfurt.de
Astrid S. Kahnt
kahnt@pharmchem.uni-frankfurt.de

† These authors have contributed
equally to this work as first authors

‡ These authors have contributed
equally to this work as last authors

Specialty section:

This article was submitted to
Translational Pharmacology,
a section of the journal
Frontiers in Pharmacology

Received: 09 November 2018

Accepted: 04 March 2019

Published: 20 March 2019

Citation:

Göbel T, Diehl O, Heering J,
Merk D, Angioni C, Wittmann SK,
Buscato E, Kottke R, Weizel L,
Schader T, Maier TJ, Geisslinger G,
Schubert-Zsilavec M, Steinhilber D,
Proschak E and Kahnt AS (2019)
Zafirlukast Is a Dual Modulator
of Human Soluble Epoxide Hydrolase
and Peroxisome Proliferator-Activated
Receptor γ .
Front. Pharmacol. 10:263.
doi: 10.3389/fphar.2019.00263

Tamara Göbel^{††}, Olaf Diehl^{††}, Jan Heering², Daniel Merk¹, Carlo Angioni³,
Sandra K. Wittmann¹, Estel.la Buscato¹, Ramona Kottke¹, Lilia Weizel¹, Tim Schader¹,
Thorsten J. Maier⁴, Gerd Geisslinger^{2,3}, Manfred Schubert-Zsilavec¹,
Dieter Steinhilber¹, Ewgenij Proschak^{1*†} and Astrid S. Kahnt^{1*‡}

¹ Institute of Pharmaceutical Chemistry/ZAFES, Goethe University Frankfurt, Frankfurt am Main, Germany, ² Branch for Translational Medicine and Pharmacology, Fraunhofer Institute for Molecular Biology and Applied Ecology IME, Frankfurt am Main, Germany, ³ Faculty of Medicine, Institute of Clinical Pharmacology, Pharmazentrum Frankfurt, ZAFES, Frankfurt am Main, Germany, ⁴ Department of Anesthesiology, Intensive Care Medicine and Pain Therapy, University Hospital Frankfurt, Goethe University Frankfurt, Frankfurt am Main, Germany

Cysteinyl leukotriene receptor 1 antagonists (CysLT1RA) are frequently used as add-on medication for the treatment of asthma. Recently, these compounds have shown protective effects in cardiovascular diseases. This prompted us to investigate their influence on soluble epoxide hydrolase (sEH) and peroxisome proliferator activated receptor (PPAR) activities, two targets known to play an important role in CVD and the metabolic syndrome. Montelukast, pranlukast and zafirlukast inhibited human sEH with IC₅₀ values of 1.9, 14.1, and 0.8 μ M, respectively. In contrast, only montelukast and zafirlukast activated PPAR γ in the reporter gene assay with EC₅₀ values of 1.17 μ M (21.9% max. activation) and 2.49 μ M (148% max. activation), respectively. PPAR α and δ were not affected by any of the compounds. The activation of PPAR γ was further investigated in 3T3-L1 adipocytes. Analysis of lipid accumulation, mRNA and protein expression of target genes as well as PPAR γ phosphorylation revealed that montelukast was not able to induce adipocyte differentiation. In contrast, zafirlukast triggered moderate lipid accumulation compared to rosiglitazone and upregulated PPAR γ target genes. In addition, we found that montelukast and zafirlukast display antagonistic activities concerning recruitment of the PPAR γ cofactor CBP upon ligand binding suggesting that both compounds act as PPAR γ modulators. In addition, zafirlukast impaired the TNF α triggered phosphorylation of PPAR γ 2 on serine 273. Thus, zafirlukast is a novel dual sEH/PPAR γ modulator representing an excellent starting point for the further development of this compound class.

Keywords: PPAR γ , soluble epoxide hydrolase, zafirlukast, montelukast, pranlukast, metabolic syndrome, polypharmacology

INTRODUCTION

In the last decades, the main intention of rational drug discovery was the design of selective ligands, following the paradigm “one drug – one target – one disease.” However, in most cases drugs interact with a multitude of targets. These interactions referred to as the polypharmacological profile of a drug can contribute either to adverse reactions or pleiotropic effects thus synergistically enhancing the efficacy of a compound (Peters, 2013). The latter is of special interest for the treatment of complex multifactorial pathophysiological conditions such as inflammation. Arachidonic acid metabolites such as leukotrienes, prostaglandins and lipoxins are important players in initiation and resolution of inflammation and the majority of anti-inflammatory drugs interfering with eicosanoid signaling are fatty acid mimetics (Proschak et al., 2017). The polypharmacology of these non-steroidal anti-inflammatory drugs has been extensively reviewed in the past and it was concluded that addressing multiple inflammatory pathways is in general beneficial for overall efficacy and safety of these anti-inflammatory compounds (Hwang et al., 2013; Meirer et al., 2014; Reker et al., 2014).

The cysteinyl leukotriene receptor 1 antagonists (CysLT₁RA) montelukast, zafirlukast and pranlukast (**Figure 1**) were initially developed for the treatment of asthma. Displaying low nanomolar inhibitory activity to their target receptor these well-tolerated compounds were designed to inhibit the vasodilatory and bronchoconstrictory activities of cysteinyl leukotrienes. In addition to their anti-inflammatory properties in asthma they were found to be effective in different animal models among them studies of chronic obstructive pulmonary disease, atherosclerosis and the metabolic syndrome (MetS). In line with this, asthmatic patients taking montelukast display lower levels of cardiovascular disease (CVD)-associated inflammatory biomarkers and blood lipids. Moreover, montelukast appears to reduce the risk for recurrent stroke and myocardial infarction (Ibrahim et al., 2014; Theron et al., 2014; Hoxha et al., 2017). Indeed, we and others could recently show that the marketed CysLT₁RA display an interesting polypharmacological profile by inhibition of additional pro-inflammatory targets such as microsomal prostaglandin E₂ synthase-1 (mPGES-1), 5-lipoxygenase (5-LO), cAMP phosphodiesterases and NF κ B (Ramires et al., 2004; Anderson et al., 2009; Woszczek et al., 2010; Fogli et al., 2013; Kahnt et al., 2013; Theron et al., 2014). Nevertheless, these already published off-target effects do not sufficiently explain their efficacy seen in models of atherosclerosis and the MetS.

The MetS is a multifactorial disease cluster consisting of central obesity, dyslipidemia, type 2 diabetes mellitus (T2D) and the increased risk for CVD that is considered a major public-health challenge (Eckel et al., 2010). Affected patients are at high risk to develop T2D and cardiovascular complications (Alberti et al., 2009; Kaur, 2014). Currently, the first-line treatment of the MetS focuses on the treatment of the accumulating risk factors. This results in a rising number of different medications increasing the pharmacologic complexity due to poorly predictable drug-to-drug interactions and raising therapy costs (Grundy, 2006). Among the frequently prescribed

medications thiazolidinediones (TZD), peroxisome proliferator activated receptor γ (PPAR γ) activating drugs, are used to reduce insulin resistance. Unfortunately, their clinical use is limited due to excessive weight gain, fluid retention and increased osteoporosis risk. Another drawback is the poor effect of TZDs on the occurrence of macrovascular events, although the equilibration of blood glucose levels reduces microvascular complications (Rohatgi and McGuire, 2008). Interestingly, PPAR γ agonism combined with soluble epoxide hydrolase (sEH) antagonism shows the potential for a beneficial outcome in terms of macrovascular events (Drew et al., 2008; Imig et al., 2012; Xu et al., 2013; Hye Khan et al., 2018). Being part of the arachidonic acid cascade, endothelial sEH promotes the hydrolysis of vasorelaxing, cytochrome P450 derived epoxyeicosatrienoic acids (EETs) to the less bioactive corresponding dihydroxyeicosatrienoic acids (DHETs) (Imig and Hammock, 2009). Thus, the increase in circulating EET levels by inhibition of sEH is vasoprotective and EET linked effects on MetS-associated disorders including CVD, dyslipidemia, diabetic neuro- and nephropathy were already shown in various studies (Fleming, 2014).

Due to the protective effects of the CysLT₁RA montelukast, zafirlukast and pranlukast seen in models of CVD we aimed at investigating their influence on human sEH and PPAR activities *in vitro*.

MATERIALS AND METHODS

Cell Culture

3T3-L1 cells were obtained from the American Type Culture Collection (ATCC, Manassas, VA, United States). HEP-G2 and HEK-293T cells were bought from the Deutsche Sammlung für Mikroorganismen und Zellkulturen (DSMZ, Braunschweig, Germany). 3T3-L1 cells were cultured in DMEM containing 10% newborn calf serum, 1% sodium pyruvate (SP) and 1% penicillin/streptomycin (PS). HEP-G2 cells were cultured in DMEM supplemented with 10% fetal calf serum (FCS), 1% non-essential amino acids, 1% SP and 1% PS. HEK-293T cells were cultured in DMEM containing 10% FCS, 1% SP, and 1% PS. All cell lines were grown in a humidified atmosphere at 37°C, 5% CO₂.

Adipocyte Differentiation

3T3-L1 cells were differentiated into adipocytes for 14 days according to the protocol of Zebisch et al. (2012). For this, cells were seeded in 6-well plates (2.5 × 10⁶/well) and differentiation was induced after 48 h by addition of a differentiation cocktail containing 1 μ g/mL insulin, 0.25 μ M dexamethasone and 0.5 mM isobutylmethylxanthine (IBMX) in DMEM supplemented with 10% FCS and 1% PS. In addition, potential PPAR γ activators (1, 5, and 10 μ M zafirlukast or montelukast) or DMSO were added and rosiglitazone (2 μ M) was used as PPAR γ positive control. After 2 days, medium was replaced by DMEM supplemented with 10% FCS, 1% PS and 1 μ g/mL insulin for 2 more days. Afterwards, cells were kept for

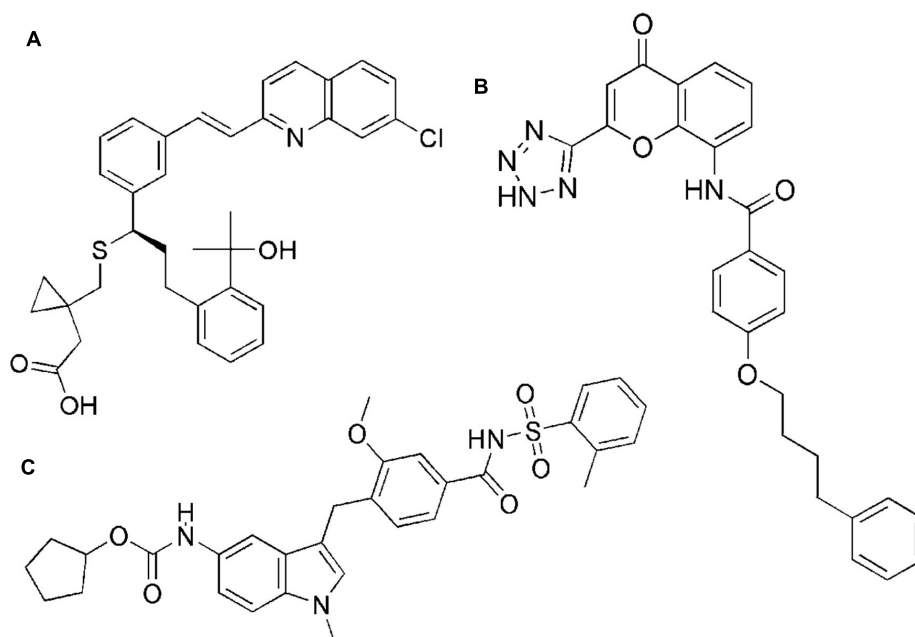


FIGURE 1 | Chemical structures of montelukast (A), pranlukast (B), and zafirlukast (C).

lipid droplet accumulation in DMEM containing 10% FCS and 1% PS until day 15. Media were replaced every other day.

For investigations on PPAR γ phosphorylation at Ser273, cells were differentiated for 10 days according to Choi et al. (2011). Cells were seeded in 6-well plates (2.5×10^6 /well) and differentiation was induced after 48 h by addition of 5 μ g/mL insulin, 1 μ M dexamethasone and 0.5 mM IBMX in DMEM supplemented with 10% FCS and 1% PS at 37°C, 5% CO₂. After 2 days, medium was replaced by DMEM supplemented with 10% FCS, 1% PS and 5 μ g/mL insulin. Medium was changed every other day until day 10. Then, cells were treated with 1 or 10 μ M zafirlukast or 2 μ M rosiglitazone for 45 min in DMEM supplemented with 10% FCS and 1% PS. After this, 50 ng/mL TNF α was added and cells were incubated for additional 30 min. Afterwards, cells were harvested, lysed and Western Blotting was performed as described below.

Oil Red O Staining

Differentiated 3T3-L1 cells were washed with PBS and subsequently fixed for 60 min with formaldehyde (4% in PBS). Afterwards, cells were thoroughly rinsed with 60% isopropanol and incubated with Oil Red O solution (0.3% in 60% isopropanol) for 120 min. This was followed by the removal of the staining solution and thorough rinsing of the cell layer with ultrapure water. Finally, the plates were dried and pictures of the stained cell layers were taken.

For quantification of the accumulated dye, 3T3-L1 cells were seeded in 24-well plates (0.55×10^5 /well) instead of 6-wells and the differentiation was carried out as described in the section 'Adipocyte differentiation'. After 14 days of differentiation, cells were fixed and stained as described above. Afterwards, cells were

incubated with 150 μ l of dye extraction solution (5% IGEPAL CA 630 in 100% isopropanol) for 30 min while gently shaking. 100 μ l of dye extract were transferred to a 96-well plate and absorbance was measured ($\lambda_{\text{abs}} = 510$ nm) by an Infinite F200 plate reader (Tecan Group Ltd., Männedorf, Switzerland). Blank wells were subtracted from samples. Values were normalized to the wells receiving the differentiation cocktail without a PPAR γ agonist (w/o).

In vitro Cell Viability Assay (WST-1)

For measurement of cell proliferation, 3T3-L1 cells were seeded in 24-well plates (0.55×10^5 /well) instead of 6-wells and the differentiation was carried out as described in the section 'Adipocyte differentiation'. After 2 days of incubation with the differentiation cocktail with or without the PPAR γ agonists, WST-1 reagent (Roche Diagnostic GmbH, Mannheim, Germany) was added (1:10) to the supernatant of the differentiating cells. Then, the cells were further incubated for 2 h at 37°C, 5% CO₂ to allow color development. After this, cell supernatant absorbance was measured ($\lambda_{\text{abs}} = 450$ nm) and corrected to a reference wavelength ($\lambda_{\text{abs}} = 690$ nm) with an Infinite F200 plate reader (Tecan Group Ltd., Männedorf, Switzerland). After this, background absorbance was subtracted from all measurements and values were normalized to the differentiated control receiving the differentiation cocktail without addition of a PPAR γ agonist (w/o).

Protein Isolation and Western Blotting

Total 3T3-L1 or HEP-G2 cell lysates were prepared in lysis buffer (20 mM Tris-HCl, pH 7.4, 150 mM NaCl, 2 mM EDTA, 1% Triton X-100, 0.5% NP-40) supplemented with protease

and phosphatase inhibitors (PhosSTOPTM + cOmpleteTM Mini, Roche Diagnostics GmbH, Mannheim, Germany). Protein concentrations were quantified using the PierceTM BCA Protein Assay Kit (Thermo Scientific, Waltham, MA, United States). Total protein (30 μ g/lane) was separated by SDS-polyacrylamide gel electrophoresis and transferred to nitrocellulose membranes (GE Healthcare Life Sciences, Little Chalfont, United Kingdom). Membranes were blocked with Odyssey blocking reagent (LI-COR Biosciences, Bad Homburg, Germany) for 1 h at room temperature. Ensuing, membranes were incubated with antibodies against CD36 (EPR6573, Abcam, Cambridge, United Kingdom), PPAR γ (E-8, Santa Cruz Biotechnology, Heidelberg, Germany), FABP-4 (C-15, Santa Cruz Biotechnology, Heidelberg, Germany) or PPAR γ Ser273 (Bioss Antibodies Inc., Woburn, MA, United States) overnight at 4°C. Afterwards, membranes were washed and incubated with fluorescence conjugated secondary antibodies (IRDye, LI-COR Biosciences, Bad Homburg, Germany). Protein antibody complexes were visualized on the Odyssey Infrared Imaging System (LI-COR Biosciences, Bad Homburg, Germany). β -actin (I-19, goat, polyclonal, Santa Cruz Biotechnology, Heidelberg, Germany) was used as loading control. The density of the immune reactive bands was analyzed using the Image Studio 5.2 software (LI-COR Biosciences, Bad Homburg, Germany).

mRNA Isolation and Quantitative RT-PCR

3T3-L1 cells were lysed using TRIzol[®] reagent (Ambion Life Technologies, Carlsbad, CA, United States). Subsequently, mRNA was isolated following the manufacturers protocol. DNA contaminations were digested using DNase (DNase I, RNase-free Kit; Thermo Scientific, Waltham, MA, United States) and mRNA concentrations were determined using a NanoDropTM2000 spectrophotometer (Thermo Scientific, Waltham, MA, United States). Afterwards, reverse transcription was performed using the High Capacity RNA-to-cDNA Kit (Applied Biosystems, Foster City, CA, United States) following the manufacturers protocol. PCR was performed with SYBR green fluorescent dye (Applied Biosystems, Foster City, CA, United States) with a StepOnePlus Real-Time PCR System (Applied Biosystems, Foster City, CA, United States) using specific primers for murine adiponectin, FABP-4, GLUT-4, and LPL (**Table 1**). Relative mRNA expression was determined by the $2^{-\Delta\Delta C_t}$ method normalized to murine non-POU domain-containing octamer binding protein (Nono). All samples were measured in triplicates and experiments were repeated independently at least three times.

PPAR Reporter Gene Assay

HEK-293T cells were seeded in 96-well plates (2.5×10^4 cells/well) and were allowed to adhere overnight. Before transfection, medium was changed to Opti-MEM without supplements. Transient plasmid transfection was carried out using Lipofectamine LTX reagent (Invitrogen, Carlsbad, CA, United States) according to the manufacturer's protocol with pFR-Luc (Stratagene, La Jolla, CA, United States), pRL-SV40

TABLE 1 | Primer sequences and nucleotide accession numbers of the genes investigated.

Murine gene	Nucleotide accession number	Primer sequence
FABP4	NM_024406.2	F: AGAAGTGGGAGTGGGCTTTG R: ACTCTCTGACCGGATGGTGA
SLC2A4 (GLUT4)	NM_009204	F: TGAAGAACGGATAGGGAGCAG R: GAAGTGCAAAGGGTGAGTGAG
LPL	NM_008509	F: CCCAGCTTCGTCATCGAGAG R: GTCCAGTGTGAGCCAGACTT
ADIPOQ (Adiponectin)	NM_009605	F: TGACGACACCAAAAGGGCTC R: CACAAGTTCCTTGGGTGGA
Nono	NM_001252518.1 NM_023144.2	F: TGCTCCTGTGCCACCTGGTACTC R: CCGGAGCTGGACGGTTGAATGC

(Promega, Fitchburg, MA, United States) and pFA-CMV-PPAR-LBD (Rau et al., 2006). 5 h after transfection, medium was changed to Opti-MEM supplemented with penicillin (100 U/mL) and streptomycin (100 μ g/mL), now additionally containing 0.1% DMSO and the respective test compound or 0.1% DMSO alone as untreated control. Each concentration was tested in triplicates and each experiment was repeated independently at least four times. Following overnight (12–16 h) incubation with the test compounds, cells were assayed for luciferase activity using the Dual-GloTM Luciferase Assay System (Promega, Fitchburg, MA, United States) according to the manufacturer's protocol. Luminescence was measured with an Infinite M200 luminometer (Tecan Group Ltd., Männedorf, Switzerland). Normalization of transfection efficiency and cell growth was done by division of firefly luciferase data by renilla luciferase data and multiplying the value by 1000 resulting in relative light units (RLU). Fold activation was obtained by dividing the mean RLU of a test compound at a respective concentration by the mean RLU of untreated control. Relative activation was obtained by dividing the fold activation of a test compound at a respective concentration by the fold activation of the respective PPAR α , γ or δ full agonist GW-7647, pioglitazone or L165,041 at 1 μ M. EC₅₀ and standard deviation were calculated with the mean relative activation values of at least four independent experiments by SigmaPlot 10.0 (Systat Software GmbH, Erkrath, Germany) using a four parameter logistic regression.

Recombinant sEH Activity

For determination of IC₅₀ values of recombinant human sEH a 96-well fluorescence-based assay system was used as described before (Blöcher et al., 2016a). In brief, non-fluorescent PHOME (3 phenylcyano-(6-methoxy-2-naphthalenyl)methyl ester 2-oxiraneacetic acid, Cayman Chemicals, Ann Arbor, MI, United States) was used as substrate, which is hydrolyzed by sEH to the fluorescent 6-methoxynaphthaldehyde (Rau et al., 2006). The formation of the fluorescent product was measured (λ_{em} = 330 nm, λ_{ex} = 465 nm) by an Infinite F200 Pro plate reader (Tecan Group Ltd., Männedorf, Switzerland). For that

purpose, 2 μ g recombinant human sEH in 100 μ l bis-Tris buffer (pH 7, 0.1 mg/mL BSA, 0.01% Triton-X 100) was applied per well. This protein solution was then incubated with different concentrations of the test compounds for 30 min at RT. After this, 10 μ L of the substrate were added (final concentration 50 μ M). The formation of 6-methoxynaphthaldehyde was monitored for 30 min. All concentrations were tested in triplicate wells.

sEH Activity in HEP-G2 Cell Lysates

Quantification of cellular sEH metabolic activity was performed as described by Zha et al. (2014). For this, HEP-G2 cells were harvested, washed twice with PBS and sonicated in PBS for disruption of cell integrity. Then, 1 μ g of total cell homogenate diluted in 100 μ l of PBS containing 0.1 mg/ml BSA was incubated with the compounds or vehicle for 15 min at 37°C. After this, 25 ng (\pm)14(15)-EET-d₁₁ (Cayman Chemical, Ann Arbor, MI, United States) were added per sample and the incubation was continued for additional 10 min at 37°C. A blank was performed using PBS (containing 0.1 mg/mL BSA). The reactions were stopped by adding 100 μ L of ice cold methanol. After centrifugation (2000 rpm, 4°C, 5 min), supernatants were analyzed by LC-MS/MS and the amounts of (\pm)14(15)-EET-d₁₁ and the corresponding (\pm)14(15)-DHET-d₁₁ were determined.

Determination of

(\pm)14(15)-EET-d₁₁/ \pm 14(15)-DHETd₁₁ by LC/MS-MS

14(15)-EET-d₁₁ and 14(15)-DHET-d₁₁ content of the extracted samples were analyzed employing liquid chromatography tandem mass spectroscopy (LC-MS/MS). The LC/MS-MS system comprised an API 5500 QTrap (Sciex, Darmstadt, Germany), equipped with a Turbo-V-source operating in negative ESI mode, an Agilent 1200 binary HPLC pump and degasser (Agilent, Waldbronn, Germany) and an HTC Pal autosampler (Chromtech, Idstein, Germany) fitted with a 25 μ L LEAP syringe (Axel Semrau GmbH, Sprockhövel, Germany). High purity nitrogen for the mass spectrometer was produced by a NGM 22-LC/MS nitrogen generator (cmc Instruments, Eschborn, Germany). All substances were obtained from Cayman Chemical, Ann Arbor, MI, United States. Stock solutions with 2,500 ng/mL of both analytes were prepared in methanol. Working standards were obtained by further dilution with a concentration range of 0.1–250 ng/mL for 14(15)-EET-d₁₁ and 14(15)-DHET-d₁₁. Sample extraction was performed with liquid–liquid-extraction. Therefore, 150 μ L of matrix homogenates were gently mixed with 20 μ L of internal standard [14(15)-EET and 14(15)-DHET all with a concentration of 100 ng/ml in methanol], and were extracted twice with 600 μ L of ethyl acetate. Samples for standard curve and quality control were prepared similarly, instead of 150 μ L of matrix homogenates, 150 μ L PBS were added. Further 20 μ L methanol, 20 μ L working standard and 20 μ L internal standard were added. The organic phase was removed at a temperature of 45°C under a gentle stream of nitrogen. The residues were reconstituted with 50 μ L of methanol/water/(50:50, v/v), centrifuged for 2 min at 10,000 g and then transferred to glass vials (Macherey-Nagel, Düren, Germany) prior to

injection into the LC-MS/MS system. For the chromatographic separation a Gemini NX C18 column and pre-column were used (150 mm \times 2 mm i.d., 5 μ m particle size and 110 Å pore size from Phenomenex, Aschaffenburg, Germany). A linear gradient was employed at a flow rate of 0.5 mL/min mobile phase with a total run time of 17.5 min. Mobile phase was A water/ammonia (100:0.05, v/v) and B acetonitrile/ammonia (100:0.05, v/v). The gradient started from 85% A to 10% within 12 min. This was held for 1 min at 10% A. Within 0.5 min the mobile phase shifted back to 85% A and was held for 3.5 min to equilibrate the column for the next sample. The injection volume of samples was 20 μ L. Quantification was performed with Analyst Software V 1.5.1 (Sciex, Darmstadt, Germany) employing the internal standard method (isotope- dilution mass spectrometry). Ratios of analyte peak area and internal standard area (y -axis) were plotted against concentration (x -axis) and calibration curves were calculated by least square regression with 1/concentration² weighting.

PPAR γ Coactivator Recruitment Assay

Recruitment of coactivator-derived peptides to the PPAR γ -LBD was studied by homogeneous time-resolved fluorescence resonance energy transfer (HT-FRET). Terbium cryptate as streptavidin conjugate (Cisbio assays, France) was used as FRET donor. Peptides derived from the coactivator cyclic AMP response element-binding protein (CREB)-binding protein (CBP) [biotin-NLVPDAASKHKQLSELLRGSGS] encompassing the coactivator consensus motif LxxLL and N-terminal biotin for stable coupling to streptavidin were purchased from Eurogentec GmbH (Cologne, Germany). Solutions containing 12 nM recombinant PPAR γ -LBD fused to N-terminal GFP as FRET acceptor and 12 nM FRET donor complex with the CBP-derived peptide as well as 1% DMSO with test compound at varying concentrations or DMSO alone were prepared in HEPES buffer [25 mM HEPES pH 7.5 adjusted with KOH, 150 mM KF, 5% (w/v) glycerol, 0.1% (w/v) CHAPS, 5 mM DTT]. After 2 h incubation at RT, the fluorescence intensities (FI) at 520 nm (acceptor) and 620 nm (donor reference) after excitation at 340 nm were recorded on a Tecan Infinite F200 (Tecan Group Ltd., Männedorf, Switzerland). FI_{520nm} was divided by FI_{620nm} and multiplied with 10,000 giving a dimensionless HTRF signal. Recruitment of coactivator-derived peptides to the PPAR γ -LBD was validated with increasing concentrations of rosiglitazone. Recruitment of CBP was referenced to recruitment in response to 1 μ M rosiglitazone (\sim EC₈₀) and reported as relative coactivator recruitment.

Molecular Docking Studies

Molecular modeling experiments were carried out using MOE (Molecular Operating Environment v. 2016.0802, Chemical Computing Group, Montreal, QC, Canada). Structure preparation of PPAR γ LBD (3WMH) and sEH c-terminal domain (5ALZ) were subjected to the Quick Preparation routine, which includes automated structure curation, determination of protonation state and restrained energy minimization. Afterwards, molecular docking of zafirlukast was performed using default settings for induced fit docking. London dG scoring function was used for initial placement of 30 poses and afterwards

refinement was performed using the MM/GBVI method (Zha et al., 2014). After visual inspection, the highest-scored pose was used to put up the binding mode hypothesis.

Drugs, Chemical Reagents and Other Materials

DMEM, OptiMEM, penicillin-streptomycin, PBS and sodium pyruvate were obtained from Gibco by Life Technologies (Carlsbad, CA, United States), SYBR green MicroAmp Fast Optical 96-well Reaction Plate 0.1 ml and StepOnePlus thermocycler were obtained from Applied Biosystems (Foster City, CA, United States). FCS was purchased from Capricorn (Ebsdorfergrund, Germany). New born calf serum was purchased from Biochrom (Berlin, Germany). All primer pairs were purchased from Eurofins (Friedrichsdorf, Germany). Cell culture flasks (T75, Cell+, vented cap) and 6-well plates for sub-culturing 3T3-L1 cells were obtained from SARSTEDT (Nümbrecht, Germany). Rosiglitazone, pioglitazone, zafirlukast, montelukast, IBMX and (\pm)14(15)-EET-d₁₁ were purchased from Cayman Chemical (Ann Arbor, MI, United States). Insulin, dexamethasone and Oil Red O were obtained from Sigma Aldrich (St. Louis, Missouri, MO, United States). Tris, Triton-X-100, NP-40, NaCl, EDTA and SDS were purchased from AppliChem (Darmstadt, Germany).

Statistical Analysis

All data are presented as mean with SEM (standard error of the mean). GraphPad Prism version 5.00 (GraphPad Software, San Diego, CA, United States) was used for statistical analysis. Data were subjected to either Repeated Measure Analysis Of Variance (ANOVA) coupled with Dunnett's post *t*-test for multiple comparisons or a two-sided paired students *t*-test. A sigmoidal concentration-response curve-fitting model with a variable slope was employed to calculate the IC₅₀ values [non-linear regression; dose-response-inhibition; log(inhibitor) vs. response- variable slope (4 parameters)].

RESULTS

Influence of the CysLT1RA on the Activation PPAR Reporter Constructs

To investigate the influence of the three marketed CysLT1RA montelukast, pranlukast, and zafirlukast on the activation of

the PPARs α , γ , or δ , a hybrid reporter gene assays specific for each isoform was utilized. For this, a hybrid receptor construct containing the respective human PPAR ligand binding domain and hinge region fused to the DNA binding domain of the yeast nuclear receptor Gal4 and a Gal4-responsive firefly luciferase construct were co-transfected into HEK-293T cells together with a plasmid constitutively expressing *Renilla* luciferase for normalization of transfection efficiency and cell growth. Activation of the PPAR isoforms was compared to 1 μ M of the well characterized agonists GW7647, L165,041, and pioglitazone for PPAR α , δ , and γ , respectively. PPAR α and PPAR δ were not activated by the CysLT1RA tested at concentrations up to 10 μ M. In contrast, PPAR γ was strongly activated by zafirlukast with an EC₅₀ value of $2.49 \pm 0.45 \mu$ M and a maximal activation of $148 \pm 15\%$ compared to pioglitazone (1 μ M). Montelukast showed PPAR γ activation as well, with an EC₅₀ of $1.17 \pm 0.08 \mu$ M but displayed only low overall activation of $21.9 \pm 0.3\%$. Pranlukast only weakly activated PPAR γ by $19.7 \pm 1.1\%$ at 10 μ M and was therefore excluded from further characterization. **Table 2** summarizes the results for activation of the different PPAR isoforms by the CysLT1RAs.

Influence of Zafirlukast and Montelukast on 3T3-L1 Adipocyte Differentiation

As master regulator of adipocyte differentiation in men and mice, PPAR γ plays a crucial role in the cell's commitment to the adipocyte lineage by controlling important functions such as intracellular biosynthesis, transport and accumulation of lipids. Murine 3T3-L1 fibroblasts are a well characterized *in vitro* tool to study PPAR γ induced adipocyte differentiation. These cells can be differentiated from fibroblasts into adipocytes by an activation cocktail (0.5 mM IBMX, 1 μ g/mL insulin, 0.25 μ M dexamethasone) together with the potential PPAR γ agonist. Upon differentiation, different parameters such as lipid accumulation and PPAR γ target gene expression can be assessed to investigate the PPAR γ activating potential of the compounds of interest. Therefore, we treated confluent 3T3-L1 cell layers with the activation cocktail (IBMX, insulin, dexamethasone) plus different concentrations of zafirlukast or montelukast for 48 h to induce differentiation. Rosiglitazone (2 μ M) was used as positive control. This was followed by insulin (1 μ g/mL) treatment for another 48 h. After this, cells were kept in growth medium for a week to complete the differentiation process and allow intracellular lipid accumulation. Subsequently, the cells

TABLE 2 | Influence of the CysLT1RA on the activation of PPAR reporter constructs.

	PPAR α	PPAR γ	PPAR δ	CysLT ₁ R
		EC ₅₀ [μ M]		IC ₅₀ [nM]
Zafirlukast	i.a. @ 10 μ M	2.49 \pm 0.45 μM ($148 \pm 15\%$)	i.a. @ 10 μ M	5
Montelukast	i.a. @ 10 μ M	1.17 \pm 0.08 μM ($21.9 \pm 0.3\%$)	i.a. @ 10 μ M	5
Pranlukast	i.a. @ 10 μ M	@ 10 μM ($19.7 \pm 1.1\%$)	i.a. @ 10 μ M	4

Employing reporter gene assays for the respective PPAR isoforms, EC₅₀ values of the CysLT1RA were determined in HEK-293T cells. PPAR activation of the positive controls GW-7647 (PPAR α), pioglitazone (PPAR γ) and L165,041 (PPAR δ) were set to 100% and receptor activation of the CysLT1RAs were calculated accordingly. Results are shown as \pm SEM of three independent experiments. i.a., inactive.

were stained with Oil Red O solution to investigate the extent of cytoplasmic lipid droplet accumulation as a measure for cell differentiation. As expected, the rosiglitazone (2 μ M) control led to strong accumulation of lipid droplets in the cytoplasm of the cells indicated by intense Oil Red O staining. Interestingly, zafirlukast induced lipid accumulation in a dose-dependent manner, but to a lesser extent compared to rosiglitazone. Montelukast did not trigger any lipid accumulation in 3T3-L1 cells (**Figure 2B**). In line with the staining results, expression levels of both PPAR γ isoforms γ_1 and γ_2 were not affected by montelukast whereas rosiglitazone and zafirlukast treatment upregulated the protein levels. Again, zafirlukast was less effective compared to rosiglitazone (**Figure 2A**).

In addition to lipid accumulation, mitochondrial activity of 3T3-L1 cells during differentiation was investigated by the turnover of the tetrazolium salt WST-1 into a formazan dye. This provides not only further information on the metabolic capacity of the cells after differentiation but can also indicate toxicity of compounds. For this, 3T3-L1 cells were treated with the differentiation cocktail in the presence or absence of PPAR γ agonists for 48 h. After this, WST-1 turnover as a measure for mitochondrial activity was assessed (**Figure 2C**). As anticipated, undifferentiated 3T3-L1 cells as well as cells differentiated in the absence of a PPAR γ agonist (w/o) displayed a third of the metabolic activity of cells treated with the PPAR γ agonist rosiglitazone (2 μ M). Montelukast potently elevated mitochondrial activity in a concentration dependent manner to over threefold of the w/o control at 10 μ M. Also, cells treated with low concentrations of zafirlukast (1 μ M) displayed potent metabolic activation (threefold) while higher concentrations (5 and 10 μ M) showed attenuated metabolic activity which was comparable to the w/o control. Of note, microscopic analysis of the cell layers showed that this was not due to any cell loss, since the monolayer cultures were confluent in all treatments applied.

Influence of Zafirlukast and Montelukast on PPAR γ Target Gene Expression in Differentiated 3T3-L1 Adipocytes

To gain further insight in PPAR γ activation after compound treatment, mature 3T3-L1 adipocytes were harvested after 14 days and mRNA was isolated, reverse transcribed and subjected to quantitative RT-PCR. mRNA expression of the PPAR γ target genes lipoprotein lipase (LPL), the glucose transporter 4 (GLUT-4), the fatty acid binding protein 4 (FABP-4) and adiponectin was monitored by quantitative PCR (**Figures 3A–D** and **Supplementary Figure S1**). Activation of gene transcription was normalized to cells treated with the activation cocktail only. Again, montelukast did not influence the expression of the PPAR γ target genes investigated while zafirlukast dose-dependently induced target gene expression although to a lesser extent compared to rosiglitazone. Of interest, zafirlukast elevated adiponectin levels more effectively compared to the other target genes.

In addition to mRNA expression, the protein expression levels of the two PPAR γ target genes FABP-4 and CD36 in differentiated 3T3-L1 cells after 14 days were investigated. For this, total protein

lysates were separated by gel electrophoresis followed by Western Blotting (**Figures 3E,F** and **Supplementary Figures S2A,B**). As anticipated, 2 μ M rosiglitazone upregulated the expression of all target genes investigated with high potency. Again, zafirlukast induced target gene expression as well but to a weaker extent and montelukast displayed no effect at all.

Influence of Zafirlukast on PPAR γ Phosphorylation and Cofactor Recruitment

Next, we analyzed the ability of zafirlukast to interfere with the phosphorylation of PPAR γ at serine 273 in 3T3-L1 cells. We induced this post-translational modification by short-term treatment of the differentiated cells with the cytokine TNF α , generating a pro-inflammatory milieu. In our hands, untreated cells already showed Serine 273 phosphorylation of PPAR γ_1 (uniprot ID: P37231-2) and this was not changed after addition of TNF α . In contrast, PPAR γ_2 (uniprot ID: P37231-1) was efficiently phosphorylated upon treatment with TNF α . The control compound rosiglitazone inhibited this phosphorylation, although this effect was not significant. Of note, zafirlukast inhibited this phosphorylation in our assay system as well (**Figure 4A** and **Supplementary Figure S3**). This indeed suggested an influence of zafirlukast on PPAR γ cofactors. Thus, we evaluated the direct influence of montelukast and zafirlukast on the recruitment of coactivators to the receptor. For this, we used an assay system in which the recruitment of the fluorescence-tagged PPAR γ coactivator CBP to the PPAR γ -LBD was assessed by time-resolved FRET technique in presence and absence of rosiglitazone. Montelukast weakly antagonized the rosiglitazone induced CBP recruitment in concentrations above 3 μ M and did not induce CBP recruitment itself in concentrations up to 20 μ M. At higher concentrations montelukast seemed to trigger recruitment but this may be due to unspecific protein aggregation. Zafirlukast did not induce CBP recruitment itself. Instead, the compound was able to antagonize the rosiglitazone (1 μ M) induced CBP recruitment with an IC₅₀ of 4.7 μ M after 2 h (**Figure 4B**).

Influence of the CysLT1RA on sEH Activity

In recent years, a number of animal studies could show that the combination of PPAR γ activation with sEH inhibition is advantageous for the treatment of the MetS. Therefore, we were interested if the CysLT1RAs zafirlukast, pranlukast, and montelukast as eicosanoid mimetics might also interfere with sEH in addition to their PPAR γ agonistic activities. For this, recombinant human sEH was incubated with zafirlukast or pranlukast in the presence of the non-fluorescent sEH substrate PHOME which is cleaved by the enzyme to form a fluorescent product. Montelukast was excluded from this assay due to its autofluorescence which interfered with product detection. Indeed, zafirlukast and pranlukast inhibited the recombinant sEH with an IC₅₀ of 1.97 ± 0.08 μ M and 8.86 ± 0.32 μ M, respectively (**Figure 5A** and **Table 3**). To confirm these results and to determine the influence of montelukast on sEH activity,

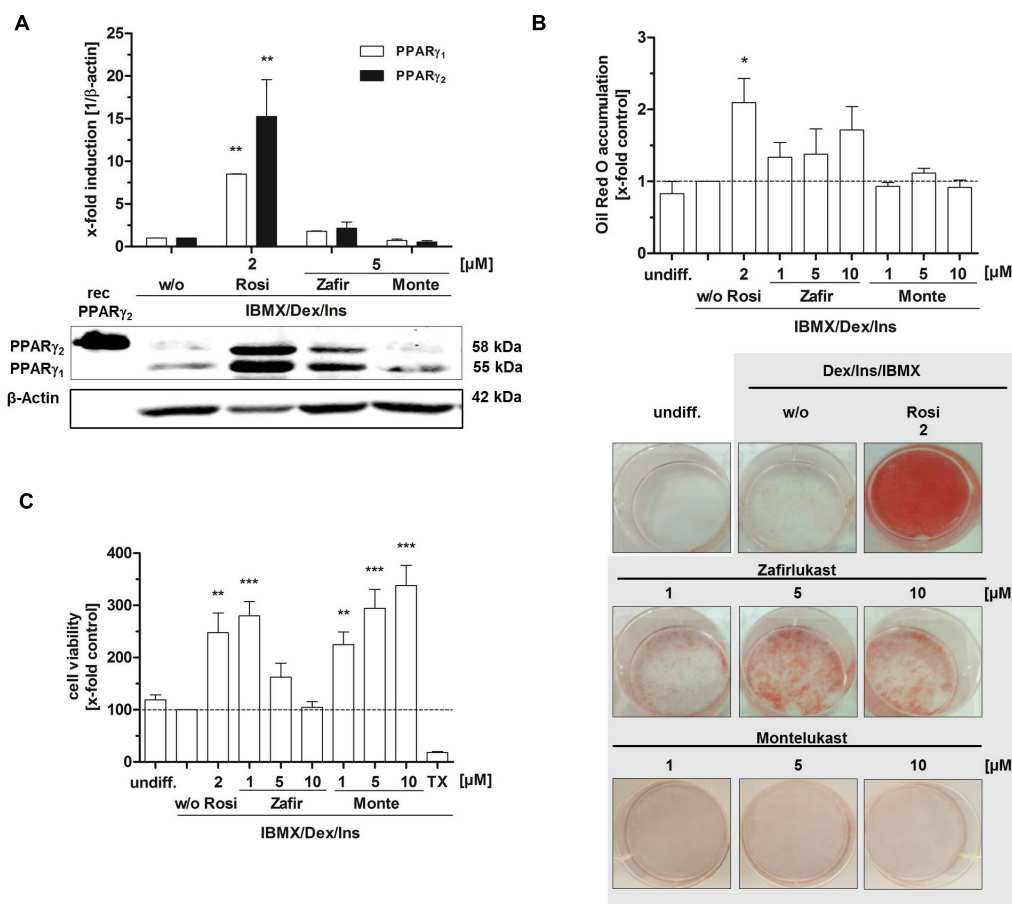


FIGURE 2 | Influence of CysLT1RA on 3T3-L1 adipocyte differentiation. **(A)** Protein expression of PPAR γ in 3T3-L1 adipocytes differentiated in the presence of 0.25 μ M dexamethasone, 0.5 mM IBMX, 1 μ g/ml insulin plus CysLT1RA or rosiglitazone (2 μ M) or DMSO (w/o). One representative western blot out of three is shown. Photographs **(B)** and densitometric analysis of the lipid accumulation in 3T3-L1 adipocytes visualized by Oil Red O staining of the differentiated cells in the presence of montelukast and zafirlukast. Rosiglitazone and DMSO (w/o) were used as positive and negative control, respectively. One representative experiment out of three is shown. **(C)** WST-1 viability assay of 3T3-L1 cells treated with the compounds plus differentiation cocktail (0.25 μ M dexamethasone, 0.5 mM IBMX, 1 μ g/ml insulin) for 48 h. Ins, Insulin; IBMX, isobutylmethylxanthine; Monte, montelukast; Rosi, rosiglitazone; w/o, without PPAR γ agonist; Zafir, zafirlukast. Significant changes versus the untreated control are indicated with an asterisk. * $P \leq 0.05$, ** $P \leq 0.01$, *** $P \leq 0.001$.

conversion of deuterated 14,15-EET to 14,15-DHET in HEP-G2 cell preparations was measured via LC-MS/MS. HEP-G2 cells express high amounts of sEH which renders them an ideal tool to investigate enzyme activity in a less artificial environment (Figure 5B and Table 3). All CysLT1RAs tested in this study inhibited the formation of 14,15-DHET from the corresponding epoxide with IC₅₀ values of $0.82 \pm 0.24 \mu$ M, $1.95 \pm 0.30 \mu$ M, and $14.11 \pm 3.22 \mu$ M for zafirlukast, montelukast, and pranlukast, respectively.

DISCUSSION

In the present report, we have investigated the sEH inhibitory as well as the PPAR activating potential of the marketed CysLT1RAs montelukast, pranlukast and zafirlukast. As expected, the chemically distinct scaffolds of these compounds resulted in different interaction profiles on the investigated

targets. Zafirlukast turned out to be a dual modulator of human sEH and PPAR γ . Montelukast and pranlukast were primarily sEH inhibitors.

CysLT₁ receptor antagonists have been developed for the treatment of atopic diseases such as asthma and allergic rhinitis. Displaying low nanomolar inhibitory activity to their target receptor these well-tolerated compounds were originally designed to inhibit the vasodilatory and bronchoconstrictory activities of cysteinyl leukotrienes. The anti-inflammatory properties of this compound class are well documented and therapy is thought to have few side-effects and therefore is considered safe. Recently, it has been shown that asthmatic patients taking montelukast display lower levels of blood lipids and CVD-associated inflammatory biomarkers (Hwang et al., 2013; Ibrahim et al., 2014; Hoxha et al., 2017). In accordance, a retrospective Swedish nationwide study suggested that regular intake of montelukast reduces the risk for recurrent stroke and myocardial infarction (Allayee et al., 2007; Ingelsson

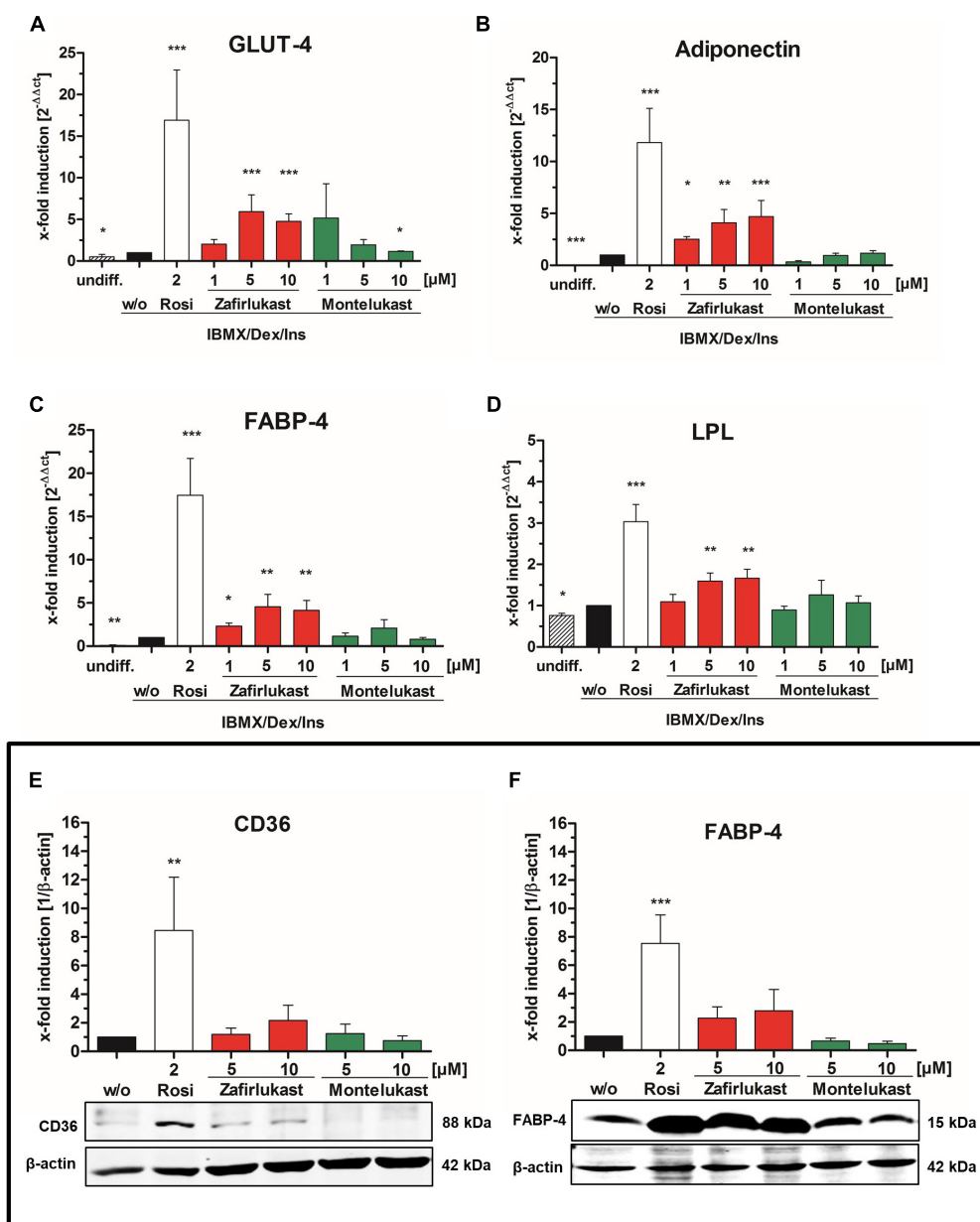


FIGURE 3 | Influence of CysLT1RA on PPAR γ target gene expression in 3T3-L1 adipocytes. Semi-quantitative mRNA expression of (A) GLUT-4, (B) adiponectin, (C) FABP-4, and (D) lipoprotein lipase in 3T3-L1 adipocytes differentiated in the presence of 0.25 μ M dexamethasone, 0.5 mM IBMX, 1 μ g/ml insulin plus the PPAR γ agonist rosiglitazone (2 μ M) or zafirlukast and montelukast. Results are shown as fold induction of the DMSO treated control ($2^{-\Delta\Delta Ct}$ method). Results are given as mean + SEM of three to six independent experiments. Western Blot experiments showing (E) CD36 and (F) FABP-4 protein expression in 3T3-L1 adipocytes differentiated in presence of 0.25 μ M dexamethasone, 0.5 mM IBMX, 1 μ g/ml insulin plus the PPAR γ agonist rosiglitazone or zafirlukast or montelukast. DMSO (w/o) treated cells were used as negative control. Densitometry results are presented as mean + SEM. One representative western blot experiment out of three is shown. Significant changes versus the untreated control are indicated with an asterisk. * $P \leq 0.05$, ** $P \leq 0.01$, *** $P \leq 0.001$.

et al., 2012). In line with these observations, higher doses of montelukast and zafirlukast are effective in several animal models of CVDs where they showed anti-atherosclerotic effects, protected from myocardial infarction and renal perfusion injury in rabbits, rats and mice (Sener et al., 2006; Jawien et al., 2008; Mueller et al., 2008; Ge et al., 2009; Liu et al., 2009). In addition, during treatment with zafirlukast (20 mg, twice

daily) rare cases of hypoglycemic events were observed and it was shown recently that the compound increases insulin secretion from pancreatic β cells (Calhoun et al., 1998; Hwang et al., 2018). These findings concerning the beneficial effects on cardiovascular and diabetic disorders clearly argue for an additional, CysLT-unrelated, mechanism of action which can be exploited for therapy in the future. Indeed, several publications

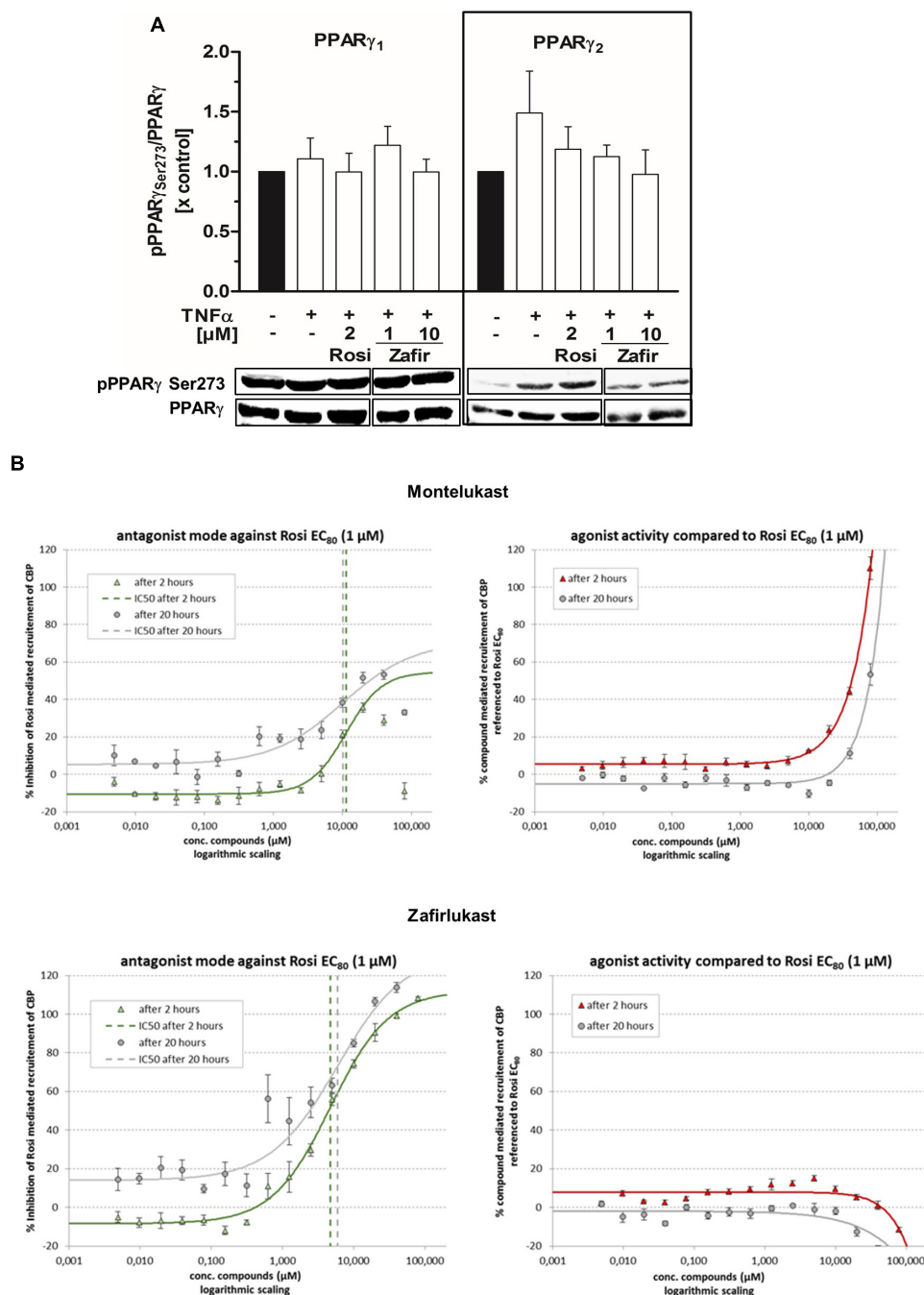


FIGURE 4 | Influence of zafirlukast on PPAR γ phosphorylation (Serine 273) and cofactor recruitment. **(A)** Differentiated 3T3-L1 adipocytes were treated with vehicle, the PPAR γ agonist rosiglitazone or zafirlukast for 45 min followed by treatment with TNF α (50 ng/mL) for 30 min. Lysates of the treated cells were analyzed afterwards for PPAR γ phosphorylation at Serine 273 by Western Blotting. Densitometry results are presented as mean \pm SEM. One representative Western Blot out of three is shown. **(B)** Recruitment of the recombinant cofactor CBP to the recombinant PPAR γ -LBD by in presence and absence of rosiglitazone via time-resolved FRET analysis. Results are presented as mean \pm SEM. Significant changes versus the untreated control are indicated with an asterisk. * $P \leq 0.05$, ** $P \leq 0.01$, *** $P \leq 0.001$.

could already show that montelukast, pranlukast as well as zafirlukast display an interesting polypharmacological profile. Already described off-target effects are inhibition of additional pro-inflammatory targets such as the PGE $_2$ down-stream

synthase mPGES-1, 5-lipoxygenase, cAMP phosphodiesterases and NF κ B (Ramires et al., 2004; Anderson et al., 2009; Fogli et al., 2013; Kahnt et al., 2013; Theron et al., 2014; Hoxha et al., 2017).

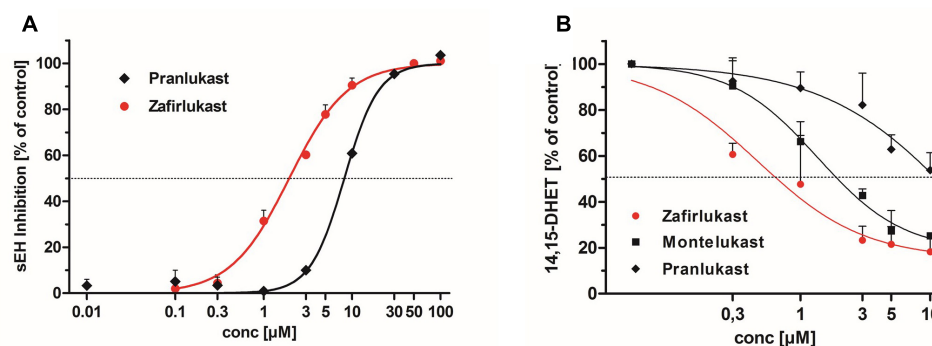


FIGURE 5 | Influence of CysLT1RA on sEH activity. **(A)** Inhibition profiles of pranlukast and zafirlukast on recombinant human sEH. PHOME was used as fluorescence substrate. Results are given as mean + SEM of three independent experiments. **(B)** sEH inhibition profiles of pranlukast, montelukast and zafirlukast in HEP-G2 lysates. (\pm)14(15)-EET- d_{11} was used as sEH substrate and the resulting DHET levels were measured via LC-MS/MS. Results are given as mean + SEM out of three independent experiments.

TABLE 3 | Inhibition of sEH by CysLT1RA.

	sEH rec.	sEH (HEP-G2)	CysLT $_1$ R
	IC $_{50}$ [μM]		[nM]
Zafirlukast	1.97 \pm 0.08 μM	0.82 \pm 0.24 μM	5
Montelukast	n.d.	1.95 \pm 0.30 μM	5
Pranlukast	8.86 \pm 0.19 μM	14.11 \pm 3.22 μM	4

sEH activities were determined with recombinant enzyme as well as HEP-G2 cell lysates. For determination of the activity of recombinant sEH, a fluorescence-based assay using PHOME as substrate was employed. In contrast, sEH activity in HEP-G2 cell lysates was measured by conversion of deuterated 14,15-EET into the corresponding diol by LC-MS/MS technique. Results are shown SEM of three independent experiments. n.d., not determined due to autofluorescence of the compound; rec, recombinant enzyme.

The combination therapy of sEH inhibition with PPAR γ agonism effectively lowers blood pressure, reduces systemic glucose, triglyceride and free fatty acid levels and is also renoprotective in animal models (Imig et al., 2012; Hye Khan et al., 2018). sEH as well as the PPAR receptors interact with a number of oxidized arachidonic acid metabolites, so-called eicosanoids. Therefore, interaction with eicosanoid mimetic compounds such as CysLT1RA suggests itself. Due to the fact that the already published off-target activities of the marketed CysLT1RAs do not sufficiently explain the beneficial effects on cardiovascular outcome and insulin secretion in man as well as their efficacy in various animal models of atherosclerosis and the MetS, we were interested if these compounds interact with sEH and PPAR isoform activities.

sEH is an enzyme that hydrolyzes cytochrome P450-derived arachidonic acid epoxides (epoxyeicosatrienoic acids, EETs) with potent vasoprotective activities into their corresponding vicinal diols (dihydroxyeicosatrienoic acids – DHETs). Upon this conversion, the beneficial effects of EETs such as vasodilation, inhibition of platelet aggregation, promotion of fibrinolysis and reduction of vascular smooth muscle cell proliferation are lost. Accordingly, it has been demonstrated in numerous studies that inhibition of sEH is antihypertensive, organ protective and

has beneficial effects on glucose metabolism (Fleming, 2014). According to the results presented in this study, all CysLT1RAs investigated inhibit human sEH. Montelukast and zafirlukast showed IC_{50} values in the nanomolar to low micromolar range which can be easily achieved with therapeutic dosage in humans as both compounds reach low micromolar plasma levels upon frequent dosing. This might explain the beneficial effects of montelukast on CVD-associated events and also raises this possibility for zafirlukast. The IC_{50} value for sEH inhibition of pranlukast was higher and might not be achieved *in vivo*.

We investigated the influence of the CysLT1RA on activation of the PPAR isoforms, γ , α , and δ . While the α and δ isoforms were not influenced by any of the tested compounds, montelukast and zafirlukast activated the PPAR γ reporter construct in our study. Zafirlukast showed potent maximal activation of the receptor compared to the reference agonist pioglitazone ($\sim 150\%$) with an IC_{50} of 2.49 μM whereas montelukast showed a reduced overall receptor activation compared to the control with an IC_{50} of 1.17 μM . Then, we investigated the influence of both compounds on PPAR γ activation further by studying the differentiation of 3T3-L1 cells into adipocytes followed by PPAR γ target gene expression analysis. Zafirlukast dose-dependently triggered 3T3-L1 differentiation judging from the lipid accumulation data and the target genes investigated. Surprisingly, the extent of lipid accumulation and target gene upregulation was lower than anticipated. Montelukast did not induce cell lipid accumulation and showed only weak effects on some target genes investigated. Nevertheless, both montelukast and low dose zafirlukast potentially upregulated the metabolic activity of 3T3-L1 cells comparable to the rosiglitazone control. In contrast, high concentrations of zafirlukast (5 and 10 μM) had no influence on mitochondrial activity.

PPAR γ is a member of the PPAR nuclear receptor family and plays a key role in adipogenesis, lipid metabolism, glucose homeostasis and anti-inflammatory processes (Tontonoz and Spiegelman, 2008). It is therefore targeted for the treatment of type II diabetes. Activation of this nuclear receptor by thiazolidinedione (TZD) compounds such as pioglitazone and

rosiglitazone influences insulin action and blood-glucose levels (Staels and Fruchart, 2005). Unfortunately, the clinical use of TZDs is limited due to excessive weight gain, edema formation and an elevated osteoporosis incidence in patients. Although the equilibration of blood glucose levels reduces microvascular complications under TZD treatment, these compounds are only poorly effective on the occurrence of macrovascular events (Rohatgi and McGuire, 2008; Ahmadian et al., 2013). In contrast to endogenous PPAR γ ligands which display moderate and selective induction of certain PPAR γ target genes, TZDs upregulate target gene expression with high potency in a global fashion. This is thought to be the cause for many of the adverse events seen under TZD treatment. At present, development of new PPAR γ activators focuses on compounds that selectively fine tune PPAR γ activity instead of exerting full blown agonism. These new modulators differentially influence cofactor recruitment or act as partial agonists that influence expression in a target gene and cell type dependent manner (Wright et al., 2014; Garcia-Vallvé et al., 2015).

In our hands, zafirlukast displayed a high maximal induction of the reporter gene construct in HEK-293T cells but its effect on 3T3-L1 lipid accumulation and PPAR γ target gene expression was way lower than anticipated from its reporter gene data. Due to this, we hypothesized that zafirlukast might additionally influence post-translational modifications of PPAR γ and thus cofactor recruitment in adipocytes. PPAR γ binds a number of cofactors depending on the target gene. For this, the receptor can be modified by phosphorylation of various serine residues which influence receptor activity and target gene transcription by altering cofactor recruitment. Among these modifications is the CDK5-mediated phosphorylation of PPAR γ that is triggered under pro-inflammatory conditions. This modification does not suppress the transcriptional activity of the receptor in general along with its overall adipogenic capacity. Instead, it modulates the recruitment of co-regulators leading to a dysregulation of various genes, among them adiponectin, whose expression is altered under chronic inflammatory conditions such as obesity.

Interestingly, this phosphorylation can be blocked by anti-diabetic PPAR γ ligands, such as rosiglitazone (Choi et al., 2011). Indeed, zafirlukast was able to completely revert this phosphorylation in TNF α treated 3T3-L1 adipocytes which shows that the compound most probably interferes with the binding of cofactors. This might explain the differing extent of target gene upregulation compared to rosiglitazone and the attenuated mitochondrial activity in cells treated with higher concentrations of zafirlukast.

Owing to the phosphorylation data, we were interested in the direct influence of montelukast and zafirlukast on PPAR γ coactivator recruitment. For this, we used an assay system in which the recruitment of the fluorescence-tagged PPAR γ coactivator CBP to the PPAR γ -LBD was assessed by time-resolved FRET technique in presence and absence of rosiglitazone. Zafirlukast did not induce CBP recruitment itself. Instead, the compound potentially antagonized the rosiglitazone induced cofactor recruitment in a non-covalent manner with an IC₅₀ of 4.7 μ M. Montelukast weakly antagonized the rosiglitazone induced CBP recruitment. At higher concentrations the compound led to an elevation of the FRET signal probably due to unspecific protein aggregation. These results clearly argue for an interesting PPAR γ modulatory role of zafirlukast rather than full agonism. In addition, this explains both the differing activation potencies of zafirlukast for adiponectin compared to the TZD control and the absence of 3T3-L1 mitochondrial activation in cells treated with high concentrations of the compound. Montelukast treatment was not able to trigger lipid accumulation in 3T3-L1 pre-adipocytes which fits to its weak PPAR γ induction measured in the reporter gene assay experiments. Nevertheless, it potentially elevated the mitochondrial activity of these cells. If this is due to its weak interference with PPAR γ cofactors and/or sEH antagonism or another off-target effect of the compound remains to be investigated in the future.

We performed *in silico* docking studies to gain further information about the possible binding modes of zafirlukast to its targets. Zafirlukast is based on an indole scaffold which is a privileged heterocycle among fatty acid mimetics

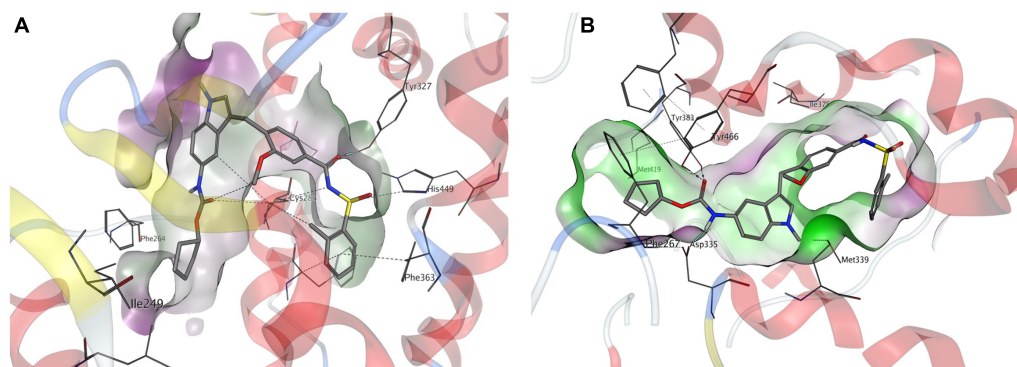


FIGURE 6 | Molecular docking of zafirlukast to human PPAR γ and sEH. **(A)** Proposed binding mode of zafirlukast (gray sticks) to the PPAR γ ligand binding domain – the acidic acyl sulphonamide moiety exhibits directed indications toward the amino acids responsible for activation of PPAR γ , while the substituted indole residue occupies a large hydrophobic sub-pocket. **(B)** Proposed binding mode of zafirlukast (gray sticks) to the sEH C-terminal domain – the carbamate moiety interacts with the catalytic triade Tyr383, Tyr466 and Asp335.

(Proschak et al., 2017). Different functional moieties are probably responsible for the interaction with the targets investigated in this study: Inhibition of sEH is most probably caused by the presence of a carbamate function, which acts as an epoxide mimetic and interacts with the enzyme's catalytic triad. This carbamate function is enclosed by two lipophilic moieties that fit well into the lipophilic pockets adjacent to the catalytic center of sEH. Indeed, molecular docking revealed that the linear shape of zafirlukast fits well into the binding site of human sEH (**Figure 6B**). While the carbamate moiety is mainly responsible for sEH binding, the acidic acyl sulfonamide linked to a lipophilic region on the opposite side of the molecule is a characteristic pharmacophore of PPAR γ agonists. Indeed, our molecular docking studies suggested that this moiety is able to interact with four amino acid residues responsible for stabilization of the AF-2 helix in PPAR γ (**Figure 6A**). Of note, this region is important for the receptor's cofactor recruitment and activation.

Taken together, zafirlukast is a marketed CysLT $_1$ receptor antagonist with additional anti-inflammatory properties such as inhibition of pro-inflammatory PGE $_2$ that also exhibits sEH inhibitory and PPAR γ modulatory properties at pharmacologically relevant concentrations. Especially in the inflammatory environment, the simultaneous inhibition of sEH and moderate activation of PPAR γ should lead to downregulation of NF κ B target genes and TGF- β 1/Smad3 as well as resolution of inflammation by the induction of anti-inflammatory and pro-resolving mediators resulting in inhibition of leukocyte influx into the inflamed tissue and promotion of alternatively activated macrophages (Kim et al., 2014; Croasdel et al., 2015). This has to be confirmed in follow-up studies employing animal models of acute and chronic inflammation which can provide new insights into how the crosstalk between sEH and PPAR γ is influenced by zafirlukast. In addition, zafirlukast is an excellent starting point for the further development of a compound class displaying superior polypharmacology for the treatment of chronic inflammatory diseases such as the MetS. High plasma protein binding has been observed for zafirlukast and peak serum levels achieved after a single oral dose of 20 mg are about 1 μ M (Brocks et al., 1996; Knorr et al., 2001; Karonen et al., 2012). This is pretty close to the EC $_{50}$ and IC $_{50}$ values assessed for PPAR γ and sEH in this study but might hamper the achievement of full activity during therapy. Due to zafirlukast's equipotent target profile and excellent pharmacokinetic properties, derivatives of zafirlukast are bearing the potential to be further optimized

through SOSA (selective optimization of side activity) strategy for various indications (Imig et al., 2012; Blöcher et al., 2016a,b). Indeed, we have recently developed a number of zafirlukast derivatives and successfully accomplished this task by developing a compound with increased bioactivity (Schierle et al., 2018). This lead compound showed improved inhibition of human sEH as well as activation of PPAR γ while it displayed favorable pharmacokinetic properties *in vivo*.

DATA AVAILABILITY

All datasets generated for this study are included in the manuscript and/or the **Supplementary Files**.

AUTHOR CONTRIBUTIONS

TG, OD, SW, DM, CA, EB, RK, LW, TS, JH, and AK performed the experiments. AK, TM, GG, MS-Z, DS, and EP contributed to the conception and design of the study as well data interpretation and analysis. AK and EP wrote the manuscript. All authors contributed to manuscript revision, read and approved the submitted version.

FUNDING

This work was supported by the Else Kröner-Fresenius Foundation (EKFS) Research Training Group Translational Research Innovation – Pharma (TRIP), Landes-Offensive zur Entwicklung Wissenschaftlich-ökonomischer Exzellenz (LOEWE) of the State of Hessen, Research Center for Translational Medicine and Pharmacology TMP, and the German Research Foundation (DFG; Sachbeihilfe PR 1405/2-2; Heisenberg-Professur PR1405/4-1; SFB 1039 Teilprojekt A02, A07, and Z01).

SUPPLEMENTARY MATERIAL

The Supplementary Material for this article can be found online at: <https://www.frontiersin.org/articles/10.3389/fphar.2019.00263/full#supplementary-material>

REFERENCES

- Ahmadian, M., Suh, J. M., Hah, N., Liddle, C., Atkins, A. R., Downes, M., et al. (2013). PPAR γ signaling and metabolism: the good, the bad and the future. *Nat. Med.* 19, 557–566. doi: 10.1038/nm.3159
- Alberti, K. G. M. M., Eckel, R. H., Grundy, S. M., Zimmet, P. Z., Cleeman, J. I., Donato, K. A., et al. (2009). Harmonizing the metabolic syndrome: a joint interim statement of the international diabetes federation task force on epidemiology and prevention; national heart, lung, and blood institute; american heart association; world heart federation; international atherosclerosis society; and international association for the study of obesity. *Circulation* 120, 1640–1645. doi: 10.1161/CIRCULATIONAHA.109.192644
- Allayee, H., Hartiala, J., Lee, W., Mehrabian, M., Irvin, C. G., Conti, D. V., et al. (2007). The effect of montelukast and low-dose theophylline on cardiovascular disease risk factors in asthmatics. *Chest* 132, 868–874. doi: 10.1378/chest.07-0831
- Anderson, R., Theron, A. J., Gravett, C. M., Steel, H. C., Tintinger, G. R., and Feldman, C. (2009). Montelukast inhibits neutrophil pro-inflammatory activity by a cyclic AMP-dependent mechanism. *Br. J. Pharmacol.* 156, 105–115. doi: 10.1111/j.1476-5381.2008.00012.x
- Blöcher, R., Lamers, C., Wittmann, S. K., Diehl, O., Hanke, T., Merk, D., et al. (2016a). Design and synthesis of fused soluble epoxide hydrolase/peroxisome proliferator-activated receptor modulators. *Med. Chem. Commun.* 7, 1209–1216. doi: 10.1039/C6MD00042H

- Blöcher, R., Lamers, C., Wittmann, S. K., Merk, D., Hartmann, M., Weizel, L., et al. (2016b). N-Benzylbenzamides: a novel merged scaffold for orally available dual soluble epoxide hydrolase/peroxisome proliferator-activated receptor γ modulators. *J. Med. Chem.* 59, 61–81. doi: 10.1021/acs.jmedchem.5b01239
- Brocks, D. R., Upward, J. W., Georgiou, P., Stelman, G., Doyle, E., Allen, E., et al. (1996). The single and multiple dose pharmacokinetics of pranlukast in healthy volunteers. *Eur. J. Clin. Pharmacol.* 51, 303–308. doi: 10.1007/s002280050202
- Calhoun, W. J., Lavins, B. J., Minkwitz, M. C., Evans, R., Gleich, G. J., and Cohn, J. (1998). Effect of zafirlukast (Accolate) on cellular mediators of inflammation: bronchoalveolar lavage fluid findings after segmental antigen challenge. *Am. J. Respir. Crit. Care Med.* 157(5 Pt 1), 1381–1389. doi: 10.1164/ajrccm.157.5.9609014
- Choi, J. H., Banks, A. S., Kamenecka, T. M., Busby, S. A., Chalmers, M. J., Kumar, N., et al. (2011). Antidiabetic actions of a non-agonist PPAR γ ligand blocking Cdk5-mediated phosphorylation. *Nature* 477, 477–481. doi: 10.1038/nature10383
- Croasdel, A., Duffney, P. F., Kim, N., Lacy, S. H., Sime, P. J., and Phipps, R. P. (2015). PPAR γ and the innate immune system mediate the resolution of inflammation. *PPAR Res.* 2015:549691. doi: 10.1155/2015/549691
- Drew, P. D., Xu, J., and Racke, M. K. (2008). PPAR-gamma: therapeutic potential for multiple sclerosis. *PPAR Res.* 2008:627463. doi: 10.1155/2008/627463
- Eckel, R. H., Alberti, K. G. M. M., Grundy, S. M., and Zimmet, P. Z. (2010). The metabolic syndrome. *Lancet* 375, 181–183. doi: 10.1016/S0140-6736(09)61794-3
- Fleming, I. (2014). The pharmacology of the cytochrome P450 epoxigenase/soluble epoxide hydrolase axis in the vasculature and cardiovascular disease. *Pharmacol. Rev.* 66, 1106–1140. doi: 10.1124/pr.113.007781
- Fogli, S., Stefanelli, F., Neri, T., Bardelli, C., Amoroso, A., Brunelleschi, S., et al. (2013). Montelukast prevents microparticle-induced inflammatory and functional alterations in human bronchial smooth muscle cells. *Pharmacol. Res.* 76, 149–156. doi: 10.1016/j.phrs.2013.08.001
- García-Vallvé, S., Guasch, L., Tomas-Hernández, S., del Bas, J. M., Ollendorff, V., Arola, L., et al. (2015). Peroxisome proliferator-activated receptor γ (PPAR γ) and ligand choreography: newcomers take the stage. *J. Med. Chem.* 58, 5381–5394. doi: 10.1021/jm501155f
- Ge, S., Zhou, G., Cheng, S., Liu, D., Xu, J., Xu, G., et al. (2009). Anti-atherogenic effects of montelukast associated with reduced MCP-1 expression in a rabbit carotid balloon injury model. *Atherosclerosis* 205, 74–79. doi: 10.1016/j.atherosclerosis.2008.11.012
- Grundy, S. M. (2006). Drug therapy of the metabolic syndrome: minimizing the emerging crisis in polypharmacy. *Nat. Rev. Drug Discov.* 5, 295–309. doi: 10.1038/nrd2005
- Hoxha, M., Rovati, G. E., and Cavanillas, A. B. (2017). The leukotriene receptor antagonist montelukast and its possible role in the cardiovascular field. *Eur. J. Clin. Pharmacol.* 73, 799–809. doi: 10.1007/s00228-017-2242-2
- Hwang, H., Park, K., Choi, J. H., Cocco, L., Jang, H., and Suh, P. (2018). Zafirlukast promotes insulin secretion by increasing calcium influx through L-type calcium channels. *J. Cell Physiol.* 233, 8701–8710. doi: 10.1002/jcp.26750
- Hwang, S. H., Weckslar, A. T., Wagner, K., and Hammock, B. D. (2013). Rationally designed multitarget agents against inflammation and pain. *Curr. Med. Chem.* 20, 1783–1799. doi: 10.2174/0929867311320130013
- Hye Khan, M. A., Kolb, L., Skibba, M., Hartmann, M., Blöcher, R., Proschak, E., et al. (2018). A novel dual PPAR- γ agonist/sEH inhibitor treats diabetic complications in a rat model of type 2 diabetes. *Diabetologia* 61, 2235–2246. doi: 10.1007/s00125-018-4685-0
- Ibrahim, M. A., Amin, E. F., Ibrahim, S. A., Abdelzahr, W. Y., and Abdelrahman, A. M. (2014). Montelukast and irbesartan ameliorate metabolic and hepatic disorders in fructose-induced metabolic syndrome in rats. *Eur. J. Pharmacol.* 724, 204–210. doi: 10.1016/j.ejphar.2013.12.024
- Imig, J. D., and Hammock, B. D. (2009). Soluble epoxide hydrolase as a therapeutic target for cardiovascular diseases. *Nat. Rev. Drug Discov.* 8, 794–805. doi: 10.1038/nrd2875
- Imig, J. D., Walsh, K. A., Hye Khan, M. A., Nagasawa, T., Cherian-Shaw, M., Shaw, S. M., et al. (2012). Soluble epoxide hydrolase inhibition and peroxisome proliferator activated receptor γ agonist improve vascular function and decrease renal injury in hypertensive obese rats. *Exp. Biol. Med.* 237, 1402–1412. doi: 10.1258/ebm.2012.012225
- Ingelsson, E., Yin, L., and Bäck, M. (2012). Nationwide cohort study of the leukotriene receptor antagonist montelukast and incident or recurrent cardiovascular disease. *J. Allergy Clin. Immunol.* 129, 702–707.e2. doi: 10.1016/j.jaci.2011.11.052
- Jawien, J., Gajda, M., Wołkow, P., Zurańska, J., Olszanecki, R., and Korb, R. (2008). The effect of montelukast on atherogenesis in apoE/LDLR-double knockout mice. *J. Physiol. Pharmacol.* 59, 633–639.
- Kahnt, A. S., Rörsch, F., Diehl, O., Hofmann, B., Lehmann, C., Steinbrink, S. D., et al. (2013). Cysteinyl leukotriene-receptor-1 antagonists interfere with PGE2 synthesis by inhibiting mPGES-1 activity. *Biochem. Pharmacol.* 86, 286–296. doi: 10.1016/j.bcp.2013.05.005
- Karonen, T., Laitila, J., Niemi, M., Neuvonen, P. J., and Backman, J. T. (2012). Fluconazole but not the CYP3A4 inhibitor, itraconazole, increases zafirlukast plasma concentrations. *Eur. J. Clin. Pharmacol.* 68, 681–688. doi: 10.1007/s00228-011-1158-5
- Kaur, J. (2014). A comprehensive review on metabolic syndrome. *Cardiol. Res. Pract.* 2014:943162. doi: 10.1155/2014/943162
- Kim, J., Imig, J. D., Yang, J., Hammock, B. D., and Padanilam, B. J. (2014). Inhibition of soluble epoxide hydrolase prevents renal interstitial fibrosis and inflammation. *Am. J. Physiol. Renal. Physiol.* 307, F971–F980. doi: 10.1152/ajprenal.00256.2014
- Knorr, B., Nguyen, H. H., Kearns, G. L., Villaran, C., Boza, M. L., Reiss, T. F., et al. (2001). Montelukast dose selection in children ages 2 to 5 years: comparison of population pharmacokinetics between children and adults. *J. Clin. Pharmacol.* 41, 612–619. doi: 10.1177/00912700122010492
- Liu, D., Ge, S., Zhou, G., Xu, G., Zhang, R., Zhu, W., et al. (2009). Montelukast inhibits matrix metalloproteinases expression in atherosclerotic rabbits. *Cardiovasc. Drugs Ther.* 23, 431–437. doi: 10.1007/s10557-009-6211-6
- Meirer, K., Steinhilber, D., and Proschak, E. (2014). Inhibitors of the arachidonic acid cascade: interfering with multiple pathways. *Basic Clin. Pharmacol. Toxicol.* 114, 83–91. doi: 10.1111/bcpt.12134
- Mueller, C. F., Wassmann, K., Widder, J. D., Wassmann, S., Chen, C. H., Keuler, B., et al. (2008). Multidrug resistance protein-1 affects oxidative stress, endothelial dysfunction, and atherogenesis via leukotriene C4 export. *Circulation* 117, 2912–2918. doi: 10.1161/CIRCULATIONAHA.107.747667
- Peters, J. (2013). Polypharmacology - foe or friend? *J. Med. Chem.* 56, 8955–8971. doi: 10.1021/jm400856t
- Proschak, E., Heitel, P., Kalinowsky, L., and Merk, D. (2017). Opportunities and challenges for fatty acid mimetics in drug discovery. *J. Med. Chem.* 60, 5235–5266. doi: 10.1021/acs.jmedchem.6b01287
- Ramires, R., Caiiffa, M. F., Tursi, A., Haeggström, J. Z., and Macchia, L. (2004). Novel inhibitory effect on 5-lipoxygenase activity by the anti-asthma drug montelukast. *Biochem. Biophys. Res. Commun.* 324, 815–821. doi: 10.1016/j.bbrc.2004.09.125
- Rau, O., Wurglics, M., Paulke, A., Zitzkowski, J., Meindl, N., Bock, A., et al. (2006). Carnosic acid and carnosol, phenolic diterpene compounds of the labiate herbs rosemary and sage, are activators of the human peroxisome proliferator-activated receptor gamma. *Planta Med.* 72, 881–887. doi: 10.1055/s-2006-946680
- Reker, D., Perna, A. M., Rodrigues, T., Schneider, P., Reutlinger, M., Mönch, B., et al. (2014). Revealing the macromolecular targets of complex natural products. *Nat. Chem.* 6, 1072–1078. doi: 10.1038/nchem.2095
- Rohatgi, A., and McGuire, D. K. (2008). Effects of the thiazolidinedione medications on micro- and macrovascular complications in patients with diabetes—update 2008. *Cardiovasc. Drugs Ther.* 22, 233–240. doi: 10.1007/s10557-008-6093-z
- Schierle, S., Flauaus, C., Heitel, P., Willems, S., Schmidt, J., Kaiser, A., et al. (2018). Boosting anti-inflammatory potency of zafirlukast by designed polypharmacology. *J. Med. Chem.* 61, 5758–5764. doi: 10.1021/acs.jmedchem.8b00458
- Sener, G., Schirli, O., Velioglu-Ogünç, A., Cetinel, S., Gedik, N., Caner, M., et al. (2006). Montelukast protects against renal ischemia/reperfusion injury in rats. *Pharmacol. Res.* 54, 65–71. doi: 10.1016/j.phrs.2006.02.007
- Staels, B., and Fruchart, J. (2005). Therapeutic roles of peroxisome proliferator-activated receptor agonists. *Diabetes* 54, 2460–2470. doi: 10.2337/diabetes.54.8.2460

- Theron, A. J., Steel, H. C., Tintinger, G. R., Gravett, C. M., Anderson, R., and Feldman, C. (2014). Cysteinyl leukotriene receptor-1 antagonists as modulators of innate immune cell function. *J. Immunol. Res.* 2014:608930. doi: 10.1155/2014/608930
- Tontonoz, P., and Spiegelman, B. M. (2008). Fat and beyond: the diverse biology of PPARgamma. *Annu. Rev. Biochem.* 77, 289–312. doi: 10.1146/annurev.biochem.77.061307.091829
- Woszczek, G., Chen, L., Alsaaty, S., Nagineni, S., and Shelhamer, J. H. (2010). Concentration-dependent noncysteinyl leukotriene type 1 receptor-mediated inhibitory activity of leukotriene receptor antagonists. *J. Immunol.* 184, 2219–2225. doi: 10.4049/jimmunol.0900071
- Wright, M. B., Bortolini, M., Tadayyon, M., and Bopst, M. (2014). Minireview: challenges and opportunities in development of PPAR agonists. *Mol. Endocrinol.* 28, 1756–1768. doi: 10.1210/me.2013-1427
- Xu, D., Davis, B. B., Wang, Z., Zhao, S., Wasti, B., Liu, Z., et al. (2013). A potent soluble epoxide hydrolase inhibitor, t-AUCB, acts through PPAR γ to modulate the function of endothelial progenitor cells from patients with acute myocardial infarction. *Int. J. Cardiol.* 167, 1298–1304. doi: 10.1016/j.ijcard.2012.03.167
- Zebisch, K., Voigt, V., Wabitsch, M., and Brandsch, M. (2012). Protocol for effective differentiation of 3T3-L1 cells to adipocytes. *Anal. Biochem.* 425, 88–90. doi: 10.1016/j.ab.2012.03.005
- Zha, W., Edin, M. L., Vendrov, K. C., Schuck, R. N., Lih, F. B., Jat, J. L., et al. (2014). Functional characterization of cytochrome P450-derived epoxyeicosatrienoic acids in adipogenesis and obesity. *J. Lipid Res.* 55, 2124–2136. doi: 10.1194/jlr.M053199

Conflict of Interest Statement: The authors declare that the research was conducted in the absence of any commercial or financial relationships that could be construed as a potential conflict of interest.

Copyright © 2019 Göbel, Diehl, Heering, Merk, Angioni, Wittmann, Buscato, Kottke, Weizel, Schader, Maier, Geisslinger, Schubert-Zsilavecz, Steinhilber, Proschak and Kahnt. This is an open-access article distributed under the terms of the Creative Commons Attribution License (CC BY). The use, distribution or reproduction in other forums is permitted, provided the original author(s) and the copyright owner(s) are credited and that the original publication in this journal is cited, in accordance with accepted academic practice. No use, distribution or reproduction is permitted which does not comply with these terms.



Soluble Epoxide Hydrolase Inhibitor: A Novel Potential Therapeutic or Prophylactic Drug for Psychiatric Disorders

Qian Ren^{1,2*}

¹Department of Human Anatomy, Hebei Medical University, Shijiazhuang, China, ²Center of Stem Cell and Immune Cell Research, Institute of Medical and Health Science, Hebei Medical University, Shijiazhuang, China

OPEN ACCESS

Edited by:

John D. Imig,
Medical College of Wisconsin,
United States

Reviewed by:

Ulrike Garscha,
Friedrich Schiller University Jena,
Germany
Xiang Fang,
The University of Texas Medical
Branch at Galveston, United States

*Correspondence:

Qian Ren
renfflnm@gmail.com;
renfflnm@126.com

Specialty section:

This article was submitted to
Translational Pharmacology,
a section of the journal
Frontiers in Pharmacology

Received: 10 November 2018

Accepted: 03 April 2019

Published: 24 April 2019

Citation:

Ren Q (2019) Soluble Epoxide
Hydrolase Inhibitor: A Novel Potential
Therapeutic or Prophylactic Drug for
Psychiatric Disorders.
Front. Pharmacol. 10:420.
doi: 10.3389/fphar.2019.00420

Psychiatric disorders, including depression and schizophrenia, affect millions of individuals worldwide. However, the precise neurobiology of psychiatric disorders remains unclear. Accumulating evidence suggests that various inflammatory processes play a key role in depression and schizophrenia, and that anti-inflammatory drugs exert a therapeutic effect in patients with psychiatric disorders. Epoxyeicosatrienoic acids (EETs) and epoxydocosapentaenoic acids (EDPs) have potent anti-inflammatory properties. These mediators are broken down into their corresponding diols by soluble epoxide hydrolase (sEH), and inhibition of sEH enhances the anti-inflammatory effects of EETs. Therefore, sEH may play a key role in inflammation, which is involved in psychiatric disorders. Recent studies have shown that abnormal levels of sEH may be involved in the pathogenesis of certain psychiatric diseases, and that sEH inhibitors exhibit antidepressant and antipsychotic activity. The present review discusses the extensive evidence supporting sEH as a therapeutic target for psychiatric diseases, and the clinical value of sEH inhibitors as therapeutic or prophylactic drugs.

Keywords: depression, antidepressant, schizophrenia, soluble epoxide hydrolase, inflammation

INTRODUCTION

Depression and schizophrenia are severe and chronic debilitating psychiatric diseases that affect millions of individuals worldwide, with >300 million individuals of all ages affected by depression and nearly 800,000 dying each year from suicide (World Health Organization, 2018a). Similarly, schizophrenia affects >21 million individuals, and the probability of death in this patient population is 2 to 3 times higher than that in the general population (World Health Organization, 2018b). Although current clinical antidepressants and antipsychotics have been shown to be effective in the treatment of depression and schizophrenia, at least one-third of individuals with depression do not fully respond to medications, and antipsychotics have no beneficial effects on negative symptoms and cognitive impairments (Hashimoto, 2014; Steinert et al., 2014; Biesheuvel-Leliefeld et al., 2015; Guidi et al., 2016). These limitations highlight the need for a new class of antidepressants and antipsychotics, particularly for patients with treatment-resistant disease.

There is ample evidence that inflammation plays a central role in the pathophysiology of depression and schizophrenia (Dantzer et al., 2008; Potvin et al., 2008; Girgis et al., 2014; Gold, 2015; Hashimoto, 2015; Steullet et al., 2016; Marques et al., 2018; Swardfager et al., 2018). In patients not undergoing antidepressant therapy, meta-analyses have reported that blood levels of proinflammatory cytokines, including tumor necrosis factor- α (TNF- α) and interleukin 6 (IL-6), are significantly higher than in healthy controls (Dowlati et al., 2010; Young et al., 2014; Haapakoski et al., 2015; Strawbridge et al., 2015). Moreover, studies of postmortem brain samples revealed increased proinflammatory cytokine gene expression in the prefrontal cortex (PFC) of individuals with a history of depression (Dean et al., 2010; Shelton et al., 2011). Studies using animal models of depression have reported lipopolysaccharide (LPS)-induced depression-like behavior and dendritic changes (Zhang et al., 2015, 2016). In studies investigating schizophrenia, the levels of proinflammatory cytokines, such as TNF- α , and IL-6, were significantly elevated in the serum and cerebrospinal fluid (Sasayama et al., 2013; Upthegrove et al., 2014; Schwieler et al., 2015; Dickerson et al., 2016). Postmortem studies and meta-analyses have demonstrated increased microglia density and activity in patients with schizophrenia (van Kesteren et al., 2017; Marques et al., 2018). Several studies have demonstrated that anti-inflammatory drugs exhibit antipsychotic activity in animal models of schizophrenia (Shirai et al., 2012, 2015). Collectively, these investigations demonstrate that inflammation is likely closely related to depression and schizophrenia, and that anti-inflammatory drugs could effectively improve the symptoms of depression and schizophrenia.

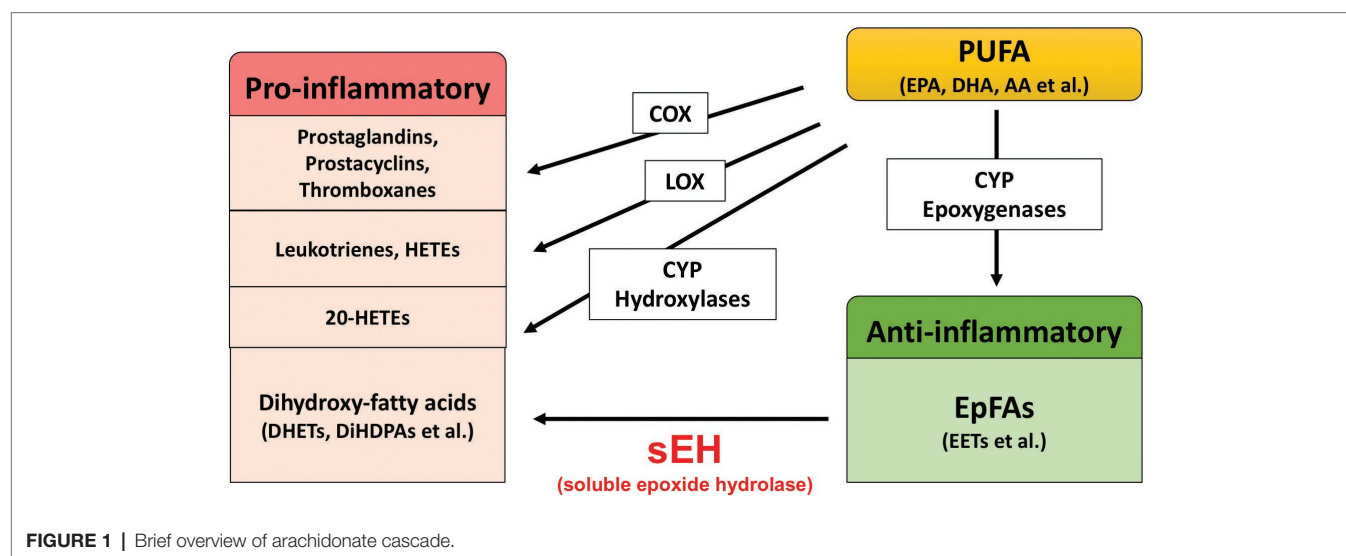
SOLUBLE EPOXIDE HYDROLASE AND THE ARACHIDONIC PATHWAY

Extensive evidence suggests that biological substances in the arachidonate cascade, such as enzymes and eicosanoid metabolites,

are involved in the etiology and pathology of inflammatory disease. Polyunsaturated fatty acids (PUFAs), such as arachidonic acid (AA), docosahexaenoic acid (DHA), and eicosapentaenoic acid (EPA), are metabolized by cyclooxygenases (COXs), lipoxygenases (LOXs), and cytochrome P450s (CYPs) (**Figure 1**; Imig and Hammock, 2009; Imig, 2012, 2018; Morisseau and Hammock, 2013). The COX and LOX pathways lead to the production of prostaglandins, leukotrienes, and hydroxyeicosatetraenoic acids (HETEs). These lipid mediators are involved in pro-inflammatory processes, while lipoxins synthesized from AA by LOX play an important role in the resolution of inflammation (Serhan and Savill, 2005; Serhan, 2017a,b). In contrast, the CYP pathway is involved in both the production of pro-inflammatory lipid mediators and anti-inflammatory lipid mediators. The CYP hydroxylases lead to 20-HETE (pro-inflammatory mediator), and CYP epoxygenases lead to epoxyeicosatrienoic acids (EETs) (anti-inflammatory mediator). Through catalyzing the epoxidation of PUFAs, such as AA, the epoxygenase CYP enzymes generate four regioisomeric EETs, including 5,6-EET, 8,9-EET, 11,12-EET, and 14,15-EET. However, the EETs are metabolized by soluble epoxide hydrolase (sEH) and converted into their corresponding diols (dihydroxyeicosatrienoic acids [DHETs]), and these molecules are considered to be less biologically active than their parent versions. Therefore, it is probable that sEH plays a role in the pathogenesis of several diseases caused by inflammation (Imig, 2005, 2012, 2016, 2018; Iliff et al., 2010; Morisseau and Hammock, 2013; Wagner et al., 2014, 2017; Zhang et al., 2014; Hashimoto, 2016).

ROLE OF sEH IN PSYCHIATRIC DISORDERS

As discussed above, inflammation is associated with psychiatric disorders such as depression and schizophrenia, and sEH plays a role in the pathogenesis of inflammatory-related diseases. Therefore, it is possible that sEH contributes to the pathophysiology of these disorders. Recently, our study



of postmortem brains revealed that the protein levels of sEH in the parietal cortex of patients with major depressive disorder, schizophrenia, and bipolar disorder were significantly elevated compared with those in the parietal cortex of healthy individuals (Ren et al., 2016). In studies involving mouse models, the brain, after inflammation or chronic social defeat stress, exhibited increased expression of sEH in the PFC and hippocampus. Meanwhile, after inflammation or social defeat stress, mice exhibited increased immobility time in tail suspension and forced swim tests, and decreased sucrose preference. These phenotypes were defined as depression-like behavior in mice (Duman and Monteggia, 2006; Dantzer et al., 2008). Studies involving behavioral tests in animal models have suggested that the sEH inhibitor 1-[1-propionylpiperidin-4-yl]-3-[4-(trifluoromethoxy) phenyl] urea (TPPU) had antidepressant effects because the inflammation and chronic social defeat stress-induced depression-like behavior was prevented by oral administration or chronic intake of TPPU (Ren et al., 2016). As such, TPPU could produce antidepressant effects in inflammation model of depression because standard antidepressants, such as selective serotonin reuptake inhibitors and serotonin norepinephrine reuptake inhibitors, do not demonstrate therapeutic effects in such models (Zhang et al., 2015). Moreover, the use of TPPU lowered serum TNF- α levels in LPS-treated mice but not control mice. Additionally, in these experiments, both TPPU and 14,15-EET potentiated nerve growth factor (NGF)-induced neuronal outgrowth in PC12 cells. Consistent with the pharmacological inhibition of sEH, despite experiencing chronic social defeat stress, sEH knockout mice did not exhibit depression-like behavior. It is likely that the deletion of the sEH gene conferred resilience to social defeat stress. Additionally, investigation of brain-derived neurotrophic factor-tropomyosin receptor kinase B (BDNF-TrkB) signaling protein expression in sEH knockout mice brains revealed that BDNF and p-TrkB-to-TrkB protein ratios were elevated in the PFC and hippocampus. Consistent with BDNF-TrkB signaling, the protein levels of glutamate receptor subunit (GluA1) and postsynaptic density protein (PSD-95), which are synaptogenesis biomarkers, were elevated in the PFC and hippocampus of sEH knockout mice. This could infer that deletion of sEH resulted in resilience to chronic social defeat stress *via* increased BDNF-TrkB signaling and synaptogenesis. Furthermore, data reported by other groups are in agreement with these results. Wu et al. reported that the sEH inhibitor TPPU decreased depression-like behavior in the novelty-suppressed feeding test, which is a test of stress-induced anxiety/depression (Wu et al., 2017). Moreover, treatment with TPPU elevated the expression of BDNF in the mouse hippocampus and PC12 cells, and the antidepressant effect of TPPU was blocked by a BDNF-TrkB signal pathway antagonist (Wu et al., 2017, 2019). This evidence suggests that BDNF is necessary for the antidepressant effects of TPPU. Collectively, these findings highlight a key function of sEH in the etiology and pathology of depression, and for its inhibitors as potential therapeutic or prophylactic drugs for depression (Ren et al., 2016; Hashimoto, 2016).

As mentioned above, patients with schizophrenia exhibit higher sEH protein levels in the parietal cortex than controls. Meanwhile, another study investigating alterations of eicosanoids in the serum of patients with schizophrenia reported that 11,12-DHETs and 14,15-DHETs were increased in patients compared with controls and were decreased post-treatment (Wang et al., 2018). This evidence suggested that EET and its metabolic enzyme sEH may play a role in schizophrenia, and studies using animal models have provided strong supportive data. Ma et al. (2013) investigated the effects of AS2586114, a potent sEH inhibitor, in an animal model of schizophrenia. In a phencyclidine (PCP)-induced model of schizophrenia, a single oral administration of AS2586114 attenuated PCP-induced hyperlocomotion in a dose-dependent manner. Furthermore, AS2586114 also improved PCP-induced prepulse inhibition deficits in a dose-dependent manner. In addition, AS2586114 exhibited a similar effect to the atypical antipsychotic drug clozapine in PCP-induced behavioral abnormalities (Ma et al., 2013). These studies suggest the therapeutic potential of sEH inhibitors for schizophrenia. However, the precise mechanism by which sEH inhibitors diminish PCP-induced acute behavioral effects in mice remains unclear. Nevertheless, some studies have provided valuable clues. Ribeiro et al. reported that omega-3 PUFAs (n3 PUFAs), but not clozapine, prevented polyinosinic:polycytidylic acid (poly I:C)-induced deficits in BDNF (Ribeiro et al., 2019). Because decreased BDNF-TrkB signaling has been suggested to play a role in the pathophysiology of schizophrenia (Giovannoli et al., 2015; Han et al., 2016), and sEH inhibitors increase the level of BDNF, it appears that sEH may play a role in schizophrenia *via* regulation of the BDNF-TrkB signaling pathway. There is ample evidence suggesting that oxidative stress also plays an important role in the pathophysiology of schizophrenia, and antioxidant agents have demonstrated antipsychotic effects in animal models of schizophrenia (Matsuzawa and Hashimoto, 2011; Reddy and Reddy, 2011; Yao and Keshavan, 2011; Shirai et al., 2012, 2015). Moreover, abnormalities in striatal dopamine levels are a hallmark of schizophrenia pathophysiology (Brisch et al., 2014; Nakao et al., 2019). Recently, Ren et al. (2018) reported that inhibition of sEH protected against MPTP (1-methyl-4-phenyl-1,2,3,6-tetrahydropyridine)-induced endoplasmic reticulum (ER) stress and oxidative stress in the brain. The immunoreactivity of sEH is present almost exclusively in astrocytes throughout the brain (Marowsky et al., 2009); however, deletion of the sEH gene suppressed MPTP-induced activation of microglia in the mouse striatum (Ren et al., 2018). Additionally, inhibition of sEH attenuated MPTP-induced dopaminergic dysfunction in the striatum (Ren et al., 2018). Other studies have consistently found that deletion of the sEH gene and pharmacological inhibition of sEH blocked MPTP-induced heme-oxygenase (HO-1) elevation (a redox-regulated protein) and caspase 12 activation (a hallmark of ER stress) (Huang et al., 2018). These findings indicate that sEH inhibitors are effective in attenuating MPTP-induced dopaminergic neurotoxicity, oxidative stress, and ER stress. Given the evidence described, there is a possibility that sEH inhibitors exert their antipsychotic properties by increasing EETs, modulating the BDNF-TrkB signaling pathway, protecting against oxidative stress, and improving dopaminergic dysfunction in the brain.

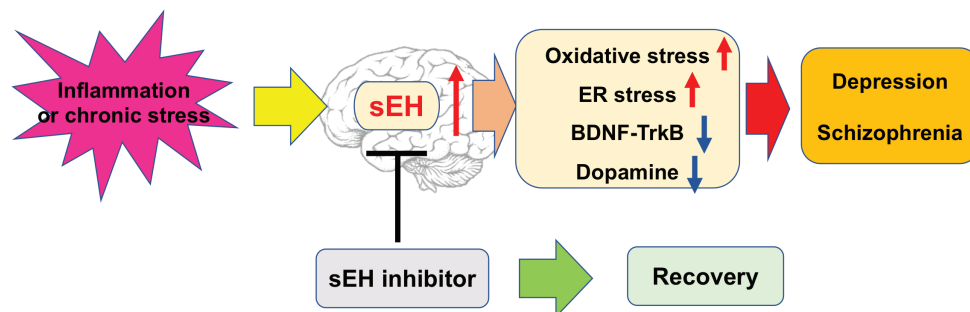


FIGURE 2 | Possible mechanisms of the role of sEH in depression and schizophrenia.

DISCUSSION

In this minireview, we highlighted recent studies that have demonstrated the potential of sEH as a therapeutic target in psychiatric disorders. Crucial data from Ren et al. (2018) and Ma et al. (2013) demonstrate that protein levels of sEH in the brains of depressed and schizophrenic patients are higher than in controls. Additionally, sEH protein levels are elevated in the brains of mice with a depression-like phenotype. These data suggest that increased levels of sEH in the brain cause enhanced metabolism of anti-inflammatory PUFA epoxides, such as EETs, EDPs, and epoxyeicosatetraenoic acids (EEQs), eventually leading to depressive symptoms. Furthermore, a single administration of sEH inhibitor has been reported to prevent depression-like phenotypes in the inflammation and chronic social defeat stress models of depression. These important findings indicate that sEH inhibitors may have a rapid onset of antidepressant action, which is similar to the rapid-acting antidepressant ketamine, but without any observable side effects (Hashimoto, 2016). Moreover, a single administration of sEH inhibitor has also been reported to rescue PCP-induced behavioral abnormality in mice. These antipsychotic effects of sEH inhibitor are similar to those of the atypical antipsychotic drug clozapine. This is noteworthy because sEH inhibitors also may have a rapid onset of antipsychotic action without any observable side effects.

Several hypotheses have postulated that inflammation may play a causative role in depression and schizophrenia (Schiepers et al., 2005; Brown and Derkits, 2010; Brown and Meyer, 2018; Chen et al., 2019). However, how do inflammatory cytokines influence behavior? In the brain, inflammatory cytokines, such as TNF- α , IL-6, and IL-1 β , are elevated in the brain during inflammation or chronic stress (Strawbridge et al., 2015; Menard et al., 2017). These cytokines have been implicated in the

activation of indoleamine-2,3-dioxygenase (IDO) and tryptophan dioxygenase (TDO), and promote the metabolism of tryptophan into formylkynurenine, a precursor of kynurenine. Furthermore, the metabolites of kynurenine, such as kynurenic acid and quinolinic acid, are involved in modulation of N-methyl-D-aspartate receptor and α -amino-3-hydroxy-5-methyl-4-isoxazolepropionic acid receptor, and can also activate monoamine oxidase. Subsequently, these metabolites are implicated in dopamine synthesis, behavioral abnormalities, and regulation of neurotrophic and metabolic signaling through BDNF and mTOR (Schiepers et al., 2005; Calcia et al., 2016; Ghasemi et al., 2017; Lima Giacobbo et al., 2018; Price et al., 2018; Chen et al., 2019).

Collectively, these studies described a potential mechanism for sEH in the pathophysiology of depression and schizophrenia. This evidence suggests that sEH inhibitors exert an antidepressant and antipsychotic effect, and may attenuate the appearance of oxidative and ER stress, dysregulation of neurotrophic and dysfunction of dopaminergic neurons in the brain (Figure 2). Nevertheless, the precise mechanism of action of sEH inhibitors remains largely unknown, thus warranting more in-depth studies in the future.

AUTHOR CONTRIBUTIONS

QR wrote the manuscript and prepared the figures.

FUNDING

This study was supported by the Japan Society for the Promotion of Science (JSPS) KAKENHI grant (18k15439).

REFERENCES

- Biesheuvel-Leliefeld, K. E., Kok, G. D., Bockting, C. L., Cuijpers, P., Hollon, S. D., van Marwijk, H. W., et al. (2015). Effectiveness of psychological interventions in preventing recurrence of depressive disorder: meta-analysis and meta-regression. *J. Affect. Disord.* 174, 400–410. doi: 10.1016/j.jad.2014.12.016
- Brisch, R., Saniotis, A., Wolf, R., Bielau, H., Bernstein, H. G., Steiner, J., et al. (2014). The role of dopamine in schizophrenia from a neurobiological and evolutionary perspective: old fashioned, but still in vogue. *Front. Psych.* 5:47. doi: 10.3389/fpsy.2014.00047
- Brown, A. S., and Derkits, E. J. (2010). Prenatal infection and schizophrenia: a review of epidemiologic and translational studies. *Am. J. Psychiatry* 167, 261–280. doi: 10.1176/appi.ajp.2009.09030361

- Brown, A. S., and Meyer, U. (2018). Maternal immune activation and neuropsychiatric illness: a translational research perspective. *Am. J. Psychiatry* 175, 1073–1083. doi: 10.1176/appi.ajp.2018.17121311
- Calcia, M. A., Bonsall, D. R., Bloomfield, P. S., Selvaraj, S., Barichello, T., and Howes, O. D. (2016). Stress and neuroinflammation: a systematic review of the effects of stress on microglia and the implications for mental illness. *Psychopharmacology* 233, 1637–1650. doi: 10.1007/s00213-016-4218-9
- Chen, K. L., Cathomas, F., and Russo, S. J. (2019). Central and peripheral inflammation link metabolic syndrome and major depressive disorder. *Physiology* 34, 123–133. doi: 10.1152/physiol.00047.2018
- Dantzer, R., O'Connor, J. C., Freund, G. G., Johnson, R. W., and Kelley, K. W. (2008). From inflammation to sickness and depression: when the immune system subjugates the brain. *Nat. Rev. Neurosci.* 9, 46–56. doi: 10.1038/nrn2297
- Dean, B., Tawadros, N., Scarr, E., and Gibbons, A. S. (2010). Regionally-specific changes in levels of tumour necrosis factor in the dorsolateral prefrontal cortex obtained postmortem from subjects with major depressive disorder. *J. Affect. Disord.* 120, 245–248. doi: 10.1016/j.jad.2009.04.027
- Dickerson, F., Stallings, C., Origoni, A., Schroeder, J., Katsafanas, E., Schweinfurth, L., et al. (2016). Inflammatory markers in recent onset psychosis and chronic schizophrenia. *Schizophr. Bull.* 42, 134–141. doi: 10.1093/schbul/sbv108
- Dowlati, Y., Herrmann, N., Swardfager, W., Liu, H., Sham, L., Reim, E. K., et al. (2010). A meta-analysis of cytokines in major depression. *Biol. Psychiatry* 67, 446–457. doi: 10.1016/j.biopsych.2009.09.033
- Duman, R. S., and Monteggia, L. M. (2006). A neurotrophic model for stress-related mood disorders. *Biol. Psychiatry* 59, 1116–1127. doi: 10.1016/j.biopsych.2006.02.013
- Ghasemi, M., Phillips, C., Fahimi, A., McEnerney, M. W., and Salehi, A. (2017). Mechanisms of action and clinical efficacy of NMDA receptor modulators in mood disorders. *Neurosci. Biobehav. Rev.* 80, 555–572. doi: 10.1016/j.neubiorev.2017.07.002
- Giovannoli, S., Notter, T., Richetto, J., Labouesse, M. A., Vuillermot, S., Riva, M. A., et al. (2015). Late prenatal immune activation causes hippocampal deficits in the absence of persistent inflammation across aging. *J. Neuroinflammation* 12:221. doi: 10.1186/s12974-015-0437-y
- Girgis, R. R., Kumar, S. S., and Brown, A. S. (2014). The cytokine model of schizophrenia: emerging therapeutic strategies. *Biol. Psychiatry* 75, 292–299. doi: 10.1016/j.biopsych.2013.12.002
- Gold, P. W. (2015). The organization of the stress system and its dysregulation in depressive illness. *Mol. Psychiatry* 20, 32–47. doi: 10.1038/mp.2014.163
- Guidi, J., Tomba, E., and Fava, G. A. (2016). The sequential integration of pharmacotherapy and psychotherapy in the treatment of major depressive disorder: a meta-analysis of the sequential model and a critical review of the literature. *Am. J. Psychiatry* 173, 128–137. doi: 10.1176/appi.ajp.2015.15040476
- Haapakoski, R., Mathieu, J., Ebmeier, K. P., Alenius, H., and Kivimäki, M. (2015). Cumulative meta-analysis of interleukins 6 and β , tumour necrosis factor α and C-reactive protein in patients with major depressive disorder. *Brain Behav. Immun.* 49, 206–215. doi: 10.1016/j.bbi.2015.06.001
- Han, M., Zhang, J. C., Yao, W., Yang, C., Ishima, T., Ren, Q., et al. (2016). Intake of 7,8-dihydroxyflavone during juvenile and adolescent stages prevents onset of psychosis in adult offspring after maternal immune activation. *Sci. Rep.* 6:36087. doi: 10.1038/srep36087
- Hashimoto, K. (2014). Targeting of NMDA receptors in new treatments for schizophrenia. *Expert Opin. Ther. Targets* 18, 1049–1063. doi: 10.1517/14728222.2014.934225
- Hashimoto, K. (2015). Inflammatory biomarkers as differential predictors of antidepressant response. *Int. J. Mol. Sci.* 16, 7796–7801. doi: 10.3390/ijms16047796
- Hashimoto, K. (2016). Soluble epoxide hydrolase: a new therapeutic target for depression. *Expert Opin. Ther. Targets* 20, 1149–1151. doi: 10.1080/14728222.2016.1226284
- Huang, H. J., Wang, Y. T., Lin, H. C., Lee, Y. H., and Lin, A. M. (2018). Soluble epoxide hydrolase attenuates MPTP-induced neurotoxicity in the nigrostriatal dopaminergic system: involvement of α -synuclein aggregation and ER stress. *Mol. Neurobiol.* 55, 138–144. doi: 10.1007/s12035-017-0726-9
- Iliff, J. J., Jia, J., Nelson, J., Goyagi, T., Klaus, J., and Alkayed, N. J. (2010). Epoxyeicosanoid signaling in CNS function and disease. *Prostaglandins Other Lipid Mediat.* 91, 68–84. doi: 10.1016/j.prostaglandins.2009.06.004
- Imig, J. D. (2005). Epoxide hydrolase and epoxyeicosanoid metabolites as therapeutic targets for renal diseases. *Am. J. Physiol. Renal Physiol.* 289, F496–F503. doi: 10.1152/ajprenal.00350.2004
- Imig, J. D. (2012). Epoxides and soluble epoxide hydrolase in cardiovascular physiology. *Physiol. Rev.* 92, 101–130. doi: 10.1152/physrev.00021.2011
- Imig, J. D. (2016). Epoxyeicosatrienoic acids and 20-hydroxyeicosatetraenoic acid on endothelial and vascular function. *Adv. Pharmacol.* 77, 105–141. doi: 10.1016/b.sapha.2016.04.003
- Imig, J. D. (2018). Prospective for cytochrome P450 epoxygenase cardiovascular and renal therapeutics. *Pharmacol. Ther.* 192, 1–19. doi: 10.1016/j.pharmthera.2018.06.015
- Imig, J. D., and Hammock, B. D. (2009). Soluble epoxide hydrolase as a therapeutic target for cardiovascular diseases. *Nat. Rev. Drug Discov.* 8, 794–805. doi: 10.1038/nrd2875
- Lima, Giacobbo, B., Doorduyn, J., Klein, H. C., Dierckx, R. A. J. O., Bromberg, E., and de Vries, E. F. J. (2018). Brain-derived neurotrophic factor in brain disorders: focus on neuroinflammation. *Mol. Neurobiol.* doi: 10.1007/s12035-018-1283-6
- Ma, M., Ren, Q., Fujit, Y., Ishima, T., Zhang, J. C., and Hashimoto, K. (2013). Effects of AS2586114, a soluble epoxide hydrolase inhibitor, on hyperlocomotion and prepulse inhibition deficits in mice after administration of phencyclidine. *Pharmacol. Biochem. Behav.* 110, 98–103. doi: 10.1016/j.pbb.2013.06.005
- Marowsky, A., Burgener, J., Falck, J. R., Fritschy, J. M., and Arand, M. (2009). Distribution of soluble and microsomal epoxide hydrolase in the mouse brain and its contribution to cerebral epoxyeicosatrienoic acid metabolism. *Neuroscience* 163, 646–661. doi: 10.1016/j.neuroscience.2009.06.033
- Marques, T. R., Ashok, A. H., Pillinger, T., Veronese, M., Turkheimer, F. E., Dazzan, P., et al. (2018). Neuroinflammation in schizophrenia: meta-analysis of *in vivo* microglial imaging studies. *Psychol. Med.* 1–11. doi: 10.1017/S0033291718003057
- Matsuzawa, D., and Hashimoto, K. (2011). Magnetic resonance spectroscopy study of the antioxidant defense system in schizophrenia. *Antioxid. Redox Signal.* 15, 2057–2065. doi: 10.1089/ars.2010.3453
- Menard, C., Pfau, M. L., Hodes, G. E., Kana, V., Wang, V. X., Bouchard, S., et al. (2017). Social stress induces neurovascular pathology promoting depression. *Nat. Neurosci.* 20, 1752–1760. doi: 10.1038/s41593-017-0010-3
- Morisseau, C., and Hammock, B. D. (2013). Impact of soluble epoxide hydrolase and epoxyeicosanoids on human health. *Annu. Rev. Pharmacol. Toxicol.* 53, 37–58. doi: 10.1146/annurev-pharmtox-011112-140244
- Nakao, K., Jeevakumar, V., Jiang, S. Z., Fujita, Y., Diaz, N. B., Pretell Annan, C. A., et al. (2019). Schizophrenia-like dopamine release abnormalities in a mouse model of NMDA receptor hypofunction. *Schizophr. Bull.* 45, 138–147. doi: 10.1093/schbul/sby003
- Potvin, S., Stip, E., Sepehry, A. A., Gendron, A., Bah, R., and Kouassi, E. (2008). Inflammatory cytokine alterations in schizophrenia: a systematic quantitative review. *Biol. Psychiatry* 63, 801–808. doi: 10.1016/j.biopsych.2007.09.024
- Price, J. B., Bronars, C., Erhardt, S., Cullen, K. R., Schwieler, L., Berk, M., et al. (2018). Bioenergetics and synaptic plasticity as potential targets for individualizing treatment for depression. *Neurosci. Biobehav. Rev.* 90, 212–220. doi: 10.1016/j.neubiorev.2018.04.002
- Reddy, R., and Reddy, R. (2011). Antioxidant therapeutics for schizophrenia. *Antioxid. Redox Signal.* 15, 2047–2055. doi: 10.1089/ars.2010.3571
- Ren, Q., Ma, M., Ishima, T., Morisseau, C., Yang, J., Wagner, K. M., et al. (2016). Gene deficiency and pharmacological inhibition of soluble epoxide hydrolase confers resilience to repeated social defeat stress. *Proc. Natl. Acad. Sci. USA* 113, E1944–E1952. doi: 10.1073/pnas.1601532113
- Ren, Q., Ma, M., Yang, J., Nonaka, R., Yamaguchi, A., Ishikawa, K. I., et al. (2018). Soluble epoxide hydrolase plays a key role in the pathogenesis of Parkinson's disease. *Proc. Natl. Acad. Sci. USA* 115, E5815–E5823. doi: 10.1073/pnas.1802179115
- Ribeiro, B. M. M., Chaves Filho, A. J. M., Costa, D. V. D. S., de Menezes, A. T., da Fonseca, A. C. C., Gama, C. S., et al. (2019). N-3 polyunsaturated fatty acids and clozapine abrogates poly I:C-induced immune alterations in primary hippocampal neurons. *Prog. Neuro-Psychopharmacol. Biol. Psychiatry* 90, 186–196. doi: 10.1016/j.pnpbp.2018.11.022

- Sasayama, D., Hattori, K., Wakabayashi, C., Teraishi, T., Hori, H., Ota, M., et al. (2013). Increased cerebrospinal fluid interleukin-6 levels in patients with schizophrenia and those with major depressive disorder. *J. Psychiatr. Res.* 47, 401–406. doi: 10.1016/j.jpsychires.2012.12.001
- Schiepers, O. J. G., Wichers, M. C., and Maes, M. (2005). Cytokines and major depression. *Prog. Neuro-Psychopharmacol. Biol. Psychiatry* 29, 201–217. doi: 10.1016/j.pnpbp.2004.11.003
- Schwieler, L., Larsson, M. K., Skogh, E., Kegel, M. E., Orhan, F., Abdelmoaty, S., et al. (2015). Increased levels of IL-6 in the cerebrospinal fluid of patients with chronic schizophrenia—significance for activation of the kynurenine pathway. *J. Psychiatry Neurosci.* 40, 126–133. doi: 10.1503/jpn.140126
- Serhan, C. N. (2017a). Discovery of specialized pro-resolving mediators marks the dawn of resolution physiology and pharmacology. *Mol. Asp. Med.* 58, 1–11. doi: 10.1016/j.mam.2017.03.001
- Serhan, C. N. (2017b). Treating inflammation and infection in the 21st century: new hints from decoding resolution mediators and mechanisms. *FASEB J.* 31, 1273–1388. doi: 10.1096/fj.201601222R
- Serhan, C. N., and Savill, J. (2005). Resolution of inflammation: the beginning programs the end. *Nat. Immun.* 6, 1191–1197. doi: 10.1038/ni1276
- Shelton, R. C., Claiborne, J., Sidoryk-Wegrzynowicz, M., Reddy, R., Aschner, M., Lewis, D. A., et al. (2011). Altered expression of genes involved in inflammation and apoptosis in frontal cortex in major depression. *Mol. Psychiatry* 16, 751–762. doi: 10.1038/mp.2010.52
- Shirai, Y., Fujita, Y., and Hashimoto, K. (2012). Effects of the antioxidant sulforaphane on hyperlocomotion and prepulse inhibition deficits in mice after phencyclidine administration. *Clin. Psychopharmacol. Neurosci.* 10, 94–98. doi: 10.9758/cpn.2012.10.2.94
- Shirai, Y., Fujita, Y., Hashimoto, R., Ohi, K., Yamamori, H., Yasuda, Y., et al. (2015). Dietary intake of sulforaphane-rich broccoli sprout extracts during juvenile and adolescence can prevent phencyclidine-induced cognitive deficits at adulthood. *PLoS One* 10:e0127244. doi: 10.1371/journal.pone.0127244
- Steinert, C., Hoffmann, M., Kruse, J., and Leichsenring, F. (2014). Relapse rates after psychotherapy for depression—Stable long-term effects? A meta-analysis. *J. Affect. Disord.* 168, 107–118. doi: 10.1016/j.jad.2014.06.043
- Stellet, P., Cabungcal, J. H., Monin, A., Dwir, D., O'Donnell, P., Cuenod, M., et al. (2016). Redox dysregulation, neuroinflammation, and NMDA receptor hypofunction: a “central hub” in schizophrenia pathophysiology? *Schizophr. Res.* 176, 41–51. doi: 10.1016/j.schres.2014.06.021
- Strawbridge, R., Arnone, D., Danese, A., Papadopoulos, A., Herane Vives, A., and Cleare, A. J. (2015). Inflammation and clinical response to treatment in depression: a meta-analysis. *Eur. Neuropsychopharmacol.* 25, 1532–1534. doi: 10.1016/j.euroneuro.2015.06.007
- Swardfager, W., Hennebelle, M., Yu, D., Hammock, B. D., Levitt, A. J., Hashimoto, K., et al. (2018). Tetabolic/inflammatory/vascular comorbidity in psychiatric disorders; soluble epoxide hydrolase (sEH) as a possible new target. *Neurosci. Biobehav. Rev.* 87, 56–66. doi: 10.1016/j.neubiorev.2018.01.010
- Upthegrove, R., Manzanares-Teson, N., and Barnes, N. M. (2014). Cytokine function in medication-naïve first episode psychosis: a systematic review and meta-analysis. *Schizophr. Res.* 155, 101–108. doi: 10.1016/j.schres.2014.03.005
- van Kesteren, C. F., Gremmels, H., de Witte, L. D., Hol, E. M., Van Gool, A. R., Falkai, P. G., et al. (2017). Immune involvement in the pathogenesis of schizophrenia: a meta-analysis on postmortem brain studies. *Transl. Psychiatry* 7:e1075. doi: 10.1038/tp.2017.4
- Wagner, K. M., McReynolds, C. B., Schmidt, W. K., and Hammock, B. D. (2017). Soluble epoxide hydrolase as a therapeutic target for pain, inflammatory and neurodegenerative diseases. *Pharmacol. Ther.* 180, 62–76. doi: 10.1016/j.pharmthera.2017.06.006
- Wagner, K., Vito, S., Inceoglu, B., and Hammock, B. D. (2014). The role of long chain fatty acids and their epoxide metabolites in nociceptive signaling. *Prostaglandins Other Lipid Mediat.* 113–115, 2–12. doi: 10.1016/j.prostaglandins.2014.09.001
- Wang, D. F., Sun, X. Y., Yan, J. J., Ren, B., Cao, B., Lu, Q. B., et al. (2018). Alterations of eicosanoids and related mediators in patients with schizophrenia. *J. Psychiatr. Res.* 102, 168–178. doi: 10.1016/j.jpsychires.2018.04.002
- World Health Organization. (2018a). Depression. 22 March 2018. Available at: <http://www.who.int/news-room/fact-sheets/detail/depression> (Accessed November 3, 2018).
- World Health Organization. (2018b). Schizophrenia. 9 April 2018. Available at: <http://www.who.int/news-room/fact-sheets/detail/schizophrenia> (Accessed November 3, 2018).
- Wu, Q., Cai, H., Song, J., and Chang, Q. (2017). The effects of sEH inhibitor on depression-like behavior and neurogenesis in male mice. *J. Neurosci. Res.* 95, 2483–2492. doi: 10.1002/jnr.24080
- Wu, Q., Song, J., Meng, D., and Chang, Q. (2019). TPPU, a sEH inhibitor, attenuates corticosterone-induced PC12 cell injury by modulation of BDNF-TrkB pathway. *J. Mol. Neurosci.* 67:364. doi: 10.1007/s12031-018-1230-z
- Yao, J. K., and Keshavan, M. S. (2011). Antioxidants, redox signaling, and pathophysiology in schizophrenia: an integrative view. *Antioxid. Redox Signal.* 15, 2011–2035. doi: 10.1089/ars.2010.3603
- Young, J. J., Bruno, D., and Pomara, N. (2014). A review of the relationship between proinflammatory cytokines and major depressive disorder. *J. Affect. Disord.* 169, 15–20. doi: 10.1016/j.jad.2014.07.032
- Zhang, G., Kodani, S., and Hammock, B. D. (2014). Stabilized epoxygenated fatty acids regulate inflammation, pain, angiogenesis and cancer. *Prog. Lipid Res.* 53, 108–123. doi: 10.1016/j.plipres.2013.11.003
- Zhang, J. C., Wu, J., Fujita, Y., Yao, W., Ren, Q., Yang, C., et al. (2015). Antidepressant effects of TrkB ligands on depression-like behavior and dendritic changes in mice after inflammation. *Int. J. Neuropsychopharmacol.* 18:pyu077. doi: 10.1093/ijnp/pyu077
- Zhang, J. C., Yao, W., and Hashimoto, K. (2016). Brain-derived neurotrophic factor (BDNF)—TrkB signaling in inflammation-related depression and potential therapeutic targets. *Curr. Neuropharmacol.* 14, 721–731. doi: 10.2174/1570159X14666160119094646

Conflict of Interest Statement: The author declares that the research was conducted in the absence of any commercial or financial relationships that could be construed as a potential conflict of interest.

Copyright © 2019 Ren. This is an open-access article distributed under the terms of the Creative Commons Attribution License (CC BY). The use, distribution or reproduction in other forums is permitted, provided the original author(s) and the copyright owner(s) are credited and that the original publication in this journal is cited, in accordance with accepted academic practice. No use, distribution or reproduction is permitted which does not comply with these terms.



Docosahexaenoic Acid Increases the Potency of Soluble Epoxide Hydrolase Inhibitor in Alleviating Streptozotocin-Induced Alzheimer's Disease-Like Complications of Diabetes

Rohit Pardeshi¹, Nityanand Bolshette², Kundlik Gadhave³, Mohammad Arfeen⁴, Sahabuddin Ahmed⁴, Rohitash Jamwal⁵, Bruce D. Hammock⁶, Mangala Lahkar² and Sumanta Kumar Goswami^{6*}

OPEN ACCESS

Edited by:

John D. Imig,
Medical College of Wisconsin,
United States

Reviewed by:

Tzong-Shyuan Lee,
National Taiwan University, Taiwan
Hui-Ching Lin,
National Yang-Ming University, Taiwan

*Correspondence:

Sumanta Kumar Goswami
sumantag@gmail.com

Specialty section:

This article was submitted to
Translational Pharmacology,
a section of the journal
Frontiers in Pharmacology

Received: 08 January 2019

Accepted: 11 March 2019

Published: 24 April 2019

Citation:

Pardeshi R, Bolshette N,
Gadhave K, Arfeen M, Ahmed S,
Jamwal R, Hammock BD, Lahkar M
and Goswami SK (2019)
Docosahexaenoic Acid Increases
the Potency of Soluble Epoxide
Hydrolase Inhibitor in Alleviating
Streptozotocin-Induced Alzheimer's
Disease-Like Complications
of Diabetes.
Front. Pharmacol. 10:288.
doi: 10.3389/fphar.2019.00288

¹ Department of Biotechnology, National Institute of Pharmaceutical Education and Research (NIPER), Gauhati Medical College and Hospital, Guwahati, India, ² Institutional Level Biotech Hub (IBT Hub), Department of Biotechnology, National Institute of Pharmaceutical Education and Research (NIPER), Gauhati Medical College and Hospital, Guwahati, India, ³ School of Basic Sciences, Indian Institute of Technology Mandi, Kamand, India, ⁴ Laboratory of Neurobiology, Department of Pharmacology and Toxicology, National Institute of Pharmaceutical Education and Research (NIPER), Gauhati Medical College and Hospital, Guwahati, India, ⁵ Biomedical and Pharmaceutical Sciences, The University of Rhode Island, Kingston, RI, United States, ⁶ Hammock Laboratory of Pesticide Biotechnology, Department of Entomology and Nematology, and Comprehensive Cancer Center, University of California, Davis, Davis, CA, United States

Diabetes is a risk factor for Alzheimer's disease and it is associated with significant memory loss. In the present study, we hypothesized that the soluble epoxide hydrolase (sEH) inhibitor N-[1-(1-oxopropyl)-4-piperidinyl]-N'-[4-(trifluoromethoxy)phenyl]-urea (also known as TPPU) could alleviate diabetes-aggravated Alzheimer's disease-like symptoms by improving memory and cognition, and reducing the oxidative stress and inflammation associated with this condition. Also, we evaluated the effect of edaravone, an antioxidant on diabetes-induced Alzheimer's-like complications and the additive effect of docosahexaenoic acid (DHA) on the efficacy of TPPU. Diabetes was induced in male Sprague-Dawley rats by intraperitoneally administering streptozotocin (STZ). Six weeks after induction of diabetes, animals were either treated with vehicle, edaravone (3 or 10 mg/kg), TPPU (1 mg/kg) or TPPU (1 mg/kg) + DHA (100 mg/kg) for 2 weeks. The results demonstrate that the treatments increased the memory response of diabetic rats, in comparison to untreated diabetic rats. Indeed, DHA + TPPU were more effective than TPPU alone in reducing the symptoms monitored. All drug treatments reduced oxidative stress and minimized inflammation in the brain of diabetic rats. Expression of the amyloid precursor protein (APP) was increased in the brain of diabetic rats. Treatment with edaravone (10 mg/kg), TPPU or TPPU + DHA minimized the level of APP. The activity of acetylcholinesterase (AChE) which metabolizes acetylcholine was increased in the brain of diabetic rats. All the treatments except edaravone (3 mg/kg) were effective in decreasing the activity of AChE and TPPU + DHA was more efficacious than TPPU alone. Intriguingly, the histological changes in hippocampus after treatment

with TPPU + DHA showed significant protection of neurons against STZ-induced neuronal damage. Overall, we found that DHA improved the efficacy of TPPU in increasing neuronal survival and memory, decreasing oxidative stress and inflammation possibly by stabilizing anti-inflammatory and neuroprotective epoxides of DHA. In the future, further evaluating the detailed mechanisms of action of sEH inhibitor and DHA could help to develop a strategy for the management of Alzheimer's-like complications in diabetes.

Keywords: Alzheimer's disease-like complications of diabetes, sEH inhibitor TPPU, DHA, Morris water maze, novel object recognition test, inflammatory cytokines

INTRODUCTION

Diabetes mellitus (DM) is a complex metabolic disorder which adversely affects multiple physiological systems including the central nervous system and cardiovascular system, and the disease is associated with altered memory function, cardiac stress, endothelial dysfunction and neuropathy (Islam et al., 2017; Bhadri et al., 2018; Minaz et al., 2018). Both type 1 and type 2 diabetes induce changes in the neurones, brain and memory as seen in the case of Alzheimer's disease (Zhao and Townsend, 2009; Ouwens et al., 2014; Rdzak and Abdelghany, 2014; King et al., 2015; Meneilly and Tessier, 2016; Morales-Corraliza et al., 2016; Chen et al., 2018; Pappas et al., 2018; Takeuchi et al., 2018; Yashkin et al., 2018).

Alzheimer's disease (AD) is the leading cause of dementia. Characterized by memory and cognitive impairment in aging populations, it poses a significant health challenge. Although, AD is reported with significant neurodegeneration by accumulation of amyloid beta (A β) and tau protein aggregates in the human brain (Kolarova et al., 2012; Peraza et al., 2016; Kim et al., 2018), its exact potential cause is still not completely understood (Gadhav et al., 2016). Recently, the World's Alzheimer's report 2018 estimated that worldwide around 50 million people are living with dementia and this number is set to reach 82 million by 2030, and more than triple to 152 million by 2050. Moreover, the total estimated worldwide cost is USD 1 trillion by 2018, and that will rise to USD 2 trillion by 2030 (Alzheimer's Disease International, 2018). Interestingly, impaired insulin signaling is linked to memory loss.

Insulin signaling is crucial for synaptogenesis, neuronal development, and survival (Apostolatos et al., 2012). The activation of GSK-3 β , inflammation, oxidative stress, and altered glucose metabolism are critical features of both Type II DM and AD (De Felice et al., 2014; Bedse et al., 2015; Pardeshi et al., 2017). Importantly, proinflammatory signaling, oxidative stress, and prolonged metabolic stress contribute to insulin resistance (Gregor and Hotamisligil, 2011; Henriksen et al., 2011). Cognitive defects in diabetes include altered psychomotor efficiency, attention, learning memory, and mental flexibility (Bakris et al., 2009). In addition to regulation of blood glucose, insulin also modulates synaptic plasticity, cognition and aging-related neurodegeneration (Zhao and Townsend, 2009). Increase in the level of blood glucose and hyperinsulinemia are known to cause neuronal death followed by neurodegeneration as

seen with AD (Zhao and Townsend, 2009). Additionally, the homeostasis of glucose and lipid affect the production and clearance of A β , phosphorylation of tau and neurodegeneration (Sato and Morishita, 2015). Insulin resistance was found to be associated with significantly lower regional cerebral glucose metabolism and impaired memory performance (Willette et al., 2015). Though insulin resistance and deficiency augment the phosphorylation of A β and tau and promote the development of AD (Garwood et al., 2015), the pathology of the process remains incompletely understood (Bedse et al., 2015). DM might facilitate the development of AD through an increase in the level of oxidative stress and advanced glycation end products (AGEs), which causes structural and functional abnormalities in the brain (Gispén and Biessels, 2000; Biessels et al., 2002).

The involvement of soluble epoxide hydrolase in vascular cognitive decline has recently been reported (Nelson et al., 2014). It was found that a soluble epoxide hydrolase inhibitor (sEHI) alleviates transmissible spongiform encephalopathies (TSEs) associated with neuronal loss and inflammation (Poli et al., 2013). Earlier, we demonstrated that the sEHI, TPPU, minimizes memory impairment in diabetic rats (Minaz et al., 2018). These lines of research suggest that sEHIs may have potential therapeutic effect in managing AD associated memory impairment. We have previously demonstrated the anti-inflammatory property (Goswami et al., 2016, 2017) of TPPU in addition to its ability to reduce oxidative stress (Goswami et al., 2016) including the diabetes-induced oxidative stress in the brain (Minaz et al., 2018), but it has not been evaluated in AD-like condition. We hypothesized that TPPU could alleviate diabetes-induced Alzheimer-like complexities by decreasing the oxidative stress and inflammation. Primarily, sEH inhibitors exert anti-inflammatory activity by preserving the levels of both ω -6 and ω -3 epoxy fatty acids including epoxyeicosatrienoic acids (EETs) which are metabolized by sEH (Morisseau and Hammock, 2013). In general, epoxy fatty acids produced from DHA, an ω -3 fatty acid are more potent anti-inflammatory agents than arachidonic acid (ω -6) derived EETs in several different bioassays. Therefore, we assessed the effect of DHA on the anti-Alzheimer activity of TPPU. For comparative analysis, we have evaluated the effect of edaravone which is known to possess anti-oxidant and anti-inflammatory properties (Watanabe et al., 2008) in diabetes-induced Alzheimer's-like complexities.

MATERIALS AND METHODS

Chemical and Reagents

TPPU was synthesized in the Hammock Laboratory of Pesticide Biotechnology, University of California, Davis, the United States as described earlier (Rose et al., 2010). DHA (TCI chemicals, United States), PEG400 (Sigma-Aldrich, United States), 3-methyl-1-phenyl-5-pyrazolone/edaravone (TCI chemicals, United States), SD Check blood glucose meter (SD Biosensor Inc., South Korea), ELISA kit for cytokine estimation (Elabscience Biotechnology Co., Ltd., Wuhan, China), HiPuraA™ Total RNA Miniprep purification kit (Himedia, India), primers (Integrated DNA Technologies, United States) were collected. All other reagents were of analytical grade.

Animal Studies

Thirty-six male Sprague-Dawley rats, 6–8 weeks old, between 200 and 250 g were used. The animals were randomized so that each group had animals of similar weight and age. Animals were maintained under standard laboratory conditions. The animal experiment protocols were approved (MC/05/2015/73) by the Institutional Animal Ethics Committee (IAEC), Gauhati Medical College and Hospital, India (CPCSEARegistration No. 351; 3/1/2001). Diabetes was induced by administration of streptozotocin (50 mg/kg body weight, i.p.) dissolved in 0.1 M cold citrate buffer (pH 4.5). Blood was collected from the tail vein, and blood glucose was quantified using SD Check blood glucose meter 48 h after STZ administration (SD Biosensor Inc., South Korea). Only animals with a blood glucose level > 250 mg/dl were used in the study. The day of diabetes assessment was considered as day 1.

Diabetic rats were randomly distributed to five groups and treated as described in **Figure 1**. Non-diabetic animals (not treated with STZ) were used as normal control whereas diabetic rats treated with the vehicle was used as positive/diabetic control. Diabetic rats were administered edaravone/EDV (3 mg/kg),

edaravone (10 mg/kg), TPPU (1 mg/kg) or TPPU + DHA (100 mg/kg). The dose of TPPU was selected based on our previous studies on anti-inflammatory and memory protective activity of the enzyme inhibitor (Goswami et al., 2016; Minaz et al., 2018). Epoxy fatty acids generated from DHA were more stable and potent in the presence of the sEHI. Therefore, DHA was selected based on previous reports (Ulu et al., 2013, 2014). The dose of DHA or its derivative to ameliorate Alzheimer's disease is 40–200 mg/kg in animal models (Cansev et al., 2008; Sugasini et al., 2017). We have selected 100 mg/kg dose of DHA for this study. The dose of edaravone was selected based on published data on its protective effect on diabetes-induced cognitive impairment (Zhou et al., 2013; Reeta et al., 2017). Two doses of edaravone were selected to evaluate if the anti-oxidant exert a dose-dependent effect.

The treatments were administered for 6 weeks after STZ injection and dosing were continued for two weeks. TPPU was dissolved in PEG400 and DHA in 5% of acacia solution. Weekly fasting blood glucose was measured by using SD Check blood glucose meter. On the day of the last dose, the blood was collected from animals through the tail vein for glucose analysis. Further, animals were sacrificed to isolate the hippocampus as well as remaining parts of the brain to perform subsequent biochemical and histopathological studies (**Figure 1**).

Behavioral and Learning Tests

The Morris water maze (MWM) test was used to assess the learning and memory function (Vorhees and Williams, 2006). Novel object recognition test (NORT) was performed to evaluate recognition memory as described previously (Singla and Dhawan, 2017).

For conducting the MWM test, a circular tank consisting of diameter 120 cm and a height of 50 cm were used. The MWM had four equal quadrants containing non-transparent water at room temperature (24–26°C). The water level was high enough to prevent the animal from touching the base of the tank and

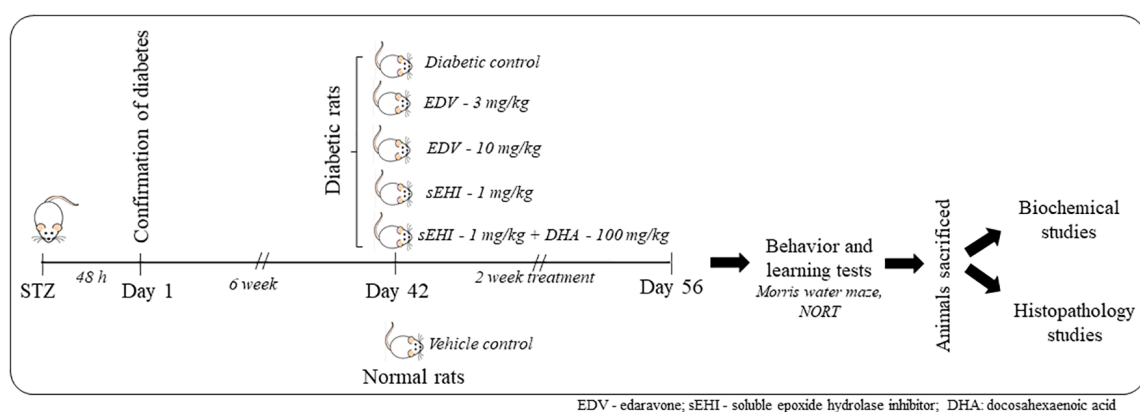


FIGURE 1 | A total number of 36 rats were included in the study containing 6 rats in 6 groups. One group was maintained as a vehicle control group, and another 5 groups of rats were dosed with STZ. Induction of diabetes was confirmed after 48 h. Animals were maintained for six weeks under the diabetic condition for the development of memory impairment. Then animals were dosed for two weeks with edaravone, sEH inhibitor TPPU or DHA + TPPU. Memory function was evaluated on the 56th day, and animals were sacrificed. Biochemical tests and histopathology were performed to evaluate the protective effect of treatments.

low enough to prevent animal from jumping out of the water. A platform measuring 10 cm, on which a rat can stand/sit, was used to assess memory function. The rats were trained for learning to locate the visible platform during the acquisition phase of training, then the memory of rats was evaluated during the evaluation phase by allowing them to discover the hidden platform. During the acquisition phase, the platform was placed 1 cm above the water level so that the rats can quickly identify the platform and sit on it when forced to explore the tank for 2 min. In case the animals failed to locate the platform, the researcher placed them on the platform for half a minute during five days of training. Daily four trials were run for each rat individually with a 5 min interval between each session in a day. During each test, the rats were placed in different quadrants. To analyze the retention of memory, the animals were positioned in the quadrant with their head facing the wall and allowed to explore the hidden platform 1 cm below the surface to avoid drowning. Retention latencies were recorded by measuring the time taken by animals to locate the hidden platform. Also, reference memories were evaluated by measuring the number of times each animal crossed over a reference point, where the platforms were kept during training phase after the animals were placed on a novel place in the quadrant. For calculating reference memory, no platforms were set during the test.

Novel object recognition test, a commonly used test, to evaluate the recognition memory were employed in this study. The ability of animals to identify the old object and to spend more time in exploring new object than the old object was considered as a marker of recognition memory. The test has 3 phases/sessions to quantify recognition index: *habituation phase* where the animals were familiarized with an open field box (36 × 50 × 36 cm), *familiarization phase* where the animals were acquainted with two objects, and finally a *test phase* where the animals were subjected to a novel object. First, the animals were habituated to a black open field box for 5 min, two times per day for a total duration of three days. Then, the animals were familiarized with a rectangular wooden block and a rubber ball in the open field box and allowed to explore for 10 min after placing them with their heads facing opposite to objects. Next day, the animals were subjects to a new and novel object, i.e., a small wooden box along with two old objects for 3 min in the open field box. Time spent on exploring the objects was recorded. Recognition index was calculated by dividing the time spent by animals in exploring known objects from the time spent in exploring novel object and presented as a percentage. The total exploratory period was also measured to validate that the recognition index calculated was not due to activation or inactivation of sensorimotor function. During the whole experiment, the open field box and objects were cleaned with 70% ethanol regularly for each animal and each session to avoid olfactory cues.

Tissue Collection, Preparation and Histopathology Studies

Animals were sacrificed by cervical dislocation under anesthesia and brains were collected. One half of the

brain including hippocampus was fixed in 10% buffered formalin. A small portion of the hippocampus was used to isolate RNA. Another half of the brain was dipped in liquid nitrogen for 30 s and later stored at -80°C until further use. A portion of each brain was homogenized (1:9, tissue: buffer, w/v) in ice-cold phosphate buffer saline (0.05 M, pH 7.0) (Heidoph, Silent Crusher S, Germany). The homogenate was centrifuged at 10000 g for 30 min at 4°C and supernatant for each tissue was collected. Supernatants were subsequently used for biochemical characterization as described below. Formalin-fixed tissue was stained with eosin using previously described procedures (Fischer et al., 2008).

Estimation of Oxidative Stress

The concentration of MDA in hippocampal homogenates as an index of lipid peroxidation was determined according to a previously described method (Ohkawa et al., 1979). Nitric oxide content in the hippocampus was determined indirectly by measuring the level of nitrite (Green et al., 1982). Glutathione concentration in the hippocampus was measured using reduced glutathione (GSH) as the reference standard as described by Ellman (1959). Total protein was estimated using Lowry's method (Waterborg and Matthews, 1984).

Quantification of Inflammatory Markers (IL-1 β , IL-6, and IL-10)

The levels of pro-inflammatory cytokines (IL-1 β and IL-6) and anti-inflammatory cytokine (IL-10) in hippocampus tissues of control and treatment groups were determined by ELISA (Elabscience Biotechnology Co. Ltd., Wuhan, China).

Gene Expression Study and Enzyme Activity

Total RNA was isolated from the freshly collected hippocampal region of the brain of mice using HiPuraATM Total RNA Miniprep purification kit (Himedia, India). The assay was performed according to kit protocol, and NCBI Primer-BLAST Tools designed primers were used. The PCR products were resolved on 1.7% agarose gel. Gel image was taken by UVI TEC Essential V4 Gel Doc XR⁺ system, and image analysis was performed with the help of Image lab-5.1 gel analysis software. See the data in Table 1. The activity of AChE was determined using acetylcholinesterase assay kit from Abcam.

TABLE 1 | PCR product size and Tm of APP and β -Actin from rat.

Sr.No	Gene (Species: <i>Rattus norvegicus</i>)	PCR Product size	Tm
1	Amyloid Precursor Protein (APP) forward primer: GCAATGATCTCCCGCTGGTA; reverse primer: AAAGTTGTTCTGTTGCCGC	90 bp	59.0°C
2	Beta Actin (β -Actin) forward primer: TCTGAACCCTAAGGCCAACC; reverse primer: TACGTACATGGCTGGGGTGT	76 bp	60.0°C

Histopathology

At the end of the study, the brain of the rat was removed after cervical dislocation and immediately fixed in 10% buffered formalin. H&E staining was performed using a standardized protocol (Bancroft and Gamble, 2008; Amin et al., 2013).

Statistical Analysis

All values are expressed as means \pm SEM and were analyzed using one-way analysis of variance (ANOVA) followed by Tukey's method for *post hoc* analysis. All the statistical analysis were performed on Prism 6 and $P < 0.05$ was considered statistically significant (GraphPad Inc., United States).

RESULTS

TPPU and TPPU + DHA Treatment Does Not Decrease the Level of Glucose in Serum

As discussed earlier, six weeks after the induction of diabetes, the animals were treated with curative doses of edaravone, TPPU or

TPPU + DHA for two weeks. The treatment did not affect the level of glucose in the serum in comparison to diabetic control animals. The serum glucose levels of diabetic control and diabetic treated animals ranged from 400 to 450 mg/dL whereas the serum glucose level of normal healthy rats was around 90 to 100 mg/dL.

TPPU and TPPU + DHA Alleviate Memory Dysfunction in Diabetes

Effect of TPPU on memory function as assessed from the Morris water maze test is summarized in **Figure 2**. In the present study, the AD-like complication was induced by administration of STZ (50 mg/kg i.p.) and confirmed by a significant decrease in “sporadic memory” and “recognition memory” in diabetic rats in comparison to healthy control animals.

Diabetic control rats spent less time (22 ± 2 s) in the target quadrant when compared with healthy vehicle control rats (46 ± 3 s). Rats treated with TPPU spent more time (33 ± 2 s) in the target quadrant of the water maze which is a result of development in sporadic memory. DHA significantly potentiated the effect of TPPU on memory function because the rats treated with DHA + TPPU spent more time in the maze

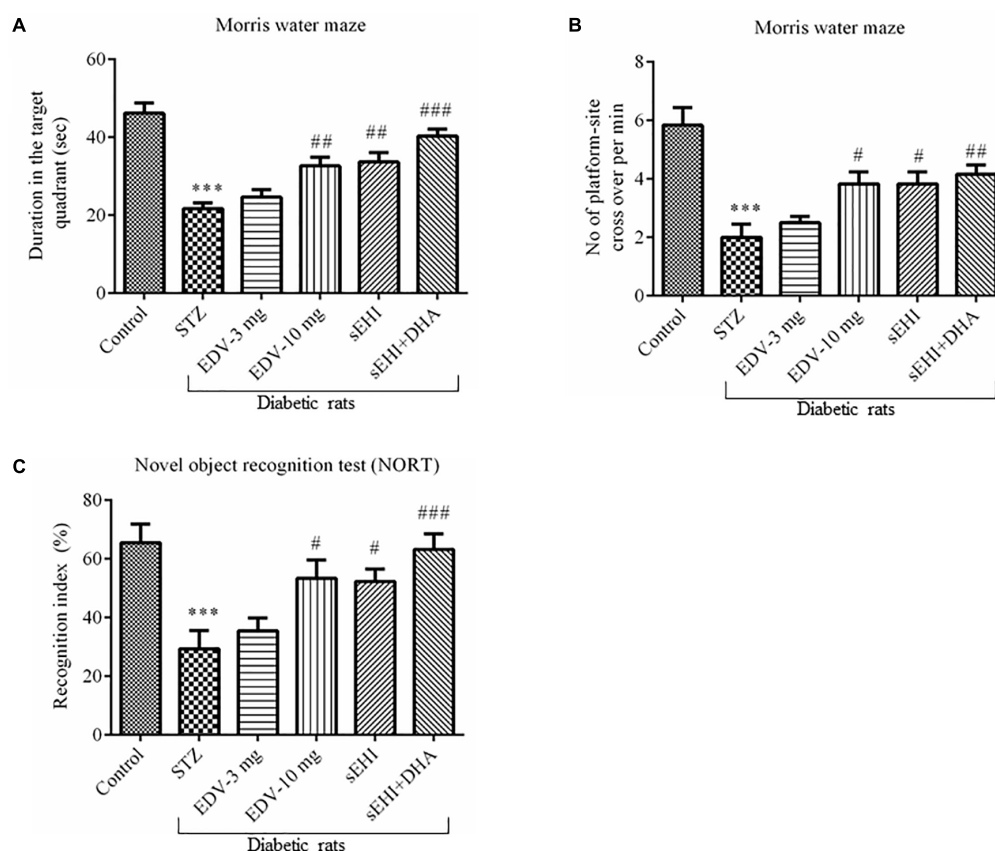


FIGURE 2 | TPPU + DHA decreases the degree of memory impairment in diabetic rats. Memory function was assessed by quantifying the (A) duration spent in target quadrant of the MWM, (B) a number of platform site crossover per minutes in MWM, and (C) recognition index. Memory impairment was observed in diabetic rats in comparison to normal healthy rats. Treatment with edaravone (only 10 mg/kg), TPPU or TPPU + DHA alleviated the memory impairment in diabetic rats. The data are presented as mean \pm SEM of 6 readings. One-way ANOVA followed by Tukey's multiple comparison test was used for statistical analysis. *** $p < 0.001$ when compared with healthy rats; $N = 6$, # $p < 0.05$, ## $p < 0.01$, ### $p < 0.001$ when compared with diabetic control rats.

(40 ± 2 s). Edaravone at higher concentration also increased sporadic memory of diabetic rats because rats spent more time in the maze (33 ± 2 ; **Figure 2A**). The number of times the diabetic rats (2 ± 0.4) crossed platform-site was less, in comparison to vehicle control rats (5.8 ± 0.6). Diabetic rats treated with edaravone (only 10 mg/kg) (3.8 ± 0.4), TPPU (3.8 ± 0.4), or DHA + TPPU (4.2 ± 0.3) significantly crossed more lines, in comparison to diabetic rats indicating an increase in the sporadic memory in the treated animals. All treatment groups showed similar results (**Figure 2B**).

A significant decrease in the recognition index was observed in diabetic rats ($29 \pm 6\%$) in comparison to normal control rats ($65 \pm 6\%$) indicating a decrease in recognition memory. An increase in the percent of recognition index in the treatment group of edaravone (only 10 mg/kg) ($53 \pm 6\%$), TPPU ($52 \pm 4\%$) and sEH + DHA ($63 \pm 5\%$) were observed in comparison to diabetic control rats. Thus, the treatment groups showed an improvement in sporadic memory, recognition memory, and learning memory (**Figure 2C**). One-way ANOVA followed by Tukey's multiple comparison test were used for calculating statistical significance. Values were presented as mean \pm SEM of 6 observations.

DHA + TPPU Minimize Oxidative Stress

An increase in the level of MDA (100 ± 7 $\mu\text{M}/\text{mg}$ protein) was observed in the diabetic rats in comparison to vehicle control rats (50 ± 5 $\mu\text{M}/\text{mg}$ protein) suggesting an increase in the oxidative stress, whereas treatment with edaravone (10 mg/kg) (72 ± 5 $\mu\text{M}/\text{mg}$ protein) or TPPU + DHA (65 ± 5 $\mu\text{M}/\text{mg}$ protein) significantly minimized an increase in the level of MDA (**Figure 3A**). The level of nitrite in the diabetic control group (10.8 ± 0.9 $\mu\text{M}/\text{mg}$ protein) significantly increased when compared with vehicle group (4.1 ± 0.5 $\mu\text{M}/\text{mg}$ protein) indicating an increase in the oxidative stress in diabetic rats. Edaravone (10 mg/kg) (7.2 ± 1 $\mu\text{M}/\text{mg}$ protein) and TPPU (7.2 ± 0.7 $\mu\text{M}/\text{mg}$ protein) prevented an increase in the level of nitrite. The combination of DHA and TPPU (5.7 ± 1 $\mu\text{M}/\text{mg}$ protein) was more effective than TPPU alone in reducing

oxidative stress in terms of decreasing the level of nitrite (**Figure 3B**). In diabetic rats (53 ± 3 $\mu\text{M}/\text{mg}$ protein), a significant decrease in the level of endogenous antioxidant GSH was observed when compared with normal control rats (79 ± 2 $\mu\text{M}/\text{mg}$ protein). Treatment of edaravone (10 mg/kg) (68 ± 5 $\mu\text{M}/\text{mg}$ protein) significantly prevented an increase in the level of GSH in diabetic rats, and when the sEH + DHA was treated along with DHA (70 ± 3 $\mu\text{M}/\text{mg}$ protein) the level of GSH was increased higher than the diabetic control (**Figure 3C**). One-way ANOVA followed by Tukey's multiple tests were used for calculating statistical significance. Values are presented as mean \pm SEM of 6 observations.

TPPU and DHA + TPPU Decrease Inflammation in the Hippocampus of Diabetic Rats

An increase in the neuroinflammation was evident in the hippocampus of diabetic rats due to the rise in the level of pro-inflammatory marker IL-1 β (**Figure 4A**) (412 ± 29 pg/ml) and IL-6 (**Figure 4B**) (180 ± 6 pg/ml) and decrease in the level of anti-inflammatory marker IL-10 (**Figure 4C**) (220 ± 7 pg/ml) in comparison to the healthy normal rats (IL-1 β , 311 ± 14 pg/ml; IL-6, 110 ± 9 pg/ml; IL-10, 261 ± 5 pg/ml). None of the treatments had any effect on the level of IL-1 β , but treatment with edaravone (10 mg/kg) (141 ± 6 pg/ml) or TPPU + DHA (139 ± 7 pg/ml) prevented an increase the level of IL-6. TPPU (245 ± 6 pg/ml) or TPPU + DHA (252 ± 6 pg/ml) prevented a decrease in the level of IL-10. Overall, the treatments decreased the degree of inflammation in diabetic rats in comparison to diabetic control rats. One-way ANOVA followed by Tukey's multiple tests were used for calculating statistical significance. Values are presented as mean \pm SEM of 6 observations.

DHA + TPPU Decreases the Expression of APP and Activity of AChE

The gene expression experimental data showed an increase in the expression of the APP gene, which is encoded for amyloid beta

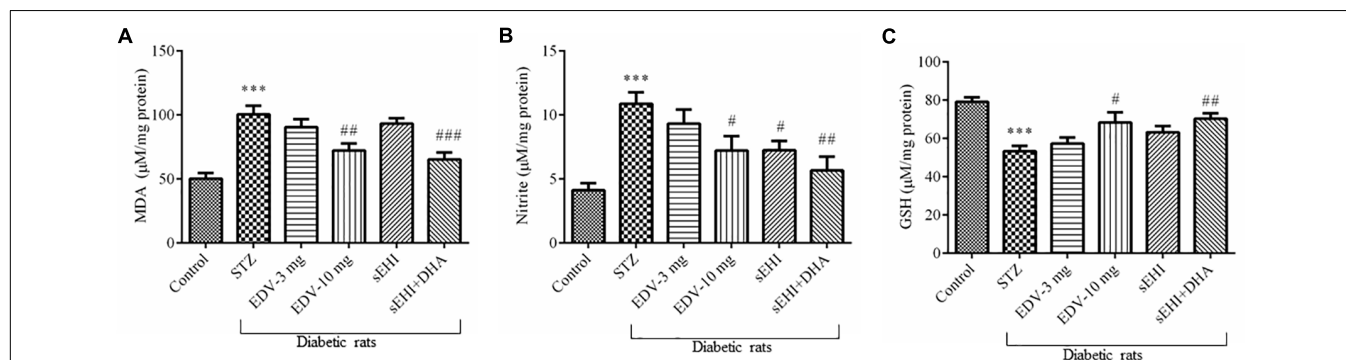


FIGURE 3 | TPPU + DHA decreases oxidative stress in the hippocampus of diabetic rats. Oxidative stress was evaluated by quantifying an increase in the levels of (A) MDA and (B) nitrite but a decrease in the level of (C) GSH. Oxidative stress was increased in the brain of diabetic rats, in comparison to normal control rats. Treatment with edaravone (10 mg/kg), TPPU or TPPU + DHA minimized the oxidative stress in the brain of diabetic rats, in comparison to diabetic control rats. The data are presented as mean \pm SEM of 6 readings. One-way ANOVA followed by Tukey's multiple comparison test was used for statistical analysis. *** $p < 0.001$ when compared with healthy rats; $N = 6$, # $p < 0.05$, ## $p < 0.01$, ### $p < 0.001$ when compared with diabetic control rats.

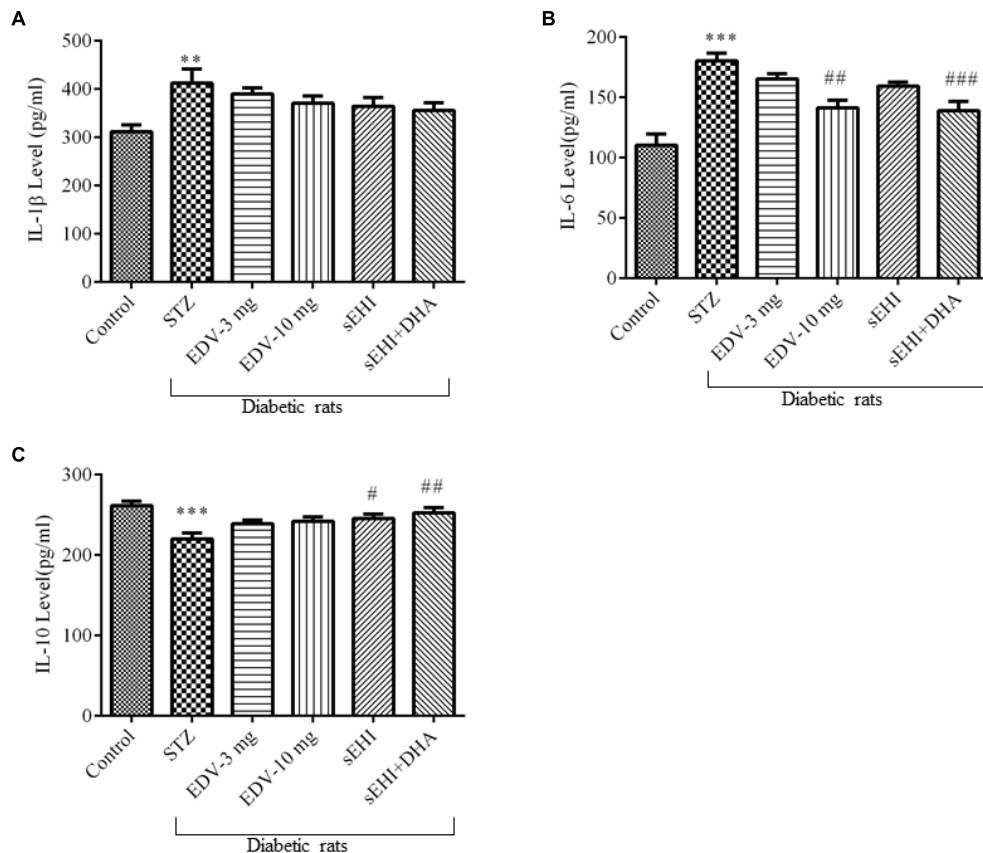


FIGURE 4 | TPPU + DHA decreases the level of neuroinflammation. **(A)** An increase in the level of IL-1 β was observed in the hippocampus of diabetic rats in comparison to normal rats. None of the treatments decreased the level of IL-1 β . **(B)** The level of IL-6 was increased in the hippocampus of diabetic rats, in comparison to normal rats. Treatment with either edaravone (10 mg/kg) or TPPU + DHA decreased the level of IL-6 in the diabetic rats. **(C)** The level of IL-10 was decreased in the brain of diabetic rats, in comparison to normal rats. TPPU increased the level of IL-10 in diabetic rats, and DHA potentiated the efficacy of TPPU in increasing the level of IL-10. The data are presented as mean \pm SEM of 6 readings. One-way ANOVA followed by Tukey's multiple comparison test was used for statistical analysis. ** p < 0.01 and *** p < 0.001 when compared with healthy rats; N = 6, # p < 0.05, ## p < 0.01, ### p < 0.001 when compared with diabetic control rats.

synthesis. Administration of STZ leads to overexpression of the APP mRNA (1.6 ± 0.0 fold) in diabetic rats, in comparison to vehicle control rats. The treatment with edaravone (10 mg/kg) (1.3 ± 0.1 fold) or TPPU (1.3 ± 0.0 fold) significantly decreased the expression of APP as compared to pathological control. DHA potentiated the effect of TPPU in decreasing (1.2 ± 0.1 fold) the level of APP (**Figure 5A**). TPPU minimized (p < 0.05) the level of mRNA of APP in diabetic rats, in comparison to diabetic control rats. DHA + TPPU was more effective in decreasing (p < 0.001) the level of mRNA of APP, in comparison to TPPU alone.

The activity of AChE was also increased (0.37 ± 0.02 μ moles/min/mg protein) in the STZ-treated group, in comparison to vehicle control rats (0.16 ± 0.00 μ moles/min/mg protein). AChE metabolizes ACh, and an increase in the activity of AChE would infer a reduction in the level of ACh, a neurotransmitter which supports cognitive function in cerebral cortex and hippocampus. Treatment with edaravone (10 mg/kg) (0.27 ± 0.01 μ moles/min/mg protein), TPPU (0.30 ± 0.02 μ moles/min/mg protein) or TPPU + DHA

(0.27 ± 0.02 μ moles/min/mg protein) decreased the activity of AChE in diabetic rats, in comparison to diabetic control rats (**Figure 5B**). One-way ANOVA followed by Tukey's multiple tests was used for calculating statistical significance. Values are presented as mean \pm SEM of 6 observations.

TPPU and TPPU + DHA Protect Hippocampal Neurons in Diabetes

H&E staining of the CA1 region of hippocampus from normal healthy rat revealed regularly arranged neurons with large, round, transparent, and intact nuclei. The pyramidal neurons in the CA1 region of the diabetic rat was severely damaged, disorderly arranged with significantly reduced in number, and characterized by pyknotic and indistinct nuclei which indicates neuron death. A decrease in the number of pyramidal neurons in the CA1 region of the hippocampus is reported in Alzheimer's disease (Davies et al., 1992). Edaravone at 3 mg/kg failed to show any neuroprotection with characteristic pyknotic nuclei still visible. Treatment with edaravone at 10 mg/kg shows

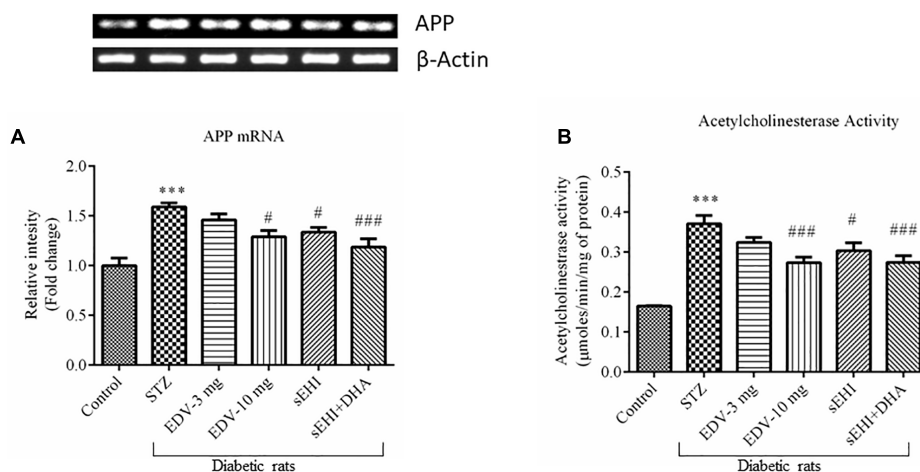


FIGURE 5 | DHA + TPPU decreases the expression of APP (A) and activity of AChE (B) in the hippocampus of diabetic rats. TPPU and both TPPU + DHA decreased the markers of Alzheimer's disease in diabetic rats. Expressions of APP and activity of AChE were quantified in the brains of normal healthy rats, diabetic rats and diabetic rats treated with either edaravone, TPPU or TPPU + DHA. The level of APP and activity of AChE were increased in the brains of diabetic rats, in comparison to normal healthy rats. Treatment with edaravone (10 mg/kg), TPPU or TPPU + DHA prevented an increase in the levels of APP, in comparison to diabetic control rats. Similarly, treatment with edaravone (10 mg/kg), TPPU or TPPU + DHA treatment minimized an increase in the activity of AChE. The data are presented as mean \pm SEM of 6 readings. One-way ANOVA followed by Tukey's multiple comparison test was used for statistical analysis. *** p < 0.001 when compared with healthy rats; N = 6, # p < 0.05, ## p < 0.01, ### p < 0.001 when compared with diabetic control rats.

some neuroprotection where neurons are orderly arranged with still indistinct nuclei visible. Treatment with TPPU resulted in good neuroprotective activity. Treatment with sEH1 + DHA resulted in better neuroprotective effect with a parallel decrease in hippocampal atrophy also to the visibility of prominent distinct nuclei (Figure 6). The qualitative neuroprotective effect of treatments was evaluated manually.

DISCUSSION

Diabetes, associated with insulin resistance and reduction in the level of insulin, mainly affects psychomotor activity, attention, learning, memory, cognition, mental flexibility in the brain (Bakris et al., 2009). Increased risk of dementia, including memory dysfunction associated with Alzheimer's disease is

prevalent among diabetic patients (Barbagallo and Dominguez, 2014). We observed a decrease in learning and memory of diabetic rats with a parallel increase in the level of inflammation, oxidative stress, APP and neuronal damage in comparison to normal healthy rats. Treatment with antioxidant (edaravone), sEH1 (TPPU) or TPPU + DHA minimized diabetes-induced memory impairment, oxidative stress, and inflammation.

Additionally, the treatment also prevented an increase in the level of APP and neuronal damage. The up-regulation, trafficking, and dysregulation of amyloid precursor protein (APP) processing facilitate the Amyloid beta ($A\beta$) production that plays a vital role in AD pathogenesis (Wang et al., 2017). APP is an integral membrane glycoprotein that undergoes sequential proteolytic cleavage by β - and γ -secretase. Moreover, genomic duplication and mutations in APP can lead to alteration in its function and consequent $A\beta$ metabolism (Dong et al., 2012).

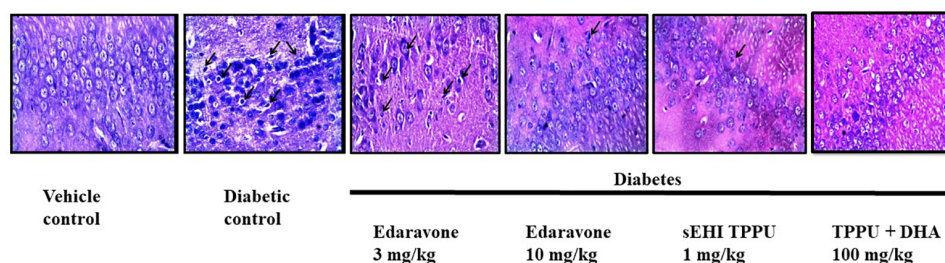


FIGURE 6 | Edaravone, TPPU, and TPPU + DHA protect the pyramidal neurons in diabetes. In addition to quantifying the level of APP, we used H&E staining to study the histology of hippocampus. In comparison to healthy rats, pyramidal neurons in the hippocampus of diabetic rats were less in number, irregularly arranged and damaged which are characterized by pyknotic and indistinct nuclei. Treatment with a low dose of edaravone i.e., 3 mg/kg did not protect pyramidal neurons, but a high dose of edaravone i.e., 10 mg/kg protected the pyramidal neurons. As expected, the protection offered by TPPU was lesser than the combination of TPPU + DHA. N = 6 in each group. The images are presented as 400 \times .

According to amyloid cascade hypothesis, the accumulation of A β peptide is the primary and sole event leading to the formation of senile plaques, then neurofibrillary tangles (NFTs), cell death, and eventually dementia (Armstrong, 2011). Senile plaques and NFTs are highly insoluble protein accumulations. A β triggers the conversion of tau from a normal to a toxic state. However, some pieces of evidence also show that toxic tau enhances A β toxicity via a feedback loop (Bloom, 2014). A β at normal physiological condition plays putative roles such as promoting recovery from injury, protecting the body from infections, regulating synaptic function (Brothers et al., 2018). But, A β acts as an initiator of progression of AD due to its overproduction or disturbed clearance, accumulation and aggregation (Sun et al., 2015). Tau is the microtubule-associated protein that regulates the assembly and structural stability of microtubules contributing to the proper function of the neuron. In AD, due to the hyperphosphorylation of tau it gets disassembles from microtubule and eventually, free tau gets to assemble and aggregates into paired helical filaments (Medeiros et al., 2011; Kolarova et al., 2012). The soluble forms of A β and tau peptides work together and independently accumulate into senile plaques and NFTs to produce neurodegeneration and synaptic loss (Bloom, 2014). Increase in A β 40 and A β 42 level has been found in the pathogenesis of AD (Findeis, 2007).

This study evaluated the effect of curative treatment of edaravone, TPPU or TPPU + DHA on diabetes-induced memory dysfunction. The work was conducted using 6-8-week-old male Sprague-Dawley rats supports our previous observation that inhibition of sEH in diabetic rats can protect memory function in 12-week-old male Wistar albino rats (Minaz et al., 2018). In the previous study, the increase in the memory function of diabetic rats was associated with a decrease in the levels of blood sugar after eight weeks of treatment with TPPU (0.1 and 0.3 mg/kg) in comparison to diabetic control rats. The memory functions were assessed by using Barne's maze and step-down test. Here, the memory function was evaluated by using Morris water maze and the novel object recognition test. Although both studies used different methods to assess memory function, we observed preservation of memory with the use of sEH TPPU. In this study, the positive effect of TPPU on memory function was not associated with a decrease in the level of blood sugar which could be due to the shorter duration of treatment, i.e., two weeks. Improvement in memory function independent of the concentration of blood glucose suggests that the sEH inhibitor can exert its positive effect on memory directly by protecting neurons via decreasing inflammation and oxidative stress.

Diabetes-induced impairment of memory is associated with an increase in the oxidative stress (Gella and Durany, 2009; Fawzy Fahim et al., 2018; Minaz et al., 2018; Rahman et al., 2018; Gomaa et al., 2019). Neuronal damage due to reactive oxygen species is known to cause memory dysfunction. Inhibition of sEH is known to reduce oxidative stress in various animal models (Goswami et al., 2016) including in STZ-induced memory dysfunction (Minaz et al., 2018). An increase in the level of MDA and nitrite, as well as a decrease in the levels of GSH, indicates an increase in oxidative stress. The anti-oxidant edaravone decreased the

level of oxidative stress, and this also supports the hypothesis that oxidative stress is involved in diabetes-induced memory dysfunction. As expected, the sEH TPPU decreased oxidative stress, and DHA potentiated the effect of TPPU presumably by the preservation of and an increase in epoxy-fatty acids such as the 19, 20-EDP from DHA.

Apart from oxidative stress, inflammation also induces neuronal damage (Aktas et al., 2007). Inflammation is also prominent in diabetes-associated memory impairment and cognition deficit (Cole et al., 2005; Chu et al., 2018; Tian et al., 2018). The increase in oxidative stress is commonly reported in Alzheimer's disease (Gella and Durany, 2009). We also observed augmentation of inflammation in the brain of diabetic rats characterized by the increase in the levels of IL-1 β and IL-6, but a decrease in the level of IL-10, in comparison to diabetic control rats. Treatment with edaravone or TPPU + DHA decreased the level of IL-6 in diabetic rats. Treatment with TPPU or TPPU + DHA increased the level of IL-10 in diabetic rats.

Association of memory loss with a parallel increase in the expression of APP in the brain of diabetic control mice suggests an association with Alzheimer's disease in the diabetes model. Additionally, with the help of H&E staining, we showed an increase in the level of neuronal damage in diabetic rats, in comparison to healthy control rats. Edaravone (10 mg/kg) or TPPU decreased the level of APP and exerted neuroprotection. This suggests that the neuroprotective effect of TPPU at this dose is mediated by interfering with the expression of APP, in addition to decreasing neuroinflammation (level of IL-6) and oxidative stress (level of nitrite). Preventative treatment with TPPU (0.1–0.3 mg/kg) for eight weeks reduced the level of MDA but increased the level of glutathione in diabetic rats (Minaz et al., 2018). In this study, curative dosing of TPPU (1 mg/kg) did not alter the levels of MDA and GSH. Treatment with TPPU + DHA decreased the expression level of APP and protected against neuronal damage. We observed an increase in the activity of AChE in the hippocampus of diabetic rats in this study, but in our earlier study (Minaz et al., 2018), we have observed a decrease in the activity of AChE. This could be due to the difference in animal strains used (Wistar Albino vs. Sprague-Dawley), glycemic status (300 vs. 400 mg/dl), the age of animals used (3 vs. 1.5–2 months) and insulin supplementation (3 IU/kg s.c. twice a week vs. no supplementation).

Nevertheless, a decrease in the level of ACh (Hu et al., 2018) in the brain and an increase in the level of AChE in the hippocampus are documented in Alzheimer's disease. Further, a reduction in the level of nicotinic receptors, one of the receptors of ACh is noticed in AD patients (Whitehouse et al., 1988; Maelicke and Albuquerque, 2000). Also, a reduction in the secretion of ACh and increase in metabolism by AChE is also implicated in AD (Maelicke and Albuquerque, 2000). Abnormality in choline transport and expression of cholinergic muscarinic receptor is also reported in AD (Terry and Buccafusco, 2003). Interestingly, splice variants of AChE are reported. Synaptic acetylcholinesterase (AChE-S) promotes AD via increasing amyloid fibril formation while "Readthrough" AChE-R protects neurons from A β . Surprisingly, an increase

in the level of AChE-R mRNA and a decrease in the AChE-S mRNA was coupled with a reduction in AChE-R protein suggesting a complex role of AChE in AD (Berson et al., 2008). Treatment with edaravone (10 mg/kg), TPPU or TPPU + DHA decreased the level of AChE in the brain of diabetic rats.

Usefulness of DHA, a ω -3 fatty in various models of Alzheimer's disease are reported (Calon et al., 2004, 2005; Lim et al., 2005; Ma et al., 2007; Kondo et al., 2013). Cole and his associates studied the effect of DHA on Alzheimer's disease. Calon et al. demonstrated that depletion of dietary ω -3 fatty acids in mice overexpressing human Alzheimer's disease gene APP_{swe} (Tg2576) via treatment with safflower oil resulted in the activation of pro-apoptotic caspase-3 and N-methyl-D-aspartate receptor subunits (NR2A and NR2B) in cortex and hippocampus, and decreased the NR1 subunit in the hippocampus in addition to the decrease in the Ca^{2+} /calmodulin-dependent protein kinase (CaMKII) in the cortex of transgenic animals. The adverse effects were minimal in wildtype mice fed with safflower oil. Supplementation of DHA minimized the changes mentioned above in the brain of transgenic mice (Calon et al., 2005).

Further, Lim et al. (2005) demonstrated that DHA rich diet (0.6%) decreased the level of A β in the cortex of Tg2576 mice shown with ELISA. Image analysis using an antibody against A β further showed that a reduction in the level of plaque in the hippocampus and parietal cortex. DHA also decreased APP and its fragments. Kondo et al. (2013) reported that *in vitro* treatment with DHA to induce pluripotent stem cell-derived neurons and astrocytes from AD patients minimized various cell stresses including endoplasmic reticulum stress. Calon et al. (2004) demonstrated that reduction in dietary DHA to Tg2576 mice did not result in loss of neuron but increased caspase-cleaved actin (fractin) which is associated with loss of neuroprotective drebrin that has a role in neuronal growth. Tg2576 mice developed behavioral deficits with DHA depleted diet. Treatment with DHA protected the mouse with a decrease in the level of fractin in the brain and protected against behavioral deficits with a parallel increase in the phosphorylation of Bcl-2-associated death promoter (BAD) which has anti-apoptotic effect unlike BAD (Calon et al., 2004). Ma et al. (2007) reported that DHA increases the level of sortilin related receptor 1 (SORL1 or LR11) which is a receptor for apolipoprotein E and minimizes the neuronal sorting of APP to secretases that generate β -Amyloid (A β). DHA increased the level of LR11 in cultured primary rat neurons, frontal cortex of 22-month C57B6/SJL and APP Tg2576 mice on DHA depleted diet and human neural SH-SY5Y cell lines. In the same study, the researchers showed that treatment with fish oil diet containing DHA and EPA to fructose-fed and insulin resistant 3–4-month-old rats increased the levels of LR11. This study demonstrated a mechanism of how DHA might regulate the level of A β because the level of LR11 is reported to be reduced in sporadic AD. Teng et al. (2015) reported that DHA prevents A β aggregation in APP/PS1 transgenic rat model of AD, but also suggested to combine DHA with other medications because DHA still increases less toxic fibrillar A β oligomers.

In a clinical trial, DHA was not able to slow the progression of AD (Quinn et al., 2010), which could be due to oxidation of DHA (Frautschy and Cole, 2011) and production of toxic levels of aldehydes and peroxides. Also, DHA's epoxy metabolite is anti-inflammatory which is metabolized by sEH. Therefore, combining sEH with DHA would be more effective in controlling AD. Provided the published literature on the effect of DHA in AD, we have not included a DHA only group. Instead, according to our hypothesis, we tested if DHA increases the potency of sEH. We observed that DHA + TPPU was more effective than only TPPU in alleviating inflammation and oxidative stress and augmented memory function. Thus, our data support the hypothesis that positive effects resulting from ω -3 supplementation of the diet are due, at least in part, to an increase in the bioactive epoxide metabolites of the ω -3 fatty acids.

Though we were supported by convincing data that sEH inhibitor TPPU ameliorates Alzheimer's-like complications, TPPU should be further evaluated using Alzheimer's disease-specific models. One of the limitations of this study is not evaluating the impact of STZ on the activity of sEH in the brain. Quantification of A β in the brain by western blot analysis and immunohistochemistry could have provided critical information. Documenting the body weight of animals and conducting glucose tolerance test and insulin tolerance test would have provided more insight into the complex biological pathology.

CONCLUSION

In the present study, we demonstrated that sEH alleviates cognitive and memory impairment associated with diabetes-induced Alzheimer-like complication. The positive effect of sEH TPPU on memory was associated with a reduction in oxidative stress and inflammation in the brain with a parallel decrease in the mRNA level of APP and activity of AChE. The DHA potentiated the effect of TPPU. Edaravone at a higher dose also alleviated memory impairment via decreasing oxidative stress and inflammation.

AUTHOR CONTRIBUTIONS

RP, MA, SA, ML, and SG planned the experiments. RP, NB, KG, MA, and SA performed the experiments. RJ and SG analyzed the data. SG, KG, RJ, and BH wrote the manuscript. All the authors reviewed and approved the manuscript.

FUNDING

The research was partly funded by following grants to BH: NIH R01 ES002710 (PI, BH), NIH superfund P42 ES04699 (PI, BH) and NIH counteract U54 NS079202-01 (PI, Lein, P.).

REFERENCES

- Aktas, O., Ullrich, O., Infante-Duarte, C., Nitsch, R., and Zipp, F. (2007). Neuronal damage in brain inflammation. *Arch. Neurol.* 64:185. doi: 10.1001/archneur.64.2.185
- Alzheimer's Disease International (2018). *World Alzheimer Report 2018 - The State of the art of Dementia Research: New frontiers; World Alzheimer Report 2018 - The state of the art of dementia research: New frontiers*. Available at: <https://www.alz.co.uk/research/WorldAlzheimerReport2018.pdf?2> [accessed December 20, 2018].
- Amin, S. N., Younan, S. M., Youssef, M. F., Rashed, L. A., and Mohamady, I. (2013). A histological and functional study on hippocampal formation of normal and diabetic rats. *F1000Research* 2:151. doi: 10.12688/f1000research.2-151.v1
- Apostolatos, A., Song, S., Acosta, S., Peart, M., Watson, J. E., Bickford, P., et al. (2012). Insulin promotes neuronal survival via the alternatively spliced protein kinase C δ II isoform. *J. Biol. Chem.* 287, 9299–9310. doi: 10.1074/jbc.M111.313080
- Armstrong, R. A. (2011). The pathogenesis of Alzheimer's disease: a reevaluation of the amyloid cascade hypothesis. *Int. J. Alzheimers Dis.* 201:630865. doi: 10.4061/2011/630865
- Bakris, G. L., Fonseca, V. A., Sharma, K., and Wright, E. M. (2009). Renal sodium-glucose transport: role in diabetes mellitus and potential clinical implications. *Kidney Int.* 75, 1272–1277. doi: 10.1038/ki.2009.87
- Bancroft, J. D., and Gamble, M. (eds) (2008). *Theory and Practice of Histological Techniques. Version details - Trove*, 6th Edn. Amsterdam: Elsevier.
- Barbagallo, M., and Dominguez, L. J. (2014). Type 2 diabetes mellitus and Alzheimer's disease. *World J. Diabetes* 5:889. doi: 10.4239/wjd.v5.i6.889
- Bedse, G., Di Domenico, F., Serviddio, G., and Cassano, T. (2015). Aberrant insulin signaling in Alzheimer's disease: current knowledge. *Front. Neurosci.* 9:204. doi: 10.3389/fnins.2015.00204
- Berson, A., Knobloch, M., Hanan, M., Diamant, S., Sharoni, M., Schuppli, D., et al. (2008). Changes in readthrough acetylcholinesterase expression modulate amyloid-beta pathology. *Brain* 131, 109–119. doi: 10.1093/brain/awm276
- Bhadri, N., Razdan, R., Goswami, S. K. (2018). Nebivolol, a β -blocker abrogates streptozotocin-induced behavioral, biochemical, and neurophysiological deficit by attenuating oxidative-nitrosative stress: a possible target for the prevention of diabetic neuropathy. *Naunyn. Schmiedeberg's Arch. Pharmacol.* 391, 207–217. doi: 10.1007/s00210-017-1450-8
- Biessels, G. J., van der Heide, L. P., Kamal, A., Bleys, R. L., and Gispen, W. H. (2002). Ageing and diabetes: implications for brain function. *Eur. J. Pharmacol.* 441, 1–14. doi: 10.1016/S0014-2999(02)01486-3
- Bloom, G. S. (2014). Amyloid- β and tau: the trigger and bullet in Alzheimer disease pathogenesis. *JAMA Neurol.* 71, 505–508. doi: 10.1001/jamaneurol.2013.5847
- Brothers, H. M., Gosztyla, M. L., and Robinson, S. R. (2018). The physiological roles of Amyloid- β peptide hint at new ways to treat Alzheimer's disease. *Front. Aging Neurosci.* 10:118. doi: 10.3389/fnagi.2018.00118
- Calon, F., Lim, G. P., Morihara, T., Yang, F., Ubeda, O., Salem, N., et al. (2005). Dietary n-3 polyunsaturated fatty acid depletion activates caspases and decreases NMDA receptors in the brain of a transgenic mouse model of Alzheimer's disease. *Eur. J. Neurosci.* 22, 617–626. doi: 10.1111/j.1460-9568.2005.04253.x
- Calon, F., Lim, G. P., Yang, F., Morihara, T., Teter, B., Ubeda, O., et al. (2004). Docosahexaenoic acid protects from dendritic pathology in an Alzheimer's disease mouse model. *Neuron* 43, 633–645. doi: 10.1016/j.neuron.2004.08.013
- Cansev, M., Wurtman, R. J., Sakamoto, T., and Ulus, I. H. (2008). Oral administration of circulating precursors for membrane phosphatides can promote the synthesis of new brain synapses. *Alzheimers Dement.* 4, S153–S168. doi: 10.1016/j.jalz.2007.10.005
- Carlson, E., Malki, M. L., and Blosser, R. (2005). Exons, introns, and DNA thermodynamics. *Phys. Rev. Lett.* 94:178101. doi: 10.1103/PhysRevLett.94.178101
- Chen, Y.-L., Weng, S.-F., Yang, C.-Y., Wang, J.-J., and Tien, K.-J. (2018). Diabetic ketoacidosis further increases risk of Alzheimer's disease in patients with type 2 diabetes. *Diabetes Res. Clin. Pract.* 147, 55–61. doi: 10.1016/j.diabres.2018.11.013
- Chu, X., Zhou, S., Sun, R., Wang, L., Xing, C., Liang, R., et al. (2018). Chrysophanol relieves cognition deficits and neuronal loss through inhibition of inflammation in diabetic mice. *Neurochem. Res.* 43, 972–983. doi: 10.1007/s11064-018-2503-1
- Cole, G. M., Lim, G. P., Yang, F., Teter, B., Begum, A., Ma, Q., et al. (2005). Prevention of Alzheimer's disease: omega-3 fatty acid and phenolic anti-oxidant interventions. *Neurobiol. Aging* 26, 133–136. doi: 10.1016/j.neurobiolaging.2005.09.005
- Davies, D. C., Horwood, N., Isaacs, S. L., and Mann, D. M. (1992). The effect of age and Alzheimer's disease on pyramidal neuron density in the individual fields of the hippocampal formation. *Acta Neuropathol.* 83, 510–517. doi: 10.1007/BF00310028
- De Felice, F. G., Lourenco, M. V., and Ferreira, S. T. (2014). How does brain insulin resistance develop in Alzheimer's disease? *Alzheimers Dement.* 10, S26–S32. doi: 10.1016/j.jalz.2013.12.004
- Dong, S., Duan, Y., Hu, Y., Zhao, Z., and Zheng, Z. (2012). Advances in the pathogenesis of Alzheimer's disease: a re-evaluation of amyloid cascade hypothesis. *Transl. Neurodegener.* 1:18. doi: 10.1186/2047-9158-1-18
- Ellman, G. L. (1959). Tissue sulfhydryl groups. *Arch. Biochem. Biophys.* 82, 70–77. doi: 10.1016/0003-9861(59)90090-6
- Fawzy Fahim, V., Wadie, W., Shafik, A. N., and Ishak Attallah, M. (2018). Role of simvastatin and insulin in memory protection in a rat model of diabetes mellitus and dementia. *Brain Res. Bull.* 144, 21–27. doi: 10.1016/j.brainresbull.2018.10.012
- Findeis, M. A. (2007). The role of amyloid β peptide 42 in Alzheimer's disease. *Pharmacol. Ther.* 116, 266–286. doi: 10.1016/j.pharmthera.2007.06.006
- Fischer, A. H., Jacobson, K. A., Rose, J., and Zeller, R. (2008). Hematoxylin and eosin staining of tissue and cell sections. *Cold Spring Harb. Protoc.* 2008:db.rot4986. doi: 10.1101/pdb.prot4986
- Frautschy, S. A., and Cole, G. M. (2011). What was lost in translation in the DHA trial is whom you should intend to treat. *Alzheimers Res. Ther.* 3:2. doi: 10.1186/alzrt61
- Gadhavi, K., Bolshette, N., Ahire, A., Pardeshi, R., Thakur, K., Trandafir, C., et al. (2016). The ubiquitin proteasomal system: a potential target for the management of Alzheimer's disease. *J. Cell. Mol. Med.* 20, 1392–1407. doi: 10.1111/jcmm.12817
- Garwood, C. J., Ratcliffe, L. E., Morgan, S. V., Simpson, J. E., Owens, H., Vazquez-Villaseñor, I., et al. (2015). Insulin and IGF1 signalling pathways in human astrocytes in vitro and in vivo; characterisation, subcellular localisation and modulation of the receptors. *Mol. Brain* 8:51. doi: 10.1186/s13041-015-0138-6
- Gella, A., and Durany, N. (2009). Oxidative stress in Alzheimer disease. *Cell Adh. Migr.* 3, 88–93. doi: 10.4161/cam.3.1.7402
- Gispen, W. H., and Biessels, G.-J. (2000). Cognition and synaptic plasticity in diabetes mellitus. *Trends Neurosci.* 23, 542–549. doi: 10.1016/S0166-2236(00)01656-8
- Gomaa, A. A., Makboul, R. M., Al-Mokhtar, M. A., and Nicola, M. A. (2019). Polyphenol-rich Boswellia serrata gum prevents cognitive impairment and insulin resistance of diabetic rats through inhibition of GSK3 β activity, oxidative stress and pro-inflammatory cytokines. *Biomed. Pharmacother.* 109, 281–292. doi: 10.1016/j.biopha.2018.10.056
- Goswami, S. K., Rand, A. A., Wan, D., Yang, J., Inceoglu, B., Thomas, M., et al. (2017). Pharmacological inhibition of soluble epoxide hydrolase or genetic deletion reduces diclofenac-induced gastric ulcers. *Life Sci.* 180, 114–122. doi: 10.1016/j.lfs.2017.05.018
- Goswami, S. K., Wan, D., Yang, J., Trindade da Silva, C. A., Morisseau, C., Kodani, S. D., et al. (2016). Anti-Ulcer efficacy of soluble epoxide hydrolase inhibitor TPPU on diclofenac-induced intestinal ulcers. *J. Pharmacol. Exp. Ther.* 357, 529–536. doi: 10.1124/jpet.116.232108
- Green, L. C., Wagner, D. A., Glogowski, J., Skipper, P. L., Wishnok, J. S., and Tannenbaum, S. R. (1982). Analysis of nitrate, nitrite, and [15N]nitrate in biological fluids. *Anal. Biochem.* 126, 131–138. doi: 10.1016/0003-2697(82)90118-X
- Gregor, M. F., and Hotamisligil, G. S. (2011). Inflammatory mechanisms in obesity. *Annu. Rev. Immunol.* 29, 415–445. doi: 10.1146/annurev-immunol-031210-101322
- Henriksen, E. J., Diamond-Stanic, M. K., and Marchionne, E. M. (2011). Oxidative stress and the etiology of insulin resistance and type 2 diabetes. *Free Radic. Biol. Med.* 51, 993–999. doi: 10.1016/j.freeradbiomed.2010.12.005

- Hu, X., Teng, S., He, J., Sun, X., Du, M., Kou, L., et al. (2018). Pharmacological basis for application of scutellarin in Alzheimer's disease: antioxidation and antiapoptosis. *Mol. Med. Rep.* 18, 4289–4296. doi: 10.3892/mmr.2018.9482
- Islam, O., Patil, P., Goswami, S. K., Razdan, R., Inamdar, M. N., Rizwan, M., et al. (2017). Inhibitors of soluble epoxide hydrolase minimize ischemia-reperfusion-induced cardiac damage in normal, hypertensive, and diabetic rats. *Cardiovasc. Ther.* 35:e12259. doi: 10.1111/1755-5922.12259
- Kim, A. C., Lim, S., and Kim, Y. K. (2018). Metal Ion Effects on A β and Tau Aggregation. *Int. J. Mol. Sci.* 19:128. doi: 10.3390/ijms19010128
- King, M. R., Anderson, N. J., Liu, C., Law, E., Cundiff, M., Mixcoatl-Zecuatl, T. M., et al. (2015). Activation of the insulin-signaling pathway in sciatic nerve and hippocampus of type 1 diabetic rats. *Neuroscience* 303, 220–228. doi: 10.1016/j.neuroscience.2015.06.060
- Kolarova, M., Garcia-Sierra, F., Bartos, A., Ricny, J., and Ripova, D. (2012). Structure and pathology of tau protein in Alzheimer Disease. *Int. J. Alzheimers Dis.* 2012, 1–13. doi: 10.1155/2012/731526
- Kondo, T., Asai, M., Tsukita, K., Kutoku, Y., Ohsawa, Y., Sunada, Y., et al. (2013). Modeling Alzheimer's disease with iPSCs reveals stress phenotypes associated with intracellular A β and differential drug responsiveness. *Cell Stem Cell* 12, 487–496. doi: 10.1016/j.stem.2013.01.009
- Lim, G. P., Calon, F., Morihara, T., Yang, F., Teter, B., Ubeda, O., et al. (2005). A diet enriched with the omega-3 fatty acid docosahexaenoic acid reduces amyloid burden in an aged Alzheimer mouse model. *J. Neurosci.* 25, 3032–3040. doi: 10.1523/JNEUROSCI.4225-04.2005
- Ma, Q.-L., Teter, B., Ubeda, O. J., Morihara, T., Dhoot, D., Nyby, M. D., et al. (2007). Omega-3 fatty acid docosahexaenoic acid increases SorLA/LR11, a sorting protein with reduced expression in sporadic Alzheimer's disease (AD): relevance to AD prevention. *J. Neurosci.* 27, 14299–14307. doi: 10.1523/JNEUROSCI.3593-07.2007
- Maelicke, A., and Albuquerque, E. X. (2000). Allosteric modulation of nicotinic acetylcholine receptors as a treatment strategy for Alzheimer's disease. *Eur. J. Pharmacol.* 393, 165–170. doi: 10.1016/S0014-2999(00)00093-5
- Medeiros, R., Baglietto-Vargas, D., and LaFerla, F. M. (2011). The Role of Tau in Alzheimer's Disease and Related Disorders. *CNS Neurosci. Ther.* 17, 514–524. doi: 10.1111/j.1755-5949.2010.00177.x
- Meneilly, G. S., and Tessier, D. M. (2016). Diabetes, Dementia and Hypoglycemia. *Can. J. Diabetes* 40, 73–76. doi: 10.1016/j.cjcd.2015.09.006
- Minaz, N., Razdan, R., Hammock, B. D., and Goswami, S. K. (2018). An inhibitor of soluble epoxide hydrolase ameliorates diabetes-induced learning and memory impairment in rats. *Prostaglandins Other Lipid Mediat.* 136, 84–89. doi: 10.1016/j.prostaglandins.2018.05.004
- Morales-Corraliza, J., Wong, H., Mazzella, M. J., Che, S., Lee, S. H., Petkova, E., et al. (2016). Brain-wide insulin resistance, tau phosphorylation changes, and hippocampal neprilysin and amyloid- β alterations in a monkey model of type 1 diabetes. *J. Neurosci.* 36, 4248–4258. doi: 10.1523/JNEUROSCI.4640-14.2016
- Morisseau, C., and Hammock, B. D. (2013). Impact of soluble epoxide hydrolase and epoxyeicosanoids on human health. *Annu. Rev. Pharmacol. Toxicol.* 53, 37–58. doi: 10.1146/annurev-pharmtox-011112-140244
- Nelson, J. W., Young, J. M., Borkar, R. N., Woltjer, R. L., Quinn, J. F., Silbert, L. C., et al. (2014). Role of soluble epoxide hydrolase in age-related vascular cognitive decline. *Prostaglandins Other Lipid Mediat.* 11, 30–37. doi: 10.1016/j.prostaglandins.2014.09.003
- Ohkawa, H., Ohishi, N., and Yagi, K. (1979). Assay for lipid peroxides in animal tissues by thiobarbituric acid reaction. *Anal. Biochem.* 95, 351–358. doi: 10.1016/0003-2697(79)90738-3
- Ouwens, D. M., van Duinkerken, E., Schoonenboom, S. N. M., Herzfeld de Wiza, D., Klein, M., van Golen, L., et al. (2014). Cerebrospinal fluid levels of Alzheimer's disease biomarkers in middle-aged patients with type 1 diabetes. *Diabetologia* 57, 2208–2214. doi: 10.1007/s00125-014-3333-6
- Pappas, C., Small, B. J., Andel, R., Laczó, J., Parizkova, M., Ondrej, L., et al. (2018). Blood glucose levels may exacerbate executive function deficits in older adults with cognitive impairment. *J. Alzheimers Dis.* 67, 81–89. doi: 10.3233/JAD-180693
- Pardeshi, R., Bolshette, N., Gadhav, K., Ahire, A., Ahmed, S., Cassano, T., et al. (2017). Insulin signaling: an opportunistic target to minimize the risk of Alzheimer's disease. *Psychoneuroendocrinology* 83, 159–171. doi: 10.1016/j.psyneuen.2017.05.004
- Peraza, L. R., Colloby, S. J., Deboys, L., O'Brien, J. T., Kaiser, M., and Taylor, J.-P. (2016). Regional functional synchronizations in dementia with Lewy bodies and Alzheimer's disease. *Int. psychogeriatr.* 28, 1143–1151. doi: 10.1017/S1041610216000429
- Poli, G., Corda, E., Martino, P. A., Dall'ara, P., Bareggi, S. R., Bondiolotti, G., et al. (2013). Therapeutic activity of inhibition of the soluble epoxide hydrolase in a mouse model of scrapie. *Life Sci.* 92, 1145–1150. doi: 10.1016/j.lfs.2013.04.014
- Quinn, J. F., Raman, R., Thomas, R. G., Yurko-Mauro, K., Nelson, E. B., Van Dyck, C., et al. (2010). Docosahexaenoic acid supplementation and cognitive decline in Alzheimer Disease. *JAMA* 304:1903. doi: 10.1001/jama.2010.1510
- Rahman, S. O., Panda, B. P., Parvez, S., Kaundal, M., Hussain, S., Akhtar, M., et al. (2018). Neuroprotective role of astaxanthin in hippocampal insulin resistance induced by A β peptides in animal model of Alzheimer's disease. *Biomed. Pharmacother.* 110, 47–58. doi: 10.1016/j.biopha.2018.11.043
- Rdzak, G. M., and Abdelghany, O. (2014). Does insulin therapy for type 1 diabetes mellitus protect against Alzheimer's disease? *Pharmacotherapy* 34, 1317–1323. doi: 10.1002/phar.1494
- Reeta, K. H., Singh, D., and Gupta, Y. K. (2017). Edaravone attenuates intracerebroventricular streptozotocin-induced cognitive impairment in rats. *Eur. J. Neurosci.* 45, 987–997. doi: 10.1111/ejn.13543
- Rose, T. E., Morisseau, C., Liu, J.-Y., Inceoglu, B., Jones, P. D., Sanborn, J. R., et al. (2010). 1-Aryl-3-(1-acylpiperidin-4-yl)urea inhibitors of human and murine soluble epoxide hydrolase: structure-activity relationships, pharmacokinetics, and reduction of inflammatory pain. *J. Med. Chem.* 53, 7067–7075. doi: 10.1021/jm100691c
- Sato, N., and Morishita, R. (2015). The roles of lipid and glucose metabolism in modulation of β -amyloid, tau, and neurodegeneration in the pathogenesis of Alzheimer disease. *Front. Aging Neurosci.* 7:199. doi: 10.3389/fnagi.2015.00199
- Singla, N., and Dhawan, D. K. (2017). Zinc improves cognitive and neuronal dysfunction during aluminium-induced neurodegeneration. *Mol. Neurobiol.* 54, 406–422. doi: 10.1007/s12035-015-9653-9
- Sugasini, D., Thomas, R., Yalagala, P. C. R., Tai, L. M., and Subbaiah, P. V. (2017). Dietary docosahexaenoic acid (DHA) as lysophosphatidylcholine, but not as free acid, enriches brain DHA and improves memory in adult mice. *Sci. Rep.* 7:11263. doi: 10.1038/s41598-017-11766-0
- Sun, X., Chen, W.-D., and Wang, Y.-D. (2015). β -Amyloid: the key peptide in the pathogenesis of Alzheimer's disease. *Front. Pharmacol.* 6:221. doi: 10.3389/fphar.2015.00221
- Takeuchi, S., Ueda, N., Suzuki, K., Shimozawa, N., Yasutomi, Y., and Kimura, N. (2018). Elevated membrane cholesterol disrupts lysosomal degradation to induce A β accumulation: the potential mechanism underlying augmentation of A β pathology by type 2 diabetes mellitus. *Am. J. Pathol.* 189, 391–404. doi: 10.1016/j.ajpath.2018.10.011
- Teng, E., Taylor, K., Bilousova, T., Weiland, D., Pham, T., Zuo, X., et al. (2015). Dietary DHA supplementation in an APP/PS1 transgenic rat model of AD reduces behavioral and A β pathology and modulates A β oligomerization. *Neurobiol. Dis.* 82, 552–560. doi: 10.1016/j.nbd.2015.09.002
- Terry, A. V., and Buccafusco, J. J. (2003). The cholinergic hypothesis of age and Alzheimer's disease-related cognitive deficits: recent challenges and their implications for novel drug development. *J. Pharmacol. Exp. Ther.* 306, 821–827. doi: 10.1124/jpet.102.041616
- Tian, S., Huang, R., Han, J., Cai, R., Guo, D., Lin, H., et al. (2018). Increased plasma Interleukin-1 β level is associated with memory deficits in type 2 diabetic patients with mild cognitive impairment. *Psychoneuroendocrinology* 96, 148–154. doi: 10.1016/j.psyneuen.2018.06.014
- Ulu, A., Harris, T. R., Morisseau, C., Miyabe, C., Inoue, H., Schuster, G., et al. (2013). Anti-inflammatory effects of ω -3 polyunsaturated fatty acids and soluble epoxide hydrolase inhibitors in angiotensin-II-dependent hypertension. *J. Cardiovasc. Pharmacol.* 62, 285–297. doi: 10.1097/FJC.0b013e318298e460
- Ulu, A., Stephen Lee, K. S., Miyabe, C., Yang, J., Hammock, B. G., Dong, H., et al. (2014). An omega-3 epoxide of docosahexaenoic acid lowers blood pressure in angiotensin-II-dependent hypertension. *J. Cardiovasc. Pharmacol.* 64, 87–99. doi: 10.1097/FJC.0000000000000094
- Vorhees, C. V., and Williams, M. T. (2006). Morris water maze: procedures for assessing spatial and related forms of learning and memory. *Nat. Protoc.* 1, 848–858. doi: 10.1038/nprot.2006.116

- Wang, X., Zhou, X., Li, G., Zhang, Y., Wu, Y., and Song, W. (2017). Modifications and Trafficking of APP in the Pathogenesis of Alzheimer's Disease. *Front. Mol. Neurosci.* 10:294. doi: 10.3389/fnmol.2017.00294
- Watanabe, T., Tahara, M., and Todo, S. (2008). The novel antioxidant edaravone: from bench to bedside. *Cardiovasc. Ther.* 26, 101–114. doi: 10.1111/j.1527-3466.2008.00041.x
- Waterborg, J. H., and Matthews, H. R. (1984). "The lowry method for protein quantitation," in *Proteins*, ed. J. M. Walker (New Jersey, NJ: Humana Press), 1–4.
- Whitehouse, P. J., Martino, A. M., Wagster, M. V., Price, D. L., Mayeux, R., Atack, J. R., et al. (1988). Reductions in [³H]nicotinic acetylcholine binding in Alzheimer's disease and Parkinson's disease: an autoradiographic study. *Neurology* 38, 720–723. doi: 10.1212/WNL.38.5.720
- Willette, A. A., Bendlin, B. B., Starks, E. J., Birdsill, A. C., Johnson, S. C., Christian, B. T., et al. (2015). Association of insulin resistance with cerebral glucose uptake in late middle-aged adults at risk for Alzheimer disease. *JAMA Neurol.* 72, 1013–1020. doi: 10.1001/jamaneurol.2015.0613
- Yashkin, A. P., Akushevich, I., Ukraintseva, S., and Yashin, A. (2018). The effect of adherence to screening guidelines on the risk of Alzheimer's disease in elderly individuals newly diagnosed with type 2 diabetes mellitus. *Gerontol. Geriatr. Med.* 4:2333721418811201. doi: 10.1177/2333721418811201
- Zhao, W.-Q., and Townsend, M. (2009). Insulin resistance and amyloidogenesis as common molecular foundation for type 2 diabetes and Alzheimer's disease. *Biochim. Biophys. Acta* 1792, 482–496. doi: 10.1016/j.bbadis.2008.10.014
- Zhou, S., Yu, G., Chi, L., Zhu, J., Zhang, W., Zhang, Y., et al. (2013). Neuroprotective effects of edaravone on cognitive deficit, oxidative stress and tau hyperphosphorylation induced by intracerebroventricular streptozotocin in rats. *Neurotoxicology* 38, 136–145. doi: 10.1016/j.neuro.2013.07.007

Conflict of Interest Statement: The University of California, Davis holds multiple patents for the use of soluble epoxide hydrolase inhibitors in humans and companion animals. BH founded EicOsis LLC to facilitate the clinical use of soluble epoxide hydrolase inhibitors.

The remaining authors declare that the research was conducted in the absence of any commercial or financial relationships that could be construed as a potential conflict of interest.

Copyright © 2019 Pardeshi, Bolshette, Gadhave, Arfeen, Ahmed, Jamwal, Hammock, Lahkar and Goswami. This is an open-access article distributed under the terms of the Creative Commons Attribution License (CC BY). The use, distribution or reproduction in other forums is permitted, provided the original author(s) and the copyright owner(s) are credited and that the original publication in this journal is cited, in accordance with accepted academic practice. No use, distribution or reproduction is permitted which does not comply with these terms.



In vitro and *in vivo* Metabolism of a Potent Inhibitor of Soluble Epoxide Hydrolase, 1-(1-Propionylpiperidin-4-yl)-3-(4-(trifluoromethoxy)phenyl)urea

Debin Wan¹, Jun Yang¹, Cindy B. McReynolds¹, Bogdan Barnych¹, Karen M. Wagner¹, Christophe Morisseau¹, Sung Hee Hwang¹, Jia Sun^{1,2}, René Blöcher¹ and Bruce D. Hammock^{1*}

OPEN ACCESS

Edited by:

Ali H. Eid,
American University of Beirut,
Lebanon

Reviewed by:

Jang Hoon Kim,
Korea Atomic Energy Research
Institute (KAERI), South Korea
Ayman Ouda El-Kadi,
University of Alberta, Canada
Xie Qishui,
China Pharmaceutical University,
China
Hong Shen,
Roche, Switzerland
Kaijing Zhao,
China Pharmaceutical University,
China

*Correspondence:

Bruce D. Hammock
bdhammock@ucdavis.edu

Specialty section:

This article was submitted to
Translational Pharmacology,
a section of the journal
Frontiers in Pharmacology

Received: 07 February 2019

Accepted: 12 April 2019

Published: 08 May 2019

Citation:

Wan D, Yang J, McReynolds CB, Barnych B, Wagner KM, Morisseau C, Hwang SH, Sun J, Blöcher R and Hammock BD (2019) *In vitro* and *in vivo* Metabolism of a Potent Inhibitor of Soluble Epoxide Hydrolase, 1-(1-Propionylpiperidin-4-yl)-3-(4-(trifluoromethoxy)phenyl)urea. *Front. Pharmacol.* 10:464. doi: 10.3389/fphar.2019.00464

¹ Department of Entomology and Nematology and UC Davis Comprehensive Cancer Center, University of California, Davis, Davis, CA, United States, ² State Forestry Administration Key Open Laboratory, International Center for Bamboo and Rattan, Beijing, China

1-(1-Propionylpiperidin-4-yl)-3-(4-(trifluoromethoxy)phenyl)urea (TPPU) is a potent soluble epoxide hydrolase (sEH) inhibitor that is used extensively in research for modulating inflammation and protecting against hypertension, neuropathic pain, and neurodegeneration. Despite its wide use in various animal disease models, the metabolism of TPPU has not been well-studied. A broader understanding of its metabolism is critical for determining contributions of metabolites to the overall safety and effectiveness of TPPU. Herein, we describe the identification of TPPU metabolites using LC-MS/MS strategies. Four metabolites of TPPU (M1–M4) were identified from rat urine by a sensitive and specific LC-MS/MS method with double precursor ion scans. Their structures were further supported by LC-MS/MS comparison with synthesized standards. Metabolites M1 and M2 were formed from hydroxylation on a propionyl group of TPPU; M3 was formed by amide hydrolysis of the 1-propionylpiperidinyl group on TPPU; and M4 was formed by further oxidation of the hydroxylated metabolite M2. Interestingly, the predicted α -keto amide metabolite and 4-(trifluoromethoxy)aniline (metabolite from urea cleavage) were not detected by the LC-MRM-MS method. This indicates that if formed, the two potential metabolites represent <0.01% of TPPU metabolism. Species differences in the formation of these four identified metabolites was assessed using liver S9 fractions from dog, monkey, rat, mouse, and human. M1, M2, and M3 were generated in liver S9 fractions from all species, and higher amounts of M3 were generated in monkey S9 fractions compared to other species. In addition, rat and human S9 metabolism showed the highest species similarity based on the quantities of each metabolite. The presence of all four metabolites were confirmed *in vivo* in rats over 72-h post single oral dose of TPPU. Urine and feces were major routes for TPPU excretion. M1, M4 and parent drug were detected as major substances, and M2 and M3 were minor substances. In blood, M1 accounted for ~9.6% of the total TPPU-related exposure, while metabolites M2, M3, and M4 accounted for <0.4%. All four metabolites were potent inhibitors of human sEH but were less potent than the parent TPPU. In conclusion, TPPU is metabolized via oxidation and amide hydrolysis without apparent

breakdown of the urea. The aniline metabolites were not observed either *in vitro* or *in vivo*. Our findings increase the confidence in the ability to translate preclinical PK of TPPU in rats to humans and facilitates the potential clinical development of TPPU and other sEH inhibitors.

Keywords: soluble epoxide hydrolase inhibitor, TPPU, drug metabolism, *in vitro*, *in vivo*, LC-MS, precursor ion scan, sEH potency

INTRODUCTION

The soluble epoxide hydrolase (sEH) is responsible for mediating the metabolism of epoxy fatty acids (EpFAs), such as epoxyeicosatrienoic acids (EETs) (Newman et al., 2005; Decker et al., 2009) and is broadly distributed throughout the mammalian body (Enayetallah et al., 2004). sEH hydrolyzes biologically active EpFAs to their less active corresponding vicinal dihydroxy fatty acids. Cytochrome P450-produced EETs from oxidation of arachidonic acid and other EpFAs are important endogenous anti-inflammatory lipid mediators that resolve inflammation in part via modulating NF- κ B signaling (Xu et al., 2006). However, sEH rapidly converts EETs and other EpFAs to their less active dihydroxy-eicosatrienoic acids (DHETs) *in vivo* (Morisseau and Hammock, 2013). Therefore, a series of potent sEH inhibitors containing a *N,N'*-disubstituted urea have been developed to stabilize the EpFA and increase their residence time to exert their beneficial effects.

Recent studies have yielded a better understanding of the role of sEH in regulating the progression of several diseases in preclinical studies (Luria et al., 2011; Imig, 2012, 2015; Wang et al., 2013, 2018; Ren et al., 2018). The inhibition of sEH demonstrates a promising approach to treat various diseases, including hypertension (Imig et al., 2005; Anandan et al., 2011), inflammation (Davis et al., 2011; Bastan et al., 2018), diabetes (Lorthioir et al., 2012; Hu et al., 2017), neuropathic pain (Hammock et al., 2011; McReynolds et al., 2016; Wagner K. et al., 2017; Wagner K. M. et al., 2017), and central nervous system (CNS) disorders (Simpkins et al., 2009; Ren et al., 2016; Zarriello et al., 2018). Growing evidence suggests that EpFAs reduce endoplasmic reticulum stress as a common underlying mechanism for these therapeutic effects (Yu et al., 2015; Inceoglu et al., 2017). In fact, several selective sEH inhibitors such as AR9281 and GSK2256294 have reached clinical trials (Chen et al., 2012; Lazaar et al., 2016). These Phase I clinical trials did not reveal any toxicity limitations for those novel drug candidates to be eventually clinically-approved.

Among the sEH inhibitors optimized for use *in vivo*, 1-(4-(trifluoro-methoxy-phenyl)-3-(1-propionylpiperidin-4-yl) urea (TPPU) is widely used because of its good potency, pharmacokinetics, and biological activity (Rose et al., 2010; Ulu et al., 2012; Liu et al., 2013) without apparent non-specific binding (Lee et al., 2014). It tightly binds to the recombinant human sEH with a low nanomolar K_i (0.9 ± 0.1 nM) and a slow k_{off} (10.5×10^{-4} s $^{-1}$) indicating its high inhibition potency and target occupancy against human sEH (Lee et al., 2014). Therefore, the pharmacological effects of TPPU have been studied extensively in a number of animal models (Qiu

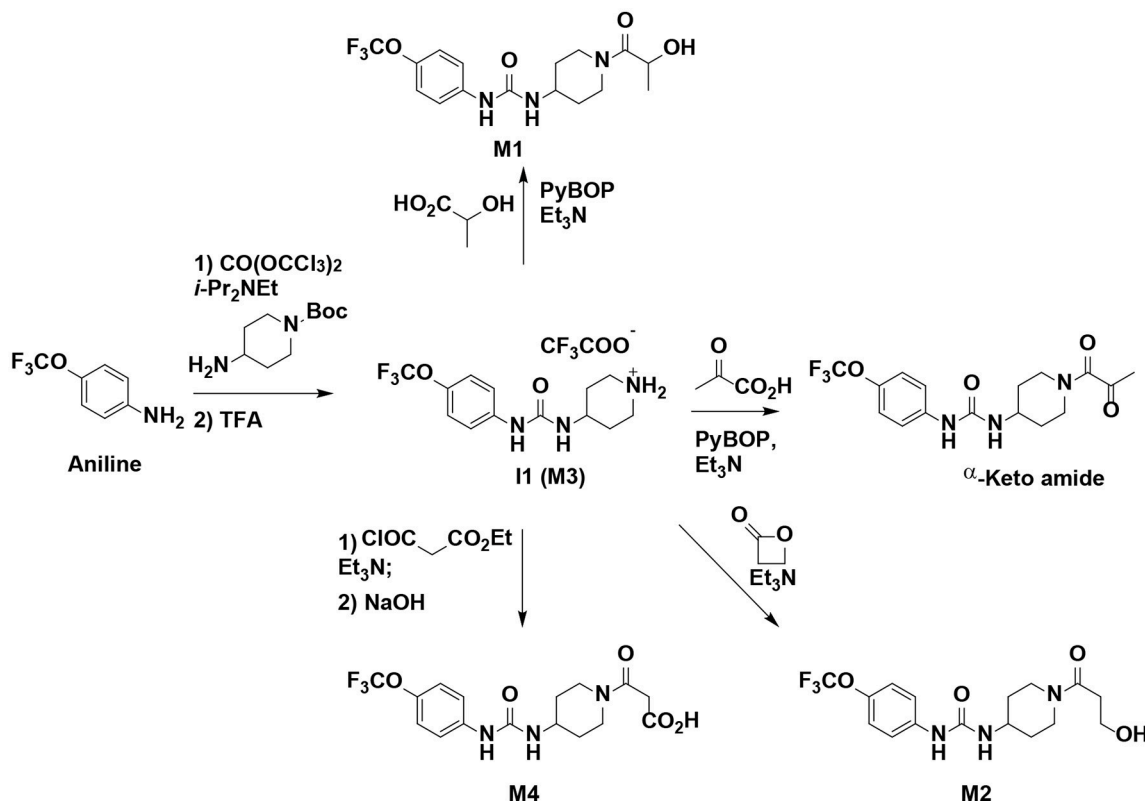
et al., 2011; Shen and Hammock, 2012; Bettaieb et al., 2015; Harris et al., 2015; Goswami et al., 2016; Hashimoto, 2016; Supp et al., 2016; Zhou et al., 2016, 2017; Chen et al., 2017; Wu et al., 2017; Huang et al., 2018; Napimoga et al., 2018; Tu et al., 2018). Notably, TPPU treatment can significantly decrease infarct volume, reduce neurologic deficits and improve sensorimotor function in transient middle cerebral artery occlusion in rats (Tu et al., 2018); reduce 1-methyl-4-phenyl-1,2,3,6-tetrahydropyridine (MPTP) induced neurotoxicity in the mouse striatum (Huang et al., 2018; Ren et al., 2018); and act as a rapid antidepressant in murine depression models (Hashimoto, 2016; Wu et al., 2017). It is also worth mentioning that TPPU both acts synergistically with and reduces the side effects of non-steroidal anti-inflammatory drugs (NSAIDs) (Qiu et al., 2011; Shen and Hammock, 2012). For instance, the severity of gastrointestinal ulcers induced by diclofenac can be prevented by TPPU (Goswami et al., 2016).

Despite its wide use in various animal disease models, the metabolism of TPPU has not been well-studied. The pharmacokinetic profile of TPPU has been investigated in several different species, and it shows high blood levels are achieved *in vivo* and are associated with long half-life of the parent compound (Tsai et al., 2010; Ulu et al., 2012; Liu et al., 2013; Lee et al., 2014). As more studies uncover the potential therapeutic benefits of sEH inhibition, it becomes essential to characterize the metabolism of this sEH inhibitor for determining appropriate dose of TPPU and the contributions of its metabolites to its overall safety and effectiveness. Therefore, we investigated the *in vitro* and *in vivo* metabolism of TPPU.

MATERIALS AND METHODS

Animals and Chemicals

Animal experiments were approved by the Animal Use and Care Committee of University of California, Davis. Male rats (Sprague Dawley, 250–300 g) were purchased from the Charles River Laboratories (CA). Liver S9 fractions from human, monkey, dog, rat, and mouse were purchased from XenoTech, LLC (Lenexa, KS). TPPU and its four metabolites as well as 1-(1-acetylpiperidin-4-yl)-3-(4-(trifluoromethyl)phenyl)urea (TAPU) and 12-(3-cyclohexyl-ureido)-dodecanoic acid (CUDA) were synthesized in house and their syntheses are described in the supplementary material. Reagents for the NADPH regeneration system, including beta-nicotinamide adenine dinucleotide phosphate sodium salt (NADP $^{+}$), D-glucose-6-phosphate dehydrogenase (G6PDH), D-glucose-6-phosphate monosodium salt (G6P), anhydrous magnesium chloride (MgCl $_2$), sodium chloride (NaCl), ethylenediaminetetraacetic acid (EDTA), and



SCHEME 1 | Synthesis of standard metabolites of TPPU.

glacial acetic acids were obtained from Sigma (St. Louis, MO). LC-MS grade water, methanol (MeOH), acetonitrile, ethyl acetate (EA), reagent grade monobasic monohydrate sodium phosphate, and anhydrous dibasic sodium phosphate were purchased from Fisher Scientific (Pittsburgh, PA).

Synthesis of TPPU Metabolites, Scheme 1

The synthesis started with preparation of the common intermediate **compound 1** (**11**) via conventional triphosgene mediated unsymmetrical urea (**M3**) formation between 4-(trifluoromethoxy)aniline and *tert*-butyl 4-aminopiperidine-1-carboxylate followed by deprotection with TFA. **M1** was synthesized in 4.5% yield by treatment of the intermediate **11** with 2-hydroxypropanoic acid and PyBOP in the presence of triethylamine. Acylation of the intermediate **11** with oxetan-2-one produced metabolite **M2**. Acylation of **11** with ethyl malonyl chloride followed by hydrolysis of the ester function provided the last metabolite **M4**. Acylation of **11** with pyruvic acid gave α -keto amide. Starting materials were purchased from one of the following commercial sources: Sigma Aldrich Chemical Co. (Milwaukee, WI), Fisher Scientific (Houston, TX), Eanmine LLC (Monmouth Jct, NJ), Oakwood Chemical (Estill, SC). All reactions were carried out under an atmosphere of dry nitrogen. All chemicals purchased from commercial sources were used as received without further purification. Analytical thin layer chromatography (TLC) was performed on Merck TLC silica

gel 60 F254 plates. Flash chromatography was performed on silica gel (230–400 mesh) from Macherey Nagel. NMR spectra were recorded on Varian VNMRs 600, Inova 400, or Bruker Avance III 800 MHz instruments. Multiplicity is described by the abbreviations b = broad, s = singlet, d = doublet, t = triplet, q = quartet, p = pentet, m = multiplet. Chemical shifts are given in ppm. ^1H NMR spectra are referenced to the residual solvent peak at $\delta = 7.26$ (CDCl_3) or 3.31 (CD_3OD). ^{13}C NMR spectra are referenced to the solvent peak at $\delta = 77.16$ (CDCl_3) or 49.00 (CD_3OD). HRMS spectra were recorded and are presented on Thermo Electron LTQ-Orbitrap XL Hybrid MS in ESI. All synthesized compounds were >95% pure based on NMR and LC-MS data.

tert-butyl 4-(3-(4-(trifluoromethoxy)phenyl)ureido)piperidine-1-carboxylate

A solution of 4-(trifluoromethoxy)aniline (1.77 g, 10 mmol, 1 equiv) and diisopropylethyl amine (1.419 g, 11 mmol, 1.1 equiv) in CH_2Cl_2 (15 mL) was added dropwise to the solution of triphosgene (1.13 g, 3.8 mmol, 0.38 equiv) in CH_2Cl_2 (20 mL) at 0°C . The reaction mixture was stirred for 40 min and then the solution of *tert*-butyl 4-aminopiperidine-1-carboxylate (2 g, 10 mmol, 1 equiv) and diisopropylethyl amine (2.58 g, 20 mmol, 2 equiv) in CH_2Cl_2 (10 mL) was added dropwise. The reaction mixture was stirred overnight, quenched with water/brine (1:1, 30 mL), and few drops of 3 M HCl (until pH \sim 3), and extracted

with CH_2Cl_2 ($3 \times 30 \text{ mL}$). Combined extracts were dried over MgSO_4 , filtered, and evaporated under reduced pressure. Purification of the residue by flash column chromatography ($\text{EtOAc}/\text{hexanes} = 1:1 \rightarrow \text{EtOAc}$) gave pure product as a pale-tan solid (3.22 g, 80 %). ^1H NMR (600 MHz, CDCl_3) δ 7.36 (bs, 1H), 7.33 (d, $J = 9.0 \text{ Hz}$, 2H), 7.11 (d, $J = 8.7 \text{ Hz}$, 2H), 5.30 (bs, 1H), 3.96 (bs, 2H), 3.79 (m, 1H), 2.85 (t, $J = 12.6 \text{ Hz}$, 2H), 1.85 (m, 3H), 1.45 (s, 9H), 1.22 (bs, 2H). ^{13}C NMR (151 MHz, CDCl_3) δ 155.2, 155.0, 144.4, 137.9, 123.2, 122.0, 121.5, 120.4, 119.8, 118.1, 80.4, 47.1, 42.8, 32.8, 28.6.

4-(3-(4-(trifluoromethoxy)phenyl)ureido)piperidin-1-ium 2,2,2-trifluoroacetate **I1**

tert-butyl 4-(3-(4-(trifluoromethoxy)phenyl)ureido)piperidine-1-carboxylate (3.2 g, 7.94 mmol, 1 equiv) was dissolved in the mixture of CH_2Cl_2 (5 mL) and TFA (5 mL) and the resulting mixture was stirred at room temperature for $\sim 3 \text{ h}$ and evaporated. The resulting product was used in the next steps without purification and had amine:TFA ratio of $\sim 1:4.48$.

1-(1-(2-hydroxypropanoyl)piperidin-4-yl)-3-(4-(trifluoromethoxy)phenyl)urea **M1**

A mixture of 4-(3-(4-(trifluoromethoxy)phenyl)ureido)piperidin-1-ium 2,2,2-trifluoroacetate **I1** (423 mg, 0.55 mmol, 1 equiv), 2-hydroxypropanoic acid (76 mg, 0.72 mmol, 1.3 equiv), PyBOP (374 mg, 0.72 mmol, 1.3 equiv), and Et_3N (391 mg, 3.87 mmol, 7 equiv) was stirred at room temperature for 16 h, quenched with water and extracted with EtOAc ($3 \times 15 \text{ mL}$). Combined extracts were dried over MgSO_4 , filtered, and evaporated under reduced pressure. Purification of the residue by flash column chromatography (EtOAc) gave pure product as a pale-tan solid (9.3 mg, 4.5 %). ^1H NMR (600 MHz, CD_3OD) δ 7.44 (d, $J = 8.9 \text{ Hz}$, 2H), 7.15 (d, $J = 8.7 \text{ Hz}$, 2H), 4.60 (q, $J = 6.6 \text{ Hz}$, 1H), 4.47–4.28 (m, 1H), 3.95 (m, 1H), 3.84 (m, 1H), 3.49–3.34 (m, 1H), 3.22 (m, 1H), 3.03–2.84 (m, 1H), 2.06–1.92 (m, 2H), 1.49–1.27 (m, 5H). ^{13}C NMR (151 MHz, CD_3OD) δ 175.93, 175.92, 174.84, 174.62, 174.57, 171.06, 171.04, 157.08, 144.98, 140.04, 124.46, 122.77, 122.62, 121.08, 120.91, 119.40, 70.17, 68.84, 67.66, 67.63, 67.01, 65.82, 65.73, 48.07, 47.98, 47.30, 47.26, 45.05, 44.77, 42.34, 42.15, 33.91, 33.69, 33.10, 32.96, 27.00, 26.95, 24.84, 24.79, 21.11, 20.84, 20.48, 20.14. HRMS (ESI), calculated for $\text{C}_{16}\text{H}_{21}\text{F}_3\text{N}_3\text{O}_4$ ($[\text{M}+\text{H}]^+$) m/z 376.1479, found m/z 376.1481.

1-(1-(3-hydroxypropanoyl)piperidin-4-yl)-3-(4-(trifluoromethoxy)phenyl)urea **M2**

A mixture of 4-(3-(4-(trifluoromethoxy)phenyl)ureido)piperidin-1-ium 2,2,2-trifluoroacetate **I1** (400 mg, 0.52 mmol, 1 equiv), oxetan-2-one (150 mg, 2.09 mmol, 2 equiv), Et_3N (634 mg, 6.27 mmol, 12 equiv) and CH_2Cl_2 (1 mL) was stirred for 4 days and directly chromatographed ($\text{EtOAc} \rightarrow \text{EtOAc}:\text{MeOH} = 99:1 \rightarrow 98:2$) to give pure product as a pale-tan solid (21.9 mg, 11 %). ^1H NMR (600 MHz, CD_3OD) δ 7.44 (d, $J = 9.1 \text{ Hz}$, 2H), 7.15 (d, $J = 8.9 \text{ Hz}$, 2H), 4.41 (d, $J = 13.7 \text{ Hz}$, 1H), 3.96 (d, $J = 13.9 \text{ Hz}$, 1H), 3.83 (t, $J = 6.1 \text{ Hz}$, 2H), 3.82 (m, 1H), 3.25 (ddd, $J = 14.1, 11.4, 2.9 \text{ Hz}$, 1H), 2.91 (t, $J = 11.4 \text{ Hz}$, 1H), 2.64 (m, 2H), 2.01 (m, 1H), 1.95 (m, 1H), 1.46 (m, 1H), 1.38 (m, 1H). ^{13}C NMR (151 MHz, CD_3OD) δ 173.0, 157.2, 145.0, 140.2,

122.8, 122.7, 120.9, 59.3, 48.1, 45.8, 41.8, 33.9, 33.1. HRMS (ESI), calculated for $\text{C}_{16}\text{H}_{20}\text{F}_3\text{N}_3\text{NaO}_4$ ($[\text{M}+\text{Na}]^+$) m/z 398.1298, found m/z 398.1300.

Ethyl 3-oxo-3-(4-(3-(4-(trifluoromethoxy)phenyl)ureido)piperidin-1-yl)propanoate

A solution of ethyl malonyl chloride (89 mg, 0.59 mmol, 1.1 equiv) in CH_2Cl_2 (0.2 mL) was added dropwise to a cooled to 0°C solution of 4-(3-(4-(trifluoromethoxy)phenyl)ureido)piperidin-1-ium 2,2,2-trifluoroacetate **I1** (412 mg, 0.54 mmol, 1 equiv) and Et_3N (326 mg, 3.23 mmol, 6 equiv) in CH_2Cl_2 (3 mL). The reaction mixture was stirred at room temperature for 3 h and directly chromatographed ($\text{EtOAc} \rightarrow \text{EtOAc}:\text{MeOH} = 99:1 \rightarrow 98:2$) to give pure product as a pale-tan solid (144 mg, 64%). ^1H NMR (600 MHz, CDCl_3) δ 7.88 (s, 1H), 7.37 (d, $J = 9.0 \text{ Hz}$, 2H), 7.07 (d, $J = 8.7 \text{ Hz}$, 2H), 5.69 (d, $J = 7.6 \text{ Hz}$, 1H), 4.38 (d, $J = 13.2 \text{ Hz}$, 1H), 4.14 (q, $J = 7.1 \text{ Hz}$, 2H), 3.89 (m, 1H), 3.64 (d, $J = 14.7 \text{ Hz}$, 1H), 3.50 (d, $J = 15.7 \text{ Hz}$, 1H), 3.43 (d, $J = 15.7 \text{ Hz}$, 1H), 3.16 (ddd, $J = 14.1, 11.4, 2.8 \text{ Hz}$, 1H), 2.85 (ddd, $J = 14.0, 11.5, 3.0 \text{ Hz}$, 1H), 2.03 (m, 1H), 1.92 (m, 1H), 1.39–1.23 (m, 2H), 1.22 (t, $J = 7.2 \text{ Hz}$, 3H). ^{13}C NMR (151 MHz, CDCl_3) δ 168.0, 165.2, 155.3, 144.0, 138.4, 123.1, 121.8, 121.4, 119.9, 119.7, 118.0, 61.9, 46.5, 45.5, 41.3, 41.2, 33.0, 31.9, 14.1.

3-oxo-3-(4-(3-(4-(trifluoromethoxy)phenyl)ureido)piperidin-1-yl)propanoic acid **M4**

A solution of ethyl 3-oxo-3-(4-(3-(4-(trifluoromethoxy)phenyl)ureido)piperidin-1-yl)propanoate (144 mg, 0.345 mmol, 1 equiv) and NaOH (10 M, 0.345 mL, 3.45 mmol, 10 equiv) in MeOH was stirred at room temperature for 20 h and evaporated. The residue was dissolved in water and acidified to $\text{pH} \sim 3$. The precipitate was filtered and dried under vacuum to give pure product as white solid (105.8 mg, 79%). ^1H NMR (600 MHz, CD_3OD) δ 7.44 (d, $J = 9.0 \text{ Hz}$, 2H), 7.15 (d, $J = 8.6 \text{ Hz}$, 2H), 4.37 (d, $J = 13.3 \text{ Hz}$, 1H), 3.83 (m, 2H), 3.58 (d, $J = 16.3 \text{ Hz}$, 1H), 3.51 (d, $J = 16.2 \text{ Hz}$, 1H), 3.26 (ddd, $J = 14.2, 11.3, 3.0 \text{ Hz}$, 1H), 2.94 (ddd, $J = 13.9, 11.4, 3.1 \text{ Hz}$, 1H), 1.98 (m, 2H), 1.51 (m, 1H), 1.40 (m, 1H). ^{13}C NMR (151 MHz, CD_3OD) δ 171.1, 167.5, 157.1, 145.0, 140.0, 122.8, 122.7, 121.1, 120.9, 47.9, 46.4, 41.9, 41.2, 33.5, 32.8. HRMS (ESI), calculated for $\text{C}_{16}\text{H}_{17}\text{F}_3\text{N}_3\text{O}_5$ ($[\text{M}-\text{H}]^-$) m/z 388.1126, found m/z 388.1094.

1-(1-(2-oxopropanoyl)piperidin-4-yl)-3-(4-(trifluoromethoxy)phenyl)urea α -keto amide

A mixture of 4-(3-(4-(trifluoromethoxy)phenyl)ureido)piperidin-1-ium 2,2,2-trifluoroacetate **I1** (347 mg, 0.45 mmol, 1 equiv), pyruvic acid (52 mg, 0.59 mmol, 1.3 equiv), PyBOP (307 mg, 0.59 mmol, 1.3 equiv), and Et_3N (321 mg, 3.18 mmol, 7 equiv) was stirred at room temperature for 20 h, and directly chromatographed ($\text{EtOAc} \rightarrow \text{EtOAc}:\text{MeOH} = 99:1 \rightarrow 98:2$) to give pure product as a pale-tan solid (71.2 mg, 42%). ^1H NMR (600 MHz, CD_3OD) δ 7.43 (d, $J = 9.0 \text{ Hz}$, 1H), 7.15 (d, $J = 8.8 \text{ Hz}$, 1H), 4.28 (d, $J = 13.5 \text{ Hz}$, 1H), 3.86 (tt, $J = 10.5, 4.1 \text{ Hz}$, 1H), 3.72 (d, $J = 14.0 \text{ Hz}$, 1H), 3.24 (ddt, $J = 14.1, 11.3, 2.3 \text{ Hz}$, 1H), 3.04–2.96 (m, 1H), 2.39 (s, 2H), 2.06–1.94 (m, 1H), 1.54–1.38 (m, 1H). ^{13}C NMR (151 MHz, CD_3OD) δ 200.2, 167.4, 157.0, 145.0, 140.0, 124.5, 122.8, 122.6, 121.1, 120.9, 119.4, 47.8, 45.7, 41.3,

33.7, 32.8, 27.6. HRMS (ESI), calculated for $C_{16}H_{18}F_3N_3NaO_4$ ($[M+Na]^+$) m/z 396.1142, found m/z 396.1160.

In vitro Study

The *in vitro* study of TPPU metabolism was conducted following previous methods as described (Watanabe and Hammock, 2001). Briefly, 1 μ L of TPPU (1 mM in DMSO; $[TPPU]_{final} = 10 \mu M$) was mixed with 94 μ L of diluted liver S9 fractions (final, 0.05 mg protein/mL) from human, monkey, dog, rat, and mouse and incubations were conducted in a 10 mL glass vial. After 5 min preincubation at 37°C, the reaction was initiated by adding 5 μ L of NADPH regeneration solution. The NADPH regeneration solution was prepared by mixing 50 μ L of NADP⁺ (100 mM), 50 μ L of G6P (500 mM), 50 μ L of G6PDH (100 Unit/mL), and 100 μ L of sodium phosphate buffer. Incubation without NADPH regeneration solution was used as control. Reactions were kept for 2 h and terminated by addition of 100 μ L of ice-cold methanol containing CUDA (200 nM) as an internal standard. The mixture was followed by vigorous mixing for 2 min and centrifuging at 10,000*g for 10 min. Each supernatant was transferred to an HPLC vial and kept under 4°C until LC-MS analysis.

In vivo Study

Healthy male rats (Sprague Dawley, $n = 4$) were housed in temperature-controlled housing with *ad libitum* standard chow and drinking water. Each rat received TPPU (dissolved in 0.5 mL PEG400) at a dose of 10 mg/kg by oral gavage in order to generate significant amounts of metabolites while corresponding to previous efficacious concentration doses. Both blood and urine samples were collected. Blood samples (10 μ L) at time points of 0 (before dosing), 0.25, 0.5, 1, 2, 4, 8, 12, 24, 48, and 72 h post dose were collected from the tail vein. Collected blood samples were transferred to Eppendorf tubes containing 90 μ L of EDTA solution (0.1% EDTA and 0.1% acetic acid) and were immediately shaken to avoid blood coagulation. The urine and feces samples were passively collected at the time points of 8, 12, 24, 48, and 72 h post dose. TAPU (10 μ L) of 1 μ M in methanol was added in each blood and urine sample as an internal standard solution. The blood sample extraction was performed with 200 μ L ethyl acetate by liquid-liquid extraction. The representative urine samples were subjected to protein precipitation prior to analysis of TPPU and Phase I metabolites. Briefly, urine (10 μ L) was treated with 50 μ L acetonitrile. After vortex mixing and centrifugation, the supernatant was collected. The feces samples (50–100 mg) were extracted using 600 μ L extraction solution (MeOH: EA = 1:1). The mixtures were kept at –20°C overnight to give efficient extraction of TPPU and its metabolites. On day 2, after vortex mixing and centrifugation, the supernatant was collected. The remaining residue was extracted an additional time with 300 μ L extraction solution, and the supernatant was combined after centrifugation. The collected supernatants were dried using a speed vacuum concentrator and reconstituted in 50 μ L of 100 nM CUDA solution in methanol. In addition, urine (10 μ L) was diluted with water (50 μ L) and then subjected to analysis of glucuronide or sulfate conjugates.

LC-MS/MS Analysis

LC-MS/MS analysis was conducted on an Agilent SL 1200 series LC system (Agilent, Palo Alto, CA) connected to a 4,000 Qtrap mass spectrometer (Applied Biosystems Instrument Corporation, Foster City, CA) with Turbo V ion source. Liquid chromatography was performed on a Kinetex® C18 column (100 \times 2.1 mm, 1.7 μ m). Three μ L solution was injected onto the column held at 45°C for analysis. Mobile phase A and B were water with 0.1% acetic acid and acetonitrile with 0.1% acetic acid, respectively. The LC flow rate was 300 μ L/min. The LC gradient for the *in vivo* study is given in Table S1. For *in vitro* study, non-volatile salts were diverted from the mass spectrometer using condition listed in Table S2.

The mass spectrometer was operated in both negative and positive modes. Ion source parameters were optimized and are listed in Table S3. Three different scan types were employed to perform mass spectrometry analysis, including product ion scan, precursor ion scan (optimized parameters in Table S4) and MRM scan (optimized parameters in Table S5).

sEH Inhibition Potency of TPPU and Its Metabolites

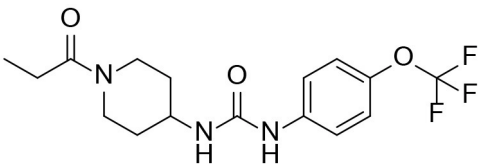
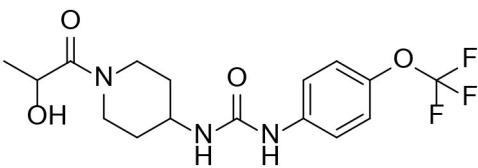
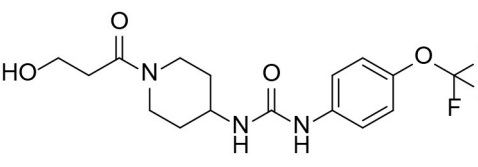
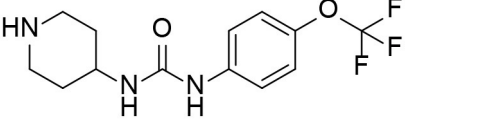
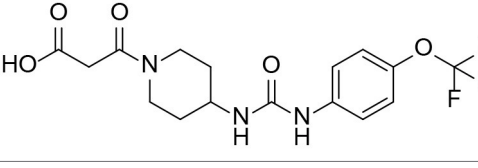
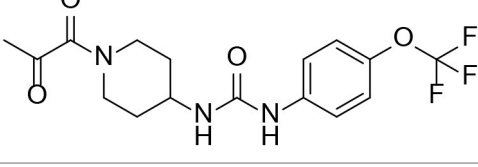
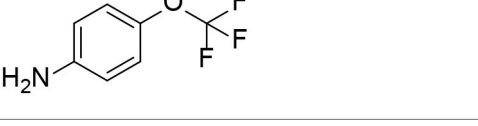
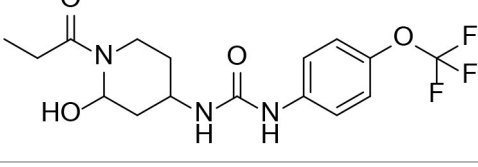
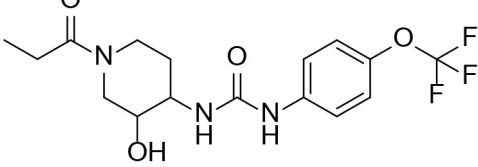
The IC₅₀ is the concentration of a compound that reduces the sEH activity by 50%. This was measured here using cyano(6-methoxynaphthalen-2-yl)methyl ((3-phenyloxiran-2-yl)methyl) carbonate (CMNPC) as substrate (Morisseau et al., 2002). Briefly, recombinant human sEH [1 nM in sodium phosphate buffer (0.1 M, pH = 7.4, 0.1 mg/mL BSA)] was incubated with each analyte ($0.1 < [I]_{final} < 10,000$ nM) at 30°C for 5 min. Then, the reaction was started with the addition to CMNPC ($[S]_{final} = 5 \mu M$). The reaction was monitored kinetically for 10 min at 30°C. The formation of the fluorescent product 6-methoxynaphthaldehyde ($\lambda_{excitation} = 330$ nm, $\lambda_{emission} = 465$ nm, 30°C) was measured every 30 s. IC₅₀ values were determined by regression of the remaining activity in function of the inhibitor concentrations. Assays were run in triplicate and IC₅₀ values are the averages of three replicates.

RESULTS

Identification of Phase I Metabolites of TPPU by LC-MS/MS

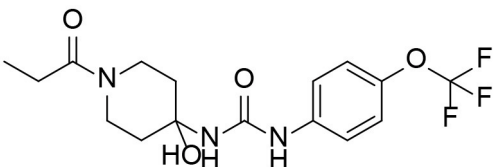
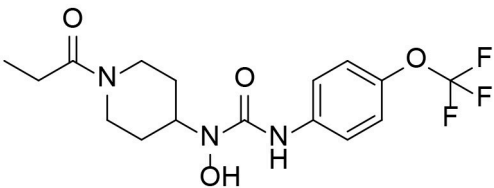
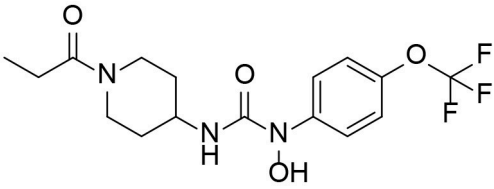
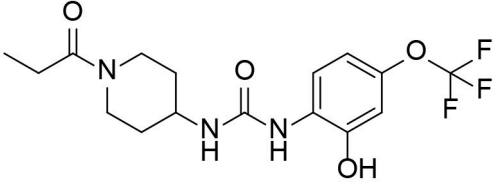
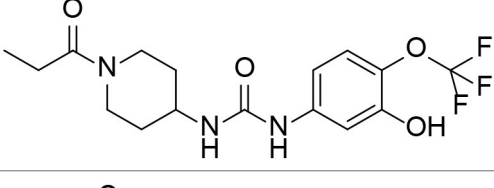
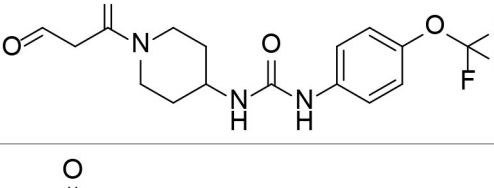
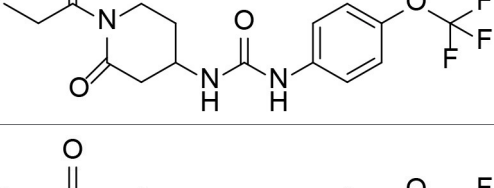
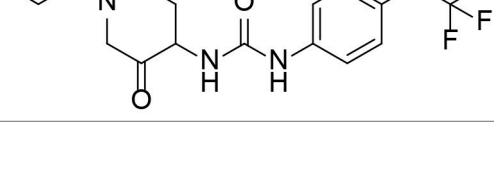
Based on chemical structure and plausible metabolic pathways, we firstly predicted possible metabolites of TPPU (Table 1). There are multiple sites that can be subject to Phase I reactions. For example, oxidation at the carbon center, including both the aliphatic groups and aromatic ring, and oxidation at a nitrogen center can generate hydroxylated TPPU metabolites. M1, M2, and compounds 1–3 are metabolites formed from hydroxylation on aliphatic groups. Compounds 4–5 are potentially formed from hydroxylation on the two nitrogen atoms in the urea. Compounds 6–7 could be formed from hydroxylation on the aromatic ring. These hydroxylated TPPU metabolites can be potentially oxidized further to yield additional TPPU metabolites (M4, α -keto amide, and compounds 8–12). In addition, hydrolysis or oxidation can occur on the amide, and urea groups

TABLE 1 | Predictive TPPU metabolites.

Compound ID	Structure	Available authentic standard
TPPU		+
M1		+
M2		+
M3		+
M4		+
α -Keto amide		+
Aniline		+
1		-
2		-

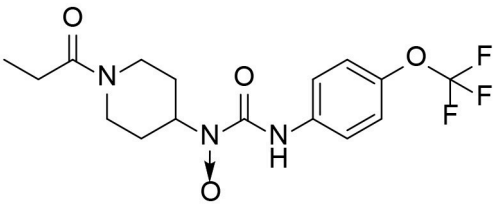
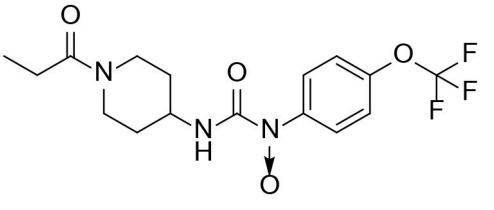
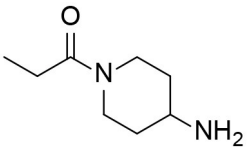
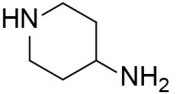
(Continued)

TABLE 1 | Continued

Compound ID	Structure	Available authentic standard
3		-
4		-
5		-
6		-
7		-
8		-
9		-
10		-

(Continued)

TABLE 1 | Continued

Compound ID	Structure	Available authentic standard
11		–
12		–
13		–
14		–

M1–M4 are detectable metabolites. α -Keto amide, aniline, and 1–14 are possible degradation products of TPPU not detected in vitro and in vivo.

⁺Standard available.

[–]Standard not available.

to form additional metabolites. M3 is formed from the amide hydrolysis of the 1-propionylpiperidine residue. The 4-trifluoromethoxy-aniline and compound 13 could result from the urea cleavage. The amide hydrolysis of compound 13 can generate compound 14. Finally, it is likely that TPPU and some of its Phase I metabolites could be conjugated to form their respective Phase II metabolites. In this study, we employed LC-MS/MS methods with assistance of synthetic standard metabolites to identify Phase I metabolites of TPPU. Analysis of Phase II metabolism of TPPU is quite complicated and beyond the scope of this study. As a preliminary study of its possible Phase II metabolites, a neutral loss scan of 176 and precursor ion scan of 97 were used to screen glucuronide and sulfonate-conjugated metabolites in rat urine, respectively. TPPU metabolites in rat feces and urine will be further analyzed after enzymatic hydrolysis and described separately.

Analysis of TPPU Metabolites Formed by Oxidation and Amide Hydrolysis

A good understanding of the fragmentation pattern of TPPU in the tandem mass spectrum is critical for screening and structural identification of the TPPU metabolites. As shown in **Figure 1**, two major dissociation pathways were observed for TPPU in the negative ion mode tandem mass spectrometric analysis of TPPU. TPPU generated one major fragment ion at m/z 176 by

lower-energy collision induced dissociation (CID, 22 eV), which is derived from the urea group cleavage (**Figure 1A**). The other minor fragment ion at m/z 85 appeared at higher-energy collision induced dissociation (CID, 38 eV) and is derived from the C-O bond cleavage on the trifluoromethoxyphenyl group (**Figure 1B**). To support the structural identification of TPPU metabolites, six putative metabolites, M1–M4, α -keto amide metabolite and 4-(trifluoromethoxy)aniline were synthesized and analyzed by LC-MS/MS (**Figure 2** and **Table 2**). In the negative ion mode, the fragment ion at m/z 176 was generated by all five synthetic putative metabolites (M1–M4 and α -keto amide metabolite). Apparently, this fragment ion (m/z 176) is a characteristic fragment that is generated by metabolites containing the 4-(trifluoromethoxy)aniline moiety. Therefore, precursor ion scan for m/z 176 can be used to screen for this kind of TPPU metabolite. The method limit of detection (LOD) is 2 ng/mL. In addition, the fragment ion at m/z 85 (from the trifluoromethoxy) was also generated by these synthetic standards. Presumably, this fragment ion at m/z 85 can be generated by metabolites resulting from oxidation and/or hydrolysis of the amide-function of TPPU regardless of the sites of metabolic conversion. Therefore, precursor ion scan for m/z 85 can unveil a large number of possible TPPU metabolites, such as the ones formed from amide hydrolysis and oxidation at aliphatic groups, aromatic ring, and nitrogen center. On the basis of different ion

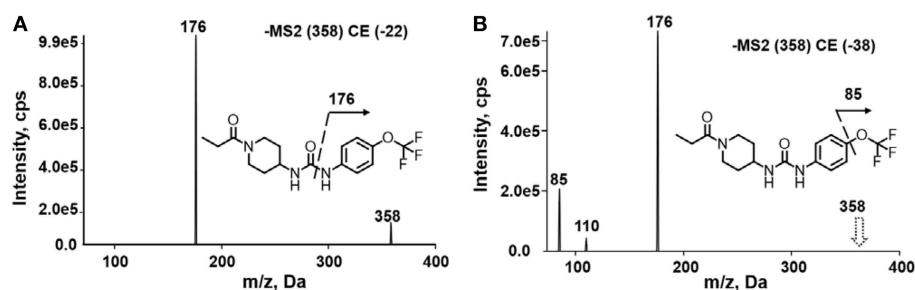


FIGURE 1 | Negative-ion mode ESI tandem mass spectra of TPPU. MS/MS fragmentation was conducted under (A) low and (B) high collision-induced dissociation (CID) energy. The CID energies were optimized to 22 and 38 eV to obtain highest signals of fragment ions at m/z 176 and 85, respectively.

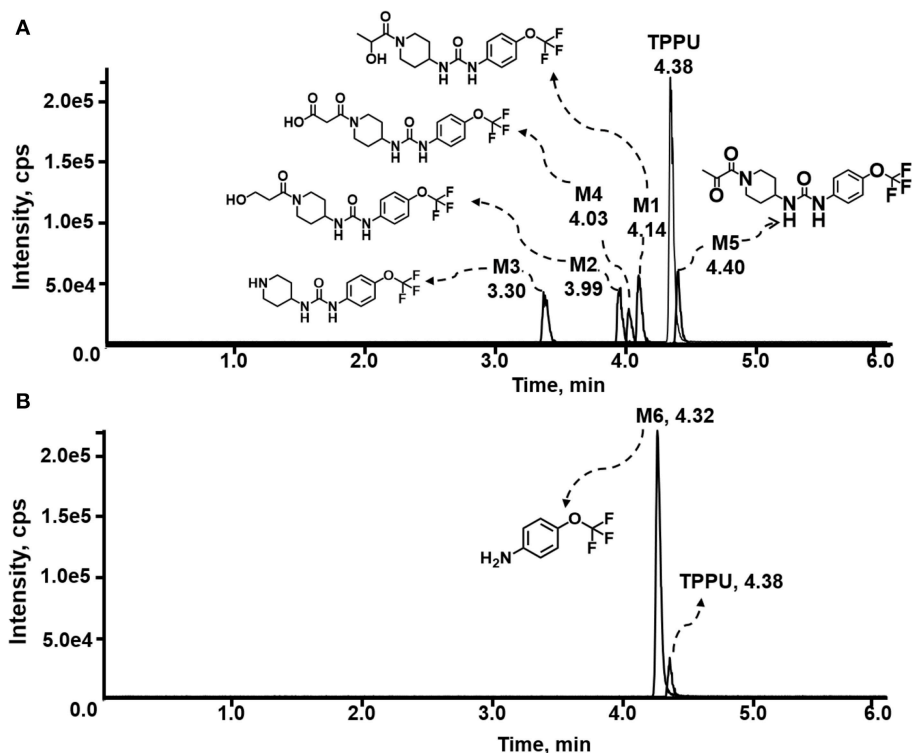


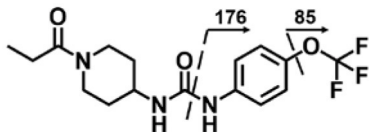
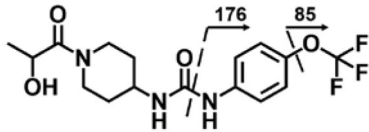
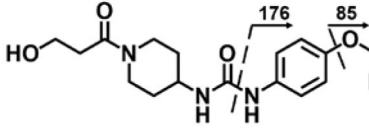
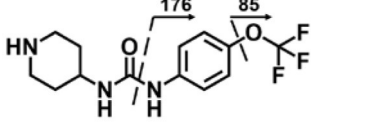
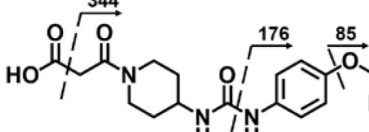
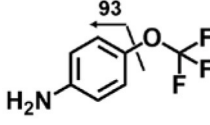
FIGURE 2 | LC-MS/MS analysis of TPPU putative and synthesized metabolites. The mass spectrometric analysis was conducted under both (A) negative and (B) positive ion modes. (A) The chromatogram of TPPU, metabolites M1–M4, and α -keto amide (M5) metabolite. (B) The chromatogram of TPPU and 4-(trifluoromethoxy)aniline (M6).

intensity, the sensitivity of precursor ion scan for m/z 85 was ~ 5 -fold lower than that of precursor ion scan for m/z 176. Therefore, an LC-MS/MS method with double precursor ion scans for both m/z 85 and m/z 176 was performed to screen metabolites, and an LC-MS/MS method with product ion scan was subsequently performed to support the structures of these metabolites.

TPPU could be excreted via different routes, including urine, bile, sweat, saliva, lachrymation, and feces. Because of the relatively small molecular weight and high level of absorption of TPPU, we anticipated that the major routes of its excretion were via urine and feces. Therefore, to identify the major metabolite of TPPU, we investigated which metabolites were detected in

urine samples collected 12 to 48 h after oral dosing. Metabolites in urine were directly analyzed by the LC-MS/MS with precursor ion scan method. As shown in Figures 3A,B, both precursor ion scan spectra for m/z 176 and m/z 85 show four peaks that were eluted earlier than TPPU, and they were M1, M2, M3, and M4, respectively. In Figure 4, TPPU eluted at 4.36 min (Figure 3A) and 4.39 min (Figure 3B) has its deprotonated ion $[M-H]^-$ at m/z 358. Both M1 and M2 (Figures 4A,B) have deprotonated molecular ions at m/z 374 ($358 + 16$) and generate the fragment ion from loss of one molecule of H_2O , suggesting that they are hydroxylated TPPU metabolites. M1 and M2 generate the same major fragment ion at m/z 176 (CID, 22 eV)

TABLE 2 | LC-MS/MS analysis of TPPU and synthetic putative TPPU metabolites.

Meta. ID	RT (min)	Molecular ion (m/z)	Key fragments (m/z)	Fragmentation pattern
TPPU	4.38	358	176, 85	
M1	4.14	374	356, 176, 85	
M2	3.99	374	356, 176, 85	
M3	3.3	302	176, 85	
M4	4.03	388	344, 176, 85	
α -Keto amide (M5)	4.4	372	176, 85	
Aniline (M6)	4.32	178	93	

Fragment ions of TPPU, M1–M4, and α -keto amide metabolite were obtained by product ion scan in negative-ion mode. Fragment ions of aniline was obtained by product ion scan in positive-ion mode.

derived from urea group cleavage (**Figures 4A,B**), indicating that hydroxylation occurred on 1-propionylpiperidinyl moiety of the TPPU molecule. By comparing the retention time of synthetic standard metabolites, M1 and M2 were elucidated to be 1-(1-(2-hydroxypropanoyl)piperidin-4-yl)-3-(4-(trifluoromethoxy)phenyl)urea (**M1**) and 1-(1-(3-hydroxypropanoyl)piperidin-4-yl)-3-(4-(trifluoromethoxy)phenyl)urea (**M2**), respectively. The metabolite at 3.54 min in the precursor ion scan spectrum of m/z 85 (**Figure 3B**) has its protonated molecular ion at m/z 374. In contrast, the metabolite eluted at 3.52 min in the precursor ion scan spectrum of m/z 176 only shows a very small peak (**Figure 3A**), which may indicate probable reaction on 4-(trifluoromethoxy)aniline moiety in

the structure of the metabolite. Because the strong electron withdrawing capabilities of the trifluoromethoxy substitute could deactivate the aromatic ring, the metabolite at 3.54 min in **Figure 3B** is presumably assigned as a metabolite from hydroxylation on nitrogen atom in urea closed to phenyl moiety (compound 5 in **Table 1**). M3 eluted at 3.23 min (**Figures 3A,B**) with its protonated molecular ion at m/z 302 (358–56) generates major fragment ion at m/z 176 and minor fragment ion at m/z 85 in its tandem mass spectrum (**Figure 4C**). These data suggest that 4-(trifluoromethoxy)phenyl moiety remained intact, and based on the molecular mass, M3 was tentatively identified as a metabolite from amide hydrolysis, and the structure elucidated by comparing the retention time, molecular ion peak and MS/MS

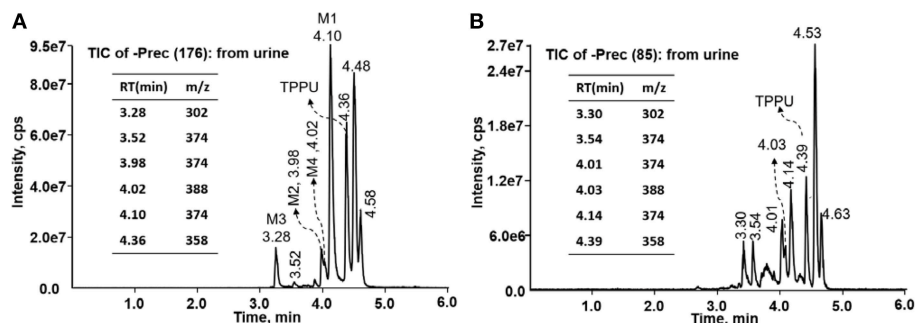


FIGURE 3 | LC-MS precursor ion scan analysis of TPPU and its metabolites in rat urine extract. Metabolites in urine were extracted directly via protein precipitation by addition of acetonitrile. **(A)** Possible TPPU metabolites containing the intact 4-(trifluoromethoxy)aniline moiety in their structures were screened by precursor ion scan for m/z 176. **(B)** TPPU metabolites if formed without urea cleavage were screened by precursor ion scan for m/z 85. Insert: the retention time and corresponding m/z of isolated metabolites.

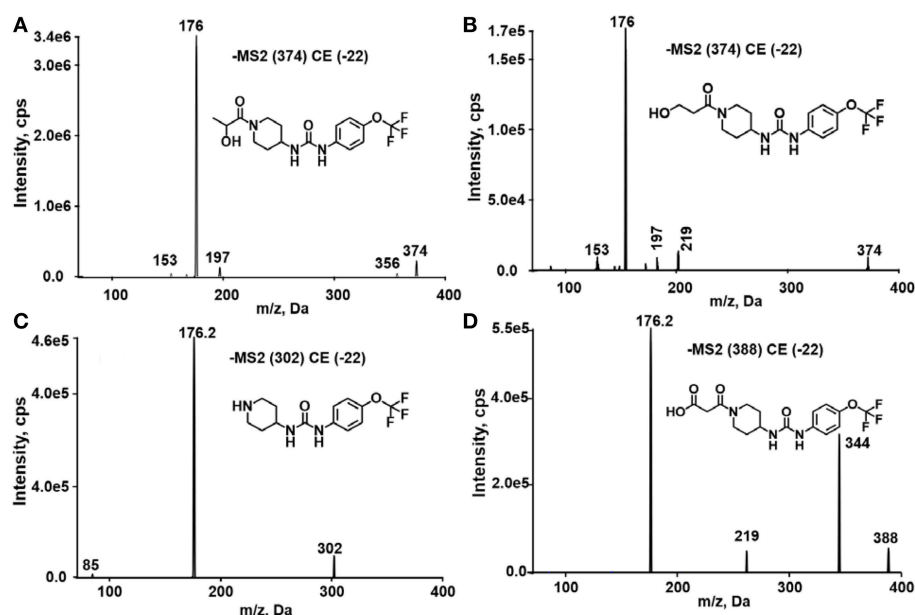


FIGURE 4 | Tandem mass spectrometric analysis of TPPU metabolites eluted in **Figure 3**. **(A)** MS/MS analysis of ion (m/z 374) eluted at 4.1 min. **(B)** MS/MS analysis of ion (m/z 374) eluted at 3.98 min. **(C)** MS/MS analysis of ion (m/z 302) eluted at 3.28 min. **(D)** MS/MS analysis of ion (m/z 388) eluted at 4.02 min.

fragmentation patterns of synthetic standard metabolite to be 1-(piperidin-4-yl)-3-(4-(trifluoromethoxy)phenyl)urea (**M3**). **M4** at 4.02 min in **Figure 3** has its molecular ion peak at m/z 388 ($358 + 30$) (**Figure 4D**). In addition to the major fragment ion at m/z 176, a minor fragment ion at m/z 344 ($388 - 44$) is observed in the tandem mass spectrum of **M4** (**Figure 4D**). The neutral loss of 44 Da is tentatively assigned as the loss of CO_2 , suggesting that there is a carboxyl functional group in **M4**. By comparing the retention time, molecular ion peak and MS/MS fragmentation patterns of the corresponding synthetic standard metabolite, it was confirmed to be 3-oxo-3-(4-(3-(4-(trifluoromethoxy)phenyl)ureido)piperidin-1-yl)propanoic acid (**M4**). Based on the molecular weight shift of 14 Da between **M2** (374) and **M4** (388), most plausibly **M4** is one of the metabolites

formed from further oxidation of the hydroxylated metabolite of TPPU (**M2**). Analysis of the urine revealed the presence of another unknown substance that eluted at 4.48 min (**Figure 3A**) with its molecular ion peak at m/z 388. This could be an unknown metabolite of TPPU. In general, drug metabolism produces more polar and water-soluble metabolites to facilitate their excretion. However, based on its relative elution time, this compound is less polar than the parent TPPU, and thus it is unlikely to be a true metabolite. Nevertheless, further studies are necessary to identify this substance.

To improve sensitivity for detection, a negative LC-MRM-MS method (**Table S5**) was established to identify the putative α -keto amide metabolite (compound 1 in **Table 1**). No peak corresponding to compound 1 was identified in urine extracts,

suggesting that the putative α -keto amide metabolite if formed is lower than the detection limitation (LOD = 0.5 ng/mL).

Analysis of TPPU Metabolites Formed by Urea Cleavage

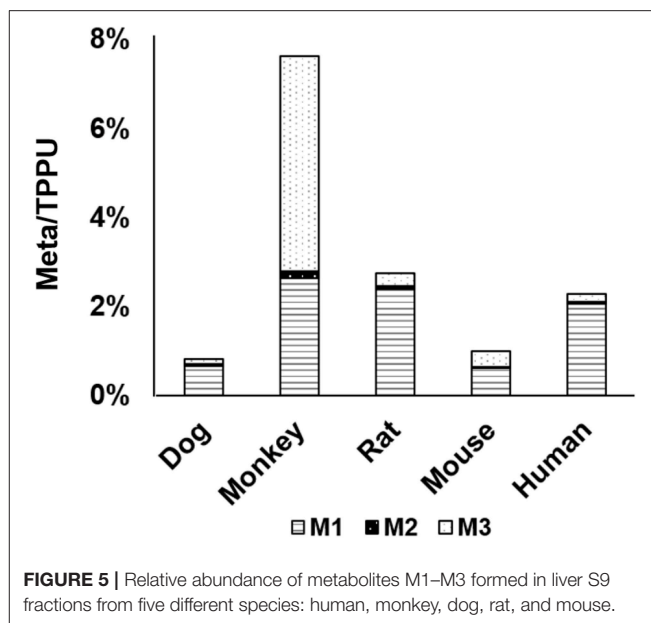
4-(Trifluoromethoxy)aniline is a putative metabolite that can be generated by urea cleavage. Therefore, a positive LC-MRM-MS method (Table S5) was developed for highly sensitive detection of 4-(trifluoromethoxy)aniline. However, there were no peaks corresponding to the expected aniline metabolite found from analysis of rat urine. Therefore, for the putative metabolites, 4-(trifluoromethoxy)aniline, if formed in rat, was either lower than the method detection limitation (0.1 ng/mL) or quickly conjugated to form Phase II metabolites. We further analyzed its presumed conjugates below.

Preliminary Study of Glucuronide Conjugates and Sulfate Conjugates in Urine

Glucuronidation is a primary Phase II metabolic pathway in mammals. Based on the chemical structure, predictive Phase I metabolites by hydroxylation, hydrolysis of amide, and breakdown of urea, as well as the TPPU molecule itself, could be further metabolized to form glucuronide or sulfate conjugates, even though sulfation is usually less extensive than glucuronidation. Biliary excretion of these conjugates can either end up in feces or be recirculated and further metabolized for urinary excretion. To assess the extent of Phase II metabolism, we did a preliminary study to directly analyze possible conjugated metabolites of TPPU by LC-MS methods. However, a detailed analysis of Phase II metabolism of TPPU is beyond the scope of the study, and we will describe it separately. A neutral loss scan for 176 in both positive and negative ion modes (Table S6) was performed with rat urine to detect glucuronide conjugated metabolites of TPPU. In addition, a precursor ion scan for m/z 97 in negative mode (Table S7) was used to detect any possible sulfate conjugates. As a result, we were not able to identify either glucuronide or sulfate conjugates from either TPPU or its Phase I metabolites in rat urine. As reported, the related urea triclocarban (TCC) forms N- and N'-glucuronides (Schebb et al., 2012), however, we specifically searched for these possible metabolites without success. It is likely that Phase II metabolites of TPPU exist, however, we were not able to visualize them using current methods. The presumed formation of Phase II conjugated metabolites in rat feces and urine will be further characterized by enzymatic hydrolysis and acid hydrolysis analysis with separate analysis using authentic standards.

In vitro Metabolism of TPPU: Species Comparisons

After identifying metabolites in rat urine, we determined the interspecies difference in the metabolism of TPPU by *in vitro* incubation with liver S9 fractions. The liver is the primary location for metabolism that drugs are likely to encounter; and therefore, it was informative to test the metabolism of TPPU *in vitro* by using liver S9 fractions. TPPU was incubated using



five liver S9 fractions obtained from different species, namely rat, mouse, dog, monkey, and human. TPPU metabolites M1, M2, and M3 were found in all species tested (Figure 5). However, M4 was not detected in the S9 fractions from any of the species. *In vitro* metabolism of TPPU varied significantly among these five different species. The S9 from monkey liver generated the greatest amount of metabolite M3. This was presumably from amide hydrolysis since it was formed in similar amounts with and without a NADPH generating system (Figure S1). The S9 fractions from rat, mouse, dog, and human generated TPPU metabolites primarily from hydroxylation, and the TPPU metabolites followed the same M1>M3>M2 order. Similar quantities of TPPU metabolites were generated by rat and human liver S9 fractions, indicating high degree of similarity of TPPU metabolism between these two species. Based on the disappearance of TPPU, the order of liver S9 activities for TPPU metabolism appeared to be monkey > rat \approx human > mouse > dog.

In vivo Metabolism of TPPU

Blood concentrations over time of TPPU and its metabolites were further investigated in rats. Consistent with the data obtained in the *in vitro* rat liver S9 studies, metabolite M1 derived from TPPU hydroxylation was the major circulating metabolite in rat blood (Figure 6). In contrast, M2 instead of M3 was found to be the second major metabolite in blood, and the oxidative metabolite (M4) was found both in urine and blood, demonstrating that the metabolite M2 was further oxidized *in vivo*. Other presumable oxidative metabolites, α -keto amide metabolite and 4-(trifluoromethoxy)aniline derived from urea breakdown were not detectable. In addition, no glucuronide and sulfate conjugated metabolites in urine were identified by LC-MS/MS analysis. TPPU was metabolized via phase I reactions, including hydroxylation (M1 and M2), amide

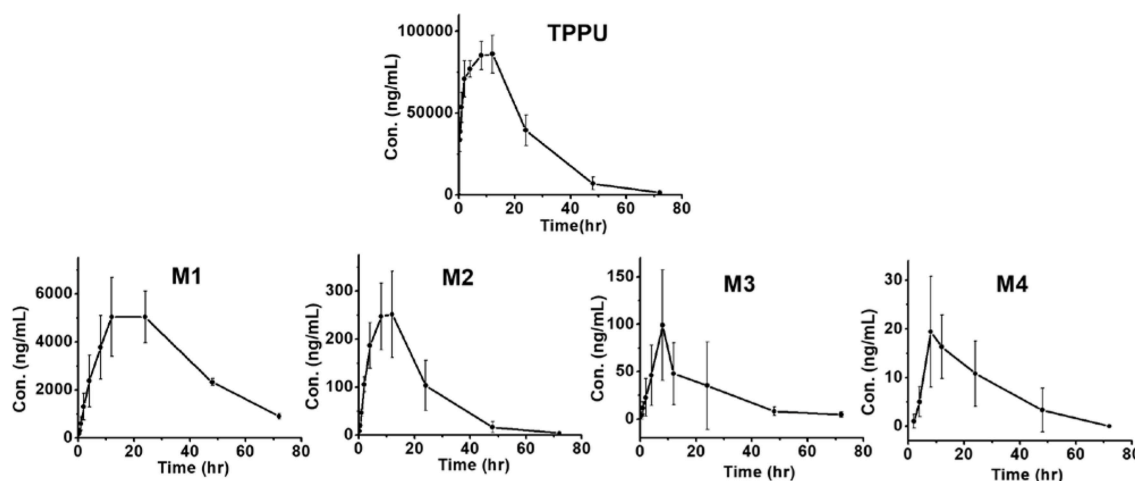


FIGURE 6 | Time course of blood TPPU and its metabolites levels in rat blood following a single oral dose of 10 mg/kg ($n = 4$).

hydrolysis (M3), and oxidation (M4). These results suggest that TPPU is metabolized predominantly via oxidation and secondary via amide hydrolysis. Furthermore, three of these four metabolites rapidly appear in the circulation because they were present 0.25 h in blood after dosage. On the other hand, over 90% the TPPU nucleus in the blood was present as the parent compound (Table 3) indicating either high stability or rapid conjugation and excretion of the more polar metabolites. Then, concentrations of TPPU metabolites as well as unchanged TPPU in both urine and feces were further determined. A large amount of TPPU metabolites (3.4×10^4 ng/mL at C_{max} of 12 h) and unchanged TPPU (5.7×10^3 ng/mL at C_{max} of 8 h) were found in urine (Table S8), while even more metabolites (5.5×10^4 ng/mL at C_{max} of 24 h) and unchanged TPPU (2.4×10^4 ng/mL at C_{max} of 12 h) were found in feces (Table S9). M1, M4 and unchanged TPPU were found to be major substances in urine and feces, shown in Figure 7. M1 was the major metabolite in urine with its C_{max} of 1.2×10^4 ng/mL at 12 h (Figure 7A and Table S8), and unchanged TPPU and M4 were determined to be the major substances in feces with their C_{max} of 2.4×10^4 ng/mL at 12 h and 2.2×10^4 ng/mL at 24 h (Figure 7B and Table S9), respectively. That more M4 than M2 found in both urine and feces further indicates M2 was probably further oxidized to M4 to facilitate its excretion. Based on the comparison of total substances in urine and feces and TPPU in blood, it seems TPPU was majorly eliminated as Phase I metabolites and parent drug via urine and feces. In general, ω - and ω -1 aliphatic hydroxylation is anticipated to be far more rapid than aromatic hydroxylation, because the strong electron withdrawing by the trifluoromethoxy substitute deactivated the aromatic ring.

The Potencies of TPPU and Its Metabolites

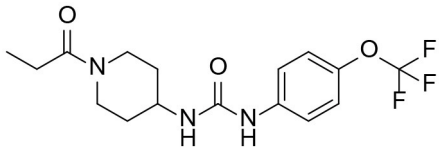
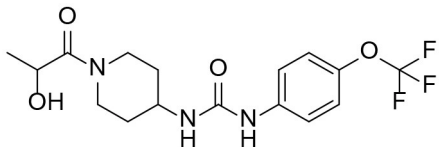
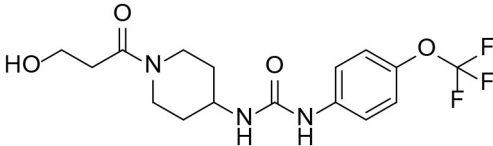
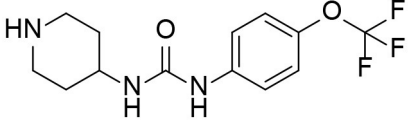
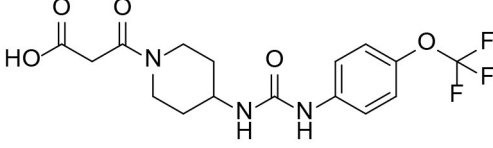
Because all four metabolites retained the central pharmacophore of N,N' -disubstituted urea in the structure, they maintained sEH inhibition and a portion of the drug effect of TPPU may be associated with these metabolites. In Table 3, these four major

TPPU metabolites still have sEH inhibitory activity, although their inhibitory potencies are weaker than that of TPPU ($IC_{50} = 1$ nM). Among all TPPU metabolites analyzed, the hydroxylated metabolite M1 has the highest inhibitory potency ($IC_{50} = 3$ nM) toward human sEH, which is ~ 5 -fold more potent than that of hydroxylated metabolite M2 ($IC_{50} = 16.7$ nM). This indicates that the hydroxylation position significantly influences the sEH inhibitory activity. M3 derived from amide hydrolysis has 80-fold lower potency ($IC_{50} = 83.5$ nM) than that of TPPU (1 nM), indicating that having the free amine of the piperidinyl group significantly reduces sEH inhibitory potency. M4 possessed the lowest potency ($IC_{50} = 158$ nM) among these four metabolites. This demonstrates that having the free carboxyl group significantly reduces sEH inhibitory potency. The comparison of sEH inhibitory activities of TPPU and its metabolites is helpful to gain knowledge of relationship between chemical structure and sEH inhibitory potency.

DISCUSSION

The sEH inhibitors were designed to inhibit the transition state of the enzyme from metabolizing the epoxide to product diol. Early chemical efforts (Rose et al., 2010) and computational studies (Waltenberger et al., 2016) found that most potent inhibitors have urea or carbamate pharmacophores. Two of the compounds, AR9281 and GSK2256294, published results from Phase I clinical trials with no significant safety concerns (Watanabe et al., 2003; Liu et al., 2015), while the third, EC5026 from EicOsis, is being prepared for human phase I safety studies. There is increasing interests in the development of sEH inhibitors for the treatment of a number of diseases. However, the metabolism of few sEHI has been studied so far, which is an important aspect of the drug development of sEHI. Previously, 1-cyclohexyl-3-dodecyl-urea (CDU) and 1-adamantan-1-yl-3-(5-(2-(2-ethoxyethoxy)ethoxy)pentyl)urea (AEPU) was studied for its Phase I metabolism and a hydroxylated metabolite

TABLE 3 | TPPU and its identified Metabolites: chemical formula, structures, inhibitory potency toward human sEH, and non-compartmental pharmacokinetic parameters after oral gavage at a 10 mg/kg in rats ($n = 4$).

Meta. ID	Formula	HsEH IC ₅₀ ^a (nM)	AUC ^b (nM·h)	C _{max} ^c (nM)	T _{1/2} ^d (h)
TPPU	 1-(1-propionylpiperidin-4-yl)-3-(4-(trifluoromethoxy)phenyl)urea	1.1 ± 0.1	6.0 ± 0.9 10 ⁶	2.0 ± 0.3 10 ⁵	9.0 ± 1.8
M1	 1-(1-(2-hydroxypropanoyl)piperidin-4-yl)-3-(4-(trifluoromethoxy)phenyl)urea	3 ± 0.5	6.0 ± 1.0 10 ⁵	1.0 ± 0.4 10 ⁴	20 ± 3
M2	 1-(1-(3-hydroxypropanoyl)piperidin-4-yl)-3-(4-(trifluoromethoxy)phenyl)urea	16 ± 2	2.0 ± 0.6 10 ⁴	7.0 ± 2.0 10 ²	9.7 ± 0.8
M3	 1-(piperidin-4-yl)-3-(4-(trifluoromethoxy)phenyl)urea	83 ± 9	6.0 ± 4.0 10 ³	3.0 ± 2.0 10 ²	14 ± 2.7
M4	 3-oxo-3-(4-(3-(4-(trifluoromethoxy)phenyl)ureido)piperidin-1-yl)propanoic acid	158 ± 10	1.0 ± 0.4 10 ³	53 ± 28	17 ± 4.7

^aIC₅₀ values were determined by CMNPC fluorescent assay.^bArea under the concentration (Time₀–72 h).^cMaximum blood concentration.^dhalf-life.

was found to be metabolically more stable than its parent and retain some potency on the sEH target (Chen et al., 2012; Lazaar et al., 2016). Published clinical trial results with AR9281 and GSK2256294 indicate that oxidative metabolism is the primary route of their metabolism in humans, and saturation at high doses reported with AR9281 results in non-linear kinetics. Although the metabolites were not reported for either compound, the formation of oxidative metabolism without presence of glucuronide metabolites was listed as the major route of elimination for both compounds, similar to the metabolites

we identified for TPPU. Because the metabolites retained the pharmacophore, it is important to understand the potency of these metabolites in order to identify an accurate therapeutic index and safety profile. More information of the relationship between chemical structure and sEH inhibitory potency of 1-Aryl-3-(1-acylpiperidin-4-yl) urea inhibitors has been reported by Rose et al. (2010).

Preclinical metabolism is often overlooked in driving small molecules to human clinical development; however, better characterization of metabolism early in development may help

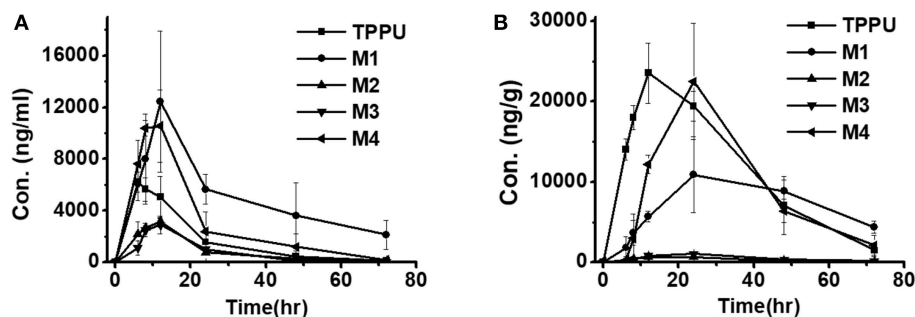


FIGURE 7 | Time course of TPPU and its metabolite levels in rat urine (A) and feces (B) following a single oral dose of 10 mg/kg (n = 3).

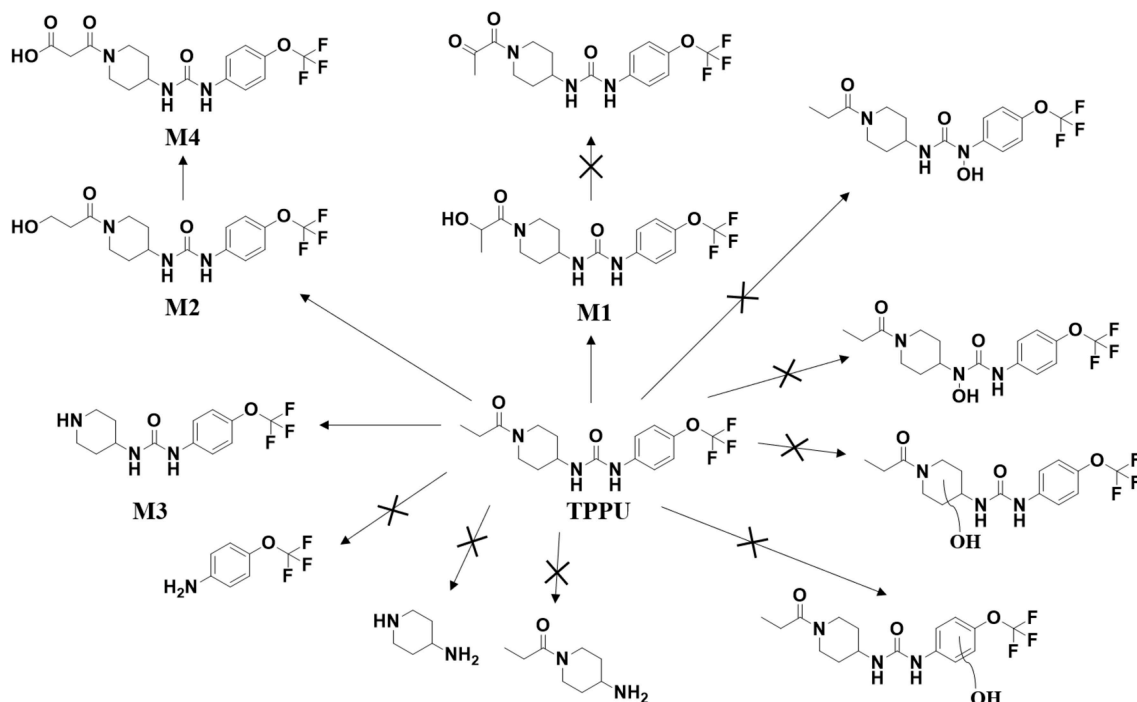


FIGURE 8 | Major routes of Phase I metabolism of the sEH TPPU detected in rat by LC-MS/MS. The pathways not detected are marked by X.

avoid unexpected consequences in clinical trials, thus preventing expensive failures late in development. The challenge to this approach is that early metabolism studies are unique to each compound and require a high level of technical expertise. This study reports methods and results for identifying unknown Phase I metabolites that can be applied to other small molecules. Although the metabolites are specific to this compound, they can be used to assess metabolism of other similar compounds. More importantly, these methods will identify potential major metabolites; and by assessing in different species, it reduces the risk of finding major metabolites in human trials, when toxicity profiles may not have been established in IND-enabling toxicity studies. Although no major metabolites were identified for TPPU in blood, understanding how metabolism affects efficacy is important for designing safe clinical trials, especially when low concentrations of a more potent metabolite could

influence safety and efficacy. For example, we found that the hydroxylation position significantly influences sEH inhibitory activity. The major metabolite M1 still has sub nanomolar potency and an *in vivo* $t_{1/2}$ that is much longer than TPPU. Therefore, even low concentrations of this metabolite may play a significant role in the efficacious profile for this drug. Similar effects of different hydroxylation positions on sEH potency have been also observed for N-adamantyl substituted urea-based sEH inhibitor (Lazaar et al., 2016). In this manuscript, we studied the relationship between different metabolites and their sEH inhibitory potency. However, further studies should be conducted to determine if the relationship is applicable for all sEH inhibitors.

In the present study, LC-MS/MS methods were employed to investigate *in vitro* and *in vivo* metabolism of TPPU. Based on the unique fragmentation pattern of TPPU and synthetic

standard metabolites in tandem mass spectrum, we employed a LC-MS/MS method with double precursor ion scans for m/z 85 (CID, 38 eV) and m/z 176 (CID, 22 eV) to identify TPPU metabolites. The LC-MS/MS method with double precursor ion scans has some distinct advantages. Most importantly, the ion chromatograms obtained by precursor ion scan showed clear peaks corresponding to these compound metabolites (**Figure 3**). Using this highly sensitive LC-MS/MS method, we identified four TPPU metabolites *in vivo*, including M1 and M2 formed from ω and ω -1 hydroxylation of TPPU, M3 from amide hydrolysis of TPPU on 1-propionylpiperidine residue, and M4 from further oxidation of terminal hydroxylated metabolite M2. Two putative metabolites, including 4-(trifluoromethoxy)aniline derived from urea cleavage and the α -keto amide metabolite, were not identified in urine even by highly sensitive LC-MRM-MS methods. In urine, neither glucuronide or sulfate conjugates formed from TPPU and its Phase I metabolites were detected by neutral loss scanning for 176 Da and precursor ion scanning for m/z 97 based LC-MS/MS methods. The other predicted metabolites of TPPU in **Table 1**, if formed, were present at a concentration lower than 2 ng/mL (LOD). Their presence was not confirmed due to their very low concentrations and lack of synthetic standards.

Both *in vitro* and *in vivo* data showed that the metabolism of TPPU mainly occurred on 1-propionylpiperidinyl moiety of the molecule but not on 4-(trifluoromethoxy)phenyl moiety. Consistent with the result from previous report (Ostermann et al., 2015), TPPU shows good metabolic stability when incubated with liver S9 fractions, as over 90% of TPPU remained after 2 h of incubation. M1, M2, and M3 were observed when TPPU was incubated in liver S9 fractions in presence of a NADPH generating solution. In the absence of a NADPH generation system, M1 and M2 failed to be detected whereas M3 could still be produced in liver S9 fractions (**Figure S1**). This suggests that hydroxylation of TPPU is mainly through CYP enzymes, while amide hydrolysis of TPPU is probably dependent on amidases or other hydrolytic enzymes. *In vivo* data showed that TPPU was predominately metabolized via three metabolic pathways, hydroxylation, amide hydrolysis and oxidation, with hydroxylation being the dominant process (**Figure 8**). On the basis of the $t_{1/2}$ values in **Table 3**, M2 was probably excreted more rapidly than M1 due to its relatively higher polarity, which is consistent with their elution order in chromatography (**Figure 2**). In rat blood, <10% of TPPU is present as its metabolites. This observation suggests that these more polar metabolites are rapidly conjugated and excreted after formation. A large amount of TPPU metabolites were found both in urine and feces. In addition, TPPU itself can be also detected in both urine and feces samples after 8 h. Therefore, the excretion of TPPU was determined to be majorly via Phase I metabolism and parent drug in urine and feces. Overall the data suggest that the pathways for TPPU excretion include primarily phase I metabolism and self-elimination. The good absorption and relatively long half-life in the blood likely contribute to its high potency and target occupancy of TPPU in multiple disease states (Kodani and Hammock, 2015). M1 with its IC_{50} at 3 nM and relatively longer

half-life (~ 20 h) could contribute to *in vivo* inhibition. The much higher IC_{50} values of M2 and M3 and relatively short half-life than M1 make them unlikely to contribute significantly to the pharmacological efficacy of TPPU *in vivo*.

In conclusion, we demonstrated species differences of TPPU metabolism using liver S9 fractions and identified TPPU metabolites in both rat blood and urine. TPPU underwent phase I metabolism, mostly through hydroxylation (M1 and M2), followed by amide hydrolysis (M3) and one of the hydroxylated metabolites (M2) was subject to further oxidation to form M4. The failure to find metabolites of TPPU hydroxylated on the aromatic ring or the piperidine ring suggests that these are likely minor pathways of metabolism. It is also possible that these putative metabolites could have been formed and rapidly metabolized to other Phase II metabolites that is not detected. As has been reported for other sEH, we failed to find possible metabolites resulting from urea cleavage. The 1-propionylpiperidinyl moiety on TPPU is the most metabolically vulnerable part in the molecule. These insights inform the predicted metabolism of other sEH inhibitors containing the acyl-piperidinyl group and a urea central pharmacophore. Therefore, it provides useful information for the optimization of future sEH inhibitors for translation to the clinical environment.

ETHICS STATEMENT

All animal studies were approved by the UC Davis IACUC committee.

AUTHOR CONTRIBUTIONS

DW, JY, CBM, and BDH designed research. DW, BB, KW, CM, JS, and RB performed research. SH contributed TPPU and 4-(trifluoromethoxy)aniline. DW, JY, CBM, BB, KW, SH, and BDH analyzed data and edited manuscript.

FUNDING

This work was supported in part by the NIEHS Grant R01 ES002710 (to BDH), NIEHS Superfund Research Program P42 ES004699 (to BDH), NIH CounterACT U54 Program NS079202 (to BDH), NIH NINDS UH2NS094258 (to BDH), NIEHS SBIR R43/R44ES025598 (to BDH) and T32GM11377004 (to CBM).

ACKNOWLEDGMENTS

The authors are grateful to Prof. Alan R. Buckpitt of UC Davis for constructive detailed discussions and revisions. Prof. Alan R. Buckpitt is serving as PI of the mEHs SBIR and NINDS Blueprint Development Grant.

SUPPLEMENTARY MATERIAL

The Supplementary Material for this article can be found online at: <https://www.frontiersin.org/articles/10.3389/fphar.2019.00464/full#supplementary-material>

REFERENCES

- Anandan, S. K., Webb, H. K., Chen, D., Wang, Y. X., Aavula, B. R., Cases, S., et al. (2011). 1-(1-Acetyl-piperidin-4-yl)-3-adamantan-1-yl-urea (AR9281) as a potent, selective, and orally available soluble epoxide hydrolase inhibitor with efficacy in rodent models of hypertension and dysglycemia. *Bioorg. Med. Chem. Lett.* 21, 983–988. doi: 10.1016/j.bmcl.2010.12.042
- Bastan, I., Ge, X. N., Dileepan, M., Greenberg, Y. G., Guedes, A. G., Hwang, S. H., et al. (2018). Inhibition of soluble epoxide hydrolase attenuates eosinophil recruitment and food allergen-induced gastrointestinal inflammation. *J. Leukoc. Biol.* 104, 109–122. doi: 10.1002/JLB.3MA1017-423R
- Bettaieb, A., Chahed, S., Bachaalany, S., Griffey, S., Hammock, B. D., and Haj, F. G. (2015). Soluble epoxide hydrolase pharmacological inhibition ameliorates experimental acute pancreatitis in mice. *Mol. Pharmacol.* 88, 281–290. doi: 10.1124/mol.114.097501
- Chen, D., Whitcomb, R., MacIntyre, E., Tran, V., Do, Z. N., Sabry, J., et al. (2012). Pharmacokinetics and pharmacodynamics of AR9281, an inhibitor of soluble epoxide hydrolase, in single- and multiple-dose studies in healthy human subjects. *J. Clin. Pharmacol.* 52, 319–328. doi: 10.1177/0091270010397049
- Chen, Y., Tian, H., Yao, E., Tian, Y., Zhang, H., Xu, L., et al. (2017). Soluble epoxide hydrolase inhibition promotes white matter integrity and long-term functional recovery after chronic hypoperfusion in mice. *Sci. Rep.* 7:7758. doi: 10.1038/s41598-017-08227-z
- Davis, B. B., Liu, J. Y., Tancredi, D. J., Wang, L., Simon, S. I., Hammock, B. D., et al. (2011). The anti-inflammatory effects of soluble epoxide hydrolase inhibitors are independent of leukocyte recruitment. *Biochem. Biophys. Res. Commun.* 410, 494–500. doi: 10.1016/j.bbrc.2011.06.008
- Decker, M., Arand, M., and Cronin, A. (2009). Mammalian epoxide hydrolases in xenobiotic metabolism and signalling. *Arch. Toxicol.* 83, 297–318. doi: 10.1007/s00204-009-0416-0
- Enayattallah, A. E., French, R. A., Thibodeau, M. S., and Grant, D. F. (2004). Distribution of soluble epoxide hydrolase and of cytochrome P450 2C8, 2C9, and 2J2 in human tissues. *J. Histochem. Cytochem.* 52, 447–454. doi: 10.1177/002215540405200403
- Goswami, S. K., Wan, D., Yang, J., Trindade da Silva, C. A., Morisseau, C., Kodani, S. D., et al. (2016). Anti-ulcer efficacy of soluble epoxide hydrolase inhibitor TPPU on diclofenac-induced intestinal ulcers. *J. Pharmacol. Exp. Ther.* 357, 529–536. doi: 10.1124/jpet.116.232108
- Hammock, B. D., Wagner, K., and Inceoglu, B. (2011). The soluble epoxide hydrolase as a pharmaceutical target for pain management. *Pain Manage.* 1, 383–386. doi: 10.2217/pmt.11.47
- Harris, T. R., Bettaieb, A., Kodani, S., Dong, H., Myers, R., Chiamvimonvat, N., et al. (2015). Inhibition of soluble epoxide hydrolase attenuates hepatic fibrosis and endoplasmic reticulum stress induced by carbon tetrachloride in mice. *Toxicol. Appl. Pharmacol.* 286, 102–111. doi: 10.1016/j.taap.2015.03.022
- Hashimoto, K. (2016). Soluble epoxide hydrolase: a new therapeutic target for depression. *Expert. Opin. Ther. Targets.* 20, 1149–1151. doi: 10.1080/14728222.2016.1226284
- Hu, J., Dziumbala, S., Lin, J., Bibli, S. I., Zukunft, S., de Mos, J., et al. (2017). Inhibition of soluble epoxide hydrolase prevents diabetic retinopathy. *Nature.* 552, 248–252. doi: 10.1038/nature25013
- Huang, H. J., Wang, Y. T., Lin, H. C., Lee, Y. H., and Lin, A. M. (2018). Soluble epoxide hydrolase inhibition attenuates MPTP-induced neurotoxicity in the nigrostriatal dopaminergic system: involvement of α -synuclein aggregation and ER stress. *Mol. Neurobiol.* 55, 138–144. doi: 10.1007/s12035-017-0726-9
- Imig, J. D. (2012). Epoxides and soluble epoxide hydrolase in cardiovascular physiology. *Physiol. Rev.* 92, 101–130. doi: 10.1152/physrev.00021.2011
- Imig, J. D. (2015). Epoxyeicosatrienoic acids, hypertension, and kidney injury. *Hypertension* 65, 476–482. doi: 10.1161/HYPERTENSIONAHA.114.03585
- Imig, J. D., Zhao, X., Zaharis, C. Z., Olearczyk, J. J., Pollock, D. M., Newman, J. W., et al. (2005). An orally active epoxide hydrolase inhibitor lowers blood pressure and provides renal protection in salt-sensitive hypertension. *Hypertension* 46, 975–981. doi: 10.1161/01.HYP.0000176237.74820.75
- Inceoglu, B., Bettaieb, A., Haj, F. G., Gomes, A. V., and Hammock, B. D. (2017). Modulation of mitochondrial dysfunction and endoplasmic reticulum stress are key mechanisms for the wide-ranging actions of epoxy fatty acids and soluble epoxide hydrolase inhibitors. *Prostaglandins Other Lipid Mediat.* 133, 68–78. doi: 10.1016/j.prostaglandins.2017.08.003
- Kodani, S. D., and Hammock, B. D. (2015). The 2014 Bernard, B. Brodie award lecture-epoxide hydrolases: drug metabolism to therapeutics for chronic pain. *Drug Metab. Dispos.* 43, 788–802. doi: 10.1124/dmd.115.063339
- Lazaar, A. L., Yang, L., Boardley, R. L., Goyal, N. S., Robertson, J., Baldwin, S. J., et al. (2016). Pharmacokinetics, pharmacodynamics and adverse event profile of GSK2256294, a novel soluble epoxide hydrolase inhibitor. *Br. J. Clin. Pharmacol.* 81, 971–979. doi: 10.1111/bcp.12855
- Lee, K. S., Liu, J. Y., Wagner, K. M., Pakhomova, S., Dong, H., Morisseau, C., et al. (2014). Optimized inhibitors of soluble epoxide hydrolase improve *in vitro* target residence time and *in vivo* efficacy. *J. Med. Chem.* 57, 7016–7030. doi: 10.1021/jm500694p
- Liu, J. Y., Lin, Y. P., Qiu, H., Morisseau, C., Rose, T. E., Hwang, S. H., et al. (2013). Substituted phenyl groups improve the pharmacokinetic profile and anti-inflammatory effect of urea-based soluble epoxide hydrolase inhibitors in murine models. *Eur. J. Pharm. Sci.* 48, 619–627. doi: 10.1016/j.ejps.2012.12.013
- Liu, J. Y., Tsai, H. J., Morisseau, C., Lango, J., Hwang, S. H., Watanabe, T., et al. (2015). *In vitro* and *in vivo* metabolism of N-adamantyl substituted urea-based soluble epoxide hydrolase inhibitors. *Biochem. Pharmacol.* 98, 718–731. doi: 10.1016/j.bcp.2015.10.013
- Lorthioir, A., Guerrot, D., Joannides, R., and Bellien, J. (2012). Diabetic CVD-soluble epoxide hydrolase as a target. *Cardiovasc. Hematol. Agents Med. Chem.* 10, 212–222. doi: 10.2174/187152512802651042
- Luria, A., Bettaieb, A., Xi, Y., Shieh, G. J., Liu, H. C., Inoue, H., et al. (2011). Soluble epoxide hydrolase deficiency alters pancreatic islet size and improves glucose homeostasis in a model of insulin resistance. *Proc. Natl. Acad. Sci. U.S.A.* 108, 9038–9043. doi: 10.1073/pnas.1103482108
- McReynolds, C., Schmidt, W. K., Wagner, K., and Hammock, B. D. (2016). Advancing soluble epoxide hydrolase inhibitors through the valley of death into phase 1 clinical trials for treating painful diabetic neuropathy by utilizing university partnerships, collaborations and NIH support. *FASEB J.* 30:Supplement 1272.1276.
- Morisseau, C., Goodrow, M. H., Newman, J., Wheelock, W. C. E., Dowdy, D. L., and Hammock, B. D. (2002). Structural refinement of inhibitors of urea-based soluble epoxide hydrolases. *Biochem. Pharmacol.* 63, 1599–1608. doi: 10.1016/S0006-2952(02)00952-8
- Morisseau, C., and Hammock, B. D. (2013). Impact of soluble epoxide hydrolase and epoxyeicosanoids on human health. *Annu. Rev. Pharmacol. Toxicol.* 53, 37–58. doi: 10.1146/annurev-pharmtox-011112-140244
- Napimoga, M. H., Rocha, E. P., Trindade-da-Silva, C. A., Demasi, A. P. D., Martinez, E. F., Macedo, C. G., et al. (2018). Soluble epoxide hydrolase inhibitor promotes immunomodulation to inhibit bone resorption. *J. Periodontol. Res.* 53, 743–749. doi: 10.1111/jre.12559
- Newman, J. W., Morisseau, C., and Hammock, B. D. (2005). Epoxide hydrolases: their roles and interactions with lipid metabolism. *Prog. Lipid. Res.* 44, 1–51. doi: 10.1016/j.plipres.2004.10.001
- Ostermann, A. I., Herbers, J., Willenberg, I., Chen, R., Hwang, S. H., Greite, R., et al. (2015). Oral treatment of rodents with soluble epoxide hydrolase inhibitor 1-(1-propanoylpiperidin-4-yl)-3-[4-(trifluoromethoxy)phenyl]urea (TPPU): resulting drug levels and modulation of oxylipin pattern. *Prostaglandins Other Lipid Mediat.* 121 (Pt A):131–7. doi: 10.1016/j.prostaglandins.2015.06.005
- Qiu, H., Li, N., Liu, J. Y., Harris, T. R., Hammock, B. D., and Chiamvimonvat, N. (2011). Soluble epoxide hydrolase inhibitors and heart failure. *Cardiovasc. Ther.* 29, 99–111. doi: 10.1111/j.1755-5922.2010.00150.x
- Ren, Q., Ma, M., Ishima, T., Morisseau, C., Yang, J., Wagner, K. M., et al. (2016). Gene deficiency and pharmacological inhibition of soluble epoxide hydrolase confers resilience to repeated social defeat stress. *Proc. Natl. Acad. Sci. U.S.A.* 113, E1944–E1952. doi: 10.1073/pnas.1601532113
- Ren, Q., Ma, M., Yang, J., Nonaka, R., Yamaguchi, A., Ishikawa, K. I., et al. (2018). Soluble epoxide hydrolase plays a key role in the pathogenesis of Parkinson's disease. *Proc. Natl. Acad. Sci. U.S.A.* 115, E5815–E5823. doi: 10.1073/pnas.1802179115
- Rose, T. E., Morisseau, C., Liu, J. Y., Inceoglu, B., Jones, P. D., Sanborn, J. R., et al. (2010). 1-Aryl-3-(1-acylpiperidin-4-yl)urea inhibitors of human and murine soluble epoxide hydrolase: structure-activity relationships, pharmacokinetics, and reduction of inflammatory pain. *J. Med. Chem.* 53, 7067–7075. doi: 10.1021/jm100691c

- Schebb, N. H., Franze, B., Maul, R., Ranganathan, A., and Hammock, B. D. (2012). *In vitro* glucuronidation of the antibacterial triclocarban and its oxidative metabolites. *Drug Metab. Dispos.* 40, 25–31. doi: 10.1124/dmd.111.042283
- Shen, H. C., and Hammock, B. D. (2012). Discovery of inhibitors of soluble epoxide hydrolase: a target with multiple potential therapeutic indications. *J. Med. Chem.* 55, 1789–1808. doi: 10.1021/jm201468j
- Simpkins, A. N., Rudic, R. D., Schreihöfer, D. A., Roy, S., Manhiani, M., Tsai, H. J., et al. (2009). Soluble epoxide inhibition is protective against cerebral ischemia via vascular and neural protection. *Am. J. Pathol.* 174, 2086–2095. doi: 10.2353/ajpath.2009.080544
- Supp, D. M., Hahn, J. M., McFarland, K. L., Combs, K. A., Lee, K. S., Inceoglu, B., et al. (2016). Soluble epoxide hydrolase inhibition and epoxyeicosatrienoic acid treatment improve vascularization of engineered skin substitutes. *Plast. Reconstr. Surg. Glob. Open.* 4:e1151. doi: 10.1097/GOX.0000000000001151
- Tsai, H. J., Hwang, S. H., Morisseau, C., Yang, J., Jones, P. D., Kasagami, T., et al. (2010). Pharmacokinetic screening of soluble epoxide hydrolase inhibitors in dogs. *Eur. J. Pharm. Sci.* 40, 222–238. doi: 10.1016/j.ejps.2010.03.018
- Tu, R., Armstrong, J., Lee, K. S. S., Hammock, B. D., Sapirstein, A., and Koehler, R. C. (2018). Soluble epoxide hydrolase inhibition decreases reperfusion injury after focal cerebral ischemia. *Sci. Rep.* 8:5279. doi: 10.1038/s41598-018-23504-1
- Ulu, A., Appt, S., Morisseau, C., Hwang, S. H., Jones, P. D., Rose, T. E., et al. (2012). Pharmacokinetics and *in vivo* potency of soluble epoxide hydrolase inhibitors in cynomolgus monkeys. *Br. J. Pharmacol.* 165, 1401–1412. doi: 10.1111/j.1476-5381.2011.01641.x
- Wagner, K., Gilda, J., Yang, J., Wan, D., Morisseau, C., Gomes, A. V., et al. (2017). Soluble epoxide hydrolase inhibition alleviates neuropathy in Akita (Ins2 Akita) mice. *Behav. Brain Res.* 326, 69–76. doi: 10.1016/j.bbr.2017.02.048
- Wagner, K. M., McReynolds, C. B., Schmidt, W. K., and Hammock, B. D. (2017). Soluble epoxide hydrolase as a therapeutic target for pain, inflammatory and neurodegenerative diseases. *Pharmacol. Ther.* 180, 62–76. doi: 10.1016/j.pharmthera.2017.06.006
- Waltenberger, B., Garscha, U., Temml, V., Liers, J., Werz, O., Schuster, D., et al. (2016). Discovery of potent soluble epoxide hydrolase (sEH) inhibitors by pharmacophore-based virtual screening. *J. Chem. Inf. Model.* 56, 747–762. doi: 10.1021/acs.jcim.5b00592
- Wang, Q., Pang, W., Cui, Z., Shi, J., Liu, Y., Liu, B., et al. (2013). Upregulation of soluble epoxide hydrolase in proximal tubular cells mediated proteinuria-induced renal damage. *Am. J. Physiol. Renal. Physiol.* 304, F168–F176. doi: 10.1152/ajprenal.00129.2012
- Wang, W., Yang, J., Zhang, J., Wang, Y., Hwang, S. H., Qi, W., et al. (2018). Lipidomic profiling reveals soluble epoxide hydrolase as a therapeutic target of obesity-induced colonic inflammation. *Proc. Natl. Acad. Sci. U.S.A.* 115, 5283–5288. doi: 10.1073/pnas.1721711115
- Watanabe, T., and Hammock, B. D. (2001). Rapid determination of soluble epoxide hydrolase inhibitors in rat hepatic microsomes by high-performance liquid chromatography with electrospray tandem mass spectrometry. *Anal. Biochem.* 299, 227–234. doi: 10.1006/abio.2001.5423
- Watanabe, T., Morisseau, C., Newman, J. W., and Hammock, B. D. (2003). *In vitro* metabolism of the mammalian soluble epoxide hydrolase inhibitor, 1-cyclohexyl-3-dodecyl-urea. *Drug Metab. Dispos.* 31, 846–853. doi: 10.1124/dmd.31.7.846
- Wu, Q., Cai, H., Song, J., and Chang, Q. (2017). The effects of sEH inhibitor on depression-like behavior and neurogenesis in male mice. *J. Neurosci. Res.* 95, 2483–2492. doi: 10.1002/jnr.24080
- Xu, D., Li, N., He, Y., Timofeyev, V., Lu, L., Tsai, H. J., et al. (2006). Prevention and reversal of cardiac hypertrophy by soluble epoxide hydrolase inhibitors. *Proc. Natl. Acad. Sci. U.S.A.* 103, 18733–18738. doi: 10.1073/pnas.0609158103
- Yu, G., Zeng, X., Wang, H., Hou, Q., Tan, C., Xu, Q., et al. (2015). 14,15-epoxyeicosatrienoic Acid suppresses cigarette smoke extract-induced apoptosis in lung epithelial cells by inhibiting endoplasmic reticulum stress. *Cell Physiol. Biochem.* 36, 474–486. doi: 10.1159/000430113
- Zarriello, S., Tuazon, J., Corey, S., Schimmel, S., Rajani, M., Gorsky, A., et al. (2018). Humble beginnings with big goals: small molecule soluble epoxide hydrolase inhibitors for treating CNS disorders. *Prog. Neurobiol.* 172, 23–39. doi: 10.1016/j.pneurobio.2018.11.001
- Zhou, C., Huang, J., Li, Q., Nie, J., Xu, X., and Wang, D. W. (2017). Soluble epoxide hydrolase inhibition protected against angiotensin II-induced adventitial remodeling. *Sci. Rep.* 7:6926. doi: 10.1038/s41598-017-07512-1
- Zhou, Y., Yang, J., Sun, G. Y., Liu, T., Duan, J. X., Zhou, H. F., et al. (2016). Soluble epoxide hydrolase inhibitor 1-trifluoromethoxyphenyl-3-(1-propionylpiperidin-4-yl) urea attenuates bleomycin-induced pulmonary fibrosis in mice. *Cell Tissue Res.* 363, 399–409. doi: 10.1007/s00441-015-2262-0

Conflict of Interest Statement: BDH and CBM are co-founders. JY and KW are employees of EicOsis, a company advancing sEH inhibitors as potential therapeutics.

The remaining authors declare that the research was conducted in the absence of any commercial or financial relationships that could be construed as a potential conflict of interest.

Copyright © 2019 Wan, Yang, McReynolds, Barnych, Wagner, Morisseau, Hwang, Sun, Blöcher and Hammock. This is an open-access article distributed under the terms of the Creative Commons Attribution License (CC BY). The use, distribution or reproduction in other forums is permitted, provided the original author(s) and the copyright owner(s) are credited and that the original publication in this journal is cited, in accordance with accepted academic practice. No use, distribution or reproduction is permitted which does not comply with these terms.



Epoxyeicosatrienoic Acid Analog EET-A Blunts Development of Lupus Nephritis in Mice

Md. Abdul Hye Khan^{1*}, Anna Stavniichuk¹, Mohammad Abdul Sattar², John R. Falck² and John D. Imig^{1*}

¹ Department of Pharmacology and Toxicology, Medical College of Wisconsin, Milwaukee, WI, United States, ² Department of Biochemistry, UT Southwestern Medical Center, Dallas, TX, United States

OPEN ACCESS

Edited by:

Richard Schulz,
University of Alberta, Canada

Reviewed by:

Anna-Marie Fairhurst,
Agency for Science, Technology
and Research (A*STAR), Singapore
Mohammed A. Nayeem,
West Virginia University, United States
Stanislaw Stepkowski,
The University of Toledo,
United States

*Correspondence:

Md. Abdul Hye Khan
abhkhan@mcw.edu
orcid.org/0000-0001-5940-9300
John D. Imig
jdimg@mcw.edu

Specialty section:

This article was submitted to
Translational Pharmacology,
a section of the journal
Frontiers in Pharmacology

Received: 16 October 2018

Accepted: 24 April 2019

Published: 10 May 2019

Citation:

Hye Khan MA, Stavniichuk A,
Sattar MA, Falck JR and Imig JD
(2019) Epoxyeicosatrienoic Acid
Analog EET-A Blunts Development
of Lupus Nephritis in Mice.
Front. Pharmacol. 10:512.
doi: 10.3389/fphar.2019.00512

Systemic lupus erythematosus (SLE) is a chronic autoimmune inflammatory disorder that causes life threatening renal disease and current therapies are limited with serious side-effects. CYP epoxygenase metabolites of arachidonic acid epoxyeicosatrienoic acids (EETs) demonstrate strong anti-inflammatory and kidney protective actions. We investigated the ability of an orally active EET analog, EET-A to prevent kidney injury in a mouse SLE model. Twenty-weeks old female NZBWF1 (SLE) and age-matched NZW/LacJ (Non SLE) were treated with vehicle or EET-A (10 mg/kg/d, p.o.) for 14 weeks and urine and kidney tissues were collected at the end of the protocol. SLE mice demonstrated marked renal chemotaxis with 30–60% higher renal mRNA expression of CXC chemokine receptors (CXCR) and CXC chemokines (CXCL) compared to Non SLE mice. In SLE mice, the elevated chemotaxis is associated with 5–15-fold increase in cytokine mRNA expression and elevated inflammatory cell infiltration in the kidney. SLE mice also had elevated BUN, serum creatinine, proteinuria, and renal fibrosis. Interestingly, EET-A treatment markedly diminished renal CXCR and CXCL renal mRNA expression in SLE mice. EET-A treatment also reduced renal TNF- α , IL-6, IL-1 β , and IFN- γ mRNA expression by 70–80% in SLE mice. Along with reductions in renal chemokine and cytokine mRNA expression, EET-A reduced renal immune cell infiltration, BUN, serum creatinine, proteinuria and renal fibrosis in SLE mice. Overall, we demonstrate that an orally active EET analog, EET-A prevents renal injury in a mouse model of SLE by reducing inflammation.

Keywords: lupus nephritis, EET analog, inflammation, chemokine, small lipid mediators, mouse

INTRODUCTION

Systemic lupus erythematosus (SLE) is an autoimmune disease characterized by abnormality in the immune system. In SLE, almost all organs in the body can be involved and clinical presentation of SLE can range from mild to severe depending on the affected organ. Involvement of the kidney is termed as lupus nephritis (LN) which affects up to 60% of the SLE patients and remains the leading cause of morbidity and mortality in SLE (Lu et al., 2012). The etiopathology of SLE as well as LN are still not fully understood and this lack of knowledge limits therapeutic options for SLE and LN (Lech and Anders, 2013).

The current therapy of LN involves the use of corticosteroids and the alkylating agent cyclophosphamide. Indeed, a combination of these agents is now considered as the standard of

care for SLE and LN and improves patient survival rate. However, serious side effects that occur with immunosuppression are common with these therapies and are associated with significant morbidity (Contreras et al., 2004; Gilkeson, 2015). As such, there is a need to develop novel therapies for LN treatment that will improve long-term renal outcomes with minimum treatment-related toxicity. Unfortunately, the success in developing novel and safer therapy for LN is still unsatisfactory and the current therapeutic approaches still depend on high-dose corticosteroids combined with broad-spectrum immunosuppressive agents (Gilkeson, 2015; Jordan and D'Cruz, 2016; Dall'Era, 2017). This lack of novel LN therapies clearly indicates an unmet need for research and development of novel LN treatment options.

One possible approach to develop novel LN therapy can be the use of epoxyeicosatrienoic acids (EETs), the cytochrome P450 epoxygenase metabolites of arachidonic acid. Several studies have demonstrated kidney protective actions for EETs and EET synthetic analogs in pre-clinical kidney disease models (Hye Khan et al., 2013, 2016; Yeboah et al., 2016). These studies determined that synthetic EET analogs reduce renal tubular and glomerular injuries (Hye Khan et al., 2013, 2016). EET analogs also demonstrated strong anti-fibrotic actions and prevented or treated kidney fibrosis in multiple pathologies that contribute to chronic kidney disease (Hye Khan et al., 2013, 2016; Khan et al., 2013; Skibba et al., 2017). We demonstrated that the biological actions of EETs and EET analogs have strong anti-inflammatory, anti-apoptotic and anti-oxidative actions that contribute to the kidney protective actions (Khan et al., 2013; Hye Khan et al., 2013, 2016).

In the present study, we investigated the ability for an orally active EET analog, EET-A, to blunt the LN development in a mouse pre-clinical SLE model. We provide evidence that EET-A anti-inflammatory actions can prevent renal injury development in SLE mice.

MATERIALS AND METHODS

Chemicals

The EET analog, EET-A, was designed and synthesized in the laboratory of JF (Department of Biochemistry, University of Texas Southwestern Medical Center, Dallas, TX). Unless mentioned otherwise, all chemicals used in the current study were obtained from Sigma Aldrich (St Louis, MO, United States).

Animal Experiments

Twenty weeks old female NZBWF1 (SLE) and NZW/LacJ (Non SLE) obtained from Jackson Laboratories (Bar Harbor, ME, United States) were used in this study. Mice had free access to food and water and were housed with 12/12h light-dark cycle in the Biomedical Resource Center at the Medical College of Wisconsin. The mice were divided into three groups based on their baseline systolic blood pressure measured by tail-cuff plethysmography. Non SLE NZW/LacJ mice received vehicle and the NZBWF1 SLE mice received either vehicle or EET-A (10 mg/kg/d) in the drinking water for 14 weeks. The dose of EET-A is based on previous experimental studies demonstrating

that appropriate EET-A plasma concentrations were achieved (Khan et al., 2013). At the end of the experimental protocol, urine, and blood samples were collected followed by kidney tissue collection for biochemical, histopathological, and other analysis. Animal experiments were performed with the approval of the Medical College of Wisconsin Institutional Animal Care and Use Committee and in accordance with National Institutes of Health guidelines.

Biochemical Analysis

Urine samples were collected at the end of the experimental protocol by placing mice in metabolic cages for 24 h. Blood samples were collected from abdominal aorta under isoflurane anesthesia followed by killing of the animal with anesthetic overdose and kidney tissue collection. Urine and serum samples were analyzed using a commercially available assay for creatinine from Cayman Chemicals (Ann Arbor, MI, United States). Urine albumin level was measured using a kit from Exocell (Philadelphia, PA, United States). Blood Urea Nitrogen (BUN) was measured using a colorimetric assay (Thermo Fisher Scientific, Waltham, MA, United States). Plasma anti-dsDNA antibodies were measured with a commercial ELISA (Alpha Diagnostic International, San Antonio, TX, United States). Urine albumin and creatinine data were used to calculate the ratio of urinary albumin and creatinine excretion, which is a measure of the kidney injury.

Real-Time PCR Analysis

Renal mRNA expression for several chemokine and chemokine receptors associated with the pathophysiology of chronic inflammatory autoimmune disease were analyzed using real-time PCR (RT-PCR). RT-PCR analysis was carried for the renal mRNA expression of CXC motif chemokine ligand 9 (CXCL9), 10 (CXCL10), 13 (CXCL13) and 16 (CXCL16). We also analyzed the mRNA expression of CXC chemokine receptors 3 (CXCR3) and 4 (CXCL4). Renal mRNA expression of several cytokines namely tumor necrosis factor- α (TNF- α), interleukin 6 (IL-6), interleukin 1- β (IL-1 β), and interferon gamma (IFN- γ) was determined. The primer sequence for the CXC chemokine, chemokine receptor and cytokines are provided in **Table 1**. Renal cortex was carefully dissected from sagittal kidney section using a dissecting microscope. Absence of any medullary tissue was confirmed using microscopic observation. Renal cortex was then homogenized for mRNA extraction and RT PCR analysis. In RT-PCR analysis, mRNA was prepared from kidney cortical tissue using RNeasy Mini Kit (QIAGEN, CA, United States) according to the manufacturer's protocol. The quality and quantity of the mRNA samples were determined spectrophotometrically. Synthesis of cDNA was carried out from the mRNA samples using iScriptTM Select cDNA Synthesis Kit (Bio-Rad, Hercules, CA, United States). Expression of the genes was quantified by iScript One-Step RT-PCR Kit with SYBR green using the MyiQTM Single Color Real-Time PCR Detection System (Bio-Rad Laboratories, Hercules, CA, United States). All mRNA samples were run in triplicate and fold change in the target gene expression compared to the expression of control genes by comparative threshold cycle (C_t) method. Target gene

TABLE 1 | Primer sequences of the target genes used in RT PCR analysis.

CXCR3	F- TCTCGTTTTCCCATATCG R- AGCCAAGCCATGTACCTTGA
CXCL9	F- CGAGGCACGATCCACTACAA R- GAGTCCGATCTAGGCAGGT
CXCL10	F- ACTGCATCCATATCGATGAC R- TTCATCGTGGCAATGATCTC
CXCR4	F- GTTGCCATGGAACCGATCA R- TGCCGACTATGCCAGTCAAGA
CXCL13	F- CAGGCCACGGTATTCTGGA R- CAGGGGGCGTAACCTGAATC
CXCL16	F-CGTTGTCCATTCTTTATCAGGTCC R- TTGCGCTCAAAGCAGTCCA
TNF- α	F- CGAGTGACAAGCCTGTAGCC R- GAGAACCTGGGAGTAGACAAGG
IL-6	F- TGTATGAACAACGATGATGCAC R- TGGTACTCCAGAAGACCAGAGG
IL-1 β	F- AAGGAGAACCAAGCAACGAC R- AACTCTGCAGACTCAAATCCAC
IFN- γ	F- AGCAAGGCGAAAAAGGATGC R- TCATTGAATGCTTGGCGCTG

expression levels were determined by normalizing the C_t values to two control genes.

Histopathology

Histopathological analysis of renal fibrosis was done using 10% formalin fixed kidney tissue. The formalin fixed kidney tissues were paraffin-embedded, sectioned (5 μ m), mounted on slides and stained with Picrosirius Red (PSR) stain (Alfa Aesar, Tewksbury, MA). PSR stained slides were examined for interstitial collagen at 200x magnification and the collagen positive fibrotic kidney area was calculated as an index of renal fibrosis using NIS Elements AR version 3.0 imaging software (Nikon instruments Inc., Melville, NY, United States). Renal fibrosis was scored in a blinded fashion by two observers as published previously (Hye Khan et al., 2016, 2018), and the scores were presented as a percentage area-fraction relative to the total area analyzed.

Immunohistopathological Analysis

Deparaffinized kidney sections mounted on slides were re-hydrated followed by overnight incubation with rat anti-mouse CD43 antibody (1:100, BD Biosciences, San Jose, CA, United States). The slides were washed and incubated with biotinylated goat anti-rat secondary antibody (1:200, abcam, Cambridge, MA, United States) for 1 h. Slides were developed with avidin-biotin and HRP complex (Vectastain ABC Elite kit, Vector Laboratories, Burlingame, CA, United States) followed by counterstaining with hematoxylin. Stained histological sections were visualized at 400 \times magnification with a light microscope and analyzed by two observers in a blinded fashion using Nikon NIS Elements Software (Nikon Instruments Inc., Melville, NY, United States).

Immunofluorescence Analysis

Formalin formalin-fixed and paraffin-embedded kidney sections (5 μ m) were de-paraffinized, re-hydrated, and incubated with rodent declocker solution (Biocare Medical, Concord, CA, United States) at 95°C for antigen retrieval. Kidney sections were then immunostained with rat monoclonal anti-F4/80 antibody (1:100; abcam, Cambridge, MA, United States) to determine renal expression of F4/80 positive inflammatory cells. Goat anti-rat IgG H&L (Alexa Fluor® 488) secondary antibody (Abcam, United States) was used for development with fluorescence quenching liquid (Vector Laboratories, United States). Immunostained sections were examined by Nikon 55i fluorescence with a green excitation (200 \times magnification) and digital images were taken for analysis using Nikon NIS Elements Software (Nikon Instruments Inc., United States). The number of glomerular F4/80 positive cells was determined in 100 glomeruli by two blinded researchers and expressed as the number of cells per glomerulus.

Statistical Analysis

All data are expressed as mean \pm S.E.M. In order to determine statistical difference between different experimental groups GraphPad Prism® Version 4.0 software was used to carry out one-way ANOVA followed by Tukey's *post hoc* test (GraphPad Software Inc., La Jolla, CA, United States).

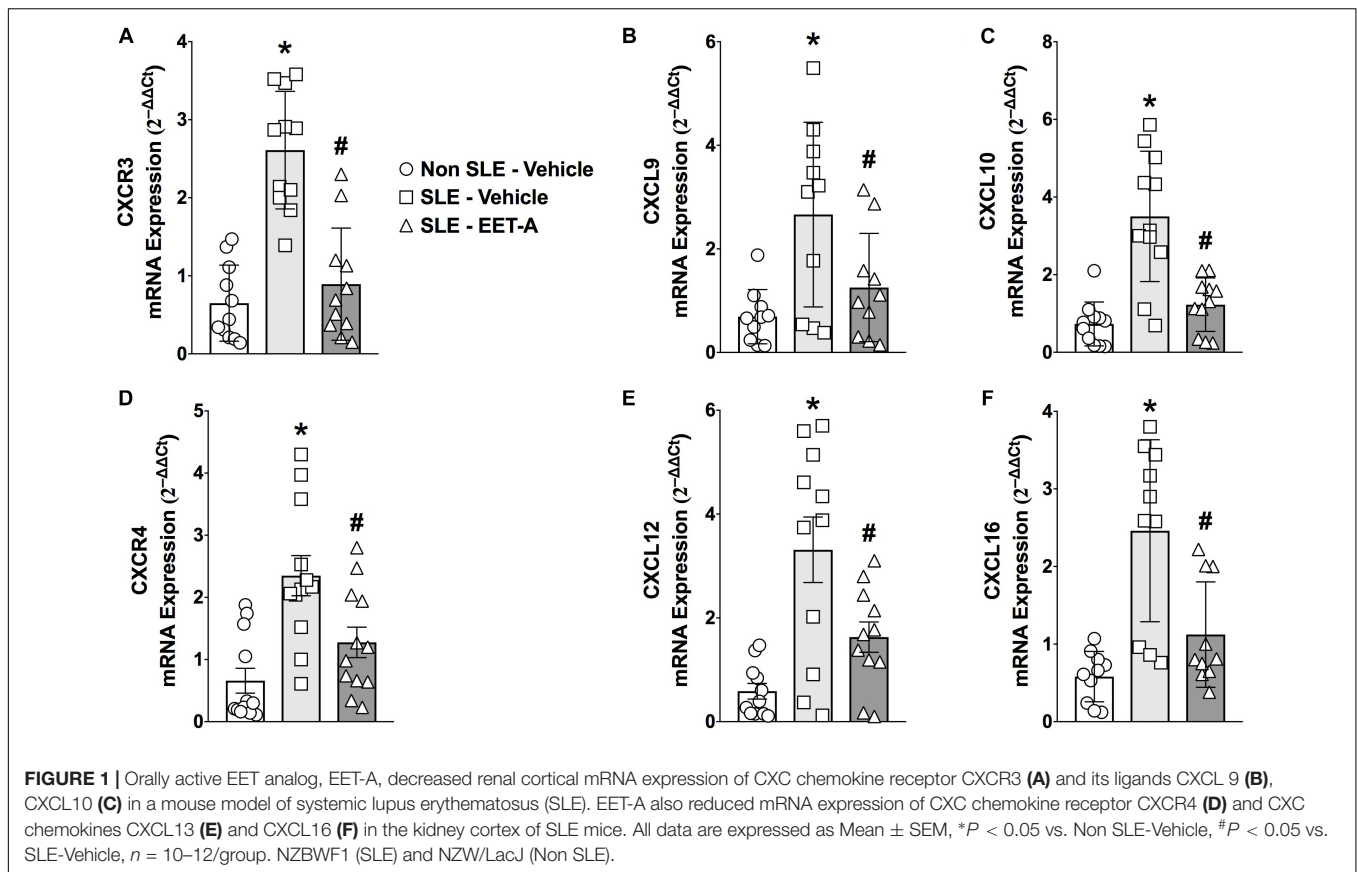
RESULTS

EET-A Treatment Reduces Blood Pressure and Body Weight Loss in SLE Mice

Systemic lupus erythematosus mice had significantly higher ($P < 0.05$) plasma anti-dsDNA antibody levels (63 ± 2 U/L, $n = 10$) compared Non SLE mice (2.3 ± 0.1 U/L, $n = 10$), and EET-A treatment did not affect plasma levels of anti-dsDNA antibodies in SLE mice (59 ± 4 U/L, $n = 10$).

Systolic blood pressure averaged 84 ± 11 mmHg ($n = 10$) in the Non SLE mice group, 94 ± 7 mmHg ($n = 10$) in the vehicle treated SLE mice group, and 96 ± 9 mmHg ($n = 10$) in EET-A treated SLE mice at the start of the experimental protocol. SLE mice systolic blood pressure was significantly increased (137 ± 10 mmHg, $n = 10$) compared to Non SLE mice (89 ± 8 mmHg, $P < 0.05$, $n = 10$) at the end of 14 week-experimental protocol. EET-A treatment to SLE mice significantly decreased systolic blood pressure (104 ± 7 mmHg, $n = 10$) compared to vehicle treated SLE mice.

Body weight averaged 28.0 ± 1.7 g ($n = 10$) in the Non SLE mice group, 28.3 ± 2.2 g ($n = 10$) in the vehicle treated SLE mice group, and 27.8 ± 3.0 g ($n = 10$) in EET-A treated SLE mice at the start of the experimental protocol. At the end of 14-week-experimental protocol, the SLE mice had a lower body weight (22.0 ± 1.3 g, $n = 10$) compared to Non SLE mice (41.7 ± 2.0 g, $P < 0.05$, $n = 10$) and EET-A treated mice (37.8 ± 1.2 g, $P < 0.05$, $n = 10$).



EET-A Treatment Decreases Renal CXCL Chemokine and CXC Receptors in SLE Mice

Systemic lupus erythematosus mice had a 3 to 5-fold higher renal cortical mRNA expression of lymphocyte-specific CXC chemokines (CXCL9,10,13, and 16) and CXC receptors (CXCR3 and 4) that contribute to SLE pathophysiology (Figure 1). Interestingly, EET-A treatment for 14 weeks markedly diminished renal CXCL chemokine and CXC receptor mRNA expression in SLE mice. Renal cortical mRNA CXCL9,10,13, and 16 expression was 40–65% lower in EET-A treated SLE mice compared to vehicle treated SLE mice. Similar to chemokines, renal cortical mRNA CXCR3 and 4 receptor expression was 40–60% lower in EET-A treated SLE mice compared to vehicle treated SLE mice (Figures 1A–F).

EET-A Treatment Reduces Renal Cytokine mRNA Expression in SLE Mice

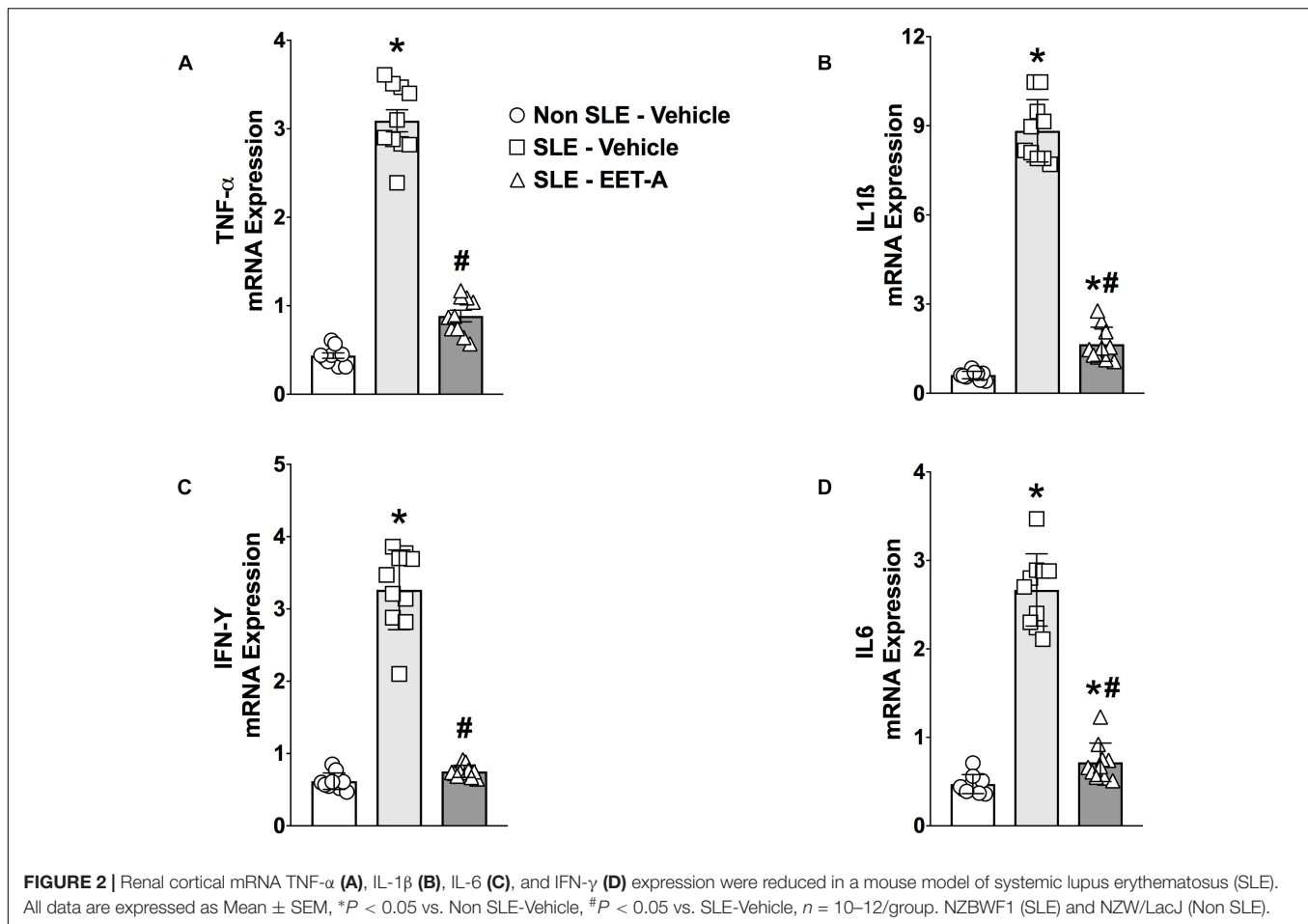
Renal cortical mRNA TNF- α , IL-6, IL-1 β , and IFN- γ cytokine expression was studied in the experimental groups. SLE mice had 5- to 15-fold increase in renal cortical cytokine mRNA expression compared to Non SLE mice (Figures 2A–D). EET-A treatment to SLE mice reduced renal mRNA TNF- α expression 70%, IL-6 expression 74%, IL-1 β expression 80% and IFN- γ expression 76% compared to vehicle treated SLE mice (Figures 2A–D).

Glomerular Inflammatory Cell Infiltration Decreases in EET-A Treated SLE Mice

Glomerular inflammatory cell infiltration was markedly higher in SLE compared to Non SLE mice. SLE mice had a 5-fold increase in glomerular CD43 positive inflammatory cells compared to Non SLE mice. Like CD43 positive cells, SLE mice had a 3-fold increase in glomerular F4/80 positive inflammatory cell levels compared to Non SLE mice. Interestingly, EET-A treated SLE mice had a 50% reduction in glomerular CD43 and F4/80 positive inflammatory cells compared to vehicle treated SLE mice (Figures 3A–D).

EET-A Treatment Decreases Albuminuria and Renal Fibrosis in SLE Mice

In the present study, SLE mice developed kidney injury a dramatic increase in albuminuria compared to Non SLE mice (Figure 4A). Interestingly, EET-A treatment to SLE mice for 14 weeks prominently attenuated renal injury in SLE mice and the albuminuria was 80% lower than vehicle treated SLE mice and at a level similar to Non SLE mice (Figure 4A). Along with albuminuria, we assessed kidney injury by measuring BUN and serum creatinine levels in the experimental groups. Serum creatinine levels were higher in vehicle treated SLE mice (5.0 ± 0.1 mg/dl, n = 10) compared to Non SLE mice (1.8 ± 0.1 mg/dl, P < 0.05, n = 10). Interestingly, serum creatinine levels in EET-A treated SLE mice were lower (3.8 ± 0.2 mg/dl,



P < 0.05, *n* = 10) than vehicle treated SLE mice. SLE mice also had higher BUN levels (54.2 ± 1.7 mg/dl, *n* = 10) compared to Non SLE mice (31.3 ± 1.4 mg/dl, *P* < 0.05, *n* = 10). EET-A treated SLE mice had decreased BUN levels (46.4 ± 2.0 md/dl, *P* < 0.05, *n* = 10) compared vehicle treated SLE mice. SLE mice developed marked renal fibrosis with higher interstitial collagen formation compared to Non SLE mice. Collagen positive renal fibrotic cortical and medullary areas were 4-fold higher in vehicle treated SLR mice compared to Non SLE mice. EET-A treatment in SLE mice significantly decreased renal fibrosis (Figures 4B–D).

DISCUSSION

Systemic lupus erythematosus presents with a diverse array of clinical symptoms, which often reflect the consequences of injury to multiple organ systems, such as the kidney, brain, and skin. The renal manifestation of SLE which is termed LN is a major risk factor for overall morbidity and mortality in SLE. Despite the use of potent anti-inflammatory and immunosuppressive therapies, LN still progresses from chronic kidney disease to end-stage renal disease for too many patients and warrants searching for new therapeutic options (Davis et al., 1996). Mice from specific lupus-prone strains spontaneously develop SLE

with renal manifestations that closely resemble LN symptoms in patients with LN. Among these mice strains, one of the most well-established murine LN models is the female NZBWF1 mice utilized in the current study (Perry et al., 2011). In the present study, we investigated the kidney protective actions of synthetic EET analog in female NZBWF1 SLE mice with LN. We have developed several orally active synthetic EET analogs and demonstrated their marked kidney protective actions in several renal pathologies. These studies indicate that these EET analogs exert potent kidney protective actions through strong anti-inflammatory action in the kidney (Khan et al., 2013; Hye Khan et al., 2013, 2016). In accord to these earlier findings, the present study found that the orally active EET analog, EET-A, demonstrated renal anti-inflammatory action in female NZBWF1 SLE mice that spontaneously develop LN symptoms comparable to that observed in LN patients.

In LN pathophysiology, elevated renal inflammation caused by autoantibody formation is an important event. Typically, LN pathophysiology is linked to autoantibody formation as presence of autoantibodies results in renal inflammation followed by the development of LN (Arbuckle et al., 2003). Because of their contribution in renal inflammation, autoantibodies to dsDNA (anti-dsDNA) are linked to the development of nephritis in SLE (Fenton and Rekvig, 2007), and what separates pathogenic

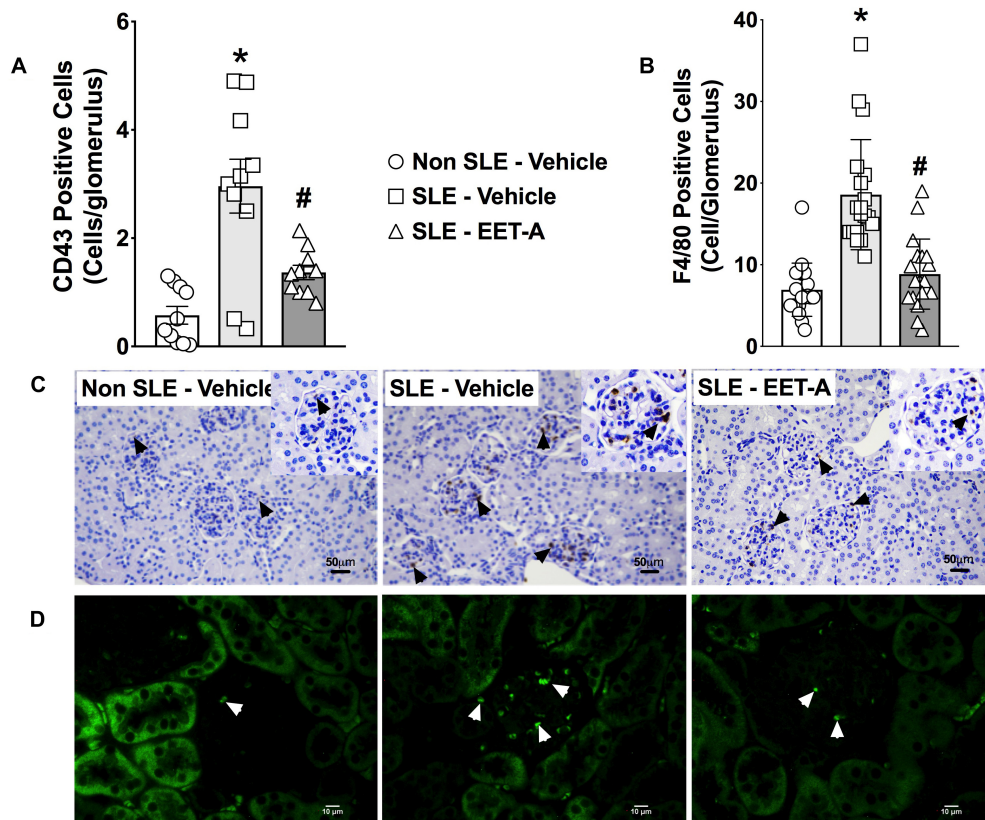
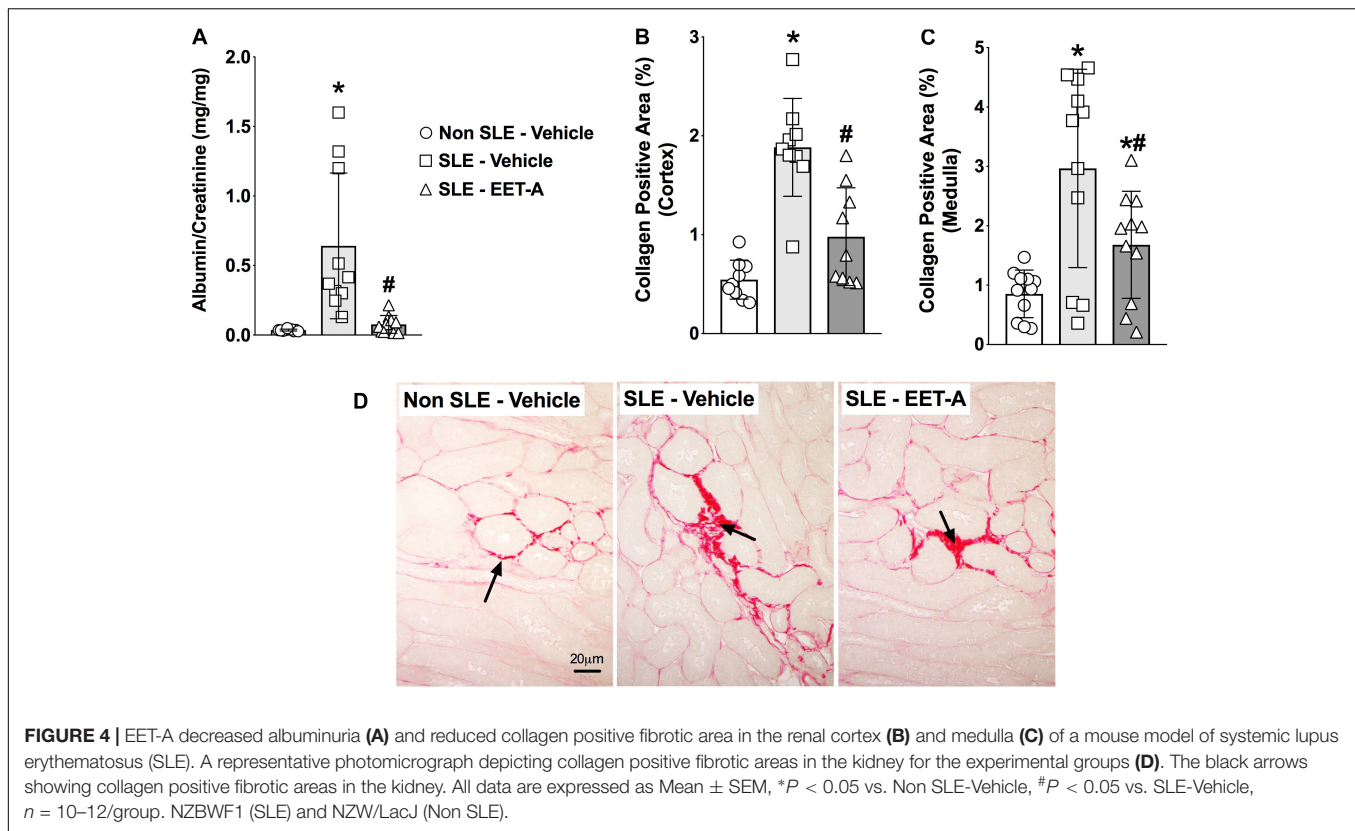


FIGURE 3 | In a mouse model of systemic lupus erythematosus (SLE), EET-A reduced glomerular infiltration of CD43 positive immune cells (A) and F4/80 positive macrophages (B). Representative photomicrographs depicting CD43 positive (black arrows) immune cells (C) and F4/80 positive (white arrows) macrophages (D) in the glomeruli for the experimental groups. All data are expressed as Mean \pm SEM, * P < 0.05 vs. Non SLE-Vehicle, # P < 0.05 vs. SLE-Vehicle, n = 10–12/group. NZBWF1 (SLE) and NZW/LacJ (Non SLE).

from non-pathogenic anti-dsDNA antibodies is not clear (Zykova et al., 2007). SLE mice with LN in the present study had elevated serum anti-dsDNA compared to Non SLE mice, and EET-A treatment to SLE mice did not affect anti-dsDNA levels. On the other hand, EET-A treated SLE mice had decreased renal inflammation, decreased proteinuria, and reduced renal fibrosis. This finding could be related to the possible presence of more non-pathogenic versus pathogenic anti-dsDNA in the SLE LN mouse model used in the present study. However, we believe this may not be the case as the SLE mice in the present study had marked renal inflammation, renal dysfunction, proteinuria, and renal fibrosis that indicate a possible contribution for pathogenic anti-dsDNA to LN pathophysiology in SLE mice. The dissociation between renal protective EET-A actions and the level of anti-dsDNA in the SLE mice could also be related to the fact that several LN models do not have elevated anti-dsDNA. In *Tlr9*-deficient MRL/+ mice that have LN, marked proteinuria and glomerular injury occurs in the absence of autoantibodies (Nickerson et al., 2017). Additionally, a neuropsychiatric SLE model, JhD/MRL/lpr mice, does not require autoantibodies to develop neuropsychiatric disease (Wen et al., 2016). Taken together, our findings provide evidence that the EET-A kidney protection in SLE LN mice does not require a reduction in

autoantibodies and is associated with the ability for EET-A to decrease renal inflammation.

Progressive kidney injury in SLE results from pathogenic anti-dsDNA antibodies that deposit as immune complexes (Cameron, 1999). Immune complex formation and/or deposition in the kidney results in the synthesis of various mediators of inflammation, cellular infiltration of immune cells, proteinuria, renal fibrosis, and progressive renal failure. We demonstrated an increase in CD43 positive immune cells in the glomeruli of SLE LN mice that was attenuated in SLE LN mice treated with EET-A. CD43 positive immune cells consist of leukocytes and dendritic cells. Leukocytes and dendritic cells are important mediators to LN progression in both mouse SLE models and human SLE patients. Renal dendritic cell infiltration is associated with poor renal outcome in SLE patients (Hill et al., 2001). Immune cells express elevated levels of molecules that are necessary for their homing that increases homing to the kidney in LN (Hase et al., 2001; Yamada et al., 2002). Mechanisms by which leukocytes contribute to tissue injury include the activation of nephritogenic antibody-producing inflammatory cells and cytokine production and recruitment (Apostolidis et al., 2011). Depleting or blocking of leukocyte activation reduces LN progression SLE mouse models (Schiffer et al., 2003). Comparable to CD43 positive



immune cell kidney infiltration, we demonstrated elevated F4/80 positive macrophage glomerular infiltration in the kidney of LN mice. Interestingly, EET-A treated SLE mice had markedly decrease glomerular macrophage infiltration. This is an important finding because macrophages contribute to LN pathogenesis and progression. Renal macrophage infiltration is associated with poor clinical outcomes LN patients (Hill et al., 2001). Several studies have shown that activated macrophage populations play an important role in the pathophysiology of LN in murine models (Schiffer et al., 2008). The contribution for macrophages in LN pathophysiology is further supported by macrophage depletion studies. These studies elegantly demonstrated that macrophages are not only present during LN but also actively contribute to the LN pathogenesis (Hasegawa et al., 2003; Shimizu et al., 2004). Findings in the current study demonstrate that EET-A treated SLE mice had decreased CD43 positive immune cell and F4/F80 positive macrophage glomerular infiltration that contributes to decreased LN pathogenesis.

Renal chemokine production during LN precedes inflammatory cell infiltration, proteinuria, and renal fibrosis (Fan et al., 1997). Chemokines promote chemotaxis and activation of selected inflammatory cell subpopulations that express specific chemokine receptors (Premack and Schall, 1996). Likewise, a role for several chemokines in several acute inflammatory renal disorders including SLE has been described (Feng et al., 1995, 1999; Wenzel et al., 1997). Chemokines play an important pathophysiological role in LN. Indeed, a common pathological finding in LN is inflammatory cell infiltration in the affected

tissue resulting from chemotaxis by chemokines and their receptors. In the present study, we demonstrated a marked increase renal cortical expression of CXC chemokines and their receptors in SLE mice. SLE mice with LN had higher CXCR3 and its ligands CXCL9 and 10 renal expression. Previous studies demonstrated that the CXCR3 receptor–ligand system is involved in chemotaxis of inflammatory cells in the affected target tissue. Evidence for the CXCR3 pathway in LN comes from the results of an extensive glomerular expression microarray analysis SLE MRL/lpr mice (Teramoto et al., 2008). Indeed, chemokines and chemokine receptors including CXCR3 and its ligands, CXCL9 and 10 play an important role in the pathogenesis of LN. Interestingly, prednisolone treatment to SLE MRL/lpr mice attenuated CXCR3 receptor upregulation inflammatory cell infiltration (Lacotte et al., 2009). In the present study, along with higher CXCR3 receptor–ligand system expression, there was marked glomerular CD43 immune cell and F4/F80 macrophage infiltration in the kidney of LN mice. This finding corroborates earlier findings on the pathophysiological role for CXCR3 and its ligands in LN. Interestingly, SLE mice treated with EET-A had markedly lower renal cortical CXCR3 receptor–ligand mRNA expression. EET-A treated SLE LN mice also had fewer CD43 immune cells and F4/F80 macrophages in the glomeruli. These findings clearly indicate a strong ability for EET-A to attenuate chemotaxis and glomerular inflammatory cell infiltration in LN.

The chemotaxis attenuating effect of EET-A was further evident from its ability to decrease several other chemokines

and receptors that contribute to LN pathophysiology. We demonstrate marked renal CXCR4 expression in SLE mice that is in agreement with earlier findings indicated that CXCR4 is crucial for SLE pathogenesis in mice (Wang et al., 2009). Elevated CXCR4 levels in SLE mice were found to prolong inflammatory cell migration to end-organs via its ligand (Wang et al., 2009). In addition, CXCR4 ligand has been shown to be selectively upregulated in kidney glomeruli of NZB/W, BXSB, and MRL/lpr SLE mice models with LN and in LN patients. (Balabanian et al., 2003; Togel et al., 2005; Chong and Mohan, 2009; Wang et al., 2010). The current findings in SLE LN mice also demonstrate a contribution for the CXC chemokines CXCL13 and CXCL16. Moreover, EET-A treated SLE mice had reduced renal mRNA expression of these important chemokines that are implicated in LN pathophysiology. CXCL13 is an important chemokine for LN pathology and several human and animal studies support its critical role in LN. Serum CXCL13 levels and kidney CXCL13 mRNA expression have been found to be higher in LN patients with increased disease severity (Lee et al., 2010; Ezzat et al., 2011). Likewise, increased CXCL13 expression has been demonstrated in female NZBWF1 LN mice (Shen et al., 2012). Our findings also demonstrate that SLE LN mice had markedly higher renal cortical CXCL16 mRNA expression that is a key mediator of the renal inflammation in LN (Norlander et al., 2013). CXCL16 has been shown to be elevated in several strains of mice and patients with LN and correlates well with elevated proteinuria and SLE disease activity index scores (Wu et al., 2007). Overall, our findings corroborate several earlier findings that clearly indicated a critical role for chemokines in LN. Most importantly, we determined that an orally active EET analog, EET-A, prevented LN in SLE mice in part by preventing chemotaxis and glomerular inflammatory cell infiltration in the kidney.

Although it is apparent that chemokines contribute significantly to inflammatory cell influx into sites of tissue injury, chemokines must be considered part of a concerted interaction involving cytokines. Indeed, renal upregulation of several proinflammatory cytokines, such as TNF- α , IFN- γ , and IL-1 β was observed in SLE LN mice. These proinflammatory cytokines have been demonstrated to participate in several pathophysiologic processes in SLE mice. For example, IFN- γ is required for LN. IFN- γ deficient MRL/lpr mice are protected from lymphadenopathy and early death, and the severity of renal damage was reduced in these mice (Balomenos et al., 1998; Schwarting et al., 1998). In kidney biopsies from LN patients, TNF- α and IL-6 mRNA expressions were elevated (Herrera-Esparza et al., 1998). In addition, administration of anti-TNF- α

antibodies was able to abrogate mercuric chloride-induced lupus-like autoimmune disease in rats (Molina et al., 1995). In our study, involvement of cytokines in LN pathophysiology was associated with elevated renal mRNA TNF- α , IL-6, IL-1 β , and IFN- γ cytokine expression in female NZBWF1 SLE mice. Indeed, these findings clearly corroborate several earlier findings on cytokine contribution to LN pathophysiology (Balomenos et al., 1998; Herrera-Esparza et al., 1998; Schwarting et al., 1998). As an important finding, EET-A treatment decreased mRNA TNF- α , IL-6, IL-1 β , and IFN- γ expression in the kidney cortex of LN mice. This finding further strengthens our findings that EET-A has strong renal anti-inflammatory action to protect the kidney in SLE from LN.

In summary, the current study demonstrates elevated renal chemotaxis that can result in cytokine production and renal glomeruli inflammatory cell infiltration in female NZBWF1 SLE LN mice. These findings clearly indicate potent EET-A kidney protective and anti-inflammatory actions in SLE LN mice which is associated with decreased chemotaxis and cytokine expression in the kidney. Most importantly, we provide unique data on the biological actions for a synthetic EET analog and the potential for an EET analog-based novel SLE LN therapy.

AUTHOR CONTRIBUTIONS

MAHK and JI conceived the study, interpreted the data, and wrote the manuscript. MAHK and AS performed the experiments. JF and MAS designed and synthesized EET-A. All authors edited the manuscript and approved the submitted version.

FUNDING

The Robert A. Welch Foundation provided support to JF (I-0011). A National Institute of Health (NIH) grant to JI (DK103616), a Medical College of Wisconsin Lupus Research Grant to JI, and a Dr. Ralph and Marian Falk Medical Research Trust Bank of America, N.A., Trustee Grant to JI and JF.

ACKNOWLEDGMENTS

The authors thank Melissa Skibba and Wojciech Jankiewicz for kidney histological analysis.

REFERENCES

- Apostolidis, S. A., Crispin, J. C., and Tsokos, G. C. (2011). IL-17-producing T cells in lupus nephritis. *Lupus* 20, 120–124. doi: 10.1177/0961203310389100
- Arbuckle, M. R., McClain, M. T., Rubertone, M. V., Scofield, R. H., Dennis, G. J., James, J. A., et al. (2003). Development of autoantibodies before the clinical onset of systemic lupus erythematosus. *N. Engl. J. Med.* 349, 1526–1533.
- Balabanian, K., Couderc, J., Bouchet-Delbos, L., Amara, A., Berrebi, D., Foussat, A., et al. (2003). Role of the chemokine stromal cell-derived factor 1 in autoantibody production and nephritis in murine lupus. *J. Immunol.* 170, 3392–3400. doi: 10.4049/jimmunol.170.6.3392
- Balomenos, D., Rumold, R., and Theofilopoulos, A. N. (1998). Interferon gamma is required for lupus-like disease and lympho accumulation in MRL-lpr mice. *J. Clin. Invest.* 101, 364–371. doi: 10.1172/jci750
- Cameron, J. S. (1999). Lupus nephritis. *J. Am. Soc. Nephrol.* 10, 413–424.
- Chong, B. F., and Mohan, C. (2009). Targeting the CXCR4/CXCL12 axis in systemic lupus erythematosus. *Expert. Opin. Ther. Targets* 13, 1147–1153. doi: 10.1517/14728220903196761

- Contreras, G., Pardo, V., Leclercq, B., Lenz, O., Tozman, E., O'Nan, P., et al. (2004). Sequential therapies for proliferative lupus nephritis. *N. Engl. J. Med.* 350, 971–980. doi: 10.1056/nejmoa031855
- Dall'Era, M. (2017). Treatment of lupus nephritis: current paradigms and emerging strategies. *Curr. Opin. Rheumatol.* 29, 241–247. doi: 10.1097/BOR.0000000000000381
- Davis, J. C., Tassioulas, I. O., and Boumpas, D. T. (1996). Lupus nephritis. *Curr. Opin. Rheumatol.* 8, 415–423.
- Ezzat, M., El-Gammasy, T., Shaheen, K., and Shokr, E. (2011). Elevated production of serum B-cell-attracting chemokine-1 (BCA-1/CXCL13) is correlated with childhood-onset lupus disease activity, severity, and renal involvement. *Lupus* 20, 845–854. doi: 10.1177/0961203311398513
- Fan, X., Oertli, B., and Wuthrich, R. P. (1997). Up-regulation of tubular epithelial interleukin-12 in autoimmune MRL-Fas(lpr) mice with renal injury. *Kidney Int.* 51, 79–86. doi: 10.1038/ki.1997.10
- Feng, L., Chen, S., Garcia, G. E., Xia, Y., Siani, M. A., Botti, P., et al. (1999). Prevention of crescentic glomerulonephritis by immunoneutralization of the fractalkine receptor CX3CR1: rapid communication. *Kidney Int.* 56, 612–620. doi: 10.1046/j.1523-1755.1999.00604.x
- Feng, L., Xia, Y., Yoshimura, T., and Wilson, C. B. (1995). Modulation of neutrophil influx in glomerulonephritis in the rat with anti-macrophage inflammatory protein-2 (MIP-2) antibody. *J. Clin. Invest.* 95, 1009–1017. doi: 10.1172/jci117745
- Fenton, K. A., and Rekvig, O. P. (2007). A central role of nucleosomes in lupus nephritis. *Ann. N. Y. Acad. Sci.* 1108, 104–113. doi: 10.1196/annals.1422.012
- Gilkeson, G. S. (2015). Complement-targeted therapies in Lupus. *Curr. Treat. Options Rheum.* 1, 10–18. doi: 10.1016/j.ekir.2016.06.005
- Hase, K., Tani, K., Shimizu, T., Ohmoto, Y., Matsushima, K., and Sone, S. (2001). Increased CCR4 expression in active systemic lupus erythematosus. *J. Leukoc. Biol.* 70, 749–755.
- Hasegawa, H., Kohno, M., Sasaki, M., Inoue, A., Ito, M. R., Terada, M., et al. (2003). Antagonist of monocyte chemoattractant protein 1 ameliorates the initiation and progression of lupus nephritis and renal vasculitis in MRL/lpr mice. *Arthritis Rheum* 48, 2555–2566. doi: 10.1002/art.11231
- Herrera-Esparza, R., Barbosa-Cisneros, O., Villalobos-Hurtado, R., and Avalos-Diaz, E. (1998). Renal expression of IL-6 and TNF α genes in lupus nephritis. *Lupus* 7, 154–158. doi: 10.1191/096120398678919949
- Hill, G. S., Delahousse, M., Nochy, D., Mandet, C., and Bariety, J. (2001). Proteinuria and tubulointerstitial lesions in lupus nephritis. *Kidney Int.* 60, 1893–1903. doi: 10.1046/j.1523-1755.2001.00017.x
- Hye Khan, M. A., Fish, B., Wahl, G., Sharma, A., Falck, J. R., Paudyal, M. P., et al. (2016). Epoxyeicosatrienoic acid analogue mitigates kidney injury in a rat model of radiation nephropathy. *Clin. Sci.* 130, 587–599. doi: 10.1042/CS20150778
- Hye Khan, M. A., Kolb, L., Skibba, M., Hartmann, M., Blöcher, R., Proschak, E., et al. (2018). A novel dual PPAR- γ agonist/sEH inhibitor treats diabetic complications in a rat model of type 2 diabetes. *Diabetologia* 61, 2235–2246. doi: 10.1007/s00125-018-4685-0
- Hye Khan, M. A., Neckár, J., Manthali, V., Errabelli, R., Pavlov, T. S., Staruschenko, A., et al. (2013). Orally active epoxyeicosatrienoic acid analog attenuates kidney injury in hypertensive Dahl salt-sensitive rat. *Hypertension* 62, 905–913. doi: 10.1161/HYPERTENSIONAHA.113.01949
- Jordan, N., and D'Cruz, D. (2016). Current and emerging treatment options in the management of lupus. *Immunotargets Ther.* 5, 9–20. doi: 10.2147/ITT.S40675
- Khan, M. A., Liu, J., Kumar, G., Skapek, S. X., Falck, J. R., and Imig, J. D. (2013). Novel orally active epoxyeicosatrienoic acid (EET) analogs attenuate cisplatin nephrotoxicity. *FASEB J.* 27, 2946–2956. doi: 10.1096/fj.12-218040
- Lacotte, S., Brun, S., Muller, S., and Dumortier, H. (2009). CXCR3, inflammation, and autoimmune diseases. *Ann. N. Y. Acad. Sci.* 1173, 310–317. doi: 10.1111/j.1749-6632.2009.04813.x
- Lech, M., and Anders, H. J. (2013). The pathogenesis of lupus nephritis. *J. Am. Soc. Nephrol.* 24, 1357–1366. doi: 10.1681/ASN.2013010026
- Lee, H. T., Shiao, Y. M., Wu, T. H., Chen, W. S., Hsu, Y. H., Tsai, S. F., et al. (2010). Serum BLC/CXCL13 concentrations and renal expression of CXCL13/CXCR5 in patients with systemic lupus erythematosus and lupus nephritis. *J. Rheumatol.* 37, 45–52. doi: 10.3899/jrheum.090450
- Lu, J., Szeto, C. C., Tam, L. S., Lai, F. M., Li, E. K., Chow, K. M., et al. (2012). Relationship of intrarenal gene expression and the histological class of lupus nephritis – a study on repeat renal biopsy. *J. Rheumatol.* 39, 1942–1947. doi: 10.3899/jrheum.120177
- Molina, A., Sa'nchez-Madrid, F., Bricio, T., Mart'n, A., Escudero, E., Alvarez, V., et al. (1995). Abrogation of mercuric chloride induced nephritis in the Brown Norway rat by treatment with antibodies against TNF α . *Med. Inflamm.* 4, 444–451. doi: 10.1155/s0962935195000718
- Nickerson, K. M., Wang, Y., Bastacky, S., and Shlomchik, M. J. (2017). Toll-like receptor 9 suppresses lupus disease in Fas-sufficient MRL Mice. *PLoS One* 12:e0173471. doi: 10.1371/journal.pone.0173471
- Norlander, A. E., Saleh, M. A., and Madhur, M. S. (2013). CXCL16: a chemokine-causing chronic kidney disease. *Hypertension* 62, 1008–1010. doi: 10.1161/hypertensionaha.113.01954
- Perry, D., Sang, A., Yin, Y., Zheng, Y. Y., and Morel, L. (2011). Murine models of systemic lupus erythematosus. *J. Biomed. Biotechnol.* 2011:271694. doi: 10.1155/2011/271694
- Premack, B. A., and Schall, T. J. (1996). Chemokine receptors: gateways to inflammation and infection. *Nat. Med.* 2, 1174–1178. doi: 10.1038/nm1196-1174
- Schiffer, L., Bethunaickan, R., Ramanujam, M., Huang, W., Schiffer, M., Tao, H., et al. (2008). Activated renal macrophages are markers of disease onset and disease remission in lupus nephritis. *J. Immunol.* 180, 1938–1947. doi: 10.4049/jimmunol.180.3.1938
- Schiffer, L., Sinha, J., Wang, X., Huang, W., von Gersdorff, G., Schiffer, M., et al. (2003). Short term administration of costimulatory blockade and cyclophosphamide induces remission of systemic lupus erythematosus nephritis in NZB/W F1 mice by a mechanism downstream of renal immune complex deposition. *J. Immunol.* 171, 489–497. doi: 10.4049/jimmunol.171.1.489
- Schwartz, A., Wada, T., Kinoshita, K., Tesch, G., and Kelley, V. R. (1998). IFN- γ receptor signaling is essential for the initiation, acceleration, and destruction of autoimmune kidney disease in MRL-Fas(lpr) mice. *J. Immunol.* 161, 494–503.
- Shen, Y., Sun, C. Y., Wu, F. X., Chen, Y., Dai, M., Yan, Y. C., et al. (2012). Association of intrarenal B-cell infiltrates with clinical outcome in lupus nephritis: a study of 192 cases. *Clin. Dev. Immunol.* 2012:967584. doi: 10.1155/2012/967584
- Shimizu, S., Nakashima, H., Masutani, K., Inoue, Y., Miyake, K., Akahoshi, M., et al. (2004). Anti-monocyte chemoattractant protein-1 gene therapy attenuates nephritis in MRL/lpr mice. *Rheumatology* 43, 1121–1128. doi: 10.1093/rheumatology/keh277
- Skibba, M., Hye Khan, M. A., Kolb, L. L., Yeboah, M. M., Falck, J. R., Amaradhi, R., et al. (2017). Epoxyeicosatrienoic acid analog decreases renal fibrosis by reducing epithelial-to-mesenchymal transition. *Front. Pharmacol.* 8:406. doi: 10.3389/fphar.2017.00406
- Teramoto, K., Negoro, N., Kitamoto, K., Iwai, T., Iwao, H., Okamura, M., et al. (2008). Microarray analysis of glomerular gene expression in murine lupus nephritis. *J. Pharmacol. Sci.* 106, 56–67. doi: 10.1254/jphs.fp0071337
- Togel, F., Isaac, J., Hu, Z., Weiss, K., and Westenfelder, C. (2005). Renal SDF-1 signals mobilization and homing of CXCR4-positive cells to the kidney after ischemic injury. *Kidney Int.* 67, 1772–1784. doi: 10.1111/j.1523-1755.2005.00275.x
- Wang, A., Fairhurst, A. M., Tus, K., Subramanian, S., Liu, Y., Lin, F., et al. (2009). CXCR4/CXCL12 hyperexpression plays a pivotal role in the pathogenesis of lupus. *J. Immunol.* 182, 4448–4458. doi: 10.4049/jimmunol.0801920
- Wang, A., Guilpain, P., Chong, B. F., Chouzenoux, S., Guillemin, L., Du, Y., et al. (2010). Dysregulated expression of CXCR4/CXCL12 in subsets of patients with systemic lupus erythematosus. *Arthritis Rheum* 2010, 3436–3446. doi: 10.1002/art.27685
- Wen, J., Doerner, J., Chalmers, S., Stock, A., Wang, H., Gullinello, M., et al. (2016). B cell and/or autoantibody deficiency do not prevent neuropsychiatric disease in murine systemic lupus erythematosus. *J. Neuroinflamm.* 13:73.
- Wenzel, U., Schneider, A., Valente, A. J., Abboud, H. E., Thaiss, F., Helmchen, U. M., et al. (1997). Monocyte chemoattractant protein-1 mediates monocyte/macrophage influx in anti-thymocyte antibody-induced glomerulonephritis. *Kidney Int.* 51, 770–776. doi: 10.1038/ki.1997.108
- Wu, T., Xie, C., Wang, H. W., Zhou, X. J., Schwartz, N., Calixto, S., et al. (2007). Elevated urinary vcam-1, p-selectin, soluble tnfr receptor-1, and

- cxcl1 chemokine ligand 16 in multiple murine lupus strains and human lupus nephritis. *J. Immunol.* 179, 7166–7175. doi: 10.4049/jimmunol.179.10.7166
- Yamada, M., Yagita, H., Inoue, H., Takanashi, T., Matsuda, H., Munechika, E., et al. (2002). Selective accumulation of CCR4+ T lymphocytes into renal tissue of patients with lupus nephritis. *Arthritis Rheum* 46, 735–740. doi: 10.1002/art.10112
- Yeboah, M. M., Hye Khan, M. A., Chesnik, M. A., Sharma, A., Paudyal, M. P., Falck, J. R., et al. (2016). The epoxyeicosatrienoic acid analog PVPA ameliorates cyclosporine-induced hypertension and renal injury in rats. *Am. J. Physiol. Renal Physiol.* 311, F576–F585. doi: 10.1152/ajprenal.00288.2016
- Zykova, S. N., Seredkina, N. E., and Rekvig, O. P. (2007). Glomerular targets for autoantibodies in lupus nephritis – an apoptotic origin. *Ann. N. Y. Acad. Sci.* 1108, 1–10. doi: 10.1196/annals.1422.001
- Conflict of Interest Statement:** JI and JF have patents that covers the composition of matter for EET-A.
- The remaining authors declare that the research was conducted in the absence of any commercial or financial relationships that could be construed as a potential conflict of interest.

Copyright © 2019 Hye Khan, Stavniichuk, Sattar, Falck and Imig. This is an open-access article distributed under the terms of the Creative Commons Attribution License (CC BY). The use, distribution or reproduction in other forums is permitted, provided the original author(s) and the copyright owner(s) are credited and that the original publication in this journal is cited, in accordance with accepted academic practice. No use, distribution or reproduction is permitted which does not comply with these terms.



Dimethyl Sulfoxide Decreases Levels of Oxylin Diols in Mouse Liver

Poonamjot Deol^{1*}, Jun Yang², Christophe Morisseau², Bruce D. Hammock² and Frances M. Sladek¹

¹ Department of Molecular, Cell and Systems Biology, University of California, Riverside, Riverside, CA, United States,

² Department of Entomology and Nematology and UCD Comprehensive Cancer Center, University of California, Davis, Davis, CA, United States

OPEN ACCESS

Edited by:

Lei Xi,
Virginia Commonwealth University,
United States

Reviewed by:

Mohammed A. Nayeem,
West Virginia University, United States
Narasimham L. Parinandi,
The Ohio State University,
United States

*Correspondence:

Poonamjot Deol
pdeol001@gmail.com

Specialty section:

This article was submitted to
Translational Pharmacology,
a section of the journal
Frontiers in Pharmacology

Received: 07 February 2019

Accepted: 06 May 2019

Published: 29 May 2019

Citation:

Deol P, Yang J, Morisseau C,
Hammock BD and Sladek FM (2019)
Dimethyl Sulfoxide Decreases Levels
of Oxylin Diols in Mouse Liver.
Front. Pharmacol. 10:580.
doi: 10.3389/fphar.2019.00580

Dimethylsulfoxide (DMSO) is widely used as a solvent and cryopreservative in laboratories and considered to have many beneficial health effects in humans. Oxylin Diols are a class of biologically active metabolites of polyunsaturated fatty acids (PUFAs) that have been linked to a number of diseases. In this study, we investigated the effect of DMSO on oxylin Diol levels in mouse liver. Liver tissue from male mice (C57Bl6/N) that were either untreated or injected with 1% DMSO at 18 weeks of age was analyzed for oxylin Diol levels using ultrahigh performance liquid chromatography tandem mass spectrometry (UPLC-MS/MS). A decrease in oxylin Diols from linoleic acid (LA, C18:2n6), alpha-linolenic acid (ALA, C18:3n3) and docosahexaenoic acid (DHA, C22:6n3) was observed 2 h after injection with DMSO. In contrast, DMSO had no effect on the epoxide precursors or other oxylin Diols including those derived from arachidonic acid (C20:4n6) or eicosapentaenoic acid (EPA, C20:5n3). It also did not significantly affect the diol:epoxide ratio, suggesting a pathway distinct from, and potentially complementary to, soluble epoxide hydrolase inhibitors (sEHL). Since oxylin Diols have been associated with a wide array of pathological conditions, from arthritis pain to obesity, our results suggest one potential mechanism underlying the apparent beneficial health effects of DMSO. They also indicate that caution should be used in the interpretation of results using DMSO as a vehicle in animal experiments.

Keywords: DMSO, antioxidant, inflammation, pain, arthritis, obesity, oxylin Diols

INTRODUCTION

Dimethyl sulfoxide [DMSO, (CH₃)₂SO] is a polar aprotic compound with a high affinity for water (Brayton, 1986). It is commonly used as a solvent in biological experiments because it has low toxicity, can solubilize both polar and non-polar substances and can readily penetrate hydrophobic barriers such as the plasma membrane. These properties make it an ideal vehicle for both *in vivo* and *in vitro* experiments, especially for pharmacologic compounds that act on an intracellular level (Brayton, 1986).

Dimethyl sulfoxide has been reported to have therapeutic effects on a number of ailments including bacterial infections (Guo et al., 2016), dermatologic conditions (Lishner et al., 1985), chronic prostatitis (Shirley et al., 1978), gastrointestinal disorders (Salim, 1991, 1992a,b), pulmonary fibrosis and amyloidosis (Pepin and Langner, 1985; Iwasaki et al., 1994) arthritis (Elisia et al., 2016) and pain (Kingery, 1997; Kelava et al., 2011; Kumar et al., 2011; Rawls et al., 2017).

Hepatoprotective effects of DMSO under various conditions of liver injury or hepatotoxicity have also been well documented (Siegers, 1978; Park et al., 1988; Achudume, 1991; Lind et al., 2000; Sahin et al., 2004). Although the physiological and pharmacological mechanisms underlying the beneficial health effects of DMSO are not fully known, they have been proposed to include its ability to increase blood flow to organs, decrease recruitment and activation of inflammatory cells and act as an antioxidant and free radical scavenger (Brayton, 1986; Beilke et al., 1987; Massion et al., 1996).

Oxylipins are biologically active, oxidized metabolites of long chain polyunsaturated fatty acids (PUFAs) that are generated by three different pathways – COX, LOX and CYP/sEH (Yang et al., 2009) (**Figure 1**). The third pathway consists of a two-step reaction involving the action of cytochrome P450s (CYPs) and soluble epoxide hydrolase (sEH) enzymes. This pathway first produces oxylipin epoxides and then diols from linoleic acid (LA, C18:2 n-6), alpha-linolenic acid (ALA, C18:3 n-3), arachidonic acid (AA, C20:4 n-6), eicosapentaenoic acid (EPA, C20:5 n-3) and docosahexaenoic acid (DHA, C22:6 n-3) (Moghaddam et al., 1997; Zeldin, 2001; Levick et al., 2007). Increased accumulation of oxylipin diols has been correlated with the pathogenesis of a number of pathological conditions including obesity, diabetes, depression, pain and cardiovascular disease (Gouveia-Figueira et al., 2015; Caligiuri et al., 2017; Deol et al., 2017; Hennebelle et al., 2017). Compounds that inhibit the formation of these lipid mediators, such as inhibitors of sEH (sEHI), have been shown to have therapeutic potential (Imig and Hammock, 2009; Morisseau et al., 2010; Wagner et al., 2017).

Dimethyl sulfoxide has been shown to attenuate the accumulation of lipids in the liver as well as free fatty acid-induced cellular lipotoxicity (Song et al., 2012). However, to our knowledge, the effect of DMSO on the hepatic levels of oxygenated fatty acid metabolites such as oxylipins has not been studied. Here, we investigate the effect of a single intraperitoneal injection of DMSO on the levels of approximately 60 oxylipin species in mouse liver. Our results show that DMSO lowers the levels of certain oxylipins, all of which are diols generated by the metabolism of omega-3 and omega-6 fatty acids LA, ALA and DHA.

MATERIALS AND METHODS

Animals

Care and treatment of animals were in accordance with guidelines from and approved by the University of California, Riverside Institutional Animal Care and Use Committee (AUP #20140014). All mice had *ad libitum* access to regular vivarium chow (Purina Test Diet 5001, Newco Distributors, Rancho Cucamonga, CA) and water. At the end of the study, mice were sacrificed by CO₂ inhalation followed by cervical dislocation, in accordance with stated NIH guidelines. C57BL/6N mice (Charles River Laboratories) were bred in-house and maintained on a 12h:12h light-dark cycle in a specific pathogen-free vivarium (SPF) with wood-chip bedding [PJ Murphy sani-chips 2.2 CF # 91100 (MFG 3-002)] and a cotton pad as an environmental stimulant. Pups were weaned at 3 weeks of age with three to four animals housed per cage.

DMSO Treatment

Male mice (~18 weeks old, *n* = 5 per group) were injected intraperitoneally with 200 µl of 1% DMSO (Sigma-Aldrich, catalog # D5879) and sacrificed 2 h later. About 200 mg of freshly excised liver tissue was rinsed in cold phosphate buffered saline (PBS), blotted with a Kimwipe and snap-frozen in liquid nitrogen for subsequent metabolomic analysis. Samples were also collected from a control group of age-matched mice that were not injected.

Oxylipin Analysis

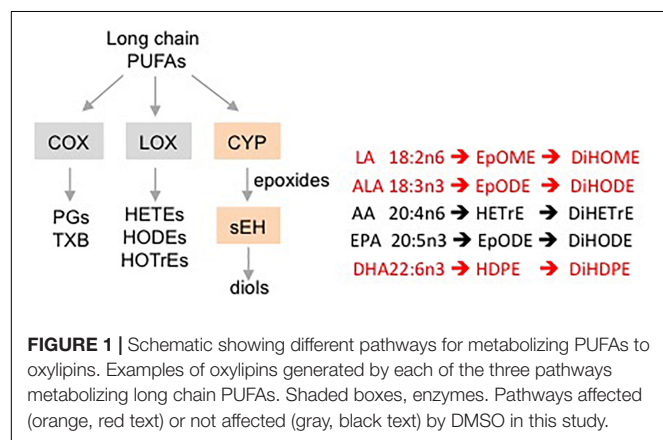
Non-esterified oxylipins were extracted by solid phase extraction from liver tissue homogenates (200 mg) and analyzed by ultrahigh performance liquid chromatography tandem mass spectrometry (UPLC-MS/MS) (Agilent 1200SL-AB Sciex 4000 QTrap) as described previously (Matyash et al., 2008; Yang et al., 2009; Deol et al., 2017). Analyst software v.1.4.2 was used to quantify peaks according to corresponding standard curves with their corresponding internal standards. Hepatic oxylipin concentrations are presented as pmol/gm tissue.

Statistical Analysis

Data are presented as mean ± standard error of mean (SEM). Statistical significance is defined as *P* ≤ 0.05 using Student's *t*-test.

RESULTS

Male mice (~18 weeks old) were injected with 1% DMSO and sacrificed 2 h later. Livers were removed and analyzed for oxylipins in the COX, LOX and CYP/sEH pathways (**Figures 1, 2A**). The 2-h time point was chosen to examine the short-term effects of DMSO and avoid potentially confounding factors that might be introduced by effects on gene expression. Not unexpectedly, the body weight and liver-to-body weight ratio at harvest did not differ between the control and injected groups (**Figure 2B**). Of the 59 oxylipin species analyzed, the DMSO-injected mice showed significantly altered levels of five species, all diols and all of which were decreased: 12,13-DiHODE, 15,16-DiHODE, 12,13-DiHOME, 16,17-DiHDPE and 19,20-DiHDPE



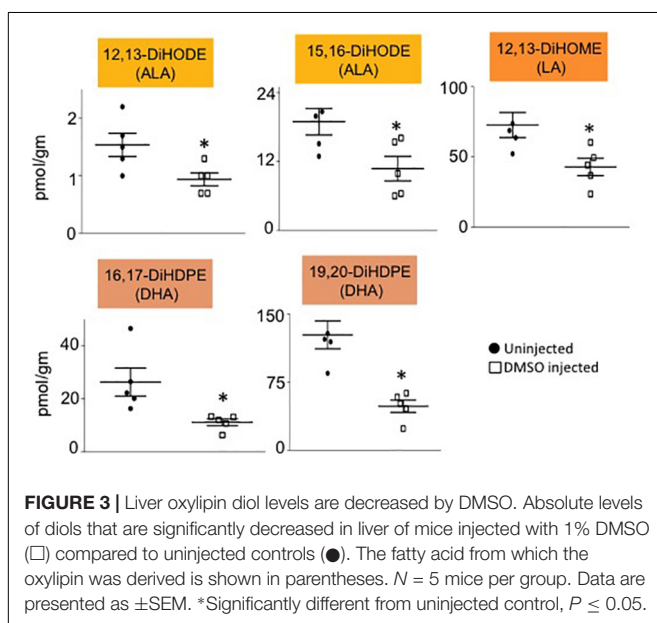
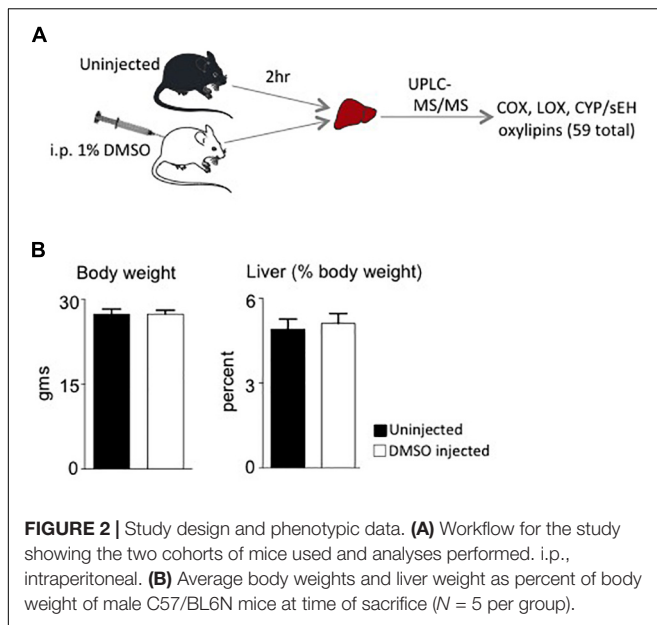


(Figure 3). In addition, levels of two diols – 14,15-DiHETrE and 13,14-DiHDPE – were also lower in the DMSO group, although the decrease did not reach statistical significance (Supplementary Table 1).

Interestingly, all of the oxylipins decreased by DMSO were in the CYP/sEH pathway and generated by hydrolysis of epoxides of LA, ALA and DHA. In contrast, levels of the epoxide precursors of these diols were not impacted by the DMSO treatment (Figure 4A). Diol:epoxide ratios, which are a reflection of sEH activity, were also not significantly different between DMSO and control, although the ratio for the DHA metabolites (DiHDPE:EpDPE) was trending toward significance (Figure 4B).

DISCUSSION

Dimethyl sulfoxide is widely used to treat numerous ailments although the underlying mechanisms remain obscure. Our results show that a single injection of DMSO can cause an immediate and pronounced decrease in oxylipin diols generated from certain omega-3 and omega-6 PUFAs (LA, ALA and DHA) by the CYP/sEH pathway in mouse liver. It was proposed early on that one potential mechanism responsible for the physiological effects of DMSO was its ability to inhibit or activate various enzymes by reversibly altering their configuration (Rammler and Zaffaroni, 1967). DMSO has subsequently been shown to have a stabilizing effect on the RNA transcript levels of CYP enzymes in rat liver hepatocytes (Su and Waxman, 2004), and varying effects on CYP enzymatic activity depending on concentration, substrate and tissue or cell fraction (Chauret et al., 1998; Hickman et al., 1998; Li et al., 2010). At very high concentrations (28% v/v) DMSO has been shown to interact with the iron center of a bacterial cytochrome P450 enzyme (Kuper et al., 2012). We did not observe an alteration in the level of the precursor epoxides, suggesting that DMSO is not acting on the CYP enzymes in our system. Similarly, the diol:epoxide ratio was not significantly altered, suggesting that sEH activity was not altered. Interestingly, oxylipin epoxide and diol levels of two other PUFAs, AA and EPA, were not affected by DMSO. Combined with the relatively short time period needed to observe these effects (2 h), these results suggest that DMSO acts directly, and selectively, on LA, ALA and DHA oxylipin diols (Figure 5). It remains to be determined whether chronic DMSO treatment would show a similar selective effect.

Since the decrease in hepatic oxylipin levels in our experiments does not appear to be due to a decrease in enzyme action, this suggests that, at least in the short term, DMSO is either decreasing the stability or somehow preventing the accumulation of these compounds in the liver. DMSO has been reported to have antioxidant and free-radical scavenging properties (Sanmartín-Suárez et al., 2011; Kabeya et al., 2013). Thus, it is possible that DMSO may be acting as a scavenger for these oxidized metabolites, converting them into products that are not present in our oxylipin panel. Indeed, it has been reported that DMSO, when used as a vehicle, enhances the anti-inflammatory effects of rosemary and ginger (Justo et al., 2015). While the authors attributed this increase to better absorption and distribution of the compounds due to DMSO, it is possible that DMSO itself could have acted as an antioxidant, as has been shown previously (Alemón-Medina et al., 2008; Jia et al., 2010). These observations, along with the current results, indicate that caution should be employed when using DMSO as a vehicle to study the pharmacological efficacy of compounds with antioxidant potential. A direct, non-enzymatic effect of DMSO also suggests that it may have a similar effect in other tissues, and hence a broad applicability to numerous pathologies.

There are two other potential explanations for the reduced levels of the oxylipin diols. The first is that DMSO affects the level of the substrates, in this case LA, ALA and DHA. However, these fatty acids are essential (or in the case of DHA, conditionally essential), meaning that they must be derived from the diet.

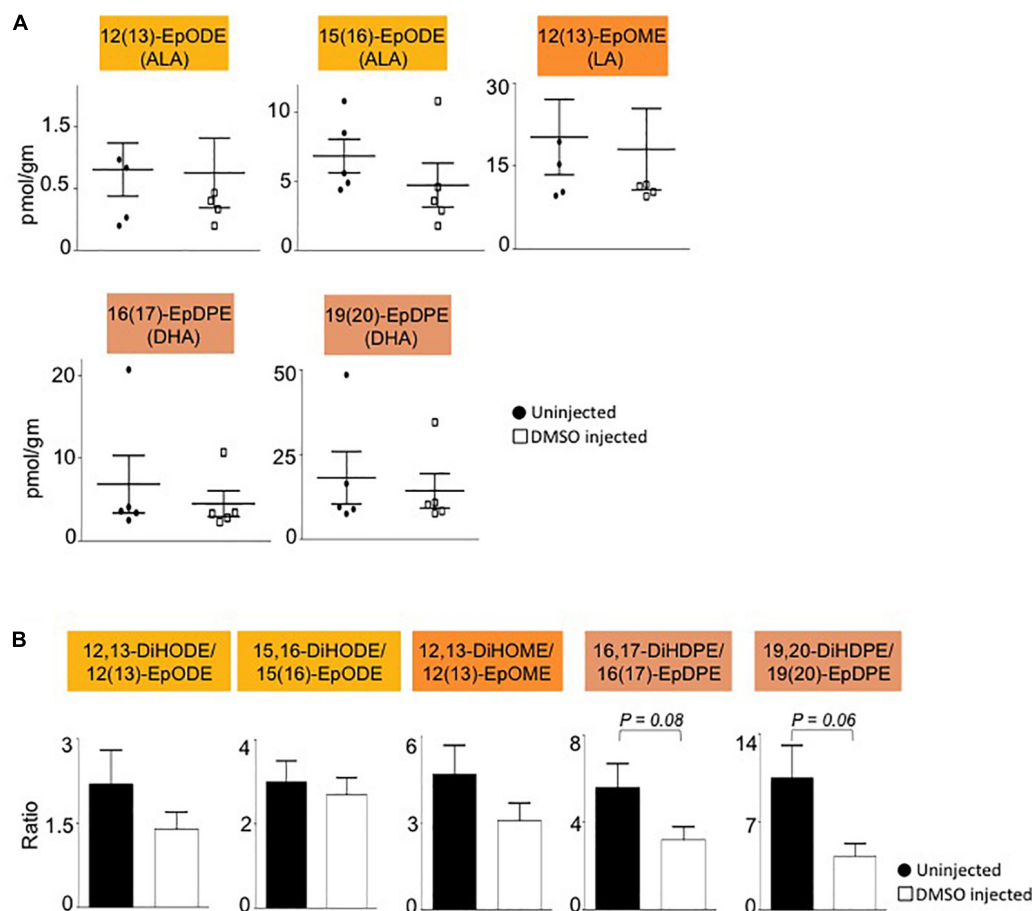
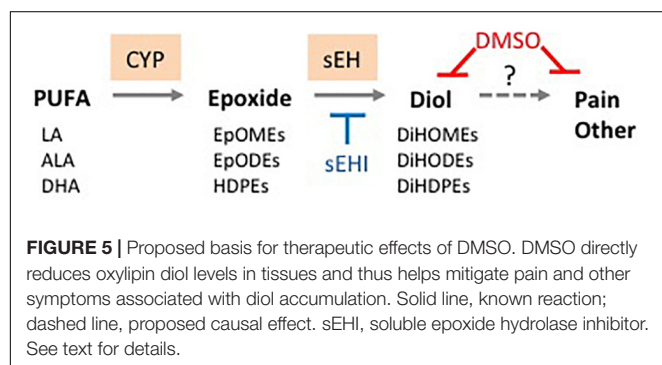


FIGURE 4 | Liver epoxide levels and diol:epoxide ratios are not affected by DMSO. **(A)** Absolute levels of parent epoxides of diols (shown in **Figure 3**) in liver of mice injected with 1% DMSO (□) compared to uninjected controls (●). The fatty acid from which the oxylipin was derived is shown in parentheses. **(B)** Ratio of diol:epoxide as a measure of soluble epoxide hydrolase (sEH) activity. Color coding for parental fatty acid is same as in panel **(A)** and **Figure 3**. $N = 5$ mice per group. Data are presented as \pm SEM. Significance is defined as $P \leq 0.05$.

Consequently, the body has robust mechanisms to maintain their levels (Tove and Smith, 1960; Lin and Conner, 1990; Lin et al., 1993; Calder, 2016) making it unlikely that within 2 h of injecting DMSO there would be a large decrease in the steady state levels of these essential fatty acids. Furthermore, if the levels of the parental fatty acids were decreased, one would also expect to

see decreased levels of the epoxides, which is not the case. The second possibility is that the diol levels decreased not because of the DMSO but because of the stress involved with the injection. However, we did not observe such effects in mock-injected mice in previous studies (Yang et al., 2009, 2013) and it is not likely that only certain oxylipins would be so significantly changed in a general stress response.

Oxylipin diols generated from omega-6 and omega-3 fatty acids have been associated with a number of pathologies including obesity, diabetes, and inflammatory and cardiovascular diseases (Kalupahana et al., 2011; Grapov et al., 2012; Tourdot et al., 2014; Deol et al., 2017). Thus, it is not surprising that limiting the production of diols with sEH inhibitors is emerging as an important therapeutic approach in disease management (Liu et al., 2012; Bettaieb et al., 2013; Wagner et al., 2017). Decreasing oxylipin diol levels by DMSO could be used as a treatment complementary to sEHI: while inhibition of sEH would help prevent the formation of new diols, DMSO would eliminate pre-existing diols that may have accumulated prior to sEHI treatment (**Figure 5**). For example, DMSO has been shown to



mitigate inflammation in arthritis (Elisia et al., 2016), a disease associated with elevated levels of oxylipins (He et al., 2015; de Visser et al., 2018; Valdes et al., 2018). In one of these studies, however, a decrease in LA-derived diols was suggested to be causal for arthritis (He et al., 2015), indicating that additional investigation is needed (Figure 5).

Another example where DMSO could play a unique therapeutic role is in reducing extreme obesity. We have shown previously that all five of the oxylipin diols decreased by DMSO in this study – 12,13-DiHODE, 15,16-DiHODE, 12,13-DiHOME, 16,17-DiHDPE and 19,20-DiHDPE – correlate positively with soybean oil-induced obesity in mice (Deol et al., 2017). Soybean oil is by far the most commonly used cooking oil in the United States and is used ubiquitously in processed foods and restaurants (Blasbalg et al., 2011; Ash, 2012). While avoiding excess soybean oil in the diet is obviously preferable to taking any sort of medication, it is intriguing to speculate that in cases of intractable obesity, a compound such as DMSO that decreases elevated levels of diols might have a therapeutic effect. For such a treatment to work, however, the DMSO would need to have more than a transient effect on diol levels. Preliminary data from our lab suggest that this might be the case for at least one of the diols (not shown).

In summary, the results reported here provide new insights into the potential health effects of DMSO, and heightens our awareness of potential complications when using it as a solvent for therapeutic compounds.

ETHICS STATEMENT

Care and treatment of animals were in accordance with guidelines from and approved by the University of California,

Riverside Institutional Animal Care and Use Committee (AUP #20140014). All mice had *ad libitum* access to regular vivarium chow (Purina Test Diet 5001, Newco Distributors, Rancho Cucamonga, CA) and water. At the end of the study, mice were sacrificed by CO₂ inhalation followed by cervical dislocation, in accordance with stated NIH guidelines.

AUTHOR CONTRIBUTIONS

PD and FS conceived and designed the experiments. FS and BH supervised the study. PD and JY performed the experiments. PD, CM, BH, and FS analyzed and interpreted the results. PD and FS wrote the manuscript with input from the other authors.

FUNDING

This work was supported by Crohn's and Colitis Foundation of America Career Development Award (#454808) to PD; NIH R01DK053892 and USDA National Institute of Food and Agriculture (Hatch project CA-R-NEU-5680) to FS; NIEHS R01 ES002710 to BH; NIEHS P42 ES004699 to BH and a WCMC Pilot Project from NIH U24 DK097154 to FS and BH.

SUPPLEMENTARY MATERIAL

The Supplementary Material for this article can be found online at: <https://www.frontiersin.org/articles/10.3389/fphar.2019.00580/full#supplementary-material>

REFERENCES

- Achudume, A. C. (1991). Effects of dimethyl sulfoxide (DMSO) on carbon (CCL₄)-induced hepatotoxicity in mice. *Clin. Chim. Acta* 200, 57–58. doi: 10.1016/0009-8981(91)90335-a
- Alemón-Medina, R., Muñoz-Sánchez, J. L., Ruiz-Azuara, L., and Gracia-Mora, I. (2008). Casiopeína IIgly induced cytotoxicity to HeLa cells depletes the levels of reduced glutathione and is prevented by dimethyl sulfoxide. *Toxicol. In Vitro* 22, 710–715. doi: 10.1016/j.tiv.2007.11.011
- Ash, M. (2012). *Soybeans & Oil Crops. USDA Economic Research Service-Related Data and Statistics*. Available at: <http://www.ers.usda.gov/topics/crops/soybeans-oil-crops.aspx#.UkJCBZLz-Y> (accessed November 1, 2016).
- Beilke, M. A., Collins-Lech, C., and Sohnle, P. G. (1987). Effects of dimethyl sulfoxide on the oxidative function of human neutrophils. *J. Lab. Clin. Med.* 110, 91–96.
- Bettaieb, A., Nagata, N., AbouBechara, D., Chahed, S., Morisseau, C., Hammock, B. D., et al. (2013). Soluble epoxide hydrolase deficiency or inhibition attenuates diet-induced endoplasmic reticulum stress in liver and adipose tissue. *J. Biol. Chem.* 288, 14189–14199. doi: 10.1074/jbc.M113.458414
- Blasbalg, T. L., Hibbeln, J. R., Ramsden, C. E., Majchrzak, S. F., and Rawlings, R. R. (2011). Changes in consumption of omega-3 and omega-6 fatty acids in the United States during the 20th century. *Am. J. Clin. Nutr.* 93, 950–962. doi: 10.3945/ajcn.110.006643
- Brayton, C. F. (1986). Dimethyl sulfoxide (DMSO): a review. *Cornell Vet.* 76, 61–90.
- Calder, P. C. (2016). Docosahexaenoic acid. *Ann. Nutr. Metab.* 69(Suppl. 1), 7–21.
- Caligiuri, S. P. B., Parikh, M., Stamenkovic, A., Pierce, G. N., and Aukema, H. M. (2017). Dietary modulation of oxylipins in cardiovascular disease and aging. *Am. J. Physiol. Heart Circ. Physiol.* 313, H903–H918. doi: 10.1152/ajpheart.00201.2017
- Chauvet, N., Gauthier, A., and Nicoll-Griffith, D. A. (1998). Effect of common organic solvents on in vitro cytochrome P450-mediated metabolic activities in human liver microsomes. *Drug Metab. Dispos.* 26, 1–4.
- de Visser, H. M., Mastbergen, S. C., Ravipati, S., Welsing, P. M. J., Pinto, F. C., Lafeber, F. P. J. G., et al. (2018). Local and systemic inflammatory lipid profiling in a rat model of osteoarthritis with metabolic dysregulation. *PLoS One* 13:e0196308. doi: 10.1371/journal.pone.0196308
- Deol, P., Fahrman, J., Yang, J., Evans, J. R., Rizo, A., Grapov, D., et al. (2017). Omega-6 and omega-3 oxylipins are implicated in soybean oil-induced obesity in mice. *Sci. Rep.* 7:12488. doi: 10.1038/s41598-017-12624-9
- Elisia, I., Nakamura, H., Lam, V., Hofs, E., Cederberg, R., Cait, J., et al. (2016). DMSO represses inflammatory cytokine production from human blood cells and reduces autoimmune arthritis. *PLoS One* 11:e0152538. doi: 10.1371/journal.pone.0152538
- Gouveia-Figueira, S., Nording, M. L., Gaida, J. E., Forsgren, S., Alfredson, H., and Fowler, C. J. (2015). Serum levels of oxylipins in achilles tendinopathy: an exploratory study. *PLoS One* 10:e0123114. doi: 10.1371/journal.pone.0123114
- Grapov, D., Adams, S. H., Pedersen, T. L., Garvey, W. T., and Newman, J. W. (2012). Type 2 diabetes associated changes in the plasma non-esterified fatty acids, oxylipins and endocannabinoids. *PLoS One* 7:e48852. doi: 10.1371/journal.pone.0048852

- Guo, Q., Wu, Q., Bai, D., Liu, Y., Chen, L., Jin, S., et al. (2016). Potential use of dimethyl sulfoxide in treatment of infections caused by *Pseudomonas aeruginosa*. *Antimicrob. Agents Chemother.* 60, 7159–7169.
- He, M., van Wijk, E., Berger, R., Wang, M., Strassburg, K., Schoeman, J. C., et al. (2015). Collagen induced arthritis in DBA/1J mice associates with oxylipin changes in plasma. *Mediat. Inflamm.* 2015:543541. doi: 10.1155/2015/543541
- Hennebelle, M., Otaki, Y., Yang, J., Hammock, B. D., Levitt, A. J., Taha, A. Y., et al. (2017). Altered soluble epoxide hydrolase-derived oxylipins in patients with seasonal major depression: an exploratory study. *Psychiatry Res.* 252, 94–101. doi: 10.1016/j.psychres.2017.02.056
- Hickman, D., Wang, J. P., Wang, Y., and Unadkat, J. D. (1998). Evaluation of the selectivity of In vitro probes and suitability of organic solvents for the measurement of human cytochrome P450 monooxygenase activities. *Drug Metab. Dispos.* 26, 207–215.
- Imig, J. D., and Hammock, B. D. (2009). Soluble epoxide hydrolase as a therapeutic target for cardiovascular diseases. *Nat. Rev. Drug Discov.* 8, 794–805. doi: 10.1038/nrd2875
- Iwasaki, T., Hamano, T., Aizawa, K., Kobayashi, K., and Kakishita, E. (1994). A case of pulmonary amyloidosis associated with multiple myeloma successfully treated with dimethyl sulfoxide. *Acta Haematol.* 91, 91–94. doi: 10.1159/000204262
- Jia, Z., Zhu, H., Li, Y., and Misra, H. P. (2010). Potent inhibition of peroxynitrite-induced DNA strand breakage and hydroxyl radical formation by dimethyl sulfoxide at very low concentrations. *Exp. Biol. Med.* 235, 614–622. doi: 10.1258/ebm.2010.009368
- Justo, O. R., Simioni, P. U., Gabriel, D. L., Tamashiro, W. M., Rosa, P. de T. V., and Moraes, Â. M. (2015). Evaluation of in vitro anti-inflammatory effects of crude ginger and rosemary extracts obtained through supercritical CO₂ extraction on macrophage and tumor cell line: the influence of vehicle type. *BMC Complement. Altern. Med.* 15:390. doi: 10.1186/s12906-015-0896-9
- Kabeya, L. M., Andrade, M. F., Piatasi, F., Azzolini, A. E. C. S., Polizello, A. C. M., and Lucisano-Valim, Y. M. (2013). 3,3',5,5'-Tetramethylbenzidine in hypochlorous acid and taurine chloramine scavenging assays: interference of dimethyl sulfoxide and other vehicles. *Anal. Biochem.* 437, 130–132. doi: 10.1016/j.ab.2013.02.020
- Kalupahana, N. S., Claycombe, K. J., and Moustaid-Moussa, N. (2011). (n-3) Fatty acids alleviate adipose tissue inflammation and insulin resistance: mechanistic insights. *Adv. Nutr.* 2, 304–316. doi: 10.3945/an.111.000505
- Kelava, T., Čavar, I., and Čulo, F. (2011). Biological actions of drug solvents. *Period. Biol.* 113, 311–320.
- Kingery, W. S. (1997). A critical review of controlled clinical trials for peripheral neuropathic pain and complex regional pain syndromes. *Pain* 73, 123–139. doi: 10.1016/s0304-3959(97)00049-3
- Kumar, S., Kumar, S., Ganesamoni, R., Mandal, A. K., Prasad, S., and Singh, S. K. (2011). Dimethyl sulfoxide with lignocaine versus eutectic mixture of local anesthetics: prospective randomized study to compare the efficacy of cutaneous anesthesia in shock wave lithotripsy. *Urol. Res.* 39, 181–183. doi: 10.1007/s00240-010-0324-z
- Kuper, J., Tee, K. L., Wilmanns, M., Roccatano, D., Schwaneberg, U., and Wong, T. S. (2012). The role of active-site Phe87 in modulating the organic co-solvent tolerance of cytochrome P450 BM3 monooxygenase. *Acta Crystallogr. Sect. F Struct. Biol. Cryst. Commun.* 68, 1013–1017. doi: 10.1107/S1744309112031570
- Levick, S. P., Loch, D. C., Taylor, S. M., and Janicki, J. S. (2007). Arachidonic acid metabolism as a potential mediator of cardiac fibrosis associated with inflammation. *J. Immunol.* 178, 641–646. doi: 10.4049/jimmunol.178.2.641
- Li, D., Han, Y., Meng, X., Sun, X., Yu, Q., Li, Y., et al. (2010). Effect of regular organic solvents on cytochrome P450-mediated metabolic activities in rat liver microsomes. *Drug Metab. Dispos.* 38, 1922–1925. doi: 10.1124/dmd.110.033894
- Lin, D. S., and Conner, W. E. (1990). Are the n-3 fatty acids from dietary fish oil deposited in the triglyceride stores of adipose tissue? *Am. J. Clin. Nutr.* 51, 535–539. doi: 10.1093/ajcn/51.4.535
- Lin, D. S., Connor, W. E., and Spenser, C. W. (1993). Are dietary saturated, monounsaturated, and polyunsaturated fatty acids deposited to the same extent in adipose tissue of rabbits? *Am. J. Clin. Nutr.* 58, 174–179. doi: 10.1093/ajcn/58.2.174
- Lind, R. C., Begay, C. K., and Gandolfi, A. J. (2000). Hepatoprotection by dimethyl sulfoxide: III. Role of inhibition of the bioactivation and covalent binding of chloroform. *Toxicol. Appl. Pharmacol.* 166, 145–150. doi: 10.1006/taap.2000.8949
- Lishner, M., Lang, R., Kedar, I., and Ravid, M. (1985). Treatment of diabetic perforating ulcers (Mal Perforant) with local dimethylsulfoxide. *J. Am. Geriatr. Soc.* 33, 41–43. doi: 10.1111/j.1532-5415.1985.tb02858.x
- Liu, Y., Dang, H., Li, D., Pang, W., Hammock, B. D., and Zhu, Y. (2012). Inhibition of soluble epoxide hydrolase attenuates high-fat-diet-induced hepatic steatosis by reduced systemic inflammatory status in mice. *PLoS One* 7:e39165. doi: 10.1371/journal.pone.0039165
- Massion, P. P., Lindén, A., Inoue, H., Mathy, M., Grattan, K. M., and Nadel, J. A. (1996). Dimethyl sulfoxide decreases interleukin-8-mediated neutrophil recruitment in the airways. *Am. J. Physiol.* 271, L838–L843.
- Matyash, V., Liebisch, G., Kurzchalia, T. V., Shevchenko, A., and Schwudke, D. (2008). Lipid extraction by methyl-tert-butyl ether for high-throughput lipidomics. *J. Lipid Res.* 49, 1137–1146. doi: 10.1194/jlr.D700041-JLR200
- Moghaddam, M. F., Grant, D. F., Cheek, J. M., Greene, J. F., Williamson, K. C., and Hammock, B. D. (1997). Bioactivation of leukotoxins to their toxic diols by epoxide hydrolase. *Nat. Med.* 3, 562–566. doi: 10.1038/nm0597-562
- Morisseau, C., Inceoglu, B., Schmelzer, K., Tsai, H.-J., Jinks, S. L., Hegedus, C. M., et al. (2010). Naturally occurring monoepoxides of eicosapentaenoic acid and docosahexaenoic acid are bioactive antihyperalgesic lipids. *J. Lipid Res.* 51, 3481–3490. doi: 10.1194/jlr.M006007
- Park, Y., Smith, R. D., Combs, A. B., and Kehrer, J. P. (1988). Prevention of acetaminophen-induced hepatotoxicity by dimethyl sulfoxide. *Toxicology* 52, 165–175. doi: 10.1016/0300-483x(88)90202-8
- Pepin, J. M., and Langner, R. O. (1985). Effects of dimethyl sulfoxide (DMSO) on bleomycin-induced pulmonary fibrosis. *Biochem. Pharmacol.* 34, 2386–2389. doi: 10.1016/0006-2952(85)90799-3
- Rammler, D. H., and Zaffaroni, A. (1967). Biological implications of dmso based on a review of its chemical properties. *Ann. N. Y. Acad. Sci.* 141, 13–23. doi: 10.1111/j.1749-6632.1967.tb34861.x
- Rawls, W. F., Cox, L., and Rovner, E. S. (2017). Dimethyl sulfoxide (DMSO) as intravesical therapy for interstitial cystitis/bladder pain syndrome: a review. *Neurourol. Urodyn.* 36, 1677–1684. doi: 10.1002/nau.23204
- Sahin, M., Avsar, F. M., Ozel, H., Topaloglu, S., Yilmaz, B., Pasaoglu, H., et al. (2004). The effects of dimethyl sulfoxide on liver damage caused by ischemia-reperfusion. *Transplant. Proc.* 36, 2590–2592. doi: 10.1016/j.transproceed.2004.09.057
- Salim, A. S. (1991). Protection against stress-induced acute gastric mucosal injury by free radical scavengers. *Intensive Care Med.* 17, 455–460. doi: 10.1007/bf01690766
- Salim, A. S. (1992a). Oxygen-derived free-radical scavengers prolong survival in colonic cancer. *Chemotherapy* 38, 127–134. doi: 10.1159/000238952
- Salim, A. S. (1992b). Role of oxygen-derived free radical scavengers in the management of recurrent attacks of ulcerative colitis: a new approach. *J. Lab. Clin. Med.* 119, 710–717.
- Sanmartín-Suárez, C., Soto-Otero, R., Sánchez-Sellero, I., and Méndez-Álvarez, E. (2011). Antioxidant properties of dimethyl sulfoxide and its viability as a solvent in the evaluation of neuroprotective antioxidants. *J. Pharmacol. Toxicol. Methods* 63, 209–215. doi: 10.1016/j.vascn.2010.10.004
- Shirley, S. W., Stewart, B. H., and Mirelman, S. (1978). Dimethyl sulfoxide in treatment of inflammatory genitourinary disorders. *Urology* 11, 215–220. doi: 10.1016/0090-4295(78)90118-8
- Siegers, C.-P. (1978). Antidotal effects of dimethyl sulphoxide against paracetamol-, bromobenzene-, and thioacetamide-induced hepatotoxicity. *J. Pharm. Pharmacol.* 30, 375–377. doi: 10.1111/j.2042-7158.1978.tb13260.x
- Song, Y. M., Song, S.-O., Jung, Y.-K., Kang, E.-S., Cha, B. S., Lee, H. C., et al. (2012). Dimethyl sulfoxide reduces hepatocellular lipid accumulation through autophagy induction. *Autophagy* 8, 1085–1097. doi: 10.4161/auto.20260
- Su, T., and Waxman, D. J. (2004). Impact of dimethyl sulfoxide on expression of nuclear receptors and drug-inducible cytochromes P450 in primary rat hepatocytes. *Arch. Biochem. Biophys.* 424, 226–234. doi: 10.1016/j.abb.2004.02.008
- Tourdot, B. E., Ahmed, I., and Holinstat, M. (2014). The emerging role of oxylipins in thrombosis and diabetes. *Front. Pharmacol.* 4:176. doi: 10.3389/fphar.2013.00176

- Tove, S. B., and Smith, F. H. (1960). Changes in the fatty acid composition of the depot fat of mice induced by feeding oleate and linoleate. *J. Nutr.* 71, 264–272. doi: 10.1093/jn/71.3.264
- Valdes, A. M., Ravipati, S., Pousinis, P., Menni, C., Mangino, M., Abhishek, A., et al. (2018). Omega-6 oxylipins generated by soluble epoxide hydrolase are associated with knee osteoarthritis. *J. Lipid Res.* 59, 1763–1770. doi: 10.1194/jlr.P085118
- Wagner, K. M., McReynolds, C. B., Schmidt, W. K., and Hammock, B. D. (2017). Soluble epoxide hydrolase as a therapeutic target for pain, inflammatory and neurodegenerative diseases. *Pharmacol. Ther.* 180, 62–76. doi: 10.1016/j.pharmthera.2017.06.006
- Yang, J., Schmelzer, K., Georgi, K., and Hammock, B. D. (2009). Quantitative profiling method for oxylipin metabolome by liquid chromatography electrospray ionization tandem mass spectrometry. *Anal. Chem.* 81, 8085–8093. doi: 10.1021/ac901282n
- Yang, J., Solaimani, P., Dong, H., Hammock, B., and Hankinson, O. (2013). Treatment of mice with 2,3,7,8-Tetrachlorodibenzo-p-dioxin markedly increases the levels of a number of cytochrome P450 metabolites of omega-3 polyunsaturated fatty acids in the liver and lung. *J. Toxicol. Sci.* 38, 833–836. doi: 10.2131/jts.38.833
- Zeldin, D. C. (2001). Epoxygenase pathways of arachidonic acid metabolism. *J. Biol. Chem.* 276, 36059–36062. doi: 10.1074/jbc.r100030200

Conflict of Interest Statement: The authors declare that the research was conducted in the absence of any commercial or financial relationships that could be construed as a potential conflict of interest.

Copyright © 2019 Deol, Yang, Morisseau, Hammock and Sladek. This is an open-access article distributed under the terms of the Creative Commons Attribution License (CC BY). The use, distribution or reproduction in other forums is permitted, provided the original author(s) and the copyright owner(s) are credited and that the original publication in this journal is cited, in accordance with accepted academic practice. No use, distribution or reproduction is permitted which does not comply with these terms.



Pharmaceutical Effects of Inhibiting the Soluble Epoxide Hydrolase in Canine Osteoarthritis

Cindy B. McReynolds^{1,2}, Sung Hee Hwang^{1,2}, Jun Yang^{1,2}, Debin Wan¹, Karen Wagner^{1,2}, Christophe Morisseau¹, Dongyang Li¹, William K. Schmidt² and Bruce D. Hammock^{1,2*}

¹ Department of Entomology and Nematology, UC Davis Comprehensive Cancer Center, University of California, Davis, Davis, CA, United States, ² EicOsis, Davis, CA, United States

OPEN ACCESS

Edited by:

Ramaswamy Krishnan,
Beth Israel Deaconess Medical
Center and Harvard Medical School,
United States

Reviewed by:

Raewyn Poulsen,
The University of Auckland,
New Zealand
Dipak Panigrahy,
Harvard Medical School,
United States

*Correspondence:

Bruce D. Hammock
bdhammock@ucdavis.edu

Specialty section:

This article was submitted to
Translational Pharmacology,
a section of the journal
Frontiers in Pharmacology

Received: 08 February 2019

Accepted: 29 April 2019

Published: 31 May 2019

Citation:

McReynolds CB, Hwang SH,
Yang J, Wan D, Wagner K,
Morisseau C, Li D, Schmidt WK and
Hammock BD (2019) Pharmaceutical
Effects of Inhibiting the Soluble
Epoxide Hydrolase in Canine
Osteoarthritis.
Front. Pharmacol. 10:533.
doi: 10.3389/fphar.2019.00533

Osteoarthritis (OA) is a degenerative joint disease that causes pain and bone deterioration driven by an increase in prostaglandins (PGs) and inflammatory cytokines. Current treatments focus on inhibiting prostaglandin production, a pro-inflammatory lipid metabolite, with NSAID drugs; however, other lipid signaling targets could provide safer and more effective treatment strategies. Epoxides of polyunsaturated fatty acids (PUFAs) are anti-inflammatory lipid mediators that are rapidly metabolized by the soluble epoxide hydrolase (sEH) into corresponding vicinal diols. Interestingly, diol levels are increased in the synovial fluid of humans with OA, warranting further research on the biological role of this lipid pathway in the progression of OA. sEH inhibitors (sEHI) stabilize these biologically active, anti-inflammatory lipid epoxides, resulting in analgesia in both neuropathic, and inflammatory pain conditions. Most experimental studies testing the analgesic effects of sEH inhibitors have used experimental rodent models, which do not completely represent the complex etiology of painful diseases. Here, we tested the efficacy of sEHI in aged dogs with natural arthritis to provide a better representation of the clinical manifestations of pain. Two sEHI were administered orally, once daily for 5 days to dogs with naturally occurring arthritis to assess efficacy and pharmacokinetics. Blinded technicians recorded the behavior of the arthritic dogs based on pre-determined criteria to assess pain and function. After 5 days, EC1728 significantly reduced pain at a dose of 5 mg/kg compared to vehicle controls. Pharmacokinetic evaluation showed concentrations exceeding the enzyme potency in both plasma and synovial fluid. *In vitro* data showed that epoxyeicosatrienoic acid (EETs), epoxide metabolites of arachidonic acid, decreased inflammatory cytokines, IL-6 and TNF- α , and reduced cytotoxicity in canine chondrocytes challenged with IL1 β to simulate an arthritic environment. These results provide the first example of altering lipid epoxides as a therapeutic target for OA potentially acting by protecting chondrocytes from inflammatory induced cytotoxicity. Considering the challenges and high variability of naturally occurring disease in aged dogs, these data provide initial proof of concept justification that inhibiting the sEH is a non-NSAID, non-opioid, disease altering strategy for treating OA, and warrants further investigation.

Keywords: soluble epoxide hydrolase, osteoarthritis, epoxyeicosatrienoic acids, analgesic, non-opioid analgesic, non-NSAID analgesic

INTRODUCTION

Arthritis is a collective term used to describe joint disease and pain; however, there are many types of arthritis with very different etiologies. The two most common forms of arthritis are rheumatoid arthritis (RA), an autoimmune disease, and osteoarthritis (OA), a degenerative disease that results in breakdown of cartilage between bone leading to joint pain, swelling, reduced mobility, and bone degradation. Cartilage is comprised of chondrocyte cells that are responsible for generating the extracellular matrix and maintaining healthy cartilage tissue. Upon injury or disease, inflammatory cytokines lead to chondrocyte cytotoxicity and if not resolved, cartilage destruction. Recent medical advances for RA target immune suppression through monoclonal antibodies against anti-inflammatory targets. These treatments have shown promise in effectively treating RA (Tanaka et al., 2014); but OA, despite also having a common inflammatory cause, remains largely untreated, and patients often turn to NSAIDs and opioids to alleviate pain with no benefit to treating or stopping the progression of the disease (Ivers et al., 2012). In addition, these treatment options have serious side effects. For example, over 100,000 people are hospitalized each year for NSAID complications, and addiction to opioids has become a national health crisis affecting over 2 million people. Considering these serious side effects, safer, and more effective options are needed for patients suffering from OA.

Osteoarthritis is characterized by an increase in both inflammatory cytokines and inflammatory metabolites of arachidonic acid (AA) (Valdes et al., 2018). AA is an omega-6 polyunsaturated fatty acid (PUFA) that is metabolized primarily by three main enzyme systems: cyclooxygenases (COX), lipoxygenases, and CYP450s. COX metabolism of AA produces proinflammatory prostaglandins (PGs) that increase inflammatory cytokines and drive the progression of OA. Blocking PG production with NSAIDs that inhibit COX function has been an important approach to treating the disease (da Costa et al., 2017). However, despite the prevalent use of NSAIDs prescribed to OA patients, the efficacy and side-effects vary widely among patients, and long-term NSAID use is associated with increased risk of life-threatening toxicities (Marcum and Hanlon, 2010). Targeting other lipid mediators, such as the CYP450 branch of the AA cascade instead of the COX branch may provide better treatment alternatives. CYP450 epoxide metabolites of AA, or epoxyeicosatrienoic acid (EETs) prevent the translocation of $\text{Nf-}\kappa\text{B}$ into the nucleus thereby resulting in decreased inflammatory cytokines (Node et al., 1999). Additionally, EETs reduce ER-stress to help maintain homeostasis and have been effective in reducing neuropathic pain (Inceoglu et al., 2017). For these reasons, EETs are viewed as largely anti-inflammatory and beneficial compounds, but are often limited in efficacy due to their rapid degradation by the sEH into diol metabolites for excretion (Shimizu, 2009; **Figure 1**). Recently, the sEH products of EET metabolism [specifically 11,12 and 14,15 dihydroxyeicosatrienoic acid (DiHET)] were found in higher concentrations in arthritic joints compared to healthy or unaffected joints (Valdes et al., 2018). Chemical inhibitors of sEH increase the concentration of EETs and other epoxides of omega-3 and -6 fatty acids in the body by decreasing

the formation of corresponding diol metabolites (Morisseau and Hammock, 2013). Increasing epoxy-fatty acid (EpFA) concentration through inhibition of the sEH resolves a variety of disease states in laboratory settings, and efforts are ongoing to evaluate inhibition of sEH as an effective treatment for pain in clinical applications (Wagner et al., 2017b).

The sEH inhibitor, EC1728 (*trans*-4-{4-[3-(4-trifluoromethoxy-phenyl)-ureido]-cyclohexyloxy}-benzoic acid, also referred to as *t*-TUCB), is a potent sEHI that has shown efficacy in several animal models (Wagner et al., 2017a), and in treating a natural, neuropathic pain condition in horses called laminitis (Guedes et al., 2017). Although EC1728 has been effective in multiple models of pain, it has poor physical properties, such as high melting point (212.2°C) and low water solubility (5 mg/L in PBS), that limits its formulation, and bioavailability. Efforts were made to develop new sEHI with improved physicochemical properties. Because optimization of sEH inhibitors demonstrated that carbamates and amides are generally less active than urea pharmacophores (Kodani et al., 2018), new compounds focused on keeping the urea pharmacophore. Attempts at improving the physicochemical characteristics of EC1728 identified EC3039 (*trans*-4-{4-[3-methyl-3-(4-trifluoromethoxy-phenyl)-ureido]-cyclohexyloxy}-benzoic acid, also referred to as *t*-MTUCB) as a structurally similar compound that differs only in the addition of a *N*-methyl group to the urea pharmacophore (**Table 1**). The results below describe the evaluation of these two sEHI in a preclinical, randomized, and blinded study for their ability to alleviate pain in dogs with natural OA. *In vitro* studies tested the hypothesis that sEH inhibition reduces pain by increasing EETs that decrease inflammation in the chondrocytes.

MATERIALS AND METHODS

sEHI (EC1728 and EC3039)

EC1728 was synthesized in-house as previously described (Hwang et al., 2007), synthesis of EC3039 and deuterated 1728 *trans*-4-{4-[3-(4-trifluoromethoxy-phenyl)-ureido]-cyclohexyloxy}-benzoic-2,3,5,6-*d*₄ acid, also referred to as 3049, *t*-TUCB-*d*₄) is described in the **Supplementary Material**.

IC₅₀ was determined as previously described (Wolf et al., 2006). Briefly, canine enzyme was partially purified on a Q-sepharose column from liver cytosol (~10-fold purification) as described in (Tsai et al., 2010). The residual esterase activity was completely inhibited with paraoxon purchased from Chem Services Inc. (West Chester, PA, catalog number 42417404) at a concentration of 100 μM in assay buffer.

EET Mixture

Epoxyeicosatrienoic acid (5,6 EET, 8,9 EET, 10,11 EET, and 13,14 EET) were purchased from Cayman Chemicals (catalog numbers 50211, 50351, 50511, and 50651) and diluted 1000-fold for a final concentration of 0.1 $\mu\text{g/mL}$ for each EET (0.4 $\mu\text{g/mL}$ total). Meloxicam iv injectable was purchased from the UC Davis veterinary pharmacy at 5 mg/mL. Stock solutions were diluted to 1 mg/mL in ethanol and added to cell cultures at a final concentration of 1 $\mu\text{g/mL}$ and 0.1% ethanol.

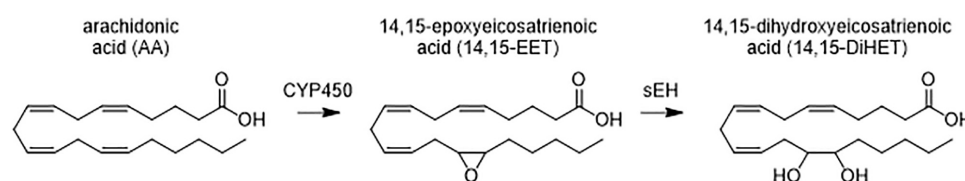


FIGURE 1 | Metabolism of arachidonic acid (AA) by cytochrome P450 (CYP450) generates anti-inflammatory fatty acid epoxides (EETs) that are degraded by the soluble epoxide hydrolase (sEH) to the corresponding 1,2 diols (DiHETs). DiHETs are more polar and diffuse out of the cells and are readily conjugated and excreted. The omega-6 fatty acid, AA, and representative metabolites on the 14, 15 carbon position are shown. Similar epoxides and vicinal diols are formed on the double bonds, and other omega-3 and 6 PUFAs are metabolized in a similar fashion.

Solubility of sEH

Solubility was determined by shaking the compounds in phosphate buffered saline (pH 7.4) at 40°C for 24 h in glass tubes. The non-dissolved compounds were filtered through a 0.22 μ m centrifuge filter at 40°C and the supernatant was further diluted 10 times with methanol. The samples were analyzed by LC/MS-MS.

HPLC/MS-MS Method

Concentrations of EC3039 and EC1728 were determined by LC/MS/MS analysis as previously described (Tsai et al., 2010) and defined in detail in the Section **Supplementary Material** “LC/MS/MS Method for PK Analyses of 1728 and 3039” and optimized parameters listed in **Supplementary Table S1**.

In vitro Model of Chondrocyte Cytotoxicity

Cell Culture

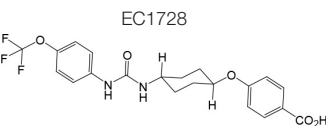
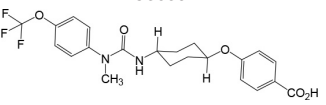
Canine chondrocytes (CnC) were purchased from Cell Applications, Inc. (catalog number Cn402-05). Cells arrived at Passage 1 and were cultured in complete growth media (Canine Chondrocyte Growth Medium supplemented with 10% Canine Chondrocyte Growth Supplement (CGS), both from Cell Applications, Inc.) and maintained at 37°C in a 5% CO₂

atmosphere. Once cells reached 80% confluence, they were passaged by removing the media, washing with PBS (warmed to room temperature) before adding 0.05% Trypsin-EDTA (Gibco Life Technologies, catalog number 25300) also warmed to room temperature. Cells were kept at room temperature and monitored for detachment (~2 min). Detached cells were added to 3 \times volume of full growth media and centrifuged to remove trypsin. Cells were reseeded at a concentration of 15,000 cells/cm² to reach 80% confluence in 3 days. Cells were expanded and frozen at the third passage in CGS containing 10% DMSO. For individual experiments, fresh cells were thawed and used at passage 5.

Chondrocyte Cytotoxicity in vitro

Canine chondrocytes cells were plated in 96-well plates at a density of 15,000 cells/cm². Optimal cell number was predetermined by a cell seeding experiment outlined in O'Brien et al. (2000). Cells were treated with recombinant canine IL1 β (Novus Biologicals catalog number 3747-CL-025) in CGS-free media for 2 h at 37°C. After 2 h, the IL1 β treated media was aspirated and replaced with complete growth media supplemented with either vehicle (0.1% ethanol), regioisomers of EETs, or meloxicam for 48-h before assessing inflammatory cytokines and cytotoxicity. Cells were also pretreated with meloxicam or EET mixture 30 min prior

TABLE 1 | EC1728 and EC3039 are potent sEH inhibitors.

Structure	Mol. Wt. (g/mol)	Melting point (°C)	Cal. LogP ¹	Canine sEH IC ₅₀ (ng/mL) ²	Solubility (mg/mL) ³	
					PBS pH 7.4	PEG300
 EC1728	438.40	240–244	5.0	0.4 \pm 0.1	0.005 \pm 0.001	97 \pm 2
 EC3039	452.43	92.4–94.7	5.0	2.0 \pm 0.3	0.130 \pm 0.015	99 \pm 1

EC3039 has a lower melting point and higher solubility but is less potent inhibiting the canine sEH enzyme compared to EC1728.

¹LogP was calculated using ChemDraw Professional version 18.0.0.231.

²IC₅₀ was measured using PHOME [(S) = 50 μ M] as fluorescent substrate with partially purified canine sEH from dog liver (Wolf et al., 2006). The residual esterase activity was completely inhibited with paraoxon (100 μ M) in assay buffer.

³Solubility was measured at 30°C as described (Hwang et al., 2007).

to adding IL1 β treatment for 2-h. After IL1 β was removed, treatments were added to complete growth media for 48-h as described above. Treatment conditions are described in the Section “Results.”

Cytotoxicity Assay

After the CnC cells were treated for 48-h under conditions described above, the media was removed and replaced with complete media containing 10% Alamar Blue (Life Technologies, catalog number DAL1025). The Alamar Blue assay relies on the metabolism of non-fluorescent resazurin to the highly fluorescent resorufin by healthy cells. Fluorescent intensity can be used to track cytotoxicity after xenobiotic treatments (Larson et al., 1997). After the addition of Alamar Blue, plates were protected from light and incubated at 30°C in a 5% CO₂ atmosphere for 8 h. The conversion of resazurin was monitored by reading fluorescence at 570 excitations and 585 emission on a plate reader (Tecan M1000 Pro) and cytotoxicity was calculated as the ratio of fluorescence from treated cells to non-treated controls.

ELISA Determination of IL-6 and TNF- α

ELISA determination of IL-6 and TNF- α : DuoSet ELISA kits (R&D Systems, **RRID:SCR_006140**) were used to quantify inflammatory cytokines, IL-6 (catalog number DY1609) and TNF- α (catalog number CATA00) in the media collected after 48-h of EET or vehicle treatments. Manufacturer's instructions were followed with adaption to improve the assay sensitivity using polymeric horseradish peroxidase (PolyHRP) according to previous work (Li et al., 2017). The following adaptations were conducted: the original two separate steps of adding standards/sample and biotinylated detection antibody with each incubated 2 h were changed to one-step simultaneous addition of both reagents with incubation time shortened to 1 h. After washing, the addition of streptavidin conjugated to horseradish peroxidase (Streptavidin-HRP) from the kit was replaced with streptavidin PolyHRP40 conjugate (25 ng/mL, 30 min) from SDT GmbH (Baesweiler, Germany). All incubations above were performed at room temperature with shaking (600 rpm, MTS 2/4 digital microtiter shaker, IKA, Germany).

Microsomal Stability

Male and female dog liver microsomes (Xenotech) were diluted in potassium phosphate buffer (0.1M, pH 7.4), MgCl₂ (3.15 mM), and sodium EDTA (1.05 mM) to a final protein concentration of 1 mg/mL. Compounds were added at 0.1 mM in methanol at 1% and microsomes were activated with 5% (v/v) NADPH regenerating system (100 μ L sodium phosphate buffer (0.1M, pH 7.4), 50 μ L, glucose-6-phosphate in sodium phosphate buffer (0.1M, pH 7.4), 50 μ L NADP⁺ in sodium phosphate (0.1M, pH 7.4), and 50 μ L of 100 Units/mL of glucose-6-dehydrogenase). Compounds were incubated for 60 min at 37°C and quenched with 4 \times volume of ice-cold methanol containing deuterated EC1728 as an internal standard. Compounds were incubated without microsomes or NADPH as negative controls.

Pain Assessment in Arthritic Dogs

In vivo Studies

Studies were contracted with InterVivo Solutions, Toronto, ON, Canada to assess pain and pharmacokinetics of E1728 and EC3039 in aged beagle dogs with OA. This study was conducted in accordance with InterVivo's approved IACUC protocol, in compliance with the Animal Welfare Act (AWA) and Public Health Service Policy on Humane Care and Use of Laboratory Animals.

Drug Administrations

There were five groups in total (placebo, 1 mg/kg EC1728, 5 mg/kg EC1728, 1 mg/kg EC3039, and 5 mg/kg EC3039). The placebo group contained 8 osteoarthritic dogs. The four drug-treated groups contained 8 osteoarthritic dogs and two satellite dogs (1 male and 1 female) of similar age and weight for PK blood sampling. Time 0 served as the pretreatment control. A total of 48 animals were on study.

PK Analysis

Eight satellite dogs (2 per each group) had whole blood collected for PK analysis on study Days 0 through 4. On Day 1, blood was collected immediately prior to dosing, and again at 0.25, 0.5, 1, 2, 4, 6, and 8 (\pm 5 min) after dosing. On Day 2 through 4, blood was collected 0.5 h (\pm 5 min) after dosing. On Day 5 blood was collected immediately prior to dosing, and again at 0.25, 0.5, 1, 2, 4, 6, 8 (\pm 5 min), 24, 48, and 72 h (\pm 30 min) post treatment. The exact sampling time was noted in the study file. For all blood samples, a minimum of 3 mL of whole blood was collected from a suitable vein as per written and approved standard operating procedures. The blood was transferred to K₂EDTA (spray dried) blood tube and inverted gently multiple times to ensure proper mixing of the blood and anticoagulant. On study Day 5, synovial fluid was collected by arthrocentesis immediately after the subject completed the questionnaire (approximately 3 h after dosing). Subjects were anesthetized as per written and approved Standard Operating Procedures. A minimum of 0.1 mL of synovial fluid was collected from each subject. Samples were frozen in an upright position and stored at $-80^{\circ}\text{C} \pm 4^{\circ}\text{C}$ before being shipped to UC Davis for analysis.

For PK analysis in the satellite group, individual parameters were calculated by fitting blood concentrations to a non-compartmental analysis using Kinetica software (Thermo Fisher Scientific version 5.1). Using the log-linear trapezoidal method, the area under the curve were calculated and were extrapolated to infinity using the last measured plasma concentration (C_{last}), defined as the timepoint collected 72 h after the last dose or 8 h after the first dose on day 1, divided by the terminal slope (λ_z).

Efficacy

The study was conducted as a blinded, parallel matched-group design. Dogs were randomized into groups based on pretreatment pain scores and each group was randomly assigned a treatment. Prior to randomization, each dog was assessed for arthritis by radiograph to assess the severity of OA by presence of osteophytes, subchondral sclerosis or joint effusion each scored on a scale of 0 (least) to 3 (worst) for each of 12 joints. Severity

of the radiograph score was included in the randomization protocol and distributed between the groups, and there were no statistical differences between the averages of each group. Individual radiograph scores can be found in **Supplementary Table S2**. Treatment groups consisted of vehicle control, 1 mg/kg EC3039, 5 mg/kg EC3039, 1 mg/kg EC1728, and 5 mg/kg EC1728. Compounds were dissolved in PEG300 to a concentration of 2.4 mg/mL (1 mg/kg) and 12 mg/mL (5 mg/kg) and administered as approximately 5 mL in size 12 gelatin capsules (Torpac) administered once daily on days 1 through 5. Vehicle group consisted of 5 mL PEG300 in capsule. Concurrent medications were not allowed and not needed during the study.

Pain and Function Assessments

Pain and function were assessed by a questionnaire answered by blinded technicians based on observation of study animals housed at InterVivo. The survey was adapted from the canine brief pain inventory (CBPI), which was developed based on clinical questionnaires in which owners score the function and pain level of their pets with existing pain conditions (Brown et al., 2007). Modifications to the questionnaire attempted to account for differences between owner pain evaluation of pets and pain evaluation of laboratory dogs by technical staff. For survey administration, blinded technicians attempted to elicit objective behavior-specific measures of function and pain level across a variety of normal canine behaviors (e.g., walking, trotting, galloping, rearing, and stair-climbing, etc.). For this, one technician was responsible for soliciting the relevant behaviors from a dog using encouragement and/or food rewards, while the evaluating technician scored function and observable pain using the modified CBPI questionnaire. Subjects were tested daily on Days -7 through -3, to develop baseline scores, and again on Days 1 through 5 administered 1.5 h after dosing. Dosing occurred in the morning, and observations were recorded 1.5 h after dosing, to limit time-of-day variability. Questions are listed in **Supplementary Table S3**. Animals in treatment groups had blood and synovial fluid collected ~2 h after the last dose on day 5 (immediately following the study questionnaire) to confirm plasma concentrations in treated animals. Full pharmacokinetic assessments were collected from a satellite group of animals so as not to interfere with pain assessment.

Statistical Analysis

Canine pain and function data were analyzed using ANOVA, linear mixed effects model, with Tukey adjustment in R and repeated measures ANOVA. Correlations coefficients were calculated in Graphpad Prism using the non-parametric Spearman correlation coefficient. *In vitro* experiments were analyzed using ANOVA in Graphpad Prism. Data are reported significant if $p < 0.05$.

RESULTS

sEHI Physicochemical Characteristics

EC3039 was synthesized and designed to have favorable physiochemical properties relative to EC1728. As crystals

or larger particles, lipophilic urea compounds have poor oral availability. Also, Chu and Yalkowsky (2009) showed an association between lower melting point and increased absorption. Thus, improving the aqueous solubility and lowering the melting point were prioritized to improve the potential for efficacy in future *in vivo* studies. EC3039 had improved solubility and lower melting point compared to EC1728 but had a slightly less potent IC₅₀ (5-times less potent than EC1728, **Table 1**). To assess the metabolic stability, both compounds were tested for stability after incubation in dog liver microsomes. Both compounds were relatively stable with EC1728 having over 95% remaining, and EC3039 having over 90% remaining in male liver microsomes and 85% remaining in female liver microsomes after 60-min incubations (**Table 2**).

In vivo Pain Evaluation

To evaluate the PK of both EC1728 and EC3039 and the ability to alleviate pain in dogs with natural arthritis, two dose levels of EC1728 and EC3039 were administered orally for five consecutive days to aged dogs with arthritis.

PK Analysis

In the satellite PK group ($n = 2$, 1 male and 1 female), concentrations of EC3039 and EC1728 increased through day 5 (**Figure 2**). Based on the reported half-life of both compounds (24–40 h, **Table 3**), it is expected that concentrations reported on day 5 represent the steady state values (Ito, 2011). Systemic exposure (C_{max} and AUC) increased in a more than dose proportional manner for EC3039 in both the male and female satellite PK dogs. On day 1, a fivefold increase in dose resulted in a 30 to 40-fold increase in C_{max} and approximate 18-fold increase in AUC for EC3039 (**Figures 2A,B**). Alternatively, a fivefold increase in dose for EC1728 resulted in a less than dose dependent increase in systemic exposure (3.25-fold increase in both C_{max} and AUC after fivefold dose increase) (**Figures 2C,D**). As the compounds reached steady-state, dose proportionality for EC1728 was less pronounced, with EC1728 having similar C_{max} and AUC for both doses (**Table 3**). This is likely due to the poor solubility of EC1728 where intestinal absorption is dependent upon the amount of drug that is in a true solution. A small portion (<10%) of 3039 was metabolized by demethylation to form EC1728 (**Figures 2A,B**).

TABLE 2 | EC3039 and EC1728 are stable after 60-minute incubations with male and female dog liver microsomes.

Compound		% Parent	
		+ NADPH	– NADPH
EC3039*	Males	90 ± 7	97 ± 4
	Females	85 ± 2	93 ± 5
EC1728	Males	103 ± 6	108 ± 8
	Females	98 ± 6	106 ± 9

*A small amount of EC1728 higher than the LOD (0.3 ng/mL) but lower than the LOQ (3 ng/mL) was detected in microsomes incubated with EC3039.

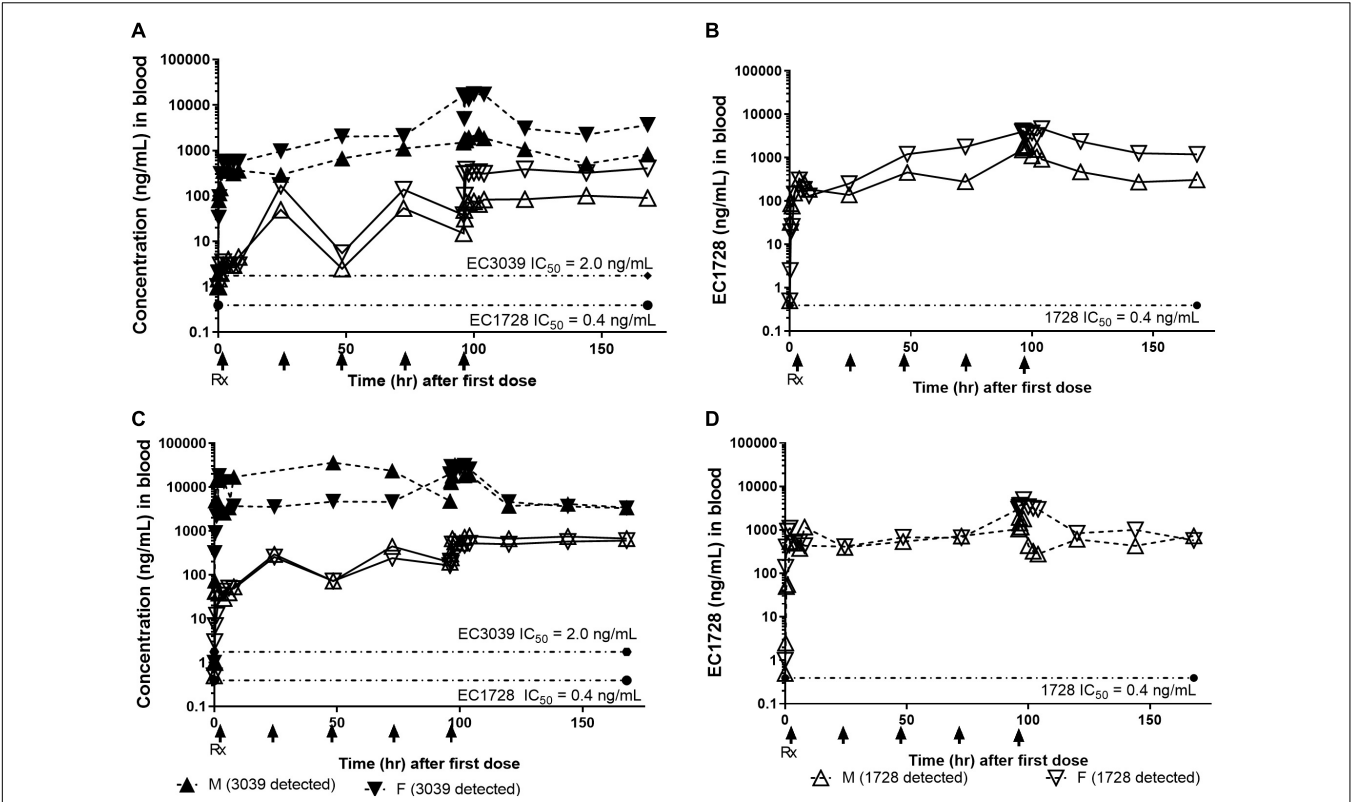


FIGURE 2 | Concentrations of EC3039 and EC1728 in the blood exceeded the IC_{50} for sEH for all treatment groups for the duration of the study. The PK profile of animals treated with EC3039 (A,C) or EC1728 (B,D) in a satellite group of $n = 2$ dogs administered 1 mg/kg or 5 mg/kg orally once daily for 5 consecutive days is shown. Blood was collected at 0.25, 0.5, 1, 2, 4, 6, and 8 h after dosing on Day 1, and again on days 2 through 4 at 0.5 h after dosing. On Day 4, blood was collected immediately prior to dosing, and again at 0.25, 0.5, 1, 2, 4, 6, 8 (± 5 min), 24, 48, and 72 h (± 30 min) post treatment. Concentrations of EC1728 and EC3039 were well above the EC_{50} for the study duration. Blood concentrations increased over the 5 days of dosing in all treatment groups, and $T_{1/2}$ calculated from the parent concentration predicts that steady-state is reached by day 5 for EC1728 and between days 5–8 for EC3039. Dogs administered EC3039 at 1 mg/kg (A) and 5 mg/kg (C) had detectable amounts of EC1728 in their blood presumably from demethylation of the urea by CYP450. The amount was proportional to EC3039 levels and above the EC_{50} for sEH, although approximately 3 \times lower than the dogs in the EC1728 treatment groups. A model could not be fitted for EC1728 detected from dogs administered EC3039 and $T_{1/2}$ were not calculated. Dogs administered EC1728 at either 1 mg/kg (B) and 5 mg/kg (D) had no detectable amounts of EC3039 in their blood. Drug concentrations did not show a clear dose response for dogs treated with EC1728, and dogs treated with 1 mg/kg of EC1728 (B) had approximately half the AUC as dogs treated with 5 mg/kg EC1728 (D).

TABLE 3 | PK parameters of EC3039 and EC1728 administered to a satellite group of dogs for 5 days by oral gavage.

	Gender	Compound detected	C_{max} (ng/mL)		AUC_{last} (h*ng/mL)		$T_{1/2}$ (h)
			Day 1	Day 5	Day 1	Day 5	
EC3039 (1 mg/kg)	M	EC3039	400	2,300	2,490	72,100	33
		EC1728 ¹	5	101	26	6,370	–
	F	EC3039	568	17,300	3,940	361,000	40
		EC1728	4	404	24	25,200	–
EC3039 (5 mg/kg)	M	EC3039	16,900	32,100	46,500	463,00	27
		EC1728	54	772	295	50,200	–
	F	EC3039	18,000	30,900	67,200	589,000	25
		EC1728	50	606	298	39,000	–
EC1728 (1 mg/kg)	M	EC1728	330	1,900	1,690	32,000	27
	F	EC1728	308	4,660	1,350	155,000	33
EC1728 (5 mg/kg)	M	EC1728	1,100	1,930	3,760	96,300	25
	F	EC1728	1,160	4,990	4,940	53,200	23

EC3039 had improved PK properties compared to EC1728. EC3039 had higher systemic exposure (C_{max} and AUC) compared to EC1728, and exposure increased in a more than dose proportional manner for EC3039 and less than dose proportional manner for EC1728. Exposure for both compounds increased over the 5-days of dosing. ¹EC1728 was detected in animals treated with EC3039, presumable from N-demethylation by CYP450; however, the $T_{1/2}$ could not be calculated because it could not be fitted to a PK model.

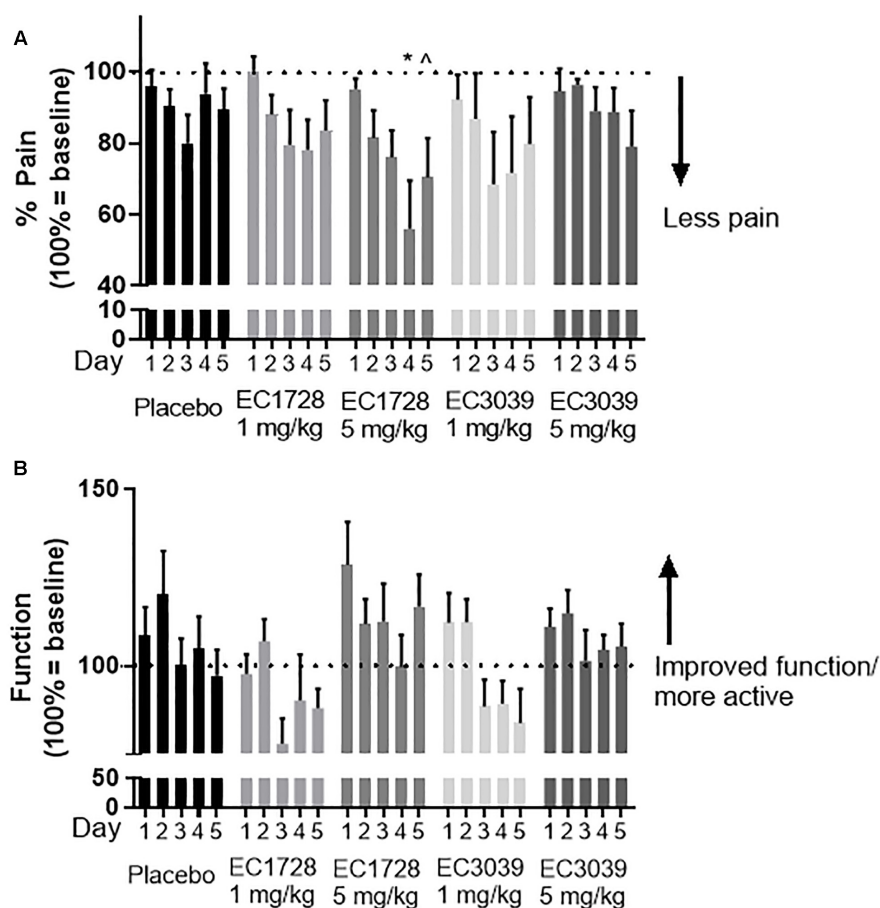


FIGURE 3 | EC1728 at 5 mg/kg reduced pain and increased function in dogs with osteoarthritis (OA). In order to assess pain, technicians blinded to treatment answered a predetermined questionnaire based on observed dog behavior (on a scale of 0–2), and activity (on a scale of 0–5) of aged beagle dogs. Score 0 was classified as least pain and most function. The composite score was normalized for each individual dog to their predose score for pain (A) and function (B) are presented. (A) Dogs treated orally, once daily with EC1728 at 5 mg/kg for 5 days had significantly less pain compared to the placebo group. Placebo control consisted of administration of an empty 100% PEG300, and size 12 capsules from Torpac. Statistical significance was reached on day 4. After 5-days of dosing, EC1728 significantly reduced pain compared to vehicle control when analyzed by repeated measures ANOVA. There were no statistical differences identified for other treatment groups. (B) While no statistical significance was observed for improvement in function with any treatment group, dogs treated with EC1728 tended to have higher function scores than other treatment groups ($p < 0.05$ for treatment effect when analyzed by repeated measures ANOVA, but there was no statistically significant interaction between treatment groups). * $p < 0.05$ compared to placebo and ^ $p < 0.05$ for cumulative treatment effects when analyzed by repeated measure ANOVA.

Efficacy

Dogs tolerated all treatments well, with no treatment related adverse events reported (a list of events recorded for the study can be found in **Supplementary Table S4**). Body weights were recorded on the day prior to dosing and again on day 5 of dosing. No dogs gained or lost more than 0.5 kg of body weight in any of the treatment groups. Dogs were assessed for pain and function based on a 12-question survey. The survey was administered for 5 days prior to dosing: the first 2 days were defined as an acclimation period and the final 3 days were averaged to provide baseline scores. One to two days prior to treatment, and after establishing baseline measurements, each dog was randomized based on age, radiograph score, and survey response. Prior to treatment, all groups averaged a score of 20 out of 24 for pain, and 14 out of 48 for function, except for the 1 mg/kg EC3039

group which averaged 15 for function. There were no significant differences between the baseline assessments of each group. One-way ANOVA analysis indicates that over the 5 days of treatment, EC1728 administered at 5 mg/kg significantly reduced pain in dogs with OA (**Figure 3A**). The maximum effect was observed on day 4 with an average of 44% reduction in pain compared to predose values. Vehicle treated animals were reported to have only a 7% reduction on this day. While there were no statistical differences between function scores for each of the treatment groups, dogs treated with EC1728 at 5 mg/kg tended to have increased function scores compared to the other groups (**Figure 3B**). After 5-days of dosing, dogs showed a 16% increase in function compared to a 3% decrease in function reported in the vehicle treated animals. Both pain and function scores showed high variability throughout the course of treatment. In

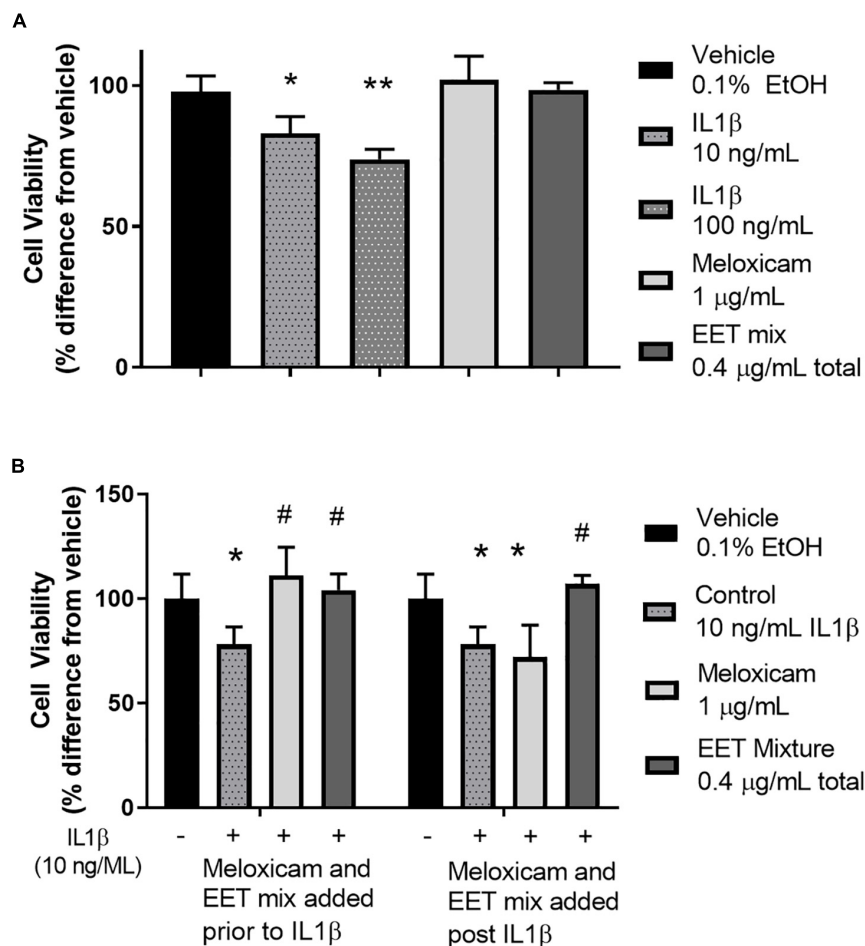


FIGURE 4 | IL1 β induced cytotoxicity was alleviated by meloxicam or EET mixture in an *in vitro* model of OA. **(A)** CnC cells treated 2 h with IL1 β showed a dose dependent increase in cytotoxicity measured by Alamar Blue. The meloxicam or EET mixture, treated for 48 h, in the absence of IL1 β , had no effect on healthy CnC cells. **(B)** Chondrocytes treated with IL1 β for 2 h before or after treatment with meloxicam (1 μ g/mL) or a mixture of EETs (5,6 EET, 8,9 EET, 11,12 EET, and 14,15 EET each at 0.1 μ g/mL for a total EET concentration of 0.4 μ g/mL). Meloxicam (added before the addition of 10 ng/mL of IL1 β) or EET mixture, added either before or after a 2-h IL1 β treatment significantly reduced IL1 β induced cytotoxicity. Meloxicam added after IL1 β did not result in significant reduction in cytotoxicity. * p < 0.05, ** p < 0.005 compared to vehicle not treated with IL1 β ; # p < 0.005 compared to vehicle treated with IL1 β .

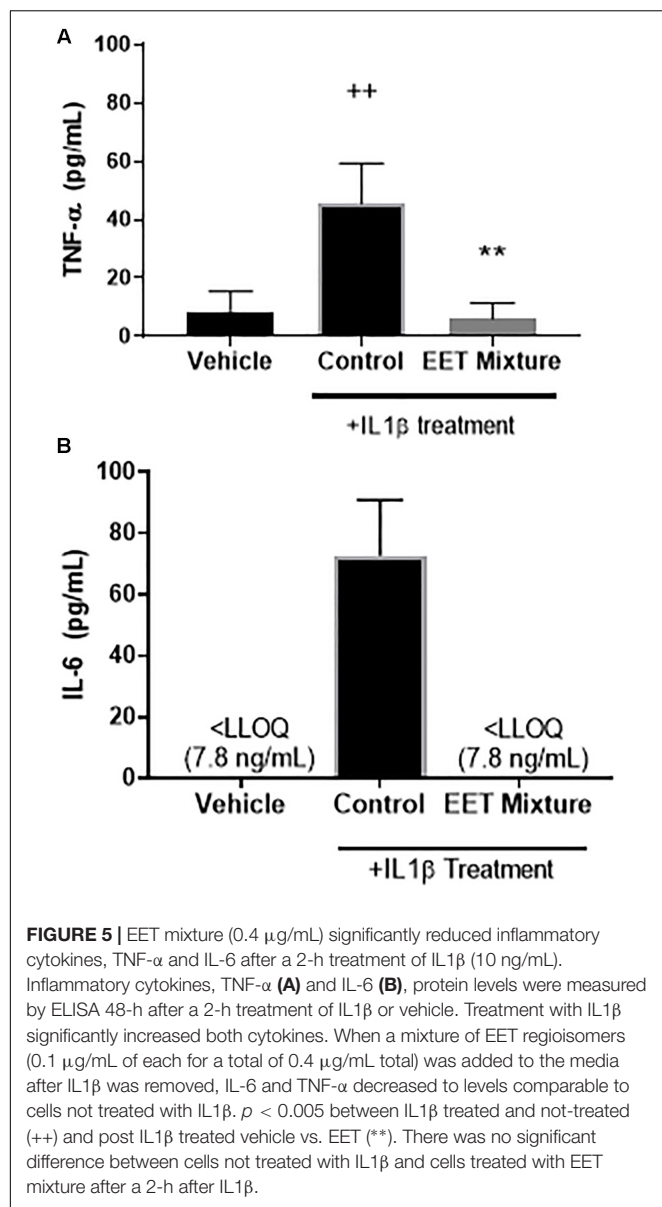
addition, we did not observe significant association between pain and function in our data when analyzed by a non-parametric Spearman correlation coefficient.

Concentrations of EC3039 and EC1728 were assessed in the whole blood and synovial fluid of dogs in each treatment group ($n = 8$). No compounds were detected in the placebo treated group. Most animals had compound concentrations measured above the IC_{50} for enzyme inhibition in both blood and synovial fluid indicating that the compound was able to penetrate into the target tissue (Supplementary Table S5). Dogs treated with EC3039 had higher C_{max} and AUC concentrations of sEHI in their blood and synovial fluid than dogs treated with EC1728 (approximately 2 \times more in the low dose group and 10 \times more in the high dose group). Dogs treated with EC3039 also had detectable levels of EC1728 in their blood and synovial fluid, presumably due to demethylation of the urea. However, these concentrations were lower than dogs administered parent

EC1728, indicating that EC3039 is acting largely as a direct sEHI, and EC3039 is a poor prodrug for EC1728. Of note, one dog (dog 2.4, Supplementary Table S5) treated with 5 mg/kg EC1728 had lower amounts of compound detected in the blood and synovial fluid (34 ng/mL in the blood on day 5 compared to 395 ng/mL average for the remainder of the group, and 80–95 ng/mL in the synovial fluid vs. 988 ng/mL averaged for the group on day 5). Due to low exposure levels, this dog was removed from analysis.

***In vitro* Model of Chondrocyte Cytotoxicity**

To elucidate the role of increasing EET concentrations in arthritic animals, EET mixtures were evaluated for their ability to decrease inflammatory cytokines and protect chondrocytes against IL1 β induced cytotoxicity. CnC cells treated with IL1 β showed a significant and dose dependent increase in cytotoxicity (Figure 4A) that was eliminated when the chondrocytes were



pretreated with either meloxicam or EETs, or treated post-IL1 β with a mixture of EETs (Figure 4B). The *in vitro* model evaluated two concentrations of IL1 β , 10, and 100 ng/mL, to simulate OA conditions in patients. A dose dependent reduction in cytotoxicity was observed (Figure 4A), and 10 ng/mL was selected as the concentration for continued experiments to better replicate *in vivo* conditions [0.288 ng/mL reported in the synovial fluid of humans with OA (McNulty et al., 2013)]. Interestingly, treating CnC cells with meloxicam after IL1 β did not result in significant improvement in cytotoxicity. IL1 β induces COX activity and an increase in PGs such as PGE2 (Attur et al., 1998); thus, it is no surprise that post treatment with a COX inhibitor would fail to attenuate inflammation in the presence of PGs (Hinson et al., 1996). Conversely, the anti-inflammatory action of EETs act downstream of PGE2 (Inceoglu et al., 2011); therefore,

it is expected that EETs would work to counter PGE2 induced inflammation post IL1 β treatment when the NSAID, meloxicam, did not. Protein measurement of inflammatory cytokines IL-6 and TNF- α were reduced in chondrocytes treated with a mixture of EETs (Figure 5); confirming that EETs protect chondrocytes through an anti-inflammatory response.

DISCUSSION

To assess the effects of sEHI on treating pain in animals with OA, arthritic dogs were treated orally with either of two sEHI (EC3039 or EC1728) for 5 days, and pain and function were measured compared to untreated placebo animals as a measure of efficacy. Although a potent inhibitor, EC1728 has poor solubility in both water and common organic solvents as well as a high melting point. EC3039 was synthesized to improve solubility without significantly altering the structure: by adding a methyl group to the urea pharmacophore, potency only slightly decreased but water solubility improved by almost 30-times and melting point was reduced from 240 to 92.4°C. Additions of N-methyl groups on the urea of sEHI are generally less active because the two hydrogens on the urea are needed to bond to the catalytic aspartic acid in the active site of the enzyme (Gomez et al., 2006). EC3039 was $\sim 5\times$ less potent than EC1728 presumably due to the addition on the urea pharmacophore; although more active than most other compounds with N-methyl additions on the urea. Improved solubility and lower melting resulted in improved PK as evident by the increase C_{max} and AUC of EC3039 compared to EC1728, and it was hypothesized that improvements in PK would compensate for decreased potency. Despite the less than ideal physiochemical properties of EC1728, the compound displayed favorable PK, and both EC3039 and EC1728 had concentration measured in the plasma and synovial fluid well above the IC_{50} of sEH. Only EC1728 at 5 mg/kg was effective in reducing pain associated with OA in dogs. While a full PK profile was conducted in satellite animals, in order to not interfere with pain assessments, study animals only had synovial fluid collected on days 1 and 5 after pain assessments were complete. Because a full timecourse of distribution in the synovial fluid was not feasible without interfering with efficacy measurements, it is unknown if EC1728 remained in the synovium longer than EC3039. It is also possible that EC1728 is more effective in penetrating the cells and interacting with the target enzyme than EC3039. In addition to differences in potency and distribution, target occupancy, or amount of time the drug is bound to the enzyme, could also influence the efficacy of the compounds. Target occupancy is a predictor of efficacy, and although the exact resonance time of the drug on the enzyme is unknown, the decrease in potency suggests an increase in K_{off} ; thus, improved efficacy observed with EC1728 could be a function of potency and target occupancy (Tonge, 2018). Further investigation is needed to test this and understand the additional benefits provided by EC1728.

The sEHI work to inhibit the metabolism of beneficial, anti-inflammatory EpFA, thereby increasing their biological concentrations. In the *in vitro* cytotoxicity assay, EETs proved to be anti-inflammatory and decreased the inflammatory

cytokines, IL-6 and TNF- α , after canine chondrocytes were incubated with IL1 β . The primary effect is hypothesized to be independent of prostaglandin production since efficacy was achieved after IL1 β incubation and reported stimulation of PG (Johnson et al., 2016). Furthermore, treatment with the NSAID, meloxicam, was only effective in protecting chondrocytes from IL1 β induced cytotoxicity if added prior to IL1 β stimulation (**Figure 4B**); however, in the longer term, EETs have been shown to down regulate induced COX-2 protein and message (Schmelzer et al., 2006a). Chondrocytes are cells in joint cartilage that produce cartilage and regulate cytokine release in response to stress stimuli, and decreased chondrocyte viability in response to injury or inflammatory stimuli has been associated with the progression of OA (Akkiraju and Nohe, 2015). IL1 β has been associated with pathological changes in OA by increasing matrix metalloproteases and inflammatory cytokines such as IL-6 and TNF- α (Pelletier et al., 1995; Kapoor et al., 2011). Chondrocytes express the receptor for IL1 β and are considered the main cellular target of this proinflammatory cytokine in cartilage (Daheshia and Yao, 2008). Thus, *in vitro* data predict that increased EET concentrations will reduce synovial inflammation *in vivo* and protect chondrocytes.

In addition to anti-inflammatory effects, EpFA also reduce ER-stress and are proposed targets for alleviating neuropathic pain (Inceoglu et al., 2017). Because OA is characterized by both inflammatory and neuropathic pain (Dimitroulas et al., 2014), a dual approach treating both inflammation, and neuropathic pain would improve patient outcomes especially considering that NSAIDs are ineffective in treating neuropathic pain (Rasmussen-Barr et al., 2016), and current neuropathic pain treatments (such as opioids and pentanoids) have serious addiction potential with debilitating and often deadly side-effects. Additionally, previously published studies demonstrated the beneficial effects of targeting dual inhibition of sEHI and COX. For example, in a mouse model of LPS, dual inhibition increased antinociception (Schmelzer et al., 2006b). In addition to synergistic efficacy, others have observed reduced ulcers in mice treated with both the NSAID, diclofenac, and sEHI compared to diclofenac treated mice alone (Goswami et al., 2016, 2017). Thus, safer and more effective treatment options are greatly needed, and the combination of sEHI and NSAID could provide a powerful approach to eliminate pain and comorbidities of patients suffering from OA without deleterious side effects. Targeting OA from two pathways of decreasing PG production, through NSAIDs, as well with sEHI to reduce ER-stress and inflammation in the presence of PG could provide an effective dual approach to reduce inflammatory and neuropathic pain in OA patients.

Osteoarthritis is a debilitating disease for both humans and companion animals. The results of this study identified a lead compound to further investigate the use of sEHI to treat OA in companion animals. In addition, natural disease in dogs is often used as a more appropriate model for human disease than rodent models (Hoffman et al., 2018), providing evidence that sEHI is a potential target for human OA as well. A limitation of the study was the high variability observed in the *in vivo* study among each treatment group in the assessments of pain,

function and PK, as well as the additional complications in using aged dogs where confounding factors could interfere with the interpretation of pain and mobility; although the limitations are somewhat offset by using a natural disease state in the animals to be treated. Variability is expected in naturally occurring disease, and as a proof of concept study, this study was designed to mimic treatment in a patient population. Future studies will identify mechanistic changes using both *in vitro* and *in vivo* models in rodents and companion animals to identify a detailed characterization of sEH activity in OA. The reduction in pain in the high dose of EC1728 provides justification for continued efforts in developing sEHI alone or in combination with NSAIDs for the treatment of OA in companion animals and humans.

ETHICS STATEMENT

This study was conducted in accordance with InterVivo's approved IACUC protocol, in compliance with the Animal Welfare Act (AWA) and Public Health Service Policy on Humane Care and Use of Laboratory Animals.

AUTHOR CONTRIBUTIONS

CBM, SH, KW, WS, and BDH conceived of the presented idea. SH synthesized the compounds and tested in these studies. CBM performed the *in vitro* cell experiments, microsomal stability, PK analysis, and analyzed the *in vivo* study results. KW and CM helped to supervise the project. JY and DW verified the analytical methods and analyzed the PK samples. DL oversaw the ELISA experiments. BDH provided overall supervision for the project. All authors discussed the results and contributed to the final manuscript.

FUNDING

This work was supported by the National Institute of Environmental Health Sciences (NIEHS) grant R01 ES002710, NIEHS Superfund Research Program P42 ES004699, and T32GM113770 (to CBM). The content is solely the responsibility of the authors and does not necessarily represent the official views of the National Institutes of Health.

ACKNOWLEDGMENTS

We thank Dr. Blythe Durbin-Johnson for statistical advice and Dr. Kin Sing Stephen Lee for solubility data.

SUPPLEMENTARY MATERIAL

The Supplementary Material for this article can be found online at: <https://www.frontiersin.org/articles/10.3389/fphar.2019.00533/full#supplementary-material>

REFERENCES

- Akkiraju, H., and Nohe, A. (2015). Role of chondrocytes in cartilage formation, progression of osteoarthritis and cartilage regeneration. *J. Dev. Biol.* 3, 177–192. doi: 10.3390/jdb3040177
- Attur, M. G., Patel, I. R., Patel, R. N., Abramson, S. B., and Amin, A. R. (1998). Autocrine production of IL-1 beta by human osteoarthritis-affected cartilage and differential regulation of endogenous nitric oxide, IL-6, prostaglandin E2, and IL-8. *Proc. Assoc. Am. Phys.* 110, 65–72.
- Brown, D. C., Boston, R. C., Coyne, J. C., and Farrar, J. T. (2007). Development and psychometric testing of an instrument designed to measure chronic pain in dogs with osteoarthritis. *Am. J. Vet. Res.* 68, 631–637. doi: 10.2460/ajvr.68.6.631
- Chu, K. A., and Yalkowsky, S. H. (2009). An interesting relationship between drug absorption and melting point. *Int. J. Pharm.* 373, 24–40. doi: 10.1016/j.ijpharm.2009.01.026
- da Costa, B. R., Reichenbach, S., Keller, N., Nartey, L., Wandel, S., Juni, P., et al. (2017). Effectiveness of non-steroidal anti-inflammatory drugs for the treatment of pain in knee and hip osteoarthritis: a network meta-analysis. *Lancet* 390, e21–e33. doi: 10.1016/s0140-6736(17)31744-0
- Daheshia, M., and Yao, J. Q. (2008). The interleukin 1beta pathway in the pathogenesis of osteoarthritis. *J. Rheumatol.* 35, 2306–2312. doi: 10.3899/jrheum.080346
- Dimitroulas, T., Duarte, R. V., Behura, A., Kitas, G. D., and Raphael, J. H. (2014). Neuropathic pain in osteoarthritis: a review of pathophysiological mechanisms and implications for treatment. *Semin. Arthritis Rheum.* 44, 145–154. doi: 10.1016/j.semarthrit.2014.05.011
- Gomez, G. A., Morisseau, C., Hammock, B. D., and Christianson, D. W. (2006). Human soluble epoxide hydrolase: structural basis of inhibition by 4-(3-cyclohexylureido)-carboxylic acids. *Protein Sci.* 15, 58–64. doi: 10.1110/ps.051720206
- Goswami, S. K., Rand, A. A., Wan, D., Yang, J., Inceoglu, B., Thomas, M., et al. (2017). Pharmacological inhibition of soluble epoxide hydrolase or genetic deletion reduces diclofenac-induced gastric ulcers. *Life Sci.* 180, 114–122. doi: 10.1016/j.lfs.2017.05.018
- Goswami, S. K., Wan, D., Yang, J., Trindade da Silva, C. A., Morisseau, C., Kodani, S. D., et al. (2016). Anti-Ulcer efficacy of soluble epoxide hydrolase inhibitor TPPU on diclofenac-induced intestinal ulcers. *J. Pharmacol. Exp. Ther.* 357, 529–536. doi: 10.1124/jpet.116.232108
- Guedes, A., Galuppo, L., Hood, D., Hwang, S. H., Morisseau, C., and Hammock, B. D. (2017). Soluble epoxide hydrolase activity and pharmacologic inhibition in horses with chronic severe laminitis. *Equine Vet. J.* 49, 345–351. doi: 10.1111/evj.12603
- Hinson, R. M., Williams, J. A., and Shacter, E. (1996). Elevated interleukin 6 is induced by prostaglandin E2 in a murine model of inflammation: possible role of cyclooxygenase-2. *Proc. Natl. Acad. Sci. U.S.A.* 93, 4885–4890. doi: 10.1073/pnas.93.10.4885
- Hoffman, J. M., Creevy, K. E., Franks, A., O'Neill, D. G., and Promislow, D. E. L. (2018). The companion dog as a model for human aging and mortality. *Aging Cell* 17:e12737. doi: 10.1111/acel.12737
- Hwang, S. H., Tsai, H. J., Liu, J. Y., Morisseau, C., and Hammock, B. D. (2007). Orally bioavailable potent soluble epoxide hydrolase inhibitors. *J. Med. Chem.* 50, 3825–3840. doi: 10.1021/jm070270t
- Inceoglu, B., Bettaieb, A., Haj, F. G., Gomes, A. V., and Hammock, B. D. (2017). Modulation of mitochondrial dysfunction and endoplasmic reticulum stress are key mechanisms for the wide-ranging actions of epoxy fatty acids and soluble epoxide hydrolase inhibitors. *Prostaglandins Other Lipid Mediat.* 133, 68–78. doi: 10.1016/j.prostaglandins.2017.08.003
- Inceoglu, B., Wagner, K., Schebb, N. H., Morisseau, C., Jinks, S. L., Ulu, A., et al. (2011). Analgesia mediated by soluble epoxide hydrolase inhibitors is dependent on cAMP. *Proc. Natl. Acad. Sci. U.S.A.* 108, 5093–5097. doi: 10.1073/pnas.1101073108
- Ito, S. (2011). Pharmacokinetics 101. *Paediatr. Child Health* 16, 535–536.
- Ivers, N., Dhalla, I. A., and Allan, G. M. (2012). Opioids for osteoarthritis pain: benefits and risks. *Can. Fam. Phys.* 58:e708.
- Johnson, C. I., Argyle, D. J., and Clements, D. N. (2016). In vitro models for the study of osteoarthritis. *Vet. J.* 209, 40–49. doi: 10.1016/j.tvjl.2015.07.011
- Kapoor, M., Martel-Pelletier, J., Lajeunesse, D., Pelletier, J. P., and Fahmi, H. (2011). Role of proinflammatory cytokines in the pathophysiology of osteoarthritis. *Nat. Rev. Rheumatol.* 7, 33–42. doi: 10.1038/nrrheum.2010.196
- Kodani, S. D., Wan, D., Wagner, K. M., Hwang, S. H., Morisseau, C., and Hammock, B. D. (2018). Design and potency of dual soluble epoxide hydrolase/fatty acid amide hydrolase inhibitors. *ACS Omega* 3, 14076–14086. doi: 10.1021/acsomega.8b01625
- Larson, E. M., Doughman, D. J., Gregerson, D. S., and Obrtsch, W. F. (1997). A new, simple, nonradioactive, nontoxic in vitro assay to monitor corneal endothelial cell viability. *Invest. Ophthalmol. Vis. Sci.* 38, 1929–1933.
- Li, D., Cui, Y., Morisseau, C., Gee, S. J., Bever, C. S., Liu, X., et al. (2017). Nanobody based immunoassay for human soluble epoxide hydrolase detection using polymeric horseradish peroxidase (PolyHRP) for signal enhancement: the rediscovery of PolyHRP? *Anal. Chem.* 89, 6248–6256. doi: 10.1021/acs.analchem.7b01247
- Marcum, Z. A., and Hanlon, J. T. (2010). Recognizing the risks of chronic nonsteroidal anti-inflammatory drug use in older adults. *Ann. Longterm Care* 18, 24–27.
- McNulty, A. L., Rothfusz, N. E., Leddy, H. A., and Guilak, F. (2013). Synovial fluid concentrations and relative potency of interleukin-1 alpha and beta in cartilage and meniscus degradation. *J. Orthop. Res.* 31, 1039–1045. doi: 10.1002/jor.22334
- Morisseau, C., and Hammock, B. D. (2013). Impact of soluble epoxide hydrolase and epoxyeicosanoids on human health. *Annu. Rev. Pharmacol. Toxicol.* 53, 37–58. doi: 10.1146/annurev-pharmtox-011112-140244
- Node, K., Huo, Y., Ruan, X., Yang, B., Spiecker, M., Ley, K., et al. (1999). Anti-inflammatory properties of cytochrome P450 epoxygenase-derived eicosanoids. *Science* 285, 1276–1279. doi: 10.1126/science.285.5431.1276
- O'Brien, J., Wilson, I., Orton, T., and Pognan, F. (2000). Investigation of the Alamar Blue (resazurin) fluorescent dye for the assessment of mammalian cell cytotoxicity. *Eur. J. Biochem.* 267, 5421–5426. doi: 10.1046/j.1432-1327.2000.01606.x
- Pelletier, J. P., McCollum, R., Cloutier, J. M., and Martel-Pelletier, J. (1995). Synthesis of metalloproteases and interleukin 6 (IL-6) in human osteoarthritic synovial membrane is an IL-1 mediated process. *J. Rheumatol. Suppl.* 43, 109–114.
- Rasmussen-Barr, E., Held, U., Grooten, W. J., Roelofs, P. D., Koes, B. W., van Tulder, M. W., et al. (2016). Non-steroidal anti-inflammatory drugs for sciatica. *Cochrane Database Syst. Rev.* 10:Cd012382. doi: 10.1002/14651858.cd012382
- Schmelzer, K. R., Inceoglu, B., Kubala, L., Kim, I. H., Jinks, S. L., Eiserich, J. P., et al. (2006a). Enhancement of antinociception by coadministration of nonsteroidal anti-inflammatory drugs and soluble epoxide hydrolase inhibitors. *Proc. Natl. Acad. Sci. U.S.A.* 103, 13646–13651. doi: 10.1073/pnas.0605908103
- Schmelzer, K. R., Wheelock, A. M., Dettmer, K., Morin, D., and Hammock, B. D. (2006b). The role of inflammatory mediators in the synergistic toxicity of ozone and 1-nitronaphthalene in rat airways. *Environ. Health Perspect.* 114, 1354–1360. doi: 10.1289/ehp.8373
- Shimizu, T. (2009). Lipid mediators in health and disease: enzymes and receptors as therapeutic targets for the regulation of immunity and inflammation. *Annu. Rev. Pharmacol. Toxicol.* 49, 123–150. doi: 10.1146/annurev-pharmtox.011008.145616
- Tanaka, T., Hishitani, Y., and Ogata, A. (2014). Monoclonal antibodies in rheumatoid arthritis: comparative effectiveness of tocilizumab with tumor necrosis factor inhibitors. *Biologics* 8, 141–153. doi: 10.2147/btt.s37509
- Tonge, P. J. (2018). Drug-target kinetics in drug discovery. *ACS Chem. Neurosci.* 9, 29–39. doi: 10.1021/acscchemneuro.7b00185

- Tsai, H. J., Hwang, S. H., Morisseau, C., Yang, J., Jones, P. D., Kasagami, T., et al. (2010). Pharmacokinetic screening of soluble epoxide hydrolase inhibitors in dogs. *Eur. J. Pharm. Sci.* 40, 222–238. doi: 10.1016/j.ejps.2010.03.018
- Valdes, A. M., Ravipati, S., Pousinis, P., Menni, C., Mangino, M., Abhishek, A., et al. (2018). Omega-6 oxylipins generated by soluble epoxide hydrolase are associated with knee osteoarthritis. *J. Lipid Res.* 59, 1763–1770. doi: 10.1194/jlr.P085118
- Wagner, K., Gilda, J., Yang, J., Wan, D., Morisseau, C., Gomes, A. V., et al. (2017a). Soluble epoxide hydrolase inhibition alleviates neuropathy in Akita (Ins2 Akita) mice. *Behav. Brain Res.* 326, 69–76. doi: 10.1016/j.bbr.2017.02.048
- Wagner, K. M., McReynolds, C. B., Schmidt, W. K., and Hammock, B. D. (2017b). Soluble epoxide hydrolase as a therapeutic target for pain, inflammatory and neurodegenerative diseases. *Pharmacol. Ther.* 180, 62–76. doi: 10.1016/j.pharmthera.2017.06.006
- Wolf, N. M., Morisseau, C., Jones, P. D., Hock, B., and Hammock, B. D. (2006). Development of a high-throughput screen for soluble epoxide hydrolase inhibition. *Anal. Biochem.* 355, 71–80. doi: 10.1016/j.ab.2006.04.045

Conflict of Interest Statement: The University of California holds patents on the sEH inhibitors used in this study as well as their use to treat inflammation, inflammatory pain, and neuropathic pain. BDH and CM are cofounders and KW, JY, and WS are employees of EicOsis L.L.C., a startup company advancing sEH inhibitors as potential therapeutics. EicOsis provided funding for studies contracted to InterVivo.

The remaining authors declare that the research was conducted in the absence of any commercial or financial relationships that could be construed as a potential conflict of interest.

The reviewer DP declared a past co-authorship with several of the authors, SH, JY, BDH, to the handling Editor.

Copyright © 2019 McReynolds, Hwang, Yang, Wan, Wagner, Morisseau, Li, Schmidt and Hammock. This is an open-access article distributed under the terms of the Creative Commons Attribution License (CC BY). The use, distribution or reproduction in other forums is permitted, provided the original author(s) and the copyright owner(s) are credited and that the original publication in this journal is cited, in accordance with accepted academic practice. No use, distribution or reproduction is permitted which does not comply with these terms.



Epoxy-Oxylipins and Soluble Epoxide Hydrolase Metabolic Pathway as Targets for NSAID-Induced Gastroenteropathy and Inflammation-Associated Carcinogenesis

Ryan D. Jones, Jie Liao, Xin Tong, Dandan Xu, Leyu Sun, Haonan Li and Guang-Yu Yang*

Department of Pathology, Feinberg School of Medicine, Northwestern University, Chicago, IL, United States

OPEN ACCESS

Edited by:

John D. Imig,
Medical College of Wisconsin,
United States

Reviewed by:

Jessica Roos,
University Hospital Frankfurt,
Germany
Guodong Zhang,
University of Massachusetts Amherst,
United States

*Correspondence:

Guang-Yu Yang
g-yang@northwestern.edu

Specialty section:

This article was submitted to
Translational Pharmacology,
a section of the journal
Frontiers in Pharmacology

Received: 18 December 2018

Accepted: 05 June 2019

Published: 25 June 2019

Citation:

Jones RD, Liao J, Tong X, Xu D,
Sun L, Li H and Yang G-Y (2019)
Epoxy-Oxylipins and Soluble Epoxide
Hydrolase Metabolic Pathway
as Targets for NSAID-Induced
Gastroenteropathy and Inflammation-
Associated Carcinogenesis.
Front. Pharmacol. 10:731.
doi: 10.3389/fphar.2019.00731

Polyunsaturated fatty acids (PUFAs) including epoxide-modified ω -3 and ω -6 fatty acids are made *via* oxidation to create highly polarized carbon-oxygen bonds crucial to their function as signaling molecules. A critical PUFA, arachidonic acid (ARA), is metabolized to a diverse set of lipids signaling molecules through cyclooxygenase (COX), lipoxygenase (LOX), cytochrome P450 epoxygenase, or cytochrome P450 hydroxylase; however, the majority of ARA is metabolized into anti-inflammatory epoxides *via* cytochrome P450 enzymes. These short-lived epoxide lipids are rapidly metabolized or inactivated by the soluble epoxide hydrolase (sEH) into diol-containing products. sEH inhibition or knockout has been a practical approach to study the biology of the epoxide lipids, and has been shown to effectively treat inflammatory conditions in the preclinical models including gastrointestinal ulcers and colitis by shifting oxylipins to epoxide profiles, inhibiting inflammatory cell infiltration and activation, and enhancing epithelial cell defense *via* increased mucin production, thus providing further evidence for the role of sEH as a pro-inflammatory protein. Non-steroidal anti-inflammatory drugs (NSAIDs) with COX-inhibitor activity are among the most commonly used analgesics and have demonstrated applications in the management of cardiovascular disease and intriguingly cancer. Major side effects of NSAIDs however are gastrointestinal ulcers which frequently precludes their long-term application. In this review, we hope to bridge the gap between NSAID toxicity and sEH-mediated metabolic pathways to focus on the role of epoxy fatty acid metabolic pathway of PUFAs in NSAIDs-ulcer formation and healing as well as inflammation-related carcinogenesis. Specifically we address the potential application of sEH inhibition to enhance ulcer healing at the site of inflammation *via* their activity on altered lipid signaling, mitochondrial function, and diminished reactive oxygen species, and further discuss the significance of dual COX and sEH inhibitor in anti-inflammation and carcinogenesis.

Keywords: oxylipin, soluble epoxide hydrolase, non-steroidal anti-inflammatory drug, inflammation, carcinogenesis

INTRODUCTION

Inflammation is a diverse and complex series of pathogenetic processes, which act to protect host organisms against infectious pathogens and damaged cells or tissues. Inflammation is initiated *via* cellular and molecular signaling, and it is necessary for clearance of infections and tissue damage and for tissue repair. On the other hand, the inflammatory process itself can cause significant harm to the host (Jaeschke and Smith, 1997). One such family of molecular mediators or signaling of inflammation is arachidonic acid (ARA) and its metabolites.

ARA is a pivotal molecule in inflammation, which when released in response to tissue injury can be metabolized into three broad pathways governed by cyclooxygenase (COX), lipoxygenase (LOX), and cytochrome P450 enzymes (including epoxigenase and hydroxylase) (as outlined in **Figure 1**) (Morisseau and Hammock, 2012). Downstream active molecules from ARA metabolism include prostaglandins (PGs), leukotrienes, epoxyeicosanoids, and hydroxyeicosatetraenoic acid. In addition to ARA, other polyunsaturated fatty acids (PUFAs) including eicosapentaenoic acid (EPA) and docosahexaenoic acid (DHA) are also substrates for these same enzymes (Hiesinger et al., 2019). Of particular interest are the epoxyeicosatrienoic acids (EETs), the metabolites of cytochrome p450 epoxigenase. EETs play important roles in gastrointestinal (GI) epithelial integrity and wound healing, and are key negative regulators of inflammation (Zhang et al., 2012; Zhang et al., 2013b; Zhang et al., 2013c). The effects of EETs have been extensively reviewed by Spector and Kim (2015).

EETs are substrates for the enzyme soluble epoxide hydrolase (sEH), which rapidly converts EETs to dihydroxyeicosatrienoic acids (DHETs) (Capdevila et al., 2000; Spector et al., 2004). The epoxide fatty acids generated from EPA and ARA are also physiologically active, and are substrates of sEH (Morisseau and Hammock, 2012). These diol-containing DHETs have drastically reduced biologic activity. Thus, inhibition of sEH has been extensively studied as a mechanism to increase the longevity of anti-inflammatory EETs *via* the discovery of sEH inhibitors, particularly in combination with other inhibitors as multi-target therapies, which were recently reviewed (Hiesinger

et al., 2019). sEH inhibitors have been shown to robustly decrease sEH activity with little to no toxicity in animal models. Further, these compounds have proven effective to 1) decrease GI ulcers induced by non-steroidal anti-inflammatory drugs (NSAIDs) (Goswami et al., 2016; Goswami et al., 2017; Yang, 2018), 2) prevent carcinogenesis in murine models of colorectal and pancreatic tumors (Liao et al., 2016a; Liao et al., 2016b; Wang et al., 2018b; Yang, 2018), and 3) decrease chronic inflammation in mouse models for both colitis and pancreatitis (Zhang et al., 2012; Zhang et al., 2013b; Zhang et al., 2013c; Goswami et al., 2016; Liao et al., 2016a; Goswami et al., 2017; Wang et al., 2018b; Yang, 2018).

Prostaglandins (PGs), produced through oxygenation of ARA *via* COX enzymes, result in a diverse family of structures that modulate many functions including vascular tone, platelet aggregation, and inflammation (Ricciotti and FitzGerald, 2011). The NSAID family of drugs act through inhibition of COX-1 and/or COX-2. Specific inhibitors against COX enzymes have also been developed. In addition to NSAIDs anti-inflammatory properties, they have been shown to decrease the risk of several cancers including colorectal adenocarcinomas (Cao et al., 2016; Chan and Ladabaum, 2016; Tsoi et al., 2018). Long-term NSAID use, however, often leads to severe GI tract ulcers and potentially life-threatening bleeding precluding their widespread use in chemoprevention (Sostres et al., 2010).

This review aims to highlight a potential strategy combining sEH and COX inhibition for chemoprevention and inflammatory conditions while also mitigating the adverse side effects of single agent sEH inhibitors and NSAIDs.

POLYUNSATURATED FATTY ACID METABOLISM AND EETS

The 20-carbon ω -6 PUFA ARA is a lipid signaling molecule that resides among phospholipids and is a key substrate for a variety of downstream cell signaling mediators known as eicosanoids. ARA is broadly metabolized into one of three main pathways: 1) by COX into prostaglandins; 2) by 5-LOX into leukotrienes; and 3) by cytochrome P450 (CYP 450) epoxigenase and hydroxylase

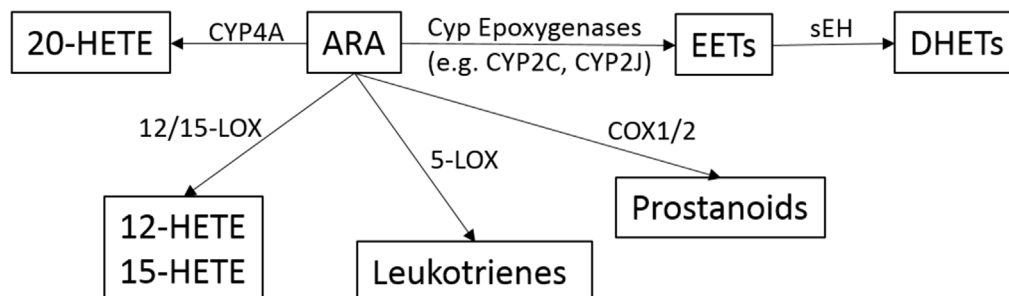


FIGURE 1 | Overview of the metabolic pathways of the arachidonic acid (ARA) cascade.

to form epoxyeicosanoids and hydroxyeicosatetraenoic acid. The EETs are signaling molecules formed within various types of cells by the metabolism of ARA (Capdevila et al., 2000; Capdevila and Falck, 2001). Several CYP 450 enzymes are involved in EET production, and include CYP2C and CYP2J, which epoxidize ARA at one of the four double bonds resulting in two different enantiomers for each EET regioisomer (Capdevila et al., 2000).

EETs can act as both autocrine and paracrine mediators of inflammation, angiogenesis, apoptosis, fibrinolysis, mitogenesis, vasodilation, and bronchodilation (Karara et al., 1990; Karara et al., 1991; Karara et al., 1992; Weintraub et al., 1999). The mechanism of their activity is not fully known, but likely involves two possible mechanisms. One postulated mechanism is that EETs function through membrane receptors such as G protein-coupled receptors or tyrosine kinase receptors to activate intracellular signaling cascades (Li and Campbell, 1997; Hoebel and Graier, 1998; Chen et al., 2000; Fukao et al., 2001; Node et al., 2001; Seubert et al., 2004; Wang et al., 2005). The other possible mechanism is that EETs directly interact with transcription factors, ion channels, or intermediary signal transduction proteins. But, the definitive EET-binding receptor/s or signaling proteins are not yet identified.

The catabolism of EETs can occur through several pathways including the main pathway of epoxide hydrolysis by sEH into DHETs, but can also occur through β -oxidation (Fang et al., 2000), fatty acid chain elongation (Fang et al., 1995; Fang et al., 1996; Fang et al., 2001), and rarely through CYP 450 ω -oxidases (Coward et al., 2002), COX (Zhang et al., 1992; Carroll et al., 1993), LOX (Pace-Asciak et al., 1983), and glutathione-S-transferase (Spearman et al., 1985). Recently, COX-derived proangiogenic metabolites of EETs were identified (Rand et al., 2017). EETs have much higher anti-inflammatory and promoting tissue repair activities compared with DHETs produced by sEH, providing a rationale for sEH inhibition (Inceoglu et al., 2007).

NON-STEROIDAL ANTI-INFLAMMATORY DRUGS, SIDE EFFECTS, AND THEIR ROLE IN CHEMOPREVENTION

Acetylsalicylic acid (aspirin) was the first NSAID synthesized and developed for commercial use in 1897 by Felix Hoffman, and it became widely used for its analgesic and anti-inflammatory effects (Sostres et al., 2010). It took approximately 40 years before it was definitively linked to GI injury. It was not until the 1970s that it was discovered that aspirin acts to inhibit prostaglandin production. Today, over 20 NSAIDs are commercially available with varied toxicities and pharmacokinetics and include non-selective COX-1/COX-2 inhibitors (e.g., aspirin, ibuprofen, naproxen, diclofenac) and COX-2 selective inhibitors (coxibs, e.g., celecoxib).

NSAIDs are among the most commonly administered drugs worldwide, as they are available by prescription and over-the-counter. Excitingly, they are also among the most promising agents for prevention of cardiovascular diseases and cancer including colorectal cancer (CRC) (Fischer et al., 2011; Wongrakpanich et al., 2018). One of the major adverse effects

of NSAIDs therapy is GI injury, including ulceration, bleeding, inflammation, and even perforation (Wolfe and Singh, 1999; Sudano et al., 2012; Tsoi, 2018). This is a serious clinical challenge causing a major burden on the health care system (specifically, in the US, >100,000 patients are hospitalized with serious NSAID-related GI complications annually, including 16,500 deaths) (Wolfe and Singh, 1999; Bjarnason et al., 2018). In addition to NSAIDs toxicity in the stomach, novel imaging techniques (e.g., capsule endoscopy) have identified the small intestine as a major target organ of toxicity, and lower GI bleeding events may even appear more frequently than upper GI events (Maiden, 2009; Sostres and Lanás, 2011). The local topical effect of NSAIDs is partially responsible for the GI-tract ulceration and bleeding, as co-prescription of aspirin and proton pump inhibitors (PPIs) or enteric-coating of NSAIDs both provide some protection against NSAID-induced gastritis and gastric ulcers; however, these treatment strategies actually increase the incidence of small-bowel ulcers. The non-topical systemic effect of NSAID use appears to be key, as enteric coating, parenteral, and rectal administration all continue to result in gastroenteropathies (Sostres et al., 2010). At least two-thirds of both long-term (>3 months) and short-term (>1 week) NSAID/coxibs users exhibit ulcers in the jejunum and ileum (Maiden, 2009). To date there is no therapy or preventive treatment for NSAIDs-induced GI ulcers available.

In contrast to the adverse ulcer-causing effects, several clinical trials and epidemiological and animal studies have clearly demonstrated that aspirin or NSAIDs actually decrease the risk and mortality of CRC and prevent colon adenoma formation (Dubois, 2009; Burn et al., 2011; Fischer et al., 2011; Cao et al., 2016). To acknowledge this supporting evidence, in 2016 the U.S. Preventive Services Task Force (USPSTF) recommended the use of aspirin to prevent CRC and cardiovascular disease for adults aged between 50 and 70 in the U.S. This recommendation distinguishes aspirin as the first pharmacologic agent to be endorsed by the USPSTF for chemoprevention of a cancer in a population not characterized as high risk (Cao et al., 2016; Chan and Ladabaum, 2016). In addition, notable chemopreventive clinical trials studied the use of aspirin for the prevention of adenomas and carcinomas in patients with Lynch syndrome (Burn et al., 2011) and the use of celecoxib for the reduction of sporadic colorectal adenoma (Dubois, 2009). To achieve significant chemoprevention while also reducing the adverse effects of GI ulcers, alternative approaches with either low doses of NSAIDs or in combination with other chemopreventive agents have been tried with little success (Fischer et al., 2011).

SOLUBLE EPOXIDE HYDROLASE

Epoxides are cyclic three atom rings which are highly reactive and are metabolized by epoxide hydrolases by adding water forming a diol group in a dihydroxylation reaction. The epoxide hydrolase family is comprised of numerous enzymes including: microsomal epoxide hydrolase (mEH), sEH, leukotriene A₄ hydrolase, cholesterol 5,6-oxide hydrolase, and epoxide hydrolase 3 (Fretland and Omiecinski, 2000; Decker et al., 2012).

The major epoxide hydrolase involved in EET metabolism is sEH, encoded by the EPHX-2 gene located on chromosome 8 (Larsson et al., 1995; Sandberg and Meijer, 1996). The 60-kDa sEH forms a homodimer with each monomer containing N-terminal domain lipid phosphatase activity with unknown physiologic significance, as well as a functionally independent C-terminal domain epoxide hydrolase activity (Argiriadi et al., 1999; Cronin et al., 2003; Newman et al., 2003).

In the early 1990s, concerns about the potential adverse effects of a chronic loss of sEH have centered around the clearance of xenobiotics, particularly the potential loss of function to clear epoxide-containing carcinogens. These concerns have been well studied and demonstrated that these xenobiotics are not the substrates of sEH (Seidegard and Ekstrom, 1997; Fretland and Omiecinski, 2000; Morisseau and Hammock, 2005; Shimada, 2006; Morisseau and Hammock, 2007; Decker et al., 2009). Studies of evolution of the microsomal EH (mEH) and sEH show that although they have common origins, they diverge at the level of prokaryotes and their substrate selectivity is vastly different (Fretland and Omiecinski, 2000). mEH rapidly degrades carcinogenic epoxides on cyclic systems (e.g., aflatoxin epoxide and benzo[a]pyrene epoxide) (Shimada, 2006). To date, sEH has not been shown to metabolize a single carcinogenic epoxide and endogenous eicosanoids are identified as its only substrates (Seidegard and Ekstrom, 1997; Decker et al., 2009). sEH inhibitors have been cross-tested on the mEH, which show a much greater selectivity for sEH (Morisseau and Hammock, 2005; Morisseau and Hammock, 2007). Most importantly, the fatty epoxides stabilized through sEH inhibition display a strong anti-inflammatory action (Norwood et al., 2010).

sEH shows high tissue expression in liver, intestine, kidneys, brain, and vasculature, with lower expression in spleen, lung, and testes (VanRollins et al., 1993; Fang et al., 1995; Johansson et al., 1995; Yu et al., 2000). The subcellular localization is variable; however, sEH is mostly localized to the cytosol with peroxisomal involvement in hepatocytes and renal proximal tubule epithelial cells (Hollinshead and Meijer, 1988; Eriksson et al., 1991; Mullen et al., 1999; Enayetallah et al., 2006). The biological activity and significance of different cell types and different subcellular localization of sEH have not been fully elucidated.

DEVELOPMENT AND APPLICATION OF SELECTIVE SEH INHIBITORS

Inhibitors have been developed for sEH, which have been instrumental in understanding the biology of EETs and sEH, as well as for testing their use in practical applications of disease. Importantly, through decades of studies, inhibitors have been selected for their stability, high selectivity against sEH, and high potency. The first iterations of sEH inhibitors were epoxide-containing *trans*-3-phenylglycidol and chalcone oxide molecules, and while these inhibitors are selective and potent, they are unstable with only temporary effects on sEH (Mullin and Hammock, 1982; Dietze et al., 1991; Dietze et al., 1993; Morisseau et al., 1998).

Newer classes of sEH inhibitors include urea- and carbamate-based molecules, which are more stable than previous inhibitors, and are also highly selective and potent (Morisseau et al., 1999). One inhibitor in this class is *N,N'*-dicyclohexylurea (DCU). DCU is the basis for several urea-based inhibitors with increased water solubility, and which bind to the active site of sEH *via* the urea subgroup with hydrogen bonds and salt bridges (Argiriadi et al., 2000; Morisseau et al., 2002; Kim et al., 2004).

The most recent and well-studied sEH inhibitors are 12-(3-adamantyl-ureido)-dodecanoic acid (AUDA) compounds. These AUDA compounds have been modified to bind the catalytic site of sEH *via* hydrogen bonds and have physical properties ideal for pharmacologic use including high water solubility, oral bioavailability, low melting point, increased stability, and high potency. *Trans*-4-[4-(3-adamantan-1-ylureido)cyclohexyl oxy]benzoic acid (t-AUCB) is another highly promising sEH inhibitor. Thus far, sEH inhibitors have been demonstrated to be safe, with very few side effects. The effective dosages show very little toxicity.

SEH INHIBITION INCREASES EETS, PROMOTES ULCER HEALING, AND INHIBITS PANCREATITIS, COLITIS, AND INFLAMMATION-ASSOCIATED CANCER IN MICE

Chronic inflammation has been demonstrated to be among the most important factors leading to carcinogenesis. Obesity, inflammatory bowel disease (IBD), and chronic colitis and pancreatitis are some specific examples of inflammatory conditions that are known risk factors for cancer with shared mechanisms involving altered epoxide fatty acid metabolites and sEH (Zhang et al., 2013; Liao et al., 2016a; Wang et al., 2018b; Yang, 2018). As a result of chronic inflammation there is overproduction of reactive oxygen and nitrogen species (RONS), as well as dysregulation of ARA metabolites. Inflammatory cell infiltration driven by neutrophils, macrophages, and subsequently lymphocytes alters tissue microenvironments with an enhanced production of RONS (e.g., superoxide) and ARA metabolites (e.g., PGE₂ and LTB₄). Leukocytes also act to modify vasculature through effects on endothelial cells (Yang et al., 2009).

Mounting evidence links EETs and sEH inhibition to treatment for chronic inflammatory conditions and inflammation-associated cancer. First, sEH has been shown to be overexpressed in human colitis and CRC (Zhang et al., 2013b). Second, recent studies demonstrated that sEH bridges obesity to colonic inflammation and potentially to colorectal carcinogenesis (Wang et al., 2018b; Yang, 2018; Yang et al., 2018). And finally, sEH inhibition blocks colitis and its associated carcinogenesis (Zhang et al., 2012; Zhang et al., 2013b; Zhang et al., 2013c) and NSAID-induced GI ulcers (Goswami et al., 2016; Goswami et al., 2017). However, the relative contribution and mechanism of sEH in sporadic colon carcinogenesis is not fully known.

Initial studies regarding the anti-inflammatory effects of EETs showed that physiologic concentration of EETs or overexpression

of CYP2J2 decreases cytokine-mediated endothelial cell adhesion molecule expression, thus preventing leukocyte recruitment *via* a mechanism involving NF- κ B (Node et al., 1999). Inhibition of EET catabolism through sEH inhibitors results in a significant increase in their anti-inflammatory properties, and effectively treat mouse models of inflammatory diseases.

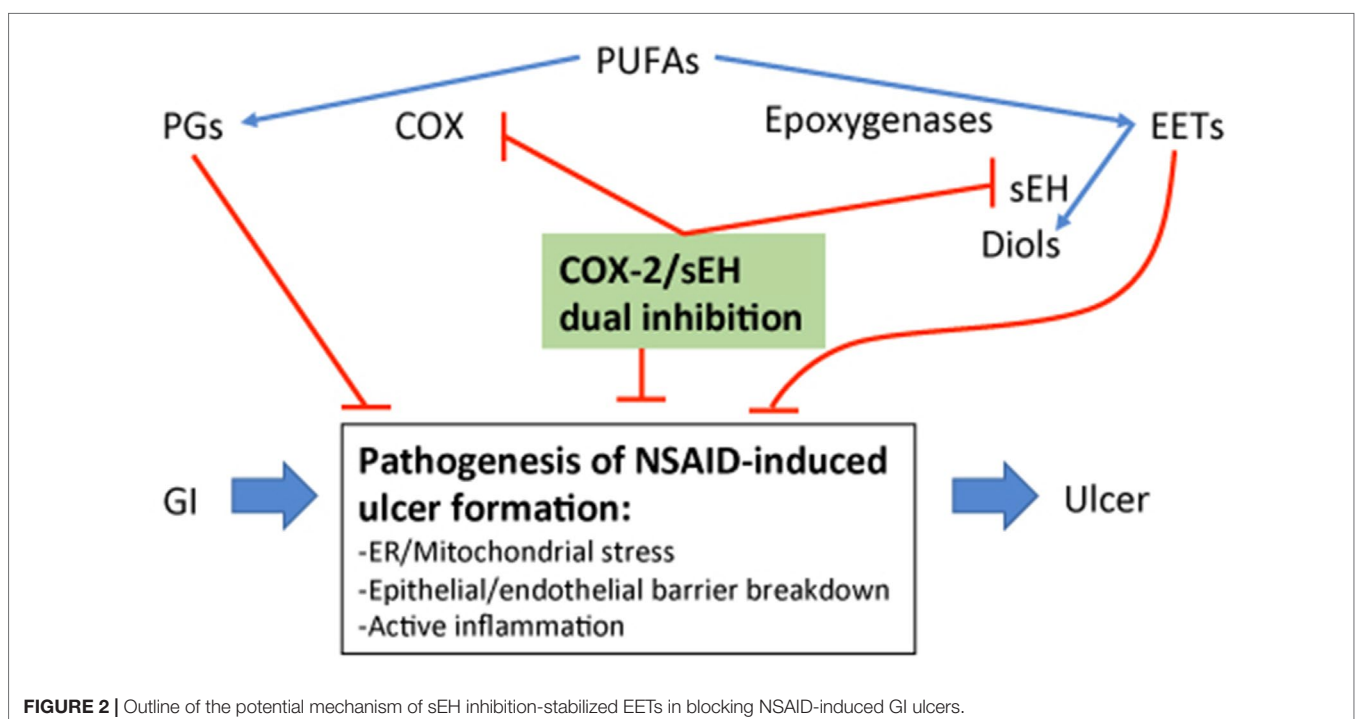
EETs cause an increased activity and expression of peroxisome proliferator-activated receptor- γ (PPAR- γ), a low-affinity nuclear hormone receptor involved in fatty acid metabolism, and inhibition of the NF- κ B pathway (Stienstra et al., 2007; Ward and Tan, 2007). It is likely that at least a portion of the anti-inflammatory effects of EETs act through PPAR- γ as cell culture models show that inhibition of this nuclear hormone receptor diminishes this effect. The role of PPAR- γ in inflammation is through inhibition of activity of pro-inflammatory transcription factors activator protein-1 (AP-1), signal transducers and activators of transcription (STAT), and nuclear factor κ B (NF- κ B). Thus, in addition to increasing EETs, ligand activation of PPAR- γ is another promising strategy for anti-inflammatory activity (Dubuquoy et al., 2006).

sEH Inhibition Can Block NSAID-Induced Gastrointestinal Ulcers

The underlying mechanisms of NSAID-induced GI ulcers are not fully understood; however, they likely involve endoplasmic reticulum (ER)/mitochondrial stress and mucinous epithelial-microvascular barrier breakdown (Hawkey, 1996; Wolfe and Singh, 1999; Cheng et al., 2015). The effects of NSAIDs/aspirin on enterocytes and on vascular endothelial cells in the lamina propria are considered toxic/pathogenic based to the findings

of i) the relatively high concentrations (mM) of conjugated NSAIDs through the enterohepatic circulation (Seitz and Boelsterli, 1998; Treinen-Moslen and Kanz, 2006), ii) direct toxic effects on intestinal mucosal epithelial and endothelial cells (break down the mucosal-vascular barrier), iii) effects on mitochondria (Somasundaram et al., 1997) and ER stress (Tsutsumi et al., 2004), and iv) mucosal injury related to active inflammation.

NSAID-induced GI ulcers can be counter-balanced by epoxides through direct administration of EETs or indirectly by increasing EETs through sEH inhibition (Goswami et al., 2016; Goswami et al., 2017; Yang, 2018). sEH inhibition increases EET bioavailability and yields significant anti-inflammatory effects (Node et al., 1999; Schmelzer et al., 2005; Imig and Hammock, 2009; Norwood et al., 2010). In addition to increasing EET availability, a partial mechanism for the anti-inflammatory effect of sEH inhibition is through a decrease of its product DHET, which has been shown to be important for monocyte chemoattractant protein-1 (MCP-1)-mediated monocyte chemotaxis (Kundu et al., 2013). Thus, co-administration of NSAIDs and a sEH inhibitor has potential synergistic effects of modulating oxylipin profile toward the resolution of inflammation (Schmelzer et al., 2006; Zhang et al., 2014a; Zhang et al., 2014b). The potential mechanistic role of sEH inhibition against NSAID-induced GI ulcers is likely either through decreasing monocyte recruitment and inflammation (Rainsford, 1993; Kundu et al., 2013), blocking NSAID-induced ER/mitochondrial stress (Hawkey, 1996; Inceoglu et al., 2017) to reduce epithelial-vascular barrier injury (Rainsford, 1993), or through enhancing the tissue repair process and angiogenesis (Panigrahy et al., 2013) as outlined in **Figure 2**.



Chronic Pancreatitis and Carcinogenesis

One of the most common conditions leading to pancreatic tumorigenesis is the inflammatory condition chronic pancreatitis. In the development of chronic pancreatitis aberrant ARA metabolism partially mediated by sEH acts to promote inflammation with a decrease of the anti-inflammatory EETs. Inhibition of sEH has been demonstrated as a successful strategy in murine models to inhibit chronic pancreatitis and the development of pancreatic intraepithelial neoplasms (PanIN) using trans-4-{4-[3-(4-chloro-3-trifluoromethyl-phenyl)-ureido]-cyclohexyloxy}-pyridine-2-carboxylic acid methylamide (t-CUPM) in KRAS-mutant mice (Liao et al., 2016a; Liao et al., 2016b). t-CUPM is a novel molecule with dual inhibition of sEH and RAF1 proto-oncogene serine/threonine kinase (c-RAF). This effect was due to both the anti-inflammatory effects of sEH inhibition and the blockade of constitutive KRAS signaling through c-RAF inhibition.

Inflammatory Bowel Disease, Colorectal Carcinogenesis, and the Role of sEH and COX2

A well-recognized risk factor for sporadic colon cancer is chronic inflammation, in which aberrant PUFA metabolism, particularly ARA, is believed to be the key inflammatory mediator contributing to carcinogenesis (Ding et al., 2003; Hermanova et al., 2008). Using IBD as an example model, studies have shown that increased prostaglandins, prostaglandin synthase activity, and mucosal expression of COX-2 all correlate with the severity of IBD activity. NSAIDs are especially promising in chemoprevention for IBD, where there is a direct relationship between inflammation and carcinogenesis. Unfortunately, the clinical application of NSAIDs with COX inhibitory activity tends to exacerbate IBD. These findings are likely multifactorial related to both delayed ulcer healing, a known side effect of NSAIDs, as well as a shunt of ARA substrates to the LOX pathway leading to overproduction of the inflammatory 5-LOX-LTB₄ pathway (Goswami et al., 2016).

Extensive epidemiological and experimental reports show COX-2 has a prominent role in carcinogenesis. Much of these observations come from the effects of aspirin and other NSAIDs resulting in the decreased rate of CRCs, including notable chemopreventive clinical trials testing the use of aspirin in the prevention of GI adenomas and carcinomas in patients with Lynch syndrome (Burn et al., 2011), and celecoxib for the reduction of colon adenomas (Dubois, 2009). COX-2 has been shown to be overexpressed by colon tumors, and COX-2 deficient mice show a decrease in APC-associated carcinogenesis. Further, under the inflammatory conditions of ulcerative colitis (UC), COX-2 is commonly overexpressed in the sequence of UC progression to carcinoma, as well as in non-dysplastic epithelium. The increased expression of COX-2 in UC has been shown to be associated with carcinogenesis rather than the inflammatory activity. PGE₂ production secondary to COX-2 activity promotes epithelial proliferation and crypt stem cell survival. Because of this, COX-2 selective inhibitors were developed with the hopes of anti-cancer effects without the development of GI ulcers; however, these agents showed significant cardiovascular risks in clinical trials,

and one trial showed a continued side effect of GI ulcers (Dubois, 2009).

Considering that sEH is overexpressed in human colitis and CRC (Zhang et al., 2013b), and that sEH inhibition blocks colonic inflammation and carcinogenesis (Wang et al., 2018b; Yang, 2018; Yang et al., 2018), sEH inhibition is a promising agent for the treatment of IBD. sEH inhibition markedly inhibits the progression of inflammation and dysplasia in mouse models of UC (Yang, 1996; Yang et al., 2008; Zhang, 2012). This is in part due to the regulation of cytokines and chemokines, but they also regulate other key enzymatic pathways in ARA metabolism. By increasing EETs, there is a reduction of COX-2 and 5-LOX and their downstream metabolites leading to a reduction of symptoms associated with severe inflammation (Schmelzer et al., 2005; Zhang, 2012). sEH inhibition can be simplistically viewed as shifting ARA metabolism to an EET-rich profile and restoring an anti-inflammatory state.

SEH INHIBITION—POTENT ANTI-INFLAMMATORY ACTIVITY VS POTENTIAL ANGIOGENESIS/TUMOR PROGRESSION ACTION, IS IT DOUBLE EDGE SWORD?

It has been well documented that sEH inhibition has high potential for anti-inflammatory, anti-hypertension, anti-diabetes, and anti-hyperalgesic activities. In addition to the anti-inflammatory activity, sEH inhibition is also associated with an indirect reduction of endotoxin-induced COX and LOX metabolite production *in vivo*, and EETs can transcriptionally inhibit COX-2 expression (Schmelzer et al., 2005; Wang et al., 2018a). However, one of the main concerns of sEH inhibition is related to the observations that EETs derived from the cytochrome p450 pathway actually promote angiogenesis and tumor progression (Elson and Yu, 1994; Panigrahy et al., 2012). This may be partly due to the specific fatty acids, which are epoxidized, as it appears that ω -3 epoxy fatty acid derivatives (e.g., epoxydocosapentaenoic acids) when stabilized by sEH inhibitors are anti-angiogenic and block tumor growth and metastasis, contrary to ω -6 ARA metabolites such as EETs (Zhang et al., 2013a). Furthermore, sEH inhibitors have been shown to promote tumor escape from dormancy and led to extensive metastases in multiple cancer models as a result of increased endothelium-derived EET concentration (Panigrahy et al., 2012). Another study aimed to reduce EETs through downregulation of the cytochrome p450 enzyme Cyp2c44 using PPAR α agonists, and demonstrated a reduction in metastatic non-small cell lung cancer growth and angiogenesis (Skrypnik et al., 2014). In spite of the association of EETs with angiogenesis and cancer progression, there is recent evidence that COX-derived products of EET metabolism may also contribute to angiogenesis, and the dual inhibition of sEH and COX results in a robust inhibition of tumor growth and a net negative effect on angiogenesis (Rand et al., 2017). This would further establish the COX-mediated EET metabolism as physiologically relevant and provides additional rationale for the sEH/COX dual inhibitor strategy. Two dual

therapy cancer models of sEH inhibition combined with either COX-2 inhibition or c-Raf inhibition show robust tumor growth and metastasis inhibition, and in the case of the dual sEH/COX-2 inhibitor (discussed below), both bladder cancers and glioblastomas were found to be inhibited with significantly decreased angiogenesis (Liao et al., 2016b; Li et al., 2017; Wang et al., 2018a).

DUAL COX2/SEH INHIBITION

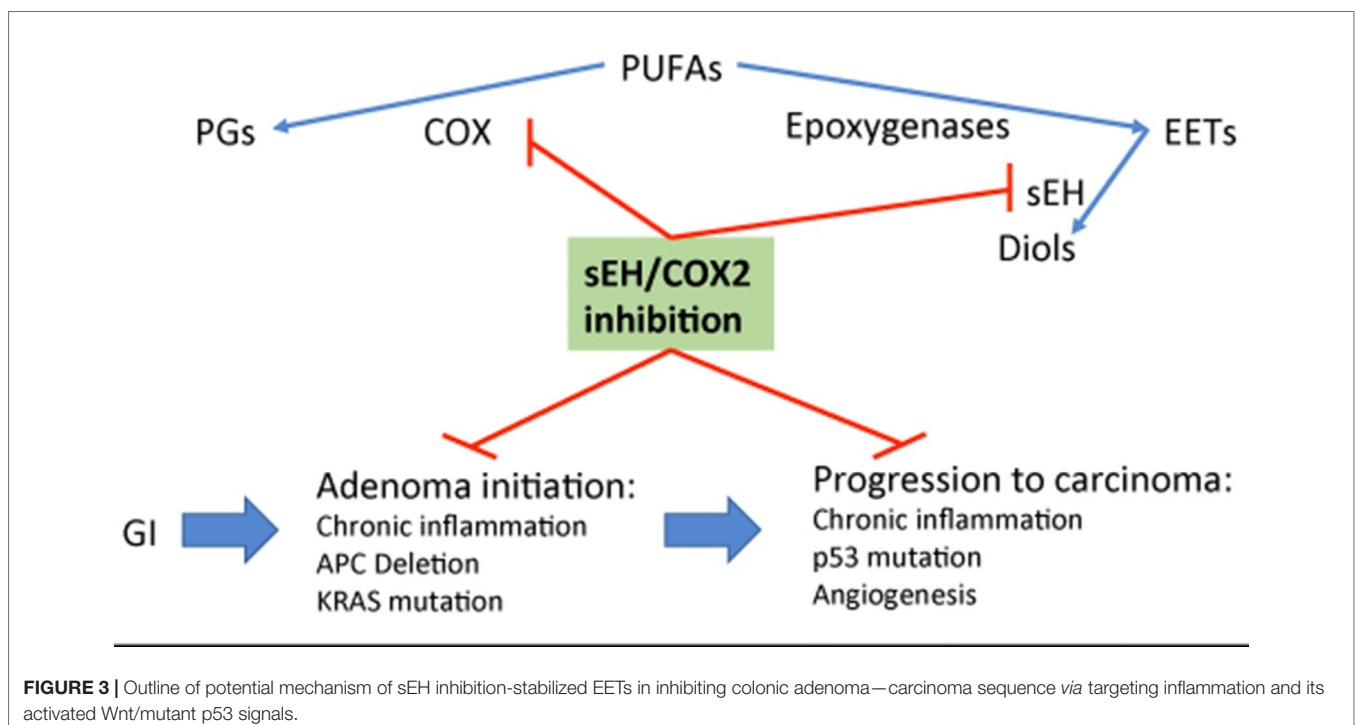
To minimize the angiogenic effect of sEH inhibitor, a novel COX-2/sEH dual inhibitor has been synthesized, 4-(5-phenyl-3-{3-[3-(4-trifluoromethyl-phenyl)-ureido]-propyl}-pyrazol-1-yl)-benzenesulfonamide (PTUPB), based on the structures of celecoxib and sEH inhibitor *trans*-4-[4-(3-adamantan-1-ylureido)cyclohexyloxy]benzoic acid (*t*-AUCB) (Hwang et al., 2011), to circumvent problems associated with formulation of two drugs for co-administration (Morphy and Rankovic, 2005). Studies related to the pharmacokinetics and safety profile have demonstrated favorable characteristics (Hwang et al., 2011; Hye Khan et al., 2016). PTUPB is potent in inhibiting sEH (IC₅₀, 0.9nM) and COX2 (IC₅₀, 1.26uM), but not COX-1 (IC₅₀, > 100uM), and is effective at suppressing inflammation (Hwang et al., 2011; Zhang et al., 2014b).

PTUPB's effects are more potent than celecoxib or *t*-AUCB alone and in combination (Hwang et al., 2011; Zhang et al., 2014b). PTUPB has been demonstrated to protect against metabolic abnormalities and retain kidney function in the Zucker diabetic fatty rat model (Hye Khan et al., 2016). In mouse models of cancer, PTUPB has been shown to be effective

to inhibit tumor growth, metastasis, and angiogenesis, and to potentiate cisplatin-based therapies without increased toxicity (Zhang et al., 2014b; Li et al., 2017; Wang et al., 2018a). Thus, a novel strategy of co-targeting both COX2 and sEH *via* the dual inhibitor PTUPB is particularly intriguing for chemoprevention in the colorectum, especially in patients with IBD. This strategy would provide an environment enriched with EETs, with the chemopreventive benefits of COX-2 inhibition while minimizing side effects including GI tract ulceration, as outlined in **Figure 3**. Taken together, these preclinical studies highly support multi-target agents against sEH and COX2, and their potential for translating into clinical trial, and toward this direction, application for clinical trials is ongoing.

SUMMARY OF SEH AND COX2 INHIBITION ON ANTI-INFLAMMATORY AND CARCINOGENESIS

The decades of studies of ARA metabolism and the sEH point to the potential of sEH inhibition and subsequent enrichment of EETs as an effective strategy for therapies in inflammatory conditions. This is particularly promising in colon and pancreas where chronic inflammatory conditions are well-documented risk factors for carcinogenesis, and therefore sEH inhibition may be ideal as a chemopreventive agent alone or in combination with other strategies. These effects have been robustly studied in mouse models, which show significant reductions in inflammation and cancer development with little to no side effects. Additionally, studies have shown that sEH inhibition can dramatically reduce the side effects of NSAIDs when



given together. Thus, we believe that sEH should be further investigated in clinical trials for inflammatory conditions and inflammation-induced cancers.

One such strategy of sEH treatment involves their co-administration with NSAIDs to further modulate ARA metabolism. NSAIDs including aspirin and celecoxib are among the most widely administered medications worldwide. While they are promising for chemoprevention and in cardiovascular diseases, they also cause significant morbidity through their side effects of gastroenteropathies. These NSAID-related ulcers and bleeding are potentially life-threatening; thus, their use in chemoprevention is not practical. This emphasizes the necessity for a novel approach to harness the beneficial aspects of NSAIDs without the side effects, and one such approach may be through the dual inhibition of COX and sEH. PTUPB is one such agent, although single agent NSAIDs combined

with sEH inhibitors may also be effective. This approach has the potential to revolutionize cancer treatment and prevention, and also has broad implications for the millions of people using NSAIDs chronically for pain and rheumatologic diseases.

AUTHOR CONTRIBUTIONS

All authors listed have made a substantial, direct, and intellectual contribution to the work and approved it for publication.

FUNDING

This study was supported by NIH R01 DK10776, CA172431, and CA164041 to G-YY.

REFERENCES

- Argiriadi, M. A., Morisseau, C., Goodrow, M. H., Dowdy, D. L., Hammock, B. D., and Christianson, D. W. (2000). Binding of alkylurea inhibitors to epoxide hydrolase implicates active site tyrosines in substrate activation. *J. Biol. Chem.* 275 (20), 15265–15270. doi: 10.1074/jbc.M000278200
- Argiriadi, M. A., Morisseau, C., Hammock, B. D., and Christianson, D. W. (1999). Detoxification of environmental mutagens and carcinogens: structure, mechanism, and evolution of liver epoxide hydrolase. *Proc. Natl. Acad. Sci. U. S. A.* 96 (19), 10637–10642. doi: 10.1073/pnas.96.19.10637
- Bjarnason, I., Scarpignato, C., Holmgren, E., Olszewski, M., Rainsford, K. D., and Lanis, A. (2018). Mechanisms of damage to the gastrointestinal tract from nonsteroidal anti-inflammatory drugs. *Gastroenterology* 154 (3), 500–514. doi: 10.1053/j.gastro.2017.10.049
- Burn, J., Gerdes, A. M., Macrae, F., Mecklin, J. P., Moeslein, G., Olschwang, S., et al. (2011). Long-term effect of aspirin on cancer risk in carriers of hereditary colorectal cancer: an analysis from the CAPP2 randomised controlled trial. *Lancet* 378 (9809), 2081–2087. doi: 10.1016/S0140-6736(11)61049-0
- Cao, Y., Nishihara, R., Wu, K., Wang, M., Ogino, S., Willett, W. C., et al. (2016). Population-wide impact of long-term use of aspirin and the risk for cancer. *JAMA Oncol.* 2 (6), 762–769. doi: 10.1001/jamaoncol.2015.6396
- Capdevila, J. H., and Falck, J. R. (2001). The CYP P450 arachidonic acid monooxygenases: from cell signaling to blood pressure regulation. *Biochem. Biophys. Res. Commun.* 285 (3), 571–576. doi: 10.1006/bbrc.2001.5167
- Capdevila, J. H., Falck, J. R., and Harris, R. C. (2000). Cytochrome P450 and arachidonic acid bioactivation. Molecular and functional properties of the arachidonate monooxygenase. *J. Lipid. Res.* 41 (2), 163–181.
- Carroll, M. A., Balazy, M., Margiotta, P., Falck, J. R., and McGiff, J. C. (1993). Renal vasodilator activity of 5,6-epoxyeicosatrienoic acid depends upon conversion by cyclooxygenase and release of prostaglandins. *J. Biol. Chem.* 268 (17), 12260–12266.
- Chan, A. T., and Ladabaum, U. (2016). Where do we stand with aspirin for the prevention of colorectal cancer? The USPSTF recommendations. *Gastroenterology* 150 (1), 14–18. doi: 10.1053/j.gastro.2015.11.018
- Chen, J. K., Capdevila, J., and Harris, R. C. (2000). Overexpression of C-terminal Src kinase blocks 14, 15-epoxyeicosatrienoic acid-induced tyrosine phosphorylation and mitogenesis. *J. Biol. Chem.* 275 (18), 13789–13792. doi: 10.1074/jbc.275.18.13789
- Cheng, Y., Lin, J., Liu, J., Wang, Y., Yan, W., and Zhang, M. (2015). Decreased vascular endothelial growth factor expression is associated with cell apoptosis in low-dose aspirin-induced gastric mucosal injury. *Am. J. Med. Sci.* 349 (2), 110–116. doi: 10.1097/MAJ.0000000000000409
- Cowart, L. A., Wei, S., Hsu, M. H., Johnson, E. F., Krishna, M. U., Falck, J. R., et al. (2002). The CYP4A isoforms hydroxylate epoxyeicosatrienoic acids to form high affinity peroxisome proliferator-activated receptor ligands. *J. Biol. Chem.* 277 (38), 35105–35112. doi: 10.1074/jbc.M201575200
- Cronin, A., Mowbray, S., Durk, H., Homburg, S., Fleming, I., Fisslthaler, B., et al. (2003). The N-terminal domain of mammalian soluble epoxide hydrolase is a phosphatase. *Proc. Natl. Acad. Sci. U. S. A.* 100 (4), 1552–1557. doi: 10.1073/pnas.0437829100
- Decker, M., Arand, M., and Cronin, A. (2009). Mammalian epoxide hydrolases in xenobiotic metabolism and signalling. *Arch. Toxicol.* 83 (4), 297–318. doi: 10.1007/s00204-009-0416-0
- Decker, M., Adamska, M., Cronin, A., Di Giallonardo, F., Burgener, J., Marowsky, A., et al. (2012). EH3 (ABHD9): the first member of a new epoxide hydrolase family with high activity for fatty acid epoxides. *J. Lipid. Res.* 53 (10), 2038–2045. doi: 10.1194/jlr.M024448
- Dietze, E. C., Casas, J., Kuwano, E., and Hammock, B. D. (1993). Inhibition of epoxide hydrolase from human, monkey, bovine, rabbit and murine liver by trans-3-phenylglycidols. *Comp. Biochem. Physiol. B.* 104 (2), 309–314. doi: 10.1016/0305-0491(93)90373-D
- Dietze, E. C., Kuwano, E., Casas, J., and Hammock, B. D. (1991). Inhibition of cytosolic epoxide hydrolase by trans-3-phenylglycidols. *Biochem. Pharmacol.* 42 (6), 1163–1175. doi: 10.1016/0006-2952(91)90250-9
- Ding, X. Z., Hennig, R., and Adrian, T. E. (2003). Lipoxigenase and cyclooxygenase metabolism: new insights in treatment and chemoprevention of pancreatic cancer. *Mol. Cancer* 2, 10. doi: 10.1186/1476-4598-2-10
- Dubois, R. N. (2009). New, long-term insights from the adenoma prevention with celecoxib trial on a promising but troubled class of drugs. *Cancer Prev. Res. (Phila)* 2 (4), 285–287. doi: 10.1158/1940-6207.CAPR-09-0038
- Dubuquoy, L., Rousseaux, C., Thuru, X., Peyrin-Biroulet, L., Romano, O., Chavatte, P., et al. (2006). PPARgamma as a new therapeutic target in inflammatory bowel diseases. *Gut* 55 (9), 1341–1349. doi: 10.1136/gut.2006.093484
- Elson, C. E., and Yu, S. G. (1994). The chemoprevention of cancer by mevalonate-derived constituents of fruits and vegetables. *J. Nutr.* 124 (5), 607–614. doi: 10.1093/jn/124.5.607
- Enayetallah, A. E., French, R. A., Barber, M., and Grant, D. F. (2006). Cell-specific subcellular localization of soluble epoxide hydrolase in human tissues. *J. Histochem. Cytochem.* 54 (3), 329–335. doi: 10.1369/jhc.5A6808.2005
- Eriksson, A. M., Zetterqvist, M. A., Lundgren, B., Andersson, K., Beijer, B., and DePierre, J. W. (1991). Studies on the intracellular distributions of soluble epoxide hydrolase and of catalase by digitonin-permeabilization of hepatocytes isolated from control and clofibrate-treated mice. *Eur. J. Biochem.* 198 (2), 471–476. doi: 10.1111/j.1432-1033.1991.tb16037.x
- Fang, X., Kaduce, T. L., VanRollins, M., Weintraub, N. L., and Spector, A. A. (2000). Conversion of epoxyeicosatrienoic acids (EETs) to chain-shortened epoxy fatty acids by human skin fibroblasts. *J. Lipid. Res.* 41 (1), 66–74. doi: 10.1074/jbc.M011761200
- Fang, X., Kaduce, T. L., Weintraub, N. L., VanRollins, M., and Spector, A. A. (1996). Functional implications of a newly characterized pathway of 11,12-epoxyeicosatrienoic acid metabolism in arterial smooth muscle. *Circ. Res.* 79 (4), 784–793. doi: 10.1161/01.RES.79.4.784

- Fang, X., VanRollins, M., Kaduce, T. L., and Spector, A. A. (1995). Epoxyeicosatrienoic acid metabolism in arterial smooth muscle cells. *J. Lipid. Res.* 36 (6), 1236–1246.
- Fang, X., Kaduce, T. L., Weintraub, N. L., Harmon, S., Teesch, L. M., Morisseau, C., et al. (2001). Pathways of epoxyeicosatrienoic acid metabolism in endothelial cells. Implications for the vascular effects of soluble epoxide hydrolase inhibition. *J. Biol. Chem.* 276 (18), 14867–14874. doi: 10.1074/jbc.M011761200
- Fischer, S. M., Hawk, E. T., and Lubet, R. A. (2011). Coxibs and other nonsteroidal anti-inflammatory drugs in animal models of cancer chemoprevention. *Cancer Prev. Res. (Phila)* 4 (11), 1728–1735. doi: 10.1158/1940-6207.CAPR-11-0166
- Fretland, A. J., and Omiecinski, C. J. (2000). Epoxide hydrolases: biochemistry and molecular biology. *Chem. Biol. Interact.* 129 (1–2), 41–59. doi: 10.1016/S0009-2797(00)00197-6
- Fukao, M., Mason, H. S., Kenyon, J. L., Horowitz, B., and Keef, K. D. (2001). Regulation of BK(Ca) channels expressed in human embryonic kidney 293 cells by epoxyeicosatrienoic acid. *Mol. Pharmacol.* 59 (1), 16–23. doi: 10.1124/mol.59.1.16
- Goswami, S. K., Rand, A. A., Wan, D., Yang, J., Inceoglu, B., Thomas, M., et al. (2017). Pharmacological inhibition of soluble epoxide hydrolase or genetic deletion reduces diclofenac-induced gastric ulcers. *Life Sci.* 180, 114–122. doi: 10.1016/j.lfs.2017.05.018
- Goswami, S. K., Wan, D., Yang, J., Trindade da Silva, C. A., Morisseau, C., Kodani, S. D., et al. (2016). Anti-ulcer efficacy of soluble epoxide hydrolase inhibitor tppu on diclofenac-induced intestinal ulcers. *J. Pharmacol. Exp. Ther.* 357 (3), 529–536. doi: 10.1124/jpet.116.232108
- Hawkey, C. J. (1996). Non-steroidal anti-inflammatory drug gastropathy: causes and treatment. *Scand. J. Gastroenterol. Suppl.* 220, 124–127. doi: 10.3109/00365529609094763
- Hermanova, M., Trna, J., Nenutil, R., Dite, P., and Kala, Z. (2008). Expression of COX-2 is associated with accumulation of p53 in pancreatic cancer: analysis of COX-2 and p53 expression in premalignant and malignant ductal pancreatic lesions. *Eur. J. Gastroenterol. Hepatol.* 20 (8), 732–739. doi: 10.1097/MEG.0b013e3282f945fb
- Hiesinger, K., Wagner, K. M., Hammock, B. D., Proschak, E., and Hwang, S. H. (2019). Development of multitarget agents possessing soluble epoxide hydrolase inhibitory activity. *Prostaglandins. Other Lipid Mediat.* 140, 31–39. doi: 10.1016/j.prostaglandins.2018.12.003
- Hoebel, B. G., and Graier, W. F. (1998). 11,12-Epoxyeicosatrienoic acid stimulates tyrosine kinase activity in porcine aortic endothelial cells. *Eur. J. Pharmacol.* 346 (1), 115–117. doi: 10.1016/S0014-2999(98)00118-6
- Hollinshead, M., and Meijer, J. (1988). Immunocytochemical analysis of soluble epoxide hydrolase and catalase in mouse and rat hepatocytes demonstrates a peroxisomal localization before and after clofibrate treatment. *Eur. J. Cell Biol.* 46 (3), 394–402.
- Hwang, S. H., Wagner, K. M., Morisseau, C., Liu, J. Y., Dong, H., Wecksler, A. T., et al. (2011). Synthesis and structure-activity relationship studies of urea-containing pyrazoles as dual inhibitors of cyclooxygenase-2 and soluble epoxide hydrolase. *J. Med. Chem.* 54 (8), 3037–3050. doi: 10.1021/jm2001376
- Hye Khan, M. A., Hwang, S. H., Sharma, A., Corbett, J. A., Hammock, B. D., and Imig, J. D. (2016). A dual COX-2/sEH inhibitor improves the metabolic profile and reduces kidney injury in Zucker diabetic fatty rat. *Prostaglandins Other Lipid Mediat.* 125, 40–47. doi: 10.1016/j.prostaglandins.2016.07.003
- Imig, J. D., and Hammock, B. D. (2009). Soluble epoxide hydrolase as a therapeutic target for cardiovascular diseases. *Nat. Rev. Drug Discov.* 8 (10), 794–805. doi: 10.1038/nrd2875
- Inceoglu, B., Bettaieb, A., Haj, F. G., Gomes, A. V., and Hammock, B. D. (2017). Modulation of mitochondrial dysfunction and endoplasmic reticulum stress are key mechanisms for the wide-ranging actions of epoxy fatty acids and soluble epoxide hydrolase inhibitors. *Prostaglandins Other Lipid Mediat.* 133, 68–78. doi: 10.1016/j.prostaglandins.2017.08.003
- Inceoglu, B., Schmelzer, K. R., Morisseau, C., Jinks, S. L., and Hammock, B. D. (2007). Soluble epoxide hydrolase inhibition reveals novel biological functions of epoxyeicosatrienoic acids (EETs). *Prostaglandins. Other Lipid Mediat.* 82 (17–4), 42–49. doi: 10.1016/j.prostaglandins.2006.05.004
- Jaeschen, H., and Smith, C. W. (1997). Mechanisms of neutrophil-induced parenchymal cell injury. *J. Leukoc. Biol.* 61 (6), 647–653. doi: 10.1002/jlb.61.6.647
- Johansson, C., Stark, A., Sandberg, M., Ek, B., Rask, L., and Meijer, J. (1995). Tissue specific basal expression of soluble murine epoxide hydrolase and effects of clofibrate on the mRNA levels in extrahepatic tissues and liver. *Arch. Toxicol.* 70 (1), 61–63. doi: 10.1007/s002040050250
- Karara, A., Dishman, E., Falck, J. R., and Capdevila, J. H. (1991). Endogenous epoxyeicosatrienoyl-phospholipids. a novel class of cellular glycerolipids containing epoxidized arachidonate moieties. *J. Biol. Chem.* 266 (12), 7561–7569.
- Karara, A., Dishman, E., Jacobson, H., Falck, J. R., and Capdevila, J. H. (1990). Arachidonic acid epoxigenase. Stereochemical analysis of the endogenous epoxyeicosatrienoic acids of human kidney cortex. *FEBS Lett.* 268 (1), 227–230. doi: 10.1016/0014-5793(90)81014-F
- Karara, A., Wei, S., Spady, D., Swift, L., Capdevila, J. H., and Falck, J. R. (1992). Arachidonic acid epoxigenase: structural characterization and quantification of epoxyeicosatrienoates in plasma. *Biochem. Biophys. Res. Commun.* 182 (3), 1320–1325. doi: 10.1016/0006-291X(92)91877-S
- Kim, I. H., Morisseau, C., Watanabe, T., and Hammock, B. D. (2004). Design, synthesis, and biological activity of 1,3-disubstituted ureas as potent inhibitors of the soluble epoxide hydrolase of increased water solubility. *J. Med. Chem.* 47 (8), 2110–2122. doi: 10.1021/jm030514j
- Kundu, S., Roome, T., Bhattacharjee, A., Carnevale, K. A., Yakubenko, V. P., Zhang, R., et al. (2013). Metabolic products of soluble epoxide hydrolase are essential for monocyte chemotaxis to MCP-1 *in vitro* and *in vivo*. *J. Lipid. Res.* 54 (2), 436–447. doi: 10.1194/jlr.M031914
- Larsson, C., White, I., Johansson, C., Stark, A., and Meijer, J. (1995). Localization of the human soluble epoxide hydrolase gene (EPHX2) to chromosomal region 8p21-p12. *Hum. Genet.* 95 (3), 356–358. doi: 10.1007/BF00225209
- Li, P. L., and Campbell, W. B. (1997). Epoxyeicosatrienoic acids activate K⁺ channels in coronary smooth muscle through a guanine nucleotide binding protein. *Circ. Res.* 80 (6), 877–884. doi: 10.1161/01.RES.80.6.877
- Li, J., Zhou, Y., Wang, H., Gao, Y., Li, L., Hwang, S. H., et al. (2017). COX-2/sEH dual inhibitor PTUPB suppresses glioblastoma growth by targeting epidermal growth factor receptor and hyaluronan mediated motility receptor. *Oncotarget* 8 (50), 87353–87363. doi: 10.18632/oncotarget.20928
- Liao, J., Hwang, S. H., Li, H., Liu, J. Y., Hammock, B. D., and Yang, G. Y. (2016a). Inhibition of Chronic Pancreatitis and Murine Pancreatic Intraepithelial Neoplasia by a Dual Inhibitor of c-RAF and Soluble Epoxide Hydrolase in LSL-KrasG(1)(2)D/Pdx-1-Cre Mice. *Anticancer Res.* 36 (1), 27–37.
- Liao, J., Hwang, S. H., Li, H., Yang, Y., Yang, J., Wecksler, A. T., et al. (2016b). Inhibition of mutant KrasG12D-initiated murine pancreatic carcinoma growth by a dual c-Raf and soluble epoxide hydrolase inhibitor t-CUPM. *Cancer Lett.* 371 (2), 187–193. doi: 10.1016/j.canlet.2015.11.042
- Maiden, L. (2009). Capsule endoscopic diagnosis of nonsteroidal antiinflammatory drug-induced enteropathy. *J. Gastroenterol.* 44 Suppl 19, 64–71. doi: 10.1016/S0006-2952(02)00952-8
- Morisseau, C., and Hammock, B. D. (2005). Epoxide hydrolases: mechanisms, inhibitor designs, and biological roles. *Annu. Rev. Pharmacol. Toxicol.* 45, 311–333. doi: 10.1146/annurev.pharmtox.45.120403.095920
- Morisseau, C., and Hammock, B. D. (2007). Measurement of soluble epoxide hydrolase (sEH) activity. *Curr. Protoc. Toxicol.* Chapter 4, Unit 4, 23. doi: 10.1002/0471140856.tx0423s33
- Morisseau, C., and Hammock, B. D. (2012). Impact of soluble epoxide hydrolase and epoxyeicosanoids on human health. *Annu. Rev. Pharmacol. Toxicol.* 2013 (53), 37–58. doi: 10.1146/annurev-pharmtox-011112-140244
- Morisseau, C., Du, G., Newman, J. W., and Hammock, B. D. (1998). Mechanism of mammalian soluble epoxide hydrolase inhibition by chalcone oxide derivatives. *Arch. Biochem. Biophys.* 356 (2), 214–228. doi: 10.1006/abbi.1998.0756
- Morisseau, C., Goodrow, M. H., Newman, J. W., Wheelock, C. E., Dowdy, D. L., and Hammock, B. D. (2002). Structural refinement of inhibitors of urea-based soluble epoxide hydrolases. *Biochem. Pharmacol.* 63 (9), 1599–1608. doi: 10.1016/S0006-2952(02)00952-8
- Morisseau, C., Goodrow, M. H., Dowdy, D., Zheng, J., Greene, J. F., Sanborn, J. R., et al. (1999). Potent urea and carbamate inhibitors of soluble epoxide hydrolases. *Proc. Natl. Acad. Sci. U. S. A.* 96 (16), 8849–8854. doi: 10.1073/pnas.96.16.8849
- Morphy, R., and Rankovic, Z. (2005). Designed multiple ligands. An emerging drug discovery paradigm. *J. Med. Chem.* 48 (21), 6523–6543. doi: 10.1021/jm058225d
- Mullen, R. T., Trelease, R. N., Duerk, H., Arand, M., Hammock, B. D., Oesch, F., et al. (1999). Differential subcellular localization of endogenous and transfected

- soluble epoxide hydrolase in mammalian cells: evidence for isozyme variants. *FEBS Lett.* 445 (2–3), 301–305. doi: 10.1016/S0014-5793(99)00142-8
- Mullin, C. A., and Hammock, B. D. (1982). Chalcone oxides—potent selective inhibitors of cytosolic epoxide hydrolase. *Arch. Biochem. Biophys.* 216 (2), 423–439. doi: 10.1016/0003-9861(82)90231-4
- Newman, J. W., Morisseau, C., Harris, T. R., and Hammock, B. D. (2003). The soluble epoxide hydrolase encoded by EPXH2 is a bifunctional enzyme with novel lipid phosphate phosphatase activity. *Proc. Natl. Acad. Sci. U. S. A.* 100 (4), 1558–1563. doi: 10.1073/pnas.0437724100
- Node, K., Huo, Y., Ruan, X., Yang, B., Spiecker, M., Ley, K., et al. (1999). Anti-inflammatory properties of cytochrome P450 epoxygenase-derived eicosanoids. *Science* 285 (5431), 1276–1279. doi: 10.1126/science.285.5431.1276
- Node, K., Ruan, X. L., Dai, J., Yang, S. X., Graham, L., Zeldin, D. C., et al. (2001). Activation of Galpha s mediates induction of tissue-type plasminogen activator gene transcription by epoxyeicosatrienoic acids. *J. Biol. Chem.* 276 (19), 15983–15989. doi: 10.1074/jbc.M100439200
- Norwood, S., Liao, J., Hammock, B. D., and Yang, G. Y. (2010). Epoxyeicosatrienoic acids and soluble epoxide hydrolase: potential therapeutic targets for inflammation and its induced carcinogenesis. *Am. J. Transl. Res.* 2 (4), 447–457.
- Pace-Asciak, C. R., Granstrom, E., and Samuelsson, B. (1983). Arachidonic acid epoxides. Isolation and structure of two hydroxy epoxide intermediates in the formation of 8,11,12- and 10,11,12-trihydroxyeicosatrienoic acids. *J. Biol. Chem.* 258 (11), 6835–6840.
- Panigrahy, D., Edin, M. L., Lee, C. R., Huang, S., Bielenberg, D. R., Butterfield, C. E., et al. (2012). Epoxyeicosanoids stimulate multiorgan metastasis and tumor dormancy escape in mice. *J. Clin. Invest.* 122 (1), 178–191. doi: 10.1172/JCI58128
- Panigrahy, D., Kalish, B. T., Huang, S., Bielenberg, D. R., Le, H. D., Yang, J., et al. (2013). Epoxyeicosanoids promote organ and tissue regeneration. *Proc. Natl. Acad. Sci. U. S. A.* 110 (33), 13528–13533. doi: 10.1073/pnas.1311565110
- Rainsford, K. D. (1993). Mechanisms of gastrointestinal damage by NSAIDs. *Agents Actions Suppl.* 44, 59–64.
- Rand, A. A., Barnych, B., Morisseau, C., Cajka, T., Lee, K. S. S., Panigrahy, D., et al. (2017). Cyclooxygenase-derived proangiogenic metabolites of epoxyeicosatrienoic acids. *Proc. Natl. Acad. Sci. U. S. A.* 114 (17), 4370–4375. doi: 10.1073/pnas.1616893114
- Ricciotti, E., and FitzGerald, G. A. (2011). Prostaglandins and inflammation. *Arterioscler. Thromb. Vasc. Biol.* 31 (5), 986–1000. doi: 10.1161/ATVBAHA.110.207449
- Sandberg, M., and Meijer, J. (1996). Structural characterization of the human soluble epoxide hydrolase gene (EPHX2). *Biochem. Biophys. Res. Commun.* 221 (2), 333–339. doi: 10.1006/bbrc.1996.0596
- Schmelzer, K. R., Kubala, L., Newman, J. W., Kim, I. H., Eiserich, J. P., and Hammock, B. D. (2005). Soluble epoxide hydrolase is a therapeutic target for acute inflammation. *Proc. Natl. Acad. Sci. U. S. A.* 102 (28), 9772–9777. doi: 10.1073/pnas.0503279102
- Schmelzer, K. R., Inceoglu, B., Kubala, L., Kim, I. H., Jinks, S. L., Eiserich, J. P., et al. (2006). Enhancement of antinociception by coadministration of nonsteroidal anti-inflammatory drugs and soluble epoxide hydrolase inhibitors. *Proc. Natl. Acad. Sci. U. S. A.* 103 (37), 13646–13651. doi: 10.1073/pnas.0605908103
- Seidegard, J., and Ekstrom, G. (1997). The role of human glutathione transferases and epoxide hydrolases in the metabolism of xenobiotics. *Environ. Health Perspect.* 105 Suppl 4, 791–799. doi: 10.1289/ehp.97105s4791
- Seitz, S., and Boelsterli, U. A. (1998). Diclofenac acyl glucuronide, a major biliary metabolite, is directly involved in small intestinal injury in rats. *Gastroenterology* 115 (6), 1476–1482. doi: 10.1016/S0016-5085(98)70026-5
- Seubert, J., Yang, B., Bradbury, J. A., Graves, J., Degraff, L. M., Gabel, S., et al. (2004). Enhanced postischemic functional recovery in CYP2J2 transgenic hearts involves mitochondrial ATP-sensitive K⁺ channels and p42/p44 MAPK pathway. *Circ. Res.* 95 (5), 506–514. doi: 10.1161/01.RES.0000139436.89654.c8
- Shimada, T. (2006). Xenobiotic-metabolizing enzymes involved in activation and detoxification of carcinogenic polycyclic aromatic hydrocarbons. *Drug Metab. Pharmacokinet.* 21 (4), 257–276. doi: 10.2133/dmpk.21.257
- Skrypnik, N., Chen, X., Hu, W., Su, Y., Mont, S., Yang, S., et al. (2014). PPARalpha activation can help prevent and treat non-small cell lung cancer. *Cancer Res.* 74 (2), 621–631. doi: 10.1158/0008-5472.CAN-13-1928
- Somasundaram, S., Rafi, S., Hayllar, J., Sigthorsson, G., Jacob, M., Price, A. B., et al. (1997). Mitochondrial damage: a possible mechanism of the “topical” phase of NSAID induced injury to the rat intestine. *Gut* 41 (3), 344–353. doi: 10.1136/gut.41.3.344
- Sostres, C., and Lanas, A. (2011). Gastrointestinal effects of aspirin. *Nat. Rev. Gastroenterol. Hepatol.* 8 (7), 385–394. doi: 10.1038/nrgastro.2011.97
- Sostres, C., Gargallo, C. J., Arroyo, M. T., and Lanas, A. (2010). Adverse effects of non-steroidal anti-inflammatory drugs (NSAIDs, aspirin and coxibs) on upper gastrointestinal tract. *Best Pract. Res. Clin. Gastroenterol.* 24 (2), 121–132. doi: 10.1016/j.bpg.2009.11.005
- Spearman, M. E., Prough, R. A., Estabrook, R. W., Falck, J. R., Manna, S., Leibman, K. C., et al. (1985). Novel glutathione conjugates formed from epoxyeicosatrienoic acids (EETs). *Arch. Biochem. Biophys.* 242 (1), 225–230. doi: 10.1016/0003-9861(85)90496-5
- Spector, A. A., and Kim, H. Y. (2015). Cytochrome P450 epoxygenase pathway of polyunsaturated fatty acid metabolism. *Biochim. Biophys. Acta* 1851 (4), 356–365. doi: 10.1016/j.bbalip.2014.07.020
- Spector, A. A., Fang, X., Snyder, G. D., and Weintraub, N. L. (2004). Epoxyeicosatrienoic acids (EETs): metabolism and biochemical function. *Prog. Lipid Res.* 43 (1), 55–90. doi: 10.1016/S0163-7827(03)00049-3
- Stienstra, R., Duval, C., Muller, M., and Kersten, S. (2007). PPARs, Obesity, and Inflammation. *PPAR Res.* 2007, 95974. doi: 10.1155/2007/95974
- Sudano, I., Flammer, A. J., Roas, S., Enseleit, F., Noll, G., and Ruschitzka, F. (2012). Nonsteroidal antiinflammatory drugs, acetaminophen, and hypertension. *Curr. Hypertens. Rep.* 14 (4), 304–309. doi: 10.1007/s11906-012-0274-7
- Treinen-Moslen, M., and Kanz, M. F. (2006). Intestinal tract injury by drugs: importance of metabolite delivery by yellow bile road. *Pharmacol. Ther.* 112 (3), 649–667. doi: 10.1016/j.pharmthera.2006.05.007
- Tsoi, K. K., Chan, F. C., Hirai, H. W., and Sung, J. J. (2018). Risk of gastrointestinal bleeding and benefit from colorectal cancer reduction from long-term use of low-dose aspirin: a retrospective study of 612 509 patients. *J. Gastroenterol. Hepatol.* 33 (10), 1728–1736. doi: 10.1111/jgh.14261
- Tsutsumi, S., Gotoh, T., Tomisato, W., Mima, S., Hoshino, T., Hwang, H. J., et al. (2004). Endoplasmic reticulum stress response is involved in nonsteroidal anti-inflammatory drug-induced apoptosis. *Cell Death Differ.* 11 (9), 1009–1016. doi: 10.1038/sj.cdd.4401436
- VanRollins, M., Kaduce, T. L., Knapp, H. R., and Spector, A. A. (1993). 14,15-Epoxyeicosatrienoic acid metabolism in endothelial cells. *J. Lipid. Res.* 34 (11), 1931–1942.
- Wang, F., Zhang, H., Ma, A. H., Yu, W., Zimmermann, M., Yang, J., et al. (2018a). COX-2/sEH dual inhibitor PTUPB potentiates the antitumor efficacy of cisplatin. *Mol. Cancer Ther.* 17 (2), 474–483. doi: 10.1158/1535-7163.MCT-16-0818
- Wang, W., Yang, J., Zhang, J., Wang, Y., Hwang, S. H., Qi, W., et al. (2018b). Lipidomic profiling reveals soluble epoxide hydrolase as a therapeutic target of obesity-induced colonic inflammation. *Proc. Natl. Acad. Sci. U. S. A.* 115 (20), 5283–5288. doi: 10.1073/pnas.1721711115
- Wang, Y., Wei, X., Xiao, X., Hui, R., Card, J. W., Carey, M. A., et al. (2005). Arachidonic acid epoxygenase metabolites stimulate endothelial cell growth and angiogenesis via mitogen-activated protein kinase and phosphatidylinositol 3-kinase/Akt signaling pathways. *J. Pharmacol. Exp. Ther.* 314 (2), 522–532. doi: 10.1124/jpet.105.083477
- Ward, J. E., and Tan, X. (2007). Peroxisome proliferator activated receptor ligands as regulators of airway inflammation and remodelling in chronic lung disease. *PPAR Res.* 2007, 14983. doi: 10.1155/2007/14983
- Weintraub, N. L., Fang, X., Kaduce, T. L., VanRollins, M., Chatterjee, P., and Spector, A. A. (1999). Epoxide hydrolases regulate epoxyeicosatrienoic acid incorporation into coronary endothelial phospholipids. *Am. J. Physiol.* 277 (5), H2098–2108. doi: 10.1152/ajpheart.1999.277.5.H2098
- Wolfe, M. M. L., and Singh, D. R. (1999). Gastrointestinal toxicity of nonsteroidal antiinflammatory drugs. *N. Engl. J. Med.* 340 (24), 1888–1899. doi: 10.1056/NEJM199906173402407
- Wongrakpanich, S. W., Melhado, A., and Rangaswami, K. (2018). A comprehensive review of non-steroidal anti-inflammatory drug use in the elderly. *Aging Dis.* 9 (1), 143–150. doi: 10.14336/AD.2017.0306
- Yang, V. W. (1996). Eicosanoids and inflammatory bowel disease. *Gastroenterol. Clin. North. Am.* 25 (2), 317–332. doi: 10.1016/S0889-8553(05)70249-1
- Yang, G. Y. (2018). Proinflammatory enzyme soluble epoxide hydrolase bridges obesity to colonic inflammation and potential carcinogenesis. *Proc. Natl. Acad. Sci. U. S. A.* 115 (23), 5827–5828. doi: 10.1073/pnas.1807520115
- Yang, J., Schmelzer, K., Georgi, K., and Hammock, B. D. (2009). Quantitative profiling method for oxylipin metabolome by liquid chromatography

- electrospray ionization tandem mass spectrometry. *Anal. Chem.* 81 (19), 8085–8093. doi: 10.1021/ac901282n
- Yang, G.-Y. Zhang, M., Chung, Y. T., Lou, C., Tsai, C., Hammock, B. D., and Liao, J. (2008). Inhibition of spontaneous colitis development in interleukin-10 knockout mice by soluble epoxide hydrolase inhibitor. *FASEB J.* 22, 479.29–479.29. doi: 10.1096/fasebj.22.1_supplement.479.29
- Yang, H., Wang, W., Romano, K. A., Gu, M., Sanidad, K. Z., Kim, D., et al. (2018). A common antimicrobial additive increases colonic inflammation and colitis-associated colon tumorigenesis in mice. *Sci. Transl. Med.* 10 (443), eaan4116. doi: 10.1126/scitranslmed.aan4116
- Yu, Z., Huse, L. M., Adler, P., Graham, L., Ma, J., Zeldin, D. C., et al. (2000). Increased CYP2J expression and epoxyeicosatrienoic acid formation in spontaneously hypertensive rat kidney. *Mol. Pharmacol.* 57 (5), 1011–1020.
- Zhang, G., Kodani, S., and Hammock, B. D. (2014a). Stabilized epoxygenated fatty acids regulate inflammation, pain, angiogenesis and cancer. *Prog. Lipid Res.* 53, 108–123. doi: 10.1016/j.plipres.2013.11.003
- Zhang, J. Y., Prakash, C., Yamashita, K., and Blair, I. A. (1992). Regiospecific and enantioselective metabolism of 8,9-epoxyeicosatrienoic acid by cyclooxygenase. *Biochem. Biophys. Res. Commun.* 183 (1), 138–143. doi: 10.1016/0006-291X(92)91619-2
- Zhang, W., Li, H., Dong, H., Liao, J., Hammock, B. D., and Yang, G. Y. (2013b). Soluble epoxide hydrolase deficiency inhibits dextran sulfate sodium-induced colitis and carcinogenesis in mice. *Anticancer Res.* 33 (12), 5261–5271.
- Zhang, W., Liao, J., Li, H., Dong, H., Bai, H., Yang, A., et al. (2013c). Reduction of inflammatory bowel disease-induced tumor development in IL-10 knockout mice with soluble epoxide hydrolase gene deficiency. *Mol. Carcinog.* 52 (9), 726–738. doi: 10.1002/mc.21918
- Zhang, G., Panigrahy, D., Hwang, S. H., Yang, J., Mahakian, L. M., Wettersten, H. I., et al. (2014b). Dual inhibition of cyclooxygenase-2 and soluble epoxide hydrolase synergistically suppresses primary tumor growth and metastasis. *Proc. Natl. Acad. Sci. U. S. A.* 111 (30), 11127–11132. doi: 10.1073/pnas.1410432111
- Zhang, G., Panigrahy, D., Mahakian, L. M., Yang, J., Liu, J. Y., Stephen Lee, K. S., et al. (2013a). Epoxy metabolites of docosahexaenoic acid (DHA) inhibit angiogenesis, tumor growth, and metastasis. *Proc. Natl. Acad. Sci. U. S. A.* 110 (16), 6530–6535. doi: 10.1073/pnas.1304321110
- Zhang, W., Yang, A. L., Liao, J., Li, H., Dong, H., Chung, Y. T., et al. (2012). Soluble epoxide hydrolase gene deficiency or inhibition attenuates chronic active inflammatory bowel disease in IL-10(−/−) mice. *Dig. Dis. Sci.* 57 (10), 2580–2591. doi: 10.1007/s10620-012-2217-1

Conflict of Interest Statement: The authors declare that the research was conducted in the absence of any commercial or financial relationships that could be construed as a potential conflict of interest.

Copyright © 2019 Jones, Liao, Tong, Xu, Sun, Li and Yang. This is an open-access article distributed under the terms of the Creative Commons Attribution License (CC BY). The use, distribution or reproduction in other forums is permitted, provided the original author(s) and the copyright owner(s) are credited and that the original publication in this journal is cited, in accordance with accepted academic practice. No use, distribution or reproduction is permitted which does not comply with these terms.



Effect Of Dual sEH/COX-2 Inhibition on Allergen-Induced Airway Inflammation

Mythili Dileepan¹, Stephanie Rastle-Simpson¹, Yana Greenberg¹, Dayanjan S. Wijesinghe², Naren Gajenthra Kumar², Jun Yang³, Sung Hee Hwang³, Bruce D. Hammock³, P. Sriramarao^{1†} and Savita P. Rao^{1*}

¹ Department of Veterinary & Biomedical Sciences, University of Minnesota, St. Paul, MN, United States, ² Department of Pharmacotherapy and Outcomes Sciences, School of Pharmacy, Virginia Commonwealth University, Richmond, VA, United States, ³ Department of Entomology, Nematology and Comprehensive Cancer Center, University of California, Davis, CA, United States

OPEN ACCESS

Edited by:

John D. Imig,
Medical College of Wisconsin,
United States

Reviewed by:

Ayman Ouda El-Kadi,
University of Alberta, Canada
Xingbin Ai,
Brigham and Women's Hospital and
Harvard Medical School,
United States

*Correspondence:

Savita P. Rao
raox099@umn.edu

†Present address:

P. Sriramarao
Department of Microbiology and
Immunology, Virginia Commonwealth
University, Richmond, VA,
United States

Specialty section:

This article was submitted to
Translational Pharmacology,
a section of the journal
Frontiers in Pharmacology

Received: 03 July 2019

Accepted: 30 August 2019

Published: 27 September 2019

Citation:

Dileepan M, Rastle-Simpson S, Greenberg Y, Wijesinghe DS, Kumar NG, Yang J, Hwang SH, Hammock BD, Sriramarao P and Rao SP (2019) Effect Of Dual sEH/COX-2 Inhibition on Allergen-Induced Airway Inflammation. *Front. Pharmacol.* 10:1118. doi: 10.3389/fphar.2019.01118

Arachidonic acid metabolites resulting from the cyclooxygenase (COX), lipoxygenase, and cytochrome P450 oxidase enzymatic pathways play pro- and anti-inflammatory roles in allergic airway inflammation (AAI) and asthma. Expression of COX-2 and soluble epoxide hydrolase (sEH) are elevated in allergic airways and their enzymatic products (e.g., prostaglandins and diols of epoxyeicosatrienoic acids, respectively) have been shown to participate in the pathogenesis of AAI. Here, we evaluated the outcome of inhibiting the COX-2 and sEH enzymatic pathways with a novel dual inhibitor, PTUPB, in *A. alternata*-induced AAI. Allergen-challenged mice were administered with 10 or 30 mg/kg of PTUPB, celecoxib (selective COX-2 inhibitor), *t*-TUCB (selective sEH inhibitor) or vehicle daily by gavage and evaluated for various features of AAI. PTUPB and *t*-TUCB at 30 mg/kg, but not celecoxib, inhibited eosinophilic infiltration and significantly increased levels of anti-inflammatory EETs in the lung tissue of allergen-challenged mice. *t*-TUCB significantly inhibited allergen-induced IL-4 and IL-13, while a less pronounced reduction was noted with PTUPB and celecoxib. Additionally, *t*-TUCB markedly inhibited eotaxin-2, an eosinophil-specific chemokine, which was only marginally reduced by PTUPB and remained elevated in celecoxib-treated mice. PTUPB or *t*-TUCB administration reversed allergen-induced reduction in levels of various lipid mediators in the lungs, with only a minimal effect noted with celecoxib. Despite the anti-inflammatory effects, PTUPB or *t*-TUCB did not reduce allergen-induced airway hyperresponsiveness (AHR). However, development of structural changes in the allergic airways, such as mucus hypersecretion and smooth muscle hypertrophy, was significantly inhibited by both inhibitors. Celecoxib, on the other hand, inhibited only airway smooth muscle hypertrophy, but not mucus hypersecretion. In conclusion, dual inhibition of COX-2 and sEH offers no additional advantage relative to sEH inhibition alone in attenuating various features associated with *A. alternata*-induced AAI, while COX-2 inhibition exerts only moderate or no effect on several of these features. Dual sEH/COX-2 inhibition may be useful in treating conditions where eosinophilic inflammation co-exists with pain-associated inflammation.

Keywords: eosinophilia, allergic airway inflammation, pharmacological inhibition, COX-2, soluble epoxide hydrolase

INTRODUCTION

Allergic airway inflammation (AAI), including allergic asthma, is associated with increased pulmonary recruitment of inflammatory cells, especially eosinophils, along with airway hyperresponsiveness (AHR) and elevated levels of Th2 cytokines, pro-inflammatory chemokines and growth factors (Hamid and Tulic, 2009; Lambrecht and Hammad, 2015). Arachidonic acid (AA) metabolites such as prostaglandins (PGs), leukotrienes (LTs) and epoxyeicosatrienoic acids (EETs) resulting from the cyclooxygenase (COX), lipoxygenase (LOX) and cytochrome P450 oxidase (CYP) enzymatic pathways, respectively (Hanna and Hafez, 2018), are known to participate in various aspects of AAI and asthma (Norton et al., 2012; Claar et al., 2015; Yang et al., 2015; Schaubberger et al., 2016; Debeuf and Lambrecht, 2018). COX-2 expression is increased in the airways of asthmatic subjects (Sousa et al., 1997; Profita et al., 2003) and in the lungs of allergen-challenged mice (Shiraishi et al., 2008; Herrerias et al., 2009). Studies to understand the importance of COX-2 during AAI in animal models using COX-2 knock-out (KO) mice or a COX-2 inhibitor have not been straightforward, with differing outcomes noted among various studies (reviewed in Peebles, 2018). Products of the COX pathway such as PGD2 and PGE2 are elevated during AAI and known to participate in the pathogenesis of airway allergic disease in humans (Profita et al., 2003; Fajt et al., 2013; Peebles, 2018) and animal models (Shiraishi et al., 2008; Herrerias et al., 2009). Additionally, COX-2-derived PGs enhance Th17 cell differentiation of naive CD4⁺ T cells during allergic inflammation in mice (Li et al., 2011) and PGD2 increases production of the Th2 cytokine IL-13 from human peripheral blood ILC2s in the presence of IL-33 and IL-25, suggesting a role for lipid mediators in regulating ILC2 function (Barnig et al., 2013; Doherty and Broide, 2018).

EETs are a class of lipid mediators generated by the CYP P450 oxidase pathway of AA metabolism that function as anti-inflammatory mediators (Christmas, 2015). However, they are rapidly converted to diol derivatives, i.e., dihydroxyeicosatrienoic acids (DiHETs) by the enzyme soluble epoxide hydrolase (sEH); thus, sEH has a pro-inflammatory role in various inflammation models (Morisseau and Hammock, 2013; Zhang et al., 2014). Expression of sEH is increased in bronchial biopsies from asthmatic patients relative to normal subjects (Morin et al., 2010). Additionally, studies have shown that inhibition of sEH with a selective inhibitor attenuates ovalbumin (OVA)-induced eosinophilia, reduces levels of Th2 cytokines and chemokines, and improves airway resistance and compliance in mice (Yang et al., 2015). Along these lines, our recent studies have shown that expression of sEH is induced by food allergens in the gastrointestinal (GI) tract and that inhibition of sEH attenuates allergen-induced eosinophilia, mast cell recruitment and mucus secretion in the jejunum (Bastan et al., 2018). As such, identification of inhibitors targeting the COX-2 and sEH enzymatic pathways in the context of allergic airway disease is likely to yield valuable information contributing to the development of novel strategies to manage this disease.

Recent studies have shown that inhibition of the COX-2 and sEH pathways using the dual inhibitor PTUPB

(4-(5-phenyl-3-{3-[3-(4-trifluoromethyl-phenyl)-ureido]-propyl}-pyrazol-1-yl)-benzenesulfonamide) has therapeutic value in reducing inflammation in models of cancer (Zhang et al., 2014; Li et al., 2017; Gartung et al., 2019) and diabetes (Hye Khan et al., 2016). Here, we investigated the effect of dual inhibition of the sEH and the COX-2 pathways in reducing eosinophilia and airway inflammation in an experimental model of AAI induced by *Alternaria alternata*.

MATERIALS AND METHODS

Mouse Model of Allergy

C57BL/6 mice (8–10 weeks, male and female) were challenged with 50 µg of an extract of *A. alternata* (Greer Laboratories, Lenoir, NC) in 50 µl of PBS on days 0, 3 and 6 or with PBS alone (control) as described previously (Ha et al., 2013). *A. alternata*-challenged mice were administered daily with PTUPB, a sEH/COX-2 dual inhibitor, *t*-TUCB (*trans*-4-{4-[3-(4-trifluoromethoxyphenyl)-ureido]-cyclohexyloxy}-benzoic acid), a highly selective sEH inhibitor, or celecoxib, a selective COX-2 inhibitor (Sigma-Aldrich Corp., St. Louis, MO). Inhibitors were dissolved in 80% Kollisolv® PEG E 300 (Sigma-Aldrich Corp., prepared in sterile water). 80% Kollisolv® PEG E 300 alone was used as the vehicle control. Synthesis and structure-activity relationship of PTUPB and *t*-TUCB have been previously described (Hwang et al., 2007; Hwang et al., 2011). Inhibitors at a dosage of 10 or 30 mg/kg were administered by gavage one hour before airway allergen challenge and mice were sacrificed 24 hours after the last challenge. Control (PBS) mice were administered with 80% Kollisolv® PEG E 300. All animal studies were performed following standards and procedures approved by the Institutional Animal Care and Use Committee at the University of Minnesota.

Sample Collection and Analysis

At the end of the study, lungs of mice were lavaged with 1 ml saline. Total and differential cell counts in the bronchoalveolar lavage fluid (BALF) were determined based on morphologic and histologic criteria after staining cytocentrifuged samples with Hema 3 System (Thermo Fisher Scientific, Pittsburgh, PA). BALF supernatants were stored at –80°C for later analysis. Right lungs were snap-frozen and left lungs were perfused with 4% paraformaldehyde (PFA) to preserve pulmonary structure, fixed in 4% PFA and paraffin embedded. Bone marrow (BM) was collected and used to determine eosinophil counts based on cell morphology after Hema 3 staining.

Histology

Lung tissue sections (4 µm thick) were stained with Hematoxylin and Eosin (Leica Biosystems, Inc., Buffalo Grove, IL) to determine cellular infiltration. Analysis of lung tissue for infiltrated eosinophils was performed by immunohistochemical staining of sections for eosinophil-specific major basic protein (MBP) with rat mAb against murine MBP as described in our previous studies (Zuberi et al., 2009). Positively stained cells (reddish brown) were counted (at 400× magnification) in randomly selected non-overlapping fields (approximately 20

fields/mouse) and expressed as the average number of MBP-positive cells/microscopic field. Sections were stained with Periodic acid-Schiff's (PAS) reagent (Sigma-Aldrich) to detect airway mucus production. PAS-positive areas (dark pink) in horizontally sectioned airways were quantitated using ImageJ image analysis program (Abramoff et al., 2004) and expressed as μm PAS-positive area/100 μm basement membrane length (BML) (Bahaie et al., 2012). Expression of α -smooth muscle actin (α -SMA) was evaluated by immunohistochemistry using mAb against α -SMA (2 $\mu\text{g}/\text{ml}$, Sigma-Aldrich) and area of the positively stained peribronchial smooth muscle layer was quantitated from captured images using ImageJ as described (Ge et al., 2010). For immunohistochemical detection of COX-2, lung sections were first permeabilized using 0.4% Triton X-100 in Tris-buffered saline containing 0.1% Tween 20 (TBST) and 1% horse serum before blocking in 5% horse serum and then incubating with a polyclonal antibody against COX-2 [5.5 $\mu\text{g}/\text{ml}$ (Novus Biologicals, Centennial, CO), 3 h at room temperature]. VECTASTAIN Elite ABC kit containing biotinylated anti-rabbit IgG (Vector Laboratories, Burlingame, CA), and the Peroxidase AEC (3-amino-9-ethylcarbazole) substrate kit (Vector Laboratories) were used for detection of bound antibodies. Expression of sEH in lungs of OVA-challenged mice (Ge et al., 2016) was detected as described previously (Bastan et al., 2018). In all cases, stained slides were examined using a Nikon Microphot EPI-FL microscope and images were captured with an Olympus DP71 camera.

Measurement of Airway Responsiveness

Pulmonary function was assessed in anesthetized control and *A. alternata*-challenged mice with or without inhibitor treatment using the FinePointe™ RC system (Buxco, Wilmington, NC) as described in our previous studies (Bahaie et al., 2012). Changes in pulmonary resistance (R_L) were monitored continuously in response to saline followed by increasing concentrations of inhaled methacholine (3–50 mg/ml) nebulized for 18–20 s and expressed as mean R_L value for each dose of methacholine.

Measurement of Lung Cytokines and Chemokines

Th1 (IL-2, IFN- γ)/Th2 (IL-4, IL-5) cytokines (including TNF α) and IL-13 were measured in the BALF by flow cytometry using CBA Flex Set kits (BD Biosciences, San Jose, CA) with a FACScan flow cytometer equipped with CellQuest Pro™ (BD Biosciences) for data acquisition and FlowJo Software (Tree Star, Inc., Ashland, OR) for analysis or a FACSCelesta flow cytometer (for IL-13) with FACSDiva™ Software (BD Biosciences) for data acquisition and analysis as described previously (Ge et al., 2013a). Eotaxin-1 (CCL11) and eotaxin-2 (CCL24) in the BALF were measured using ELISA kits (R & D Systems, Minneapolis, MN) according to the manufacturer's recommendations. Results were expressed as pg/ml BALF in each case.

Measurement of Total IgE

Total IgE in serum was measured using a mouse IgE ELISA MAX kit (BioLegend, San Diego, CA) as per the manufacturer's recommendation.

Analysis of Lung Eicosanoids

Eicosanoids in lung tissue were analyzed as previously reported (Al-Husseini et al., 2015) with minor modifications. Briefly, lung tissues were homogenized in ice-cold water in the presence of 50 μM indomethacin (Thermo Fisher Scientific) to obtain a 10% (w/v) solution. Volume of the tissue homogenate was brought up to 9 ml with ice-cold water followed by addition of 1 ml of 100% methanol to obtain a 10% (v/v) methanol in water solution. 100 μl of a stock of internal standards (Cayman Chemicals, Ann Arbor, MI, containing the following deuterated standards, (d_4) thromboxane B2 (TxB2), (d_5) 5(S),6(R)-lipoxin A4, (d_4) LTB4, (d_8) 5(S)-hydroxyeicosatetraenoic acid (HETE), (d_8) 15(S)-HETE, (d_6) 20-HETE, (d_8) 12(S)-HETE, (d_9) PGD2, (d_9) PGE2, (d_4) 6-keto PGF1 α (the stable metabolite of PGI2), (d_4) 15-deoxy- Δ 12,14-PGJ2, (d_5) eicosapentaenoic acid (EPA), (d_5) docosahexaenoic acid (DHA), (d_8) AA, (d_5) Resolvin D1, and (d_5) Resolvin D2) and 50 μl of acetic acid were added to the samples and mixed by vortexing. The resultant mixture was centrifuged for 10 min at 4°C and 5,000 $\times g$. Solid phase extraction was performed on the clarified supernatant using StrataX-C18 (Phenomenex, Torrance CA) solid phase extraction cartridges (30 mg). The analytes bound to the column were eluted in isopropanol *via* vacuum assisted percolation. The resultant eluant was vacuum dried, resuspended in 100 μl of 1:1 water:ethanol and analyzed *via* liquid chromatography tandem mass spectrometry. Chromatographic separation of eicosanoids was performed *via* a Shimadzu Nexera Ultra-high Performance Liquid Chromatography system (Shimadzu, Columbia, MD) using a Phenomenex Kinetex C18 2.1 \times 100 mm reverse phase column (Phenomenex, Torrance CA). The eluting eicosanoids were analyzed *via* a Sciex QTRAP 6500+ Hybrid Triple Quadrupole Linear Ion Trap Mass Spectrometer (Sciex, Redwood City CA). Only eicosanoids demonstrating a signal to noise (s/n) ratio of at least 3 were considered for further analysis. Semi-quantitative analysis of the eicosanoids was undertaken *via* the method of isotope dilution. A full quantitation was impractical due to the commercial lack of analytical grade standards. For those eicosanoids where an internal standard was unavailable, the standard that is closest in structure was used for quantitation. Values are reported as ng of relevant eicosanoid per mg of tissue or as fold change relative to the level of the eicosanoid in control non-allergen challenged mice.

Culture of BM-Derived Murine Eosinophils

Eosinophils were cultured from BM of naïve mice as described previously (Dyer et al., 2008; Bahaie et al., 2011). Cells between days 12–14 of culture that were 99% Hema 3-positive and expressed both MBP and Siglec-F determined as described (Bastan et al., 2018) were used in studies.

To examine the effect of inflammatory mediators on expression of COX-2, cells ($\sim 5 \times 10^6/\text{well}$) were cultured in medium containing 10% FBS and IL-4, TNF α or eotaxin-1 (all at 50 ng/ml, PeproTech, Rocky Hill, NJ) for 24 h at 37°C. Treated cells were lysed and used to evaluate COX-2 expression by q-PCR.

q-PCR

Total RNA was extracted from eosinophils using *Quick*-RNA mini-prep (Zymo Research, Irvine, CA) and reverse-transcribed into cDNA using M-MLV Reverse Transcriptase (Promega, Madison, WI). Gene expression was examined by qPCR with primers specific for mouse COX-2 (Cheng et al., 2016) (FP: CAGGTCATTGGTGGAGAGGTGTAT; RP: CCAGGCACCAGACCAAGACTT) and β -actin (Ha et al., 2013). Primers for both genes were synthesized by Integrated DNA Technologies (Coralville, IA). qPCR was performed using a Mx3000P qPCR System (Agilent, Santa Clara, CA). The amount of target mRNA was calculated based on its threshold cycle (Ct) normalized to the Ct of the housekeeping gene β -actin and results were expressed as fold change relative to expression of the target gene in untreated control cells using the ddCt method ($2^{-\Delta\Delta Ct}$) (Schmittgen and Livak, 2008).

Migration Assay

To examine the effect of PTUPB, celecoxib and *t*-TUCB on eosinophil migration, cells treated with each drug (5 or 10 μ M, 20 min at 37°C) or DMSO were added to the upper wells of Transwell® 96-well plates (Corning Life Sciences, Tewksbury, MA) and migration towards murine eotaxin-1 (100 nM, PeproTech) in the lower wells of the chambers was assessed after 3–4 h at 37°C (Ge et al., 2013b). The number of migrating cells was determined using an Olympus CK2 inverted microscope ($\times 200$ magnification). Cells in ten randomly selected non-overlapping fields were counted for each well and expressed as percent migration relative to vehicle-treated cells.

Statistical Analysis

All experiments were repeated at least three times. Statistical significance between various groups was assessed by Brown-Forsythe and Welch ANOVA or ordinary one-way ANOVA (for analysis of lipid mediator levels to compare vehicle-treated allergen-challenged group with every other group and for analysis of COX-2 induction in inflammatory mediator-treated eosinophils compared to untreated control group) followed by Dunnett's T3 *post hoc* test for multiple comparisons using GraphPad Prism Software (8.1.2). A *p* value < 0.05 was considered significant.

RESULTS

Effect of PTUPB, Celecoxib and *t*-TUCB on Allergen-Induced Airway Cellular Inflammation and Eosinophilia

WT mice were challenged with *A. alternata*, an airborne fungal allergen, as outlined in **Figure 1A**, and examined for expression of COX-2 by immunohistochemical staining. While COX-2 expression in control (PBS-exposed) mice was noted mostly in the airway epithelium, exposure to *A. alternata* led to increased expression of COX-2 in the peribronchial areas of the lungs and was mostly associated with alveolar macrophages (**Supplementary Figure 1A**). Allergen-challenged mice were administered with PTUPB (sEH/COX-2 dual inhibitor), *t*-TUCB

(sEH inhibitor) or celecoxib (COX-2 inhibitor) as shown in **Figure 1A**. A dosage of 30 mg/kg/day was selected for PTUPB based on previous studies in mice demonstrating its effectiveness at this dose without exerting any adverse effects (Zhang et al., 2014). Since this was a comparative study evaluating the effect of the three inhibitors, *t*-TUCB and celecoxib were also used at 30 mg/kg/day to maintain a consistent dosage. PTUPB was additionally tested at a lower dose of 10 mg/kg/day to determine the outcome of dual inhibition of the sEH and COX-2 pathways relative to inhibition of the two pathways independently (i.e., with TUCB or celecoxib) at 30 mg/kg/day. Administration of PTUPB at 10 mg/kg (PTUPB-10) or *t*-TUCB at 30 mg/kg (TUCB-30) had no effect on mortality in comparison to allergen-challenged mice that received vehicle alone. However, administration of celecoxib at 30 mg/kg (Celecoxib-30) or PTUPB at 30 mg/kg (PTUPB-30) resulted in 45% (5/11) and 23% (3/13) of the animals dying, respectively, before the end of the study (**Figure 1B**).

A. alternata-exposed mice treated with vehicle alone demonstrated a marked increase in recruitment of inflammatory cells to the airways relative to control mice (PBS-exposed and treated with vehicle) as indicated by the total number of cells in the BALF (**Figure 1C**) and cellular infiltration in lung tissue sections by H&E staining (**Figure 1D**). PTUPB-10 did not alter airway cellular inflammation in the allergen-challenged mice; a significant reduction in the number of BALF inflammatory cells was noted only at the higher dose, i.e., PTUPB-30, relative to mice that received vehicle alone (**Figure 1C**). This reduction in cellular inflammation was also evident in the lung tissue of these mice (**Figure 1D**). Celecoxib-30 did not affect airway cellular inflammation in the surviving mice. Administration of TUCB-30, on the other hand, significantly attenuated recruitment of inflammatory cells to BALF and lung tissue of allergen-challenged mice. Evaluation of lipid mediators in the lung tissue of these mice indicated that *A. alternata* challenge reduced levels of the anti-inflammatory lipid mediators 11,12- and 14,15-EET in the lungs compared to control mice, although the reduction was not statistically significant (**Figure 1E**). However, administration of PTUPB-30 and TUCB-30, but not PTUPB-10 or celecoxib-30, to allergen-challenged mice significantly increased levels of both these lipid mediators relative to allergen-challenged mice that received vehicle alone confirming the dose-dependent and specific inhibitory effect of these compounds on sEH. Level of 5,6-EET and 8,9-EET were extremely low and unaffected by *A. alternata* challenge with no further change after treatment with the inhibitors (data not shown).

Analysis of differential cell counts in the BALF demonstrated a marked reduction in recruitment of eosinophils in allergen-challenged mice treated with PTUPB-30, celecoxib-30, or TUCB-30 compared to vehicle-treated mice (**Figure 2A**). Exposure to *A. alternata* did not induce an influx of monocyte/macrophages or neutrophils to the airways, which remained unaffected by administration of PTUPB-30 or TUCB-30 (**Figures 2B, C**). The effect of PTUPB-10 and celecoxib-30 on the number of monocyte/macrophages and neutrophils in the BALF was variable, with some mice exhibiting increased numbers of these cell types relative to allergen-challenged mice treated with vehicle. This variable effect on the number of macrophages and

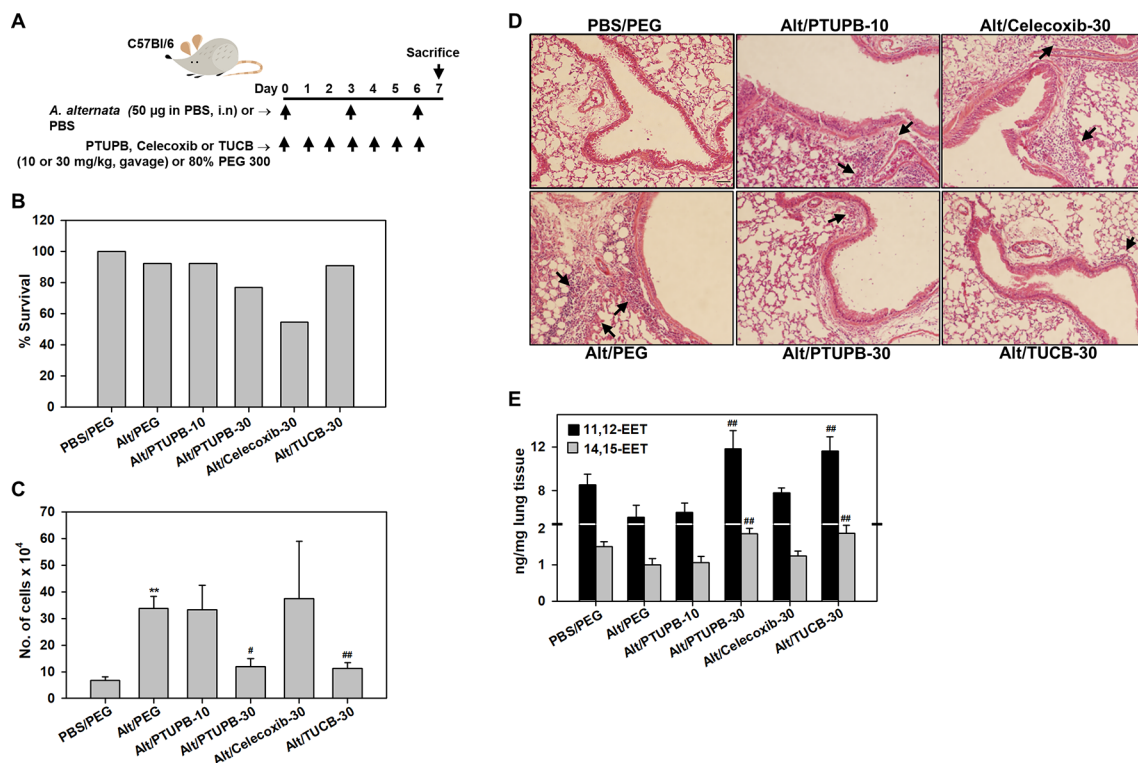


FIGURE 1 | Effect of PTUPB, celecoxib and *t*-TUCB on allergen-induced airway cellular inflammation. **(A)** Outline of protocol for challenge with *A. alternata* and administration of PTUPB (dual sEH and COX-2 inhibitor), celecoxib (COX-2 inhibitor), *t*-TUCB (sEH inhibitor) or vehicle. i.n, intranasal. **(B)** Effect of inhibitors on survival of allergen-exposed mice. Alt, *A. alternata*. **(C)** Total cell counts in the BALF of control and *A. alternata*-challenged mice with or without administration of inhibitors. **(D)** H & E staining of lung tissue from mice identified in C. Representative image for each group is shown. Arrows indicate infiltrating inflammatory cells. **(E)** Concentration of EETs in lungs of control and *A. alternata*-challenged mice with or without administration of inhibitors. Scale bar, 50 μ m in D. Data shown in C and E represent mean \pm SEM. $n = 6$ mice for Alt/Celecoxib-30 group and 9–10 mice for all other groups in C and 5–6 mice/group in E. ** $p < 0.01$ compared to PBS/PEG, # $p < 0.05$ and ## $p < 0.01$ compared to Alt/PEG.

neutrophils noted with PTUPB-10 and celecoxib-30 may explain the absence of an effect on total airway cellular inflammation by these compounds (Figures 1C, D). The number of lymphocytes in mice administered with PTUPB-10, PTUPB-30 and celecoxib-30 was lower than in vehicle-treated mice, although not statistically significant (Figure 2D). A significant reduction in the number of lymphocytes was noted only in mice that received TUCB-30.

The effect of these inhibitors on lung tissue eosinophils was examined by immunohistochemistry based on expression of eosinophil-specific MBP. As expected, quantitation of MBP-positive cells demonstrated a significantly increased number of eosinophils in lung sections of vehicle-treated allergen-exposed mice relative to the number detected in control lung sections (Figures 3A, B). Consistent with the decreased number of eosinophils in the BALF (Figure 2A), there was a marked reduction in the number of MBP-positive cells detected in the lungs of allergen-challenged mice administered with PTUPB-30 or TUCB-30. A modest reduction in number of MBP-positive cells was also noted in mice that received PTUPB-10 or celecoxib-30, although the decrease was not statistically significant compared to vehicle-treated allergen-challenged mice in either case. The effect of these inhibitors on eosinophil

proliferation in the BM was evaluated. Allergen-challenged mice had an increased number of eosinophils compared to unchallenged mice, albeit not statistically significant. None of the inhibitors significantly altered BM eosinophil proliferation relative to untreated mice (Figure 3C) suggesting that the effect of the inhibitors on reducing eosinophilia is at the level of cell recruitment. Overall, while allergen-challenged mice administered with PTUPB-30, celecoxib-30 or TUCB-30 demonstrated reduced eosinophil recruitment to a similar extent in the BALF, only PTUPB-30 and TUCB-30 treatment inhibited eosinophil infiltration in the lung tissue.

Effect of PTUPB, Celecoxib, and *t*-TUCB on Th2 Cytokines, Eotaxins, and IgE

AAI and asthma is associated with elevated Th2 cytokine levels (Lambrecht et al., 2019). IL-4, IL-5 and IL-13 levels in the BALF were evaluated. Compared to control PBS-exposed mice, allergen-challenged mice treated with vehicle alone had significantly higher levels of IL-4 and IL-13 with a modest increase in IL-5 (Figure 4A). Administration of PTUPB-10 did not alter IL-4 or IL-5 levels but moderately reduced IL-13 (not statistically significant). While PTUPB-30 and celecoxib-30 reduced IL-4,

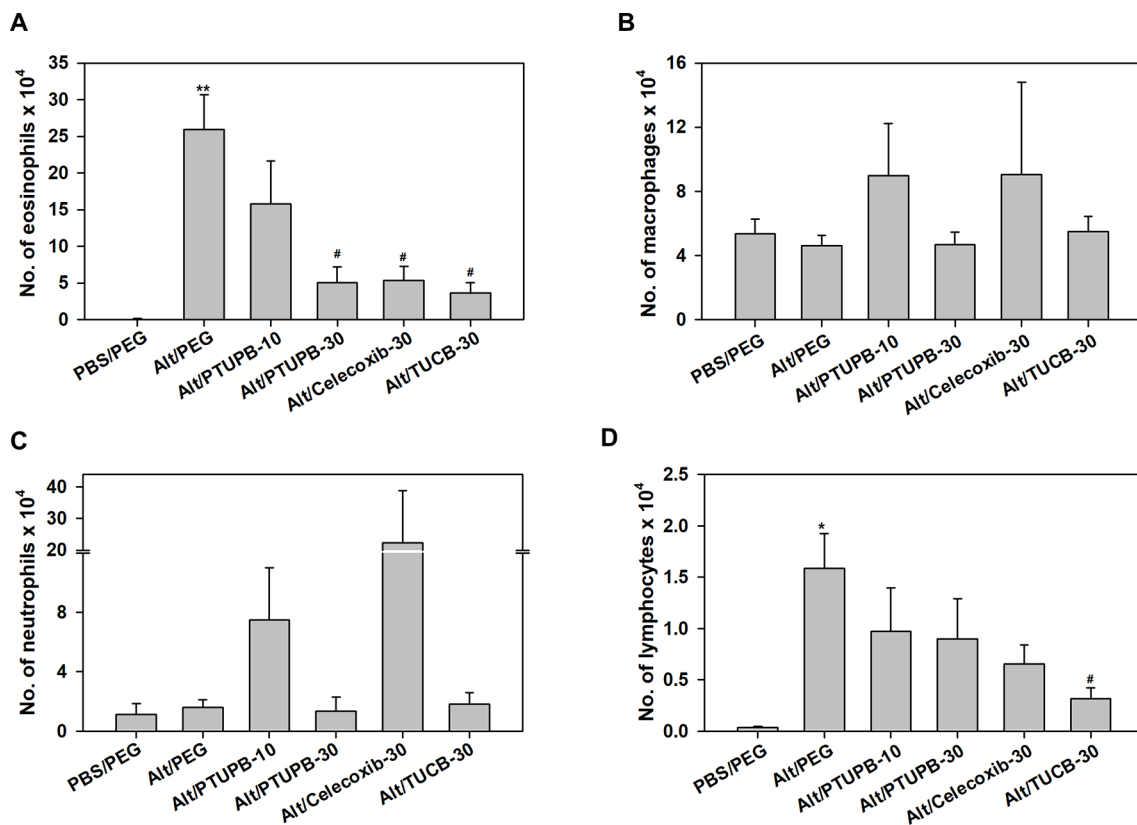


FIGURE 2 | Airway eosinophil recruitment in allergen-challenged mice administered with PTUPB, celecoxib or *t*-TUCB. **(A)** Eosinophil, **(B)** macrophage, **(C)** neutrophil and **(D)** lymphocyte counts in the BALF of control and *A. alternata*-challenged mice with or without administration of PTUPB, celecoxib or *t*-TUCB. Data represent mean \pm SEM. $n = 6$ mice for Alt/Celecoxib-30 group and 9–10 mice for all other groups. * $p < 0.05$ and ** $p < 0.01$ compared to PBS/PEG, # $p < 0.05$ compared to Alt/PEG.

IL-5 and IL-13 levels compared to vehicle-treated allergen-challenged mice, the reduction was not statistically significant. On the other hand, in mice administered with TUCB-30, IL-4 and IL-13 levels were significantly lower compared to vehicle-treated mice. IL-5 levels were also lower in these mice, although the reduction was not significant. *A. alternata* challenge did not increase TNF- α levels compared to control mice and remained unaltered by administration of inhibitors, while IL-2 and IFN- γ levels were below detection limit in all groups (data not shown).

Since PTUPB-30, celecoxib-30, and TUCB-30 inhibited recruitment of eosinophils in the BALF, levels of the eosinophil-active chemokines, eotaxin-1 and -2 (Pope et al., 2005), were measured. Eotaxin-1 in allergen-challenged mice that received vehicle alone was marginally higher than in control mice and was not significantly altered by any of the inhibitors (Figure 4B). Eotaxin-2 levels were significantly higher in vehicle-treated allergen-challenged mice relative to control mice. PTUPB-10 and celecoxib-30 had no effect, while a marginal reduction in eotaxin-2 was noted with PTUPB-30 relative to vehicle-treated mice. TUCB-30 on the other hand, significantly inhibited eotaxin-2 levels (Figure 4B). Since elevated IgE is a distinguishing feature of allergic inflammation, we examined the effect of these inhibitors on allergen-induced IgE levels in

the serum. Consistent with the allergic disease phenotype, IgE levels in allergen-challenged mice were higher than in control mice, although the increase was not statistically significant. None of the inhibitors significantly altered IgE levels in the allergen-challenged mice (Figure 4C).

Effect of PTUPB, Celecoxib, and *t*-TUCB on Allergen-Induced Changes in Lung Lipid Mediators

Eicosanoids resulting from AA metabolism contribute to the pathogenesis of allergic asthma by playing both pro-inflammatory as well as anti-inflammatory roles (Sanak, 2016; Peebles, 2018). Eicosanoid levels in the lung tissue of allergen-challenged mice administered with PTUPB-30, celecoxib-30, *t*-TUCB-30 or vehicle alone were analyzed. Exposure to *A. alternata* reduced levels of AA as well as various COX and LOX metabolites such as 6-keto-PGF 1α , PGD $_2$, 11- and 15-HETE, and the omega 3 polyunsaturated fatty acid EPA, with a significant reduction noted in the levels of 5-HETE and DHA (Figure 5A). Administration of PTUPB-30 and TUCB-30 increased levels of all these lipid mediators, in some cases to levels noted in lungs of control mice. Level of 6-keto-PGF 1α and 11-HETE were significantly higher in allergen-challenged mice treated with PTUPB-30 relative to

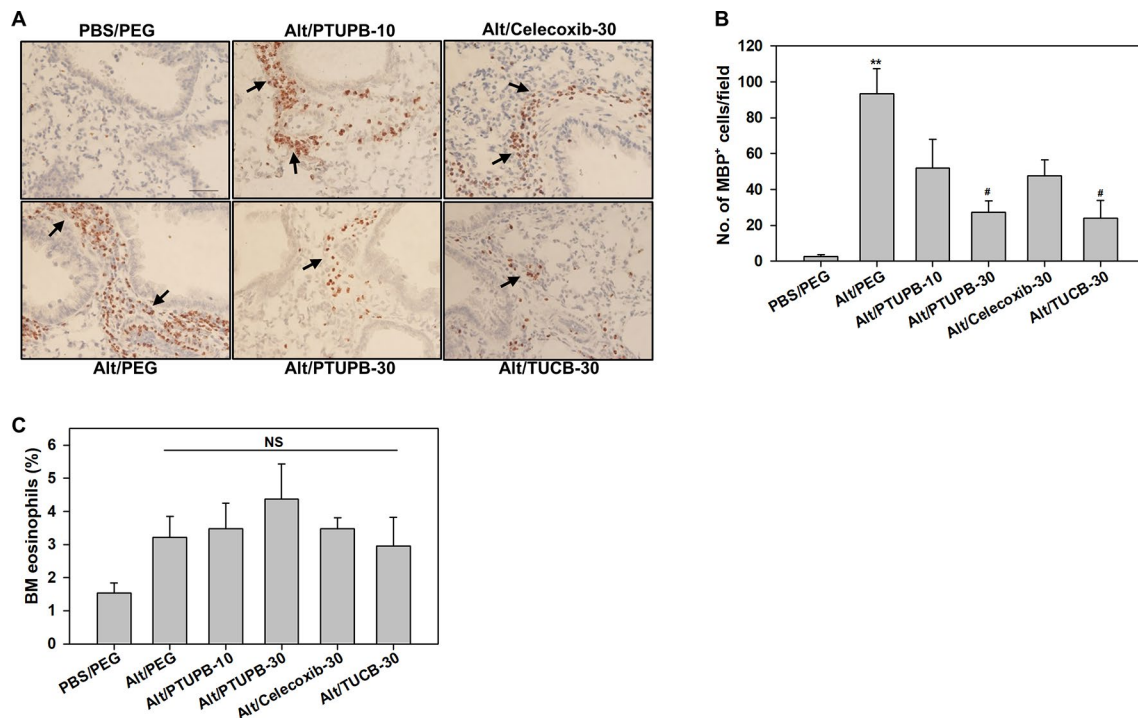


FIGURE 3 | PTUPB and *t*-TUCB inhibit eosinophil recruitment in the lung tissue of allergen-challenged mice. **(A)** Immunohistochemical staining for expression of eosinophil-specific MBP (stained dark brown, black arrows) in the lung tissue of control and *A. alternata*-challenged mice with or without administration of PTUPB, celecoxib or *t*-TUCB. A representative image for each group is shown. Scale bar, 50 μ m. **(B)** Quantitation of infiltrated lung tissue eosinophils (i.e., MBP-positive cells) in mice described in A. **(C)** Percentage of eosinophils in the BM of mice identified in A based on cell morphology after Hema3 staining. Data represent mean \pm SEM. $n = 6$ -7 mice/group in B, 6 mice for Alt/Celecoxib-30 group and 7-9 mice for all other groups in C. ** $p < 0.01$ compared to PBS/PEG, # $p < 0.05$ compared to Alt/PEG. NS, not significant.

allergen-challenged mice treated with vehicle alone. In the case of TUCB-30, levels of 6-keto-PGF 1α , 11- and 15-HETE as well as DHA were significantly higher than in mice treated with vehicle alone. Administration of celecoxib-30 only increased levels of AA, 11-HETE, EPA, and DHA, although the increase was not found to be statistically significant in the case of any of the mediators. *A. alternata* challenge increased TxB $_2$ levels but not that of PGE $_2$ or LTB $_4$, which remained unaltered by administration of PTUPB-30, celecoxib-30 or TUCB-30 (Figure 5B).

Effect of PTUPB, Celecoxib, and *t*-TUCB on Allergen-Induced AHR and Airway Structural Changes

AHR is one of the hallmark features of allergic asthma and is associated with structural changes in the airways such as increased mucus production and airway smooth muscle hyperplasia/hypertrophy that contribute to airflow obstruction (Bai and Knight, 2005). Vehicle-treated allergen-challenged mice displayed elevated AHR with significantly higher pulmonary resistance (R_L) relative to control mice (Figure 6A). Administration of PTUPB-30 and TUCB-30 had no effect on allergen-induced AHR. The effect of celecoxib-30 could not be examined in the current study due to mice dying during the procedure thus resulting in small sample size. Associated with the elevated AHR, vehicle-treated allergen-challenged mice

exhibited significantly increased airway mucus secretion and smooth muscle thickening compared to control mice based on PAS staining and α -SMA immunohistochemical staining, respectively (Figures 6B–E). Despite the lack of an effect on AHR, administration of PTUPB-30 or TUCB-30 strongly inhibited allergen-induced airway mucus production (Figures 6B, C) and smooth muscle hyperplasia (Figures 6D, E) in these mice. Interestingly, while substantial levels of mucus secretion were detectable in the airways of allergen-challenged mice that received celecoxib-30, smooth muscle thickening was significantly inhibited.

Effect of PTUPB, Celecoxib, and *t*-TUCB on Eosinophil Migration

We have previously demonstrated that pro-inflammatory mediators such as TNF- α and eotaxin-1 induce expression of sEH in eosinophils (Bastan et al., 2018). Here, we examined the effect of IL-4, TNF- α or eotaxin-1 on expression of COX-2 in BM eosinophils by qPCR. IL-4 and TNF- α marginally increased COX-2 expression in eosinophils. Eotaxin-1 on the other hand significantly induced COX-2 expression in these cells (Figure 7A). Next, we examined whether PTUPB, celecoxib or *t*-TUCB exert a direct effect on eosinophils migration. Celecoxib significantly inhibited eotaxin-1-induced eosinophil migration at 5 and 10 μ M, while a significant

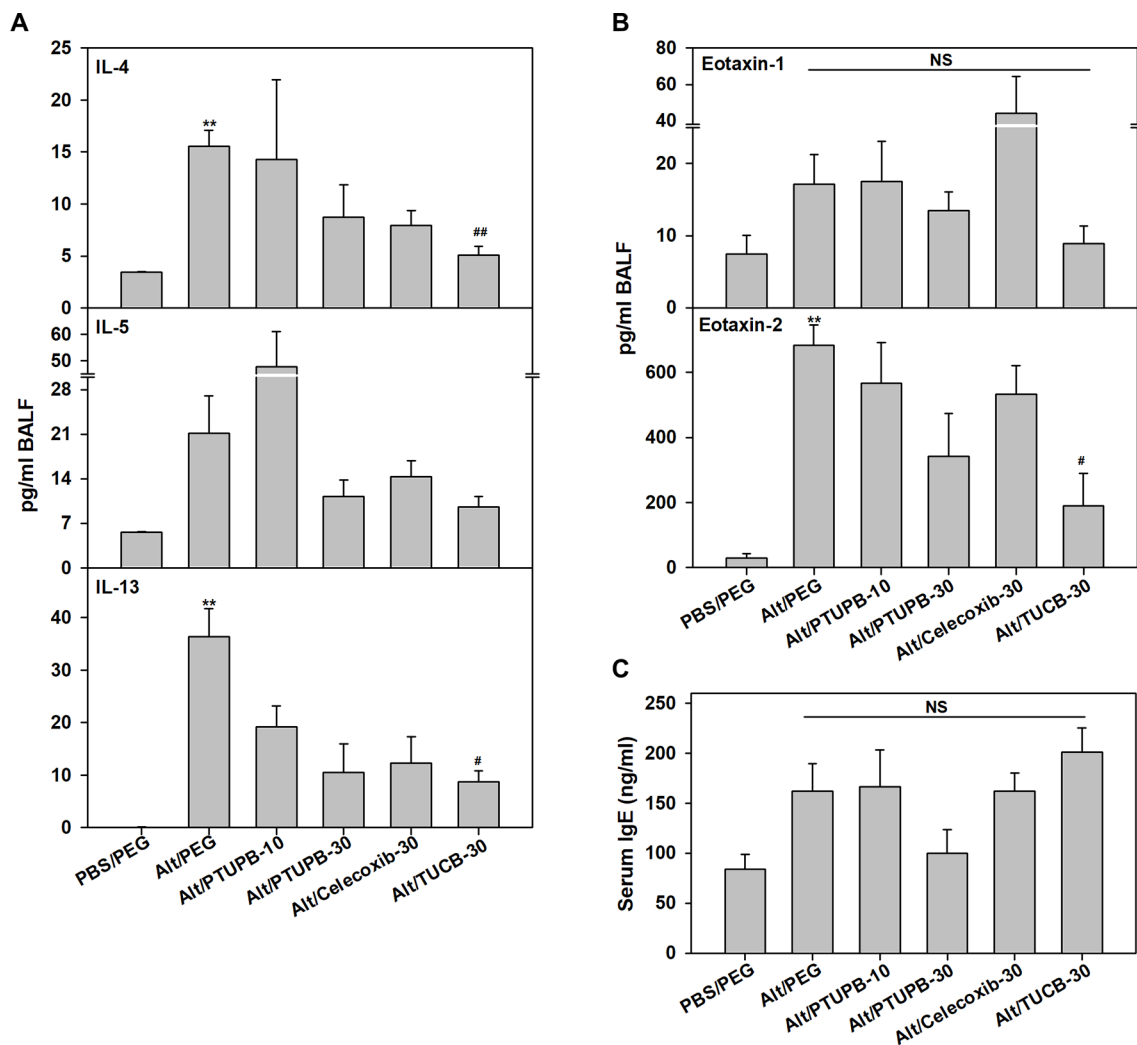


FIGURE 4 | Effect of PTUPB, celecoxib and *t*-TUCB on Th2 cytokines, eotaxins and IgE. **(A)** Th2 cytokine levels in BALF from control and *A. alternata*-challenged mice with or without administration of PTUPB, celecoxib or *t*-TUCB. **(B)** Eotaxin-1 and -2 levels in BALF, and **(C)** total IgE levels in the serum of mice identified in A. Data represent mean \pm SEM. $n = 5$ –7 mice per group. ** $p < 0.01$ compared to PBS/PEG, # $p < 0.05$ and ## $p < 0.01$ compared to Alt/PEG. NS, not significant.

inhibition of migration was noted at a concentration of 10 μ M with PTUPB and *t*-TUCB (Figure 7B).

DISCUSSION

COX-2 expression in asthmatic subjects (Sousa et al., 1997; Profita et al., 2003) and in models of AAI (Oguma et al., 2002; Shiraishi et al., 2008; Herrerias et al., 2009), including the current study (Supplementary Figure 1A), is increased relative to controls. Although it is recognized that products of the COX pathway, e.g., PGD₂, play a pro-inflammatory role in AAI (Shiraishi et al., 2008; Domingo et al., 2018), selective inhibition of COX-2 has yielded mixed outcomes towards resolution of airway inflammation (reviewed in Peebles, 2018). Like COX-2, sEH expression is increased in asthmatic airways (Morin et al., 2010) and lungs of allergen-challenged mice (Supplemental Figure

1B). Inhibition of sEH with *t*-TUCB attenuates various aspects of AAI (Yang et al., 2015) and food allergen-driven GI inflammation (Bastan et al., 2018), specifically allergen-induced eosinophilia, thus demonstrating its pro-inflammatory role in allergic inflammation. Eosinophilia is a hallmark of airway inflammation in asthma (George and Brightling, 2016). Eosinophils are a source of various cytokines, chemokines, growth factors and highly cytotoxic cationic granule proteins that are secreted upon activation (Davoine and Lacy, 2014) and known to exert various pro-inflammatory effects (reviewed in Acharya and Ackerman, 2014). Further, eosinophils are thought to contribute to asthma exacerbation (Nakagome and Nagata, 2018). Thus, identifying antagonists for specific mediators and/or pathways involved in promoting airway eosinophilic inflammation is critical for the identification of novel therapeutic strategies.

The efficacy of dual sEH/COX-2 inhibition with PTUPB relative to selective inhibition of COX-2 with celecoxib or sEH

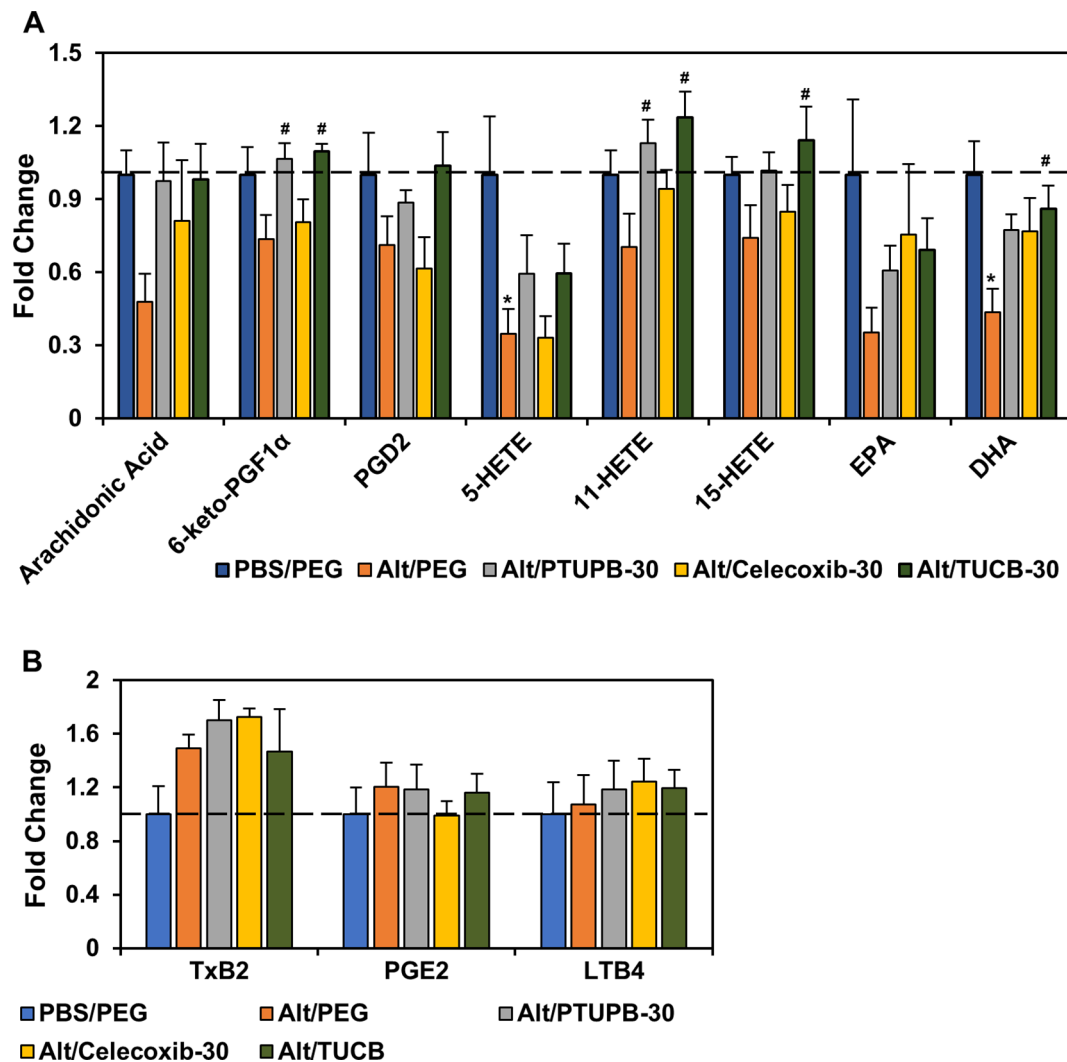


FIGURE 5 | Effect of PTUPB, celecoxib and *t*-TUCB on allergen-induced changes in lung lipid mediators. Eicosanoid levels in control and *A. alternata*-challenged mice with or without administration of PTUPB, celecoxib or *t*-TUCB shown as fold change relative to unchallenged mice. Eicosanoids that were decreased by allergen exposure are shown in panel (A) and those that increased or remained unchanged are shown in panel (B). *n* = 5–6 mice per group. **p* < 0.05 compared to PBS/PEG, #*p* < 0.05 compared to Alt/PEG.

with *t*-TUCB independently in reducing eosinophilia and airway inflammation in a clinically relevant model of AAI induced by the fungal allergen *A. alternata* (Gabriel et al., 2016) was investigated. In our studies, increased mortality was noted in allergen-challenged mice administration with celecoxib (45%), a finding not reported previously. Only a slight increase in mortality was noted in mice administered with the dual sEH/COX-2 inhibitor PTUPB at the higher dose, while *t*-TUCB at the higher dose did not affect survival. While this effect of COX-2 inhibition on survival of mice is not entirely clear, previous studies have shown increased blood pressure and leukocyte adherence to the endothelium in animal models (Muscará et al., 2000) and increased cardiovascular disease in patients with suppression of COX-2, which may be due to inhibition of the synthesis of the vasodilator PGI₂ (FitzGerald, 2004). Celecoxib has been administered to mice at doses close to or higher than 30 mg/

kg/day with no report of toxicity, albeit in models other than AAI (Park et al., 2008; Zhang et al., 2017). Our observation of increased mortality in allergen-challenged mice treated with celecoxib raises the question whether inhibition of COX-2 in a setting of AAI/asthma might be associated with harmful effects. Additional studies are needed to understand the effect of selective inhibition of COX-2 on survival during AAI. BALF eosinophilia was significantly reduced in mice administered with PTUPB at the higher dose, celecoxib and *t*-TUCB, while in the lung tissue only PTUPB and *t*-TUCB, but not celecoxib, strongly inhibited eosinophil recruitment. It is possible that administration of celecoxib does not affect allergen-induced eosinophil recruitment to the lungs and the recruited eosinophils are retained in the lung tissue, thus accounting for the lower eosinophil numbers detected in the BALF of these mice. Other studies have reported that selective COX-2 inhibition with lumiracoxib (Swedin

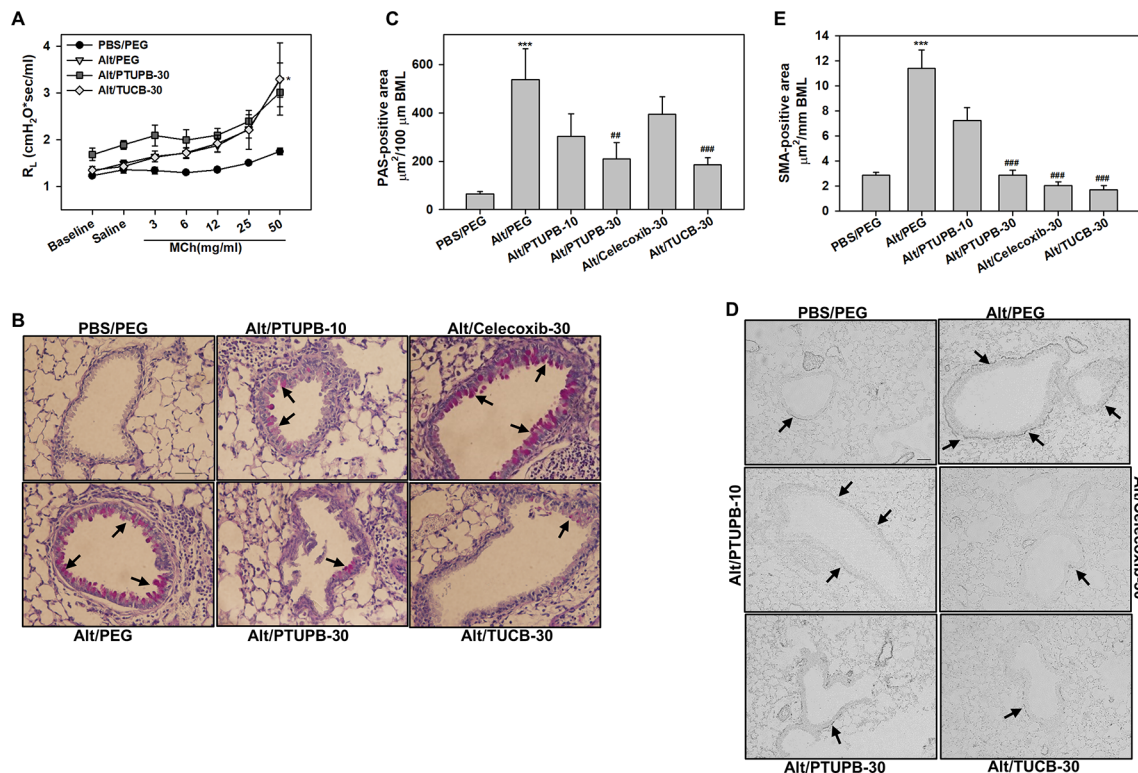


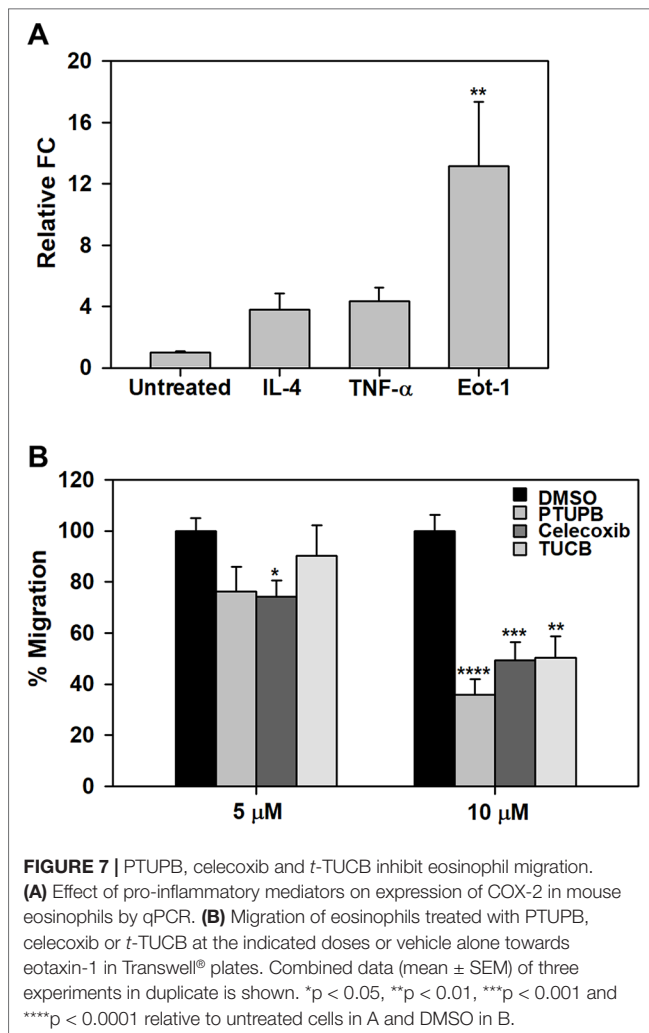
FIGURE 6 | Administration of PTUPB or *t*-TUCB attenuates allergen-induced mucus secretion and smooth muscle thickening but not AHR. **(A)** Measurement of pulmonary resistance (RL) following exposure to increasing concentrations of aerosolized methacholine (MCh) in mechanically ventilated control and *A. alternata*-challenged mice with or without administration of PTUPB or *t*-TUCB. **(B and C)** Airway mucus secretion based on PAS staining (stained dark-pink, black arrows) in control and *A. alternata*-challenged mice administered with vehicle or with PTUPB, celecoxib or *t*-TUCB and quantitation of PAS-positive area in the airways, respectively. **(D and E)** Airway smooth muscle thickening in mice described in B assessed by immunohistochemical staining for α -SMA expression and quantitation of α -SMA-positive area, respectively. Scale bar, 50 μ m. Data represent mean \pm SEM. $n = 5$ –7 mice per group. *** $p < 0.001$ compared to PBS/PEG, ** $p < 0.01$ and *** $p < 0.001$ compared to Alt/PEG.

et al., 2010) or COX-2 knock-down (Carey et al., 2003) does not affect airway eosinophilia during AAI.

EETs derived from AA metabolism via the CYP450 enzyme pathway are well-known anti-inflammatory mediators (Morisseau and Hammock, 2013; Christmas, 2015). In the current study, levels of 11,12- and 14,15-EETs in the lung tissue were reduced by *A. alternata* challenge. Administration of PTUPB at the higher dose or *t*-TUCB, but not PTUPB at the lower dose or celecoxib, significantly increased levels of these EETs. Importantly, this increase in levels of 11,12- and 14,15-EETs was associated with decreased lung tissue eosinophilia. Additionally, Th2 cytokines IL-4, IL-5, and IL-13 were lower in the BALF of mice administered with PTUPB at the higher dose, celecoxib or *t*-TUCB, although a statistically significant reduction was noted only in IL-4 and IL-13 levels in allergen-challenged mice administered with *t*-TUCB. This may be linked to the observation that lymphocyte counts were significantly lower only in the TUCB-treated mice but not in PTUPB- or celecoxib-treated mice. Levels of the eosinophil-specific chemokines eotaxin-1 and -2 were also reduced in *t*-TUCB-treated mice, with a marked decrease noted for eotaxin-2. On the other hand, both eotaxins were moderately reduced with PTUPB at the higher dose but remained elevated in celecoxib-treated mice. It is likely that COX-2 inhibition

does not affect expression of eotaxins, which may be another contributing factor to the higher number of eosinophils in the lung tissue of celecoxib-treated mice. Our findings with administration of *t*-TUCB are similar to those from a previous study where OVA-challenged mice administered with *t*-TUCB demonstrated increased levels of EETs (5,6-, 11,12-, and 14, 15-) associated with decreased eosinophilia and reduced IL-4 and IL-5 levels (Yang et al., 2015). Overall, our studies suggest that PTUPB at the higher dose and *t*-TUCB are equally effective in reducing eosinophilic inflammation, while *t*-TUCB alone but not PTUPB or celecoxib appears to be more effective at significantly reducing levels of specific Th2-promoting inflammatory mediators, i.e., IL-4, IL-13 and eotaxin-2.

Exposure to *A. alternata* resulted in reduction of various lipid mediators (AA, 6-keto-PGF1 α , PGD2, 11,12-EET, 14,15-EET, 5-, 11- and 15-HETE, EPA and DHA) in lung tissue homogenates. Our findings with respect to levels of some of these lipid mediators, e.g., PGD2, 6-keto-PGF1 α , are different (lower in allergen-challenged mice) than those observed in OVA- (Swedin et al., 2010) or HDM-induced (Herrerias et al., 2009) models of AAI. These differences may be due to the nature of the allergen (fungal versus non-fungal), duration of allergen challenge (6 days versus 10–46 days) and sample used for measurement of lipid mediators (lung tissue versus BALF).



Nonetheless, administration of PTUPB at the higher dose or *t*-TUCB increased levels of all of these mediators, in some cases to levels noted in lungs of control mice and significantly higher than in allergen-challenged mice that received vehicle alone. Celecoxib on the other hand, increased levels of only some of the mediators (AA, 11-HETE, EPA, and DHA), although not in a statistically significant manner. In the context of eosinophil recruitment, we have previously shown that 11,12-EET, which was significantly increased after treatment with PTUPB at the higher dose or *t*-TUCB, can directly inhibit eotaxin-induced migration of eosinophils (Bastan et al., 2018). 14,15-EETs, which were also elevated after treatment with PTUPB at the higher dose or *t*-TUCB, have been shown to exert anti-inflammatory effects in human bronchi by inhibiting I κ B α degradation resulting in lower NF κ B-dependent transcription (Morin et al., 2008). In the current study, 6-keto-PGF1 α , the stable metabolite of PGI $_2$, was restored to levels seen in the lungs of control unchallenged mice by PTUPB at the higher dose and *t*-TUCB (but not celecoxib). Studies in experimental models suggest that PGI $_2$ restrains AAI by inhibiting dendritic cell-mediated immune activation effects including inhibition of Th2 cytokines from Th2 polarized CD4 $^+$ cells (Debeuf and Lambrecht, 2018). Lipid mediators such as AA, HETEs, EPA and DHA can play an important role in regulating

acute inflammation by serving as a source of potent lipid-derived pro-resolving mediators (Serhan, 2014; Antonio Gonçalves et al., 2018). While lipoxin A4, resolvins D1 and D2 were not detected at measurable levels in this model, it is possible that other pro-resolving mediators that were not analyzed in this study could be generated from these lipid mediators. Nonetheless, the reversal of various lipid mediator levels to that noted in non-allergen-challenged controls by PTUPB at the higher dose and *t*-TUCB appears to be directly associated with attenuation of airway cellular inflammation and suppression of a Th2 phenotype.

Regardless of their ability to reduce eosinophil recruitment to the airways significantly, PTUPB at the higher dose and *t*-TUCB failed to inhibit allergen-induced AHR. Our observation with *t*-TUCB is in contrast to previous studies in an OVA-induced model of AAI where administration of *t*-TUCB at 1 mg/kg rescued methacholine-induced AHR in allergen-challenged mice (Yang et al., 2015). This difference may be due to the type and duration of allergen exposure as well as concentration, frequency and route of administration of the inhibitor. Previous studies have shown that 14,15-EET can relax airway smooth muscle cells (Benoit et al., 2001) and that inhibition with a selective sEH inhibitor [12-(3-adamantan-1-yl-ureido)-dodecanoic acid] different than the one used in the current study significantly reduces TNF α -induced hyperreactivity of human bronchi to methacholine (Morin et al., 2010). Although levels of 14,15-EETs were increased in allergen-challenged mice after administration of PTUPB at the higher dose or *t*-TUCB in the current study, it is possible that the concentrations are not sufficient to exert a suppressive effect on AHR. Further TxB2, a metabolite of TxA2, was increased in allergen-challenged mice and remained elevated after administration of inhibitors. Studies in animal models of AAI and asthmatics using TxA2 antagonists suggest a role for this lipid mediator in allergen-induced airway reactivity (reviewed in Peebles, 2018). Additional studies are needed to further understand the persistence of AHR in spite of attenuated eosinophilic inflammation. Alternatively, airway inflammation as noted in the BALF/lung tissue and AHR may be dissociated, and differently regulated, events during *A. alternata*-induced AAI. Despite the sustained AHR in allergen-challenged mice treated with PTUPB or *t*-TUCB, airway mucus secretion and smooth muscle thickening, both distinguishing features associated with increased airway reactivity, were significantly inhibited. Interestingly, celecoxib had no effect on allergen-induced airway mucus secretion but reduced airway smooth muscle mass. These findings are somewhat different from those reported in an OVA-model of AAI using a different COX-2-selective inhibitor (Swedin et al., 2010), wherein mice treated with the inhibitor continued to show not only increased airway mucus secretion but also smooth muscle mass along with exaggerated AHR. Based on various studies in the literature, it is clear that a particular eicosanoid can have a pro-inflammatory or anti-inflammatory effect depending on the cell type. Further, *in vivo* a certain cell type is exposed to both pro- and anti-inflammatory eicosanoids and the cellular response is likely to be determined by a balance between the effects.

Inflammatory mediators such as IL-4, TNF α , and/or eotaxin-1 induced expression of COX-2 (in the present study) and sEH (as shown previously Bastan et al., 2018) by eosinophils. Induction of COX-2 expression by inflammatory mediators has been reported

in other cells of the airways such as smooth muscle and epithelial cells and is associated with increased release of PGs from these cells (Belvisi et al., 1997). Increased expression of COX-2 and/or sEH by eosinophils as noted in the present study can lead to increased synthesis of eosinophil-activating mediators. For example, studies have shown that eosinophils synthesize and secrete PGD₂, which in turn can act in an autocrine manner to activate eosinophils (Luna-Gomes et al., 2011). In the current study, we found that treatment of eosinophils with PTUPB, celecoxib or *t*-TUCB inhibits eotaxin-induced migration *in vitro*, with maximum inhibition noted with PTUPB. We have previously shown that sEH inhibition with *t*-TUCB inhibits eotaxin-induced migration of eosinophils *in vitro* (Bastan et al., 2018). *t*-TUCB has been shown to exert anti-inflammatory effects on human monocytes by increasing the EET to DiHET ratio (Sanders et al., 2012) and also blocking migration in response to MCP-1 (Kundu et al., 2013). Thus, blockade of eosinophil migration by PTUPB and *t*-TUCB at a cellular level may contribute to the overall reduction in eosinophilia noted in allergen-challenged mice administered with these inhibitors. The ability of celecoxib to inhibit eosinophil migration effectively *in vitro* but not *in vivo* is not entirely clear and may in part be due to the elevated eotaxin levels in allergen-challenged mice even after administration of this inhibitor.

In summary, dual inhibition of the COX-2 and sEH pathways was as effective as inhibition of sEH alone with respect to reducing eosinophilia, restoring various lipid mediator levels and decreasing airway structural changes but not with inhibiting levels of Th2-promoting inflammatory mediators in a significant manner (IL-4, IL-13, and eotaxin-2) in an *A. alternata*-induced model of AAI. Inhibiting the COX-2 pathway alone had only moderate or no effect on several of these features associated with *A. alternata*-induced AAI. While these studies provide valuable information on the role of sEH/COX-2 dual inhibition in preventing the development of eosinophilia and several features of AAI, future studies will focus on investigating the therapeutic effect of dual sEH/COX-2 inhibition in a model of established allergic airway disease. However, since allergen-induced AHR remained elevated, dual inhibition of the COX-2 and sEH pathways may be useful in the treatment of conditions where eosinophilic inflammation with no bronchial reactivity, e.g., eosinophilic esophagitis, dermatologic disorders, and pain-associated

inflammation co-exist, with the additional advantage of reducing side effects associated with COX inhibitors.

DATA AVAILABILITY STATEMENT

The datasets generated for this study are available on request to the corresponding author.

ETHICS STATEMENT

The animal study was reviewed and approved by Institutional Animal Care and Use Committee at the University of Minnesota.

AUTHOR CONTRIBUTIONS

MD, SR-S, and YG performed the experiments and analyzed the data. DW and NK performed the lipid mediator measurement using mass spectrometry and the data analysis. JY, SH, and BH contributed to study design pertaining to drug administration to animals and provided essential reagents (sEH and dual sEH/COX-2 inhibitors). PS assisted with study design, manuscript review and secured funding for the studies. SR designed experiments, prepared figures and wrote the manuscript. All authors read and approved the final manuscript.

FUNDING

This work was supported by the University of Minnesota College of Veterinary Medicine (to PS) and in part by NIEHS (River Award R35ES030443 to BDH) and NIH (HD087198 to DW). The content is solely the responsibility of the authors and does not necessarily represent the official views of the NIH.

SUPPLEMENTARY MATERIAL

The Supplementary Material for this article can be found online at: <https://www.frontiersin.org/articles/10.3389/fphar.2019.01118/full#supplementary-material>

REFERENCES

- Abramoff, M. D., Magalhaes, P. J., and Ram, S. J. (2004). Image processing with ImageJ. *Biophotonics Int.* 11, 36–42.
- Acharya, K. R., and Ackerman, S. J. (2014). Eosinophil granule proteins: form and function. *J. Biol. Chem.* 289, 17406–17415. doi: 10.1074/jbc.R113.546218
- Al-Husseini, A., Wijesinghe, D. S., Farkas, L., Kraskauskas, D., Drake, J. I., Van Tassel, B., et al. (2015). Increased eicosanoid levels in the Sugen/chronic hypoxia model of severe pulmonary hypertension. *PLoS One* 10, e0120157. doi: 10.1371/journal.pone.0120157
- Antonio Gonçalves, W., Reis, A., Teixeira, M., Rezende, B., and Pinho, V. (2018). "Pro-resolving mediators," in *Immunopharmacology and inflammation*, (Switzerland: Springer International Publishing) 133–175. doi: 10.1007/978-3-319-77658-3_6
- Bahaie, N. S., Kang, B., Frenzel, E. M., Hosseinkhani, M. R., Ge, X., Greenberg, Y., et al. (2011). N-glycans differentially regulate eosinophil and neutrophil recruitment during allergic airway inflammation. *J. Biol. Chem.* 286, 38231–38241. doi: 10.1074/jbc.M111.279554
- Bahaie, N. S., Hosseinkhani, R. M., Ge, X. N., Kang, B. N., Ha, S. G., Blumenthal, M. N., et al. (2012). Regulation of eosinophil trafficking by SWAP-70 and its role in allergic airway inflammation. *J. Immunol.* 188, 1479–1490. doi: 10.4049/jimmunol.1102253
- Bai, T. R., and Knight, D. A. (2005). Structural changes in the airways in asthma: observations and consequences. *Clin. Sci.* 108, 463–477. doi: 10.1042/CS20040342
- Barnig, C., Cernadas, M., Dutile, S., Liu, X., Perrella, M. A., Kazani, S., et al. (2013). Lipoxin A4 regulates natural killer cell and type 2 innate lymphoid cell activation in asthma. *Sci. Transl. Med.* 5, 174ra26. doi: 10.1126/scitranslmed.3004812
- Bastan, I., Ge, X. N., Dileepan, M., Greenberg, Y. G., Guedes, A. G., Hwang, S. H., et al. (2018). Inhibition of soluble epoxide hydrolase attenuates eosinophil

- recruitment and food allergen-induced gastrointestinal inflammation. *J. Leuk. Biol.* 104, 109–122. doi: 10.1002/JLB.3MA1017-423R
- Belvisi, M. G., Saunders, M. A., Haddad, el-B., Hirst, S. J., Yacoub, M. H., Barnes, P. J. et al. (1997). Induction of cyclo-oxygenase-2 by cytokines in human cultured airway smooth muscle cells: novel inflammatory role of this cell type. *Br. J. Pharmacol.* 120, 910–916. doi: 10.1038/sj.bjp.0700963
- Benoit, C., Renaudon, B., Salvail, D., and Rousseau, E. (2001). EETs relax airway smooth muscle via an EpDHF effect: BKCa channel activation and hyperpolarization. *Am. J. Physiol. Lung Cell. Mol. Physiol.* 280, L965–L973. doi: 10.1152/ajplung.2001.280.5.L965
- Carey, M. A., Germolec, D. R., Bradbury, J. A., Gooch, R. A., Moorman, M. P., Flake, G. P., et al. (2003). Accentuated T helper Type 2 airway response after allergen challenge in cyclooxygenase-1-/- but not cyclooxygenase-2-/- mice. *Am. J. Respir. Crit. Care Med.* 167, 1509–1515. doi: 10.1164/rccm.200211-1383OC
- Cheng, K. P., Kiernan, E. A., Eliceiri, K. W., Williams, J. C., and Watters, J. J. (2016). Blue light modulates murine microglial gene expression in the absence of optogenetic protein expression. *Sci. Rep.* 6, 21172. doi: 10.1038/srep21172
- Christmas, P. (2015). "Role of cytochrome P450s in inflammation," in *Advances in pharmacology*, 74. Ed. J. P. Hardwick Waltham, MA, USA; San Diego, CA, USA; London, UK; Oxford, UK: Academic Press), 163–192. doi: 10.1016/bs.apha.2015.03.005
- Claar, D., Hartert, T. V., and Peebles, R. S. (2015). The role of prostaglandins in allergic lung inflammation and asthma. *Expert Rev. Respir. Med.* 9, 55–72. doi: 10.1586/17476348.2015.992783
- Davoine, F., and Lacy, P. (2014). Eosinophil cytokines, chemokines, and growth factors: emerging roles in immunity. *Front. Immunol.* 5, 570. doi: 10.3389/fimmu.2014.00570
- Debeuf, N., and Lambrecht, B. N. (2018). Eicosanoid control over antigen presenting cells in asthma. *Front. Immunol.* 9, 2006. doi: 10.3389/fimmu.2018.02006
- Doherty, T. A., and Broide, D. H. (2018). Lipid regulation of group 2 innate lymphoid cell function: moving beyond epithelial cytokines. *J. Allergy Clin. Immunol.* 141, 1587–1589. doi: 10.1016/j.jaci.2018.02.034
- Domingo, C., Palomares, O., Sandham, D. A., Erpenbeck, V. J., and Altman, P. (2018). The prostaglandin D(2) receptor 2 pathway in asthma: a key player in airway inflammation. *Respir. Res.* 19, 189–189. doi: 10.1186/s12931-018-0893-x
- Dyer, K. D., Moser, J. M., Czapiaga, M., Siegel, S. J., Percopo, C. M., and Rosenberg, H. F. (2008). Functionally competent eosinophils differentiated ex vivo in high purity from normal mouse bone marrow. *J. Immunol.* 181, 4004–4009. doi: 10.4049/jimmunol.181.6.4004
- Fajt, M. L., Gelhaus, S. L., Freeman, B., Uvalle, C. E., Trudeau, J. B., Holguin, F., et al. (2013). Prostaglandin D₂ pathway upregulation: relation to asthma severity, control, and TH2 inflammation. *J. Allergy Clin. Immunol.* 131, 1504–1512. doi: 10.1016/j.jaci.2013.01.035
- FitzGerald, G. A. (2004). Coxibs and cardiovascular disease. *New Eng. J. Med.* 351, 1709–1711. doi: 10.1056/NEJMp048288
- Gabriel, M. F., Postigo, I., Tomaz, C. T., and Martinez, J. (2016). *Alternaria alternata* allergens: markers of exposure, phylogeny and risk of fungi-induced respiratory allergy. *Environ. Int.* 89–90, 71–80. doi: 10.1016/j.envint.2016.01.003
- Gartung, A., Yang, J., Sukhatme, V. P., Bielenberg, D. R., Fernandes, D., Chang, J., et al. (2019). Suppression of chemotherapy-induced cytokine/lipid mediator surge and ovarian cancer by a dual COX-2/sEH inhibitor. *Proc. Natl. Acad. Sci. U. S. A.* 116, 1698–1703. doi: 10.1073/pnas.1803999116
- Ge, X. N., Bahaie, N. S., Kang, B. N., Hosseinkhani, R. M., Ha, S. G., Frenzel, E. M., et al. (2010). Allergen-induced airway remodeling is impaired in galectin-3 deficient mice. *J. Immunol.* 185, 1205–1214. doi: 10.4049/jimmunol.1000039
- Ge, X. N., Greenberg, Y., Hosseinkhani, M. R., Long, E. K., Bahaie, N. S., Rao, A., et al. (2013a). High-fat diet promotes lung fibrosis and attenuates airway eosinophilia after exposure to cockroach allergen in mice. *Exp. Lung Res.* 39, 365–378. doi: 10.3109/01902148.2013.829537
- Ge, X. N., Ha, S. G., Liu, F. T., Rao, S. P., and Sriramarao, P. (2013b). Eosinophil-expressed galectin-3 regulates cell trafficking and migration. *Front. Pharmacol.* 4, 37. doi: 10.3389/fphar.2013.00037
- Ge, X. N., Ha, S. G., Greenberg, Y. G., Rao, A., Bastan, I., Blidner, A. G., et al. (2016). Regulation of eosinophilia and allergic airway inflammation by the glycan-binding protein galectin-1. *Proc. Natl. Acad. Sci. U. S. A.* 113, E4837–E4846. doi: 10.1073/pnas.1601958113
- George, L., and Brightling, C. E. (2016). Eosinophilic airway inflammation: role in asthma and chronic obstructive pulmonary disease. *Ther. Adv. Chronic Dis.* 7, 34–51. doi: 10.1177/2040622315609251
- Ha, S., Ge, X. N., Bahaie, N. S., Kang, B. N., Rao, A., Rao, S. P., et al. (2013). ORMDL3 promotes eosinophil trafficking and activation via regulation of integrins and CD48. *Nat. Commun.* 4, 2479. doi: 10.1038/ncomms3479
- Hamid, Q., and Tulic, M. (2009). Immunobiology of asthma. *Ann. Rev. Physiol.* 71, 489–507. doi: 10.1146/annurev.physiol.010908.163200
- Hanna, V. S., and Hafez, E. A. A. (2018). Synopsis of arachidonic acid metabolism: a review. *J. Adv. Res.* 11, 23–32. doi: 10.1016/j.jare.2018.03.005
- Herrerias, A., Torres, R., Serra, M., Marco, A., Pujols, L., Picado, C., et al. (2009). Activity of the cyclooxygenase 2-prostaglandin-E prostanoïd receptor pathway in mice exposed to house dust mite aeroallergens, and impact of exogenous prostaglandin E₂. *J. Inflamm.* 6, 30. doi: 10.1186/1476-9255-6-30
- Hwang, S. H., Tsai, H.-J., Liu, J.-Y., Morisseau, C., and Hammock, B. D. (2007). Orally bioavailable potent soluble epoxide hydrolase inhibitors. *J. Med. Chem.* 50, 3825–3840. doi: 10.1021/jm070270t
- Hwang, S. H., Wagner, K. M., Morisseau, C., Liu, J. Y., Dong, H., Weckslar, A. T., et al. (2011). Synthesis and structure-activity relationship studies of urea-containing pyrazoles as dual inhibitors of cyclooxygenase-2 and soluble epoxide hydrolase. *J. Med. Chem.* 54, 3037–3050. doi: 10.1021/jm2001376
- Hye Khan, M. A., Hwang, S. H., Sharma, A., Corbett, J. A., Hammock, B. D., and Imig, J. D. (2016). A dual COX-2/sEH inhibitor improves the metabolic profile and reduces kidney injury in Zucker diabetic fatty rat. *Prostaglandins Other Lipid Mediat.* 125, 40–47. doi: 10.1016/j.prostaglandins.2016.07.003
- Kundu, S., Roome, T., Bhattacharjee, A., Carnevale, K. A., Yakubenko, V. P., Zhang, R., et al. (2013). Metabolic products of soluble epoxide hydrolase are essential for monocyte chemotaxis to MCP-1 in vitro and in vivo. *J. Lipid Res.* 54, 436–447. doi: 10.1194/jlr.M031914
- Lambrecht, B. N., and Hammad, H. (2015). The immunology of asthma. *Nat. Immunol.* 16, 45–56. doi: 10.1038/ni.3049
- Lambrecht, B. N., Hammad, H., and Fahy, J. V. (2019). The cytokines of asthma. *Immunity* 50, 975–991. doi: 10.1016/j.immuni.2019.03.018
- Li, H., Bradbury, J. A., Dackor, R. T., Edin, M. L., Graves, J. P., DeGraff, L. M., et al. (2011). Cyclooxygenase-2 regulates Th17 cell differentiation during allergic lung inflammation. *Am. J. Respir. Crit. Care Med.* 184, 37–49. doi: 10.1164/rccm.201010-1637OC
- Li, J., Zhou, Y., Wang, H., Gao, Y., Li, L., Hwang, S. H., et al. (2017). COX-2/sEH dual inhibitor PTUPB suppresses glioblastoma growth by targeting epidermal growth factor receptor and hyaluronan mediated motility receptor. *Oncotarget* 8, 87353–87363. doi: 10.18632/oncotarget.20928
- Luna-Gomes, T., Magalhães, K. G., Mesquita-Santos, F. P., Bakker-Abreu, I., Samico, R. F., Molinaro, R., et al. (2011). Eosinophils as a novel cell source of prostaglandin D₂: autocrine role in allergic inflammation. *J. Immunol.* 187, 6518–6526. doi: 10.4049/jimmunol.1101806
- Morin, C., Sirois, M., Echave, V., Gomes, M. M., and Rousseau, E. (2008). EET displays anti-inflammatory effects in TNF- α -stimulated human bronchi. *Am. J. Respir. Cell Mol. Biol.* 38, 192–201. doi: 10.1165/rcmb.2007-0232OC
- Morin, C., Sirois, M., Echave, V., Albadine, R., and Rousseau, E. (2010). 17,18-epoxyeicosatetraenoic acid targets PPAR γ and p38 mitogen-activated protein kinase to mediate its anti-inflammatory effects in the lung. *Am. J. Respir. Cell Mol. Biol.* 43, 564–575. doi: 10.1165/rcmb.2009-0155OC
- Morisseau, C., and Hammock, B. D. (2013). Impact of soluble epoxide hydrolase and epoxyeicosanoids on human health. *Ann. Rev. Pharmacol. Toxicol.* 53, 37–58. doi: 10.1146/annurev-pharmtox-011112-140244
- Muscará, M. N., Vergnolle, N., Lovren, F., Triggle, C. R., Elliott, S. N., Asfaha, S., et al. (2000). Selective cyclo-oxygenase-2 inhibition with celecoxib elevates blood pressure and promotes leukocyte adherence. *Br. J. Pharmacol.* 129, 1423–1430. doi: 10.1038/sj.bjp.0703232
- Nakagome, K., and Nagata, M. (2018). Involvement and possible role of eosinophils in asthma exacerbation. *Front. Immunol.* 9, 2220. doi: 10.3389/fimmu.2018.02220
- Norton, S. K., Wijesinghe, D. S., Dellinger, A., Sturgill, J., Zhou, Z., Barbour, S., et al. (2012). Epoxyeicosatrienoic acids are involved in the C(70) fullerene derivative-induced control of allergic asthma. *J. Allergy Clin. Immunol.* 130, 761–769. doi: 10.1016/j.jaci.2012.04.023
- Oguma, T., Asano, K., Shiomi, T., Fukunaga, K., Suzuki, Y., Nakamura, M., et al. (2002). Cyclooxygenase-2 expression during allergic inflammation in

- guinea-pig lungs. *Am. J. Respir. Crit. Care Med.* 165, 382–386. doi: 10.1164/ajrccm.165.3.2103093
- Park, W., Oh, Y. T., Han, J. H., and Pyo, H. (2008). Antitumor enhancement of celecoxib, a selective cyclooxygenase-2 inhibitor, in a Lewis lung carcinoma expressing cyclooxygenase-2. *J. Exp. Clin. Cancer Res.* 27, 66. doi: 10.1186/1756-9966-27-66
- Peebles, R. S. (2018). Prostaglandins in asthma and allergic diseases. *Pharmacol. Ther.* 193, 1–19. doi: 10.1016/j.pharmthera.2018.08.001
- Pope, S. M., Zimmermann, N., Stringer, K. F., Karow, M. L., and Rothenberg, M. E. (2005). The eotaxin chemokines and CCR3 are fundamental regulators of allergen-induced pulmonary eosinophilia. *J. Immunol.* 175, 5341–5350. doi: 10.4049/jimmunol.175.8.5341
- Profita, M., Sala, A., Bonanno, A., Riccobono, L., Siena, L., Melis, M. R., et al. (2003). Increased prostaglandin E2 concentrations and cyclooxygenase-2 expression in asthmatic subjects with sputum eosinophilia. *J. Allergy Clin. Immunol.* 112, 709–716. doi: 10.1016/S0091-6749(03)01889-X
- Sanak, M. (2016). Eicosanoid mediators in the airway inflammation of asthmatic patients: what is new? *Allergy Asthma Imm. Res.* 8, 481–490. doi: 10.4168/aair.2016.8.6.481
- Sanders, W. G., Morisseau, C., Hammock, B. D., Cheung, A. K., and Terry, C. M. (2012). Soluble epoxide hydrolase expression in a porcine model of arteriovenous graft stenosis and anti-inflammatory effects of a soluble epoxide hydrolase inhibitor. *Am. J. Physiol. Cell Physiol.* 303, C278–C290. doi: 10.1152/ajpcell.00386.2011
- Schauberger, E., Peinhaupt, M., Cazares, T., and Lindsley, A. W. (2016). Lipid mediators of allergic disease: pathways, treatments, and emerging therapeutic targets. *Curr. Allergy Asthma Rep.* 16, 48–48. doi: 10.1007/s11882-016-0628-3
- Schmittgen, T. D., and Livak, K. J. (2008). Analyzing real-time PCR data by the comparative C(T) method. *Nat. Protoc.* 3, 1101–1108. doi: 10.1038/nprot.2008.73
- Serhan, C. N. (2014). Pro-resolving lipid mediators are leads for resolution physiology. *Nature* 510, 92–101. doi: 10.1038/nature13479
- Shiraishi, Y., Asano, K., Niimi, K., Fukunaga, K., Wakaki, M., Kago, J., et al. (2008). Cyclooxygenase-2/prostaglandin D2/CRTH2 pathway mediates double-stranded RNA-induced enhancement of allergic airway inflammation. *J. Immunol.* 180, 541–549. doi: 10.4049/jimmunol.180.1.541
- Sousa, A., Pfister, R., Christie, P. E., Lane, S. J., Nasser, S. M., Schmitz-Schumann, M., et al. (1997). Enhanced expression of cyclo-oxygenase isoenzyme 2 (COX-2) in asthmatic airways and its cellular distribution in aspirin-sensitive asthma. *Thorax* 52, 940–945. doi: 10.1136/thx.52.11.940
- Swedin, L., Ellis, R., Neimert-Andersson, T., Ryrfeldt, Å., Nilsson, G., Inman, M., et al. (2010). Prostaglandin modulation of airway inflammation and hyperresponsiveness in mice sensitized without adjuvant. *Prostaglandins Other Lipid Mediat.* 92, 44–53. doi: 10.1016/j.prostaglandins.2010.02.004
- Yang, J., Bratt, J., Franzi, L., Liu, J. Y., Zhang, G., Zeki, A. A., et al. (2015). Soluble epoxide hydrolase inhibitor attenuates inflammation and airway hyperresponsiveness in mice. *Am. J. Respir. Cell Mol. Biol.* 52, 46–55. doi: 10.1165/rcmb.2013-0440OC
- Zhang, G., Panigrahy, D., Hwang, S. H., Yang, J., Mahakian, L. M., Wettersten, H. I., et al. (2014). Dual inhibition of cyclooxygenase-2 and soluble epoxide hydrolase synergistically suppresses primary tumor growth and metastasis. *Proc. Natl. Acad. Sci. U. S. A.* 111, 11127–11132. doi: 10.1073/pnas.1410432111
- Zhang, G., Kodani, S., and Hammock, B. D. (2014). Stabilized epoxygenated fatty acids regulate inflammation, pain, angiogenesis and cancer. *Prog. Lipid Res.* 53, 108–123. doi: 10.1016/j.plipres.2013.11.003
- Zhang, B., Jin, K., Jiang, T., Wang, L., Shen, S., Luo, Z., et al. (2017). Celecoxib normalizes the tumor microenvironment and enhances small nanotherapeutics delivery to A549 tumors in nude mice. *Sci. Rep.* 7, 10071. doi: 10.1038/s41598-017-09520-7
- Zuberi, R. I., Ge, X., Jiang, S., Bahaie, N. S., Kang, B. N., Hosseinkhani, R. M., et al. (2009). Deficiency of endothelial heparan sulfates attenuates allergic airway inflammation. *J. Immunol.* 183, 3971–3979. doi: 10.4049/jimmunol.0901604

Conflict of Interest: The authors declare that the research was conducted in the absence of any commercial or financial relationships that could be construed as a potential conflict of interest.

The reviewer, AH, declared a past co-authorship with one of the authors, BH, to the handling editor at the time of the review.

Copyright © 2019 Dileepan, Rastle-Simpson, Greenberg, Wijesinghe, Kumar, Yang, Hwang, Hammock, Sriramara and Rao. This is an open-access article distributed under the terms of the Creative Commons Attribution License (CC BY). The use, distribution or reproduction in other forums is permitted, provided the original author(s) and the copyright owner(s) are credited and that the original publication in this journal is cited, in accordance with accepted academic practice. No use, distribution or reproduction is permitted which does not comply with these terms.

Advantages of publishing in Frontiers



OPEN ACCESS

Articles are free to read
for greatest visibility
and readership



FAST PUBLICATION

Around 90 days
from submission
to decision



HIGH QUALITY PEER-REVIEW

Rigorous, collaborative,
and constructive
peer-review



TRANSPARENT PEER-REVIEW

Editors and reviewers
acknowledged by name
on published articles

Frontiers

Avenue du Tribunal-Fédéral 34
1005 Lausanne | Switzerland

Visit us: www.frontiersin.org

Contact us: info@frontiersin.org | +41 21 510 17 00



REPRODUCIBILITY OF RESEARCH

Support open data
and methods to enhance
research reproducibility



DIGITAL PUBLISHING

Articles designed
for optimal readership
across devices



FOLLOW US

@frontiersin



IMPACT METRICS

Advanced article metrics
track visibility across
digital media



EXTENSIVE PROMOTION

Marketing
and promotion
of impactful research



LOOP RESEARCH NETWORK

Our network
increases your
article's readership